

Serial No. 09/104340

#11
ucont
PATENT

IN THE UNITED STATES PATENT AND TRADEMARK OFFICE

Applicant: Boyd *et al.* Examiner: NIRMAL S. BASI
Serial No.: 09/104340 Group Art Unit: 1646
Filed: June 25, 1998 Docket No.: FISHR11.001AUS
Title: "RECEPTOR-LIGAND SYSTEM AND ASSAY"

DECLARATION OF ANDREW WALLACE BOYD

Assistant Commissioner for Patents
Washington, D.C., 20231

1. I, ANDREW WALLACE BOYD of 110 Kitchener Road, Ascot Queensland, 4007, Australia, am an inventor with respect to the abovementioned United States patent application. I am currently Senior Principal Research Fellow and Head of the Leukaemia Foundation Laboratory at the Queensland Institute of Medical Research, Brisbane, Queensland, Australia. I am also Professor of Experimental Haematology at The University of Queensland, St Lucia, Queensland, Australia, an appointment I have held since 1996. I am an expert in the field of Eph receptor biology and **attach** herewith a copy of my *Curriculum Vitae* which attests to my numerous publications in this area.
2. I am aware of the Examiner's reasons for rejecting all claims of the instant application as outlined in the Office Action dated October 25 1999. I consider that major concerns of the Examiner are:-
 - i. that it is not clear what comprises an Eph family receptor tyrosine kinase; and
 - ii. that while the instant specification is enabling for polypeptides which bind LERK7, such as HEK polypeptides according to SEQ

ID NO: 4, enablement is not provided for other polypeptides and ligands.

3. As will be discussed in more detail hereinafter, it is my contention that it is now currently accepted in the field that as a general rule, exon III of any Eph family receptor tyrosine kinase gene encodes a polypeptide capable of ligand binding, which polypeptide may, optimally, include amino acids encoded by exon II. This general rule is not limited to HEK and LERK7, but extends to other members of the well-defined Eph family of receptor tyrosine kinases. This general rule was first set forth in the instant application.
4. Included in Appendix A is a bibliographic reference to publications D1-D23 which support my arguments in rebuttal of the abovementioned concerns of the Examiner. A copy of publications D1-D23 is attached herewith.
5. With regard to (i) above, I contend that the term "Eph family receptor tyrosine kinase" has a precise and definite meaning in the art. The structure and function of Eph family receptor tyrosine kinases has been extensively reviewed, as has their ligands (originally called LERKS but hereinafter referred to as ephrins in accordance with current nomenclature; D1) and their high degree of structural conservation (D2-D7). The conserved structural features common to all Eph family members, and which serve to define this family are:-
 - an extracellular domain having an outer, globular, cysteine-rich region, a classical EGF-like domain and two fibronectin type III repeats
 - a highly conserved spacing of cysteine residues within the extracellular domain
 - conserved regions of amino acid identity, a feature which has

- been exploited to identify new Eph family members (D8, D9)
- a cytoplasmic domain having conserved tyrosine motifs, and an absolutely conserved YEDP motif in a juxtamembrane region
- a C-terminal conserved sterile alpha motif (SAM) domain
- a typical tyrosine kinase catalytic domain

This highly conserved structure is represented at both the nucleotide and amino acid sequence level in all vertebrate species and in *Drosophila* (D10) and *C. elegans* (D11). In fact, inter-species conservation is extremely high: typically greater than 90% amino acid identity between mammalian species and at least 80% identity between mammals and lower vertebrates (D12). In particular, mammalian Eph receptor tyrosine kinases share high sequence identity with fish and amphibian homologs (D13), and function in these species (D12, D14). A unifying nomenclature first set forth in D1 allows an unambiguous identification of Eph family members and their ligands in vertebrates and invertebrates. Therefore, the Eph family of receptor tyrosine kinases, and their ligands, is a well-defined family of molecules.

6. With regard to (ii) above, I contend that the experimental detail provided in the instant specification enunciates a broad principle which is readily adaptable to other Eph family members by a skilled person. A well recognized feature of the Eph-ephrin system is that there is a degree of degeneracy, such that any given Eph family RTK is capable of binding several ephrins, and *vice versa* (D15). In general, type A receptors preferentially bind type A ephrins, type B receptors preferentially bind type B ephrins and so on. As first shown for HEK in Example 4 of the instant specification, in reality there is a hierarchy of affinities of each Eph family receptor for a number of ephrin ligands (D16). An extreme example of this is EphA4, which binds ephrin A and ephrin B ligands (D14, D17). Consistent with Examples 8-11 of the instant specification, human EphA3 (referred to as HEK in the instant specification) binds a

number of zebrafish ligands with similar affinities to that of their human ephrin homologs (D12).

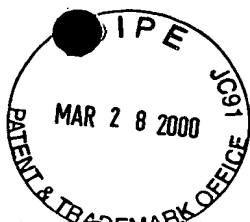
7. Further to the above, the exon III-encoded LERK-binding domain first described in Example 7 of the instant application was identified by producing recombinant proteins following exon structure studies, as shown in Example 1 (D18). The generalization proposed therein of the absolute requirement for the exon III-encoded polypeptide in binding ephrins has been confirmed by subsequent studies showing conservation of genomic organization and function among Eph receptors (D19-D21). Furthermore, the evidence presented at page 7 of the instant application that amino acids flanking the exon III-encoded domain may contribute to structural integrity, and hence assist ligand binding, has also been confirmed. The strongest confirming evidence comes from a study of mouse EphB2 (D22). A deletion mutant strategy identified a polypeptide domain encoded by exon III and exon II of the EphB2 gene as a domain both necessary and sufficient for ephrin binding. This publication also demonstrated that the corresponding domain of chicken EphA3 was necessary and sufficient for ephrin binding (D22). These data were then used as the basis for crystallization and structure determination (D23). This structural study showed that the domain encoded by exons II and III comprised a complex β jelly roll structure and a C-terminal region, with some features of an EGF-like domain as had been discussed in the instant application and in D18. This publication also identified a H-I loop which is structurally distinct in the EphA and EphB receptors studied, and is responsible for ligand preference. On the basis of this, and other reports, all investigators in the field accept that exon III of Eph family receptor tyrosine kinase genes encode a polypeptide capable of ligand binding, and that exon II encodes additional amino acids which contribute to this function.
8. I further declare that all statements made herein of my own knowledge

are true and that all statements made on information and belief are believed to be true, and further that these statements are made with the knowledge that willful false statements and the like are punishable by fine or imprisonment, or both, under Section 1001 of Title 18 of the United States Code, and that such willful false statements may jeopardize the validity of this application or any patent issuing therefrom.

Dated:

1/3/2000


Andrew Wallace BOYD



APPENDIX A

- D1: Eph Nomenclature Committee [letter] ,1997, Cell **90** 403-4
- D2: Drescher, U. 1997, Curr. Biol. **7** 799-807
- D3: Holder & Klein, 1999, Development **126** 2033-44
- D4: Lemke, 1997, Mol. Cell. Neurosci **9** 331-2
- D5: O'Leary & Wilkinson, 1999, Curr. Opin. Neurobiol. **9** 65-73
- D6: Pasquale, 1997, Curr. Opin. Neurobiol. **9** 608-15
- D7: Tuzi & Gullick, 1994, Britsh. J. Cancer **69** 417-21
- D8: Bohme *et al.*, 1993, Oncogene **8** 2857-62
- D9: Lickliter *et al.*, 1996, Proc. Natl. Acad. Sci. USA **93** 145-50
- D10: Scully *et al.*, 1999, Mol. Cell. Neurosci. **13** 337-47
- D11: George *et al.*, 1998, Cell **92** 633-43
- D12: Oates *et al.*, 1999, Mech. Dev. **83** 77-94
- D13: Suga *et al.*, 1999, J. Mol. Evol. **49** 601-8
- D14: Xu *et al.*, 1995, Development **121** 4005-16
- D15: Gale *et al.*, 1996, Neuron **17** 9-19
- D16: Lackmann *et al.*, 1997, J. Biol. Chem. **272** 16521
- D17: Dottori *et al.*, 1998, Proc. Natl. Acad. Sci. USA **95** 13248-13253
- D18: Lackmann *et al.*, 1998, J. Biol. Chem. **273** 20228-37
- D19: Connor & Pasquale, 1995, Oncogene **11** 2929-38
- D20: Henkemeyer *et al.*, 1996, Cell **86** 35-46
- D21: Owshalimpur & Kelley, 1999, Mech. Dev. **83** 77-94
- D22: Labrador *et al.*, 1997, EMBO J. **16** 3889-97
- D23: Himanen *et al.*, 1998, Nature **396** 486-91



ANDREW WALLACE BOYD BMedSc MB BS PhD FRACP

PLACE & DATE OF BIRTH:

Melbourne, Australia - 22nd June, 1948

DEGREES AND PROFESSIONAL QUALIFICATIONS:

1970	B.Med.Sc. Melbourne University.
1973	M.B.,B.S. Melbourne University.
1981	Ph.D. Melbourne University.
1983	Fellow of the Royal Australasian College of Physicians

PRESENT APPOINTMENTS:

Assistant Director (Clinical Sciences), Queensland Institute of Medical Research
Unit Head, Leukocyte Biology Unit, Queensland Institute of Medical Research
Head, Leukaemia Foundation Laboratory, Queensland Institute of Medical Research
Senior Principal Research Fellow, Queensland Institute of Medical Research
Professor of Experimental Haematology, University of Queensland
Chairman, Joint Program for Experimental Haematology, Queensland Institute of Medical Research & University of Queensland
Consultant Haematologist, Department of Haematology, Royal Brisbane Hospital

PREVIOUS APPOINTMENTS:

1974- 1976	Resident Medical Officer, Royal Melbourne Hospital.
1976-1977	Medical Registrar, Royal Melbourne Hospital.
1977-1978	Haematology Registrar, Austin Hospital.
1978-1981	National Health and Medical Research Council Postgraduate Fellowship, Cellular Immunology Unit, Walter and Eliza Hall Institute.
1978-1982	Associate, Department of Medical Biology, Melbourne University.
1979-1982	Clinical Instructor, Department of Medicine, Melbourne University.
1982-1983	Lyndal Skea Leukaemia Research Fund Fellowship in Clinical Oncology, the Haematology-Oncology Unit, Royal Melbourne Hospital.
1983-1985	Research Fellow, Division of Tumor Immunology, Dana-Farber Cancer Institute, Harvard Medical School, Boston, MA, U.S.A.
1983-1985	Research Associate, Department of Medicine, Harvard University, U.S.A.
1985-1996	Head, Lions Cancer Research Laboratory, Cellular Immunology Unit, Walter and Eliza Hall Institute
1985-1989	Senior Research Fellow, Department of Medical Biology, Melbourne University.
1985-1986	Visiting Associate, Department of Medical Oncology, Royal Melbourne Hospital.
1985-1987	Assistant Physician, Clinical Research Unit, Royal Melbourne Hospital.
1986-1996	Physician, Department of Medical Oncology, Royal Melbourne Hospital.
1987-1996	Associate, Royal Melbourne Hospital Clinical School.
1989-1996	Principal Research Fellow, Dept of Medical Biology, Melbourne University.
1990-1996	Assistant Haematologist, Department of Diagnostic Haematology, Royal Melbourne Hospital
1992-1996	Head, Monoclonal Antibody Laboratory, Collaborative Research Centre for Cellular Growth Factors
1992-1996	Senior Associate, Department of Medical Biology Melbourne University.

AWARDS AND DISTINCTIONS:

1970	Research Scholarship, Dept of Medicine, University of Melbourne
------	---

1973	Dame Kate Campbell Prize in Paediatrics
1978-1981	National Health and Medical Research Council Postgraduate Scholarship.
1983-1985	Neil Hamilton Fairley Travelling Fellowship, National Health and Medical Research Council.
1994-1995	Ramaciotti-Wellcome Fellowship

MEMBERSHIP OF PROFESSIONAL SOCIETIES:

Royal Australasian College of Physicians
Australasian Society for Immunologists
Haematology Society of Australia
International Cytokine Society
American Society for Haematology
Australasian Society for Developmental Biology

COMMITTEE APPOINTMENTS:

Regional Grant Interviewing Committees, National Health & Medical Research Council Assessors Panel (1988-1989, 1991-1992, 1996)
Scientific Secretary, Ethics Committee, Walter & Eliza Hall Institute Ethics Committee (1986-1996).
Ethics Committee, Royal Melbourne Hospital (1988-1993).
Assessor for National Association of Testing Authorities (1994-1995).
Scientific Advisory Committee, CRC for Vaccine Technology (1995-1999)
Australian Health Technology Advisory Committee Working Party on Molecular Biology (1995-1998)
Scientific Advisory Committee, Queensland Institute of Medical Research
Program Grant Interview Committee, National Health & Medical Research Council (1996)
Oncology Discipline Panel, National Health & Medical Research Council (1999)
Management Executive Committee, Queensland Institute of Medical Research (1999-)
Chairman, Clinical Protocol Review Committee, Queensland Institute of Medical Research (1999-)

MAJOR SCIENTIFIC CONTRIBUTIONS

- Tumour models for immune function - mechanism of effector cell blockade, induction of cell death by anti-immunoglobulin, phenotype switch from B cell to macrophage
- The role of membrane proteins in B lymphocyte differentiation - altered expression in tumours, link between cell surface phenotype and tumour type
- first demonstration of lineage switching within the hemopoietic compartment
- Role of ICAM-1 and other adhesion molecules in immune function and in inflammation
- Characterisation of human haemopoietic progenitor cells from umbilical cord blood
- Bone marrow stromal cell activity in support of human haemopoiesis
- Identification of a novel tyrosine kinase (HEK) as one of the first members of a unique class of receptor tyrosine kinase proteins, the EPH-like kinases
- characterisation of the HEK ligand and elucidation of receptor-ligand promiscuity
- role of Eph receptors in cell movement in early development
- role of Eph receptors in cancer

THESIS SUPERVISION AND EXAMINING

Examiner of 19 theses from the Universities of Adelaide, Flinders, Melbourne, Monash, Newcastle, Queensland and Sydney. I have supervised the following students:

Dr Stefan Wawryk	PhD	1989	Pathologist, Peter Macallum Hospital, Melbourne
Dr Ian Wicks	PhD	1991	Professor of Rheumatology, University of Melbourne
Dr Flavia Cicuttini	PhD	1993	Senior Lecturer, Dept of Medicine, Monash University
Dr Darryl Maher	PhD	1994	Clinical Director, Commonwealth Serum Laboratories
Ms Kirilee Wilson	BSc(Hons)	1994	PhD student, Melbourne University
Dr Nadesapillai Subanesan	BMedSc	1995	Resident Medical Officer, Royal Melbourne Hospital

44. Nadler LM, BOYD AW, Park E, Anderson KC, Fisher D, Slaughenhaupt B, Thorley-Lawson DA, Schlossman SF. The B cell restricted glycoprotein (B2) is the receptor for Epstein-Barr virus. In: Reinherz EL, Haynes B, eds. Proceedings of 2nd International Workshop on leukocyte differentiation antigens. Springer-Verlag, 1985
45. Anderson KC, BOYD AW, Fisher DC, Daley JF, Schlossman SF, Nadler LM. Human B cell populations defined by the B1 and B2 antigens. In: Reinherz EL, Haynes B, eds. Proceedings of 2nd International Workshop on human leukocyte antigens. Springer-Verlag, 1985
46. BOYD AW, Freedman A, Anderson KC, Fisher DC, Schlossman SF, Nadler LM. Phenotypic changes occurring during *in vitro* B cell activation. In: Reinherz EL, Haynes B, eds. Proceedings of 2nd International Workshop on leukocyte differentiation antigens. Springer-Verlag, 1985
47. Freedman AS, BOYD AW, Anderson KC, Fisher DC, Schlossman SF, Nadler LM. B5, a new B cell specific activation antigen. J Immunol 134:2048, 1985
48. BOYD AW, Anderson KC, Freedman AS, Fisher DC, Slaughenhaupt B, Schlossman SF, Nadler LM. Studies on the *in vitro* activation and differentiation of normal human B cells. I. Phenotypic and functional characterization of the B cell response to anti-Ig antibody. J Immunol 134:1516, 1985
49. BOYD AW, Griffin JD. Detection of non-random clustering of colonies in agar culture. Exp Hematol 13:696, 1985
50. Morimoto C, Letvin NL, BOYD AW, Hagen M, Brown HM, Kornacki MM, Schlossman SF. The isolation and characterization of the helper inducer T cell subset. J Immunol 134:3762, 1985
51. Tedder TF, BOYD AW, Freedman AS, Nadler LM, Schlossman SF. B cell activation and differentiation is linked to the cell surface B1 molecule. Fed Proc 44:1296, 1985
52. BOYD AW, Tedder TF, Anderson KC, Freedman AS, Nadler LM, Schlossman SF. The role of the 145Kd B2 antigen in B cell differentiation. Fed Proc 44:1296, 1985
53. Burns GF, Triglia T, Werkmeister JA, Begley CG, BOYD AW. TLiSA1, a human T lineage specific activation antigen involved in the differentiation of cytotoxic T lymphocytes and anomalous killer cells from their precursors. J Exp Med 161:1063, 1985
54. Tedder TF, BOYD AW, Freedman AS, Nadler LM, Schlossman SF. The B cell surface molecule B1 is functionally linked with B cell activation and differentiation. J Immunol 135:973, 1985
55. Berrebi A, Freedman AS, BOYD AW, Schlossman SF, Nadler LM. Phenotypic and functional analysis of the nodular poorly differentiated lymphoma cells. Exp Hematol 13:418, 1985
56. Freedman AS, BOYD AW, Slaughenhaupt B, Horowitz J, Nadler LM. Neoplastic counterparts of activated B cell states. Blood (Suppl) 66:187A, 1985
57. Ewan VA, Cieplinski W, Hancock WW, Goldschneider I, BOYD AW, Rickles FR. Production of a monoclonal antibody (A1-3) that binds selectively to activated monocytes and inhibits monocyte procoagulant activity. J Immunol 136:2408, 1986
58. BOYD AW, Freedman AS, Horowitz JC, Anderson KC, Fisher DC, Rosen KJ, Schlossman SF, Nadler LM. Studies on the *in vitro* activation and differentiation of human B lymphocytes. II. Analysis of the role of autocrine effects on B cell proliferation and of T cell-help in B cell differentiation. Cell Immunol 99:228, 1986
59. Tedder TF, Forsgren A, BOYD AW, Nadler LM, Schlossman SF. Antibodies reactive with the B1 molecule inhibit cell cycle progression of activated human B cells. Eur J Immunol 16:881, 1986
60. Freedman AS, BOYD AW, Berrebi A, Horowitz JC, Levy DN, Rosen KJ, Daley J, Slaughenhaupt B, Levine H, Nadler LM. Expression of B cell activation antigens on normal and malignant B cells. Leukemia 1:9, 1987
61. BOYD AW, Tedder TF, Griffin JD, Freedman AS, Fisher DC, Nadler LM. Pre-exposure of resting B cells to gamma-interferon enhances their proliferative response to subsequent activation signals. Cell Immunol 106:355, 1987

62. Burns GF, BOYD AW, Lucas CM, Werkmeister JA. The LFA-1 antigen and the glycolipid GD3 are involved in substrate attachment by melanoma cells. In: M^cMichael AJ, et al, eds. Leukocyte typing III: White cell differentiation antigens. 1987:849-851
63. BOYD AW, Lauriola F, Burns GF. Phenotypic analysis of human pre-B and B cells after *in vitro* culture. In: M^cMichael AJ, et al eds. Leukocyte typing III: White cell differentiation antigens. 1987:488
64. BOYD AW. Human leukocyte antigens: an update on structure, functional and nomenclature. Pathology 19:329-337, 1987
65. Freedman AS, BOYD AW, Bieber FR, Daley J, Rosen K, Horowitz JC, Levy DN, Nadler LM. Normal cellular counter parts of B cell chronic lymphocytic leukemia. Blood 70:418-427, 1987
66. BOYD AW, Wawryk S, Sheridan W. B cell differentiation: aspects relevant to the pathogenesis of autoimmune thrombocytopaenia. In: Immunoglobulins: the present and future. Excerpta Medica, Asian Pacific Congress Series No 67:29-44, 1987
67. Clutterbuck E, Shields JG, Gordon J, Smith SH, BOYD AW, Callard RE, Campbell HD, Young IG, Sanderson CJ. Recombinant human interleukin-5 is an eosinophil differentiation factor but has no activity in standard human B cell growth factor assays. Eur J Immunol 17:1743-1750, 1987
68. Morstyn G, Dührsen U, Campbell L, Villeval J, Kannourakis G, BOYD AW, Keech J, Abbot M, Nicola N, Bond J, Green M, Sheriden, W, Cebon T, Thomas R, Metcalf D, Fox RM. Granulocyte-colony stimulating factor (G-CSF) in patients with advanced cancer receiving Melphalan. Blood 70:(Suppl 1) 140a, 1987
69. BOYD AW, Ellis DW, Kannourakis G, Begley CG, Mackay IR, Burns GF. Activated killer cell lymphoma: an erythrophagocytic syndrome stimulating histiocytic medullary reticulosis. Pathology 20:265-270, 1988
70. BOYD AW, Fecondo J. The role of the CD21 antigen in lymphocyte transformation by Epstein Barr virus. Immunol Cell Biol 66:159-165, 1988
71. Morstyn G, Campbell L, Dührsen U, Souza LM, Alton NK, Villeval JL, Nicola N, BOYD AW, Kannourakis G, Cebon J, Thomas R, Boyd, J, Keech, J, Green M, Sheridan W, Metcalf D, Fox RM. Clinical studies with granulocyte colony stimulating factor (G-CSF) in patients receiving cytotoxic chemotherapy. Behring Inst Mitt 83:234-239, 1988
72. BOYD AW, Wawryk SO, Burns GF, Fecondo JV. Intercellular adhesion molecule 1 (ICAM-1) has a central role in cell-cell contact mediated immune mechanisms. Proc Natl Acad Sci USA 85:3095-3098, 1988
73. Maher D, BOYD AW. Interleukin 4 inhibits interleukin 2-induced growth of chronic lymphocytic leukemia cells *in vitro*. Blood 72:(Suppl) 124A, 1988
74. BOYD AW, Novotny JR, Wicks IP, Salvaris E, Welch K, Wawryk SO. The role of accessory molecules in lymphocyte activation. Transplant Proc 21:38-40, 1989
75. Sheridan WP, Green M, Fox RM, BOYD AW, Morstyn G. Autologous bone marrow transplantation: present status and future prospects. Aust NZ J Med 17:274, 1989
76. Sheridan W, BOYD AW, Green M, Morstyn G, Russell D, Thomas, R, Varigos G, McGrath K, Vaughan S, Scarlett J, Griffiths J, Brodie G, Januszewicz H, Fox R. High dose chemotherapy with Busulphan and Cyclophosphamide for drug-sensitive malignancies in adults: preliminary results. Med J Aust 15:379-386, 1989
77. Lieschke GJ, Maher D, Cebon J, O'Connor M, Green M, Sheridan W, BOYD AW, Rallings M, Bonnem E, Metcalf D, Burgess AW, McGrath K, Fox RM, Morstyn G. Effects of subcutaneously administered bacterially synthesised recombinant granulocyte-macrophage colony-stimulating factor in patients with advanced malignancy. Annals Int Med 110:357-364, 1989
78. Dunn SM, Hillam AJ, Stomski F, Jin B, Lucas CM, BOYD AW, Krissansen GW, Burns GF. Leukocyte adhesion molecules involved in inflammation. Transplant Proc 21:31-34, 1989
79. BOYD AW, Dunn SM, Fecondo JV, Culvenor JG, Dührsen U, Burns, GF, Wawryk SO. Regulation of expression of a human intercellular adhesion molecule (ICAM-1) during lymphohemopoietic differentiation. Blood 73:1896-1903, 1989

80. Ellis D, Marks D, Sheridan W, BOYD AW, Morstyn G. Diffuse large cell lymphoma: a teaching hospital experience. *Aust NZ J Med* 17:274-278, 1989
81. Deans JP, BOYD AW, Pilarski LM. Transitions from high to low molecular weight isoforms of CD45 involve rapid activation of alternative mRNA splicing and slow turnover of surface CD45R. *J Immunol* 143:1233-1238, 1989
82. Wawryk SO, Novotny JR, Wicks IP, Wilkinson D, Maher D, Salvaris E, Welch K, Fecondo J, BOYD AW. The role of LFA-1/ICAM-1 interaction in human leukocyte homing and adhesion. *Immunol Rev* 108:135-161, 1989
83. Campbell I, Cutri A, Wilkinson D, BOYD AW, Harrison LC. Induction of expression of ICAM-1 on human pancreatic islet cells. *Proc Natl Acad Sci USA* 86:4282-4286, 1989
84. Newman JD, Eckhardt GS, BOYD AW, Harrison LC. Induction of insulin receptor expression in the Burkitt lymphoma cell Raji by butyrate. *Biochem Biophys Res Comm* 161:101-106, 1989
85. BOYD AW, Wicks IP, Wilkinson D, Campbell I, Novotny JR, Wawryk SO, Harrison LC, Burns GF. Intracellular adhesion molecule 1 (ICAM-1): regulation and role in cell contact-mediated lymphocyte function. *Leukocyte Typing IV*. Ed. Knapp W, et al, Oxford U.P. 1989:684-686
86. Shimizu Y, Luce GG, Wahl L, BOYD AW, Shaw S. Molecular basis of T/monocyte adhesion. *Leukocyte Typing IV*. Ed Knapp W., et al, Oxford U.P., pp 689-693, 1989
87. BOYD AW, Wicks IP, Wawryk SO, Burns GF, Salvaris E, Wilkinson D and Novotny JR. Functional studies of intercellular adhesion molecule-1 (ICAM-1). *Tissue Antigens* 33:279, 1989
88. Novotny JR, Duehrsen U, Welch K and BOYD AW, Characterization of stromal cells and cell lines derived from long term bone marrow cultures. *Tissue antigens* 33:180, 1989
89. Wawryk SO, Salvaris E, Sandrin M and BOYD AW. Functional studies of stable L cell transfectants expressing intercellular adhesion molecule-1 (ICAM-1). *Immunol Cell Biol* 67:391-401, 1989
90. Krissansen GW, Lucas CM, Stomski FC, Elliot MJ, Berndt MC, BOYD AW, Horton MA, Cheresch DA, Vadas MA, Burns GF. Blood leukocytes bind platelet glycoprotein (IIb-IIIa)' but do not express the vitronectin receptor. *Int Immunol* 2:267-277, 1990
91. BOYD AW, Wicks IP, Wilkinson D, Novotny JR, Welch K, Salvaris E, Campbell IL, Harrison LC and Wawryk SO. The role of LFA-1/ICAM-1 linkage in immune function; Implications for the pathogenesis of diabetes mellitus. In: *Endothelial cell function in diabetic microangiopathy*. Ed., Molinatti GM et al, Karger press 1990:164-174
92. Novotny JR, Duehrsen U, Welch K, Layton JE, Cebon JS and BOYD AW. Clonal stromal cell lines derived from human Whitlock-Witte long term bone marrow cultures. *Exp Hematol* 18: 775-784, 1990
93. BOYD AW, Salvaris E, Wicks LP, Welch K and Novotny JR. Tyrosine kinase proteins expressed by human pre B cell leukemia cell lines. *J Cell Biochem Suppl* 14D:251, 1990
94. Biggs B-A, Gooze L, Wycherley K, Wilkinson D, BOYD AW, Forsyth KP, Edelman L, Brown GV and Leech JH. Knob-independent cytoadherence of *Plasmodium Falciparum* to the leukocyte differentiation antigen CD36. *J Exp Med* 171:1883-1892, 1990
95. Maher DW, Pike BL, BOYD AW. The response of human B cells to IL-4 is determined by their stage of activation and differentiation. *Scand J Immunol* 32:631-640, 1990
96. Maher DW, Welch K, Pike BL, Morstyn G, BOYD AW. The Biology and Potential Clinical Role of Interleukin 4 In: *Biological Agents in the Treatment of Cancer*. (Conference Proceedings) Newcastle pp 454-473, 1990
97. Maher D, BOYD AW, McKendrick J, Begley CG, Lieschke M, Green M, Fox R, Rallings M, Bonnem E and Morstyn G. Rapid response of B cell malignancies induced by Interleukin 4. *Blood* 76 (suppl. 1): 152a, 1990
98. Wawryk SO, Cockerill P, BOYD AW. Analysis of the promoter region of Intercellular Adhesion molecule 1 (ICAM-1). *International Immunol* 3:83-93, 1991
99. Fecondo JV, Kent SBH, BOYD AW. Inhibition of Intercellular adhesion molecule-1 (ICAM-1) - dependent biological activities by a synthetic peptide analog. *Proc Natl Acad Sci USA* 88:2879-2882, 1991

100. Wawryk SO, Aykerk H, BOYD AW, Rode J. Analysis of Adhesion molecules in the Immunopathogenesis of Giant Cell Arteritis. *J Clin Path* 44:497-501, 1991
101. Maher DW, Davis I, BOYD AW, Morstyn G., Human interleukin-4; An immunomodulator with potential therapeutic applications. *Prog. Growth Factor Res.* 3:43-56, 1991
102. Duguid IGM, BOYD AW, Mandel TE. The expression of adhesion molecules in the human retina and choroid. *Aust. NZ J Ophthalmol.* 19:309-316, 1991
103. Agrez MV, Bates RC, BOYD AW and Burns GF. ARG-GLY-ASP-containing peptides expose novel collagen receptors on fibroblasts: implications for wound healing. *Cell. Regul.* 2:1035-1044, 1991.
104. Cicuttini FM, Martin M, Maher DW and BOYD AW. Long term human hematopoiesis in vitro using cloned stromal cell lines and highly purified progenitor cells. In: Miller, JFAP, ed. *Advances in molecular and cell biology - Vol 5.* JAI Press, Greenwich Connecticut, 1992. pp1-35
105. Salvaris E, Novotny JR, Welch K, Campbell, L, BOYD AW. Characterisation of two novel pre B cell lines (LK63 and LiLa-1): Potential models of pre B cell differentiation. *Leukemia Res* 16:655-663, 1992
106. Wicks IP, Leizer T, Wawryk SO, Novotny JR, Hamilton J, Vitti G and BOYD AW. The effect of cytokines on the expression of MHC antigens and ICAM-1 by normal and transformed synoviocytes. *Autoimmunity* 12:13-20, 1992
107. Cicuttini F, Begley CG, BOYD AW. The effect of recombinant stem cell factor (SCF) on purified human umbilical cord blood progenitor cells. *Growth Factors* 6:31-39, 1992.
108. BOYD AW, Ward LD, Wicks IP, Simpson RJ, Salvaris E, Wilks A, Welch K, Loudovaris M, Rockman S and Busmanis I. Isolation and characterisation of a novel receptor-type protein tyrosine kinase (hek) from a human pre B cell line. *J Biol Chem* 267:3262-3267, 1992.
109. Campbell LJ, Maher DW, Tay DLM, BOYD AW, Rockman S, McGrath K, Fox RM and Morstyn G. Marrow proliferation and the appearance of giant neutrophils in response to recombinant human granulocyte colony stimulating factor (rhG-CSF) *Br. J. Haematol.* 80:298-304, 1992
110. Cicuttini, FM, Martin M, Salvaris E, Ashman L, Begley CG, Novotny JR, Maher D, and BOYD AW. Support of human cord blood progenitor cells on stromal cell lines transformed by SV40 large T antigen under the influence of an inducible (Metallothionein) Promoter. *Blood*, 80:102-112, 1992.
111. Wicks IP, Wilkinson D, Salvaris E and BOYD AW. Molecular cloning of *hek*, a novel receptor tyrosine kinase expressed by human lymphoid tumour cell lines. *Proc. Natl. Acad. Sci. USA* 89:1611-1615, 1992.
112. Maher DW, Pike BL, Kountouri N, Boyd AW. Human IL-10 promotes B cell differentiation and increases the frequency of human B cells induced to secrete IgG *in vitro*. *Blood (suppl.)* (in press).
113. Fecondo JV, Pavuk NC, Silburn KA, Read DMY, Mansell AS, BOYD AW, McPhee DA. Synthetic peptide Analogs of Inter cellular Adhesion Molecule-1 (ICAM-1) inhibit HIV-1 replication of MT-2 cells. *AIDS Res. Hum. Retro.* 9:733-740, 1993
114. Martin M, Strasser A, Baumgarth N, Cicuttini FM, Welch K, Salvaris E, and BOYD AW. SPGM1: a novel model for pre B cell to monocyte switching. *J Immunol.* 150:4395-4406, 1993.
115. Whittingham S, Naselli G, Harrison LC, BOYD AW, Cebon J, Jack I. Cytokine production in response to Epstein Barr virus infection of peripheral blood mononuclear cells *in vitro*. *Immunol. Cell. Biol.* 71:259-264, 1993.
116. Cicuttini FM, Martin M, Petrie H, BOYD AW. A novel population of NK precursors isolated from umbilical cord blood. *J Immunol.* 151:29-37, 1993.
117. Zola H, Siderius N, Flego N, Sparrow R, van der Weyden NB, Nimmo J, Hart DNJ, Houghton S and BOYD AW. Expression of CD45 isoforms in chronic B cell leukaemia. *Leukemia Res.* 17:209-216, 1993.
118. Cicuttini FM, Loudovcris ML and BOYD AW. Interactions between purified human cord blood haemopoietic progenitor cells and accessory cells. *Brit J Haematol.* 84:365-373, 1993.

119. Nicola NA, Wycherley K, BOYD AW, Layton JE, Cary D and Metcalf D. Neutralizing and non-neutralizing monoclonal antibodies to the human GM-CSF receptor α chain. *Blood*. 82:1724-1731, 1993.
120. BOYD AW, Olsson JE, Wilkinson D, and Wicks IP. Hek, a human receptor tyrosine kinase hyper-expressed on human leukaemic cell lines. *Tissue Antigens* 42:342, 1993.
121. McKinstry WJ, Welch KL, Martin M, Moritz RL, Ward LD, Simpson RJ, Boyd AW, Nicola NA. Purification of a fragment of human complement factor Bb having self-renewal activity on a murine haemopoietic progenitor cell line. *Exp. Hematol.* 21: 1148a, 1993.
122. Robb LG, Rockman S, Begley CG, BOYD AW and McGrath K. A study of Granular lympho-proliferative disorders including a CD3-negative case with a rearrangement of the T cell receptor locus. *Leukaemia and Lymphoma* 13:143-150; 1994.
123. Wicks, IP, Lapsys N, Baker E, Campbell L, BOYD AW, Sutherland G. Localization of a human receptor tyrosine kinase (ETK1) to chromosome region 3p11.2. *Genomics* 19:38-41, 1994.
124. Cicuttini FM, Martin M and BOYD AW. Cytokine induction of adhesion molecules on synovial type B cells. *J Rheumatol.* 21: 406-412, 1994.
125. Sotzik F, BOYD AW and Shortman K. Surface antigens of human thymocyte populations defined by CD3, CD4 and CD8 expression. CD 1a is expressed by mature thymocyte but not peripheral T cells. *Immunol. Letters.* 36:101-106, 1994
126. Sotzik F, Rosenberg Y, BOYD AW, Honeyman M, Metcalf D, Scollay R and Shortman KD. Assessment of CD4 expression by early T precursor cells and by dendritic cells in the human thymus. *J. Immunol* 152: 3370-3377, 1994.
127. Martin M, Spencker T, Cicuttini F, Welch K, BOYD AW and Strasser A. SPGM-1: A novel cellular model for interleukin 3 induced lineage switch. *Proceedings of the 3rd International Symposium on Cytokines in Hematology, Oncology and Immunology*, Springer-Verlag, 1994.
128. Cicuttini FM and BOYD AW. Hemopoietic and lymphoid progenitor cells in human umbilical cord blood. *Developmental Immunol.* 4:1-11, 1994.
129. Duhrsen U, Novotny J and BOYD AW. Self renewal of a transplantable murine leukemia induced by co-culture with human stromal cell lines. *Leukemia* 8:490-497, 1994
130. Lickliter JD, Begley CG, BOYD AW, Szer J, and Grigg AP. Combined chemotherapy and granulocyte stimulating factor (G-CSF) mobilise large numbers of peripheral blood progenitor cells in pre-treated patients. *Leukemia and Lymphoma* 15:91-71; 1994
131. Cicuttini FM, Welch K, BOYD AW. Characterisation of CD34⁺ CD 38⁺ and CD34⁺, CD38⁻ progenitor cells from Human Umbilical Cord blood. *Growth factors* 10:127-134; 1994.
132. Cicuttini FM, Welch K, BOYD AW. The effect of cytokines on CD34⁺Rh-123^{high} and CD34⁺Rh-123^{low} progenitor cells from human umbilical cord blood. *Exp. Hematol.* 22:1244-1251; 1994.
133. Grigg A, O'Flaherty E, Begley CG & BOYD AW. The relationship between the number of GM-CFC, CD34⁺ cells and mononuclear cells in PBL and leucapheresis products after chemotherapy and Growth Factor Mobilization. *Blood* (in press).
134. BOYD AW, Olsson JE, Wilkinson D, Bucci T, Smith F, Dottori M, Lickliter J, Welch K and Zaiss M. The role of the Hek RTK in hematopoiesis and oncogenesis. *Cytokine* 6: 552; 1994.
135. BOYD AW, Olsson JE, Wilkinson D, Bucci T, Carter WM, Wilson KA, Welch K, Dottori M, and Wicks IP. Isolation and characterisation of hek - an oncogenic receptor tyrosine kinase. In: *Leukocyte Typing V*, Vol 2, pp1928-1930, OUP, 1995
136. Grigg AP, Roberts AW, Raunow, H, Houghton, S, Layton, JE, BOYD, AW, McGrath, K & Maher, D. Defining the optimal dose and scheduling of Granulocyte Colony Stimulating Factor for mobilisation and collection of peripheral blood progenitor cells in normal volunteers. *Blood* 86:4437-4445; 1995.
137. de Nichilo MO, Shaffren DR, Carter WM, Berndt MC, Burns GF and BOYD AW. A common epitope on platelet integrin α IIb β 3 (glycoprotein IIb IIIa; CD41b/CD61) and α Mb2 (Mac-1; CD11b/CD18) *J.Immunol.* 156:284-288; 1996.
138. Lickliter JD, Smith FM, Olsson JE & BOYD AW. Embryonic stem cells express multiple Eph-subfamily tyrosine kinases. *Proc. Natl. Acad. Sci. USA* 93:145-150; 1996.

139. Lackmann M, Bucci T, Mann RJ, Kravets LA, Viney E, Smith M, Moritz RL, Carter W, Simpson RJ, Nicola N, Mackwell K, Nice EC, Wilks AF & BOYD AW. Purification of a ligand for the Eph-like receptor HEK using a novel biosensor-base affinity detection approach. *Proc. Natl. Acad. Sci. USA* 93:2523-2527; 1996.
140. Hair, GA, Padula, S, Zeff, R, Schmeizl, M, Contrino, J, Kreutzer, DL, de Moerloose, P, BOYD, AW, Stanley, I, Burgess, AW & Rickles, FR
Tissue factor expression in human leukemic cells. *Leukemia Res.* 20:1-11; 1996.
141. Davis, ID, Maher, DW, Cebon, JS, Green, MR, Fox, RM, McKendrick, JJ, Rybak, ME & BOYD AW Phase I and pharmacokinetic study of subcutaneously administered recombinant human interleukin-4(rhu-IL-4) in patients with advanced cancer. *Growth Factors* (in press).
142. Roberts, AW, Zaiss, M, BOYD, AW & Nicola, NA G-CSF-mobilised peripheral blood progenitor cells: in vitro growth pattern & hematopoietic growth factor receptor profile. *Exp Hematol* 25: 298-305; 1997.
143. Lackmann, M, Mann, RJ, Kravets, L, Smith, FM, Bucci, TA, Maxwell, KF, Howlett, GJ, Olsson, JE, Cerretti, DP and BOYD, AW Biomolecular interaction analysis of ligand binding to the HEK receptor exodomain shows that LERK7 is the preferred high affinity ligand. *J.Biol.Chem.* 272:16521-30;1997.
144. Zaiss,M, Andreesen,R & BOYD AW A method for single cel RT-PCR allowing multiple amplifications from single hematopoietic progenitor cells. *Blood (Suppl)* 90:153b; 1997.
145. Smith, SI, Weil, D, Johnson, GR, BOYD, AW & Li, CL Expression of the Wilms' Tumor Suppressor Gene, WT1, Is Upregulated by Leukemia Inhibitory Factor and Induces Monocytic Differentiation in M1 Leukemic Cells *Blood* 91: 764-773; 1998
146. Dottori, M, Hartley, L, Galea, M, Paxinos, G, Polizzotto,M, Kilpatrick, T, Bartlett, PB, Murphy, M, Köntgen, F & BOYD, AW. EphA4 (Sek1) receptor tyrosine kinase is required for the development of the corticospinal tract. *Proc Natl. Acad. Sci. USA* 95:13248-53; 1998.
147. Lackmann,M, Oates, A, Dottori, M, Power, M, Smith, FM, Do, C, Kravets, L, & BOYD, AW Distinct subdomains of the EphA3 receptor mediate ligand binding and receptor dimerisation. *J. Biol. Chem.* 273:20228-37; 1998
148. Oates, AC, Lackmann,M, Power, M-A, Brennan, C, Smith, FM, Do, C, Evans,B, Holder, N & BOYD, AW An early developmental role for Eph-ephrin interaction during vertebrate gastrulation. *Mech. Dev.* 83:77-94; 1999.
149. Dottori, M, Down, M, Hüettnann, A, Fitzpatrick, DR & BOTD, AW Cloning and characterization of the EphA3 gene promoter: DNA methylation regulates expression in hemopoietic tumor cells. *Blood* 94:2477-2486;1999.
150. Smith, SI, Down, M, BOYD, AW & Li, CL. Expression of the Wilm's Tumor Suppressor Gene, WT1, reduces the tumorigenicity of the leukemic cell line M1 in C.B-17 *scid/scid* mice. *Cancer Res* 60:808-814.

The Eph family of receptors

Elena B Pasquale

Eph receptor tyrosine kinases have recently been identified as instructive molecules that guide the topographic movement of cells and growth cones. The activation of Eph receptors by their ligands, which are membrane-anchored molecules, involves a cell-cell recognition event that often causes cell repulsion. Therefore, Eph receptors mediate signals that can override cell adhesion. Transmembrane ligands for Eph receptors also exhibit properties of signal transducing molecules, suggesting that bidirectional signaling occurs when receptor-expressing cells contact ligand-expressing cells.

Addresses

The Burnham Institute, 10901 N Torrey Pines Road, La Jolla, CA 92037, USA; e-mail: elenap@ljcrf.edu

Current Opinion in Cell Biology 1997, 9:608-615

<http://biomednet.com/elecref/0955067400900608>

© Current Biology Ltd ISSN 0955-0674

Abbreviations

GAP	GTPase-activating protein
GPI	glycosylphosphatidylinositol
PI 3-kinase	phosphatidylinositol 3-kinase
SH2	Src homology 2
SLAP	Src-like adaptor protein

Introduction

Directional movement of cells and cell processes requires molecules with permissive and instructive functions [1]. Recently identified families of instructive molecules include the netrins, semaphorins, and Eph family receptors and ligands [1]. In this review, I summarize new developments in the study of the role of Eph receptors in contact-mediated cell guidance.

The Eph family comprises fourteen structurally related transmembrane receptor tyrosine kinases (Table 1). The extracellular region of Eph receptors is composed of a series of modules, namely, a putative immunoglobulin (Ig) domain at the amino terminus, followed by a cysteine-rich region and two fibronectin type III repeats near the single membrane-spanning segment. The cytoplasmic region contains a highly conserved tyrosine kinase domain flanked by a juxtamembrane region and a carboxy-terminal tail, which are less conserved [2]. Many receptor variant forms also exist that do not conform to the prototypical domain structure, as they contain deletions, truncations, substitutions, or insertions (see [3] and references therein). One Eph receptor, Mep, lacks kinase activity [4].

Because so many Eph receptor genes have been identified in different species within a brief period of time, each gene has been assigned multiple names (Table 1).

According to a unified nomenclature, which has been published elsewhere [5], the Eph receptors are divided into two groups on the basis of sequence homologies. Receptors of the EphA group preferentially interact with glycosylphosphatidylinositol (GPI)-linked ligands (of the ephrin-A subclass, which comprises five ligands), while receptors of the EphB group preferentially interact with transmembrane ligands (of the ephrin-B subclass, which comprises three ligands) (Table 1). In either case, binding of a ligand results in Eph receptor autophosphorylation on tyrosine residues and activation of the kinase activity of the Eph receptor [6-8].

Spatially restricted Eph receptor activation

As, *in vitro*, each Eph receptor binds multiple ligands and each ligand binds multiple receptors, determination of the expression patterns of the Eph receptors and ligands is crucial to identifying which interactions occur *in vivo*. In addition, it provides clues to how the Eph receptors and their ligands function.

There are numerous examples of reciprocal expression of Eph receptors and their ligands (summarized in Table 2 and shown schematically in Figure 1a,b). Reciprocal distributions allow for only limited receptor activation, restricted to sites where ligand and receptor come into contact in significant numbers. Recent evidence suggests that Eph receptors guide the movement of growth cones and cells in which they are expressed in order to avoid regions of excessive ligand concentration, thereby influencing axon pathfinding and the segregation of subpopulations of cells. As discussed below, repulsive interactions between receptor- and ligand-expressing cells are presumably responsible for these activities.

An example of Eph receptor mediated axon guidance is the specification of retinotectal topography. Even before the Eph receptors were found to be involved in this process, it was established that the precise targeting of retinal ganglion cell axons in the optic tectum relies upon repulsive activities mediated by molecules expressed in a graded manner on the ingrowing retinal axons and in the tectum [9,10]. Consistent with this model, retinal ganglion cells from different portions of the retina express different levels of the Eph receptor Cck4 (Table 2) [11]. Temporal retinal axons, which have high levels of Cck4 expression, grow to the anterior tectum, where expression of the two GPI-linked ligands, ELF1 and RAGS (see Table 1), is low [11,12]. These two ligands are distributed in superimposed increasing anterior to posterior gradients in the tectum, with the higher affinity ligand for Cck4, RAGS, restricted to more posterior regions than the lower affinity ligand, ELF1 [13]. *In vitro* experiments have confirmed that both ELF1 and RAGS behave as repulsive guidance molecules.

Table 1

The Eph receptors and their ligand specificities.

Receptors					Ligands*
Unified nomenclature	Human	Mouse	Rat	Chicken/Quail	
EphA receptors					
EphA1	Eph	Esk	—	—	Ephrin-A1
EphA2	Eck	mEck/Myk2/Sek2	—	—	Ephrin-A3, -A1, -A5, -A4
EphA3	Hek	Mek4	Tyro4	Cek4	Ephrin-A5, -A2, -A3, -A1
EphA4	Hek8	Sek1	Tyro1	Cek8	Ephrin-A5, -A1, -A3, -A2, -B2, -B3
EphA5	Hek7	Bsk	Ehk1/Rek7	Cek7	Ephrin-A5, -A1, -A2, -A3, -A4
EphA6	—	mEhk2	Ehk2	—	Ephrin-A2, -A1, -A3, -A4, -A5
EphA7	Hek11	Mdk1/Ebk	Ehk3	—	Ephrin-A2, -A3, -A1
EphA8	Eek	mEek	Eek	—	Ephrin-A5, -A3, -A2
EphB receptors					
EphB1	Net	—	Elk	Cek6	Ephrin-B2, -B1, -A3
EphB2	Erk/Hek5/Drt	Nuk/Sek3	Tyro5	Cek5, Qek5	Ephrin-B1, -B2, -B3
EphB3	Hek2	Sek4/Mdk5	Tyro6	Cek10, Qek10	Ephrin-B1, -B2, -B3
EphB4	Htk	Myk1/Mdk2	Tyro11	—	Ephrin-B2, -B1
EphB5	—	—	—	Cek9	?
EphB6	Hep	Mep	—	—	?

*Ligands are listed in approximate order of decreasing affinity for receptor according to a recently published unified nomenclature [5]. Other names for these ligands are as follows: ephrin-A1, B61; ephrin-A2, ELF1; ephrin-A3, Ehk1-L, Lerk3; ephrin-A4, Lerk4; ephrin-A5, AL1, RAGS; ephrin-B1, Lerk2, Elk-L, Cek5-L; ephrin-B2, Htk-L, ELF2, Lerk5; ephrin-B3, Nlerk2, Elk-L3. Please note that not all possible ligand-receptor interactions have been tested. Long dashes indicate that homologs of some receptors in other species have not yet been found. Question marks indicate that the ligands for Cek9 and Hep/Mep are unknown.

The growth cones of cultured temporal retinal neurons collapse when exposed to soluble forms of these ligands, and in 'stripe assays' temporal retinal axons, grown on stripes containing RAGS or ELF1 alternating with stripes without ligand, avoid extending on the stripes coated with ligand [12,13,14**]. The *in vivo* repulsive activity of ELF1 was demonstrated when the distribution of ELF1 in the chicken tectum was modified by retroviral expression: temporal axons followed aberrant trajectories that avoided ectopic areas of abnormally high ELF1 expression in the anterior tectum [14**].

Other examples where the reciprocal expression patterns of Eph receptors and their ligands suggest that Eph receptors and ligands guide axons by repulsive mechanisms are summarized in the top half of Table 2. Interestingly, the confinement of spinal axon growth to rostral somite halves had been attributed to repulsive activities located in caudal somite halves [15]. As it turns out, the transmembrane Eph receptor ligands Htk-L and Lerk2 (see Table 1) are restricted to caudal somite halves [16*,17**], whereas several Eph receptors, including Nuk/Cek5 and Cek8, are found on axons of spinal neurons [7,17**,18]. Repulsive activities of these transmembrane ligands (Htk-L and Lerk2) toward axons extending from neural tube explants has been demonstrated *in vitro* in both growth cone collapse assays and stripe assays [17**].

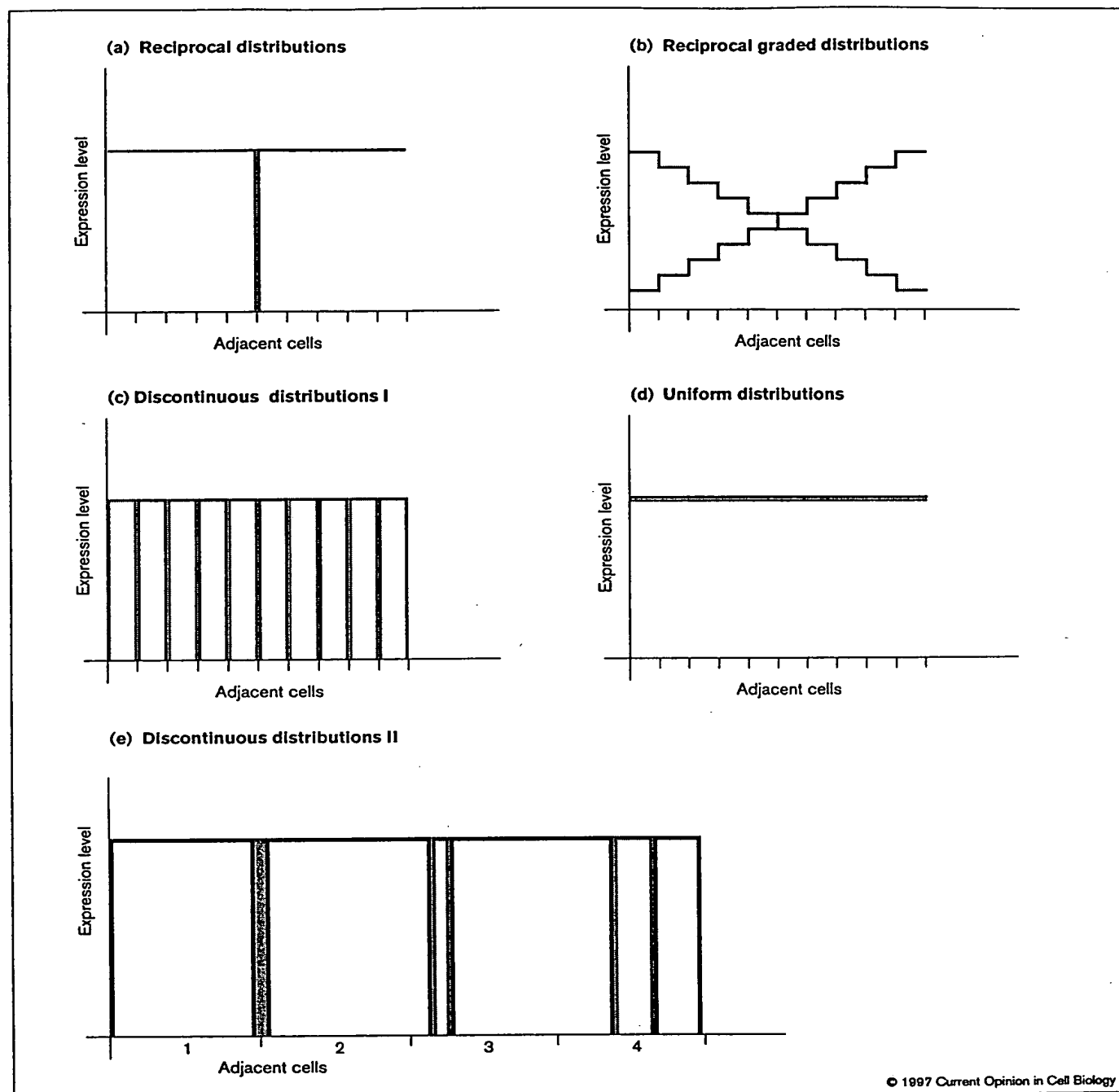
Examples of where Eph receptors and their ligands are expressed in adjacent populations of cells, suggesting that they restrict cell movement across boundaries of ligand and receptor expression, are summarized in the bottom half of Table 2. Experimental evidence supports a role

for Eph receptors in restricting and guiding cell migration. Exposure of chicken embryo trunk explants to a soluble dimeric form of the ligand Elk-L (see Table 1) perturbed the routing of trunk neural crest cells, which express a receptor, Qek10/Cek10, for Elk-L [19*]. Although the motility of neural crest cells was not appreciably affected, their movement no longer exhibited a persistent directional component, nor was it restricted to the normal route across rostral somite halves. Similarly, in *Xenopus* embryos the migration of third branchial arch neural crest cells, which express the receptors Sek1 and Elk, was perturbed by the ectopic uniform expression of a ligand for these receptors, Htk-L, which is normally restricted to the adjacent second arch neural crest [20*]. Ectopic expression in *Xenopus* embryos of dominant-negative forms of the receptors Sek1 and Elk, which lacked the kinase domain and were thus unable to transduce signals, also interfered with the directional migration of third arch neural crest cells. Furthermore, the boundaries of rhombomeres 3 and 5, which express Sek1, became blurred in the presence of ectopic dominant-negative Sek1 [21].

Persistent Eph receptor activation

Overlapping distributions of Eph receptors and their ligands have also been observed; this may cause persistent receptor activation. For example, in the 11-day chicken embryonic retina the receptor Cek5 and its ligand, Cek5-L, have overlapping expression patterns; binding of Cek5-L to Cek5 results in enhanced Cek5 phosphorylation on tyrosine [22,23]. During the first half of chicken embryonic development, Cek9 is highly phosphorylated on tyrosine, possibly reflecting extensive interactions with its as yet unidentified ligand [24]. In the developing

Figure 1



Schematic representation of the possible relative distributions of Eph receptors and their ligands in a series of adjacent cells. Each subdivision on the X axis indicates a cell; the Y axis indicates the level of ligand or receptor expression, in arbitrary units. Ligand expression levels are indicated in gray and receptor expression levels in black. (a,b) Illustrate reciprocal and reciprocal graded patterns of expression, respectively. (c-e) Illustrate hypothetical distributions in tissues in which receptor and ligand have overlapping expression patterns. In (c) each cell expresses either receptor or ligand, and receptor-bearing cells and ligand-bearing cells are interspersed. In (d) each cell expresses both receptor and ligand, and receptor and ligand have uniform distribution over the surface of the cell. In (e) each cell (depicted at higher magnification and indicated by a number) expresses both receptor and ligand, but receptor and ligand do not co-localize. Rather, they are confined to separate cell surface domains: for example, the ligand is in the region of contact between cell 1 and cell 2 and in subdomains of cell 3 and cell 4 that could represent a presynaptic or postsynaptic region. In contrast, the receptor would be on the extrasynaptic portions of the cell surface. High resolution localization experiments will be required to determine which of the distributions shown in (c-e) actually occurs *in vivo*.

Table 2

Examples of reciprocal expression patterns of Eph family receptors and ligands.

Receptor(s)	Receptor distribution	Ligand(s)	Ligand distribution	Proposed function	References
Cek4	Increasing nasal to temporal gradient in the developing retina	ELF1, RAGS	Increasing anterior to posterior gradients in the developing optic tectum	Targeting of retinotectal projection	[11-13,14**]
Bsk	Increasing lateral to medial gradient in the developing and adult hippocampus	ELF1, RAGS, Lerk3	Increasing dorsomedial to ventrolateral gradient (of the three ligands considered in combination) in the developing and adult lateral septum	Targeting and remodeling of hippocamposeptal projection	[45*]
Bsk	Increasing ventral to dorsal gradient in the subiculum	AL1	Increasing caudal to rostral gradient in the hypothalamus	Targeting of projections from subiculum to hypothalamus	[45*]
Bsk	Subpopulation of mitral and tufted cells in the embryonic and adult olfactory bulb	Lerk3	Subpopulation of olfactory sensory neurons in the nasal epithelium	Specification of synapses between olfactory neurons and mitral or tufted cells	[45*]
?	Caudally derived (lumbar) sensory and motor axons?	AL1	Higher expression in rostral (head and neck) embryonic muscles than in caudal (trunk and limb) muscles	Regulating position-dependent connectivity along the rostrocaudal axis between spinal cord axons and target muscles	[26]
Cek8	Lumbar and brachial embryonic motor neurons	?	?	Guiding lumbar and brachial embryonic motor neurons to their target muscles	[46]
Cek4/Mek4/Tyro4	Cervical and thoracic motor neurons of the medial motor column. These neurons innervate receptor-positive axial musculature	ELF1?	Limb buds	ELF1 may repel receptor-positive myoblasts and axons away from the limb bud and direct them jointly into the body wall	[47]
Nuk	Brain regions immediately ventral to the anterior commissure	Lerk2	Axons of the posterior portion of the anterior commissure	Guiding the axons of the posterior portion of the anterior commissure	[42**]
Nuk/Cek5, Cek8	Spinal nerves	Lerk2, Htk-L	Caudal somite halves	Restricting the growth of spinal nerves to the rostral somite halves	[7,16*,17**,18]
Nuk, Cek10/Cek10	Trunk neural crest cells and rostral somite halves	Elk-L/Lerk2, Htk-L	Caudal somite halves	Restricting the migration of trunk neural crest cells to the rostral somite halves	[17**,19*,25]
Sek1, Elk	Third branchial arch neural crest cells and mesoderm along their presumptive migratory pathways	Htk-L	Second branchial arch neural crest cells and mesoderm along their presumptive migratory pathways	Guiding the migration of third branchial arch neural crest cells	[20*]
Sek1, Nuk EphA receptors	Hindbrain rhombomeres 3 and 5 Mouse E10.5 limb: distal tip (prospective autopod) and body-proximal areas (prospective stylopod)*	Transmembrane ligands GPI-linked ligands	Hindbrain rhombomeres 2, 4, and 6 Mouse E10.5 limb: central portion (prospective zeugopod)*	Defining rhombomere boundaries Limb patterning: specification of domains with different fates	[18,21,25,48-50] [16*]
EphA receptors	Mouse E13 limb: cartilaginous digits*	GPI-linked ligands	Mouse E13 limb: interdigital zone*	Limb patterning: segregation of condensing cartilage from surrounding mesenchyme Segregating dorsal and ventral retinal cells, organizing the retinotectal pathway	[16*,25,51,52]
Cek5	E8 chicken ventral retina*	Cek5-L	E8 chicken dorsal retina*	Segregating dorsal and ventral retinal cells, organizing the retinotectal pathway	[23,53]
Cek4	Embryonic temporal retina	RAGS	Embryonic nasal retina*	Segregating nasal and temporal retinal cells, organizing the retinotectal pathway	[25,54] (a)
Htk	Erythroid progenitor cells	Htk-L	Bone marrow stromal cells	Regulating erythropoiesis by providing positional information in the bone marrow microenvironment	[44]

(a) RJ Connor, P Menzel, EB Pasquale, unpublished data. *E refers to embryonic day of development. Question marks indicate that receptor, ligand or ligand distribution is not yet known. Examples where the reciprocal expression patterns of Eph receptors and their ligands suggest that Eph receptors and ligands guide axons by repulsive mechanisms are shown in the top half of the table. Examples where the Eph receptors and their ligands are expressed in adjacent populations of cells, suggesting that they restrict cell movement across boundaries of ligand and receptor expression, are shown in the bottom half of the table.

mouse embryo, expression of the receptor Sek1 in the dorsal portion of the somites overlaps with that of the ligands AL1 and Lerk4, which are localized throughout the somites [25]. It is not known, however, whether in regions of overlapping expression ligand and receptor are found on distinct but mixed subpopulations of cells (Figure 1c), or on the same cells either with uniform distribution over the surface of the cell (Figure 1d) or confined to complementary subcellular domains (Figure 1e).

Uniform ligand concentrations should presumably provide signals other than directional cues and their effects may be more subtle. Uniformly presented ligands did not prevent the growth of neurites from retinal or neural tube explants [14**,17**] nor did they prevent *in vitro* or *in vivo* motility of trunk neural crest cells [17**,19*]. However, the GPI-linked ligands AL1 and ELF1, expressed on a continuous

monolayer of cells, appreciably inhibited outgrowth of neurites from neurons expressing the receptors [26,27]. Effects on axon fasciculation and cell-cell adhesion have also been demonstrated. Soluble AL1 ligand promoted axon fasciculation in cultures of cortical neurons, which express the Eph receptor Rek7 [28]. Ectopic expression of an activated form of the receptor Pag (*Xenopus* Sek1) in *Xenopus* embryos caused decreased cell-cell adhesion, possibly by affecting cadherin function [29]. Effects of Eph receptors such as Cek5 on neuronal recognition events or fasciculation could result from the tyrosine phosphorylation of the neural cell adhesion molecule L1 [30]. However, the functional consequences of L1 phosphorylation by Cek5 remain to be determined.

Activation of Eph receptors may also be relevant in angiogenesis. When activated by their ligands, the re-

ceptors Eck and Elk mediate the *in vitro* assembly of human umbilical vein endothelial cells and human renal microvascular endothelial cells, respectively, into capillary-like structures [31,32]. Furthermore, a soluble dimeric form of the Eck ligand, B61, has been shown to act as an angiogenic factor *in vivo* [32].

Receptor signaling

Cell-cell recognition mediated by Eph receptors results in signals that override adhesive mechanisms mediated by cell adhesion molecules, integrins, and possibly the receptor-ligand interaction itself [33]. Furthermore, growth cone collapse induced by ligands for Eph receptors such as AL1 is accompanied by disruption of the actin cytoskeleton in the growth cone [34]. In contrast, proliferative signals generated by Eph receptors are at best modest [35]. Like other receptor tyrosine kinases, the Eph receptors autophosphorylate in response to ligand binding [2]. Only membrane-anchored ligands, however, efficiently activate their receptors [6]. Monomeric soluble ligands that are released into the culture medium generally do not cause receptor signaling, even though they retain high binding affinity [6].

A number of signaling molecules that bind by means of their SH2 (Src homology 2) domains to tyrosine-phosphorylated sequences of Eph receptors have been identified (Table 3). Their associations with Eph receptors have been demonstrated by using the two-hybrid system and/or biochemical assays. Grb2, Grb10, and Src-like adaptor protein (SLAP) are adaptor molecules that presumably link Eph receptors to downstream signaling pathways, such as, in the case of Grb2, the Ras pathway [2]. Phosphatidylinositol 3-kinase (PI 3-kinase), Src family kinases, and p120Ras GTPase-activating protein (GAP) have intrinsic catalytic activities. PI 3-kinase activity is increased following activation of the receptor Eck [36], but it is not known whether the catalytic activities of Src and p120RasGAP are affected by activation of the Eph receptors to which they bind.

It appears that the Eph receptors engage downstream molecules that were previously known as components in signaling pathways of other families of receptor tyrosine

kinases, such as growth factor receptors [2]. The only novel protein identified so far by virtue of its interaction with an Eph receptor is SLAP [37]. Src family kinases, PI 3-kinase, and p120RasGAP have been previously implicated in neurite outgrowth, cell migration, and cytoskeletal organization (Table 3). In particular, given their co-localization with Eph receptors in growth cones and axons [38], Src family kinases are promising candidates as mediators of signals involved in axon guidance.

Ligand signaling?

Three ligands for Eph receptors, Lerk2, Htk-L, and Elk-L3/NLerk2, contain a transmembrane segment and a highly conserved cytoplasmic region of approximately 80 amino acids. Evidence has suggested that the cytoplasmic domain of the ligand Lerk2, although not required for receptor activation, has signaling activities, as it inhibits signaling pathways activated by tyrosine kinases [39,40*]. Tyrosine phosphorylation of the ligands Lerk2 and Htk-L has indeed been observed *in vivo* in the mouse embryo, demonstrating the physiological relevance of such phosphorylation, and has also been observed in actively growing cultured fibroblasts and v-Src-transformed cells [40*,41**]. Tyrosine phosphorylation of transmembrane ligands for Eph receptors is also rapidly upregulated by activation of growth factor receptors and, notably, upon interaction with EphB receptors. Ligand phosphorylation is presumably mediated by an as yet unknown ligand-associated tyrosine kinase and may promote the formation of complexes of ligands with SH2 and phosphotyrosine-binding domains of signaling molecules. Hence, contact between cells expressing ligand and cells expressing receptor probably results in activation of bidirectional signaling pathways.

Genetic analyses of Eph receptor functions

Gene knockout experiments substantiated the importance of Eph receptors in axon guidance and fasciculation. Disruption of the Nuk receptor gene affected axons of the anterior commissure, which did not follow their normal route to the contralateral side of the brain and incorrectly grew toward the ventral forebrain [42**]. Disruption of the closely related Sek4 receptor gene affected the axons of the corpus callosum, which did not follow their normal

Table 3

Signaling molecules that bind to Eph receptors through their SH2 domains.

Signaling molecule	Eph receptor	Binding site in Eph receptor	Possible role of signaling molecule in	Reference
p85 subunit of PI 3-kinase	Eck	n.d.	Cell migration, cytoskeletal organization	[36]
SLAP	Eck	n.d.	n.d.	[37]
Grb10	Elk	Tyr929	Neuronal cell migration	[55]
Grb2	Elk	In kinase domain	Neuronal differentiation, linkage to Ras pathway	[55]
Fyn	Sek1	Tyr602	Cytoskeletal organization	[56]
Src	Cek5, Cek8	Tyr611 of Cek5	Cytoskeletal organization	(a)
p120RasGAP	Nuk	Tyr604, Tyr610	Cytoskeletal organization, linkage to Ras pathway	[57]

(a) AH Zisch, MS Kalo, EB Pasquale, unpublished data. n.d., not determined.

trajectories to the contralateral side of the brain [43**]. In the absence of both Nuk and Sek4, pathfinding abnormalities were more severe, and other brain projections were also abnormal, indicating that the receptors Nuk and Sek4 have partially redundant roles [42**,43**]. Interestingly, in at least one axon tract—the habenular–interpeduncular tract, in which transmembrane ligands are co-expressed with Nuk and Sek4 receptors—axon fasciculation rather than pathfinding was affected.

Genetic evidence also supports the physiological relevance of signaling through the cytoplasmic domain of ligands [42**]. The axons of the brain anterior commissure, which are abnormal in Nuk knockout mice, were surprisingly found to express not Nuk but the Nuk ligand Lerk2. Interestingly, areas of Nuk expression are adjacent to the pathway followed by these axons (Table 2), suggesting that Nuk provides guidance cues that are transduced through the cytoplasmic domain of Lerk2. Consistently, Nuk mutant receptors lacking the kinase domain are able to properly guide anterior commissure axons [42**].

Conclusions and perspectives

What we have learnt so far about the distributions and activities of Eph family receptors and their ligands predicts that their roles are not restricted to developmental processes. Their expression in adult neural structures, such as the hippocampus and olfactory bulb, suggests a role in synaptic remodeling. The repulsive activities of ligands toward axons expressing Eph receptors predicts that these ligands may contribute to the failure of the adult central nervous system to regenerate. Finally, the expression of ligands and receptors in tumor cells may downregulate cell adhesion, thereby favoring the dissemination of metastases, while the expression of the ligands B61 and Lerk2 in the vasculature [31,32] and Htk-L in the bone marrow [44] may influence the targeting of metastatic cells expressing Eph receptors. Because of the existence of so many Eph receptors (and of alternatively spliced forms), the redundancy in ligand–receptor interactions, and the possible importance of the spatial coordinates of their signaling activities, elucidating how the Eph receptors signal will be a particularly challenging task.

Acknowledgements

The author thanks Andreas Zisch and Matthew Kalo for helpful comments on the manuscript. The author's work is supported by National Institutes of Health grants EY10576, HD25938 and HD26351, and by a grant from the March of Dimes.

References and recommended reading

Papers of particular interest, published within the annual period of review, have been highlighted as:

- of special interest
 - of outstanding interest
1. Tessier-Lavigne M, Goodman CS: The molecular biology of axon guidance. *Science* 1996, 274:1123-1133.

2. Van der Geer P, Hunter T, Lindberg RA: Receptor protein-tyrosine kinases and their signal transduction pathways. *Annu Rev Cell Biol* 1994, 10:251-337.
3. Connor RJ, Pasquale EB: Genomic organization and alternatively processed forms of Cdk5, a receptor protein-tyrosine kinase of the Eph subfamily. *Oncogene* 1995, 11:2429-2438.
4. Gurniak CB, Berg LJ: A new member of the Eph family of receptors that lacks protein tyrosine kinase activity. *Oncogene* 1996, 13:777-786.
5. Eph Nomenclature Committee: Flanagan JG, Gale NW, Hunter T, Pasquale EB, Tessier-Lavigne M: Unified nomenclature for Eph receptors and their ligands, the ephrins. *Cell* 1997, 90:403-404.
6. Davis S, Gale NW, Aldrich TH, Maisonpierre PC, Lhotak V, Pawson T, Goldfarb M, Yancopoulos GD: Ligands for EPH-related receptor tyrosine kinases that require membrane attachment or clustering for activity. *Science* 1994, 266:816-819.
7. Soans C, Holash JA, Pasquale EB: Characterization of the expression of the Cdk8 receptor-type tyrosine kinase during development and in tumor cell lines. *Oncogene* 1994, 9:3353-3361.
8. Bartley TD, Hunt RW, Welcher AA, Boyle W, Parker VP, Lindberg RA, Lu HS, Colombero AM, Elliot RL, Guthrie BA *et al.*: Receptor affinity techniques: Identification of a ligand for the ECK receptor protein-tyrosine kinase. *Nature* 1994, 368:558-560.
9. Sperry RW: Chemoaffinity in the orderly growth of nerve fiber patterns and connections. *Proc Natl Acad Sci USA* 1963, 50:703-710.
10. Walter J, Kern-Veits B, Huf J, Stolze B, Bonhoeffer F: Recognition of position-specific properties of tectal cell membranes by retinal axons *in vitro*. *Development* 1987, 101:685-696.
11. Cheng HJ, Nakamoto M, Bergemann AD, Flanagan JG: Complementary gradients in expression and binding of ELF-1 and Mek4 in development of the topographic retinotectal projection map. *Cell* 1995, 82:371-381.
12. Drescher U, Kremoser C, Handwerker C, Loschinger J, Noda M, Bonhoeffer F: *In vitro* guidance of retinal ganglion cell axons by RAGS, a 25 kDa tectal protein related to ligands for Eph receptor tyrosine kinases. *Cell* 1995, 82:359-370.
13. Monschau B, Kremoser C, Ohta K, Tanaka H, Handwerker C, Hornberger MR, Loschinger J, Pasquale EB, Siever DA, Verderame MF *et al.*: Shared and distinct functions of RAGS and ELF-1 in guiding retinal axons. *EMBO J* 1997, 16:1258-1267.
14. Nakamoto M, Cheng HJ, Friedman GC, McLaughlin T, Hansen MJ, Yoon CH, O'Leary DD, Flanagan JG: Topographically specific effects of ELF-1 on retinal axon guidance *in vitro* and retinal axon mapping *in vivo*. *Cell* 1996, 86:755-766.
- The ability of the ligand ELF-1 to influence the trajectories in the optic tectum of retinal ganglion cell axons expressing the receptor Cdk4 was demonstrated for the first time.
15. Keynes RJ, Stern CD: Segmentation in the vertebrate nervous system. *Nature* 1984, 310:413-429.
16. Gale NW, Holland SJ, Valenzuela DM, Flenniken A, Pan L, Ryan TE, Henkemeyer M, Strebhardt K, Hirai H, Wilkinson DG *et al.*: Eph receptors and ligands comprise two major specificity subclasses and are reciprocally compartmentalized during embryogenesis. *Neuron* 1996, 17:9-19.
- This was the first report to point out that the Eph receptors can be divided into two groups on the basis of sequence homologies and binding specificities for either transmembrane or glycosylphosphatidylinositol-linked ligands. The authors also show that expression patterns of receptors and their ligands are often complementary in the embryo.
17. Wang HU, Anderson DJ: Eph family transmembrane ligands can mediate repulsive guidance of trunk neural crest migration and motor axon outgrowth. *Neuron* 1997, 18:383-396.
- The authors of this paper are the first to indicate that the Eph family transmembrane ligands can mediate repulsive cell interactions. The authors describe the segmented expression of transmembrane ligands for Eph receptors in the caudal somite halves and show that, *in vitro*, these ligands can guide both spinal axons and trunk neural crest cells, both of which express receptors for these ligands.

18. Henkemeyer M, Marengere LE, McGlade J, Olivier JP, Conlon RA, Holmyard DP, Letwin K, Pawson T: Immunolocalization of the Nuk receptor tyrosine kinase suggests roles in segmental patterning of the brain and axonogenesis. *Oncogene* 1994, 9:1001-1014.
19. Krull CE, Lansford R, Gale NW, Collazo A, Marcelle C, Yancopoulos GD, Fraser SE, Bronner-Fraser M: Interactions of Eph-related receptors and ligands confer rostrocaudal pattern to trunk neural crest migration. *Curr Biol* 1997, 7:571-580.
- The authors are the first to demonstrate *in vivo* the functional significance of the asymmetric expression of transmembrane ligands for Eph receptors in the developing somites.
20. Smith A, Robinson V, Patel K, Wilkinson DG: The EphA4 and EphB1 receptor tyrosine kinases and ephrin-B2 ligand regulate the targeted migration of branchial neural crest cells. *Curr Biol* 1997, 7:561-570.
- The authors show that *in vivo* inhibition of Sek1 and Elk receptor function, or ectopic activation by overexpression of one of their ligands, Htk-L, disrupts the targeting of third arch crest cells in *Xenopus* embryos.
21. Xu Q, Alldus G, Holder N, Wilkinson DG: Expression of truncated *Sek-1* receptor tyrosine kinase disrupts the segmental restriction of gene expression in the *Xenopus* and zebrafish hindbrain. *Development* 1995, 121:4005-4016.
22. Pasquale EB, Connor RJ, Rocholl D, Schnurch H, Risau W: Cdk5, a tyrosine kinase of the Eph subclass, is activated during neural retina differentiation. *Dev Biol* 1994, 163:491-502.
23. Holash JA, Soans C, Chong LD, Shao H, Dixit VM, Pasquale EB: Reciprocal expression of the eph receptor Cdk5 and its ligand(s) in the early retina. *Dev Biol* 1997, 182:256-269.
24. Soans C, Holash JA, Pavlova Y, Pasquale EB: Developmental expression and distinctive tyrosine phosphorylation of the Eph-related receptor tyrosine kinase Cdk9. *J Cell Biol* 1996, 135:781-795.
25. Flenniken AM, Gale NW, Yancopoulos GD, Wilkinson DG: Distinct and overlapping expression patterns of ligands for Eph-related receptor tyrosine kinases during mouse embryogenesis. *Dev Biol* 1996, 179:382-401.
26. Donoghue MJ, Lewis RM, Merlie JP, Sanes JR: The Eph kinase ligand AL-1 is expressed by rostral muscles and inhibits outgrowth from caudal neurons. *Mol Cell Neurosci* 1996, 8:185-198.
27. Gao PP, Zhang JH, Yokoyama M, Racey B, Dreyfus CF, Black IB, Zhou R: Regulation of topographic projection in the brain: ELF-1 in the hippocampal system. *Proc Natl Acad Sci USA* 1996, 93:11161-11166.
28. Winslow JW, Moran P, Valverde J, Shih A, Yuan JQ, Wong SC, Tsai SP, Goddard A, Henzel WJ, Hefti F et al.: Cloning of AL-1, a ligand for an Eph-related tyrosine kinase receptor involved in axon bundle formation. *Neuron* 1995, 14:973-981.
29. Winning RS, Scales JB, Sargent TD: Disruption of cell adhesion in *Xenopus* embryos by Pagliaccio, an Eph-class receptor tyrosine kinase. *Dev Biol* 1996, 179:309-319.
30. Zisch AH, Stallcup WB, Chong LD, Dahlin-Hippe K, Voshol J, Schachner M, Pasquale EB: Tyrosine phosphorylation of L1 family adhesion molecules: Implication of the Eph kinase Cdk5. *J Neurosci Res* 1997, 47:655-665.
31. Daniel TO, Stein E, Cerretti DP, St John PL, Robert B, Abrahamson DR: ELK and LERK-2 in developing kidney and microvascular endothelial assembly. *Kidney Int* 1996, Suppl 57:73-81.
32. Pandey A, Shao H, Marks RM, Polverini PJ, Dixit VM: Role of B61, the ligand for the Eck receptor tyrosine kinase, in TNF-alpha-induced angiogenesis. *Science* 1995, 268:567-569.
33. Heaysman JEM: Contact inhibition of locomotion: a reappraisal. *Int Rev Cytol* 1978, 55:49-66.
34. Meima L, Kjavlin U, Moran P, Shih A, Winslow JW, Caras I: AL-1-induced growth cone collapse of rat cortical neurons is correlated with REK7 expression and rearrangement of the actin cytoskeleton. *Eur J Neurosci* 1997, 9:177-188.
35. Lhotak V, Pawson T: Biological and biochemical activities of a chimeric epidermal growth factor-Elk receptor tyrosine kinase. *Mol Cell Biol* 1993, 13:7071-7079.
36. Pandey A, Lazar DF, Saltiel AR, Dixit VM: Activation of the Eck receptor protein tyrosine kinase stimulates phosphatidylinositol 3-kinase activity. *J Biol Chem* 1994, 269:30154-30157.
37. Pandey A, Duan H, Dixit VM: Characterization of a novel Src-like adapter protein that associates with the Eck receptor tyrosine kinase. *J Biol Chem* 1995, 270:19201-19204.
38. Bixby JL, Jabvala P: Tyrosine phosphorylation in early embryonic growth cones. *J Neurosci* 1993, 13:3421-3432.
39. Brambilla R, Schnapp A, Casagrande F, Labrador JP, Bergemann AD, Flanagan JG, Pasquale EB, Klein R: Membrane-bound LERK2 ligand can signal through three different Eph-related receptor tyrosine kinases. *EMBO J* 1995, 14:3116-3126.
40. Brückner K, Pasquale EB, Klein R: Tyrosine phosphorylation of transmembrane ligands for Eph receptors. *Science* 1997, 275:1640-1643.
- This article reports that the cytoplasmic domain of the Eph receptor ligand Lerk2 inhibits tyrosine kinase signaling pathways in the ligand-bearing cells, suggesting a direct signaling function for this ligand.
41. Holland SJ, Gale NW, Mbamalu G, Yancopoulos GD, Henkemeyer M, Pawson T: Bidirectional signalling through the EPH-family receptor Nuk and its transmembrane ligands. *Nature* 1996, 383:722-725.
- This was the first report indicating that the transmembrane ligands for Eph receptors become tyrosine-phosphorylated as a consequence of interacting with the Eph receptors.
42. Henkemeyer M, Orioli D, Henderson JT, Saxton TM, Roder J, Pawson T, Klein R: Nuk controls pathfinding of commissural axons in the mammalian central nervous system. *Cell* 1996, 86:35-46.
- This is the first report of inactivation of an Eph receptor gene, the Nuk gene. Defects in the trajectories of anterior commissure neurons indicated a role for the Nuk receptor in axon pathfinding. Unexpectedly, Nuk was detected not in these axons but in the brain regions surrounding their pathway. It is a ligand for Nuk, Lerk2, that is present in the axons and which may respond to guidance cues provided by the Nuk extracellular domain.
43. Orioli D, Henkemeyer M, Lemke G, Klein R, Pawson T: Sek4 and Nuk receptors cooperate in guidance of commissural axons and in palate formation. *EMBO J* 1996, 15:6035-6049.
- This is the first report of the simultaneous inactivation of two Eph receptor genes, Nuk and Sek4. Defects in axon pathfinding and fasciculation and in palate formation were observed. Double mutant mice were more severely affected than would be expected from the phenotypes of single receptor mutants, indicating that the two Eph receptor genes have redundant functions during development. Both transmembrane ligands and their Eph receptors were found to be expressed in cortical neurons.
44. Inada T, Iwama A, Sakano S, Ohno M, Sawada K, Suda T: Selective expression of the receptor tyrosine kinase, HTK, on human erythroid progenitor cells. *Blood* 1997, 89:2757-2765.
45. Zhang JH, Cerretti DP, Yu T, Flanagan JG, Zhou R: Detection of ligands in regions anatomically connected to neurons expressing the Eph receptor Bsk: potential roles in neuron-target interaction. *J Neurosci* 1996, 16:7182-7192.
- This report indicates that Eph receptors and their ligands may specify topographic projections in various regions of the nervous system, in addition to in the visual system.
46. Ohta K, Nakamura M, Hirokawa K, Tanaka S, Iwama A, Suda T, Ando M, Tanaka H: The receptor tyrosine kinase, Cdk8, is transiently expressed on subtypes of motoneurons in the spinal cord during development. *Mech Dev* 1996, 54:59-69.
47. Kilpatrick TJ, Brown A, Lai C, Gassmann M, Goufing M, Lemke G: Expression of the Tyro4/Mek4/Cek4 gene specifically marks a subset of embryonic motor neurons and their muscle targets. *Mol Cell Neurosci* 1996, 7:62-74.
48. Bergemann AD, Cheng HJ, Brambilla R, Klein R, Flanagan JG: ELF-2, a new member of the Eph ligand family, is segmentally expressed in mouse embryos in the region of the hindbrain and newly forming somites. *Mol Cell Biol* 1995, 15:4921-4929.
49. Gilardi-Hebenstreit P, Nieto MA, Frain M, Mattei MG, Chestier A, Wilkinson DG, Charnay P: An Eph-related receptor protein tyrosine kinase gene segmentally expressed in the developing mouse hindbrain. *Oncogene* 1992, 7:2499-2506. [Published erratum appears in *Oncogene* 1993, 8:1103.]

50. Gale NW, Fenniken A, Compton DC, Jenkins N, Copeland NG, Gilbert DJ, Davis S, Wilkinson DG, Yancopoulos GD: Elk-L3, a novel transmembrane ligand for the Eph family of receptor tyrosine kinases, expressed in embryonic floor plate, roof plate and hindbrain segments. *Oncogene* 1996, 13:1343-1352.
51. Cheng HJ, Flanagan JG: Identification and cloning of ELF-1, a developmentally expressed ligand for the Mek4 and Sek receptor tyrosine kinases. *Cell* 1994, 79:157-168.
52. Patel K, Nittenberg R, D'Souza D, Irving C, Burt D, Wilkinson DG, Tickle C: Expression and regulation of Cek-8, a cell to cell signalling receptor in developing chick limb buds. *Development* 1996, 122:1147-1155.
53. Holash JA, Pasquale EB: Polarized expression of the receptor protein tyrosine kinase Cek5 in the developing avian visual system. *Dev Biol* 1995, 172:683-693.
54. Marcus RC, Gale NW, Morrison ME, Mason CA, Yancopoulos GD: Eph family receptors and their ligands distribute in opposing gradients in the developing mouse retina. *Dev Biol* 1996, 180:786-789.
55. Stein E, Cerretti DP, Daniel TO: Ligand activation of ELK receptor tyrosine kinase promotes its association with Grb10 and Grb2 in vascular endothelial cells. *J Biol Chem* 1996, 271:23588-23593.
56. Ellis C, Kasmi F, Ganju P, Walls E, Panayotou G, Reith AD: A juxtamembrane autophosphorylation site in the Eph family receptor tyrosine kinase, Sek, mediates high affinity interaction with p59fyn. *Oncogene* 1996, 12:1727-1736.
57. Holland SJ, Gale NW, Gish GD, Roth RA, Songyang Z, Cantley LC, Henkemeyer M, Yancopoulos GD, Pawson T: Juxtamembrane tyrosine residues couple the Eph family receptor EphB2/Nuk to specific SH2 domain proteins in neuronal cells. *EMBO J* 1997, 13:3877-3888.

REVIEW

***eph*, the largest known family of putative growth factor receptors**

N.L. Tuzi & W.J. Gullick

Molecular Oncology Laboratory, ICRF Oncology Unit, Royal Postgraduate Medical School, Hammersmith Hospital, Du Cane Road, London W12 0NN, UK.

Receptor tyrosine kinases (RTKs) and their ligands are involved in many different processes including cellular differentiation, proliferation, embryonic development and some cases of neoplastic growth (Ullrich & Schlessinger, 1990; Pawson & Bernstein, 1990). The RTKs all have a similar structure consisting of an extracellular ligand-binding domain, a hydrophobic transmembrane region and an intracellular domain that contains the tyrosine kinase catalytic activity (Yarden & Ullrich, 1988). Receptors of this type may be categorised according to their overall layout, their regions of sequence homology and on the similarity of their ligands. Several subclasses or families of RTKs can be defined using this approach. One such subclass is the recently discovered family of RTKs termed *eph*, which currently consists of seven distinct members, *eph*, *eck*, *elk*, *cek5*, *mek4/cek4/hek*, *sek* and *hek2*, all of whose cDNAs have been fully sequenced. The relationships between the Eph family members is illustrated in a phylogenetic tree (Figure 1) constructed using the amino acid sequence from the consensus sequence Gly-X-Gly-X-X-Gly, found towards the amino terminus of the catalytic region (Hanks *et al.*, 1988), to the carboxy-terminal tail. The tree was constructed using the De Soete Tree Fit program (De Soete, 1983, 1984). There are at least another five *eph*-related putative receptors reported in the literature that have not yet been fully sequenced. Taken together, this appears to be the largest known family of RTKs. The pattern of expression of mRNA or protein of the full and partial length *eph*-like receptors is summarised in Table I.

***eph* family characteristics**

The shared characteristics of the Eph family which allow it to be considered as a subclass of RTKs are depicted in Figure 2. The extracellular domain contains an immunoglobulin-like (Ig) loop (although this homology is very weak) and two fibronectin type III repeats. Ig loops are found in several RTK extracellular domains, notably in the fibroblast growth factor (FGF) receptor and platelet-derived growth factor receptor families. Fibronectin type III repeats are found in many proteins, including some RTKs and a number of neural cell adhesion molecules. The function of these motifs in growth factor receptors is unclear, however they may be involved in cell-cell interactions. There is also one cysteine-rich region, containing 13 cysteine residues, in the extracellular domain. The spacing of the cysteines is different to the cysteine-rich region found in the type I RTK family, which includes the epidermal growth factor (EGF) receptor, *c-erbB-2*, *c-erbB-3* (Prigent & Lemoine, 1992) and *c-erbB-4* receptors (Plowman *et al.*, 1993), and the type II family, which consists of the insulin receptor, IGF-1 and the insulin receptor-related receptor.

So far no ligands for any of the Eph RTK family have been reported, and therefore they should be considered 'putative' growth factor receptors. Lack of known ligands

severely restricts the studies that can be performed on their functions. However, several reports on the expression pattern of the mRNA and protein of the various members have been performed, and this may ultimately aid in the discovery of the ligands for this family and help unravel their normal cellular functions.

eph

eph, the first receptor to be discovered, was isolated from human hepatocellular carcinoma cell line cDNA library (Hirai *et al.*, 1987). The *eph* gene has been well conserved throughout evolution as the human *eph* cDNA protein detected specific bands on a Southern blot of DNA from mouse, chicken, rat and *Drosophila melanogaster*. The human *eph* gene has been mapped to chromosome 7 and codes for 3.5 kb mRNA. *eph* has been found to be most highly expressed at the mRNA level in adult rat liver, lung and kidney and to a lesser extent in the testis (Table I). It was also noted that some human breast, lung, liver and colon carcinomas overexpress *eph* mRNA compared with normal tissues, but no gene amplification was seen (Maru *et al.*, 1988). The observation of overexpression without gene amplification has been reported for several RTKs, e.g. *c-erbB-3* in breast carcinomas (Lemoine *et al.*, 1992). When the human breast cancer cell line MCF-7 was analysed for the expression of

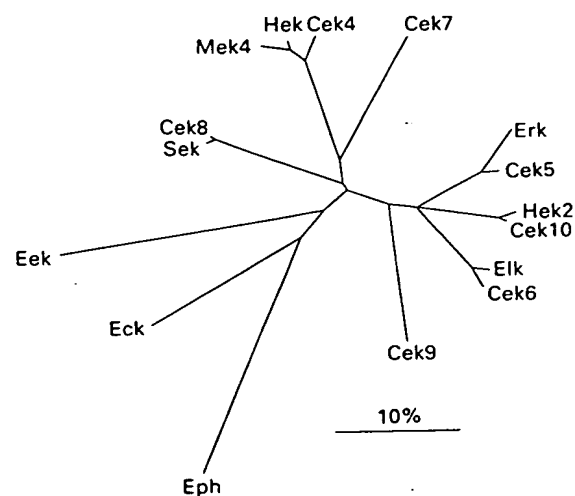


Figure 1 Phylogenetic tree of the Eph family of receptor tyrosine kinases. The tree was constructed using the De Soete Tree Fit program. The amino acid sequence from the consensus sequence GXGXXG, of the catalytic region, to the carboxy-terminal tail was used. The predicted amino acid sequences of human Eph, Hek, Hek2, Erk and Eck, rat Eek and Elk, chicken Cek4, Cek5, Cek6, Cek7, Cek8, Cek9 and Cek10 and mouse Mek4 and Sek were used in the construction for the above tree. The following partially sequenced Eph-like receptors were of insufficient length to be included; rat Tyro 1, Tyro 4, Tyro 5, Tyro 6 and Tyro 1 and human Tk2.

Table 1 Summary of the expression of mRNA or protein of all fully and partially sequenced *eph*-like receptors

Name	Species	Homologue(s)	mRNA (kb)	Normal distribution of mRNA or protein	Overexpression of mRNA in human cancers
<i>eph</i>	Human	NI	3.5	Highest in adult rat liver, lung and kidney. Lower in testes	Some lung, liver, breast and colon carcinomas
<i>elk</i>	Rat	<i>cek6*</i>	4.0	Highest in adult rat brain and embryonic day 14–16 stomach. Lower in adult rat testes	2/3 gastric carcinomas
<i>cek</i>	Human	NI	4.7	Highest in rat lung, skin, small intestine and ovary. Lower in kidney, brain, spleen and submaxillary gland	
<i>cek5</i>	Chicken	<i>erk*</i> / <i>tyro5*</i>	4.4 and 10	Highest in chicken embryonic day 10 and adult brain. Lower in kidney, lung, thigh and intestine	
<i>sek</i>	Mouse	<i>cek8*</i> / <i>tyro1*</i>	7.0	Highest in adult mouse brain. Lower in heart, lung and kidney. Expressed during embryonic brain development	
<i>cek4</i>	Chicken	<i>mek4/hek/tyro4*</i>	7.5	Highest in adult chicken brain and retina, but detectable in all adult tissue, except liver	
<i>mek4</i>	Mouse	<i>cek4/hek/tyro4*</i>	6.0 and 3.4	Highest in adult mouse brain. Lower in testes (3.4 kb)	
<i>hek</i>	Human	<i>cek4/mek4/tyro4*</i>	5.5–6.0	Undetectable at the protein level	1/28 CLL and 2/39 AML
<i>hek2</i>	Human	<i>cek10*</i> / <i>tyro6*</i>	4.6	Highest in human pancreas, lung, placenta, brain and kidney. Lower in heart, skeletal muscle and liver	
<i>EEK*</i>	Rat	NI	ND	Rat brain	
<i>erk*</i>	Human	<i>cek5/tyro5*</i>	4.0	Highest in adult rat lung. Lower in placenta, brain and kidney. Expressed in 16 day rat embryo stomach	3/3 gastric carcinomas
<i>tyro1*</i>	Rat	<i>sek/cek8*</i>	ND	Constant expression from rat embryonic day 12 to adulthood in CNS	
<i>tyro4*</i>	Rat	<i>cek4/mek4/hek</i>	ND	Constant expression from rat embryonic day 12 to birth in CNS	
<i>tyro5*</i>	Rat	<i>cek5/erk*</i>	ND	Constant expression from rat embryonic day 12 to birth in neural tissue	
<i>tyro6*</i>	Rat	<i>hek2/cek10*</i>	ND	Maximal in rat embryonic day 12 brain	
<i>tyro11*</i>	Rat	NI	ND	Highest in rat heart and kidney, lower in neural tissue	
<i>cek6*</i>	Chicken	<i>elk</i>	4.4 and 6.5	Highest in chicken embryonic day 10 and adult brain, lung, heart and skeletal muscle. Low level of 6.5 kb in adult brain	
<i>cek7*</i>	Chicken	NI	4.4, 7.0 and 8.5	Chicken embryonic day 10 brain. Low level of 8.5 kb transcript in adult brain	
<i>cek8*</i>	Chicken	<i>sek/tyro1*</i>	6.0	Highest in adult chicken brain and retina. Lower in adult kidney, lung, skeletal muscle and thymus	
<i>cek9*</i>	Chicken	NI	4.4	Highest in chicken adult thymus. Lower in brain, retina, kidney, lung and heart. Expressed in embryonic day 10 brain	
<i>cek10*</i>	Chicken	<i>hek2/tyro6*</i>	4.4 and 6.0	Highest in adult chicken kidney. Lower in adult lung. Expressed in embryonic day 10 brain and body tissues	

*Partially sequenced. NI, none identified. ND, not determined.

tyrosine kinase mRNAs using the polymerase chain reaction (PCR), 17/76 tyrosine kinase clones isolated and sequenced coded for *eph* (Lehtola *et al.*, 1992). It has also been observed that when the *eph* gene is artificially overexpressed in the mouse fibroblast cell line, NIH 3T3, it allows the transfected cells to grow in an anchorage-independent manner (determined by their ability to grow in soft agar) and to form tumours in nude mice (Maru *et al.*, 1990). Taken together these data suggest that overexpression of the *eph* gene may have a role to play in certain human carcinomas. However only 50 tumours of different tissue types were examined and no clinical data were presented to allow the comparison of tumour characteristics with overexpression to be made. Larger studies must therefore be performed to allow the prevalence of overexpression of *eph* mRNA in human carcinomas to be more accurately determined.

elk

The second member of this family to be identified was termed *elk* for *eph*-like kinase and was isolated from a rat brain cDNA library (Letwin *et al.*, 1988; Lhotak *et al.*, 1991). This gene appears to have a different pattern of expression from *eph*. *elk* mRNA is 4.0 kb in size and can only be detected in adult rat brain and to a lesser degree in the testis. A partial *elk* cDNA clone was isolated by Iwase *et al.* (1993) and used to screen a Northern blot of mRNA isolated from the stomach of adult, newborn and embryonic rats. It was found that *elk* expression increased in the stomach between embryonic days 14 and 16 but was very low by embryonic day 18 and in newborn rats. No expression was seen in the stomach of adults. RNA was also prepared from three cases of human gastric cancer and it was found that *elk*

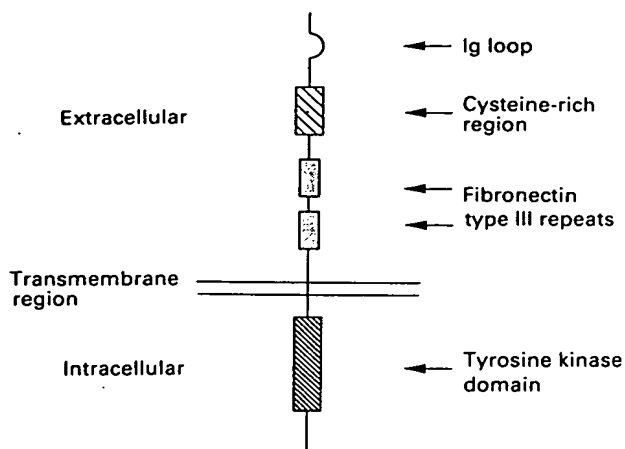


Figure 2 Schematic representation of the *eph* subclass of putative receptor tyrosine kinases.

mRNA levels were several times higher in 2/3 cases when compared with RNA prepared from normal gastric tissue (Table I). *elk* may therefore have a role to play in human gastric cancer; however, a larger study must be undertaken before any firm conclusions may be drawn.

eck

The third member, isolated from a human keratinocyte cDNA library, has been termed *eck* (epithelial cell kinase), and as the name suggests is expressed primarily in cells of epithelial origin (Lindberg & Hunter, 1990). The mRNA is 4.7 kb in size and was shown to be most highly expressed in rat lung, skin, small intestine and ovary, with lower levels seen in the kidney, brain, spleen and submaxillary gland (Table I). *Eck* was the first member of this family to be shown to have intrinsic tyrosine kinase activity. This was demonstrated by immunoprecipitating the 130 kDa *Eck* protein from A431 cells (a human vulva carcinoma-derived cell line) using an antibody raised against a TrpE fusion protein containing 101 amino acids from the C-terminal tail of *Eck* and then performing an *in vitro* kinase reaction on the immune complex. The phosphorylated protein was subjected to phosphoamino acid analysis, which confirmed that the majority of the phosphate was on tyrosine.

cek5

cek5 (chicken embryo kinase) was isolated from a 10 day chicken embryo cDNA expression library probed with anti-phosphotyrosine antibodies (Pasquale, 1991). Antibodies to the *Cek5* protein were raised against a β -gal fusion protein consisting of 759 amino acid residues (including all of the intracellular domain) and a synthetic peptide consisting of the ten amino acids from the C-terminal tail. Using these antibodies the *Cek5* protein was found to have an apparent molecular mass of 120 kDa and its pattern of expression in the 10 day chicken embryo, determined by Western blotting, was found to be highest in the brain, marginally lower in the kidney, lung, thigh, gizzard and intestine, and lower still in the liver, heart and lens (Table I). In the adult chicken protein expression was found to be most abundant in the brain and detectable in most of the tissues seen in the embryo, but at a lower level. A more detailed study on the embryonic and newly hatched chicken brain revealed that expression decreases gradually during embryonic development and after hatching. Immunocytochemical staining showed that the *Cek5* protein is expressed in regions that are rich in nerve cell processes especially in the hippocampus and the cerebellum (Pasquale *et al.*, 1992). *Cek5* is specifically

expressed in neurons and may play a role in neuronal maintenance in the chicken brain.

A variant of *cek5* was isolated from the same 10 day chicken embryo cDNA library and is termed *cek5+* (Sajjadi & Pasquale, 1993). This partial length cDNA variant codes for an *eph*-like receptor with an insert of 16 amino acids in the juxtamembrane region, which may be the result of alternative splicing. A Northern blot of 10-day-old chicken embryo brain and body tissue was screened with a probe specific for *cek5+* and one that would recognise both *cek5* and *cek5+*. Using the probe that recognises both *cek5*s a 4.4 kb transcript was detected in 10 day embryonic brain and body tissues, with a 10 kb transcript also being detected in the brain. The *cek5+* probe detected the 4.4 kb transcript only, and this was expressed exclusively in the CNS. *cek5+* therefore appears to be a neuronal-specific variant of *cek5*.

sek

Another *eph* family member, *sek* (segmentally expressed kinase), seems to be involved in the development of the mouse hindbrain. *sek* was isolated from an 8.5 day mouse embryo cDNA library and the gene has been mapped to mouse chromosome 1 and human chromosome 2 (Gilardi-Hebenstreit *et al.*, 1992). Murine *sek* mRNA is 7.0 kb in size and was found to be most highly expressed in the adult mouse brain. However it was also detectable in the heart and lung, with a lower level of expression being seen in the kidney (Table I). A detailed study of the expression of mRNA in the developing mouse brain revealed *sek* is expressed initially in the forebrain and hindbrain but not in the midbrain, with expression becoming more restricted within the developing forebrain (Nieto *et al.*, 1992). *sek* also appears to be expressed in the developing neural tube of the spinal cord and *sek* may therefore have a role to play in the initial steps of neuronal differentiation in the spinal cord of the mouse. Later on in development *sek* may play a role in neuronal maintenance as is suggested for *cek5*.

cek4/mek4/hek

Chicken *cek4* (isolated at the same time as *cek5*) encodes a 7.5 kb mRNA which was detectable in brain, head structures and body tissues of an 8 day chicken embryo (Sajjadi *et al.*, 1991). Expression of the 7.5 kb transcript was most pronounced in adult brain and retina, but was detectable in all other adult tissue except the liver (Sajjadi & Pasquale, 1993). *cek4* was used to isolate the mouse homologue termed *mek4* (mouse embryo kinase) (Sajjadi *et al.*, 1991), not to be confused with MAP kinase/ERK kinase (MEK), which is responsible for phosphorylating the extracellular signal regulated kinases (ERK) (Crews *et al.*, 1992). A cDNA coding for a soluble form of *mek4* was isolated at the same time as the usual membrane-spanning form. The soluble form consists of the extracellular domain only and possesses no transmembrane coding region. The *mek4* gene that codes for the full-length and secreted form of the receptor possesses an internal exon which encodes a polyadenylation signal. Use of this exon would result in the secreted form of *mek4* being transcribed. This phenomenon has been noted for various RTKs, including the EGF receptor, *c-erbB-2* and some of the FGF receptors. There is evidence to suggest that expression of truncated receptor tyrosine kinases are developmentally regulated (Vu *et al.*, 1989), however the function of these secreted extracellular domains has not been determined. One suggestion is that they may help regulate the levels of growth factors surrounding the cell or alternatively they could bind to the full-length receptor and inhibit activation by preventing productive dimerisation (Petch *et al.*, 1990).

The *mek4* mRNA is 6.0 kb in length and expression is similar to *elk* in that the highest level is seen in the brain and a lower level is detected in the testis, but the mRNA found

here is only 3.4 kb in length and may represent a third form of this receptor, which may again be the result of alternative splicing (Table I). No mRNA of the soluble form of *mek4* was detected, and it may be that this form is expressed in a tissue-specific and/or a stage-specific manner. Further studies are required to confirm this.

The human homologue of *cek4/mek4* is termed *hek*. This was cloned from a cDNA library prepared from mRNA obtained from a human pre-B-cell line LK63/C20⁺ (a variant of the parental cell line, LK63) (Wicks *et al.*, 1992). A monoclonal antibody, IIIA4, which recognises the human Hek protein, was made by immunising Balb/c mice with the LK63 cell line. This was then used to perform biochemical analysis on the Hek protein. Immunoprecipitation of labelled Hek from LK63 cells showed the mature protein to have a molecular mass of 135 kDa, and 95 kDa when deglycosylated. When Hek was immunoprecipitated from LK63 cells labelled *in vivo* with ³²P, a weak band of 135 kDa was detected, suggesting that Hek had been phosphorylated to a low level. However, in attempts to find a specific ligand, no increase in phosphorylation of Hek was observed when cells were treated with a variety of cytokines (Boyd *et al.*, 1992).

Two approaches were taken to determine the distribution of the Hek protein in normal and tumour tissue. The first was using immunocytochemistry on frozen sections of solid human biopsy tissues and the second was immunofluorescence followed by flow cytometry on single-cell suspensions of haemopoietic cells and solid human tissues. The results showed that normal tissue (spleen, lymph node, bone marrow, tonsil, breast and brain) and some acute lymphoblastic leukaemia, breast, cervical, prostate, ovarian and renal carcinomas were negative for Hek protein expression, whereas 1/28 chronic lymphocytic leukaemias and 2/39 acute myeloid leukaemias were positive. These data suggest that Hek may play a role in some human haematopoietic cell tumours.

Northern blots of mRNA from LK63 and the T-cell line JM probed with the *hek* cDNA revealed a band of 5.5–6.0 kb. When Southern blot analysis was performed on DNA prepared from LK63 and LK63/C20⁺, which express higher levels of *hek* than LK63 cells, no amplification or rearrangement of the *hek* gene was detected. Further studies should be undertaken to determine whether the *hek* gene is overexpressed and/or amplified in human haematopoietic cell tumours and/or solid human tumours.

hek2

The *hek2* gene was isolated using PCR technology. Human cDNAs from embryonic tissue were used as templates and the primers were designed to specifically recognise *eph*-like receptors. The predicted amino acid sequence on the *hek2* gene is most similar to the partially sequenced *eph*-like receptor, *cek10* (Figure 1), and the gene has been located to the distal end of human chromosome 3. Northern blot analysis of human tissue, using the *hek2* probe, recognised a transcript of 4.6 kb. Expression was highest in pancreas, lung, placenta, brain and kidney, with lower expression being noted in heart, skeletal muscle and liver (Table I). *hek2* transcripts were also detected in tumour cell lines of squamous and breast origin but not from epithelial cells of the lung or HeLa cells. A *hek2* transcript was detected in A431 cells and lysate from these cells was used in an *in vitro* kinase assay using polyclonal antibodies which were raised against a synthetic peptide to the C-terminal end of the predicted Hek2 protein sequence. The phosphorylated Hek2 protein was determined to be approximately 130 kDa (Bohme *et al.*, 1993).

Partially sequenced *eph* family members

Many partial cDNA sequences of putative receptors belonging to the *eph* family have been reported. *EEK* (*eph*-and

elk-related kinase) was isolated from a rat brain cDNA library and was used to isolate human *erk* (*elk*-related kinase) (Chan & Watt, 1991). This should not be confused with the ERK proteins, which are extracellular signal-regulated kinases which become phosphorylated by MEK (Crews *et al.*, 1992). *EEK* mRNA was only detectable in the rat brain, whereas *erk* mRNA was highest in lung and lower in rat placenta, brain and kidney. Recently a longer clone of *erk* was isolated from a human gastric cancer cDNA library and found to differ from the original clone in one predicted amino acid residue (Iwase *et al.*, 1993). Northern blots of RNA prepared from the stomach of embryonic and adult rats plus mRNA from three cases of human gastric cancer were probed with this longer *erk* clone. It was found that *erk* was preferentially expressed in 16 day rat embryo stomach and weakly, if at all, in the adult forestomach and glandular stomach. *erk* expression was much higher in 3/3 human gastric cancers examined when compared with normal gastric tissue. *erk* may therefore play a role in human gastric cancer.

In another study using PCR technology five partial sequences coding for *eph*-like receptors, *tyro1*, 4, 5, 6 and 11, were identified using rat cDNA as the template (Lai & Lemke, 1991). When their predicted amino acid sequences are compared with all other *Eph*-like receptors it is noted that 100% identity exists between rat *Tyro1* and mouse *Sek/chicken Cek8* (see below). One hundred per cent identity is also shared between *Tyro4* and human *Hek*, *Tyro5* and human *Erk* and *Tyro6* and human *Hek2*. *Tyro11* is most closely related (93% identical) at the predicted amino acid level to human *Hek2*. These partial clones may therefore represent rat homologues of the given full-length *Eph*-like receptors. The expression of the various *tyro* mRNAs in adult and neonatal rat tissues was examined. *tyro1* and 4 are preferentially expressed in the cells of the CNS and the level is fairly constant from embryo day 12 to adulthood for *tyro1*, whereas *tyro4* expression drops sharply at birth. *tyro5* mRNA is found exclusively in the neural tissue, and the level of expression falls shortly after birth. *tyro6* mRNA is found in the brain, where expression is maximal at embryonic day 12, after which it gradually falls and by 10 days after birth is fairly constant. *tyro11* has a different expression pattern and is found predominantly in the heart and kidney, with a lower level being detectable in neural tissue. Five partial length *eph*-like receptor cDNAs were isolated from the 10 day chicken embryo cDNA library, used to isolate *cek4* and 5, and a 13 day chicken embryo brain cDNA library (Sajjadi & Pasquale, 1993). These have been termed *cek6*, *cek7*, *cek8*, *cek9* and *cek10*. *cek6* is thought to be the avian homologue of rat *elk*, while *cek8* is considered to be the avian homologue of rat *tyro1* and murine *sek*. *cek10* is thought to be the avian homologue of human *hek2*, whereas *cek7* and *cek9* appear to be new *eph*-like receptors (see the phylogenetic tree in Figure 1). *cek7* mRNAs were found to be mainly expressed in embryonic and adult brain. The highest level of *cek8* mRNA expression is found in the adult chicken brain and retina. *cek9* mRNA levels were highest in the adult chicken thymus, and lower in the brain, retina, kidney, lung and heart (Table I).

A variant form of *cek10*, termed *cek10**, was isolated. This variant possesses an insert of 15 amino acids in the juxtamembrane domain, similar to that seen with the *cek5* variant, *cek5**. This variation may be the result of alternative splicing, but the significance of this is as yet unclear.

A partial *eph*-like receptor sequence was isolated using PCR technology. mRNA from a human breast cancer cell line was used as the template and the primers were degenerate oligonucleotides to protein kinases. One out of 32 tyrosine kinase-coding PCR products was found to belong to the *eph* family and was termed *tk2* (Cance *et al.*, 1993). At the predicted amino acid level, 91% identity is shared between *Tk2* and human *Eck*. The level of *tk2* expression was beyond the limits of detection of a Northern blot of RNA prepared from various epithelial cell lines. However, *tk2* expression could be detected in some of these cell lines

when PCR technology was used, but when nine human primary and metastatic breast cancers were examined using this technique *tk2* was undetectable.

Conclusions

Owing to modern molecular biology techniques the *eph* family is rapidly expanding, and is presently the largest known family of RTKs. However, at present only very limited information as to their possible functions is available. It appears that *sek*, *cek5*, *elk*, *EEK* and possibly *tyr1*, 4, 5 and 6 may have roles to play in the development of the brain and CNS; and in the maintenance of these tissues. As to the functions of the remaining family members, further studies must be undertaken before any conclusions can be made. Although there is preliminary evidence to suggest that *eph*, *hek*, *erk* and *elk* may be involved in some forms of human cancers, larger studies are necessary to confirm this. Other

family members should also be investigated for mutation gene amplification and/or overexpression in human carcinomas.

There is evidence to suggest that *cek5*, *cek10* and *mek* may exist as alternatively spliced variants. The significance of the resulting truncated receptor, in the case of *mek4*, receptors possessing inserts in the juxtamembrane region, is seen with *cek5*⁺ and *cek10*⁺, is as yet unknown, however, this warrants further investigation. The other *eph*-like receptors should also be examined for splice variants.

Once the ligands for the Eph-like receptors have been identified, biochemical studies will be possible and the functions of this large family of 'putative' growth factor receptors will begin to be unravelled.

We wish to thank Alex Whittaker in the Biomedical Informatics Unit, ICRF, Lincoln's Inn Fields, London, for constructing the *Eph* family phylogenetic tree.

References

- BOHME, B., HOLTRICH, U., WOLF, G., LUZIUS, H., GRZESCHIK, K.H., STREBHARDT, K. & RUBSAMEN-WAIGMANN, H. (1993). PCR mediated detection of a new human receptor-tyrosine-kinase, HEK 2. *Oncogene*, **8**, 2857–2862.
- BOYD, A.W., WARD, L.D., WICKS, I.P., SIMPSON, R.J., SALVARIS, E., WILKS, A., WELCH, K., LOUDOVARIS, M., ROCKMAN, S. & BUSMANIS, I. (1992). Isolation and characterisation of a novel receptor-type protein tyrosine kinase (*hek*) from a human pre-B cell line. *J. Biol. Chem.*, **267**, 3262–3267.
- CANCE, W.G., CRAVEN, R.J., WEINER, T.M. & LIU, E.T. (1993). Novel protein kinases expressed in human breast cancer. *Int. J. Cancer*, **54**, 571–577.
- CHAN, J. & WATT, V.M. (1991). *EEK* and *ERK*, new members of the *eph* subclass of receptor protein tyrosine kinases. *Oncogene*, **6**, 1057–1061.
- CREWS, C.M., ALESSANDRINI, A. & ERIKSON, R.L. (1992). The primary structure of MEK, a protein kinase that phosphorylates the ERK gene product. *Science*, **258**, 478–480.
- DE SOETE, G. (1983). A least squares algorithm for fitting additive trees to proximity data. *Psychometrika*, **48**, 621–626.
- DE SOETE, G. (1984). Additive tree representations of incomplete dissimilarity data. *Qual. Quant.*, **18**, 387–393.
- GILARDI-HEBENSTREIT, P., NIETO, M.A., FRAIN, M., MATTEI, M.G., CHESTIER, A., WILKINSON, D.G. & CHARNAY, P. (1992). An *eph*-related receptor protein tyrosine kinase gene segmentally expressed in the developing mouse hindbrain. *Oncogene*, **7**, 2499–2506.
- HANKS, S.K., QUINN, A.M. & HUNTER, T. (1988). The protein kinase family: conserved features and deduced phylogeny of the catalytic domains. *Science*, **241**, 42–52.
- HIRAI, H., MARU, Y., HAGIWARA, K., NISHIDA, J. & TAKAKU, F. (1987). A novel putative tyrosine kinase receptor encoded by the *eph* gene. *Science*, **238**, 1717–1720.
- IWASE, T., TANAKA, M., SUZUKI, M., NAITO, Y., SUGIMURA, H. & KINO, I. (1993). Identification of protein-tyrosine kinase genes preferentially expressed in embryo stomach and gastric cancer. *Biochem. Biophys. Res. Commun.*, **194**, 698–705.
- LAI, C. & LEMKE, G. (1991). An extended family of protein tyrosine kinase genes differentially expressed in the vertebrate nervous system. *Neuron*, **6**, 691–704.
- LEHTOLA, L., PARTANEN, J., SISTONEN, L., KORHONEN, J., WARRI, A., HARKONEN, P., CLARKE, R. & ALITALO, K. (1992). Analysis of tyrosine kinase mRNAs including four FGF receptor mRNAs expressed in MCF-7 breast-cancer cells. *Int. J. Cancer*, **50**, 598–603.
- LEMOINE, N.R., BARNES, D.M., HOLLYWOOD, D.P., HUGHES, C.M., SMITH, P., DUBLIN, E., PRIGENT, S.A., GULLICK, W.J. & HURST, H.C. (1992). Expression of the *ERBB3* gene product in breast cancer. *Br. J. Cancer*, **66**, 1116–1121.
- LETWIN, K., YEE, S.P. & PAWSON, T. (1988). Novel protein tyrosine kinase cDNAs related to *spfses* and *eph* cloned using anti phosphotyrosine antibody. *Oncogene*, **3**, 621–627.
- LHOTAK, V., GREER, P., LETWIN, K. & PAWSON, T. (1991). Characterization of *elk*, a brain-specific receptor tyrosine kinase. *Mol. Cell Biol.*, **11**, 2496–2502.
- LINDBERG, R.A. & HUNTER, T. (1990). cDNA cloning and characterization of *eck*, an epithelial cell receptor protein-tyrosine kinase in the *eph/elk* family of protein kinases. *Mol. Cell Biol.*, **10**, 6316–6324.
- MARU, Y., HIRAI, H., YOSHIDA, M.C. & TAKAKU, F. (1988). Evolution, expression, and chromosomal location of a novel receptor-tyrosine kinase gene. *eph. Mol. Cell Biol.*, **8**, 3770–3776.
- MARU, Y., HIRAI, H. & TAKAKU, F. (1990). Overexpression confers an oncogenic potential upon the *eph* gene. *Oncogene*, **4**, 445–447.
- NIETO, M.A., GILARDI-HEBENSTREIT, P., CHARNAY, P. & WILKINSON, D.G. (1992). A receptor protein tyrosine kinase implicated in the segmental patterning of the hindbrain and mesoderm. *Development*, **116**, 1137–1150.
- PASQUALE, E.B. (1991). Identification of chicken embryo kinase 5, developmentally regulated receptor-type tyrosine kinase of the *eph* family. *Cell Regul.*, **2**, 523–534.
- PASQUALE, E.B., DEERINCK, T.J., SINGER, S.J. & ELLISMAN, M.J. (1992). *cek5*, a membrane receptor-type tyrosine kinase, is expressed in neurons of the embryonic and postnatal avian brain. *J. Neurosci.*, **12**, 3956–3967.
- PAWSON, T. & BERNSTEIN, A. (1990). Receptor tyrosine kinase: genetic evidence for their role in *Drosophila* and mouse development. *Trends Genet.*, **6**, 350–356.
- PETCH, L.A., HARRIS, J., RAYMOND, V.W., BLASBAND, A., LE DUC, D.C. & EARP, H.S. (1990). A truncated, secreted form of the epidermal growth factor receptor is encoded by an alternative spliced transcript in normal rat tissue. *Mol. Cell Biol.*, **10**, 2973–2982.
- PLOWMAN, G.D., CULOUSCOU, J.M., WHITNEY, G.S., GREEN, J.M., CARLTON, G.W., FOY, L., NEUBAUER, M.G. & SHOYAB, M. (1993). Ligand-specific activation of HER4/p180^{erbB4}, a four-member of the epidermal growth factor receptor family. *Proc. Natl. Acad. Sci. USA*, **90**, 1746–1750.
- PRIGENT, S.A. & LEMOINE, N.R. (1992). The type 1 (EGFR-related) family of growth factor receptors and their ligands. *Prog. Growth Factor Res.*, **4**, 1–24.
- SAJJADI, F.G., PASQUALE, E.B. & SUBRAMANI, S. (1991). Identification of a new *eph*-related receptor tyrosine kinase gene from mouse and chicken that is developmentally regulated and encodes at least two forms of the receptor. *New Biol.*, **3**, 769–778.
- SAJJADI, F.G. & PASQUALE, E.B. (1993). Five novel avian *eph*-related tyrosine kinases are differentially expressed. *Oncogene*, **7**, 1807–1813.
- ULLRICH, A. & SCHLESSINGER, J. (1990). Signal transduction by receptors with tyrosine kinase activity. *Cell*, **61**, 202–212.
- VU, T.H., MARTIN, G.R., LEE, P., MARK, D., WANG, A. & WILLIAM L.T. (1989). Developmentally regulated use of alternative promoters creates a novel platelet-derived growth factor receptor transcript in mouse teratocarcinoma and embryonic stem cell. *Mol. Cell Biol.*, **9**, 4563–4567.
- WICKS, I.P., WILKINSON, D., SALVARIS, E. & BOYD, A.W. (1992). Molecular cloning of HEK, the gene encoding a receptor tyrosine kinase expressed by human lymphoid tumor cell lines. *Proc. Natl. Acad. Sci. USA*, **89**, 1611–1615.
- YARDEN, Y. & ULLRICH, A. (1988). Growth factor receptor tyrosine kinases. *Annu. Rev. Biochem.*, **57**, 443–478.

D8

SHORT REPORT

PCR mediated detection of a new human receptor-tyrosine-kinase, HEK 2

Beatrix Böhme, Uwe Holtrich, Georg Wolf, Heike Luzius, Karl-Heinz Grzeschik¹, Klaus Strebhardt & Helga Rübsamen-Waigmann

Chemotherapeutisches Forschungsinstitut, Georg-Speyer-Haus, Paul-Ehrlich-Str. 42-44, 6000 Frankfurt 70, Germany

We have previously amplified cDNA subfragments of protein-tyrosine-kinases (PTKs) by using the polymerase chain reaction (PCR) and specific sets of oligonucleotide primers derived from nucleotide sequences of their kinase domain. In this study we have used a more directed approach to identify new members of the EPH/elk-family by PCR of human embryonic cDNA: we utilized oligonucleotide primers specifically designed to a highly conserved N-terminal motif and the kinase region of EPH/elk-PTKs in RNA-PCRs. The 5' and 3' elongation of the primary PCR product was achieved by the RACE (rapid amplification of cDNA ends)-technique. Sequence analysis of 3.8 kb of overlapping PCR products allowed to identify a novel receptor-PTK, HEK 2 (human embryo kinase 2), as an additional member of this family, without the need to screen a cDNA library. This approach should be useful for the rapid isolation of other PTK-genes as well. Analysis of genomic DNA placed HEK 2 on chromosome 3. Northern blot analysis demonstrated the expression of a 4.6 kb HEK 2-mRNA in lung, brain, pancreas, liver, placenta, kidney, skeletal muscle, heart and several human cells. In a protein kinase assay with HEK 2-specific immunoprecipitates from the human epidermoid carcinoma cell line A431, a protein of 130 kDa was found phosphorylated.

Receptor-tyrosine-kinases (RTK) represent a family of proteins that transmit signals from the external environment into the cytoplasm of the cell after binding specific ligands. Binding of a ligand to their extracellular domain activates the catalytic domain inside the cell. Interaction of this domain with cytosolic proteins allows to transmit the signal further. Alterations of growth factors and their receptors have been shown to disturb the network of growth control and in some cases to be linked to malignant transformation (Bishop, 1987). The epidermal growth factor receptor (EGFR), colony stimulating factor 1 receptor (CSF-1R) and *ros* achieve transforming potential by truncation or mutation (*v-erbB*, *v-fms* and *v-ros*, respectively) due to retroviral transduction (Downward *et al.*, 1984; Matsushine *et al.*, 1986; Sherr, 1990). Alternatively, overexpression and structural rearrangement may also render oncogenic potential to RTKs. Given the key role of

PTKs in controlling cell proliferation and their potential oncogenic activation, identification of members of this family, which participate in the development of human cancer is of utmost interest. PTKs are often poorly expressed in cells. Here, we applied reverse transcription of RNA and subsequent amplification of the cDNA by the polymerase chain reaction (PCR) to detect low levels of PTK-transcripts. With this approach, we identified a new RTK, whose sequence is related to the EPH/elk-family.

Isolation and characterization of an EPH/elk-related gene

The comparison of the amino acid sequences of the catalytic domains of human PTKs has previously led to the identification of short, highly conserved regions. These coding sequences are suitable for the design of degenerate oligonucleotide primers which can be used in PCR reactions to identify new PTKs (Hanks *et al.*, 1988; Wilks, 1989; Partanen *et al.*, 1990; Holtrich *et al.*, 1991). This approach had two disadvantages: (i) Only small segments (approx. 200 bp) of carboxyterminal kinase domains were amplified in PCR reactions. (ii) The amplification of specific PTK-genes could not be achieved by this technique. To circumvent these obstacles we analysed N-terminal amino acid sequences for conserved regions. For EPH/elk-family members the motif CKETFNL in the N-terminus was found. Oligonucleotide primers (N1-N8) to the potential corresponding nucleic acid sequences were used in combination with primers (P6[1-4]) derived from the catalytic domain (SDVWS-motif, Figure 1a) in PCR reactions with cDNA templates from human embryonic tissues. Several combinations of primers gave rise to the anticipated amplification products of 2 kb, which represented a number of different sequences. One was shown to be identical to the previously described gene HEK (Wicks *et al.*, 1992). A second PCR product, called B1, was found to contain 2079 bp and encoded a portion of an unknown gene. Since this cDNA did not encompass the entire open reading frame, specific primers from the 5' region of B1 were utilized for cDNA synthesis. The cDNA was subsequently ligated to a 3' modified oligonucleotide (EB) and amplified using primer EB(com) and the B1 specific primer E8, resulting in the extension of 560 bp of upstream sequence (Figure 1b). To complete the missing 3' portion of B1 anchored PCR was performed: a cDNA, starting at the poly A-tail, was synthesized with P12(T+). Subsequent PCR amplification

Correspondence: H. Rübsamen-Waigmann

¹Present address: Klinikum der Philipps-Universität Marburg, Medizinisches Zentrum für Humangenetik, Bahnhofstr. 7a, 3550 Marburg, Germany

Received 1 March 1993; accepted in revised form 18 May 1993

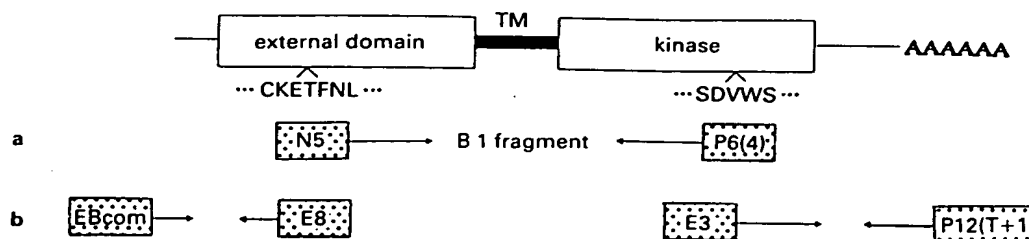


Figure 1 Position of PCR-primers with respect to the isolated cDNA. The figure shows the domain topology of the EPH/elk-RTKs; highly conserved motifs are indicated below the domains. (a and b) indicate localization of PCR-primers used for the isolation of HEK 2. TM = transmembrane domain. First strand cDNA synthesis was carried out using 1 μ g total RNA from human embryonic cells and 5 U M-MuLV reverse transcriptase in 50 mM Tris-HCl pH 8.3, 75 mM KCl, 10 mM DTT, 3 mM MgCl₂, 500 μ M dNTPs, 100 μ g ml⁻¹ BSA, and 0.2 μ M PTK specific primer P6(4). One half of the first strand synthesis was used as a template in a PCR (30 cycles) in 8.3 mM Tris-HCl pH 8.8, 41.7 mM KCl, 1.25 mM MgCl₂, 0.01% gelatine, 166.7 μ M dNTPs, 0.2 μ M each primer and 2.5 U Taq (Cetus). Each cycle consisted of 1 min 95°C, 2 min 70°C (or 50–60°C annealing temperature for less homologous primers) and 3 min at 72°C. For oligonucleotide ligation 10 U RNA ligase and 2 μ M 3' modified primer EB was added to 0.5–100 pg cDNA in 50 mM Tris-HCl pH 8.0, 10 mM MgCl₂, 10 μ g ml⁻¹ BSA, 40% PEG 6000, 1 mM hexamine cobalt chloride and 20 μ M ATP and incubated at 22°C for 48 h. The ligation product was subsequently purified and used as template in a PCR (30 cycles) with 0.2 μ M primer EB(com) and the specific E5 primer in 10 mM Tris-HCl pH 8.8, 50 mM KCl, 1.5 mM MgCl₂, 0.01% gelatine, 0.2 mM dNTPs and 2.5 U Taq. From this reaction, 1 μ l (out of 50 μ l) was used as template in a second PCR using the specific primer E8. Anchored PCR was similar to a previously described technique (Loh *et al.*, 1989). Briefly, cDNA was synthesized using primer P12(T+). Half of a tailing reaction was used as template in a PCR (30 cycles) as described above, with 0.2 μ M of the anchor primer P12(T-) and the specific HEK 2 primer E3. The following primers were used: P6(4)-5'-CCATAGGTCCAGACATCACT/P12(T+)-5'-GCAGAATTCGTGAAGTGGCGCCGCA(dT)₁₂/P12(T-)-5'-GCAGAATTCGTGAAGTGGCGCCGCA/EB-5'-CTGAATTCGGATCCGACTGGTCTGACTCG-P-CH₂-CHOH-CH₂-NH₂/EBcom-5'-CGAGTCA-GACCAATCGGATCCGAATTCAG/N5-5'-TGCAAGGAGACATTCAACCT/E3-5' (nt 2347–2378)/E5-5' (nt 616–594)/E7-5' (nt 2055–2031)/E8-5' (nt 560–535)/E13-5' (nt 1769–1743)/E16-5' (nt 1242–1222)/E18-5' (nt 1034–1009)/E19-5' (nt 801–777)

with the specific primer E3 located at the 3' end of B1 and primer P12(T-) provided the complete 3' coding region of the gene and 784 bp of 3' untranslated sequence (Figure 1b). Both, upstream and downstream extension products of B1 (later renamed HEK 2) were sequenced directly. To verify the sequence overlapping fragments were amplified from embryonic cDNA and analysed again.

HEK 2 represents a new member of the EPH/elk-family

The analysis of the combined sequences showed that HEK 2 has an open reading frame encoding 998 amino acids preceded by a 5' untranslated region of 27 nucleotides and followed by a 3' untranslated region of 784 nucleotides (Figure 2). A motif in the 5' noncoding region is in agreement with Kozak's rule for the initiation of translation (Kozak, 1984). The presence of two hydrophobic stretches of amino acids, probably representing a cleavage signal sequence (residues 1–33) and a transmembrane region (residues 557–582) followed by a basic stop transfer motif suggests that the putative protein is an integral membrane protein (von Heijne, 1986; Singer, 1990) with an extracellular domain of 556 amino acids and a cytoplasmic domain of 416 amino acids. Two potential N-linked glycosylation sites were found in the extracellular portion. In the N-terminal subdomain of the extracellular region clustering of 13 cysteine residues (aa 269–392) forms a cysteine rich box (Lindberg & Hunter, 1990). The carboxyterminal portion of the external domain is mostly devoid of cysteine residues but contains two regions (aa 336–556) which are homologous to fibronectin type III repeats (Skorstengaard *et al.*, 1986; Ruoslahti, 1988). The cytoplasmic domain of HEK 2 contains a typical catalytic domain of PTKs. The consensus sequence Gly-X-Gly-X-X-Gly found in many nucleotide-binding

proteins and in PTKs is perfectly conserved in HEK 2 at amino acid positions 640–645 (Wierenga & Hol, 1983). A highly conserved lysine residue, which is believed to be directly involved in the phosphotransfer reaction possibly mediating proton transfer is located at position 665 (Kamps *et al.*, 1984). In addition, the invariant amino acids (Asp-Phe-Gly) implicated in ATP-binding are located at residues 776–778 and a putative autophosphorylation site is found at position 792. The 3' untranslated sequence contains 784 nucleotides and a potential polyadenylation signal.

The new gene has the following overall protein sequence identity with each of the fully sequenced members of the EPH/elk-family: chicken cek 5 (Pasquale, 1991), 70%; rat elk (Lhotak *et al.*, 1991), 70%; human HEK (Wicks *et al.*, 1992), 55%; human ECK (Lindberg & Hunter, 1990), 47% and human EPH (Hirai *et al.*, 1987), 42%. In addition to the close relationship of their sequences; the domain topology of HEK 2 is quite comparable to that of the other members of the EPH/elk-family (Figure 3). The clustering of the cysteine residues in a single cysteine rich box distinguishes HEK 2 from other RTK-families like FGFR, EGFR or insulin receptor. Furthermore, like the other members of the EPH/elk-family HEK 2 contains a kinase domain, which is not interrupted by an insert. Because of its highest homology to the chicken gene cek 5 (chicken embryo kinase), we propose to call our new gene HEK 2 (human embryo kinase).

Southern blot analysis

Southern blot analysis of 10 μ g of human genomic DNA digested by various restriction enzymes and hybridized with an aminoterminal HEK 2-specific probe under stringent conditions resulted in two bands with PstI digested DNA (2.6 kb and 2.4 kb). EcoRI-

GGCTCGGCTCCTAGAGCTGCCACGGCCATGGCCAGAGCCGCGCGCGCGCGCGCTGCGCGCGCGCGGGGCTTTCGCGCTGCTCCCT 90
 H A R A R P P P P P S P P P G L L P L L P
 CGCTGCTGCTGCTGCGCGCTGCTGCTGCTGCTGCCCGCGCGCTGCGCGCGCGCTGGAAGAGACCTCATGGACACAAATGGGTAACTCTGAG 180
 P L L L L L P L P A G C R A L E E T L M D T K W V T S E
 TTGGCGTGGACATCTCATCCAGAAAGTGGGTGGGAAGAGGTGAGTGGCTACGATGAGGCCATGAATCCCATCCGCACATACCAGGTGTGT 270
 L A W T S H P E S G W E E V S G Y D E A M N P I R T Y Q V C
 AATGTCGCGAGTCAAGCCAGAACAAGTGGCTTCGACGCGGGTTCATCTGCGCGCGGGATGTGCAGCGGGTCTACGTGGAGCTCAAGTTT 360
 N V R S S Q N N W L R T G A T I W R R D V Q R V Y G A L K F
 ACTGTGCGTGAAGTCAACAGCATCCCAACATCCCGGCTCTGCAAGGAGACCTTCAACCTCTTCTACTAGAGGCTGACAGCGATGTG 450
 T V R D C N S I P N I P G S C K E T F N L F Y E A D S D V
 GCCTCAGCTCTCTCCCTCTCTGGATGGAGAACCCCTACGTGAAAGTGACACCATGACCCGATGAGAGCTTCTCGCGCTGGATGCC 540
 A S A S S P F W M E N P Y V K V D T I A P D E S F S R L D A
 GCGCTGTCAACCAAGTGGCGAGCTTTGGGGCCATTTCCAAAGTGGCTTCTACCTGGCCTTCCAGGACAGGCGCGCTGCMATGCG 630
 G R V P T K V R S F G P L S S K A G F Y L A F Q G A C M S
 CTCATCTCCGTGCGCGCTTCTACAAGAAGTGTGATCCACACCGAGGCTTCGCACTCTTCCCGAGACCTCAGTGGCGGGAGGCC 720
 L I S V R A F Y K K C A S T T A G F A L F P E T L T G A E P
 ACCTGCTGGTCAATGCTCTGGCAGCTGCATCCCTAACCGGTGGAGGTGCGGTGCCACTCAAGCTCTACTGCAACGGCGATGGGGAG 810
 T S L V I A P G T C I P N A V E V S V P L K L Y C N G D G E
 TGGATGGTGGCTGTGGGTGCTGCACCTGTGCACCGGCTGAGCCAGTGCACAGGAGTCCAGTGGCGCGCTGCTCCCTGGGAGC 900
 W M V P V G A C T C A T G H E P A A K E S Q C R P P G S
 TACAAGCGAAGCAGGAGAGGGGCGCTGCTCCCATGTCCCCCAACAGCGGTACCACTCCCGAGCGCGAGCATCTGCACCTGCCAC 990
 Y K A K Q G E G P C L P C P P N S R T T S P A A S I C T C H
 AATACTTCTACCTGTCAGACTCGGACTTGCAGGAGTGCCTTACCGCTGCTTCCACCGAGGTGTGATCTCAATGTGAAT 1080
 N N F Y R A D S D S A D S A C T T V P S P P R G V I S N V
 GAACTCTACTGATCTCGAGTGGAGTGACCCCGGACCTGGGTGTCTCGGAGTGACCTCTGTACAATGTATCTCAAGAAGTCCAT 1170
 E T S L I L E W S E P R D L D L L Y N I C K K C H
 GGGGCTGGAGGGGCTCAGCTGTCTACGCTGTGATGACAACGTGGAGTTTGTGCTCGGCGCTGGGCTGTGGAGCGCGGGTCCAC 1260
 G A G G A S A C S R C D D N V E F V P R Q L G L S E P R V H
 ACCAGCATCTGCTGGCGGACGCTACCTTTCAGGTGACGGGTGCTGCGGGCAGAGGCTTTCGCGCGCTGCTGCTTAT 1350
 T S L L L A H T R Y T F E V Q A V N G V S G K S P L P P R Y
 GCGGCTGGAATCACCACAAACAGGCTGCGCCGCTGGAAGTCCCTACCTACGCTGCACAGCAGCTCAGGCGAGCGCTCACCTA 1440
 A A V N I T T N Q A A P S E V P T A C T R L H S S S G S L T L
 TCCTGGGACCGCCAGAGCGGCGCAACGGAGTTCCTGGACTACGAGATGAAGTACTTTGAGAAGAGCGAGGGCATCGCTCCACAGTG 1530
 S W A P P E R P N G V I L D Y E M K Y F E K S E G I A S T V
 ACCAGCAGATGAATCCGTCAGCTGGACGGGCTTCGGCTGACGGCGCTGAGTGTGCTGCTGCTGCTGCTGCTGCTGCTGCTGCTGCT 1620
 T S Q M N S V Q L D G L R P D A R Y V V Q V R A R T V A G Y
 GGGCAGTACAGCGCGCTGCGAGTTTGAAGACCAAGTGAAGAGGCTCTGGGCGCGAGCAGCTCCAGGAGCAGCTTCCCTCATCGTG 1710
 G Q Y S R P A E F E T S E R G S G A Q Q L Q L I V
 GGCTCGCTACAGCTGGGCTTGTCTCTGCTGGTGGTGTCTGCTGCTGCTGCTGCTGCTGCTGCTGCTGCTGCTGCTGCTGCTGCTGCT 1800
 G S A T A G L V F V V A V V I A I V C L R K Q R H G S D S
 GAGTACAGGAGAGCTGCAGCAGTACCTGCTCCTGGAATGAAGTATTATGACCTTTTACCTACGAGGACCTTAATGAGGCTGT 1890
 E Y T E K L Q Q Y I A P G M K V Y I D P F T Y E D P N E A V
 CGGGAGTTTGCAGAGGATCGACGTGTCTCGCTCAAGATCGAGGAGTGTGCGAGCTGGGGAATTTGGGGAAGTGTGCGGTGCGA 1980
 R E F A K E I D V S C V K I E E V I G A G E F G V C R G R
 CTGAAACAGCTGGCGCGGAGAGGTGTTTGTGGCCATCAAGAGCTGAAGGTGGGCTACACCGAGAGGCGAGCGCGGGAGCTTCTAAGC 2070
 L K Q P G R R E V F V A I K T L K V G Y T E R Q R R D F L S
 GAGGCTCCATCGGTGCTGATCAGCCCAATATATCGGCTCAGGCGGTGCTGACCAAAAGTGTGCTGCTGCTGCTGCTGCTGCTGCTGCT 2160
 E A S I M G Q F D H P N I I R L E G V V T K S R P V M I L T
 GAGTTCATGAAAAGTGCAGCGCTGCTCCTCGGCTCAACGATGGGAGTTCACGGTTCATCCAGCTGCTGCTGCTGCTGCTGCTGCTGCTGCT 2250
 E F M E N C A L D S F L R L N D G Q F T V I Q L V G M L R G
 ATTGTGCGCGCATGAAGTACCTGTCCGAGATGAATATGTGCACCGGACCTGGCTGCTGCGAACATCTTGTCAACAGCAACCTGGTC 2340
 I A A G M K Y L S E M N Y V H R D L A A R N I L V N S N L V
 TGCAAGTCTCAGACTTTGGCTCTCCCGCTTCTGGAGGATGACCCCTACCTACCACTTCCCTGCGGCGGAGATCCCC 2430
 C K V S D F G L S R F L E D D P S D P T Q T S S L G G K I P
 ATCCGCTGAGTGCAGGAGGCGCATAGCCTTCCGGAAGTTCATCTGCTAGTGTCTGAGCTACGAGTTCGGAATGTCTGCTGCTGCTGCT 2520
 I R W T A P E A I A Y R K F T S A S D V W S Y G I V M W E V
 ATGAGCTATGAGAGCGACCTACTGGGACATGAGCAACAGGATGTATCAATGCCGTGGAGCAGGATTACCGGCTGCCACCAACCTG 2610
 M S Y G E R P Y W D M S N Q D V I N A V E Q D Y R L P P M
 GACTGTCCACAGCACTGCACAGGCTCATGCTGGAGTGTGGGTGGGCGGCGGAGCTTCCAGGCTTCCAGATGTCAATACC 2700
 D C P T A L H Q L M L D C W V R D R N L R P K F S Q I V N T
 CTGGCAAGCTCATCCGCAATGCTGCCAGCTCAAGGTCATGCGCGCTCAGTGTGGCATGTACAGGCCCTCTGGAGCGGCGGTC 2790
 L D K A L I R N A L S L K V I A S A Q S G M S P L L D R T V
 CCAGATTACACAACCTTACGACAGTTGGTGATTGGCTGGATGCCATCAAGATGGGCGGTACAAGGAGAGCTTCTGTCAGTGGCGGTTT 2880
 P D Y T T F T T V G D W L D A I K M G R Y K E S F V S A G F
 GCATCTTTGACCTGGTGGCCAGATGACGGCAGAAGACCTGCTCCGTAATTGGGGTCAACCTGGCGCGGACCAAGAGATCCTGAGC 2970
 A S F D L V A Q M T A E D L L R I G V T L A G H Q K K I L S
 AGTATCCAGGACATGGCGCTGCAGATGAACAGAGCTGCTGCTGCTGCTGCTGCTGCTGCTGCTGCTGCTGCTGCTGCTGCTGCTGCT 3060
 S I Q D M R L Q M N Q T L P V Q V
 GATGCCAAGCAGCGCGCTGGAGTTTTCGAGCTTTCGAGCTTTTGGATGCTGCGCTTAGGCTGTGGCCAGAAGCTGGAAGTTTGGGAAAG 3150
 GCCCAAGCTGGAGCTTCTCAGGCTGTGCTCCCTCCCGAGAGTGGCGCCCAACCTCTTCAATTTGAAGATGAGATTAGGAGAGGGG 3240
 TGAATGACCTGAGCTTCTCAGGCT 3330
 GCTGAGCTCTGCGGAGGTGAGCTGCGGTTCCACAGGCGGCGGCTGCGGAGGCTGCGGCGGCTGCGGCGGCTGCGGCGGCTGCGGCGG 3420
 AGCAGTCTCTCTCAGGAAGTGGAGGAGGGGAGCTCAGGAATGGGAAATGTGACACCACTCTGAAGCCAGCTTGCACCTCCAGTT 3510
 TGCACAGGGAATTTGCTGCGGCTGAGGGGCTGCTCCCGCGGCTTGGTGTGCTGCTGCTGCTGCTGCTGCTGCTGCTGCTGCTGCTGCT 3600
 AGTTGCGGCTTGCCTCCAGAGCTGCTCAGAGCCAGAGATGGGATGTGAGT 3690
 TGTGTGTGACGCACTGGCTGCACAGAGAGCATGGGTGAGCGTGTAAAGCTTGGCCCTGTGCTGCTGCTGCTGCTGCTGCTGCTGCTGCTGCT 3780
 AGCAGATAAAGCAATAAGTGA

Figure 2 Nucleotide sequence and deduced amino acid sequence of the putative HEK 2 protein including partial untranslated sequences. The putative signal peptide and the transmembrane region are underlined. Possible sites for N-glycosylations are boxed. The motives involved in ATP-binding are marked by dots. The putative autophosphorylation site is indicated by a grey circle. Shaded domains show conserved regions among PTKs. The polyadenylation signal AATAAA is underlined. Numbers at the right indicate positions of nucleotides. For DNA sequencing primers and unincorporated dNTPs were removed from PCR-products by ultrafiltration through Millipore UFC3 TTK00 filters. Sequencing was done using 0.6 pmol of purified DNA and a Taq DyeDeoxy Terminator Cycle Sequencing Kit from Applied Biosystems according to the manufacturer's protocol except that the labelling reaction was performed for 30 cycles at 96°C - 30 s, 50°C - 15 s, 60°C - 4 min. The products of the sequencing reactions were analysed on an Applied Biosystem 373 A DNA sequencer

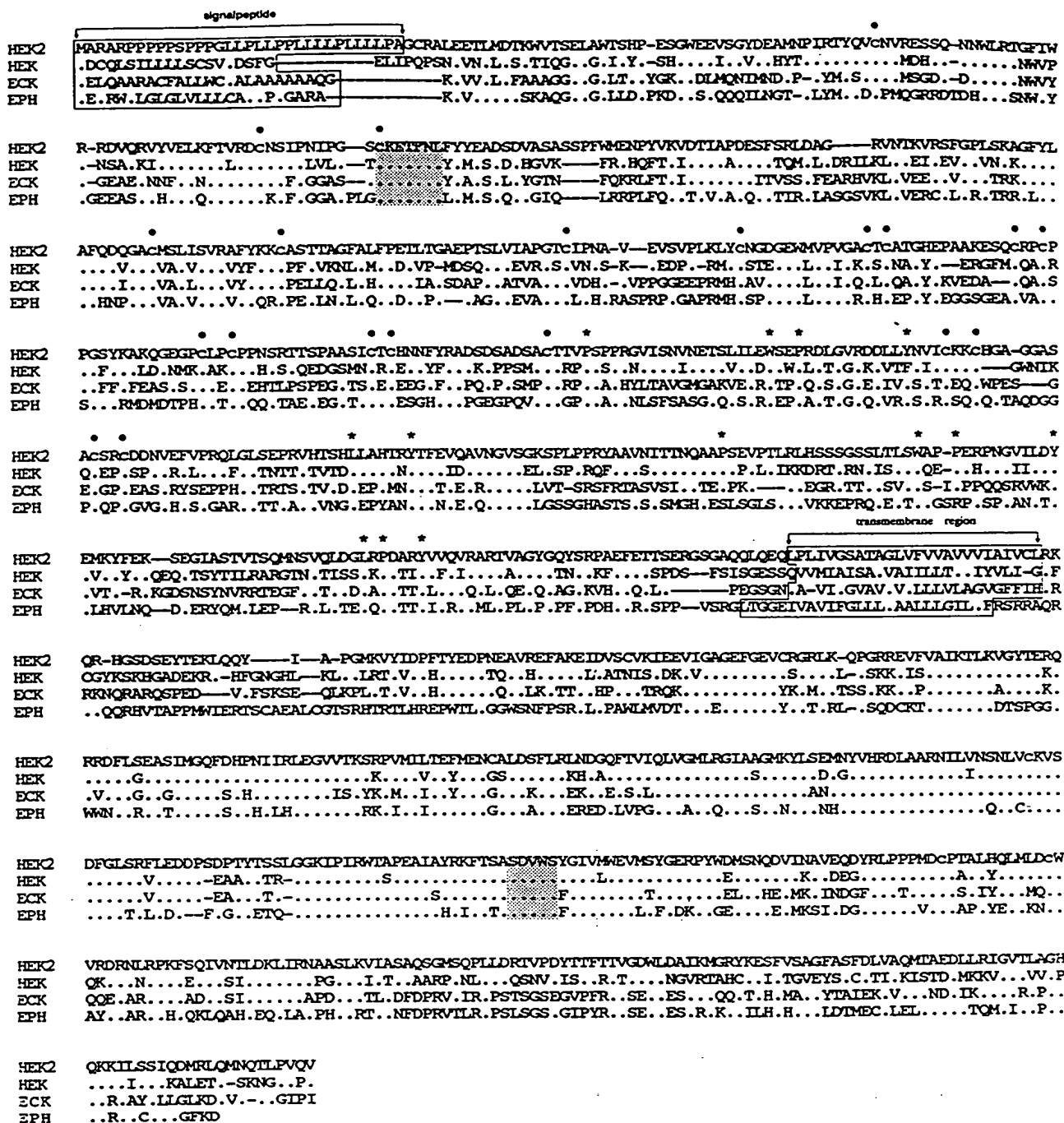


Figure 3 Comparison of amino acid sequences of the human EPH/elk-family: HEK 2, HEK, ECK and EPH. Amino acid sequences were aligned by the TREE program of HUSAR, based on a progressive alignment method of Feng and Doolittle (1987). The putative signal sequences and the transmembrane domains are boxed. Conserved cysteine residues are marked by dots above the sequences. Stars indicate amino acids corresponding to conserved residues of the fibronectin repeat III. Dashes within the sequences indicate gaps introduced to optimize alignment. Motifs for the initial PCR-amplification appear on grey background

and HindIII-digested DNA gave rise to a single band of 20 kb and 9.4 kb, respectively (data not shown). This suggests that HEK 2 is a single-copy gene. Furthermore, our Southern analysis of genomic DNA indicates that probe specificity and hybridization stringency are sufficient for discrimination between the highly homologous members of the EPH/elk-family.

Chromosomal location

We used two different sets of primers for the localization of the HEK 2 gene in human-mouse somatic cell hybrids (Willecke *et al.*, 1990). In PCR reactions with human genomic DNA both combinations of primers generated products of appropriate size, which were

visible as a single band on agarose gels. In contrast, amplifications with mouse DNA did not yield PCR-products. HEK 2 segregates with the human chromosome 3. The gene marker is present in clone GM194 RAG 7 which contains chromosome 3q21-3qter. Since it is missing in clone GM194 RAG 5-5 which contains the remaining part of chromosome 3, the locus is on the distal half of 3q.

Expression of the HEK 2 gene in human adult tissues and cell lines

We examined several human tissues in a Northern blot analysis to determine the pattern of HEK 2 expression. Using a probe representing a portion of the aminoterminal domain (nt positions 423–2055), a single mRNA of 4.6 kb was detected. HEK 2 transcripts were noted in lung, pancreas, placenta, brain and kidney. In heart, skeletal muscle and liver, HEK 2 mRNA was found to be less frequent (Figure 4). A similar distribution has been reported for ECK (Lindberg & Hunter, 1990). EPH transcripts were detected in rat kidney, lung and liver and in smaller amounts in testis (Maru *et al.*, 1988).

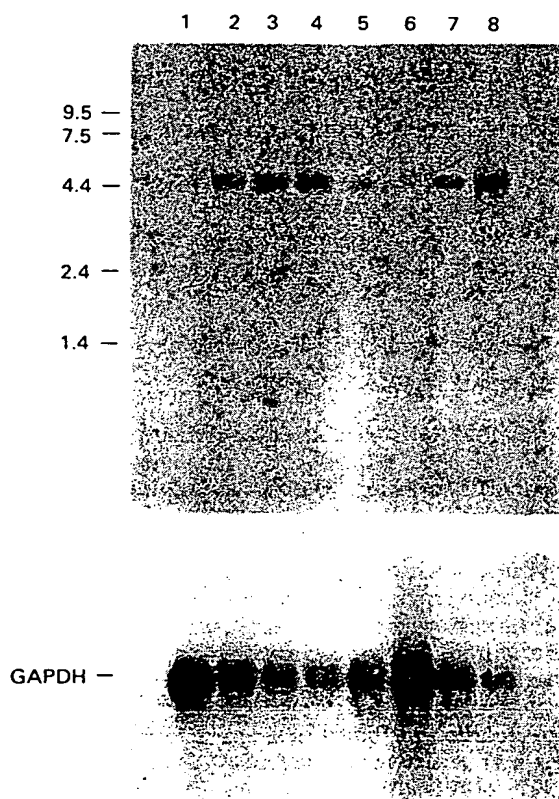


Figure 4 Northern blot analysis of the HEK 2 gene. Each lane of the multiple tissue blot contains 2 μ g of human poly(A)⁺ RNA. Lanes 1–8: heart, brain, placenta, lung, liver, skeletal muscle, kidney and pancreas. PCR was used to obtain a single-stranded specific probe of HEK 2 (nt 423–2055). Radiolabelling of the antisense strand was performed using primers E19, E18, E16, E13, E8, E7 and 150 μ Ci [α -³²P]dCTP (6000 Ci mmol⁻¹). Hybridization was performed with a specific HEK 2 probe and with a human glyceraldehyde-3-phosphate dehydrogenase (GAPDH) probe, to indicate the amount of RNA. The size marker (kb) is indicated

Applying the RNA-PCR we were also able to demonstrate HEK 2 transcripts in cultured human macrophages, but not in T-lymphocytes. The expression of HEK 2 in macrophages, however, was at the limit of detection of Northern blot experiments. Low levels of HEK 2 transcripts were also found in spleen and thymus (data not shown). In contrast to HEK 2, the expression of HEK was previously shown to be restricted to lymphoid tumor cell lines only (one pre-B- and two T-cell lines) (Wicks *et al.*, 1992). In normal human lymphoid and bone marrow cells HEK expression was not detectable. Since HEK expression was observed on a small number of fresh hemopoietic tumor specimens, the possibility was raised that HEK is a sporadically over-expressed gene. According to our data HEK 2 appears to play a minor role in the lymphoid system.

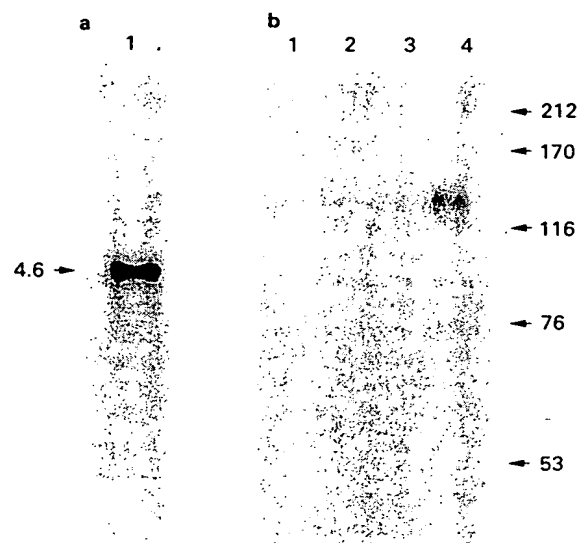


Figure 5 Expression of HEK 2 in the epidermoid carcinoma cell line A431. (a) Northern blot analysis of RNA from A431 cells with a HEK 2-specific probe. The lane contains 10 μ g total RNA. Total RNA was isolated by the guanidinium isothiocyanate/CsCl cushion technique (Chirgwin *et al.*, 1979). RNA was separated on an agarose/formaldehyde gel (Lehrach *et al.*, 1977) and transferred to a nitrocellulose membrane (Amersham). RNA hybridization was performed as described in Figure 4. The size (kb) of HEK 2-transcripts is indicated by an arrow. (b) Protein kinase activity of HEK 2 from A431 cells. For protein extraction A431 cells were grown to 70% confluency, washed twice in phosphate-buffered saline (PBS) and lysed in ice-cold modified RIPA buffer (0.1% sodium dodecyl sulfate (SDS), 1% Nonidet P-40, 0.5% sodium deoxycholate, 20 mM Tris-HCl (pH 7.5), 0.15 M NaCl, 2 mM ϵ -aminocaproic acid, 1 mM EDTA, 50 mM NaF, 1 mM phenylmethylsulfonyl fluoride and 10 μ g ml⁻¹ aprotinin, leupeptin and pepstatin A, for 30 min. The lysates were centrifuged at 100 000 g for 45 min at 4°C. Protein concentration was measured by the Bradford-assay (BioRad, München). Lysate containing 640 μ g protein was incubated with 10 μ l preimmune serum or rabbit anti-HEK 2 serum for 1 h at 4°C. The HEK 2-antibody-complexes were precipitated with 100 μ l of 10% protein-A-Sepharose (Pharmacia-LKB). The immunoprecipitates were washed five times and incubated for 15 and 30 min at 30°C in 20 μ l of buffer containing 20 mM Bis/Tris-propane (pH 5.9), 10 mM MnCl₂ and 6 μ Ci of [γ -³²P]ATP (3000 Ci mmol⁻¹, DuPont NEN). Immune complexes of preimmune serum (lane 1: 15 min, lane 2: 30 min) and rabbit anti-HEK 2 serum (lane 3: 15 min, lane 4: 30 min) were analysed on a 7% SDS-polyacrylamide gel. Radiolabeled proteins were detected with Fuji RX film with an intensifying screen for 15 min at -80°C. The molecular weight in kDa of marker proteins is indicated

In addition to tissues, several human cell lines were examined for the expression of the HEK 2 gene. HEK 2 transcripts were detected in tumor cell lines of breast and epidermoid origin, but not in HeLa cells and epithelial cells of the lung. Figure 5 shows HEK 2-RNA and -protein expression in the epidermoid carcinoma cell line A431. Polyclonal antibodies against a peptide from the carboxyterminal region of the HEK 2-protein (amino acids 897–998) were raised in rabbits. In immunoprecipitates with lysates from the

A431 cell line and these antibodies followed by a kinase reaction a 130 kDa protein was found to be phosphorylated (Figure 5b).

Acknowledgements

The Georg-Speyer-Haus is supported by the Bundesgesundheitsministerium and the Hessisches Ministerium für Wissenschaft und Kunst. This work was supported by the Hermann-Schlösser-Stiftung (U.H.), the Deutsche Forschungsgemeinschaft Ru 242/11-1 (B.B.) and Gr 373/16-2 (K.-H.G.).

References

- Bishop, J.M. (1987). *Science*, **235**, 305–311.
- Chirgwin, J.M., Przybyla, A.E., MacDonald, R.J. & Rutter, W.J. (1979). *Biochemistry*, **18**, 5294–5299.
- Downward, J., Yarden, Y., Mayes, G., Scrace, G., Totty, N., Stockwell, P., Ullrich, A., Schlessinger, J. & Waterfield, M.D. (1984). *Nature*, **307**, 521–527.
- Feng, D.-F. & Doolittle, R.F. (1987). *J. Mol. Evol.*, **25**, 351–360.
- Hanks, S.K., Quinn, A.M. & Hunter, T. (1988). *Science*, **241**, 42–52.
- Hirai, H., Maru, Y., Hagiwara, K., Nishida, J. & Takaku, F. (1987). *Science*, **238**, 1717–1720.
- Holtrich, U., Bräuninger, A., Strebhardt, K. & Rübsamen-Waigmann, H. (1991). *Proc. Natl. Acad. Sci. USA*, **88**, 10411–10415.
- Kamps, M.P., Taylor, S.S. & Sefton, B.M. (1984). *Nature*, **310**, 589–592.
- Kozak, M. (1984). *Nucleic Acids Res.*, **12**, 857–872.
- Lehrach, H., Diamond, D., Wozney, J.M. & Boedtker, H. (1977). *Biochemistry*, **16**, 4743–4748.
- Lhotak, V., Greer, P., Letwin, K. & Pawson, T. (1991). *Mol. Cell. Biol.*, **10**, 2496–2502.
- Lindberg, R.A. & Hunter, T. (1990). *Mol. Cell. Biol.*, **10**, 6316–6324.
- Loh, E.Y., Elliott, J.F., Cwirla, S., Lanier, L.L. & Davis, M.M. (1989). *Science*, **234**, 217–220.
- Maru, Y., Hirai, H., Yoshida, M.C. & Takaku, F. (1988). *Mol. Cell. Biol.*, **8**, 3770–3776.
- Matsushine, H., Wang, L.H. & Shibuya, M. (1986). *Mol. Cell. Biol.*, **6**, 3000–3004.
- Partanen, J., Mäkelä, T.P., Alitalo, R., Lehtväslaiho, H. & Alitalo, K. (1990). *Proc. Natl. Acad. Sci. USA*, **87**, 8913–8917.
- Pasquale, E.B. (1991). *Cell Regul.*, **2**, 523–534.
- Ruoslahti, E. (1988). *Annu. Rev. Biochem.*, **57**, 375–413.
- Sherr, C.J. (1990). *Blood*, **75**, 1–12.
- Singer, S.J. (1990). *Annu. Rev. Cell. Biol.*, **6**, 247–296.
- Skorstengaard, K., Jensen, M.S., Sahl, P., Petersen, T.E. & Magnusson, S. (1986). *Eur. J. Biochem.*, **161**, 441–453.
- von Heijne, M. (1986). *Nucleic Acids Res.*, **14**, 4683–4690.
- Wicks, I.P., Wilkinson, D., Salvaris, E. & Boyd, A.W. (1992). *Proc. Natl. Acad. Sci. USA*, **89**, 1611–1615.
- Wierenga, R.K. & Hol, W.G.J. (1983). *Nature*, **302**, 842–844.
- Wilks, A.F. (1989). *Proc. Natl. Acad. Sci. USA*, **86**, 1603–1607.
- Willecke, K., Jungbluth, S., Dahl, E., Hennemann, R., Heynkes, R. & Grzeschik, K.-H. (1990). *Eur. J. Cell Biol.*, **53**, 275–280.

D9

Embryonic stem cells express multiple Eph-subfamily receptor tyrosine kinases

JASON D. LICKLITER*, FIONA M. SMITH, JANE E. OLSSON, KAREN L. MACKWELL, AND ANDREW W. BOYD

Lions Cancer Research Laboratory, Walter and Eliza Hall Institute of Medical Research, P.O. Royal Melbourne Hospital, Victoria 3050, Australia

Communicated by G. J. V. Nossal, The Walter and Eliza Hall Institute of Medical Research, Victoria 3050, Australia, September 29, 1995

ABSTRACT Eph and its homologues form the largest subfamily of receptor tyrosine kinases. Normal expression patterns of this subfamily indicate roles in differentiation and development, whereas their overexpression has been linked to oncogenesis. This study investigated the potential role of Eph-related molecules during very early embryonic development by examining their expression in embryonic stem (ES) cells and embryoid bodies differentiated from ES cells *in vitro*. By use of a strategy based on reverse transcriptase-mediated PCR, nine clones containing Eph-subfamily sequence were isolated from ES cells. Of these, eight were almost identical to one of four previously identified molecules (Sek, Nuk, Eck, and Mek4). However, one clone contained sequence from a novel Eph-subfamily member, which was termed embryonic stem-cell kinase or Esk. Northern analysis showed expression of Esk in ES cells, embryoid bodies, day 12 mouse embryos, and some tissues of the adult animal. Levels of expression were similar in ES cells and embryoid bodies. By comparison, Mek4 showed no significant transcription in the ES cell cultures by Northern analysis, whereas Eck displayed stronger signals in ES cells than in the embryoid bodies. These results suggest that Eph-subfamily molecules may play roles during the earliest phases of embryogenesis. Furthermore, the relative importance of different members of this subfamily appears to change as development proceeds.

The receptor tyrosine kinases (RTKs) are transmembrane molecules which transduce signals from the extracellular environment into the cytoplasm. They include well-studied regulators of cell proliferation and differentiation, such as c-Kit and the receptors for epidermal growth factor, platelet-derived growth factor, and macrophage colony-stimulating factor (1). Signaling by an RTK is initiated when its ligand binds to the extracellular domain of the receptor. This leads to the formation of receptor dimers, which activate their catalytic domains by reciprocal phosphorylation on tyrosine residues (2). Once activated, RTKs can bind and phosphorylate specific intracellular proteins that act as second messengers.

Eph was the first isolated member of what is currently the largest subfamily of RTKs (3-20). This group is distinguished by a cysteine-rich region and two fibronectin type III repeats in the extracellular domain (4). Eph-subfamily kinases have been found in diverse species, including zebrafish (17), frogs (19), chickens (4, 8, 12), mice (8, 11, 14-16, 20), rats (5, 7), and humans (3, 6, 10, 13, 18). Features of their expression pattern suggest key functions during embryonic development. First, strong expression in the embryo is characteristic (4, 8, 11, 12, 15, 21). Second, *in situ* hybridization and immunolocalization studies show associations between the expression of specific Eph-subfamily molecules and particular events in morphogenesis. For example, Eck is transiently expressed in cells adjacent to the primitive streak during gastrulation, and later its transcripts are found in specific rhombomeres of the developing

hindbrain and in the ectoderm of the second and third branchial arches (22). The expression of Nuk protein on growing peripheral nervous system axons, which disappears when the axons have ceased migrating, and the segment-restricted pattern of Nuk and Sek expression during hindbrain morphogenesis are other examples (11, 15). Preferential expression at interfaces between embryonic cell populations and in intercellular junctions has led to the suggestion that Eph-subfamily molecules influence embryonic differentiation and cellular migration by interactions involving direct cell-cell contact (15, 22). The recent finding that ligands for some members of this group are cell membrane bound supports this notion (23-26). Eph-related molecules also have a potential role in oncogenesis. Eph and Eck overexpression was reported in epithelial tumor cell lines and some human carcinomas (3, 27), and Hek overexpression occurs sporadically in leukemia (9). Furthermore, artificial overexpression of Eph transforms NIH 3T3 cells, allowing them to form colonies in agar and produce tumors in nude mice (28). In transgenic models of murine mammary cancer, overexpression of the Eph-subfamily members Myk-1 and Myk-2 correlates with the development of poorly differentiated and invasive tumors, suggesting a role in tumor progression (20).

In this study, reverse transcriptase-mediated PCR (RT-PCR) was used to identify Eph-subfamily RTKs expressed by embryonic stem (ES) cells. These are undifferentiated, totipotent cells derived from the inner cell mass of the blastocyst (29). We speculated that Eph-related molecules expressed by ES cells may be involved in the initial differentiation and organization of embryonic tissues, thus helping to establish the blueprint for later development. Nine positive clones were isolated by this method, including one which encoded sequence from a novel molecule.† We also cultured ES cells under conditions which induced *in vitro* differentiation into embryoid bodies containing a variety of primitive tissue lineages (30). Expression of selected Eph-related molecules was then examined in both the ES cells and embryoid bodies by Northern analysis.

MATERIALS AND METHODS

ES Cell Cultures. The murine 129/Sv-derived ES cell line W9.5 (provided by F. Koentgen of the Walter and Eliza Hall Institute, Melbourne, Australia) was routinely passaged on underlayers of irradiated embryonic fibroblasts in Dulbecco's modified Eagle's medium supplemented with leukemia inhibitory factor (LIF, 1000 units/ml; AMRAD, Melbourne), 0.1 mM 2-mercaptoethanol, and 15% fetal bovine serum. Cultures were incubated in a 10% CO₂ atmosphere at 37°C. In preparation for the studies described below, ES cells were subcul-

Abbreviations: RTK, receptor tyrosine kinase; ES cells, embryonic stem cells; RT-PCR, reverse transcriptase-mediated PCR; LIF, leukemia inhibitory factor; GAPDH, glyceraldehyde-3-phosphate dehydrogenase.

*To whom reprint requests should be addressed.

†The sequence reported in this paper has been deposited in the GenBank database (accession no. MMU18084).

The publication costs of this article were defrayed in part by page charge payment. This article must therefore be hereby marked "advertisement" in accordance with 18 U.S.C. §1734 solely to indicate this fact.

tured into gelatin-coated flasks, and four passages without a feeder layer were performed to deplete the embryonic fibroblasts. In some of the cultures, LIF was withdrawn 11 days prior to harvesting, to allow differentiation into embryoid bodies to take place (30). Control cultures of embryonic fibroblasts alone were also prepared.

RT-PCR. Prior to RNA extraction, cultures of undifferentiated ES cells were disrupted with trypsin and the cells were washed in phosphate-buffered saline. Cell pellets were resuspended in buffer containing guanidinium isothiocyanate and total RNA was extracted with the use of organic solvents (31). cDNA was then synthesized from 1 μ g of total RNA by use of an oligo(dT) primer and avian myeloblastosis virus reverse transcriptase (Promega). PCR amplifications were performed with degenerate primers derived from three regions of sequence which are relatively conserved in the Eph subfamily (13) (Fig. 1). Reaction mixtures (30 μ l) contained 50 mM KCl, 10 mM Tris-HCl (pH 8.3), 1.25 mM MgCl₂, 0.2 mM each dNTP, 2.5 units of *Taq* polymerase (Perkin-Elmer), 30 pmol of sense primer (P1 or P2), 30 pmol of antisense primer (P3 or P4), and 3 μ l of the ES cell cDNA synthesis reaction. In addition, mRNA was directly extracted from ES cells with oligo(dT)-coated magnetic beads (Dyna, Oslo) and cDNA was synthesized from 1 μ g of mRNA with an oligo(dT) primer and Superscript II reverse transcriptase (Life Technologies, Grand Island, NY). Half of the reverse transcription reaction was then amplified with primers P1 and P4, with other reaction conditions identical to those described above. PCR products were electrophoretically separated, purified with the GeneClean II kit (Bio 101), and then subjected to a second round of PCR. Products initially amplified with primers P1 and P4 were reamplified with the same primers, while those amplified with P2 and P4 were reamplified with P2 and P3. All reactions were carried out in a PTC-100 programmable thermal controller (MJ Research, Cambridge, MA) employing cycle programs specific to each primer combination, as follows: 1 min at 95°C, 2 min at 70°C, and 3 min at 72°C for 30 cycles (primers P1 and P4); 1 min at 95°C, 1 min at 51°C, and 1 min at 72°C for 35 cycles (primers P2 and P4); 1 min at 95°C, 1 min at 41°C, and 1 min at 72°C for 35 cycles (primers P2 and P3).

Cloning and Sequencing. Reamplified, gel-purified PCR fragments were cloned into the *Sma* I site of pUC18 with the SureClone ligation kit (Pharmacia). Recombinant clones were sequenced with the *Taq* DyeDeoxy Terminator Cycle sequencing kit (Applied Biosystems); a Perkin-Elmer GeneAmp PCR System 2400 was used to perform the sequencing reactions and an Applied Biosystems 373 DNA sequencer was used for their subsequent analysis. Sequences were compared against se-

quence databank entries with the FASTA sequence analysis program.

Northern Blots. Poly(A)⁺ RNA from ES cells, embryoid bodies, embryonic fibroblasts, day 12 mouse embryos, and adult mouse tissues (5 μ g per sample) was electrophoresed through 1.2% agarose gels containing 2.2 M formaldehyde and transferred to nylon membranes (Zeta-Probe, Bio-Rad). The Northern blots were then probed with cDNA inserts from selected ES cell recombinants cloned by the methods described earlier. Sequence analysis (see Table 1) showed that clone 35C4 encoded murine Eck (21), clone 35C11 encoded Mek4 (8), and clone 35C15 encoded an apparently novel sequence. Inserts were digested from these clones with *Eco*RI and *Xba*I and used as templates for synthesizing ³²P-labeled probes with the Prime-It II random primer labeling kit (Stratagene). A labeled probe was also made from glyceraldehyde-3-phosphate dehydrogenase (GAPDH) cDNA. All blots were initially hybridized to the 35C15 probe. Subsequently, the membrane containing RNA from ES cells, embryoid bodies, and embryonic fibroblasts was reprobbed with the Eck and Mek4 probes. Between each reprobing, hybridized probe was stripped from the membrane by pouring boiling 0.1% SDS on the membrane and cooling to room temperature. Exposure to x-ray film overnight confirmed effective removal of the probe. Hybridization to the GAPDH probe was performed last. In all cases, hybridizations took place in 50% formamide at 42°C and washes were performed under stringent conditions, with the final wash at 65°C in 0.1× SSC/0.1% SDS (SSC is 0.15 M NaCl/0.015 M sodium citrate, pH 7.6). Autoradiographs were exposed at -70°C.

RESULTS

Eph-Subfamily Molecules Expressed by ES Cells. Primers P2 and P4 were expected to amplify ≈350 bp from the catalytic domain of Eph-subfamily molecules. In contrast, it was anticipated that primers P1 and P4 would amplify about 2.1 kb including much of the extracellular and intracellular domain (Fig. 1). RT-PCR was initially performed on total RNA derived from ES cells. Reactions using primers P2 and P4 amplified a band of the expected size, which reamplified with primers P2 and P3. However, no PCR product of the anticipated size was observed when primers P1 and P4 were used. Subsequently, when magnetically separated poly(A)⁺ RNA was substituted for total RNA, reactions with primers P1 and P4 successfully amplified a 2.1-kb product. Cloning of this 350-bp product resulted in four recombinants containing Eph-subfamily sequences (Table 1). These were highly homo-

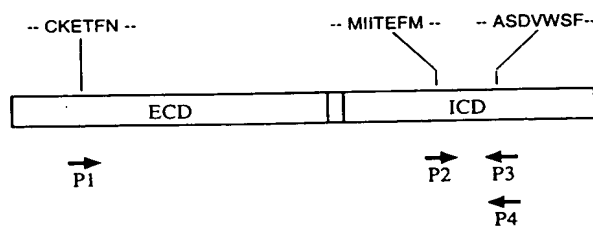


FIG. 1. Position of the four degenerate oligonucleotide primers used for RT-PCR. Relatively conserved peptide motifs on which the primers were based are shown above a schematic representation of the basic domain structure of Eph-subfamily molecules. ECD, extracellular domain; ICD, intracellular domain. The particular amino acid sequences shown are from Eph. Two sense primers (P1 and P2) and two antisense primers (P3 and P4) were synthesized. Their sequences were as follows: P1, 5'-GTAGGCATGCAAGGAGAC(A/C)TT(C/T)AACC-3'; P2, 5'-GCGATGATCAT(C/G)AC(A/G/T)GA(A/G)TA(C/T)ATGG-3'; P3, 5'-GTAGGAATTCCA(C/G/T)A-CATC(A/G)CT(A/G)GC-3'; P4, 5'-CCA(T/A)A(A/G)CTCCA(C/

Table 1. Eph-subfamily cDNA clones isolated from ES cells by RT-PCR

Clone	Closest homologue	Homology, %
<i>Primers P2 and P4*</i>		
25C5	Sek	97.8
33C1.1	Nuk	97.2
33C1.2	Eck	99.1
33C1.5	Eck	100
<i>Primers P1 and P4*</i>		
35C4	Eck	97.2
35C6	Mek4	97.3
35C10	Mek4	99.7
35C11	Mek4	99.7
35C15	Eph	83

Homologues were identified by screening nucleic acid databases with the FASTA program. Sek (11), Nuk (15), Eck (21), and Mek4 (8) are murine Eph-subfamily molecules; Eph (3) is a human molecule. *Refers to the primers used in the initial amplification during RT-PCR.

ogous to either Sek (11), Nuk (15), or Eck (21)—members of the Eph subfamily previously isolated from murine sources. When the 2.1-kb product was cloned, five recombinants containing sequences of this subfamily were identified. Four of these showed high levels of homology with either murine Eck or Mek4 (8), but one clone (35C15) contained 1602 bp of sequence which appeared novel after comparative databank analysis (GenBank and GenBank Cumulative Updates, November 1995). The novel molecule was termed embryonic stem cell kinase or Esk.

Sequence and Structural Features of Esk. The sequence of the partial Esk cDNA is shown in Fig. 2. Its shortfall of about 500 bp from the expected length of 2.1 kb is due to a 5'-end deletion, which presumably occurred during cloning. The deduced amino acid sequence of Esk was obtained by using an open reading frame spanning the entire cDNA fragment. This encoded a sequence of 533 amino acids (Fig. 2). Sequence homology strongly suggests that Esk is a new Eph-subfamily member. Its closest relative is the human kinase Eph, which displays 83.0% identity in its nucleotide sequence and 78.8% identity at the amino acid level. Eck is the closest murine relative, showing 44.9% amino acid identity. An alignment of the peptide sequences of Esk, Eph, and Eck is shown in Fig. 3. Included in the Esk sequence is a group of hydrophobic residues (amino acids 269–289) which form a putative transmembrane domain, dividing the molecule into extracellular and intracellular portions. Two fibronectin type III repeats are arranged in series in the C-terminal part of the extracellular domain. Similar repeats are found in all other Eph subfamily molecules (4, 10, 18). Also highly conserved in this group is a cysteine-rich box (6, 18) in the N-terminal region. All of the expected cysteine residues were encoded by the 35C15 sequence, except for the anticipated cysteine at position 104, which was replaced by an arginine. Since 35C15 was cloned after a total of 60 cycles of amplification using *Taq* polymerase,

a small number of base misincorporations would be expected. To check whether this was responsible, cDNA was reverse transcribed from ES cell poly(A)⁺ RNA and subjected to 35 cycles of PCR using *Taq* polymerase and two Esk-specific primers 519 bp apart. A product of the expected size was amplified and directly sequenced with the PCR primers. Unambiguous sequence data were obtained over a region corresponding to bases 45–397 of clone 35C15, and this contained four base differences compared with the cloned PCR fragment. The differences included a thymine instead of a cytosine at base 311, which would result in a cysteine at residue 104. All analyses and figures in this report employ the bases observed by direct sequencing of PCR product where they are different from those in clone 35C15.

Several features of the deduced peptide sequence of Esk imply protein-tyrosine kinase activity. The putative intracellular domain contains a kinase consensus region, beginning at residue 343 (32). This includes the presumed ATP-binding-site motif Gly-Xaa-Gly-Xaa-Xaa-Gly at residues 352–357 and a lysine at position 377, thought to be involved in the phosphotransfer reaction and highly conserved among protein-tyrosine kinases (32). However, the partial cDNA sequence ends before a complete catalytic domain is encoded. Esk also displays the motifs Asp-Leu-Ala-Ala-Arg-Asn (positions 470–475) and Pro-Ile-Arg-Trp-Thr-Ala-Pro (positions 510–516), which indicate substrate specificity for tyrosine (32). However, the latter sequence is followed by a conserved glutamate in other protein-tyrosine kinases, while in Esk this residue is a glycine. This could indicate another PCR artifact. Finally, the tyrosine residue at position 502 is a potential autophosphorylation site.

Esk Expression. Northern analysis revealed expression of a 4.2-kb Esk transcript in day 12 mouse embryo and adult mouse thymus, liver, kidney, lung, and placenta (Fig. 4). Faint bands at ≈6.0 kb observed in the liver, kidney, and lung samples may be due to alternatively spliced transcripts, although weak

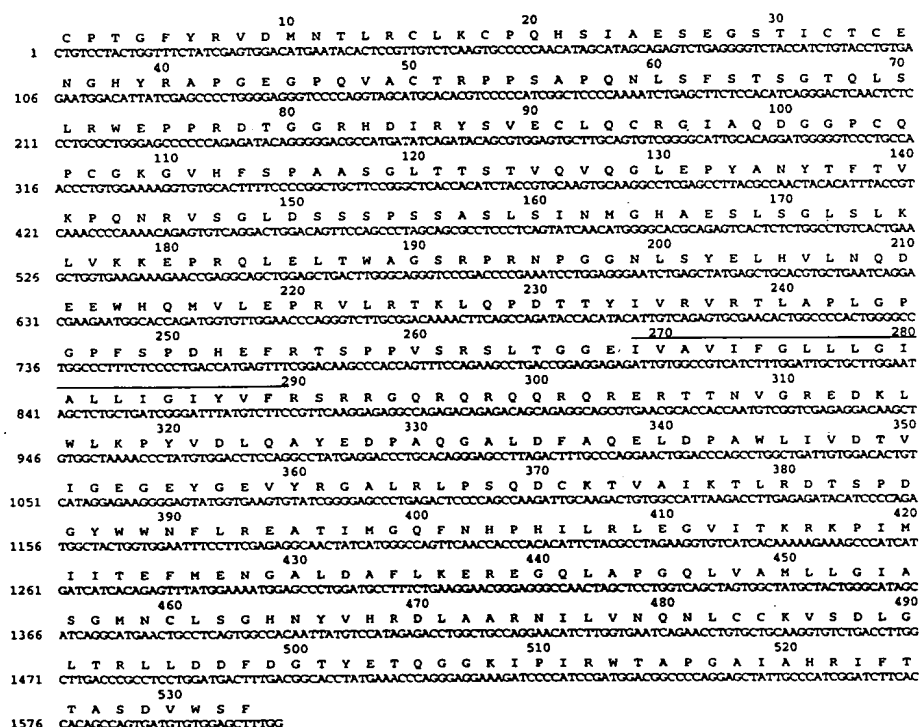


Fig. 2. Partial nucleotide and deduced amino acid sequences of Esk. Nucleotides are numbered down the left side of the figure; amino acids are numbered above the peptide sequence. The putative transmembrane domain is overlined. Clone 35C15 showed the following differences when compared with directly sequenced PCR product over nucleotides 45–397: nt 86 = C, aa 29 = Pro; nt 232 = G, aa 77 = Arg (unchanged); nt 254 = G, aa 85 = Val; nt 311 = C, aa 104 = Arg.

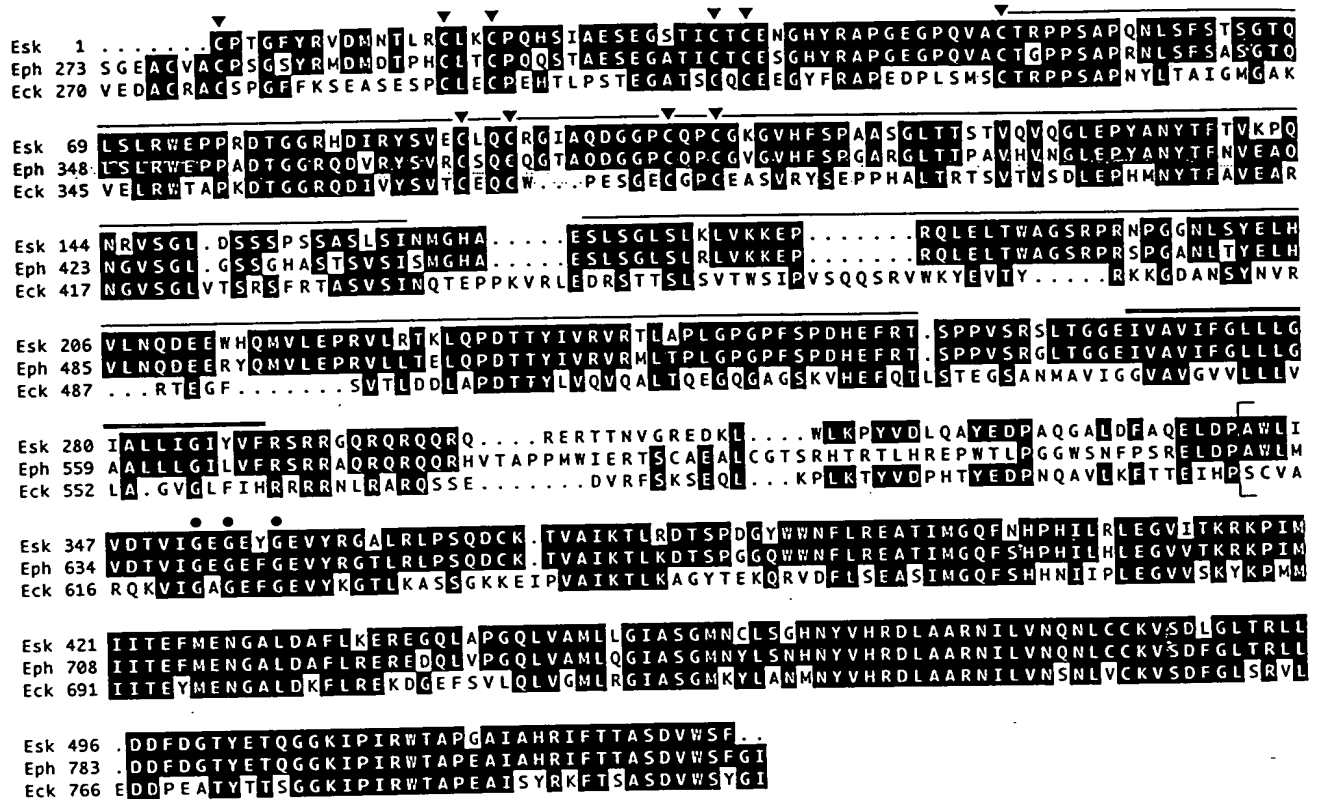


FIG. 3. Peptide sequence of Esk aligned with two close homologues, Eph and Eck. Conserved cysteine residues are marked with arrowheads. The fibronectin type III repeats are indicated with a single overline and the transmembrane domain with a double overline. The bracket shows the beginning of the catalytic domain, and the ATP-binding motif is marked with dots.

hybridization to related molecules cannot be excluded. No signal was detected from lymph node, spleen, heart, brain, or skeletal muscle.

Comparative Expression of Esk, Mek4, and Eck in ES Cells and Embryoid Bodies. To determine whether expression of Eph-subfamily molecules occurred in ES cells at a significant level and to investigate potential changes in expression as ES cells differentiated *in vitro*, a Northern blot containing ES cell and embryoid body RNA was sequentially hybridized to Esk, Mek4, and Eck probes. Embryonic fibroblast RNA was included as a control on this blot, because some fibroblast

contamination of the ES cell and embryoid body samples could not be excluded. As shown in Fig. 5, the Esk probe hybridized to all three samples, approximately in proportion to the amount of RNA present. This indicates significant levels of Esk expression in ES cells and embryoid bodies and could not be accounted for by fibroblast contamination alone. In contrast, expression of Mek4 was barely detectable in the ES cell

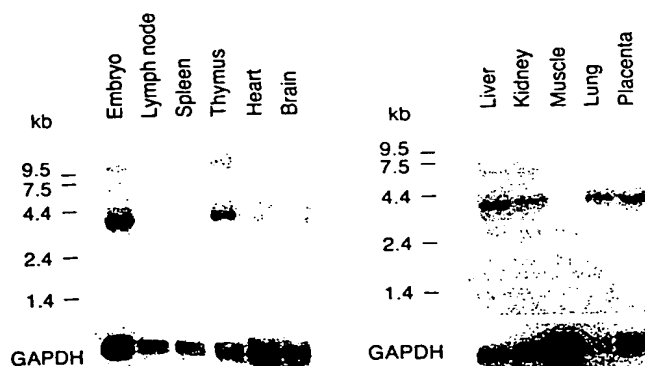


FIG. 4. Expression of Esk. Northern blots were prepared with poly(A)⁺ RNA (5 µg per lane) extracted from day 12 mouse embryo and the adult mouse tissues shown. Hybridization was performed in turn to a ³²P-labeled probe derived from clone 35C15 and a GAPDH probe. The positions of RNA size markers are indicated to the left of

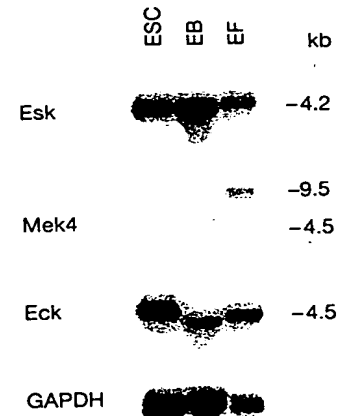


FIG. 5. Comparative expression of Esk, Mek4, and Eck during *in vitro* differentiation of ES cells. Cultures of ES cells were induced to differentiate into embryoid bodies by the withdrawal of LIF 11 days prior to harvesting. The Northern blot was prepared with poly(A)⁺ RNA (5 µg per lane) extracted from undifferentiated ES cells (ESC), embryoid bodies (EB), and embryonic fibroblasts (EF). ³²P-labeled probes synthesized from Esk, Mek4, Eck, and GAPDH were then sequentially hybridized to the membrane. The sizes of transcripts are

cultures. A 9.5-kb Mek4 transcript was expressed by the embryonic fibroblasts, however, suggesting that the faint bands seen in the ES cell lane may be due to contaminating fibroblast RNA. Finally, the Eck probe hybridized to all three samples, but expression was relatively greater in the undifferentiated ES cells. Transcripts were of slightly different sizes in the different lanes.

DISCUSSION

Nine Eph-subfamily cDNA clones were isolated from ES cells by use of RT-PCR with degenerate primers specific for this subfamily (Table 1). Of these, eight showed >97% homology to one of four previously reported molecules (Sek, Nuk, Eck, and Mek4). Given that clones were isolated after 60–70 amplification cycles using *Taq* polymerase, PCR artifacts are a likely reason for the less than complete identity with published sequences. In support of this, when sequence from Esk obtained by direct sequencing of PCR product was compared with clone 35C15, a misincorporation rate of 4/353 bases (1.1%) was observed in the latter. However, it remains possible that clones amplified from the catalytic domain with primers P2 and P4 could be derived from novel RTKs. This region is highly conserved within the Eph subfamily and may be close to identical in molecules which have markedly divergent sequence elsewhere (13).

A novel molecule, Esk, was also identified in ES cells. The deduced peptide sequence of Esk contains the conserved cysteine residues and fibronectin type III repeats characteristic of the Eph subfamily. It also shows typical protein-tyrosine kinase catalytic domain motifs. These findings define Esk as a member of the Eph subfamily of RTKs. Esk most closely resembles the human kinase Eph, with an overall amino acid sequence identity of 78.8%. When the most disparate region of Esk (residues 302–338) is excluded, the identity is 85.7%. However, this remains less than the similarity between other Eph-subfamily molecules considered to be interspecies homologues. For example, Mek4 shows 95.5% amino acid sequence identity to Hek, and murine Eck is 92% identical to its human homologue (21). Although a definitive answer awaits further data, it appears that Esk may not be the murine homologue of Eph.

Northern analysis of Esk revealed strong expression in ES cells, embryoid bodies, and day 12 embryo, suggesting that Esk, like other Eph-related kinases, has a role in development. Expression was also observed in adult mouse thymus, liver, kidney, and lung, which implies ongoing roles in these tissues. In contrast to the situation for the majority of its subfamily, Esk transcripts were not observed in adult brain. Eph and Eck show a similar propensity for expression in epithelial tissues and, together with Esk, may form a subgroup within the Eph subfamily.

When expression of two other Eph-related molecules in the ES cell cultures was investigated, contrasting patterns were observed. Mek4 demonstrated no significant expression by Northern analysis, while Eck was preferentially expressed by undifferentiated ES cells. These results suggest that Esk and Eck are likely to be more important than Mek4 in the *in vitro* differentiation of ES cells to embryoid bodies. A corollary is that they may also be more important in very early embryogenesis *in vivo*. The identification of Eck protein in gastrula-stage embryos (22) provides additional support for this conclusion.

While the specific functions of Eph-related RTKs in development require further study, several findings indicate involvement in signaling processes mediated by direct cell–cell contact (15, 23–26). Therefore, although stimulation of protein-tyrosine kinase activity is the final common pathway of signal transduction, this may be critically linked to the adhesive interactions of these molecules. One possibility is that the

extensive family of Eph-related proteins convey positional information between embryonic cells, which regulates their migration and differentiation. Given the oncogenic potential of some Eph-like RTKs (3, 9, 20, 27, 28), the attainment of correct position within the embryo might be communicated by signals which induce proliferation and/or prevent apoptosis. In this context, it is interesting that Esk, Eck, and Mek4 were all present in embryonic fibroblasts. Expressing multiple Eph-related molecules may permit fibroblasts to migrate into all developing tissues.

The normal functions of Eph-related proteins in adult tissues remain unclear but may be an extension of their functions in development. For example, thymocyte maturation requires direct cell–cell interactions and a specific migration pathway within the thymus (33). Eph-subfamily molecules expressed in thymus, such as Esk, are possible mediators of some of these interactions. In this context, it is interesting that Esk transcripts were not observed in lymph node and spleen, suggesting expression by thymus-specific populations such as CD4⁺CD8⁺ T-cell progenitors or thymic epithelial cells. Studies of the ligands of Eph-related RTKs, and potentially the outcome of gene targeting experiments, will be required to better define the biological function of these molecules.

We thank David Vaux, Christine Hawkins, and Steve Gerondakis for helpful discussions. We acknowledge the assistance of Vladimir Brusich with the sequence analysis and John Wilkins and Philip Vernon with the graphic artwork. This study was supported by the National Health and Medical Research Council, the Anti-Cancer Council of Victoria, and the Cooperative Research Centre for Cellular Growth Factors. J.D.L. is a National Health and Medical Research Council Postgraduate Scholar.

- Yarden, Y. & Ullrich, A. (1988) *Annu. Rev. Biochem.* 57, 443–478.
- Schlessinger, J. & Ullrich, A. (1992) *Neuron* 9, 383–391.
- Hirai, H., Maru, Y., Hagiwara, K., Nishida, J. & Takaku, F. (1987) *Science* 238, 1717–1720.
- Pasquale, E. B. (1991) *Cell Regul.* 2, 523–534.
- Letwin, K., Yee, S. P. & Pawson, T. (1988) *Oncogene* 3, 621–627.
- Lindberg, R. A. & Hunter, T. (1990) *Mol. Cell. Biol.* 10, 6316–6324.
- Chan, J. & Watt, V. M. (1991) *Oncogene* 6, 1057–1061.
- Sajjadi, F. G., Pasquale, E. B. & Subramani, S. (1991) *New Biol.* 3, 769–778.
- Boyd, A. W., Ward, L. D., Wicks, I. P., Simpson, R. J., Salvaris, E., Wilks, A., Welch, K., Loudovaris, M., Rockman, S. & Busmanis, I. (1992) *J. Biol. Chem.* 267, 3262–3267.
- Wicks, I. P., Wilkinson, D., Salvaris, E. & Boyd, A. W. (1992) *Proc. Natl. Acad. Sci. USA* 89, 1611–1615.
- Gilardi, H. P., Nieto, M. A., Frain, M., Mattei, M. G., Chestier, A., Wilkinson, D. G. & Charnay, P. (1992) *Oncogene* 7, 2499–2506.
- Sajjadi, F. G. & Pasquale, E. B. (1993) *Oncogene* 8, 1807–1813.
- Bohme, B., Holtrich, U., Wolf, G., Luzius, H., Grzeschik, K. H., Strebhardt, K. & Rubsamen, W. H. (1993) *Oncogene* 8, 2857–2862.
- Maisonpierre, P. C., Barrezaeta, N. X. & Yancopoulos, G. D. (1993) *Oncogene* 8, 3277–3288.
- Henkemeyer, M., Marengere, L. E., McGlade, J., Olivier, J. P., Conlon, R. A., Holmyard, D. P., Letwin, K. & Pawson, T. (1994) *Oncogene* 9, 1001–1014.
- Zhou, R., Copeland, T. D., Kromer, L. F. & Schulz, N. T. (1994) *J. Neurosci. Res.* 37, 129–143.
- Xu, Q., Holder, N., Patient, R. & Wilson, S. W. (1994) *Development (Cambridge, U.K.)* 120, 287–299.
- Bennett, B. D., Wang, Z., Kuang, W. J., Wang, A., Groopman, J. E., Goeddel, D. V. & Scadden, D. T. (1994) *J. Biol. Chem.* 269, 14211–14218.
- Winning, R. S. & Sargent, T. D. (1994) *Mech. Dev.* 46, 219–229.
- Andres, A. C., Reid, H. H., Zurcher, G., Blaschke, R. J., Albrecht, D. & Ziemiecki, A. (1994) *Oncogene* 9, 1461–1467.
- Ganju, P., Shigemoto, K., Brennan, J., Entwistle, A. & Reith, A. D. (1994) *Oncogene* 9, 1613–1624.
- Ruiz, J. C. & Robertson, E. J. (1994) *Mech. Dev.* 46, 87–100.

23. Bartley, T. D., Hunt, R. W., Welcher, A. A., Boyle, W. J., Parker, V. P., Lindberg, R. A., Lu, H. S., Colombero, A. M., Elliott, R. L., Guthrie, B. A., Holst, P. L., Skrine, J. D., Toso, R. J., Zhang, M., Fernandez, E., Trail, G., Varnum, B., Yarden, Y., Hunter, T. & Fox, G. M. (1994) *Nature (London)* 368, 558-560.
24. Beckmann, M. P., Cerretti, D. P., Baum, P., Vanden, B. T., James, L., Farrah, T., Kozlosky, C., Hollingsworth, T., Shilling, H., Maraskovsky, E., Fletcher, F. A., Lhotak, V., Pawson, T. & Lyman, S. D. (1994) *EMBO J.* 13, 3757-3762.
25. Cheng, H. J. & Flanagan, J. G. (1994) *Cell* 79, 157-168.
26. Shao, H., Lou, L., Pandey, A., Pasquale, E. B. & Dixit, V. M. (1994) *J. Biol. Chem.* 269, 26606-26609.
27. Kiyokawa, E., Takai, S., Tanaka, M., Iwase, T., Suzuki, M., Xiang, Y. Y., Naito, Y., Yamada, K., Sugimura, H. & Kino, (1994) *Cancer Res.* 54, 3645-3650.
28. Maru, Y., Hirai, H. & Takaku, F. (1990) *Oncogene* 5, 445-449.
29. Abbondanzo, S. J., Gadi, I. & Stewart, C. L. (1993) *Meth. Enzymol.* 225, 803-823.
30. Keller, G., Kennedy, M., Papayannopoulou, T. & Wiles, M. (1993) *Mol. Cell. Biol.* 13, 473-486.
31. Chomczynski, P. & Sacchi, N. (1987) *Anal. Biochem.* 162, 156-159.
32. Hanks, S. K., Quinn, A. M. & Hunter, T. (1988) *Science* 241, 42-46.
33. Anderson, G. & Jenkinson, E. J. (1995) *Semin. Immunol.* 177-183.

Isolation and Characterization of Dek, a *Drosophila* Eph Receptor Protein Tyrosine Kinase

Audra L. Scully,^{*,1} Mike McKeown,[†] and John B. Thomas^{*,2}

^{*}Molecular Neurobiology Laboratory, and [†]Molecular Biology and Virology Laboratory,
The Salk Institute, P.O. Box 85800, San Diego, California 92186

Copied by uni. of Qld Library

Herston Medical Library for Supply

under S.50 of Copyright Act 1968

22 FEB 2000

We have isolated a *Drosophila* receptor protein tyrosine kinase (RTK) of the Eph subfamily. Dek, for *Drosophila* Eph kinase, possesses all the domains characteristic of the Eph subfamily of RTKs and is equally similar in sequence to both the EphA and the EphB subclasses. Antibody staining and promoter fusions to axon-targeted reporters reveal that Dek is expressed by a large subset of developing embryonic interneurons and is targeted to their axons and growth cones at the time of axon pathfinding. Dek is also expressed by photoreceptor cells of third-instar larvae as they project axons into the optic brain lobe. Misexpression and overexpression of full-length Dek or kinase-inactive Dek do not grossly affect axon pathfinding.

INTRODUCTION

The Eph receptors comprise the largest subfamily of receptor tyrosine kinases and have been implicated in pattern formation, cell migration, and axon pathfinding (for review see Brückner and Klein, 1998; Drescher, 1997; Drescher *et al.*, 1997; Holland *et al.*, 1998). Over 15 distinct Eph receptors and 8 of their ligands, the ephrins, have been identified to date. Members of the Eph subfamily are characterized by their extracellular structure consisting of a globular domain, a cysteine-rich region unrelated to those of other receptor protein tyrosine kinases (RTKs), and two fibronectin (FN) type III repeats. The cytoplasmic structure of Eph receptors contains conserved catalytic domains and a unique sterile alpha motif (SAM) domain which is thought to be involved in binding SH2 proteins and is not found in

other RTKs (Ponting, 1995; Schultz *et al.*, 1997; Stein *et al.*, 1998a). The subfamily is divided into two classes, EphA and EphB, based upon the amino acid sequence homology of their extracellular domains. Ligands of the Ephrin-A subclass are attached to the membrane via a glycosylphosphatidylinositol linkage, while the Ephrin-B ligands span the membrane via a transmembrane domain.

Genetic analyses of Eph receptors demonstrate their involvement in establishing axon pathways in the developing nervous system. Null mutations of murine EphA8 (Park *et al.*, 1997), EphB2 (Henkemeyer *et al.*, 1996) and EphB3 (Orioli *et al.*, 1996), and EphA4 (Dottori *et al.*, 1998) have revealed mild axon pathfinding and fasciculation defects. The only identified *Caenorhabditis elegans* Eph receptor, VAB-1, has been suggested to have a role in axonal outgrowth and fasciculation (George *et al.*, 1998).

We report here the isolation and characterization of Dek, the first identified Eph receptor tyrosine kinase in *Drosophila*. Dek possesses all the conserved domains of the Eph RTKs and shares equal homology to both the EphA and the EphB receptor subclasses. Dek is expressed on the growth cones and axons of embryonic interneurons and larval photoreceptor cells. We show that over- and misexpression of Dek or kinase-inactive Dek do not grossly alter axon pathfinding.

RESULTS

Isolation of the *Drosophila* dek Gene

To isolate novel *Drosophila* RTKs, we screened an adult cDNA library by polymerase chain reaction (PCR) using degenerate primers (Lai and Lemke, 1991) corresponding to amino acid sequences HRDLAARN and DVWSYGV within the conserved catalytic domain (Fig.

¹ Present address: Department of Cell Biology, The Scripps Research Institute, 10550 N. Torrey Pines Road, La Jolla, CA 92037.

² To whom correspondence should be addressed. Fax: (619) 450-2172. E-mail: jthomas@salk.edu.

1A). Several novel partial cDNAs were isolated (see Experimental Methods). Amino acid comparison of the open reading frame (ORF) of one of these clones to known RTKs revealed homology to the vertebrate Eph subfamily. We next isolated the corresponding full-length 4.1-kb cDNA and found it to encode a novel fly Eph family member that we have named Dek for *Drosophila* Eph kinase. We mapped the *dek* gene by *in situ* hybridization to polytene chromosome band 102C6, a region of the genome for which there are no deficiencies.

Like other members of the family, the predicted Dek protein possesses a single globular domain, a cysteine-rich region, and two FN type III repeats in the extracellular domain, as well as a putative transmembrane domain and conserved catalytic region (Fig. 1B). Dek also contains a conserved stretch of amino acids in the juxtamembrane region that includes two tyrosine residues known to be major sites of autophosphorylation in vertebrate Eph receptors and which appear to interact with SH2-containing proteins (Ellis *et al.*, 1996; Holland *et al.*, 1997; Stein *et al.*, 1998a; Zisch *et al.*, 1998). The cytoplasmic region of Dek contains the conserved SAM domain (Ponting, 1995) found in all vertebrate Eph receptors (Fig. 1B). A conserved tyrosine present in the SAM domain of EphB1, also conserved in Dek, has been shown to be required for the interaction of EphB1 with the adapter protein Grb10 and the low-molecular-weight protein tyrosine phosphatase (LMW-PTP; Stein *et al.*, 1996; Stein *et al.*, 1998b). The last three residues of Dek, T-I-I, follow immediately after the SAM domain (Fig. 1A). This sequence fits the consensus motif of S/T-X-V/I that binds one group of PDZ domains (Doyle *et al.*, 1996). Many PDZ-domain-containing proteins have been shown to be involved with clustering or localization of membrane proteins (Sheng, 1996), while some allow for the assembly of signaling complexes (Tsunoda *et al.*, 1997).

The Eph subfamily is classified into two groups, EphA and EphB, based upon amino acid similarity within the extracellular domain. The extracellular portion of Dek from the globular domain through the FN

type III repeats shows 32 and 35% identity to EphA3 and EphB2, respectively, and the cytoplasmic region spanning the catalytic domain shows an equal 71% identity to both EphA3 and EphB2 (Fig. 1B). Thus, Dek cannot readily be placed in either the A or the B Eph subclass based on amino acid similarity.

Dek Is Expressed in the Embryonic Central Nervous System (CNS)

In situ hybridization to whole-mount embryos revealed that *dek* transcripts are present in precellular blastoderm stage embryos (Fig. 2A), as well as in unfertilized eggs (data not shown), demonstrating that *dek* RNA is maternally supplied. A higher concentration of *dek* transcripts is evident in the posterior pole of the embryo. In the embryo zygotic transcription of *dek* is confined to the nervous system. Expression commences in a large subset of neurons within the brain and ventral nerve cord (VNC) at stage 13 when neurons begin elongating axons (Figs. 2C and 2D; Fig. 3A). *dek* continues to be expressed in the larval CNS and imaginal discs, as well as pupal and adult stages as assayed by Northern blot analysis (data not shown).

To further define which neurons express Dek, we generated antibodies to the cytoplasmic portion of the Dek protein (see Experimental Methods). Immunostaining with an affinity-purified mouse antibody revealed that Dek is highly targeted to axons and growth cones of developing neurons within the VNC (Fig. 3B). Highest levels are present on axons within the connectives; lower levels are detectable in the commissures. Based upon the numbers and morphology of the staining axons, Dek is expressed by a large subset of interneurons and does not appear to be expressed by motor neurons.

Analysis of the *dek* Gene Structure

To further establish the identity of the *dek*-expressing neurons, we generated transgenic lines carrying the *dek*

FIG. 1. Alignment of Dek with EphA and EphB receptors. (A) Amino acid alignment of the cytoplasmic portions of Dek to the murine EphA3 and EphB2 receptors, corresponding respectively to amino acids 700–1080, 596–983, and 573–963. Identical amino acids are shaded in black. Conserved tyrosine residues in the juxtamembrane region are marked with arrowheads. The highly conserved RTK catalytic subdomains are present in Dek. Shaded in gray are subdomains I, the critical lysine of II, the catalytic loop of VIb, and subdomain IX (van der Geer *et al.*, 1994). The boundaries of the SAM domain are bracketed and Dek amino acids matching the SAM domain consensus are marked by an asterisk (*). (B) Schematic diagram comparing Dek to mouse Eph receptors EphA3 and EphB2. Alignment of the globular domain through the FN type III repeats reveals 32 and 37% identity to Dek, respectively, while the catalytic domains are both 71% identical to Dek. The transmembrane domain is represented by a double line (=). Sequence of mouse Eph receptors EphA3/Mek4 and EphB2/Nuk was obtained using GenBank Nos. M68513 and L25890, respectively.

A

```

Y      Y
YVDPHTYEDPNOATREFAREIDANYITIEAIGGGGEGFDVCRGRLKIPPN Dek
YVDPHTYEDPTDAVHEFAKELDATNISLQKVVGAGEGFEVCSGRLKLEPK EphA3
YLDPTTYEDPNEAVREFAKEIDITSCVKIEQVIGAGEGFEVCSGRLKLEPK EphB2

FVQDIDVAIKTLKPSSEKARCOFLTEASIMQOFDHPNVIYLGQVVTNRN Dek
--KEISVAIKTLKVSYTEKORROFLGEASIMQOFDHPNIIIRLEGVVTNRN EphA3
--REIFVAIKTLKVSYTEKORROFLGEASIMQOFDHPNVIHLEGVVTNRN EphB2

PVMIIITEYMENGSLDSELRVNDGKFQTLQILVHLRGIASGNSYLSDMNYV Dek
PEMIVTEYMENGSLDSELRKHDAQFTVIQLVGHLRGIASGMKYLSDMGIV EphA3
PVMIIITEYMENGSLDSELRONDGQFTVIQLVGHLRGIAAGMKYLADMNYV EphB2

HRDLAARNVLVNAQELCKIAQFGLSREIENASDA--Y--TTRGGKIPVNRW Dek
HRDLAARNVLVNSNVCKVSDFGLSRVLEDDPEAA--Y--TTRGGKIPVNRW EphA3
HRDLAARNVLVNSNVCKVSDFGLSRVLEDDTSDPTYTSALSGKIPVNRW EphB2

APEAIAFRKETSASDVWSYGVVLWEVMSYGERPYWNWSNODVIKSIKGV Dek
SPEAMSYRKETSASDVWSYGVVLWEVMSYGERPYWQMSNODVIKAVDERI EphA3
APEAIOYRKETSASDVWSYGVVLWEVMSYGERPYWDMTNODVINALEQDY EphB2

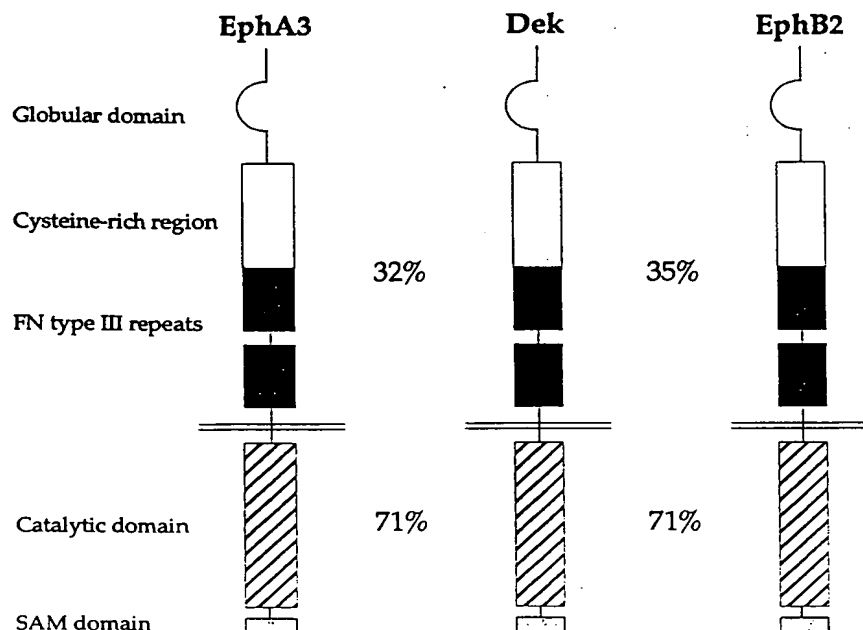
RLPAPMDCPEALYQLMLDCWOKORTHRPTFASIVSTLDNEARQPSLETT Dek
RLPAPMDCPEALYQLMLDCWOKORNNRPKEQIVSILDKELRNPGSLKII EphA3
RLPAPMDCPEALYQLMLDCWOKORNNRPKEQIVNLDKMLRNPNLSIKAM EphB2

RESPESDGHILDGQGGQ-NIEISDLVLEHKKSRICHHEKEANLINAQ Dek
TSAAARPSILLDQSNVDIATFHTIGDNLNGMRTAHCKEITGVVEYSSD EphA3
AELSSGINLPLDRTIPDYTSNTVDENLEALKMGQIKESFANAGTSPD EphB2

* * * * *
QISRLTAQQLSDMSTELVGHOKKILHQAQQLD-----II Dek
TIAKISTDDMKVGVVVGQKKIISTIKALEIQ-SKNGPVPV EphA3
VVSQMMMEDILRVGVLEAGHOKKILNSIQVMRAQMNIQSVEV EphB2

```

B



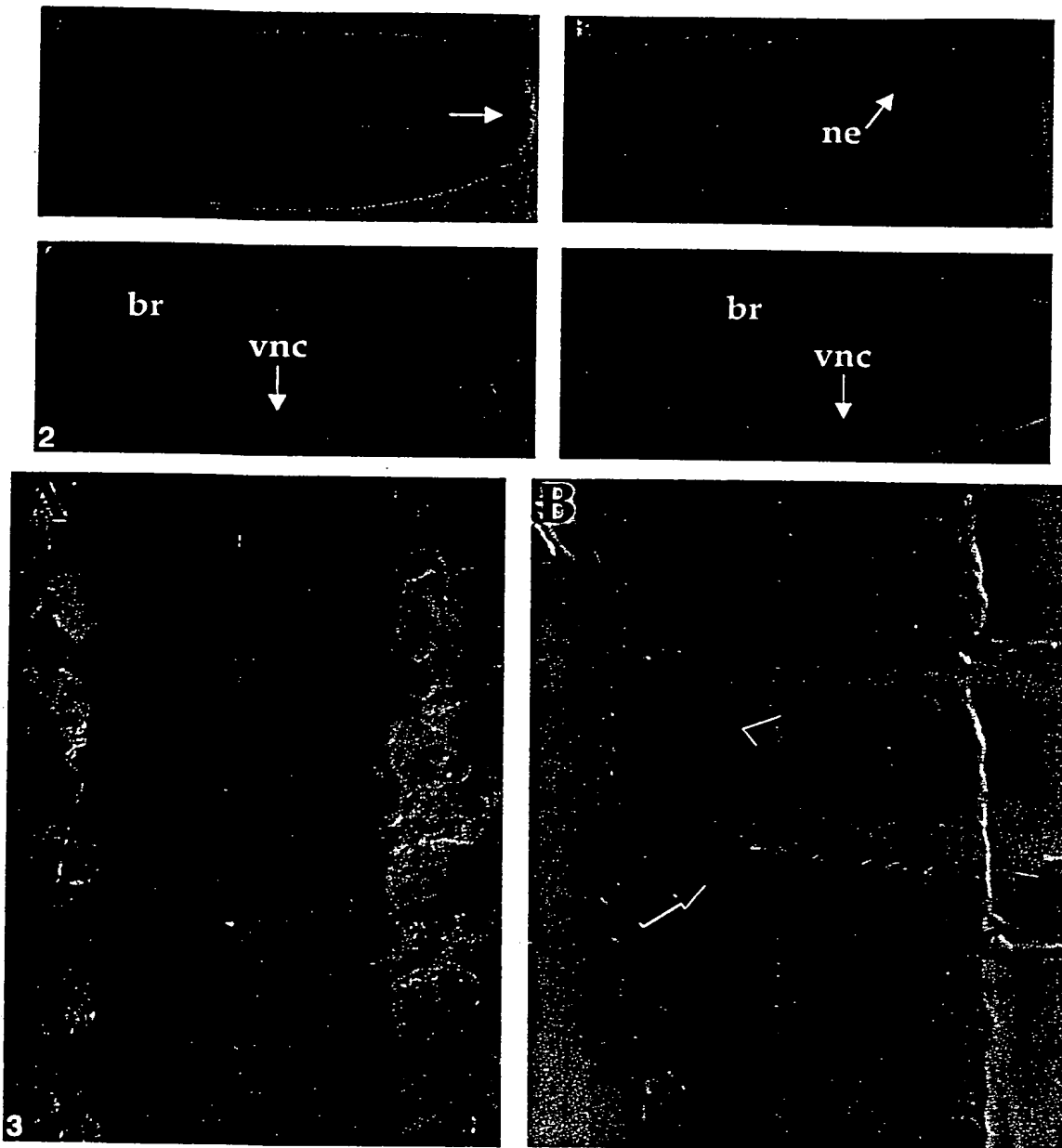


FIG. 2. Expression of *dek* during embryogenesis. Lateral view of *in situ* hybridization of *dek* to whole-mount wild-type embryos showing expression of *dek*. (A) Maternal contribution of *dek* transcripts in a stage 3 embryo. A higher concentration of *dek* transcripts is evident at the posterior pole (arrow). (B) *dek* expression is evident in the neural ectoderm (ne) of a stage 10 embryo. In stage 14 (C) and stage 17 (D) embryos, *dek* expression is confined to the nervous system, including the brain (br) and ventral nerve cord (vnc). Anterior is to the left and dorsal is up.

FIG. 3. RNA and protein expression of *dek* in the VNC. (A) Higher magnification of the VNC from *in situ* hybridization of *dek* to a stage 16 embryo (ventral view). *dek* is expressed in a large subset of neurons. (B) Dorsal view of the VNC of a dissected stage 16 embryo immunostained with affinity-purified antibodies directed against a nonconserved cytoplasmic portion of Dek. Highest levels of Dek are seen within the connectives on the axons (arrow) from a large subset of interneurons. Dek is also present on axons in the commissures (arrowhead). Anterior is up.

neural enhancer fused to an axon-targeted reporter gene. The *dek* transcription unit is composed of 10 exons spanning approximately 10 kb (Fig. 4). We tested eight genomic fragments covering 20 kb (Fig. 4) for enhancer activity by examining transgenic individuals each carrying a fragment fused to either tau(τ)-myc (Thor and Thomas, 1997) or τ -lacZ (Callahan and Thomas, 1994). As judged by reporter gene expression, genomic fragments dekD through dekH do not demonstrate any enhancer activity. Fragments dekA and dekB drive reporter gene expression in patterns completely unrelated to that of *dek* and thus appear to contain enhancers for a different gene located upstream of the *dek* locus (data not shown). In contrast, dekC, a 5.5-kb fragment located 2.2 kb upstream of the putative transcriptional start site of *dek*, contains the *dek* neural enhancer. In *dekC*- τ -lacZ embryos, τ - β -gal expression closely resembles the pattern of Dek expression and is confined to a large subset of interneurons that project axons in the commissures and connectives of the VNC (Fig. 5A). Similar to the antibody result, we could detect no reporter expression in motor neurons. dekC also drives expression of τ - β -gal in third-instar larval photoreceptor cells and their axon projections into the optic brain lobes (Fig. 5B).

Misexpression and Overexpression of Dek Have Little Effect on Axon Pathfinding

In order to begin to address its potential role in axon pathfinding, we misexpressed Dek using the *UAS*-*GAL4*

system (Brand and Perrimon, 1993). To reliably follow the complete translation of Dek, five c-myc epitopes were added in frame to the C-terminal end of the Dek coding sequence. Transformants carrying the full-length myc-tagged *dek* construct, *UAS-dek-myc*, were initially screened for high expression levels of the c-myc epitope by crossing them to a panneuronal *GAL4* line (data not shown). Individuals carrying four copies of the highest-expressing *UAS-dek-myc* insertions were crossed to a number of *GAL4* lines that drive expression in various tissues at different developmental times and assayed for phenotypes at embryonic, larval, and adult stages (Table 1 and data not shown). Immunostaining with anti-Dek and anti-myc antibodies revealed that Dek-myc is expressed at high levels when crossed to these *GAL4* lines and the protein is targeted to axons and growth cones in a manner indistinguishable from endogenous Dek protein (Figs. 6A and 6B). The axonal targeting of Dek-myc allowed us to examine subsets of neurons and their processes without an additional τ -based axon-targeted reporter. Despite our observation that Dek-myc protein is being expressed at robust levels, misexpression in motor neurons or overexpression in interneurons of Dek-myc protein does not appear to generate a phenotype in any of our *GAL4* assays (Figs. 6A and B; Table 1).

The SAM domain, as well as the terminal PDZ binding motif, may have biological functions in Dek (Hock *et al.*, 1998; Stein *et al.*, 1996; Stein *et al.*, 1998b) and may be disrupted by the addition of the c-myc epitopes. We thus tested a full-length version of Dek without an

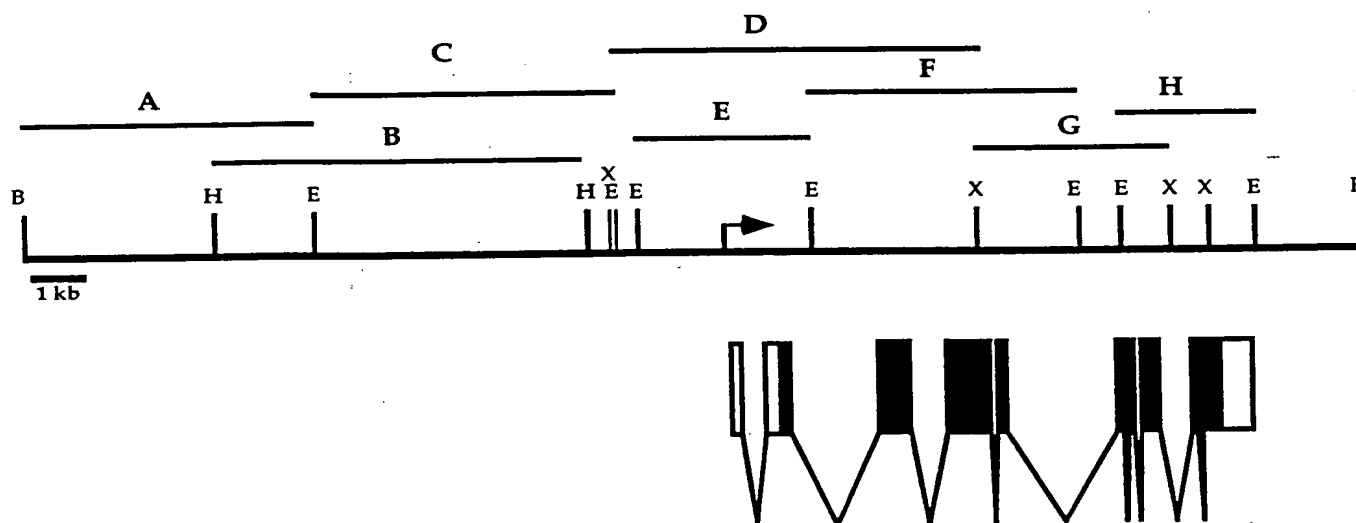


FIG. 4. Genomic organization of the *dek* gene. The *dek* gene consists of 10 exons. Coding region is shaded in black. The arrow denotes the putative transcriptional start site. Fragments A–H were tested for enhancer activity using the τ -myc (Thor and Thomas, 1997) or τ - β -gal reporters (Callahan and Thomas, 1994). Restriction sites for *Bam*HI (B), *Hind*III (H), *Eco*RI (E), and *Xba*I (X) are shown.

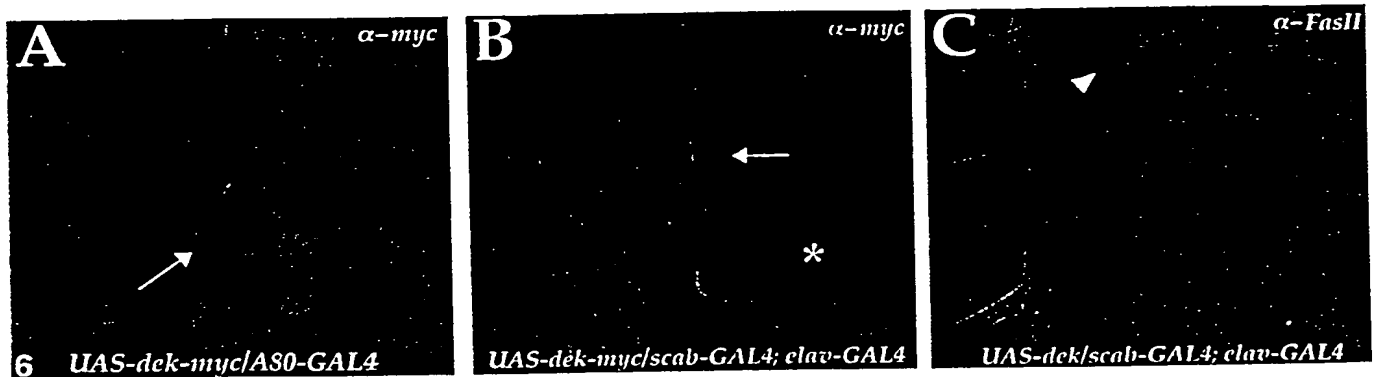
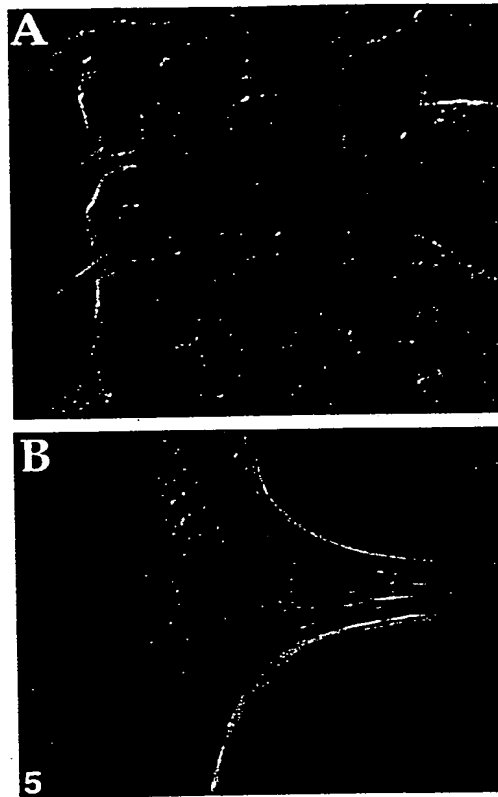


FIG. 5. *dek* promoter fusion to τ -*lacZ* reporter. Immunostainings for τ - β -gal in embryos and larvae carrying the *dekC*- τ -*lacZ* transgene. (A) Staining of a dissected stage 15 embryo labels a large subset of axons within the VNC. Anterior is up. (B) Larval eye disc staining shows expression of τ - β -gal in photoreceptor cells and on axon tracts from the eye disc to the optic lobe. Anterior is to the left.

FIG. 6. Analysis of GAL4-driven expression of Dek-myc and Dek in the nervous system. Anti-myc immunostaining of dissected stage 16 embryos carrying four copies of *UAS-dek-myc* in trans to (A) *A80-GAL4* and (B) *sca-GAL4; elav-GAL4*. Dek-myc is efficiently targeted to axons (arrows). The white asterisk marks the intersegmental and segmental nerves containing motor axons expressing Dek-myc. (C) Anti-FasII (FasII) immunostaining of a dissected stage 15 embryo with two copies of *UAS-dek* in trans to *sca-GAL4; elav-GAL4*. Overall structure of the FasII bundles is normal, although occasional defasciculation is observed (arrowhead).

TABLE 1

Over- and Misexpression of Dek, Dek-myc, and Dek-K759M-myc in the Developing Nervous System

GAL4 line ^a	GAL4-driven expression pattern	UAS construct tested ^b	Phenotypic analysis
<i>elav</i> ^{C155}	All postmitotic neurons	<i>dek-myc; dek-K759M-myc</i>	c
<i>sca</i>	All neuronal precursor cells	<i>dek-myc; dek-K759M-myc; dek</i>	c
<i>elav</i>	All postmitotic neurons	<i>dek-myc; dek-K759M-myc; dek</i>	c
<i>sca; elav</i>	As described above	<i>dek-myc; dek-K759M-myc; dek</i>	c,d
<i>ftz_{ng}-20</i>	Subset of GMCs and their progeny	<i>dek-myc; dek-K759M-myc; dek</i>	c,d
<i>A80</i>	Subset of midline neurons and glia	<i>dek-myc; dek-K759M-myc</i>	c,d
<i>GMR</i>	Photoreceptor cells	<i>dek-myc; dek-K759M-myc; dek</i>	c,e

^a See Experimental Methods for references of GAL4 lines.^b *UAS-dek-myc* and *UAS-dek-K759M-myc* were tested with four copies in *trans* to different GAL4 lines expressing in neural tissue. Several independent single insertions of *UAS-dek* as well as double insertions were also tested with GAL4-expressing lines.^c All crosses were scored for viability and general motor coordination as well as the morphology of adult wings, bristles, and eyes. Extra macrochaete on the scutellum were observed in flies with *UAS-dek* in combination with *sca-GAL4*; however, this phenotype is not specific to Dek overexpression, since the same phenotype was also observed in flies with *UAS-derailed*, and RTK, in *trans* to *sca-GAL4*.^d Interneuron and/or motor neuron axon morphology of dissected embryos immunostained with α -myc or α -Fasciclin II.^e Axon projections into lamina and medulla.

epitope tag. As with Dek-myc, *UAS-dek* individuals over- and misexpressing Dek with the panel of GAL4 drivers were viable and appeared normal. The non-myc-tagged Dek does not grossly affect axon pathfinding in the VNC, although axon fascicles appeared somewhat defasciculated when *UAS-dek* was driven by *scabrous* (*sca*)-GAL4 plus *elav*-GAL4 (Fig. 6C). This *sca*-GAL4; *elav*-GAL4 combination initiates GAL4 expression at the neuroblast stage and continues its expression in postmitotic neurons throughout the CNS (Klaes *et al.*, 1994; Luo *et al.*, 1994). Overexpression of Dek with *pGMR*-GAL4, which drives expression in the photoreceptor cells of the larval eye disc (Hay *et al.*, 1994), does not affect axon pathfinding in the developing visual system (Table 1). These results indicate that altering the levels or patterns of Dek in the CNS by ectopic expression has little effect on axon pathfinding.

We attempted to alter the normal function of endogenous Dek by expressing a kinase-inactive form of the protein containing the critical lysine (K759) changed to

methionine. To assay expression levels, we myc-tagged the mutant derivative at the C-terminus. Flies were transformed with *UAS-dek-K759M-myc* and screened as described above for high expression levels. Individuals carrying four copies of the highest-expressing *UAS-dek-K759M-myc* insertions were crossed to a panel of GAL4 lines and assayed for phenotypes at embryonic, larval, and adult stages. Although Dek-K759M-myc protein, like Dek-myc, is being expressed at robust levels, its expression does not appear to generate a phenotype in any of the assays (Table 1 and data not shown).

DISCUSSION

Dek is the first identified *Drosophila* member of the Eph subfamily of RTKs. Given that it exhibits equal sequence similarity to both the EphA and the EphB subclasses, Dek may represent a prototypical Eph family member from which the two vertebrate subclasses evolved. The highly localized expression of Dek on axons in the developing nervous system suggests that this kinase will have a role in axon pathfinding, especially in light of the evidence from vertebrate Eph studies which have demonstrated a role for Eph RTKs in axon guidance (Dottori *et al.*, 1998; Henkemeyer *et al.*, 1996; Orioli *et al.*, 1996; Park *et al.*, 1997). Nevertheless, overexpression and misexpression of full-length Dek does not grossly perturb axon pathfinding.

Signaling via the SAM domain may be an important part of the biological function of the Eph receptors. A conserved tyrosine residue in the SAM domain at the carboxy-terminal tail appears to mediate the interaction of EphB1 with adapter protein Grb10 and the LMW-PTP (Stein *et al.*, 1996; Stein *et al.*, 1998b). Our initial *UAS-GAL4* studies used a C-terminal myc epitope tag to easily follow the transgenic expression of Dek. Since two codons separate the SAM domain and the C-terminal myc epitopes, the myc-tag may be interfering with the binding of cytoplasmic proteins necessary for proper signaling. In addition, the vertebrate Eph receptor subfamily has a conserved carboxy-terminal sequence that is suspected to be a docking site for PDZ-domain-containing proteins. Studies have shown that PDZ domains do not bind to internal sequences (Songyang *et al.*, 1997). Most recently, internalization of the PDZ motif of the EphB3 receptor prevents interaction with the PDZ domain of the ras-binding protein AF6 (Hock *et al.*, 1998). Therefore, if PDZ-domain-containing proteins do not recognize the internal T-I-I motif in Dek-myc, then potential clustering and/or signaling may not occur. To eliminate any potential

interference with Dek function, we constructed *UAS-dek*. Misexpressing this non-myc-tagged version of Dek in a wide variety of tissues and developmental times does not grossly affect the organism. In all of our *UAS-GAL4* assays Dek-myc and Dek gave similar results. In combination with *sca-GAL4*; *elav-GAL4* or *ftz_{ng}-GAL4.20*, which drive GAL4 expression in neural precursor cells and postmitotic neurons, and subsets of GMCs or their progeny, respectively, Dek does not appear to strongly perturb axon pathfinding in the embryo (Table 1; Fig. 6C; and data not shown).

There could be several reasons for the lack of phenotypes with full-length Dek. First, the level of Dek expression may not be sufficiently high to affect axon pathfinding or other putative biological functions in which Dek may be involved. Second, for misexpression in motor neurons, the Dek ligand may not be present on those cells that interact with motor neurons; therefore, the signaling cascade of Dek might not be initiated upon misexpression of Dek in those cells. Third, for overexpression in interneurons, the levels of Dek may not be critical, in contrast to systems in which disturbing gradients of Eph receptors or ephrins gives rise to pathfinding phenotypes. Finally, though less likely considering the evidence from vertebrate Eph receptor studies, the endogenous Dek receptor may not play a role in axon guidance in which case misexpression of Dek would not be expected to perturb axon pathfinding.

We also observed no overt phenotypes as a consequence of expressing Dek-K759M-myc, the kinase-inactive form of Dek. One interpretation of this result is that Dek-K759M-myc is indeed interfering with endogenous Dek function, but that Dek is involved in developmental events other than axonal guidance. Alternatively, Dek-K759M-myc might not be acting in a dominant-negative fashion. Although kinase-defective forms of growth factor receptors, such as the insulin receptor or c-kit receptor, can cause negative effects (Giebel and Spritz, 1991; Moller and Flier, 1991; Tan *et al.*, 1990), there are examples of kinase-inactive receptors that can participate in signal transduction. For example, a kinase-inactive PDGF β -receptor is able to mediate activation of the MAP kinase signaling cascade using endogenous PDGF α -receptor (Vaillancourt *et al.*, 1996). Furthermore, there is evidence that some Eph family members can retain partial function even in the absence of their kinase domains. In *Nuk^{lacZ}* homozygous mutant mice, EphB2 retains some functions required for proper axon pathfinding despite the fact that its catalytic domain is replaced with β -galactosidase (Henkemeyer *et al.*, 1996). Additionally, mutations that truncate the kinase domain of the *C. elegans* Eph receptor VAB-1

result in weak phenotypes compared to those of *vab-1*-null alleles (George *et al.*, 1998). Thus, if Dek-K759M-myc was interfering in a dominant-negative fashion with Dek function, the resulting phenotype could be mild in comparison to the null mutant phenotype.

Although studies in vertebrates have generated insight into the functions of the Eph RTK subfamily, some analyses have been hampered by the functional overlap of the many vertebrate Eph receptors. Most of the single-receptor knockouts in mice have resulted in subtle phenotypes and the mutant mice are completely viable and fertile (Dottori *et al.*, 1998; Henkemeyer *et al.*, 1996; Orioli *et al.*, 1996; Park *et al.*, 1997). Analysis of the mouse null mutation of the EphA2 receptor reveals no detectable phenotypes (Chen *et al.*, 1996). However, when both the EphB2 and the EphB3 receptors are absent, mice display a marked increase in the severity of axonal pathfinding phenotypes (Orioli *et al.*, 1996). Thus, in vertebrates redundancy has been an issue in uncovering the function of the Eph RTK subfamily and its signaling pathway(s). Analysis of Eph receptors and their ligands may be more amenable in a simpler genetic system such as *C. elegans* or *Drosophila*. Currently 14 distinct vertebrate Eph receptors have been identified, but Dek represents the only *Drosophila* Eph receptor isolated to date. A single Eph receptor, VAB-1, has been identified in the *C. elegans* genome (George *et al.*, 1998), the sequence of which is complete (Ruvkun and Hobert, 1998). Therefore, although additional *Drosophila* Eph receptors may exist, it is unlikely that this organism will have the large number of Eph receptors present in vertebrates. Further studies of Dek function in *Drosophila* employing loss-of-function mutants may produce insight into the roles of Eph receptors in the developing nervous system.

EXPERIMENTAL METHODS

cDNA Isolation

A *Drosophila* adult *tudor* female cDNA library (Stratagene) was screened by PCR using degenerate primers (Lai and Lemke, 1991) to the kinase domains HRD-LAARN and DVWS(F/Y)G(I/V) (M. McKeown, unpublished results). The generated fragments approximately 220 bp in length were subsequently cloned into pGEM3 (Promega). The fragment termed K2, which shows significant homology to the Eph RTK subfamily, was subcloned into pBluescript (Stratagene) and used to isolate a 4.1-kb full-length clone from a *Drosophila* embryonic cDNA plasmid library (Brown and Kafatos, 1988). This cDNA was sequenced on both strands using

the T7 sequencing kit (Pharmacia). The cDNA contains a long ORF, the beginning of which contains three putative methionine start codons all of which closely resemble the *Drosophila* translational start site consensus; therefore, the precise start of translation has not been determined. Arbitrarily using the first methionine of the ORF as the start codon, the encoded protein is predicted to be 1080 aa in length. Locations of the exon-intron boundaries correspond to breaks between cDNA nucleotide numbers 179–180, 630–631, 1297–1298, 2185–2186, 2362–2363, 2492–2493, 2588–2589, 2959–2960, and 3106–3107.

In Situ Hybridization

In situ hybridization of whole-mount embryos was carried out as previously described (Bourgouin *et al.*, 1992) using the *dek* cDNA to generate digoxigenin-labeled antisense RNA probes (Boehringer Mannheim). The sense (control) probe revealed no signal in the embryos.

Antibody Production

Mouse polyclonal antiserum was raised against glutathione S-transferase fusion proteins (Pharmacia) containing aa 994–1022 of the Dek intracellular domain. Mouse serum was diluted approximately 1:10 and antibodies against the intracellular portion of Dek were affinity purified on a column of Dek-maltose binding fusion protein containing aa 994–1058 of intracellular Dek created by cloning the corresponding *dek* sequence into the vector pMAL-c2 (New England Biolabs).

Immunostaining

Dek protein was detected using purified serum diluted 1:10. For the detection of τ -myc expression, monoclonal antibody (MAb) 9E10 anti-c-myc was used at 1:30 (Evan *et al.*, 1985). Rabbit anti- β -gal polyclonal antibody (Cappel) was used at 1:10,000 to detect τ - β -gal expression and MAb ID4 α -FasII was used at 1:30 (Van Vactor *et al.*, 1993). Embryo dissections and immunostainings were carried out as previously described (Callahan and Thomas, 1994; Thomas *et al.*, 1984). Primary antibody incubation was followed by a biotinylated goat anti-mouse antibody at 1:1500 (Vector Laboratories), then incubation with an avidin-biotin-horseradish peroxidase complex (Vectastain ABC Elite kit; Vector Laboratories). The figures were compiled using Adobe Photoshop.

Chromosomal in Situ

Polytene chromosomes were prepared as described (Ashburner, 1989). Chromosomal *in situ* were performed essentially as described (Wallrath and Elgin, 1995) using a *dek* digoxigenin-labeled antisense RNA probe.

Isolation of dek Genomic Clones

Genomic clones were isolated from a cosmid library (Tamkun *et al.*, 1992), and fragments spanning the *dek* locus were subcloned into pBluescript. The exon-intron structure was determined by PCR and sequencing of these cosmid fragments, as well as by Southern blot analysis of the cosmids and chromosomal DNA.

Generation of Transformants

P-element transformation was carried out as previously described (Rubin and Spradling, 1982) using *w¹¹¹⁸* as host. The *dek* genomic fragments were inserted upstream of the hsp70 minimal promoter of either the C4P τ -lacZ vector (Callahan and Thomas, 1994) or the pCaSpEr2/17 τ -myc vector (Thor and Thomas, 1997). For each genomic fragment multiple independent insertions were generated and tested for expression. Four independent *dekC*- τ -lacZ lines were examined. Three of these displayed identical expression patterns, while the fourth most likely reported on expression of a local enhancer and was discarded. Two of the three remaining insertions were placed *in cis* to each other so that a homozygous line containing four copies of *dekC*- τ -lacZ was created.

UAS-dek Constructs

UAS-*dek* constructs were made by inserting the modified *dek* cDNAs into pUAS (Brand and Perrimon, 1993) and were confirmed by sequencing across junctions and modified sites. It is possible that negative regulatory elements are present in the 5' and 3' untranslated ends of the *dek* cDNA (A.L.S. and J.B.T., unpublished results) and the three putative start methionines may cause inefficient translation of Dek protein. Therefore, for all the various UAS-*dek* constructs, nt 1–474 and 3538–4120 of the *dek* cDNA were deleted. Furthermore, nt 475–486 were replaced with a Cavener consensus start site (Cavener, 1987) placed directly in front of the putative signal sequence of *dek* (TTTCGAGAATGT changed to CAATCAAAATGG). The lysine permuted construct, UAS-*dek*-K759M-myc, is identical to UAS-*dek*-myc except

lysine 759 has been altered to a methionine (AAG changed to ATG). For *UAS-dek-myc* and *UAS-dek-K759M-myc* five c-myc epitopes from vector pCS2+MT (Turner and Weintraub, 1994) followed by two stop codons were placed in frame directly downstream of nt 3537. Independent insertions of *UAS-dek-myc* and *UAS-dek-K759M-myc* were screened by α -c-myc immunostaining to determine those with robust expression. Of these lines, those that were healthy as homozygotes were mated to each other to generate stocks with multiple copies via recombination. Two independent insertions on the second chromosome and two independent insertions on the third chromosome, generated by recombination, were then made homozygous in one fly strain. *UAS-dek* contains the native stop codon plus one additional stop codon instead of the c-myc epitopes, and fly lines containing independent single and multiple insertions on the second and third chromosomes were used.

Fly Strains and Crosses

All stocks were raised on standard cornmeal and agar medium. *UAS-GAL4* crosses were performed at 25 and 29°C. *GAL4* fly strains used were *scabrous-GAL4* (*sca-GAL4*; Klaes *et al.*, 1994); *elav-GAL4* (Luo *et al.*, 1994); *pGMR-GAL4* (Hay *et al.*, 1994); *sca-GAL4*; *elav-GAL4* (obtained from S. Thor); and *ftz_{ng}-GAL4.20*, which is the neurogenic enhancer of *fushi tarazu* driving *GAL4* (Lin and Goodman, 1994; Thor *et al.*, 1999); plus *elav^{C155}-GAL4* and *A80-GAL4* (gifts from C. S. Goodman).

ACKNOWLEDGMENTS

We are indebted to Dr. Stefan Thor for his invaluable discussions and technical advice and Dr. Andrew Zelhof for his support and stimulating discussions. We thank Phil Edeen for excellent technical assistance with the degenerate PCR screen and Dr. Sanford Madigan for initial Blast analysis of the cDNA sequences isolated in the screen. We thank the Bloomington Stock Center and Dr. C. S. Goodman for fly stocks. Special appreciation to Drs. D. van Meyel, A. Zelhof, and S. Thor for critically reading the manuscript. This work was supported by grants from the NIH to J.B.T. A.L.S. was supported in part by a predoctoral training grant from The National Institutes of Health and a Chapman Fellowship from The Salk Institute. The GenBank accession number for *dek* is AF132028.

REFERENCES

- Ashburner, M. (1989). *Drosophila: A Laboratory Manual*. Cold Spring Harbor Laboratory Press, Cold Spring Harbor, NY.
- Bourgouin, C., Lundgren, S. E., and Thomas, J. B. (1992). *apterous* is a *Drosophila* LIM domain gene required for the development of a subset of embryonic muscles. *Neuron* 9: 549–561.
- Brand, A. H., and Perrimon, N. (1993). Targeted gene expression as a means of altering cell fates and generating dominant phenotypes. *Development* 118: 401–415.
- Brown, N. H., and Kafatos, F. C. (1988). Functional cDNA libraries from *Drosophila* embryos. *J. Mol. Biol.* 203: 425–437.
- Brückner, K., and Klein, R. (1998). Signaling by Eph receptors and their ephrin ligands. *Curr. Opin. Neurobiol.* 8: 375–382.
- Callahan, C. A., and Thomas, J. B. (1994). Tau-beta-galactosidase, an axon-targeted fusion protein. *Proc. Natl. Acad. Sci. USA* 91: 5972–5976.
- Cavener, D. R. (1987). Comparison of consensus flanking translational start sites in *Drosophila* and vertebrates. *Nucleic Acids Res.* 15: 1353–1361.
- Chen, J., Nachabiah, A., Scherer, C., Ganju, P., Reith, A., Bronson, R., and Ruley, H. E. (1996). Germ-line inactivation of the murine Eck receptor tyrosine kinase by gene trap retroviral insertion. *Oncogene* 12: 979–988.
- Dottori, M., Hartley, L., Galea, M., Paxinos, G., Polizzotto, M., Kilpatrick, T., Bartlett, P. F., Murphy, M., Kontgen, F., and Boyd, A. W. (1998). EphA4 (Sek1) receptor tyrosine kinase is required for the development of the corticospinal tract. *Proc. Natl. Acad. Sci. USA* 95: 13248–13253.
- Doyle, D. A., Lee, A., Lewis, J., Kim, E., Sheng, M., and MacKinnon, R. (1996). Crystal structures of a complexed and peptide-free membrane protein-binding domain: Molecular basis of peptide recognition by PDZ. *Cell* 85: 1067–1076.
- Drescher, U. (1997). The Eph family in the patterning of neural development. *Curr. Biol.* 7: R799–807.
- Drescher, U., Bonhoeffer, F., and Muller, B. K. (1997). The Eph family in retinal axon guidance. *Curr. Opin. Neurobiol.* 7: 75–80.
- Ellis, C., Kasmi, F., Ganju, P., Walls, E., Panayotou, G., and Reith, A. D. (1996). A juxta membrane autophosphorylation site in the Eph family receptor tyrosine kinase, Sek, mediates high affinity interaction with p59fyn. *Oncogene* 12: 1727–1736.
- Evan, G. I., Lewis, G. K., Ramsay, G., and Bishop, J. M. (1985). Isolation of monoclonal antibodies specific for human c-myc proto-oncogene product. *Mol. Cell. Biol.* 5: 3610–3616.
- George, S. E., Simokat, K., Hardin, J., and Chisholm, A. D. (1998). The VAB-1 Eph receptor tyrosine kinase functions in neural and epithelial morphogenesis in *C. elegans*. *Cell* 92: 633–643.
- Giebel, L. B., and Spritz, R. A. (1991). Mutation of the KIT (mast/stem cell growth factor receptor) protooncogene in human piebaldism. *Proc. Natl. Acad. Sci. USA* 88: 8696–8699.
- Hay, B. A., Wolff, T., and Rubin, G. M. (1994). Expression of baculovirus p35 prevents cell death in *Drosophila*. *Development* 120: 2121–2129.
- Henkemeyer, M., Orioli, D., Henderson, J. T., Saxton, T. M., Roder, J., Pawson, T., and Klein, R. (1996). Nuk controls pathfinding of commissural axons in the mammalian central nervous system. *Cell* 86: 35–46.
- Hock, B., Böhme, B., Karn, T., Yamamoto, T., Kaibuchi, K., Holtrich, U., Holland, S., Pawson, T., Rübsamen-Waigmann, H., and Strebhardt, K. (1998). PDZ-domain-mediated interaction of the Eph-related receptor tyrosine kinase EphB3 and the ras-binding protein AF6 depends on the kinase activity of the receptor. *Proc. Natl. Acad. Sci. USA* 95: 9779–9784.
- Holland, S. J., Gale, N. W., Gish, G. D., Roth, R. A., Songyang, Z., Cantley, L. C., Henkemeyer, M., Yancopoulos, G. D., and Pawson, T. (1997). Juxtamembrane tyrosine residues couple the Eph family

- receptor EphB2/Nuk to specific SH2 domain proteins in neuronal cells. *EMBO J.* 16: 3877-3888.
- Holland, S. J., Peles, E., Pawson, T., and Schlessinger, J. (1998). Cell-contact-dependent signalling in axon growth and guidance: Eph receptor tyrosine kinases and receptor protein tyrosine phosphatase beta. *Curr. Opin. Neurobiol.* 8: 117-127.
- Klaes, A., Merne, T., Stollewerk, A., Scholz, H., and Klambt, C. (1994). The Ets transcription factors encoded by the Drosophila gene pointed direct glial cell differentiation in the embryonic CNS. *Cell* 78: 149-160.
- Lai, C., and Lemke, G. (1991). An extended family of protein-tyrosine kinase genes differentially expressed in the vertebrate nervous system. *Neuron* 6: 691-704.
- Lin, D. M., and Goodman, C. S. (1994). Ectopic and increased expression of Fasciclin II alters motoneuron growth cone guidance. *Neuron* 13: 507-523.
- Luo, L., Liao, Y. J., Jan, L. Y., and Jan, Y. N. (1994). Distinct morphogenetic functions of similar small GTPases: Drosophila Drac1 is involved in axonal outgrowth and myoblast fusion. *Genes Dev.* 8: 1787-1802.
- Moller, D. E., and Flier, J. S. (1991). Insulin resistance—Mechanisms, syndromes, and implications [see comments]. *N. Engl. J. Med.* 325: 938-948.
- Orioli, D., Henkemeyer, M., Lemke, G., Klein, R., and Pawson, T. (1996). Sek4 and Nuk receptors cooperate in guidance of commissural axons and in palate formation. *EMBO J.* 15: 6035-6049.
- Park, S., Frisen, J., and Barbacid, M. (1997). Aberrant axonal projections in mice lacking EphA8 (Eek) tyrosine protein kinase receptors. *EMBO J.* 16: 3106-3114.
- Ponting, C. P. (1995). SAM: A novel motif in yeast sterile and Drosophila polyhomeotic proteins. *Protein Sci.* 4: 1928-1930.
- Rubin, G. M., and Spradling, A. C. (1982). Genetic transformation of Drosophila with transposable element vectors. *Science* 218: 348-353.
- Ruvkun, G., and Hobert, O. (1998). The taxonomy of developmental control in Caenorhabditis elegans. *Science* 282: 2033-2041.
- Schultz, J., Ponting, C. P., Hofmann, K., and Bork, P. (1997). SAM as a protein interaction domain involved in developmental regulation. *Protein Sci.* 6: 249-253.
- Sheng, M. (1996). P Γ Zs and receptor/channel clustering: Rounding up the latest suspects. *Neuron* 17: 575-578.
- Songyang, Z., Fanning, A. S., Fu, C., Xu, J., Marfatia, S. M., Chishti, A. H., Crompton, A., Chan, A. C., Anderson, J. M., and Cantley, L. C. (1997). Recognition of unique carboxyl-terminal motifs by distinct PDZ domains. *Science* 275: 73-77.
- Stein, E., Cerretti, D. P., and Daniel, T. O. (1996). Ligand activation of ELK receptor tyrosine kinase promotes its association with Grb10 and Grb2 in vascular endothelial cells. *J. Biol. Chem.* 271: 23588-23593.
- Stein, E., Huynh-Do, U., Lane, A. A., Cerretti, D. P., and Daniel, T. O. (1998a). Nck recruitment to Eph receptor, EphB1/ELK, couples ligand activation to c-Jun kinase. *J. Biol. Chem.* 273: 1303-1308.
- Stein, E., Lane, A. A., Cerretti, D. P., Schoecklmann, H. O., Schroff, A. D., Van Etten, R. L., and Daniel, T. O. (1998b). Eph receptors discriminate specific ligand oligomers to determine alternative signaling complexes, attachment, and assembly responses. *Genes Dev.* 12: 667-678.
- Tamkun, J. W., Deuring, R., Scott, M. P., Kissinger, M., Pattatucci, A. M., Kaufman, T. C., and Kennison, J. A. (1992). brachy: A regulator of Drosophila homeotic genes structurally related to the yeast transcriptional activator SNF2/SWI2. *Cell* 68: 561-572.
- Tan, J. C., Nocka, K., Ray, P., Traktman, P., and Besmer, P. (1990). The dominant W42 spotting phenotype results from a missense mutation in the c-kit receptor kinase. *Science* 247: 209-212.
- Thomas, J. B., Bastiani, M. J., Bate, C. M., and Goodman, C. S. (1984). From grasshopper to Drosophila: A common plan for neuronal development. *Nature* 310: 203-207.
- Thor, S., Andersson, S. G., Tomlinson, A., and Thomas, J. B. (1999). A LIM-homeodomain combinatorial code for motor-neuron pathway selection. *Nature* 397: 76-80.
- Thor, S., and Thomas, J. B. (1997). The Drosophila islet gene governs axon pathfinding and neurotransmitter identity. *Neuron* 18: 397-409.
- Tsunoda, S., Sierralta, J., Sun, Y., Bodner, R., Suzuki, E., Becker, A., Socolich, M., and Zuker, C. S. (1997). A multivalent PDZ-domain protein assembles signaling complexes in a G-protein-coupled cascade. *Nature* 388: 243-249.
- Turner, D. L., and Weintraub, H. (1994). Expression of achaete-scute homolog 3 in Xenopus embryos converts ectodermal cells to a neural fate. *Genes Dev.* 8: 1434-1447.
- Vaillancourt, R. R., Gardner, A. M., Kazlauskas, A., and Johnson, G. L. (1996). The kinase-inactive PDGF beta-receptor mediates activation of the MAP kinase cascade via the endogenous PDGF alpha-receptor in HepG2 cells. *Oncogene* 13: 151-159.
- van der Geer, P., Hunter, T., and Lindberg, R. A. (1994). Receptor protein-tyrosine kinases and their signal transduction pathways. *Annu. Rev. Cell Biol.* 10: 251-337.
- Van Vactor, D., Sink, H., Fambrough, D., Tsou, R., and Goodman, C. S. (1993). Genes that control neuromuscular specificity in Drosophila. *Cell* 73: 1155-1164.
- Wallrath, L. L., and Elgin, S. C. (1995). Position effect variegation in Drosophila is associated with an altered chromatin structure. *Genes Dev.* 9: 1263-1277.
- Zisch, A. H., Kalo, M. S., Chong, L. D., and Pasquale, E. B. (1998). Complex formation between EphB2 and Src requires phosphorylation of tyrosine 611 in the EphB2 juxtamembrane region. *Oncogene* 16: 2657-2670.

Received January 14, 1999

Revised March 4, 1999

Accepted March 9, 1999

The VAB-1 Eph Receptor Tyrosine Kinase Functions in Neural and Epithelial Morphogenesis in *C. elegans*

D 11

Sean E. George,* Kristin Simokat,†
Jeff Hardin,†‡ and Andrew D. Chisholm*§

*Department of Biology
Sinsheimer Laboratories
University of California
Santa Cruz, California 95064

†Program in Cellular and Molecular Biology

‡Department of Zoology
University of Wisconsin
Madison, Wisconsin 53706

Summary

Mutations in the *C. elegans vab-1* gene disrupt the coordinated movements of cells during two periods of embryogenesis. *vab-1* mutants are defective in the movement of neuroblasts during closure of the ventral gastrulation cleft and in the movements of epidermal cells during ventral enclosure of the embryo by the epidermis. We show that *vab-1* encodes a receptor tyrosine kinase of the Eph family. Disruption of the kinase domain of VAB-1 causes weak mutant phenotypes, indicating that VAB-1 may have both kinase-dependent and kinase-independent activities. VAB-1 is expressed in neurons during epidermal enclosure and is required in these cells for normal epidermal morphogenesis, demonstrating that cell-cell interactions are required between neurons and epidermal cells for epidermal morphogenesis.

Introduction

The shape of an organism is determined by the morphogenetic behavior of its cells. While we know much about the process of morphogenesis at the descriptive level and from experimental embryology and biochemistry, relatively little is known of the genetic mechanisms underlying morphogenetic movements (Bard, 1992). Many common types of morphogenetic movements involve epithelia, such as invagination and spreading (epiboly). One approach to understanding the molecular mechanisms underlying such movements is to use genetic analysis to identify mutants defective in such movements. Genetic analysis in *Drosophila melanogaster* has identified cell signaling pathways required for dorsal epidermal closure (Knust, 1997), including a JNK pathway that regulates cell shape changes in the leading edge (Glise et al., 1995; Riesgo-Escovar et al., 1996; Sluss et al., 1996), and TGF β signaling pathways that may transmit signals to cells behind the leading edge. Another type of epithelial morphogenesis that has been analyzed genetically is ventral furrow invagination during *Drosophila* gastrulation. Genetic screens have identified two loci required for cell shape changes in gastrulation: the G α subunit *concertina* (*cta*) (Parks and Wieschaus, 1991) and the novel secreted protein *folded*

gastrulation (*fog*) (Costa et al., 1994). Thus, both these types of epithelial morphogenesis involve cell signaling, either via JNK and TGF β pathways in epiboly or via *cta* and *fog* pathways in invagination.

The epidermis of the nematode *Caenorhabditis elegans* is a simple system in which to analyze epithelial morphogenesis. The epidermis, also known as hypodermis, begins as a set of cells born in the dorsal part of the embryo (Sulston et al., 1983) that forms an epithelial sheet. Ventral enclosure of the embryo by the epidermis occurs in two steps (Williams-Masson et al., 1997). Four anterior epidermal cells lead the migration of the epidermis to the ventral midline by extending actin-rich filopodia over substrate neurons. Once these leading cells have reached the midline, the remainder of the ventral midline appears to be enclosed by an actin-mediated purse-string mechanism. After enclosure is complete, circumferential constriction in the epidermis squeezes the embryo longitudinally (Priess and Hirsh, 1986).

To identify genes involved in epidermal morphogenesis, we have analyzed mutants in which morphogenesis is defective. *vab-1* mutants were originally isolated by Brenner (1974) based on their morphogenetic defects in head epidermis. Here, we show that *vab-1* is also required for cell movements following gastrulation and during ventral closure of the epidermis. We show that *vab-1* encodes an Eph receptor expressed in neuroblasts and neuronal cells and that *vab-1* function in these neuronal cells is required for epidermal morphogenesis. Our results provide an example of interactions between neuronal substrate cells and a migrating epithelial sheet in morphogenesis.

Results

vab-1 Mutants are Defective in Morphogenesis

The most striking defect of *vab-1* mutant larvae is the deformation of head epidermis, the "Notched head" phenotype (Brenner, 1974; Figures 1A and 1B); epidermal morphogenesis is often also abnormal in the tail region (Figure 1B). Morphology of the body is normal in most *vab-1* mutants. The phenotypes caused by *vab-1* alleles are incompletely penetrant and variably expressed, hence the gene name *vab* (variable abnormal). The number of head epidermal cells and nuclei is normal in Notched head *vab-1* mutants, as determined by Nomarski microscopy and expression of epidermal markers (data not shown), indicating that the Notched head phenotype results specifically from abnormal morphogenesis of head epidermal syncytia (Figures 1C and 1D).

Seventeen recessive zygotic *vab-1* mutant alleles have been isolated by various workers (see Experimental Procedures). We classified *vab-1* alleles as strong, intermediate, or weak, based on the penetrance of mutant phenotypes (Table 1); most animals mutant for strong *vab-1* alleles arrest during embryogenesis due to defects in epidermal enclosure (see below), whereas weak *vab-1* mutants are almost fully viable. By genetic and molecular criteria (Tables 1 and 2), the strong *vab-1* alleles cause complete loss of function.

§To whom correspondence should be addressed.

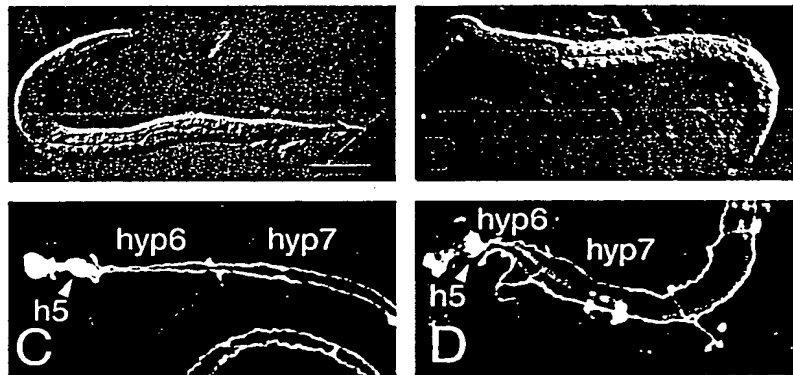


Figure 1. Morphogenetic Phenotypes of *vab-1* Mutant Larvae

(A) Wild-type first stage (L1) larva. Anterior is to the left, and dorsal is up. Bar, 20 μ m.
 (B) Abnormal Notched head and abnormal tail morphogenesis of *vab-1(e2027)* L1 larva.
 (C) Wild-type L1 larva stained with the MH27 monoclonal antibody to show junctions between epidermal cells; the head epidermal syncytia hyp5 (h5), hyp6, and hyp7 are marked.
 (D) *vab-1(dx14)* mutant L1 larva, MH27 staining, showing malformation of hyp5, hyp6, and hyp7 cells.

vab-1 Null Mutations Cause Variable Defects in Cell Movements following Gastrulation and during Embryonic Ventral Enclosure of the Epidermis

To determine the role of *vab-1* in embryonic development of the epidermis, we analyzed the embryogenesis of *vab-1* mutant embryos using conventional and four-dimensional Nomarski microscopy. We found that *vab-1* null mutant embryos are variably defective in the movements of neuroblast cells during closure of the ventral gastrulation cleft and in the migrations of epidermal cells during ventral enclosure of the epidermis. These defects in cell movements result in failure of enclosure of the embryo by epidermal cells, and such embryos arrest because internal cells leak out at the ventral midline.

The variable phenotypes of *vab-1* null mutants can be described in terms of five phenotypic classes (Figure 2 legend).

Approximately 35% of *vab-1* null mutant animals displayed defects in cell movements following gastrulation. During normal *C. elegans* gastrulation, a ventral cleft is formed by the movement of endoderm, mesoderm, and germline precursors into the interior of the embryo; this cleft is gradually closed by the short-range lateral movements of many neuroblasts (Figures 2A and 2C) (Sulston et al., 1983). In 20% of *vab-1* embryos (phenotypic classes I and II), the ventral cleft is deeper than normal and remains for longer (Figure 2E); in 15% of embryos the cleft is of normal depth and lasts longer (class III). These phenotypes appear to result from delays in the

Table 1. Strength of *vab-1* Mutations and Molecular Lesions

Allele	Embryonic Arrest	Larval Arrest	Adult, Vab	Adult, Non-Vab	Wild-Type Sequence	Mutant Sequence	Predicted Effect
Strong							
<i>e2027</i>	58.2%	31.3%	8.9%	2.5%	—	74 bp deletion removing first 7 bp of exon 5	
<i>e721</i>	58.2%	29.3%	11.4%	1.0%	ND	ND	
<i>dx14</i>	56.1%	29.6%	9.5%	4.7%	—	deletion of exon 4, part of exon 5	
<i>ju8</i>	53.3%	32.5%	13.2%	0.8%	CAA	AAA	E62K
<i>dx31</i>	50.8%	33.2%	14.0%	2.0%		deletion of exons 1–4	
<i>e1059</i>	49.9%	36.0%	12.5%	1.4%	CAG	TAG	Q21amber
Intermediate							
<i>tn2</i>	30.3%	14.9%	33.4%	21.3%	TGG	TAG	W932amber
<i>e856</i>	19.9%	26.7%	45.0%	8.4%	GAG	AAG	E195K
<i>e699</i>	9.0%	20.9%	51.2%	19.8%	ACT	ATT	T63I
Weak							
<i>e118</i>	10.1%	8.6%	45.6%	35.8%	—	326 bp deletion in exon 10	
<i>e2</i>	10.2%	5.5%	31.4%	51.4%	GGA	GAA	G917E
<i>ju63</i>	9.2%	7.0%	52.1%	31.5%	CAG	TAG	W964amber
<i>ju22</i>	8.5%	6.4%	53.8%	31.2%	TGT	TTT	C966F
<i>e1063</i>	8.3%	6.6%	51.0%	34.0%	TGT	TAT	C966Y
<i>e116</i>	6.4%	17.5%	50.7%	25.3%	TGG	TGA	W921opal
<i>e200</i>	5.6%	3.1%	44.4%	46.7%	tttcag AAG	tttcaa AAG	exon 2 splice acceptor
<i>e1029</i>	5.9%	1.9%	45.7%	46.5%	ND	ND	

Mutant phenotypes were quantitated as described in Experimental Procedures. We classify *vab-1* mutations as strong (>50% lethality), intermediate (25%–50% lethality), or weak (<25% lethality). Most larval arrest animals arrested during L1 or L2 stages; some *vab-1* larvae rupture at the rectum. Some (<5%) adult animals showed egg-laying defects. Wild-type and mutant *vab-1* genomic DNA sequences are shown with the predicted effects on VAB-1 protein.
 ND, not determined.

Table 2. The *vab-1* Null Phenotype Is a Variable Defect in Morphogenesis

Parental Genotype (n)	Arrest at or before 2-Fold	Arrest Later Than 2-Fold	Hatched, Abnormal Head or Tail	Hatched, Normal Head and Tail
<i>vab-1</i> (133)	18.0% (24)	23.3% (31)	58.6% (78)	0% (0)
<i>vab-1/+</i> (152)	8.5% (13)	7.8% (12)	11.2% (17)	72% (110)
<i>vab-1/+</i> × <i>ccDf4/+</i> (81)	8.6% (7)	5% (4)	11.1% (9)	75.3% (61)
<i>ccDf4/+</i> × <i>maDf4/+</i> (105)	12.3% (13)	7.6% (8)	3.8% (4)	76.2% (80)

Arrest stages of *vab-1* mutants were scored as described in Experimental Procedures. Arrest at or before 2-fold stages corresponds to phenotypic Classes I-III and some Class IV phenotypes, arrest later than 2-fold corresponds to a subset of Class IV phenotypes, embryos that hatch correspond to Class V. Data for the strong *vab-1* allele *e2027* are shown; similar results were obtained for other strong *vab-1* alleles. Similar ranges of phenotypes are seen in progeny from homozygous *vab-1(e2027)* mothers and in one quarter of the progeny of *vab-1(e2027)/+* mothers, indicating that there is no maternal effect for *vab-1*. The range of phenotypes of *vab-1(e2027)*, *vab-1(e2027)/Df*, and *Df/Df* animals are similar, consistent with *vab-1(e2027)* being a null mutation.

lateral movements of the neuroblasts that normally close the gastrulation cleft. Thus, *vab-1* function is required for neuroblast movements following gastrulation.

Approximately 35% of *vab-1* null mutant embryos displayed severe defects in cell movements during the process of epidermal enclosure. During ventral enclosure of the epidermis in wild-type embryos, leading cells of the epidermis migrate over neurons, from lateral positions to the ventral midline (Figures 2B and 2D) (Williams-Masson et al., 1997). The epidermal leading edge cells fail to migrate or migrate more slowly than normal in *vab-1* animals (phenotypic class I: Figure 2F), or they migrate to the ventral midline and fail to form junctions correctly (class II). The leading cells in class I and II embryos often send actin-rich processes to abnormally anterior regions, as determined by phalloidin staining (data not shown), and migrate to abnormally anterior positions (Figure 2F). As a result, ventral closure is incomplete, and internal cells ooze through a hole in the ventral midline of the epidermis when elongation begins, resulting in rupture and arrest of the embryo. In other embryos (class III) the leading cells meet up normally, but internal cells ooze from the region of the posterior leading cells after elongation (Figure 2I), suggesting that the cells do not properly connect with their partners. In 65% of *vab-1* embryos, closure of the gastrulation cleft appears normal, and the embryos elongate to the 1.5-fold or 2-fold stage (classes IV and V); about one-third of these embryos rupture along the ventral midline at the 2-fold stage or later (Figure 2J), indicating a late defect in ventral enclosure; and the remaining two-thirds do not rupture (class V; data not shown). The phenotype of class IV embryos, in which closure of the ventral gastrulation cleft is normal but epidermal enclosure is defective, suggests that the ventral enclosure defects in *vab-1* embryos are not merely a consequence of the defects in ventral cleft closure.

In *vab-1* embryos, internal organs and tissues differentiate normally, as judged by Nomarski microscopy. Several markers of neuronal and epidermal cell fates were examined and showed normal expression in *vab-1* mutants (data not shown). Thus, the morphogenetic defects in *vab-1* embryos do not appear to be due to improper specification of neural or epidermal fates.

vab-1 Encodes an Eph Receptor Protein-Tyrosine Kinase

We cloned *vab-1* using genetic mapping and transformation rescue. We mapped *vab-1* close to the right

of *hlh-1*, tested genomic DNA clones from this region (Figure 3A) for their ability to rescue *Vab-1* phenotypes in transgenic lines, and found that the cosmid M03A1 fully rescued *vab-1(e2027)* mutant phenotypes. Genomic sequence available from the *C. elegans* genome consortium predicted a gene from this cosmid that could encode a receptor protein-tyrosine kinase (RPTK) of the Eph subfamily. This RPTK gene is mutated in *vab-1* mutants (see below), establishing that this gene is *vab-1*. *vab-1* produces a 4 kb transcript expressed throughout development (data not shown). We determined the cDNA sequence corresponding to this *vab-1* transcript as described in Experimental Procedures.

The predicted VAB-1 protein (Figure 4A) is most similar to Eph-related RPTKs, recently renamed Eph receptors (Eph Nomenclature Committee, 1997). The Eph receptor subfamily is the largest subfamily of RPTKs (Orioli and Klein, 1997). EphA receptors bind GPI-linked ephrin ligands, and EphB receptors bind transmembrane ephrins (Gale et al., 1996); VAB-1 shows equal sequence similarity to EphA and EphB subclasses. VAB-1 contains all hallmark features of Eph receptors (Figures 3B and 3C), including in its extracellular domain an N-terminal globular domain with weak similarity to immunoglobulin domains (O'Bryan et al., 1991), a cysteine rich domain, in which the positions of the cysteine residues are highly conserved among Eph family members, and two fibronectin type III repeats. The intracellular domain of VAB-1 contains the juxtamembrane motif Y(I/V)DPXTYEDP found in all vertebrate Eph receptors and a tyrosine kinase catalytic domain most similar (59% identical) to that of human EphA3/Hek and between 51% and 58% identical to those of other Eph receptors (Figure 3E). Unlike other Eph receptor kinase domains, the VAB-1 kinase domain contains an insert sequence (A719-E743) between subdomains I and II.

Mutations in the VAB-1 Extracellular Domain Cause Strong or Intermediate Mutant Phenotypes

To identify functionally important parts of the VAB-1 protein, we determined the molecular lesions of *vab-1* mutant DNAs (Table 1). Several of the strong alleles had lesions consistent with their genetic behavior as null mutations. Three strong alleles, *dx14*, *dx31*, and *e2027*, cause deletions of sequences encoding parts of the extracellular domain (Figure 3A), and *e1059* is an amber stop in the signal peptide. One strong and two intermediate alleles cause missense alterations in the extracellular

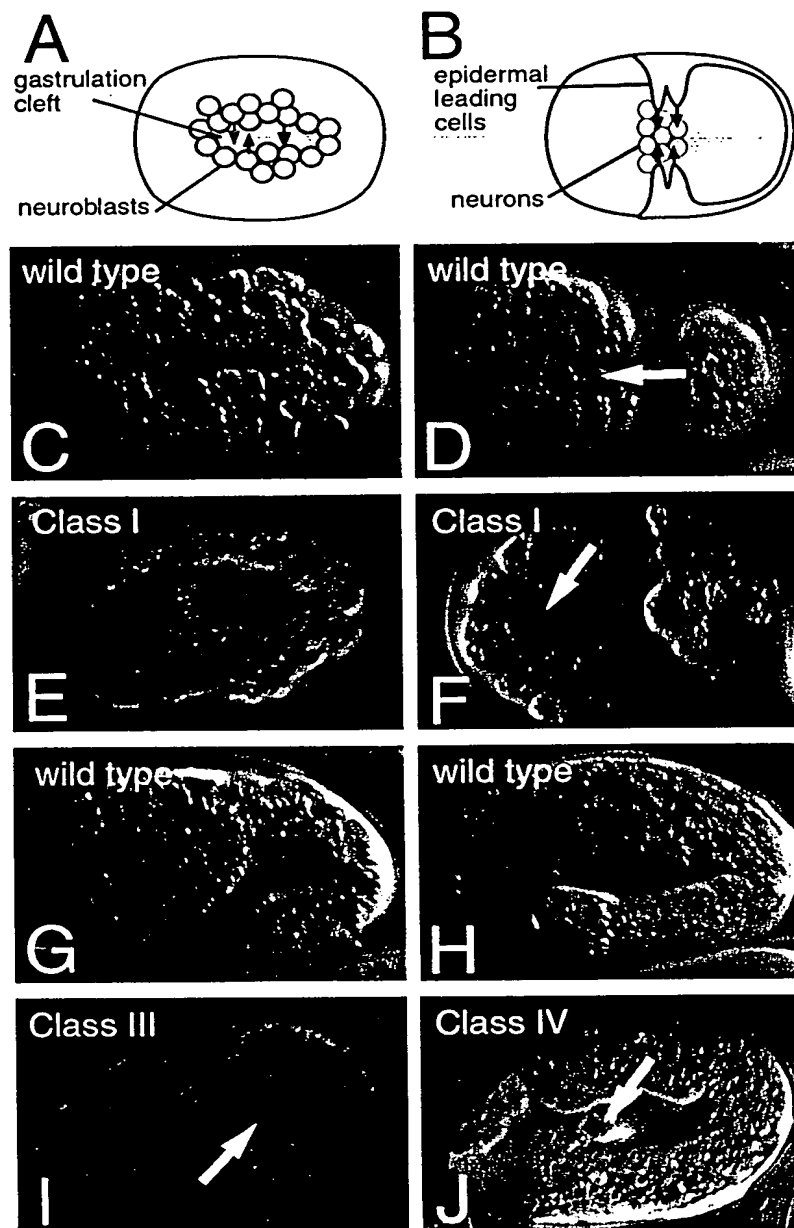


Figure 2. Cell Movement Defects following Gastrulation and during Ventral Closure in *vab-1* Embryos

In wild-type embryos the gastrulation cleft (A and C) is normally 1–2 μm deep and closes 230–290 min postfertilization; epidermal enclosure (B and D) occurs between 310–340 min. (C–F), ventral Nomarski views, anterior to left. Bar, 15 μm . (G–H), lateral views.

vab-1 class I phenotype (~14% of animals): embryo is rounded, double ventral gastrulation cleft forms single cleft (arrow in [E]) 4–5 μm deep that persists throughout enclosure. Ventral closure fails early (F): leading cells (arrow) fail to migrate or migrate slowly. In class I embryos the ventral pocket attempts to form, and the embryos display muscular twitching. The class II phenotype (~5% of animals, data not shown) is similar, only weaker. (G and H) Wild-type comma stage and 2-fold stage embryos. Animals displaying a class III phenotype (~15% of animals) show a transient 1–2 μm deep cleft, similar to wild-type but persisting approximately 30 min longer. The leading edge cells zip up normally, and the ventral pocket forms. The embryo oozes from the region of the posterior leading edge after elongation begins (arrow, [I]). Class IV animals (~23% of animals) initially appear normal and elongate to the 1.5-fold or 2-fold stage, then ooze along the ventral midline in the head or tail (arrow, [J]). Class V embryos (~43% of animals; data not shown) show no embryonic abnormality and hatch. Some class III, IV, and V embryos have enlarged buccal cavities and develop a Notched head.

domain and might define functionally important residues in Eph receptors. The strong allele *ju8* and the intermediate allele *e699* affect residues (E62K and T63I, respectively) in the N-terminal globular domain, and the *e856* mutation affects the cysteine-rich domain (Figure 3D); these domains have been implicated in ephrin-Eph receptor interactions (Labrador et al., 1997).

Mutations in the VAB-1 Kinase Domain Cause Weak Mutant Phenotypes

Seven *vab-1* mutations disrupt the kinase domain of VAB-1 (Figure 3E) and are likely to cause severe loss of kinase activity (see Discussion). Strikingly, six of these seven alleles cause weak mutant phenotypes. The weak

alleles *e2*, *e1063*, and *ju22* cause missense alterations of conserved residues that function to stabilize the structure of other kinase domains (Hubbard et al., 1994). Three weak alleles should truncate the kinase domain: *ju63* and *e116* cause stop codons, and *e118* is a deletion of the C-terminal 202 residues of VAB-1. One allele, *tn2*, causes a stop codon in kinase subdomain IX yet causes an intermediate mutant phenotype; it is unclear why the *tn2* phenotype is stronger than those of the other kinase domain alleles. The above mutations would be predicted to abolish catalytic activity of VAB-1, yet none appears to cause complete loss of *vab-1* function, suggesting that VAB-1 may possess both kinase-dependent and kinase-independent functions.

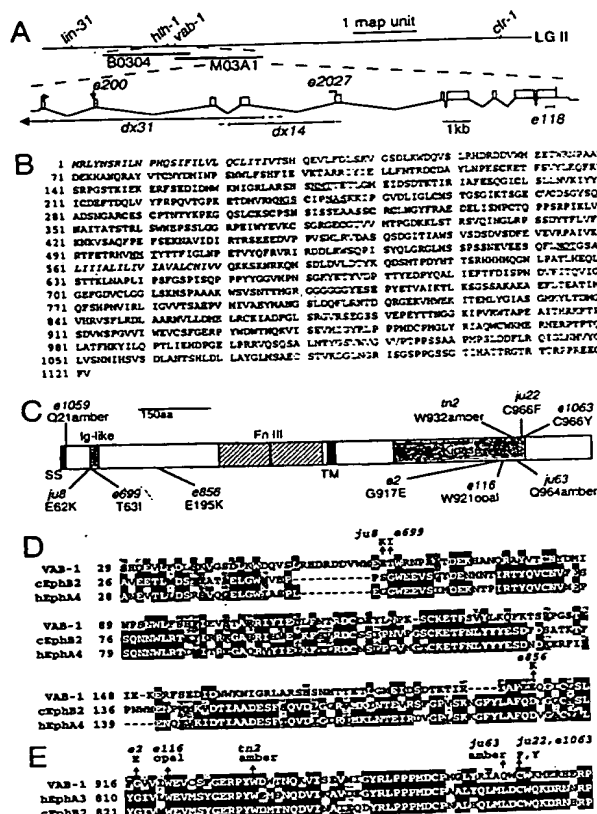


Figure 3. Molecular Cloning and Sequence Analysis of *vab-1*

(A) Genetic and physical maps of the *vab-1* region and structure of the *vab-1* transcription unit. Genetic mapping placed *vab-1* 0.07 map units to the right of *hih-1*. Cosmid clones were mapped by the *C. elegans* genome project. B0304 contains *hih-1*; M03A1 contains *vab-1*. The position of the intron between exons 2 and 3 is conserved between *vab-1* and chicken EphB2 (Connor and Pasquale, 1995), and the position of the intron between exons 6 and 7 is conserved between *vab-1*, chicken EphB2, and rat EphA5 (Maisonpiere et al., 1993), suggesting that these genes might share a common ancestor. Locations of the deletions *dx14*, *dx31*, *e2027*, *e118*, and the splice site mutation *e200* are shown.

(B) Sequence of the predicted VAB-1 protein. The signal sequence (residues 1-28) and transmembrane domain (residues 559-581) are italicized. Potential N-linked glycosylation sites (NX(T/S)) are underlined. The conserved cysteines in the cysteine-rich domain are in boldface and shaded.

(C) Domains of VAB-1 and locations of point mutations. SS, signal sequence; TM, transmembrane domain.

(D) Alignment of the VAB-1 N-terminal globular domain and part of the cysteine-rich domain with those of the closest vertebrate EphA and EphB receptors. The VAB-1 extracellular domain (residues 55-550) is most similar (27% identity, 42% similarity) to chicken EphB2/Cek5 (Pasquale, 1991); within the EphA subfamily the extracellular domain of human EphA4/Hek8 (Fox et al., 1995) is most similar to VAB-1 (27% identity, 41% similarity). Sequences were aligned using ClustalW; identities are in black and conserved residues in gray. *ju8*, which changes a glutamate to a lysine (charge reversal), and the intermediate allele *e699*, which changes a polar residue (threonine) to a nonpolar residue (isoleucine) affect a poorly conserved part of the N-terminal globular domain. The intermediate allele *e856* changes a glutamate to a lysine; the equivalent residue is aspartate (negatively charged) in most vertebrate Eph receptors.

(E) Alignment of VAB-1 kinase subdomains IX-XI with the most similar vertebrate EphA and EphB kinase domains and location of *vab-1* kinase domain mutations. The VAB-1 kinase domain (residues 665-

vab-1 Reporter Constructs Are Widely Expressed in Early Embryos but Only in Nonepidermal Cells during Ventral Enclosure

To determine the pattern of expression of *vab-1*, we used reporter constructs containing translational fusions of the *vab-1* locus to green fluorescent protein (GFP; see Experimental Procedures). Such *vab-1::GFP* constructs fully rescued *vab-1(e2027)* mutant phenotypes, indicating that these constructs reflect the endogenous *vab-1* expression pattern. Expression from one such construct, *ju1s24*, was analyzed in detail.

VAB-1::GFP was expressed in many cells during late gastrulation; based on their positions these cells include the neuroblasts whose movement is defective in *vab-1* mutants (Figure 4A) and may also include some epidermal precursors. During ventral enclosure of the epidermis, VAB-1::GFP was expressed in clusters of cells of the head and tail regions (Figures 4B-4F). In the head region, VAB-1::GFP was expressed in clusters of presumptive neuronal cells. Early in enclosure these cells appear to lie beneath the epidermal leading cells (Figures 4C and 4D); later in enclosure, the VAB-1-expressing cells lie anterior to the leading cells (Figure 4E). VAB-1::GFP was not detectably expressed in the epidermal leading cells at any stage during ventral enclosure. In the posterior of the embryo, VAB-1::GFP was expressed in several cells, including QV5 and the ventral hyp7 cells posterior to the rectum (data not shown); VAB-1::GFP was also expressed in several pharyngeal cells (Figure 4G). In late embryogenesis and throughout larval and adult development, VAB-1::GFP was localized to the axons of many neurons throughout the nervous system (Figures 4G and 4H). Thus, in most stages following gastrulation, VAB-1::GFP is widely expressed in the developing nervous system. Expression of VAB-1::GFP in the larval nervous system suggested that *vab-1* might function in neural development; although *vab-1* mutants do not display obvious behavioral defects, we have found that *vab-1* mutants display defects in axonal outgrowth and fasciculation (S. E. G. and A. D. C., unpublished data).

Vab-1 Function Is Required in Nonepidermal Cells for Epidermal Morphogenesis

The expression of VAB-1::GFP reporter constructs in nonepidermal cells during epidermal enclosure led us to ask whether the epidermal morphogenetic defects in *vab-1* mutants are due to a requirement for *vab-1* function in neurons. We used genetic mosaic analysis (Herman, 1995) to determine in which cells *vab-1* is necessary for normal morphogenesis. Because genetic mosaics could not be identified during embryogenesis, we analyzed viable *vab-1* genetic mosaics. We identified 83 *vab-1* genetic mosaics, 56 of which displayed morphogenetic defects in head epidermis (the *Vab* phenotype). All such *Vab* mosaics proved to have lost *vab-1* within the AB lineage, which generates head epidermal

991) is most similar (59% identity, 72% similarity) to that of human EphA3/Hek (Wicks et al., 1992); the EphB with highest similarity to VAB-1 in the kinase domain is chicken EphB2/Cek5 (58% identity, 72% similarity).

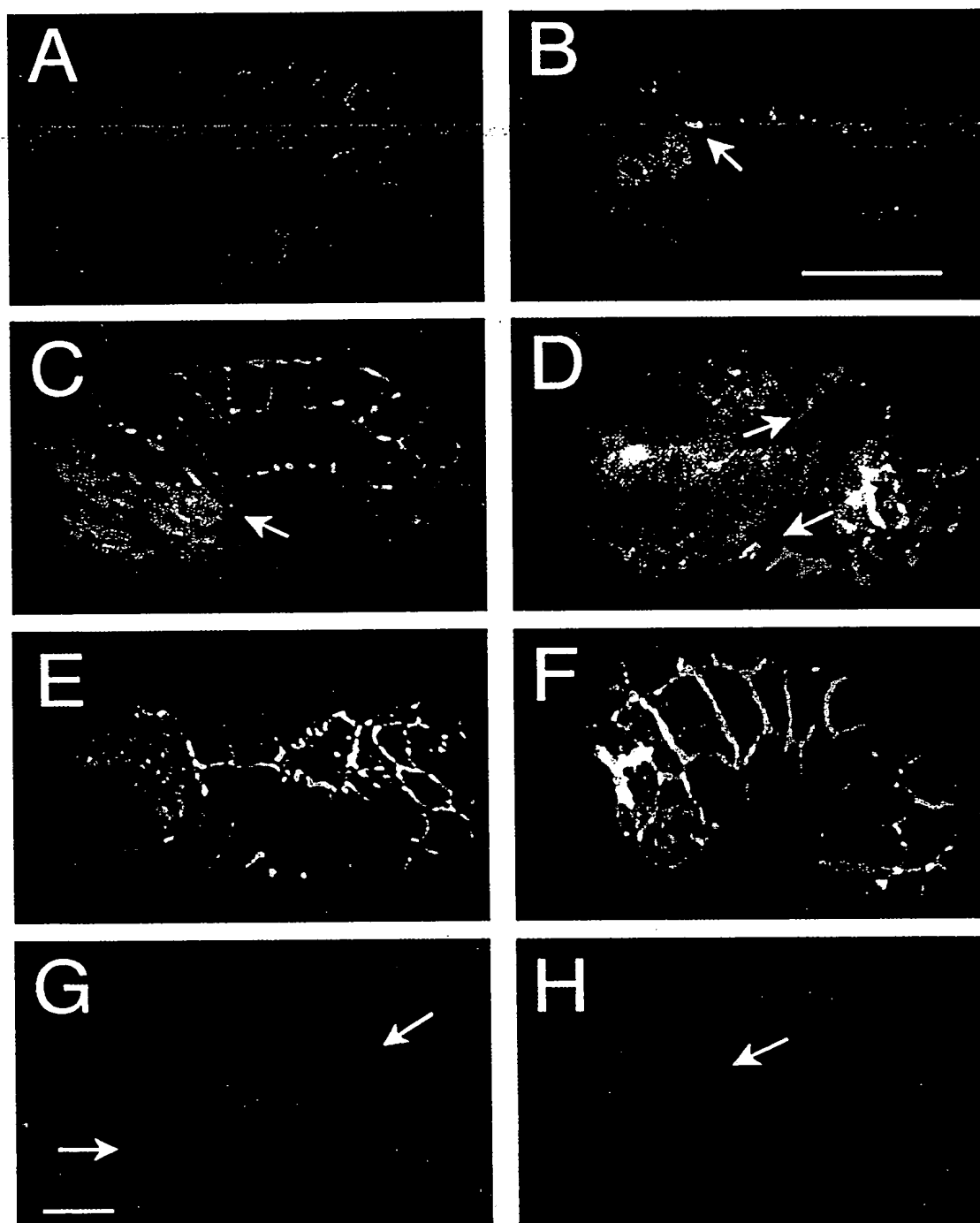


Figure 4. Expression Pattern of *vab-1* Reporter Constructs

Confocal images of VAB-1::GFP expression from the *juls24* transgene (visualized using anti-GFP antibodies [green]) and epidermal cell junctions (MH27 antigen [red]). Bars, 15 μ m. (A) VAB-1::GFP expression in postgastrulation embryo (~200–250 min). Ventral view. Not all VAB-1-expressing cells have been identified at this stage; based on position most of the cells are neuroblasts. Some epidermal precursors may also express VAB-1::GFP. (B and C) Beginning of ventral closure, ventrolateral and ventral views (D). Later in ventral closure, leading epidermal cells are marked (arrows). (E) Midventral closure; leading cells have met at ventral midline, ventral view; ventral pocket has not yet closed. (F) Completed ventral closure (comma stage). (G) L1 larval animal showing expression of VAB-1::GFP (*juls33* transgene) in the nervous system; nerve ring and ventral nerve cord are arrowed. Strong expression is also seen in the procorpus and terminal bulb of the pharynx. (H) Expression of VAB-1::GFP in axons in late larval animal; lateral view, close-up of expression in D neuron axon commissure (arrowed) and ventral cord.

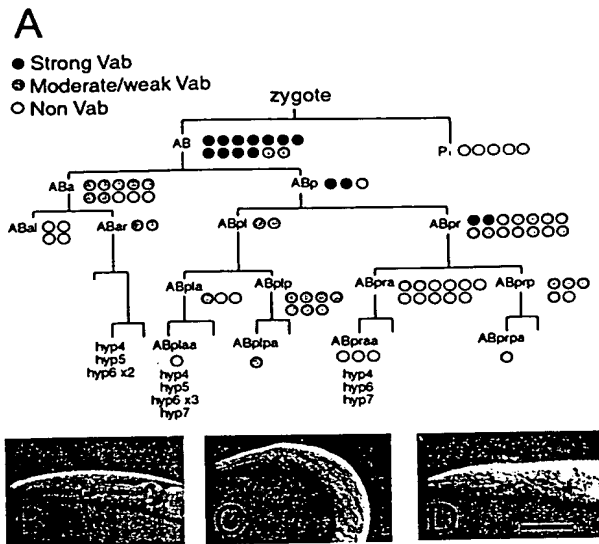


Figure 5. Mosaic Analysis of *vab-1*

(A) Partial lineage of *C. elegans* showing points at which arrays were lost in *vab-1* mosaic animals. The origin of the main head epidermal syncytia (hyp4, hyp5, hyp6, and anterior of hyp7) is shown. Black circle, strong head morphogenetic defect; gray circle, moderate or weak morphogenetic defect (Figures 6C and 6D). Open circle, wild-type morphology. (B) Wild-type (N2) head morphology. (C and D) Vab phenotypes resulting from losses of *vab-1* function outside of the epidermis. (C) Head region of typical ABprp mosaic, L4 stage, displaying moderate Vab phenotype. (D) Typical ABplp mosaic displaying moderate Vab phenotype. Bar, 20 μ m.

cells, neuronal cells, and neuronal support cells (Figure 5A). In general, only early losses (in AB or ABp) of *vab-1* function caused strong morphogenetic defects, suggesting that *vab-1* functions in many AB-derived cells. Five losses of *vab-1* function outside the AB lineage did not cause morphological defects (Figure 5A).

The early focus of *vab-1* function in the AB lineage might reflect a requirement for *vab-1* in many epidermal cells, in many nonepidermal cells, or both. To determine whether *vab-1* was required in epidermal or nonepidermal cells, we identified mosaics in which *vab-1* had been lost from precursors at the AB⁸ stage or later; at this stage three precursors (ABprp, ABpra, and ABprp) generate the head epidermal cells hyp4, hyp5, and hyp6. Three of 18 mosaic animals in which *vab-1* was lost in epidermal precursors (in ABpla, ABplaa, ABpra, or ABpraa) displayed Vab phenotypes. By contrast, 12 of 14 mosaic animals in which *vab-1* had been lost only from nonepidermal precursors (ABplp, ABplpa, ABprp, and ABprpa) displayed Vab phenotypes (Figures 5B and 5C). Our data clearly show that losses of *vab-1* function in neuronal lineages cause non-cell-autonomous defects in epidermal morphogenesis, consistent with our data showing that VAB-1::GFP is mostly expressed in neurons from the ventral enclosure stage onward. However, we cannot exclude the possibility that *vab-1* has additional cell-autonomous roles in the epidermal cells.

Discussion

We show here that *vab-1*, which functions in epidermal morphogenesis in *C. elegans*, encodes an Eph receptor

tyrosine kinase. The phenotypes of null and kinase domain mutations in VAB-1 suggest that the VAB-1 RTK has both kinase-dependent and kinase-independent functions. Our analysis of *vab-1* mutant phenotypes, expression pattern, and genetic mosaics suggests that *vab-1* functions in neuronal cells to regulate normal morphogenesis of the epidermis.

Evolutionary Conservation of Eph Signaling Pathways
VAB-1 is most similar to receptor tyrosine kinases of the Eph subfamily. Eph receptors were first isolated from vertebrates by homology in the kinase domain (Hirai et al., 1987) and are the largest subfamily of RPTK (Orioli and Klein, 1997). Previously, Eph receptors have only been reported from vertebrates. Our findings show that the Eph receptor family is ancient and likely to be conserved among all animals.

Eph receptors bind membrane-bound protein ligands, recently renamed ephrins (Eph Nomenclature Committee, 1997). Ephrins are either membrane-anchored in cell membranes via glycosylphosphatidylinositol (GPI) anchors (ephrin-As) or are integral membrane proteins (ephrin-Bs). Eph receptors can be grouped into two subclasses: the EphA receptors, which bind ephrin-A ligands, and the EphB receptors, which bind transmembrane ephrin-B ligands (Gale et al., 1996). VAB-1 is equally similar in sequence to EphA and EphB receptors and thus may be similar to a common ancestor of the two vertebrate subclasses. We have also identified ephrin-related genes in the *C. elegans* genomic sequence (A. D. C. and S. E. G., unpublished data), indicating that potential ligands for VAB-1 exist in *C. elegans* and thus that ephrin signaling pathways may be conserved between nematodes and vertebrates.

VAB-1 Might Participate in Forward and Reverse Signaling

Vertebrate Eph receptors may participate in both kinase-dependent "forward" signaling and in kinase-independent "reverse" signaling. For example, deletion of the kinase domain of murine Nuk/EphB2 did not affect its function in axonal guidance in the anterior commissure (Henkemeyer et al., 1996). EphB2 is not expressed on anterior commissure axons but on substrate cells over which the axons navigate. A transmembrane ligand for EphB2, ephrin-B1/LERK-2, is expressed on anterior commissure axons, and EphB2 binding to ephrin-Bs can induce phosphorylation of tyrosines on the intracellular domain of the ephrin-B, thus potentially activating a signaling cascade in the ligand-expressing cell (Holland et al., 1996; Brückner et al., 1997).

VAB-1 likely has some forward signaling functions, because missense alterations of conserved residues in the kinase domain cause partial reduction in *vab-1* function. However, none of the VAB-1 kinase alleles causes complete loss of *vab-1* function. It is possible that the weak phenotype of these mutants is due to residual kinase activity. However, the kinase subdomains deleted in *e118* mutants contain residues essential for catalytic activity (Yaciuk and Shalloway, 1986); also, lesions equivalent to those of *vab-1(e2)* and *vab-1(e116)* were found in the null alleles *sy7* and *sy5* of the *C. elegans let-23* RPTK, indicating that such mutations

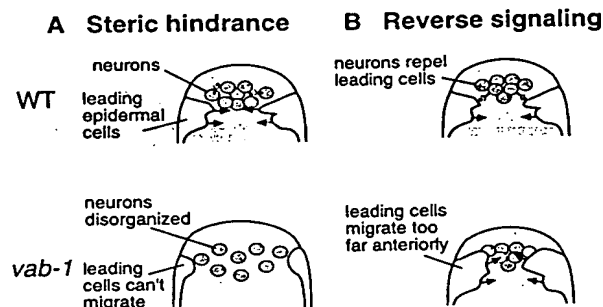


Figure 6. Two Models for the Function of VAB-1 in Epidermal Morphogenesis
See discussion for details.

cause complete loss of activity of the LET-23 kinase (Aroian et al., 1994). Thus, the VAB-1 kinase domain mutations should abolish kinase activity.

An alternative explanation for the weak phenotypes of *vab-1* kinase mutants is that VAB-1, in addition to kinase-dependent forward signaling functions, has kinase-independent reverse signaling functions. Such functions presumably require the VAB-1 extracellular domain, possibly interacting with ephrin ligands, and would explain why only mutations disrupting the VAB-1 extracellular domain would cause null phenotypes. As discussed below, VAB-1 reverse signaling could account for the nonautonomous role of *vab-1* in epidermal morphogenesis. As both weak and strong *vab-1* alleles appear to cause similar ranges of phenotypes with different penetrances, the kinase-dependent and kinase-independent functions of *vab-1* may be required for related aspects of morphogenesis.

The Role of VAB-1 in Signaling from Neurons to Epidermis during Epidermal Morphogenesis

vab-1 mutants are defective in the movements of neuroblasts that close the ventral gastrulation cleft and the movements of the epidermal leading cells that initiate epidermal enclosure. Unexpectedly, *vab-1* is not expressed in the epidermal leading cells but in neurons underlying or adjacent to the leading cells. In addition, our mosaic analysis has shown that loss of *vab-1* function in nonepidermal precursors causes epidermal morphogenetic defects. Our results suggest that a major function of *vab-1* is in neuronal cells and that the epidermal morphogenesis defects of *vab-1* mutants in part result from defects in neuronal cells. Thus, despite its similarity to receptors, VAB-1 acts in signaling rather than responding cells.

Our observations raise two questions: what signals do underlying neurons provide to migrating epidermal cells, and does VAB-1 function directly in such neuronal-to-epidermal signaling? We propose two models for this process (Figure 6). These two models are not mutually exclusive, and the phenotypes of *vab-1* mutants suggest that both models might apply. In the "steric hindrance" model (Figure 6A), VAB-1 signaling only occurs between neuronal precursors, and the epidermal defects in *vab-1* mutants are a result of defects in neuronal precursors

that normally provide a permissive substrate for epidermal cell movements. Mispositioned neuronal precursors resulting from the gastrulation cleft defects seen in *vab-1* mutant embryos could interfere with normal epidermal migration and likely contribute to the epidermal defects seen in severely mutant *vab-1* animals (class I-III). However, we often observe defects in enclosure in the absence of obvious defects in cleft closure (class IV phenotype). Thus, defects in epidermal enclosure do not appear to be solely due to defects in neuroblast movements following gastrulation.

In the "reverse signal" model (Figure 6B), neurons signal directly to epidermal cells, potentially providing cues for their migration. As discussed above, VAB-1 could participate directly in such reverse signaling, analogous to that observed for vertebrate Eph receptors. Alternatively, VAB-1 could receive a signal from epidermal cells and thereby activate a second signaling pathway in the reverse direction. Two observations further suggest that VAB-1-expressing cells might provide an inhibitory signal to epidermal cells. First, in wild-type embryos the leading cells migrate posteriorly and adjacently to VAB-1-expressing cells (Figures 4B-4E). Second, in some *vab-1* mutant embryos the leading cells migrate anteriorly to their normal positions, possibly a result of a lack of anterior repulsive cues. Identification and localization of ligands for VAB-1 is necessary to distinguish between these two models for VAB-1.

Our genetic analysis of *vab-1* has shown that the null phenotype of *vab-1* is a variable defect in epidermal morphogenesis. As a small percentage of *vab-1* null mutants develop into apparently normal adults, *vab-1* function is not essential. *vab-1* signaling may be partly redundant with other signaling pathways, as found for some vertebrate Eph receptors (Orioli et al., 1996), although no additional Eph receptors have yet been identified in the *C. elegans* genomic sequence.

Eph Signaling in Vertebrate Morphogenesis

Signaling via Eph receptors and ligands has been implicated in axon guidance and topographic mapping (Cheng et al., 1995; Gao et al., 1996; Henkemeyer et al., 1996; Nakamoto et al., 1996). Ephrin signaling can function as a repulsive cue for axon guidance by promoting growth cone collapse (Drescher et al., 1995). Ephrin signaling has also been shown to promote axon fasciculation (Winslow et al., 1995), formation of rhombomere boundaries (Xu et al., 1995), and to inhibit cell-cell adhesion (Winning et al., 1996). A common feature of Eph-mediated signaling is thus the modulation of cell shape and cell adhesion, processes critical to epithelial morphogenesis.

The expression patterns of many vertebrate Eph receptors suggest they may be functioning in epithelial morphogenesis. For example, EphB2/Nuk is expressed in midline epithelial cells of the palatal shelves as they begin to fuse in the midline. Mice lacking both the EphB2 and EphB3/Sek4 receptors have cleft palates as a result of failure in closure of the secondary palate, possibly due to defective epithelial morphogenesis (Orioli et al., 1996). Many other Eph receptors are expressed in epithelial or endothelial organs undergoing morphogenesis, such as lung, heart (Ruiz et al., 1994), or in migrating cells (Brändli and Kirschner, 1995). Determining the

roles of vertebrate Eph receptors in these processes may be complicated by redundancy between members of this gene family; for example, EphA2/Eck is specifically expressed during mouse gastrulation (Ruiz and Robertson, 1994), yet Eck mutant mice show no discernible phenotype (Chen et al., 1996). *vab-1* may provide a relatively simple model for understanding the functions of Eph receptors in these aspects of vertebrate morphogenesis.

Experimental Procedures

Genetic Analysis of *vab-1*

C. elegans strains were cultured using standard methods (Brenner, 1974). Mutations used were as follows: LG1, *unc-29(e1072)*; LG II, *lin-31(n301)*, *hlh-1(cc450)*, *dpy-25(e817sd)*, and *tra-2(q122dm)* (Schedl and Kimble, 1988); LGIII, *ncl-1(e1865)*; and LGX, *lin-15(n765ts)*. Rearrangements used were *ccDf4II* and *maDf4II*. Mutations are described in Hodgkin (1997) or in references above.

vab-1 alleles were isolated in general screens for visible mutations by S. Brenner (e2, e116, e118, e200, e699, e721, e856, and e1059), J. Lewis (e1029), J. Hodgkin (e1063), A. Fire (e2027), E. Lambie (*dx14*, *dx31*), M. Zhen (*ju8*), D. Ostertag (*ju22*, *ju63*), and D. Greenstein (*tn2*). All alleles were EMS-induced except *dx14* and *dx31*, which were UV-induced, and e2027, which arose spontaneously. All mutations fail to complement *vab-1(e2)*. Map data showing that *vab-1* lies close to the right of *hlh-1* are available from the Caenorhabditis Genetics Center.

Phenotypic Analysis

We determined the penetrance of *vab-1* mutant phenotypes by picking L4 animals from homozygous strains to separate plates, allowing them to self, and transferring them every 24 hr. Eggs unhatched after 24 hr were scored as embryonic arrest. Larvae that failed to develop into adults after 48 hr were scored as larval arrest. Any morphological abnormality of the head region was scored as abnormal. At least 500 individuals were scored for each genotype.

We determined the stages at which *vab-1* embryos arrest by following the development of *vab-1* embryos using Nomarski microscopy. Embryos were followed from comma stage or before until either development arrested or the embryo hatched. To generate embryos heterozygous for *vab-1* alleles and the deficiency *ccDf4*, we mated males carrying the dominant feminizing mutation *tra-2(q122)* with *ccDf4/dpy-25* hermaphrodites; non-Dpy cross progeny are *ccDf4/tra-2* females. These females were mated with *vab-1/+* males. One quarter of the F₁ animals from this cross will be of genotype *vab-1/ccDf4*.

To generate animals transheterozygous for deficiencies that uncover *vab-1*, *tra-2(q122)* males were mated with *ccDf4/dpy-25* hermaphrodites and *maDf4/dpy-25* hermaphrodites in separate crosses. Non-Dpy female cross progeny (genotype *ccDf4/q122*) from the first cross were mated with non-Dpy male cross progeny (genotype *maDf4/q122*) from the second cross. One quarter of the progeny of this cross were *ccDf4/maDf4* heterozygotes.

Analysis of Cell Movements by Time-Lapse

Nomarski Microscopy

Four-dimensional microscopy was used to record and follow cell movements as described (Williams-Masson et al., 1997). To generate the movies analyzed, 30 focal planes 0.5 μ m apart were recorded every 60 s. A total of 58 *vab-1(e2027)* embryos were recorded from early gastrulation until they had reached a terminal phenotype. We found that some *vab-1* embryos develop more slowly than wild-type embryos following gastrulation and morphogenesis. Wild-type embryos took 320 min to develop from the eight-cell stage to the beginning of elongation. *vab-1* embryos took up to 55 min longer to develop to this stage, with the developmental delay correlating with the severity of the morphogenetic defects.

Transformation Rescue of *vab-1*

vab-1(e2027) animals were injected with cosmid M03A1 (15 μ g/ml) and the plasmid pRF4 (50 μ g/ml), which confers a dominant Roller

(Rol) phenotype (Mello et al., 1991). Transgenic lines carrying pRF4 and M03A1 in extrachromosomal arrays were established and scored for rescue of the *Vab-1* phenotypes. Five of six lines showed rescue of the *vab-1* embryonic lethality and head morphology defects (2.8% of Rols were *Vab* in rescued lines), compared with 0/2 control lines bearing pRF4 alone (86.5% of Rols were *Vab*).

Analysis of *vab-1* cDNA Sequence

cDNAs from the *vab-1* locus had been isolated in a genome-wide EST project (Y. Kohara, personal communication). The longest cDNA clone, yk18c8, contains a 2992 bp insert that we sequenced, corresponding to bases 700–3962 of the composite *vab-1* cDNA. We determined the 5' end (bases 1–699) of the *vab-1* transcript in RT-PCR experiments; RT-PCR using the SL1 *trans*-spliced leader sequence as upstream primer (Krause and Hirsh, 1987) generated products, indicating that the *vab-1* message is *trans*-spliced to SL1. The *vab-1* cDNA sequence is 3962 bp in length, consistent with the 4 kb band observed on Northern blots (data not shown), including an SL1 *trans*-spliced leader, an 89 bp 5' UTR, a 3354 bp open reading frame, and a 458 bp 3' UTR. No evidence was found for alternative *vab-1* transcripts either by Northern blot or RT-PCR experiments.

Determination of Mutant DNA Sequences

We determined the sequences of genomic DNAs from *vab-1* mutants as described previously (Chisholm and Horvitz, 1995). *vab-1* exons and splice sites were amplified from all *vab-1* mutants (except the deletion alleles *dx14*, *dx31*, e118, and e2027) and PCR products sequenced using ³²P labeled primers and the fmol kit (Promega). All mutations were confirmed on both strands and in independent PCRs. The molecular lesions of two *vab-1* mutations (e721 and e1029) have not yet been found. Sequences of primers used are available upon request.

The *vab-1* alleles *dx14* and *dx31* result from rearrangements, based on Southern blot analysis of mutant genomic DNA (data not shown). *dx31* causes a deletion of at least 7 kb, removing exons 1–4. *dx14* appears to be a complex rearrangement, resulting in an approximately 2 kb deletion that deletes exon 4 and the first half of exon 5.

vab-1::GFP Reporter Constructs

The VAB-1::GFP construct pCZ55 used for expression studies is a translational fusion of GFP to a *vab-1* minigene and contains 4.2 kb of genomic sequence 5' to the *vab-1* start codon, exons 1–5 (to the SmaI site in exon 5) as genomic DNA, exons 6–10 as cDNA, GFP inserted in frame at the XhoI site near the VAB-1 N terminus, the *vab-1* 3' UTR, and 0.4 kb of genomic DNA 3' to the polyadenylation site.

Transgenic lines were generated by transformation of *vab-1(e2027); lin-15* animals with pCZ55 and the *lin-15* rescuing plasmid pLin-15EK (Clark et al., 1994); four independent chromosomal integrants (*juls24*, *juls31*, *juls32*, and *juls33*) were identified following X-ray mutagenesis. Expression was analyzed in the strain CZ723 of genotype *vab-1(e2027); lin-15(n765); juls24(vab-1::GFP; lin-15[+])* by staining fixed transgenic animals with anti-GFP antibodies. Embryos were fixed in 1% paraformaldehyde and incubated with anti-GFP polyclonal antisera (Clontech) at 1:100 to 1:500 dilution and with MH27 monoclonal (1:1500). Staining was visualized with fluorescently conjugated secondary antibodies using a confocal microscope. VAB-1::GFP staining patterns in all four lines were indistinguishable.

Analysis of *vab-1* Genetic Mosaics

We used two approaches to identify *vab-1* mosaic animals. In both approaches we generated transgenic arrays bearing wild-type copies of *vab-1* and cell-autonomous marker genes (Herman, 1995). First, we generated strains of genotype *unc-29; vab-1; juEx(unc-29[+] vab-1[+] sur-5-GFP)* by transformation of *unc-29; vab-1* worms with cosmid DNAs C45G10 (*unc-29[+]*) [Miller et al., 1996], M03A1 (*vab-1[+]*) and the *sur-5-GFP* plasmid pTG96.1. *sur-5-GFP* is expressed in most somatic cell nuclei (T. Gu and M. Han, personal communication) and is a cell-autonomous marker for the array; *unc-29(+)* is required in body muscles (derived from P.) [Miller et al.,

1996). From such strains, three Unc non-Vab mosaics were identified and found to have lost the array in P₁. We then screened for Vab non-Unc animals (putative mosaics with losses in AB). Twenty-three of such animals were found that had patterns of *sur-5-GFP* interpretable as resulting from losses of the array within AB.

We used the cell-autonomous marker *ncl-1* (Hedgecock and Herman, 1995) in additional mosaic analysis experiments. We generated the strain CZ712 *vab-1; ncl-1; juEx39(vab-1[+] ncl-1[+] rol-6[dm])* by transformation with cosmids containing the wild-type copies of *vab-1* (M03A1), *ncl-1* (C33D3 [Miller et al., 1996]) and *prf4*. Expression of *rol-6(dm)* in cells contributing to the epidermal syncytium *hyp7* confers a Rol phenotype. Transgenic animals are thus Rol non-Vab non-Ncl. We screened CZ712 Rols for rare Rol Vab animals, predicted to be mosaics in which the array had been lost from a subset of *hyp7* precursors. We found 15 mosaics with patterns of Ncl cells resulting from single losses of the array. Ncl cannot be scored in syncytial nuclei unless all precursors of the syncytium have lost the array, so we assessed the loss point by scoring identifiable cell nuclei, as described (Clark et al., 1993).

Of the 15 Rol Vab mosaic animals, 4 had losses in the nonepidermal precursors ABprp and ABppl. As these mosaics had been selected on the basis of their Vab phenotype, it was possible that they were rare double loss mosaics in which the Vab phenotype was due to loss of the array in epidermal cells (which we could not directly score), rather than the observed loss in nonepidermal precursors. To address this caveat we screened CZ712 Rols directly for mosaicism of the Ncl marker. From 800 Rols screened we identified 42 animals with mosaic Ncl expression. Of these 42 mosaics, 8 had lost the array in nonepidermal precursors, of which 6 were Vab, and 13 had lost the array in head epidermal precursors, of which 1 was Vab. Thus, loss of *vab-1* function in nonepidermal precursors can frequently cause Vab phenotypes.

Acknowledgments

We thank the colleagues above for *vab-1* mutants, the *C. elegans* genome consortium for cosmid and sequence data, and Yuji Kohara for *vab-1* cDNAs. We thank Chuck Wilson for use of his oligo synthesizer, Dawne Shelton for oligo synthesis, Bill Sullivan for help with confocal microscopy, and Doug Kellogg for the motherode. We thank Yishi Jin for extensive advice, Mei Zhen for invaluable help, Derek Ostertag and Inessa Grinberg for help with allele sequencing, Andy Fire for advice, Jeff Simske for help with phalloidin staining, and members of the Chisholm, Jin, and Hardin labs for discussions. We thank Cori Bargmann, Gian Garriga, Ian Chin-Sang, and John Tamkun for comments on the manuscript. Some strains were provided by the *Caenorhabditis* Genetics Center, which is funded by the National Institutes of Health (NIH). K. S. was supported by an NIH training grant. Part of this work was supported by grants to J. H. (NSF IBN9357246 and a Lucille P. Markey Scholar Award) and by a grant to A. D. C. (NIH GM54657). A. D. C. is an Alfred P. Sloan Research Fellow.

Received December 17, 1997; revised January 29, 1998.

References

- Aroian, R.V., Lesa, G.M., and Sternberg, P.W. (1994). Mutations in the *Caenorhabditis elegans* *let-23* EGFR-like gene define elements important for cell-type specificity and function. *EMBO J.* 13, 360-366.
- Bard, J. (1992). *Morphogenesis*. (Cambridge, England: Cambridge University Press).
- Brändli, A.W., and Kirschner, M.W. (1995). Molecular cloning of tyrosine kinases in the early *Xenopus* embryo: identification of Eck-related genes expressed in cranial neural crest cells of the second hyoid arch. *Dev. Dynam.* 203, 119-140.
- Brenner, S. (1974). The genetics of *Caenorhabditis elegans*. *Genetics* 77, 71-94.
- Brückner, K., Pasquale, E.B., and Klein, R. (1997). Tyrosine phosphorylation of transmembrane ligands for Eph receptors. *Science* 275, 1640-1643.

- Chen, J., Nachabiah, A., Scherer, C.P.G., Reith, A., Bronson, R., and Ruley, H.E. (1996). Germ-line inactivation of the murine Eck receptor tyrosine kinase by gene trap retroviral insertion. *Oncogene* 12, 979-988.
- Cheng, H.-J., Nakamoto, M., Bergemann, A.D., and Flanagan, J.G. (1995). Complementary gradients in expression and binding of ELF-1 and Mek4 in development of the topographic retinotectal projection map. *Cell* 82, 371-381.
- Chisholm, A.D., and Horvitz, H.R. (1995). Patterning of the head region of *Caenorhabditis elegans* by the Pax-6 family member *vab-3*. *Nature* 377, 52-55.
- Clark, S.G., Chisholm, A.D., and Horvitz, H.R. (1993). Control of cell fates in the central body region of *C. elegans* by the homeobox gene *lin-39*. *Cell* 74, 43-55.
- Clark, S.G., Lu, X., and Horvitz, H.R. (1994). The *Caenorhabditis elegans* locus *lin-15*, a negative regulator of a tyrosine kinase signaling pathway, encodes two different proteins. *Genetics* 137, 987-997.
- Connor, R.J., and Pasquale, E.B. (1995). Genomic organization and alternatively processed forms of Cdk5, a receptor protein-tyrosine kinase of the Eph subfamily. *Oncogene* 11, 2429-2438.
- Costa, M., Wilson, E.T., and Wieschaus, E. (1994). A putative cell signal encoded by the folded gastrulation gene coordinates cell shape changes during *Drosophila* gastrulation. *Cell* 76, 1075-1089.
- Drescher, U., Kremoser, C., Handwerker, C., Löscherer, J., Noda, M., and Bonhoeffer, F. (1995). In vitro guidance of retinal ganglion cell axons by RAGS, a 25 kDa tectal protein related to ligands for the eph receptor tyrosine kinases. *Cell* 82, 359-370.
- Eph Nomenclature Committee (1997). Unified nomenclature for Eph family receptors and their ligands, the ephrins. *Cell* 90, 403-404.
- Fox, G.M., Holst, P.L., Chute, H.T., Lindberg, R.A., Janssen, A.M., Basu, R., and Welcher, A.A. (1995). cDNA cloning and tissue distribution of five human EPH-like receptor protein-tyrosine kinases. *Oncogene* 10, 897-905.
- Gale, N.W., Holland, S.J., Valenzuela, D.M., Flenniken, A., Pan, L., Ryan, T.E., Henkemeyer, M., Strebhardt, K., Hirai, H., Wilkinson, D.G., et al. (1996). Eph receptors and ligands comprise two major specificity subclasses and are reciprocally compartmentalized during embryogenesis. *Neuron* 17, 9-19.
- Gao, P.-P., Zhang, J.-H., Yokoyama, M., Racey, B., Dreyfuss, C.F., Black, I.B., and Zhou, R. (1996). Regulation of topographic projection in the brain: Elf-1 in the hippocamposeptal system. *Proc. Natl. Acad. Sci. USA* 93, 11161-11166.
- Glise, B., Bourbon, H., and Noselli, S. (1995). *hemipterous* encodes a novel *Drosophila* MAP kinase, required for epithelial cell sheet movement. *Cell* 83, 451-461.
- Hedgecock, E.M., and Herman, R.K. (1995). The *ncl-1* gene and genetic mosaics of *Caenorhabditis elegans*. *Genetics* 141, 989-1006.
- Henkemeyer, M., Orioli, D., Henderson, J.D., Saxton, T.M., Roder, J., Pawson, T., and Klein, R. (1996). Nuk controls pathfinding of commissural axons in the mammalian central nervous system. *Cell* 86, 35-46.
- Herman, R.K. (1995). Mosaic analysis. In *Caenorhabditis elegans: Modern Biological Analysis of an Organism*, H.F. Epstein and D.C. Shakes, eds. (San Diego, California: Academic Press), pp. 123-146.
- Hirai, H., Maru, Y., Hagiwara, K., Nishida, J., and Takaku, F. (1987). A novel putative tyrosine kinase receptor encoded by the *eph* gene. *Science* 238, 1717-1720.
- Hodgkin, J.A. (1997). Appendix 1: genetics. In *C. elegans* II, D.L. Riddle, T. Blumenthal, B.J. Meyer, and J.R. Priess, eds. (Cold Spring Harbor, New York: Cold Spring Harbor), pp. 881-1048.
- Holland, S.J., Gale, N.W., Mbalamu, G., Yancopoulos, G.D., Henkemeyer, M., and Pawson, T. (1996). Bidirectional signaling through the EPH-family receptor Nuk and its transmembrane ligands. *Nature* 383, 722-725.
- Hubbard, S.R., Wei, L., Ellis, L., and Hendrickson, W.A. (1994). Crystal structure of the tyrosine kinase domain of the human insulin receptor. *Nature* 372, 746-754.
- Knust, E. (1997). *Drosophila* morphogenesis: movements behind the edge. *Curr. Biol.* 7, R558-R561.

- Krause, M., and Hirsh, D. (1987). A trans-spliced leader sequence on actin mRNA in *C. elegans*. *Cell* 49, 753-761.
- Labrador, J.P., Brambilla, R., and Klein, R. (1997). The N-terminal globular domain of Eph receptors is sufficient for ligand binding and receptor signaling. *EMBO J.* 16, 3889-3897.
- Maisonpierre, P.C., Barrezuela, N.X., and Yancopoulos, G.D. (1993). Etk-1 and Etk-2: two novel members of the Eph receptor-like tyrosine kinase family with distinctive structures and neuronal expression. *Oncogene* 8, 3277-3288.
- Mello, C.C., Kramer, J.M., Stinchcomb, D., and Ambros, V. (1991). Efficient gene transfer in *C. elegans*: extrachromosomal maintenance and integration of transforming sequences. *EMBO J.* 10, 3959-3970.
- Miller, L.M., Waring, D.A., and Kim, S.K. (1996). Mosaic analysis using a *ncl-1(+)* extrachromosomal array reveals that *lin-31* acts in the Pn.p cells during *Caenorhabditis elegans* vulval development. *Genetics* 143, 1181-1191.
- Nakamoto, M., Cheng, H.-J., Friedman, G.C., McLaughlin, T., Hansen, M.J., Yoon, C.H., O'Leary, D.D.M., and Flanagan, J.G. (1996). Topographically specific effects of ELF-1 on retinal axon guidance in vitro and retinal axon mapping in vivo. *Cell* 86, 755-766.
- O'Bryan, J.P., Frye, R.A., Cogswell, P.C., Neubauer, A., Kitch, B., Prokop, C., Espinosa, R., III, Le Beau, M.M., Earp, H.S., and Liu, E.T. (1991). *axl*, a transforming gene isolated from primary human myeloid Leukemia cells, encodes a novel receptor tyrosine kinase. *Mol. Cell Biol.* 11, 5016-5031.
- Orioli, D., and Klein, R. (1997). The Eph receptor family: axonal guidance by contact repulsion. *Trends Genet.* 13, 354-359.
- Orioli, D., Henkemeyer, M., Lemke, G., Klein, R., and Pawson, T. (1996). Sek4 and Nuk receptors cooperate in guidance of commissural axons and in palate formation. *EMBO J.* 15, 6035-6049.
- Parks, S., and Wieschaus, E. (1991). The *Drosophila* gastrulation gene *concertina* encodes a G α -like protein. *Cell* 64, 447-458.
- Pasquale, E.B. (1991). Identification of chicken embryo kinase 5, a developmentally regulated receptor-type tyrosine kinase of the Eph family. *Cell Reg.* 2, 523-534.
- Priess, J., and Hirsh, D. (1986). *Caenorhabditis elegans* morphogenesis: the role of the cytoskeleton in the elongation of the embryo. *Dev. Biol.* 117, 156-173.
- Riesgo-Escovar, J.R., Jenni, M., Fritz, A., and Hafen, E. (1996). The *Drosophila* Jun-N-terminal kinase is required for cell morphogenesis but not for DJun-dependent cell fate specification in the eye. *Genes Dev.* 10, 2759-2768.
- Ruiz, J.C., and Robertson, E.J. (1994). The expression of the receptor-protein tyrosine kinase gene, *eck*, is highly restricted during early mouse development. *Mech. Dev.* 46, 87-100.
- Ruiz, J.C., Conlon, F.L., and Robertson, E.J. (1994). Identification of novel protein kinases expressed in the myocardium of the developing mouse heart. *Mech. Dev.* 48, 153-164.
- Schedl, T., and Kimble, J. (1988). *fog-2*, a germ-line-specific sex determining gene required for hermaphrodite spermatogenesis in *Caenorhabditis elegans*. *Genetics* 119, 43-61.
- Sluss, H.K., Han, Z., Barrett, T., Davis, R.J., and Ip, Y.T. (1996). A JNK signal transduction pathway that mediates morphogenesis and an immune response in *Drosophila*. *Genes Dev.* 10, 2745-2758.
- Sulston, J.E., Schierenberg, E., White, J.G., and Thomson, J.N. (1983). The embryonic cell lineage of the nematode *Caenorhabditis elegans*. *Dev. Biol.* 100, 64-119.
- Wicks, I.P., Wilkinson, D., Salvaris, E., and Boyd, A.W. (1992). Molecular cloning of *HEK*, the gene encoding a receptor tyrosine kinase expressed by human lymphoid tumor cell lines. *Proc. Natl. Acad. Sci. USA* 89, 1611-1615.
- Williams-Masson, E.M., Malik, A.N., and Hardin, J. (1997). An actin-mediated two-step mechanism is required for ventral enclosure of the *C. elegans* hypodermis. *Development* 124, 2889-2901.
- Winning, R.S., Scales, J.B., and Sargent, T.D. (1996). Disruption of cell adhesion in *Xenopus* embryos by Pagliaccio, an Eph-class receptor tyrosine kinase. *Dev. Biol.* 179, 309-319.
- Winslow, J.W., Moran, P., Shih, A., Valverde, J., Yuan, J.Q., Beck, K.D., Wong, S.C., Tsai, S.P., Goddard, A., Henzel, W.J., et al. (1995). Cloning of AL-1, a ligand for an Eph-related tyrosine kinase receptor involved in axon bundle formation. *Neuron* 14, 973-981.
- Xu, Q., Alldus, G., Holder, N., and Wilkinson, D.G. (1995). Expression of truncated *Sek-1* receptor tyrosine kinase disrupts the segmental restriction of gene expression in the *Xenopus* and zebrafish hindbrain. *Development* 121, 4005-4016.
- Yaciuk, P., and Shalloway, D. (1986). Features of the pp60^{src} carboxyl terminus that are required for transformation. *Mol. Cell Biol.* 6, 2807-2819.

Genbank Accession Number

The Genbank accession number for the *vab-1* cDNA sequence is AF040269.

An early developmental role for Eph-ephrin interaction during vertebrate gastrulation[☆]

Andrew C. Oates^{a,1,2}, Martin Lackmann^{a,b,1,*}, Mary-Anne Power^c, Caroline Brennan^d,
L. Michelle Down^c, Cuong Do^a, Betty Evans^c, Nigel Holder^d, Andrew W. Boyd^c

^aLudwig Institute for Cancer Research (Melbourne Branch) Post Office, Royal Melbourne Hospital, Victoria 3050 Australia

^bCooperative Research Centre for Cellular Growth Factors, Post Office, Royal Melbourne Hospital, Victoria 3050 Australia

^cQueensland Institute for Medical Research, The Bancroft Centre, Post Office, Royal Brisbane Hospital, 4029 Queensland Australia

^dDepartment of Anatomy and Developmental Biology, University College, Gower Street, London WC1E 6BT, UK

Received 15 October 1998; received in revised form 11 February 1999; accepted 12 February 1999

Abstract

Eph receptor tyrosine kinases (RTK) and their ephrin ligands are involved in the transmission of signals which regulate cytoskeletal organisation and cell migration, and are expressed in spatially restricted patterns at discrete phases during embryogenesis. Loss of function mutants of Eph RTK or ephrin genes result in defects in neuronal pathfinding or cell migration. In this report we show that soluble forms of human EphA3 and ephrin-A5, acting as dominant negative inhibitors, interfere with early events in zebrafish embryogenesis. Exogenous expression of both proteins results in dose-dependent defects in somite development and organisation of the midbrain-hindbrain boundary and hindbrain. The nature of the defects as well as the distribution and timing of expression of endogenous ligands/receptors for both proteins suggest that Eph-ephrin interaction is required for the organisation of embryonic structures by coordinating the cellular movements of convergence during gastrulation. © 1999 Elsevier Science Ireland Ltd. All rights reserved.

Keywords: Vertebrate embryogenesis; Development; Eph; Ephrin; EphA3; EphA1; EphB1; Ephrin-A5; L1; HEK; LERK-7; Gastrulation; Somitogenesis; CNS patterning; Mesoderm; Boundary formation; Zebrafish; Danio rerio; RNA microinjection; BIAcore analysis; Fc-fusion; Whole-mount in situ hybridisation

1. Introduction

Complex and cellular movements form the three primary germ layers lay out the architecture of the vertebrate body during gastrulation (reviewed in Ho, 1992; Slack et al., 1992; Tam and Quinlan, 1996; Harland and Gerhart, 1997). Cell-fate inducing signals, which are released initially from the vegetal mass of the blastula (in *Xenopus*) and later from the dorsal organiser (embryonic shield in zebrafish) to induce dorso-ventral and anterior-posterior polarities in the blastula and gastrula, include members of the TGF- β , *wnt* and FGF superfamilies of growth factors (reviewed: Kessler and Melton, 1994; Heasman, 1997). In

contrast, little is known about the mechanisms and signals by which gastrulating cells coordinate involution and/or ingression, guide their migration as they converge to the midline, and finally intercalate along the dorsal axis.

Eph receptors and their ephrin ligands, along with other protein families, including netrins, semaphorins and cadherins, guide the migration of growth cones to the correct target location for synaptogenesis (for review see Kennedy and Tessier-Lavigne, 1995; Müller et al., 1996; Nieto, 1996; Tessier-Lavigne and Goodman, 1996; Flanagan and Vanderhaeghen, 1998) and the targeted migration of neural crest cells in streams from the dorsal neural tube (reviewed in Robinson et al., 1997). On the basis of sequence homology, members of the Eph subfamily of receptor tyrosine kinases (RTKs) fall into two receptor subclasses. EphA and EphB, which display affinities for either GPI-linked (ephrin A) or transmembrane (ephrin B) ligands, respectively. The current model of Eph-ephrin signalling in growth cone pathfinding involves the migration of an Eph-bearing growth cone into a gradient of ephrin expression (reviewed in: Friedman and O'Leary, 1996; Pasquale, 1997; Flanagan and Vanderhaeghen, 1998), leading to cell

[☆] This manuscript is dedicated to our dear friend and collaborator Nigel Holder who tragically died during submission of this manuscript.

* Corresponding author. Tel.: + 61-3-9341-3171; fax: + 61-3-9341-3104.

E-mail address: martin.lackmann@ludwig.edu.au (M. Lackmann).

¹ Current address: Moffett Laboratories 323, Department of Molecular Biology, Princeton University, Washington Road, Princeton, New Jersey 08544, USA.

² The first two authors made equal contributions to this manuscript.

contact-dependent Eph receptor activation (Davis et al., 1994; Bruckner and Klein, 1998) which instructs the growth cone to change direction and avoid the ligand-rich area. Eph-ephrin interactions thus deliver a growth cone repulsion signal. For the EphA3 receptors (HEK/MEK4/CEK4) and their ephrin-A2 and A5 ligands (ELF1 and AL-1/RAGS/zEphL4), nerve guidance functions during the development of the retinotectal projection map have been established (Cheng et al., 1995; Drescher et al., 1995; Nakamoto et al., 1996; Brennan et al., 1997; Monschau et al., 1997; Frisen et al., 1998). In addition to the retinal axon guidance defects in the midbrain of mice lacking ephrin-A5, a significant proportion of these ephrin-deficient mice display additional defects in dorsal midline structures, resulting in anencephaly or open crania with cleft nose and palate (Frisen et al., 1998). This extreme phenotype suggests functions for the ephrin-A5/EphA receptor signalling system in addition to those in growth cone pathfinding.

It is noteworthy that members of the Eph and ephrin families are also expressed earlier in vertebrate development, during gastrulation. EphA2 is expressed in the primitive streak of mouse embryos (Ganju et al., 1994; Ruiz et al., 1994), and the *Xenopus* EphA4 homolog, *pagaliaccio*, is expressed during gastrulation in the involuting mesoderm (Winning and Sargent, 1994). The *Xenopus* ephrin-B1 homolog is also expressed during gastrulation, and ectopic expression of this protein causes a loss of cell adhesion prior to the onset of gastrulation (Jones et al., 1998), similar to the effect of activated *pagaliaccio* (Winning et al., 1996). In contrast, the ectopic expression of EphB2 in the ventral blastomeres of *Xenopus* causes dorsalisation of the embryo before the onset of gastrulation (Tanaka et al., 1998). In zebrafish, there are seven *Eph* genes, *rtkl-3*, *rtk5*, 6, 8, and *zdk1* known to be expressed in a regulated manner during gastrulation (Xu et al., 1994; Taneja et al., 1996; Cooke et al., 1997). However, sequence alignment reveals significant differences to human EphA3 (A. Boyd, unpublished data), suggesting that a zebrafish EphA3 homologue had not yet been isolated.

The high degree of structural and functional conservation of Ephs and ephrins in vertebrate evolution has enabled the use of dominant negative mammalian EphA receptors to study the function of these proteins during zebrafish development, and as a read-out for receptor structure-function studies (Xu et al., 1995; Xu et al., 1996; Lackmann et al., 1998). The expression of Eph and ephrins during vertebrate gastrulation prompted us to examine potential functions of Eph-ephrin interaction in this process. We have previously established that human EphA3 interacts with a distinct hierarchy of affinities with all ephrin-A ligands tested, whereby the highest affinity was determined between EphA3 and ephrin-A5 (Lackmann et al., 1996; Lackmann et al., 1997). In subsequent experiments with dominant negative human EphA3 constructs we demonstrated a role for the ephrin-binding domain of EphA receptors in embryonic axis organisation and somite formation (Lackmann et al.,

1998). The present study examines the developmental basis of this phenomenon. We demonstrate that expression of soluble forms of either human EphA3 or its high affinity ligand ephrin-A5 in zebrafish embryos produce indistinguishable patterns of disruption of the notochord, somites and brain. These effects are preceded by apparent cell migration defects throughout gastrulation, as indicated by perturbed *ntl* expression patterns around the blastula margin and during formation of the presumptive notochord. We report the identification of the zebrafish homologue of EphA3 and describe the expression pattern of the corresponding mRNA during gastrulation that is consistent with the timing and location of the dominant-negative effects. Our observations imply that EphA-ephrin-A signalling is active during involution and convergence movements and thus is required for the correct execution of gastrulation.

2. Results

2.1. Expression of active soluble human EphA3 and ephrin-A5 protein in the zebrafish embryo

To evaluate the role and specificity of Eph-ephrin interactions during early vertebrate embryogenesis we adopted a previously established dominant negative approach (Lackmann et al., 1998). We introduced capped mRNA encoding FLAG (refers to the amino acid sequence DYKDDDDK) epitope-tagged forms of either soluble EphA3 (HEK) extracellular domain (ECD, mRNA encoding the FLAG-tagged human EphA3 ECD (sh EphA3-RNA), 10 pg per embryo) or soluble human ephrin-A5 (Lackmann et al., 1997) (mRNA encoding the soluble, FLAG-tagged form of human ephrin-A5 (sh ephrin-A5-RNA), 100 pg/embryo) into zebrafish embryos at the 1–2 cell stage, by microinjection into the blastoderm or into the yolk cell directly under the blastoderm. Injected in this manner mRNA became widely distributed throughout the embryo (as shown by co-injection of mRNA encoding green fluorescent protein (GFP), see Lackmann et al., 1998) and was translated into the expected proteins (Fig. 1a,b). A marginally increased apparent molecular weight was observed for the zebrafish-expressed sh ephrin-A5 relative to sh ephrin-A5 produced by CHO cells, suggesting increased glycosylation of the zebrafish-produced protein (Fig. 1a). Importantly, BIAcore analysis of zebrafish extracts using sensorchips coated with the EphA3 ECD (for ephrin-A5 analysis) or a native conformation-specific anti-EphA3 MAbs (for EphA3 ECD analysis) demonstrated that correctly folded and functionally-active proteins were expressed in the embryos throughout early development (Fig. 1b). The approximate concentrations of sh EphA3 (soluble human EphA3 extracellular domain) and sh ephrin-A5 at the onset of gastrulation were 0.5 and 10 ng/embryo respectively, rising to 3 and 25 ng/embryo respectively from 15 h post fertilisation (hpf) onwards.

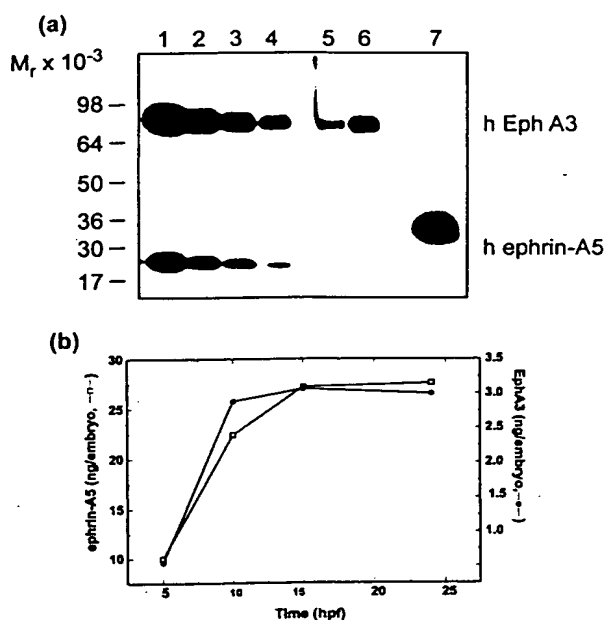


Fig. 1. Detection of exogenous sh EphA3 and sh ephrin-A5 in zebrafish embryos by Western blot and BIAcore analysis. (a) Comparison of CHO-cell derived sh EphA3 and sh ephrin-A5 (lanes 1–4) with the corresponding proteins extracted from injected zebrafish embryos (lanes 5–7). Samples of zebrafish lysates (10 embryos/0.1 ml) containing 25, 12.5, 6.25, 3.125 ng of CHO cell-derived sh EphA3 and sh ephrin-A5 (lanes 1–4, respectively) were immunoprecipitated with anti-FLAG MAb (M2) agarose and analysed by Western blot. Zebrafish embryos which had been injected with sh EphA3-RNA (10 pg/embryo) or sh ephrin-A5-RNA (100 pg/embryo) were lysed after 5h (lane 5) or 10 h (lanes 6,7) and analysed in parallel lanes of the gel. sh ephrin-A5 extracted from zebrafish embryos had an increased size compared to its CHO cell-produced counterpart. (b) BIAcore analysis of lysates from sh EphA3-RNA or sh ephrin-A5-RNA-injected (100 pg/embryo) zebrafish embryos. Samples were prepared 5, 10, 15 and 24 hpf and analysed on a sensorchip containing the conformation-specific anti-EphA3 MAb IIIA4 (Boyd et al., 1992; Lackmann et al., 1996) to detect the intact exogenous receptor ECD (—●—), and a sh EphA3-derivatised sensorchip to monitor functionally-intact ephrin-A5 (—□—). The responses were compared to samples of zebrafish lysates containing known amounts of the purified, CHO cell expressed proteins.

2.2. Soluble human EphA3 and ephrin-A5 cause indistinguishable defects in the organisation of neur ectoderm and mesoderm during early embryonic zebrafish development

Inspection of developing zebrafish injected with 100 pg of sh EphA3 RNA revealed the presence of a distinctive syndrome of defects in approximately 50% of individuals (see also Fig. 4, below). During gastrulation, an uneven retardation of epiboly was observed, resulting in an irregular gastrula margin relative to control embryos (data not shown). In early segmentation stages, between 11 and 15 hpf, the dorsal axis was reduced in height above the yolk surface and tailbud formation was dramatically retarded (compare Figs. 2a and 2b). Viewed dorsally, the animals displayed a range of defects in paraxial mesoderm, including disorganisation and/or loss of somites and their bound-

aries, and an extension of the somitic boundary clefts into lateral regions of the embryos (compare Figs. 2d and 2e). The notochord was often twisted (Figs. 2e and 7 below). In addition, the organisation of the anterior neur ectoderm was affected, with laterally broadened and twisted mid- and hindbrain regions. Although the height of the forebrain above the yolk surface was reproducibly reduced (Fig. 2b), the formation of the optic vesicle was not noticeably disrupted (data not shown). Exogenously expressed sh ephrin-A5 resulted in an indistinguishable phenotype in approximately 50% of zebrafish embryos injected with 100 pg of the corresponding mRNA at all stages examined (Fig. 2c,f and see below, Fig. 4) consistent with a disruption of the same signalling processes inhibited by exogenous sh EphA3.

The array of differentiated embryonic structures existing by segmentation stages present a sensitive readout of the processes of gastrulation that underly their formation. Therefore, to analyse the effects of ectopic EphA3 and ephrin-A5 expression on cell fate and position in greater detail, embryos injected with a range of concentrations of sh EphA3 or sh ephrin-A5 RNA (see below, Fig. 4) were fixed in early segmentation stages between 12 and 13 hpf. Whole mount in situ hybridisation was used to monitor the expression of developmentally important regulatory genes marking ventral fore- and midbrain (*hlx1*, Fjose et al., 1994), midbrain-hindbrain boundary (MHB, or isthmus) (*pax2.1*, Krauss et al., 1991), rhombomeres 3 and 5 of the hindbrain (*krox20*, Oxtoby and Jowett, 1993), and adaxial and paraxial muscle (*myoD*, Weinberg et al., 1996). The expression patterns of these genes in normal embryos at this developmental stage is illustrated in Fig. 3a,b.

In both sh EphA3 and sh ephrin-A5 RNA injected embryos there was a consistent disorganisation of the paraxial mesoderm. A highly irregular pattern in the lateral stripes of *myoD* expressing cells in the paraxial mesoderm confirmed the observation in live embryos (Figs. 2e,f) that somite formation is affected. Many somites were missing or out of register across the midline (Fig. 3d,f), whereas other *myoD* expressing cells were arrayed in a pattern consistent with the fusion of a somite across expected somite boundaries (Fig. 3f). The paraxial *myoD* expression domains were extended more laterally from the midline (Fig. 3f). Furthermore, the distance between *myoD* positive cells of the adaxial mesoderm was increased across the midline (Fig. 3d), which was often twisted, suggesting a defect in the positioning of adaxial cells prior to somitogenesis (Weinberg et al., 1996).

Examination of anterior neur ectodermal structures of embryos injected with sh EphA3 and sh ephrin-A5 RNA revealed that the limits of groups of cells in the MHB and hindbrain expressing respectively *pax2.1* and *krox20*, were extended laterally, often accompanied by irregular anterior and posterior boundaries (Fig. 3c,e). Defects in the hindbrain, as revealed by *krox20* expression, were always more severe than defects in the MHB; further, the rhombo-

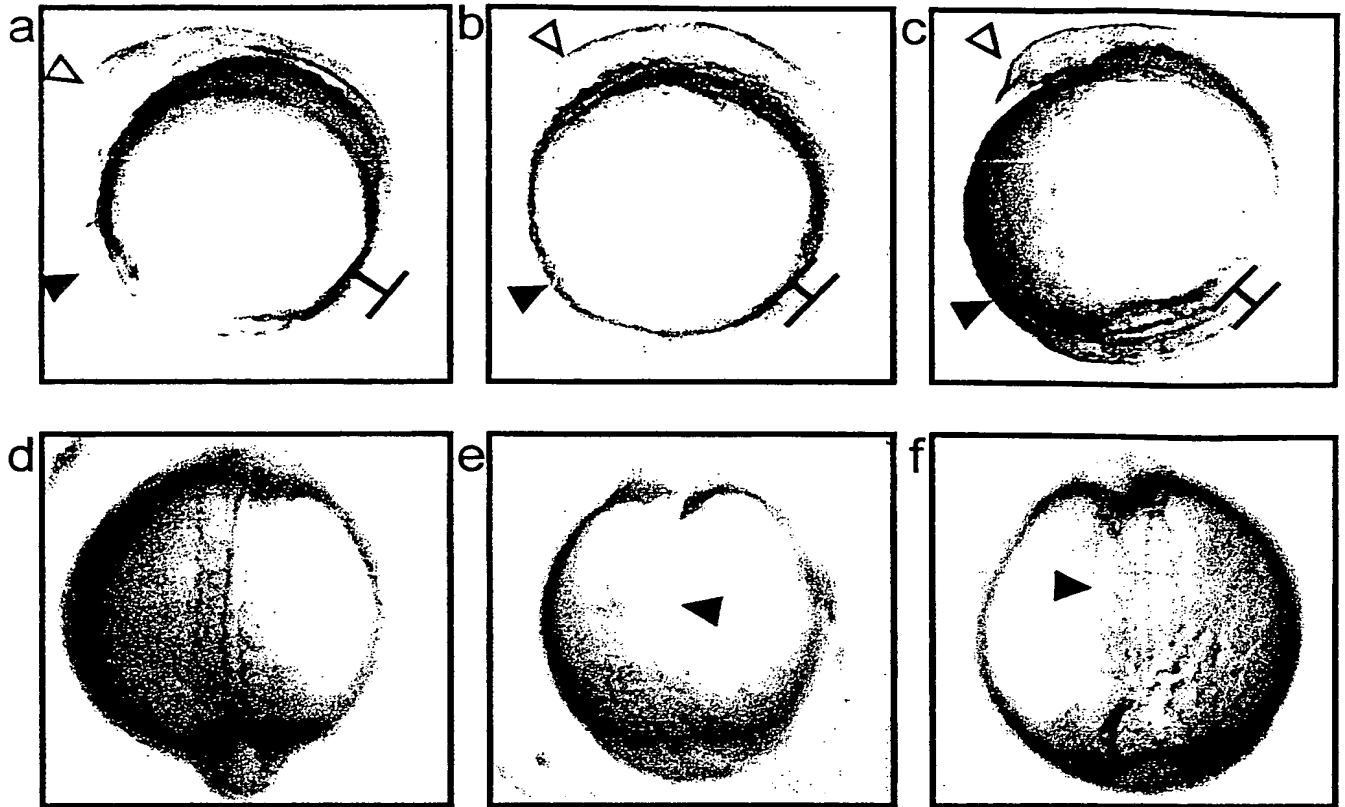


Fig. 2. Effect of ectopic expression of human sh EphA3 ECD or the soluble form of its ligand sh ephrin-A5 on the development of zebrafish embryos. (a–f) Zebrafish embryos, uninjected or injected with 5 pg marker mRNA and with 10 pg of either sh EphA3-RNA or sh ephrin-A5 mRNA during the first two cleavage divisions, were raised at 28°C. After 12–13 h embryos were photographed from a lateral perspective in a,b,c with dorsal to the right and anterior up, and from a dorsal perspective (d–f) with anterior up in each frame. (a) A non-injected zebrafish embryo at 12 hpf showing normally developed forebrain (open arrowhead) and tailbud (closed arrow head) and revealing a normal dorsal height of the trunk from the yolk surface (H). (b) A zebrafish embryo at 12 h after microinjection with 10 pg sh EphA3-RNA displaying reduced development of the mid- and hindbrain, poorly developed forebrain (open arrowhead), reduced height of the trunk from the yolk surface (H) and absence of intersomitic grooves and tailbud (closed arrowhead). (c) A zebrafish embryo at 12 hpf after microinjection with 10 ng sh ephrin-A5-RNA displaying an indistinguishable phenotype to embryos injected with the sh EphA3-RNA. (d) Dorsal view of the non-injected embryo illustrated in (a), revealing well-developed somitic boundaries, lining up in register along the midline. (e,f) Dorsal views of embryos shown in (b) and (c), respectively, showing disorganisation and/or loss of somite boundaries (closed arrowheads), and crooked notochord (e).

mere five domain of *krox20* was always more severely affected, i.e. laterally displaced than rhombomere three. Occasionally, a cluster of *krox20* expressing cells was seen separated from rhombomere three or five (Fig. 3c). In contrast, a single axially located stripe of *hlx1* expressing cells appeared unaffected in the sh EphA3 or sh ephrin-A5 RNA injected embryos, suggesting wildtype development of the ventral diencephalon and midbrain (Fig. 3c,e). In these dominant negative experiments we noted a spectrum in the intensity of these defects, whereby the most severely affected embryos displayed a median gap at the midline, demarcated with *krox20* and *myoD* expressing cells on either side (data not shown). Thus, examination of gene expression *in situ* in embryos injected with either sh EphA3 or sh ephrin-A5 RNA indicates defects in the organisation of mesodermal and ectodermal derivatives that suggest a disturbance of the convergence movement of cells to the dorsal midline during gastrulation. Further,

using the markers available, the effects of the expression of sh EphA3 and sh ephrin-A5 on development cannot be distinguished, implying that the same developmental process(es) are disrupted in each case.

2.3. Coexpression of soluble human EphA3 and ephrin-A5 rescues defective development

We next performed experiments to address the possibility that the observed defects could be due to non-specific effects of the microinjections on development. Embryos were injected with mRNAs coding for proteins unrelated to Ephs or ephrins to control for disruption of development due to production of exogenous protein. Non-injected control embryos, or embryos injected with mRNA encoding GFP at a concentration of 250 pg/embryo did not display any developmental defects (Fig. 3a,b and Lackmann et al., 1998). Embryos were also injected with mRNA encoding a

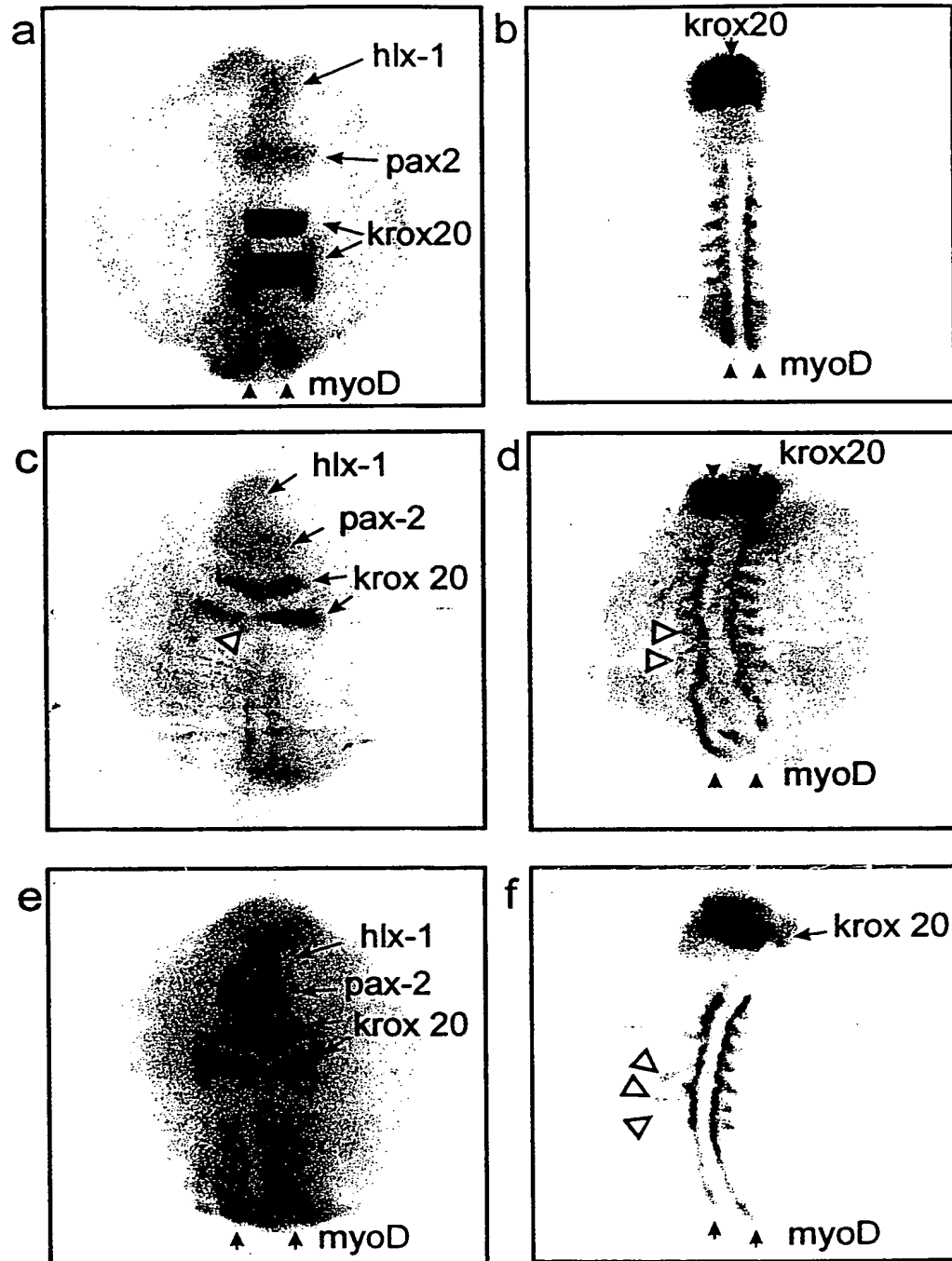


Fig. 3. In situ hybridisation reveals somitic, mid-hindbrain boundary (MHB) and hindbrain defects upon ectopic sh EphA3 or sh ephrin-A5 expression. Embryos were injected with 10 pg of either sh EphA3-RNA or sh ephrin-A5-RNA, allowed to develop for 12.13 hpf and fixed for in situ hybridisation with *pax2.1*, *hlx1*, *krox20* and *myoD* DIG-labelled riboprobes. Embryos are photographed from a dorsal perspective with anterior to the top and posterior to the bottom of each frame: (a,c,e) antero-dorsal view; (b,d,f) posterior-dorsal view. (a,b) Uninjected embryo at 12 hpf showing normal expression of *hlx1* in the ventral fore- and midbrain, *pax2.1* in the MHB, *krox20* in rhombomeres three and five of the hindbrain and *myoD* in the paraxial and adaxial mesoderm. Note the sharp boundaries between regions of expressing and non-expressing cells. (c,d) sh EphA3-RNA (10 pg) injected embryo at 12 hpf showing *pax2.1* and *krox20* expressing cells in the MHB and hindbrain with irregular boundaries. A cluster of *krox20* expressing cells is found posterior to rhombomere five the normal site of expression (open arrowhead in (c)). *myoD* expressing cells of the paraxial mesoderm in the posterior part of the embryo show disorganisation (open arrowheads in d). In contrast, an intact *hlx1* stripe is present anteriorly (e). (e,f) sh ephrin-A5-RNA (10 pg) injected embryo at 12 hpf demonstrating a phenotype which is indistinguishable from the sh EphA3-RNA injected embryos. Note the presence of *myoD* expressing cells (open arrowheads in (f)) which do not align either across the midline, or parallel to each other.

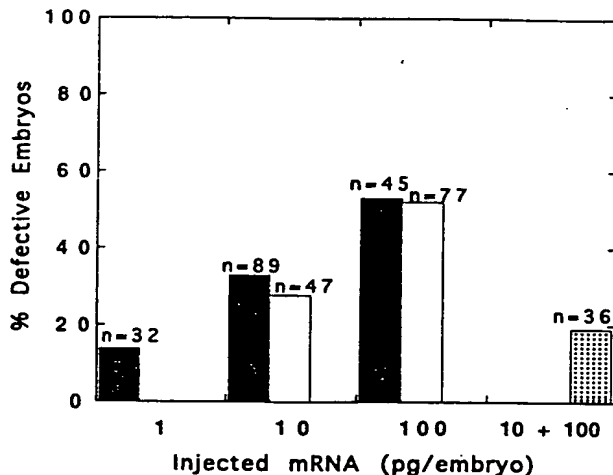


Fig. 4. Dose response and phenotypic rescue of sh EphA3 and sh ephrin-A5-induced developmental defects. Batches of embryos, injected with indicated amounts sh EphA3-RNA (■), sh ephrin-A5-RNA (□) or a combination of 10 pg sh EphA3-RNA and 100 pg sh ephrin-A5-RNA (▨) and a constant amount of E-GFP mRNA (5 pg) were allowed to grow for 12,13 hpf before fixation and hybridisation with *pax2.1*, *hlx1*, *krox20* and *myoD* DIG-labelled riboprobes. Embryos were analysed under a dissecting microscope and scored for disrupted patterns of gene expression. Non-injected control embryos were scored after an identical developmental period and identical handling to the injected embryos to control for defects due to the genetic background of particular parents in our strain. None of these embryos showed any reproducible or significant defects.

FLAG epitope-tagged, soluble form of murine deleted in colon carcinoma (DCC) (Cooper et al., 1995). The resulting protein was detected in embryo extracts at comparable levels to sh EphA3 and sh ephrin-A5 throughout development (not shown). Although expression of exogenous soluble DCC in *Xenopus* embryos induces a distinct axonal guidance defect (R.A. Anderson, H.M. Cooper et al., submitted), there was no detectable disruption of adaxial and paraxial mesoderm, or mid- and hindbrain organisation in zebrafish.

Dose-response experiments were performed to further address the possibility that the observed defects could be due to a novel, non-physiological action of EphA3 and ephrin-A5 or due to non-specific toxicity of the injected material. In either of these cases co-injection of sh EphA3 and sh ephrin-A5 RNA should lead to an additive increase in the number of defective embryos. A partial reduction or rescue of the defects would be expected if expression of either sh EphA3 or sh ephrin-A5 interfered specifically with Eph-ephrin signalling processes, as the binding of exogenous receptor and ligand would titrate the specific activity of both proteins. Previously we have demonstrated that the injection of increased amounts of mRNA leads to increased production of the corresponding functionally active protein (Lackmann et al., 1998). When increasing concentrations of either sh EphA3 or sh ephrin-A5 RNA were injected into embryos, a dose-dependent increase in the number of embryos displaying the developmental

syndrome described above was observed (Fig. 4). Thus, injection of 100 pg sh ephrin-A5-RNA caused defective axis and somite organisation in approximately 50% of embryos, and injection of 10 pg sh EphA3 RNA resulted in indistinguishable defects in 35% of the treated embryos. In contrast, co-injection of sh ephrin-A5 and sh EphA3 RNA at these concentrations caused defects in only 20% of the treated embryos (Fig. 4). Together these data demonstrate that disruption of adaxial and paraxial mesoderm and of mid- and hindbrain organisation in zebrafish embryos injected with sh EphA3 and sh ephrin-A5 RNA is mediated by expression and specific activity of the corresponding proteins, and suggests that both dominant negative proteins interfere with the same endogenous Eph-ephrin mediated processes.

2.4. Soluble human EphA3 expression causes defects in the presumptive notochord during gastrulation

Our observations suggesting aberrant morphology during gastrulation, combined with the apparent defects in convergence evident by the early segmentation stage in embryos injected with sh EphA3 or sh ephrin-A5 RNA, led us to monitor cell convergence during gastrulation more closely. We used the expression of the notochord-specific gene *ntl* (Halpern et al., 1993; Schulte-Merker et al., 1994) measured by in situ hybridisation as a marker for mesodermal convergence to the midline in sh EphA3 RNA injected embryos between onset and completion of gastrulation (6–10 hpf). In untreated shield-stage (50–60% epiboly) embryos, *ntl* expressing cells are arranged in a uniform radial pattern, following the germ ring and marking the embryonic shield (Fig. 5a) (Schulte-Merker et al., 1994). Defects in the expression pattern of the *ntl* expressing cells were noted in approximately 50% of sh EphA3 RNA injected embryos, ranging from a diffuse, poorly converged shield and irregular shaped blastula margin (Fig. 5b) to lack of shield formation and scattered *ntl* expressing cells around the dorsal midline (Fig. 5c). By 80–90% epiboly, *ntl* expressing cells of the epiblast of the non-injected embryos have converged and extended anteriorly and posteriorly along the dorsal midline (Warga and Kimmel, 1990; Concha and Adams, 1998) to form a tight band of the presumptive notochord (Fig. 5d). In contrast, *ntl* expressing cells of injected embryos at the same developmental stage had not converged equivalently and appeared as a broadened stripe which extended over the anterior-posterior length of the dorsal midline (Fig. 5e,f). Furthermore, the progress of the gastrula margin at this stage and later seemed to be retarded. Experimental and control embryos derived from the same clutch were co-hybridised with *pax2.1*, which is expressed with increasing level in the area of the presumptive midbrain (Fig. 5g–i), demonstrating that the illustrated embryos were analysed at equivalent stages of their development. By the end of gastrulation (95–100% epiboly) the difference between the *ntl* expression pattern of non-injected embryos

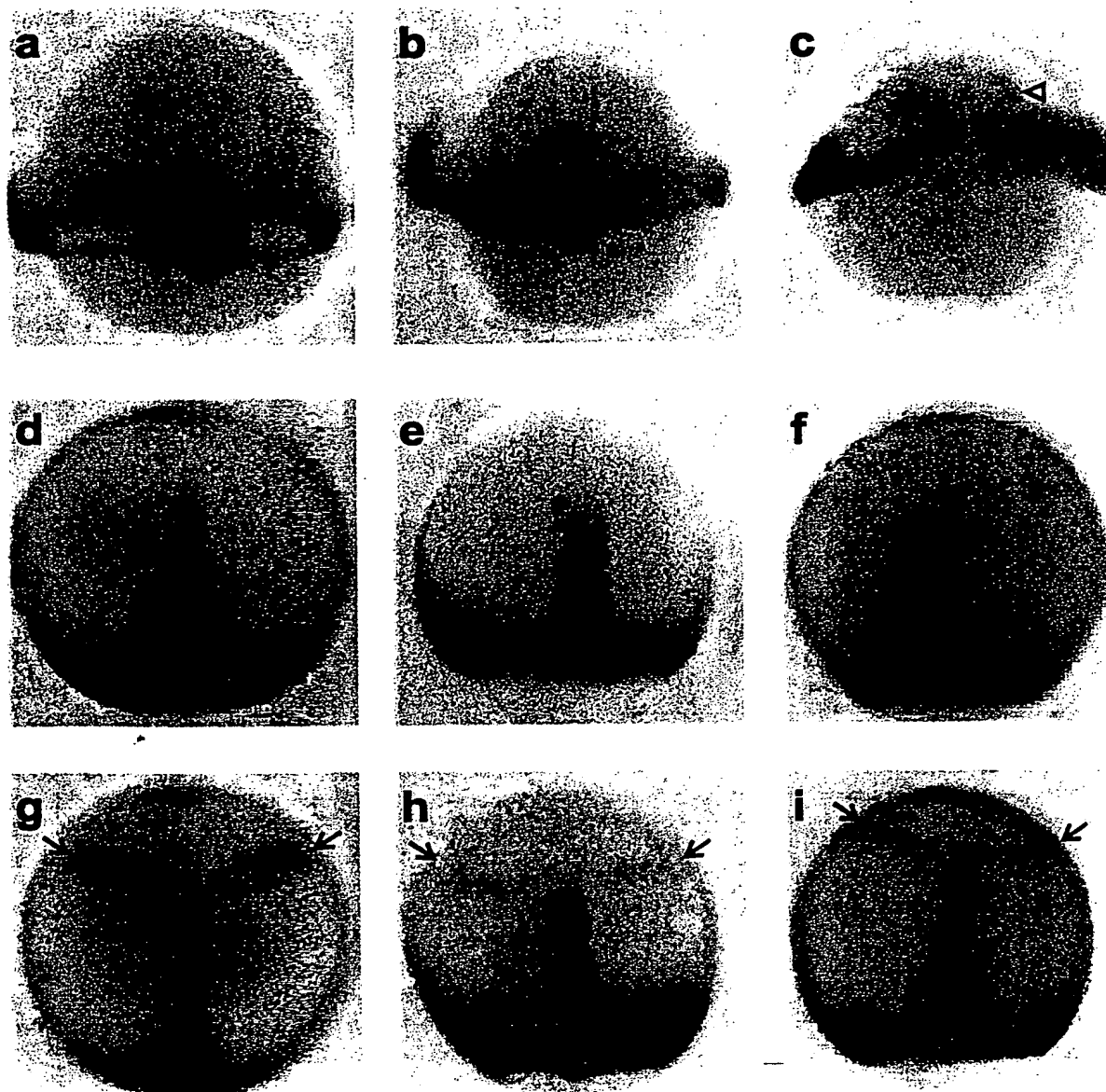


Fig. 5. *ntl* in situ hybridisation reveals convergence defects during gastrulation in *hs EphA3*-expressing embryos. Batches of zebrafish embryos were injected with 10 pg *sh EphA3* mRNA and analysed at various time points during gastrulation by in situ hybridisation with a DIG-labelled riboprobes specific for *ntl* and *pax2.1* (b,c,e,f,h,i). Non-injected control embryos from the same clutch were analysed in parallel (a,d,g). Embryos are oriented dorsally with anterior up, whereby examples of injected embryos with moderate (b,e,h) and severe (c,f,i) gastrulation defects are shown. (a–c) Embryos at 50–60% epiboly: *ntl*-staining illustrates the newly formed shield and an even path around the blastula margin in non-injected embryos (a). Closed arrows in these panels and in panels (d–f) indicate the approximate position, at which the presumptive notochord -width was determined (see Fig. 5). Moderately (b) and severely-affected (c) embryos reveal an uneven margin and retarded or absent formation of a shield. The open arrow in (c) indicates *ntl* expressing cells that are separated from the shield area. (d–f) 80–90% epiboly embryos with distinct *ntl* staining of the presumptive notochord and of the closing yolk plug (d). Anteriorly, faint bands of *pax2.1*-staining are discernable. The phenotype of affected embryos ranges from a substantially widened median stripe of *ntl*-expressing cells and a 'kinked' shape of the presumptive notochord (e) to diffuse *ntl* staining extending in a broad band from the yolk plug to the posterior base of *pax2.1* staining (f). (g,h) Towards the end of gastrulation (95–100% epiboly) *ntl* staining marks the notochord as a straight line of cells from the posterior, medial tips of the *pax2.1* domains (marked by arrows) to the closed yolk plug in control embryos (g), while affected embryos reveal a distinctively twisted notochord (h,i).

(Fig. 5g; Schulte-Merker et al., 1994) and injected embryos had become less pronounced with respect to the width of the presumptive notochord (Fig. 5h,i and see below, Fig. 6a). On the other hand, injected embryos could be distinguished

by a distinctively kinked appearance of the *ntl*-stained notochord at this stage (Fig. 5h,i).

In order to quantitate the effect of dominant negative *hs EphA3* on the convergence of early mesodermal cells at

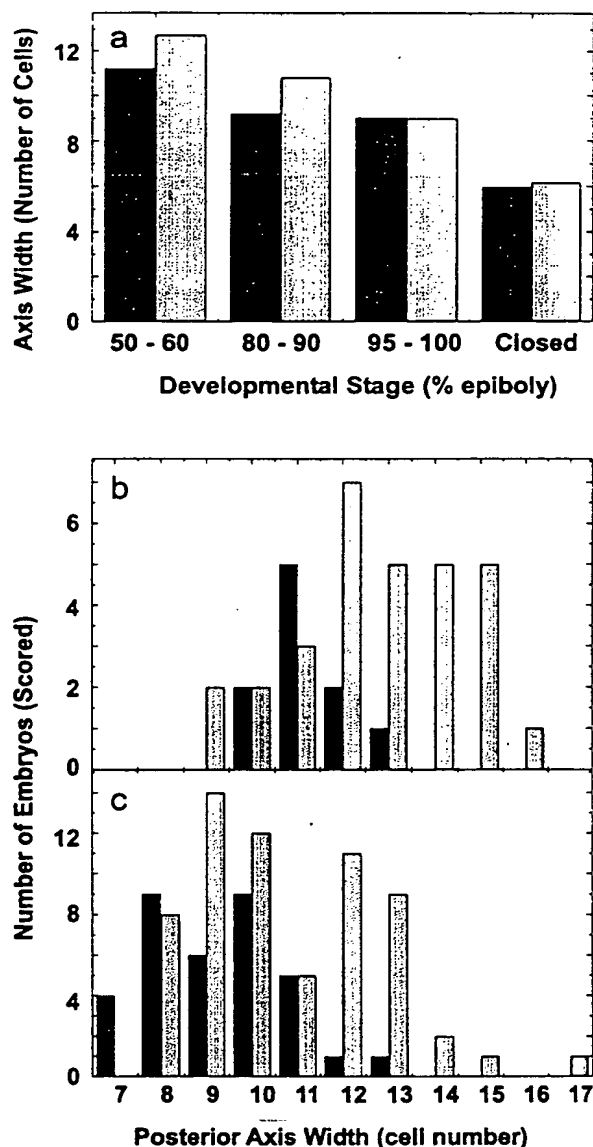


Fig. 6. The width of presumptive notochord is significantly increased in embryos injected with sh EphA3-RNA. Batches of sh EphA3 mRNA-injected and control embryos analysed at various time points during gastrulation as indicated by *in situ* hybridisation with a *ntl*-specific riboprobe and the posterior width (in number of cells) across the presumptive notochord determined (a). The mean axis width of non-injected control embryos (■) and of injected embryos (▨) is shown. (b,c) Untreated (■) and injected (▨) embryos are grouped by their posterior axis width, which is plotted against the number of scored individuals. The distribution of the axis width around a statistical mean was ranked by Mann–Whitney *U*-test, suggesting an additional population with increased notochord width at 50–60% epiboly ($P < 0.01$, panel (b)) and at 80–90% epiboly ($P < 0.003$, panel (c)).

varying stages during gastrulation, we estimated the width across the posterior end of the presumptive notochord by counting the number of *ntl*-positive cells at this position in sh EphA3-RNA injected and in uninjected embryos (Fig. 6). In agreement with the findings illustrated above, we observed significant differences by this criterion for

embryos at 50–60% and 80–90% epiboly, whereas towards the end of gastrulation (95–100% epiboly) the mean notochord width was essentially the same in injected and non-injected embryos (Fig. 6a). A more detailed analysis of the data suggests that during early and late gastrulation injected embryos can be grouped into wildtype and affected populations by the number of *ntl*-expressing cells across the developing notochord (Fig. 6b,c). At 50–60% epiboly some 50% of the injected embryos displayed a wildtype distribution of 11 ± 2 cells across the presumptive notochord, whereas the affected phenotype was characterised by a significantly (Mann–Whitney *U* test, $P < 0.01$) increased width of 14 ± 2 *ntl*-expressing cells (Fig. 6b). Later during gastrulation (80–90% epiboly), the wildtype notochord width had decreased to 9 ± 2 cells, while some 50% of the injected embryos display a significantly (Mann–Whitney *U*-test, $P < 0.003$) increased posterior axis width of 13 ± 2 cells (Fig. 6c).

By early segmentation stages of development, the notochord of affected embryos injected with sh EphA3 RNA was severely deformed. In contrast to the wildtype expression of the *ntl* gene (Fig. 7a), the affected phenotype of 12 hpf embryos injected with sh EphA3 RNA ranged from a distinctly twisted and shortened notochord (Fig. 7b) to structures where *ntl*-expressing cells formed two twisted tracks for short stretches along the anterior/posterior axis (Fig. 7c). Parallel staining of these embryos with *pax2* and *krox20* probes demonstrated failure of the convergence of the presumptive mid- and hindbrain in the same embryos (Fig. 7b,c). The appearance of *ntl* expression patterns during gastrulation are consistent with the twisted and broadened axial structures observed in living embryos (Fig. 2e) and inferred from the increased distance across the midline between *myoD*-expressing adaxial cells (Fig. 3d). These findings indicate that ectopic expression of dominant-negative EphA3 affects development from the onset of gastrulation, with defects in the convergence of cells to the midline also found in the axial mesoderm.

2.5. Expression and activity during gastrulation of zebrafish EphA3 and ephrin-A-L1

We next assessed which EphA or ephrin-A family members are expressed during gastrulation, and hence might be subject to interference by the dominant negative hs'EphA3 and ephrin-A5 constructs. Significant differences in the primary protein structure of EphA3 and the known zebrafish EphAs suggest that the zebrafish EphA3 homologue had not been described yet. Therefore, we screened a zebrafish library with a human EphA3 probe and isolated a cDNA clone containing partial EphA3-related DNA sequences (A. Boyd, in preparation) including the predicted C-terminal third of exon 3 (ligand binding domain), exons 4, 5 and 6 and the beginning of exon 7 (Lackmann et al., 1998). Alignment of the corresponding amino acid sequence with homologous sequences from human (h) EphA3 and chick (en

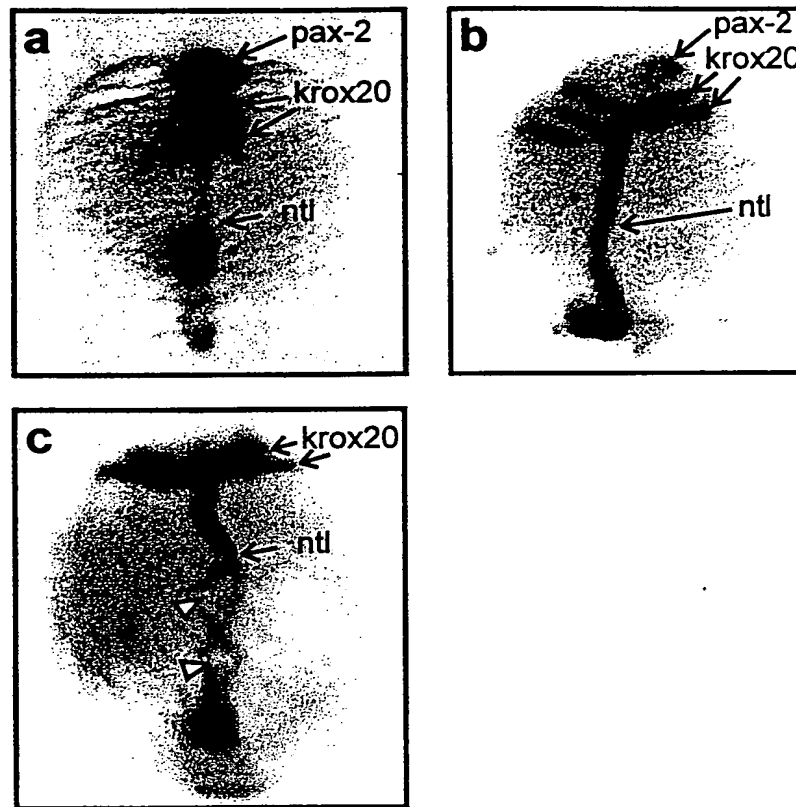


Fig. 7. The notochord is severely distorted in sh EphA3-expressing segmentation-stage embryos. Embryos were injected with sh EphA3 mRNA (b,c) or left untreated (a) and the expression of *pax2.1*, *krox20* and *ntl* analysed by *in-situ* hybridisation. Defects due to expression of sh EphA3 include a kinked notochord and the failure of *pax2.1*, *krox20* and *ntl* (open arrow heads in (c)) expressing cells to meet at the midline (b,c).

(c) EphA3 (Sajjadi et al., 1991) indicated an amino acid identity of 78% (85% similarity) with human, and 77% (similarity 86%) with chicken sequences over this region. In contrast, other known zebrafish and mammalian Eph sequences gave identity scores of less than 60%. We concluded that this clone encoded partial sequences of the zebrafish EphA3 homologue and used the cDNA sequence to generate probes for *in situ* analysis of whole-mount embryos during gastrulation (Fig. 8).

Beginning with the shield stage (6 hpf), transcripts were detectable throughout the embryo (Fig. 8a), with marginally higher levels in the future dorsal side of the embryo (Fig. 8a,b). Examination of later developmental stages revealed that transcripts were present in both epi- and hypoblast, although at higher levels in hypoblast (Fig. 8c,e,g). An elevated dorsal expression in the hypoblast became more obvious at 70–90% epiboly (7–9 hpf) (Fig. 8c–f), revealing a faint longitudinal dorsal stripe of EphA3 transcript in the region of the presumptive notochord (Fig. 8f). At the end of gastrulation (10 hpf) the expression became most pronounced in the anterior hypoblast, including the prechordal plate (Fig. 8g), while the fainter signal along the presumptive notochord persisted (Fig. 8g,h). Thus the putative zebrafish EphA3 homologue is expressed throughout

gastrulation, and is a candidate for interference by the dominant negative hs EphA3 and ephrin-A5 constructs.

The homologue of human ephrin-A5, zebrafish ephrin-A-L4, is not expressed during gastrulation (Brennan et al., 1997; C. Brennan and N. Holder, unpublished data), however a recently characterised zebrafish A-class ligand, ephrin-A-L1, is expressed in the gastrula margin and ventral hypoblast (Durbin et al., 1998). Towards the end of gastrulation strong ephrin-A-L1 expression remains in a region corresponding to the presumptive tailbud, with weak expression lateral to the presumptive notochord. We initially established the ability of recombinant, CHO-cell-expressed ephrin-A-L1 protein to bind to human EphA3 by BIAcore analysis. Together with recombinant, FLAG-tagged zebrafish ephrins-A-L3 and L4, ephrin-A-L1 was expressed in CHO cells and, following purification to homogeneity, passed over a sensorchip derivatized with sh EphA3 (Fig. 9). Deconvolution of the binding reactions confirmed the previously-described 1:1 interaction (Lackmann et al., 1997) for all analysed ligands and revealed an affinity of ephrin-A-L4 binding to sensorchip-coupled sh EphA3 of 50 nM, which is similar to the previously reported affinity of 12 nM of the ephrin-A5/EphA3 interaction (Table 1; Lackmann et al., 1997). Ephrin-A-L1 and ephrin-A-L3 (zebrafish

ephrin-A2) bound to immobilised sh EphA3 with 9 and 6-fold reduced affinities, respectively, primarily due to markedly decreased association rate constants (Table 1).

We next assessed if zebrafish ephrin-A-L1 would also interact with sh EphA3 *in vivo*, by injecting mRNA encoding sh EphA3 or soluble (s) ephrin-A-L1 proteins either separately or in combination into 1–2 cell embryos, and scoring developmental defects by *in situ* hybridisation analysis of *myo D* gene expression (Fig. 10). Injection of mRNA encoding s ephrin-A-L1 at 60 pg/embryo resulted in 67% of the injected embryos ($n = 48$) displaying defects reminiscent of the sh EphA3-mediated developmental defects (Fig. 10, and Durbin et al., 1998; Lackmann et al., 1998). At this concentration of sh EphA3 RNA, 52% ($n = 46$) of the injected embryos displayed similar defects. Co-injection of the s ephrin-A-L1 and sh EphA3 RNAs resulted in reduction of affected embryos to 34% ($n = 49$). The rescue by s ephrin-A-L1 of the sh EphA3-induced developmental defect is thus similar to that observed with sh ephrin-A5 (compare Fig. 4) and indicates that s ephrin-L1 is also capable of binding to sh EphA3 *in vivo*. Together our experiments suggest the newly isolated zebrafish EphA3, and ephrin-A-L1 as strong candidates for components of the endogenous Eph-ephrin signalling system that are disrupted during zebrafish gastrulation by the expression of sh EphA3 and sh ephrin-A5.

3. Discussion

The fate of cells and cell layers during gastrulation has been studied in considerable detail in the zebrafish (Kimmel et al., 1990; Ho, 1992; Shih and Fraser, 1995; Woo and Fraser, 1995; Melby et al., 1996), but little is known about the molecular mechanisms which guide the migration of these cells. We previously reported a characteristic, dose-dependent syndrome, which is evident in early segmentation stage embryos and is induced by the expression of a series of truncated, soluble versions of the human EphA3 extracellular domain (Lackmann et al., 1998). Specifically, truncated extracellular domains containing the ephrin-binding domain displayed biological activity, suggesting that an interaction between the EphA3 receptor and an ephrin-A ligand was responsible for the developmental defects. In this study we have extended this observation, showing that this developmental syndrome can be mimicked by the expression of the soluble human ephrin-A5. We have examined the development of these embryos in detail and present evidence that the Eph and ephrin families of cell-cell signalling proteins may have important roles in the process of gastrulation, potentially by regulating cell movements during involution and convergence.

3.1. Soluble forms of Eph and ephrins cause defects in zebrafish development

It is well established that signalling through RTKs can be

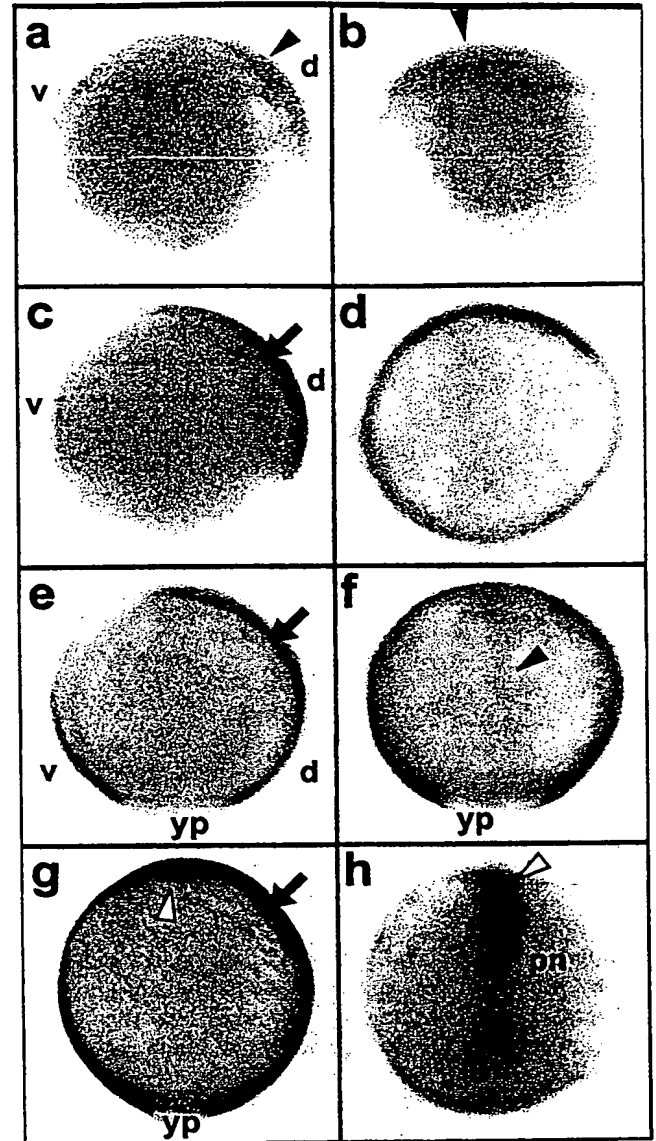


Fig. 8. Expression of EphA3 during zebrafish gastrulation. Whole-mounted embryos were labelled with an antisense RNA probe to zebrafish EphA3. The embryos are viewed lateral, with dorsal to the right in (a,c,e,g) viewed from the animal pole with dorsal to the top in (b,d) and viewed dorsal with anterior to the top in (f,h). (a,b), shield stage (6 hpf): low level expression throughout the embryo, with higher levels observed in the future dorsal side (closed arrow heads). (c,d), 70% epiboly (7 hpf), expression on the dorsal half of the embryo is more pronounced and the boundary between hypoblast and epiblast becomes apparent as discontinuity, whereby EphA3 expression is notably higher in the hypoblast (arrow in panels (c,e,g)). (e,f), 90% epiboly (9 hpf), showing higher expression in the future brain area as compared to the trunk (e, arrow). A faint stripe of expression extends longitudinally along the axial midline (panel f, closed arrowhead). (g,h), 10 hpf, prominent anterior expression including the prechordal plate (panel g, open arrow head). A continuous stripe of axial midline expression in a laterally decreasing gradient has developed, with markedly increased expression in the head (panel h, open arrow heads). d, dorsal; pn, presumptive notochord; v, ventral; yp, yolk plug.

Table 1
High-affinity binding of recombinant mammalian and zebrafish ephrins to sh EphA3

Sample	Sequence identity with mammalian ephrins	Association rate constant, k_a ($M^{-1}s^{-1}$) ^a	Dissociation rate constant, k_d (s^{-1}) ^a	Dissociation constant, K_D (M) ^a	Dissociation constant (global fit), K_D (M) ^b
Ephrin-A5		9.27×10^5	7.75×10^{-3}	1.2×10^{-8}	1.1×10^{-8}
Ephrin-A-L1	Ephrin-A1 (50%)	1.77×10^4	5.15×10^{-3}	4.6×10^{-7}	3.2×10^{-7}
Ephrin-A-L3	Ephrin-A2 (58%)	1.30×10^3	5.00×10^{-3}	3.1×10^{-7}	3.1×10^{-7}
Ephrin-A-L4	Ephrin-A5 (78%)	5.11×10^5	2.50×10^{-2}	5.0×10^{-8}	7.6×10^{-8}

^a Association and dissociation rate constants and dissociation constants were estimated for a single-site interaction model as described previously (Lackmann et al., 1997) using the BIAevaluation software, versions 2.1 and 3.0.

^b The affinity was also determined by global fitting to a 1:1 interaction model using the BIAevaluation 3.0 software.

inhibited by coexpression of kinase deleted or truncated forms of the receptor (Honegger et al., 1990; Frattali et al., 1992; Spritz et al., 1992; Reith et al., 1993; Dumont et al., 1994; Peters et al., 1994). These findings suggest that heterodimerisation between an intact endogenous receptor and an exogenous inactive counterpart will antagonise signalling in a dominant negative manner (reviewed in van der Geer and Hunter, 1994). A dominant negative approach was successful in the analysis of zebrafish EphA4 (*rtk1*) function, in which the kinase-inactive form of the murine EphA4 receptor (Sek1) antagonised zebrafish EphA4 receptor-regulated cell movements during rhombomere boundary formation (Xu et al., 1995; Xu et al., 1996). Studies using the extracellular domain of the human EphA3 in vitro and in vivo as signalling antagonist have confirmed the utility of the approach (Lackmann et al., 1998).

In the case of the Eph family and their membrane-associated ephrin ligands, cell-cell contact is essential for signalling (Davis et al., 1994), hence the soluble form of the ligand can also inhibit signalling through the receptor (Winslow et al., 1995). In agreement with this notion, we reproduced the effect of the soluble EphA3 receptor on development (see Section 3.2) by injecting mRNA encoding sh ephrin-A5 into 1–4 cell stage zebrafish embryos. Using BIAcore technology and western blotting, we confirmed that both zebrafish expressed human proteins were functionally active and abundantly expressed over the time course of our experiments (Fig. 1). The morphology of live embryos, and the expression pattern of the *hlx1*, *pax2.1*, *krox20* and *myoD* genes in embryos injected with sh ephrin-A5 RNA were indistinguishable from those displayed by embryos injected with sh EphA3 RNA (Figs. 2 and 3). This correspondence of developmental effects indicates that the same signalling process(es) were blocked by the expression of sh EphA3 and sh ephrin-A5. This conclusion is strongly supported by the ability of co-expressed receptor and ligand to correct the defects produced by either in isolation (Fig. 4).

The high expression levels of the human proteins detected in injected embryos (Fig. 1b), combined with the previously demonstrated specificity of EphA class receptors for ephrin-A class ligands (Cheng and Flanagan, 1994; Brambilla et al., 1995; Lackmann et al., 1997; Monschau et al., 1997)

precludes the conclusion that these effects are necessarily specific for the zebrafish homologues of human EphA3 and ephrin-A5. In this regard, it is important to note that a consistent syndrome was observed for all concentrations of mRNA introduced into the embryo, though with increasing frequency and intensity at higher levels of mRNA (Fig. 4). Additional categories of defective features would have been expected if additional low-affinity receptor ligand interactions, for example with the Eph-ephrin B class, were successively disrupted with increasing concentration

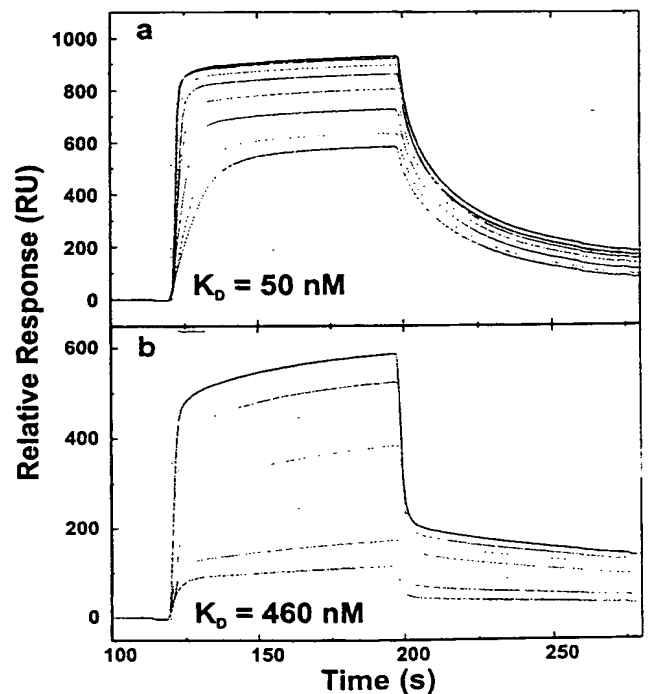


Fig. 9. BIAcore binding curves illustrating the interaction of ephrin-A-L1 and ephrin-A-L4 with sh EphA3. Homogenous preparations of CHO cell-expressed ephrin-A-L4 (a) or ephrin-A-L1 (b) at increasing concentrations (0.1, 0.2, 0.4, 0.6, 0.8, 1.0, 2.0, 4.0, 6.0 μ M) were injected across a sh EphA3-coated sensor chip surface and the plasmon resonance signal (response units, RU) used to estimate the kinetic rate constants (k_a , k_d) and the affinity of the interactions (K_D) as detailed in section 4.

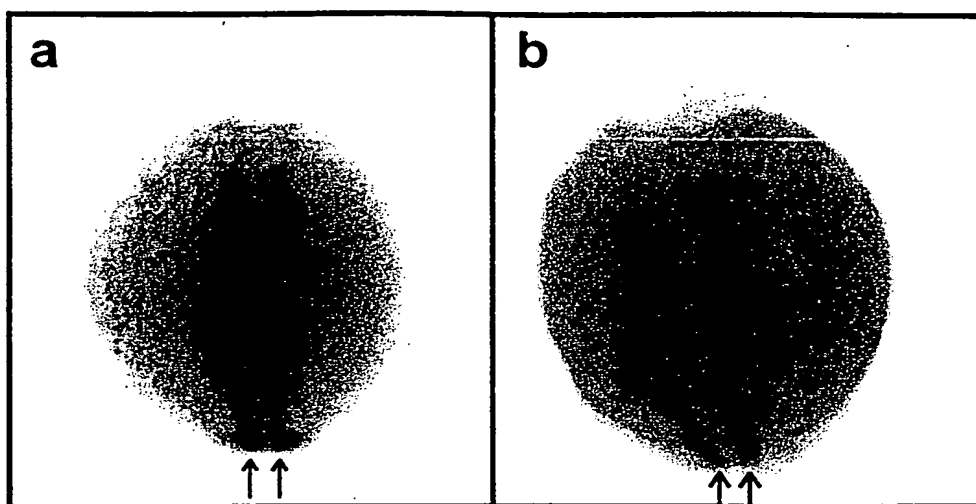


Fig. 10. Developmental defects in expression of soluble ephrin-A-L1 induces defects reminiscent of sh ephrin-A5 mediated defects. Embryos were injected with 60 pg of s ephrin-A-L1-RNA, allowed to develop for 12–13 hpf and fixed for in situ hybridisation with a *myoD* DIG-labelled riboprobe. Embryos are photographed from a dorsal perspective with anterior to the top and posterior to the bottom of each frame. (a) Uninjected embryo at 12 hpf showing normal expression of *myoD* in the paraxial and adaxial mesoderm. Note the exactly-parallel pattern of *myoD*-positive cells (arrows). (b) mRNA encoding the soluble, FLAG-tagged form of zebrafish ephrin-A-L1 (s ephrin-A-L1-RNA) (60 pg) injected embryo at 12 hpf illustrating a phenotype reminiscent with the sh ephrin-A5-RNA injected embryos shown in Fig. 3(e,f). *myoD* expressing cells do not form the parallel pattern of paraxial and adaxial mesoderm seen in non-injected embryos (arrows) and reveal areas of missing *myoD* expression in the somites (open arrow head) and an unevenly increased distance across the midline.

of dominant negative protein. For example, defects involving the generation of ectopic secondary embryonic axes are seen in *Xenopus* embryos expressing dominant negative EphB2 or ephrin-B1 constructs (Tanaka et al., 1998), indicating a role in dorsal specification for these proteins. However, this type of defect was never observed in our studies, indicating that any potential homologous function for EphB signaling in the zebrafish was not perturbed by a disruption of EphA3/ephrin-A5 signaling. Further, convergence defects in the zebrafish hindbrain or paraxial mesoderm were not observed after injection of a dominant negative EphA4 construct (Xu et al., 1996; Durbin et al., 1998). Instead, ventral diencephalon cells became incorporated into the eye fields, losing midline neural markers such as *rtk1* and *zash1* (Xu et al., 1996). Our data showing normal expression of *hlx1* in the ventral diencephalon indicates that this structure is not grossly affected by a disruption of EphA3/ephrin-A5 signalling, suggesting that the defects observed here are distinct from those produced by blocking EphA4 function. From these considerations, we suggest that the early effects of ectopic expression of sh EphA3 and ephrin-A5 may be restricted to a subset of the EphA/ephrin-A class of interactions.

3.2. Endogenous targets of disrupted EphA-ephrin-A interactions in the zebrafish embryo

What are the endogenous targets of the exogenous sh EphA3 and ephrin-A5 proteins in the gastrula stage zebrafish embryo? To date, eight of the 11 Eph family members described in zebrafish, (*rtk1-3*, 5, 6, 8, *zdk1*, and EphA3) are

expressed in spatially restricted patterns at this time (Fig. 8) (Xu et al., 1994; Taneja et al., 1996; Cooke et al., 1997) whereas the expression of only one zebrafish ephrin, ephrin-A-L1, has been demonstrated during gastrulation (Durbin et al., 1998). Our data is consistent with the novel zebrafish EphA3 being a target of the exogenous sh EphA3 and ephrin-A5 proteins. Firstly, EphA3 is expressed in a pattern that matches the site and timing of the defects, i.e. during gastrulation in the epiblast and at higher levels in the dorsal hypoblast. Secondly, as discussed in section 3.1, our disruption of Eph/ephrin signalling does not phenocopy previously described abnormalities in the early embryo caused by perturbation of (1) EphB class signalling (Winning et al., 1996; Jones et al., 1998; Tanaka et al., 1998) or (2) other members of the EphA class (Xu et al., 1996; Durbin et al., 1998 #537). Finally, the novel EphA3 has a higher similarity in its ligand binding domain to human EphA3 than any other known zebrafish Eph protein, and thus would likely represent a preferential high affinity binding partner for sh ephrin-A5. However, on the basis of their expression patterns we acknowledge the possibility of interaction with other EphA receptors, for example *rtk2*, 3, or 6 (Xu et al., 1994; Cooke et al., 1997).

The zebrafish ephrin-A5 orthologue, ephrin-A-L4 (Brennan et al., 1997) interacts with the human EphA3 receptor with an affinity that is comparable to the interaction between the corresponding human proteins (Table 1). However, it is clear from in situ expression studies that ephrin-A-L4 is expressed only after gastrulation (Brennan et al., 1997), in contrast to ephrin-A-L1, which is expressed at sites and times (Durbin et al., 1998) that match the observed defects.

In this study we demonstrate high affinity binding of s ephrin-A-L1 to human EphA3 in vitro. Further, the developmental defects resulting from overexpression of dominant negative s ephrin-A-L1 (Fig. 8) are indistinguishable from the sh EphA3 and sh ephrin-A5-induced defects, consistent with a functional role for EphA3/ephrin-A1 interaction in mammalian systems (Beckmann et al., 1994; Gale et al., 1996). Importantly, coexpression of a soluble form of ephrin-A-L1 with sh EphA3 during zebrafish gastrulation partially neutralises the effects of sh EphA3 expression, similar to the activity of sh ephrin-A5 in this context. Combined, our results strongly suggest that ephrin-A-L1 is an endogenous target for the dominant negative effects of sh EphA3 expression, and that zebrafish EphA3 is likely to be an endogenous target for sh ephrin-A5.

3.3. The developmental syndrome associated with blocking EphA-ephrin-A interaction is consistent with a disruption of gastrulation

Extensive convergence movements during zebrafish gastrulation bring cells from lateral positions of the epiblast and the hypoblast in the early gastrula toward the dorsal midline of the embryo (Warga and Kimmel, 1990; Woo and Fraser, 1995; Concha and Adams, 1998). Cells that have involuted from the epiblast at the onset of gastrulation to form the hypoblastic mesoderm (Schulte-Merker et al., 1992) are marked by the *ntl* gene, a zebrafish *Brachyury* homologue (Schulte-Merker et al., 1994). Our observations of perturbed gastrula morphology, combined with defects in early mesodermal *ntl* expression (Figs. 5–7) indicate that the antagonistic effects of sh EphA3 and sh ephrin-A5 are evident with the onset of gastrulation. As cells from lateral positions of the hypoblast converge to the dorsal margin to form the shield or dorsal organiser, an accumulation of *ntl* transcript is normally observed at this location. The loss of *ntl* expression from this marginal region in embryos with a block in EphA-ephrin-A interaction implies that involution has been locally perturbed (Fig. 5c). Further, the increase in mediolateral width of the shield and presumptive notochord, as gauged by *ntl* expression, appears to indicate a significant retardation of early convergence movements in embryos with disrupted EphA-ephrin-A interactions (Fig. 5b,e,f). The notochord derives from cells within or very close to the shield region of the early gastrula (Melby et al., 1996), and presumptive notochord cells continue to express *ntl* as the notochord elongates towards the animal pole by the movements of extension (Schulte-Merker et al., 1992). Two alternative interpretations could explain why disruption of EphA-ephrin-A interactions affect convergence most markedly early in gastrulation (Figs. 5 and 6). Firstly, early and late phases of convergence, which differ with respect to cell movement, morphology and orientation of cell division (Concha and Adams, 1998), may be differentially affected by a block of Eph-ephrin interactions. Alternatively, the early defects may reflect a delayed completion of involution

and ingression at the margin rather than resulting from a perturbation of convergence. Thus the correction in notochord width seen in embryos by 10 hpf (Figs. 6a and 7b,c) may indicate cells converging correctly, but late, at the midline.

Cells of the epiblast fated to contribute to the mid- and hindbrain also undergo extensive convergence movements during gastrulation (Warga and Kimmel, 1990; Woo and Fraser, 1995; Concha and Adams, 1998), whereby the more posterior cells in the neuraxis come from more lateral positions in the early gastrula, and hence have further to migrate (Woo and Fraser, 1995). The observed lateral displacement of *krox20* expressing cells of the presumptive hindbrain, and to a lesser extent, *pax2.1* positive cells of the presumptive MHB, from the midline of affected embryos (Figs. 3 and 7), suggests a correlation between the degree of disruption we observe (with rhombomere five, more medio-laterally displaced than rhombomere three, and rhombomere three, more strongly displaced than the MHB), and the probable distance, the affected cells migrated during gastrulation. Notably, *hlx1*-expressing cells in the ventral forebrain and midbrain (Fjose et al., 1994) which are derived from a contiguous domain centered about the midline at the beginning of gastrulation (Woo and Fraser, 1995) remain relatively insulated from the effects of a blockade of EphA-ephrin-A interaction. Thus the correspondingly shorter convergence distance of ventral *hlx1* expressing forebrain and midbrain cells over the cells of the MHB may account for the normal appearance of the *hlx1* domain in embryos exhibiting MHB and hindbrain defects.

Using an early marker of muscle commitment, *myoD* (Weinberg et al., 1996), we have demonstrated that a disruption of EphA/ephrin-A interaction leads to a range of defects in the organisation of cells in the paraxial mesoderm. The elongation of lateral somite boundaries away from the midline (Fig. 3f) is readily explained by a retardation of convergence, similar to that seen in the gastrulation defective mutants *trilobite* and *knypeck* (Solnica-Krezel et al., 1995). The localised absence of paraxial *myoD* expression in some embryos (Fig. 3f) may result from a failure of ingression and involution of a particular region of the somitic anlage. Alternatively it may reflect a later migration defect, similar to the effect of the *spadetail* mutation on *myoD* expression, where mesoderm fated to migrate into developing trunk somites appears in the tailbud, resulting in animals with greatly enlarged tails and lacking somitic structures (Kimmel et al., 1989; Ho, 1992; Weinberg et al., 1996). Finally, disturbance of paraxial *myoD* expression may result from an aberrant positioning of the paraxial mesoderm at a distance from the notochord which is outside the inductive activity of *shh*. Transcription of *myoD* throughout the paraxial mesoderm is known to be induced by *Shh* (Weinberg et al., 1996) and recently it has been shown, that loss of *shh*, as found in *sonic you* mutants, dramatically reduces *myoD* levels in adaxial cells and more lateral somitic mesoderm (Schauerte et al., 1998).

The fusion of somite boundaries and loss of register between boundaries across the midline that we observed in some of the injected embryos (Fig. 3d,f) is reminiscent of treatments and mutations that affect the anterior-posterior segmentation process of the paraxial mesoderm (van Eeden et al., 1996; van Eeden et al., 1998; for review, see: McGrew and Pourquie, 1998), raising the possibility that the disruption of EphA-ephrin-A signalling may perturb segmentation or somitogenesis directly. The expression patterns in mice and rats would support the possibility of Eph-ephrin interactions during somitogenesis (Cheng and Flanagan, 1994; Donoghue et al., 1996; Gale et al., 1996; Kilpatrick et al., 1996; Flenniken et al., 1997). Indeed, we have demonstrated recently, that expression of dominant negative EphB2, EphA4 or ephrin-A-L1 affects somite boundary formation (Durbin et al., 1998). Thus a contribution of EphA4 or ephrin-A-L1 to some of the observed defects in somite organisation seems likely. Importantly, although the segmental expression of *myoD* in the paraxial mesoderm was lost in the most severe dominant negative EphA4 phenotypes (Durbin et al., 1998), in no instance was an effect on the adaxial cells observed. By contrast, the twisted appearance of the notochord and adaxial cells of early segmentation stage embryos with disrupted EphA/ephrin-A interactions in the present study suggests dramatically disturbed convergence movements in the trunk of these animals which would result in a perturbation of paraxial mesoderm prior to the localised somite boundary formation of segmentation.

3.4. Potential mechanisms of EphA-ephrin-A activity during gastrulation

As described above, interference in Eph-ephrin signalling appears to perturb multiple processes during gastrulation. The evidence is consistent with a disruption of involution and/or ingression, as well as the later convergence of both epi- and hypoblast. The current view of the role of EphA/ephrin-A interactions during growth cone and neural crest cell migration is the delivery of a repulsive signal that causes the moving cell to select a path that avoids high concentrations of ligand (for review: Flanagan and Vanderhaeghen, 1998). It is not clear how the endogenous EphA3 and ephrin-A-L1 proteins, likely to be disrupted by our treatment, would be mediating this type of behaviour during early gastrulation, but it is intriguing that the two genes appear in complementary expression gradients in the late gastrula (70% epiboly). This does not preclude the involvement of other, as yet unknown, EphA or ephrin-A family members with appropriate expression patterns in specific contact repulsion based guidance tasks during gastrulation.

Importantly, depending on the Eph-ephrin interaction and the cell type involved, biological responses other than repulsion have been noted for Eph receptors. For example, ephrin-A1 is competent to cause endothelial cell chemotaxis and capillary assembly (Pandey et al., 1995; Daniel et al., 1996), and mice lacking ephrin-B2 do not remodel vascular

plexi into properly branched vessels (Wang et al., 1998). Stein et al. (1998) have demonstrated that the adhesive properties, but not receptor phosphorylation, of endothelial cells expressing EphB receptors are dependent upon higher order clustering of the ephrin-B ligand, indicating that Eph receptors can distinguish between different ligand oligomer states and deliver alternate signals. These results suggest that Eph/ephrin interactions can also deliver attractive and adhesive signals.

Multiple cell adhesion molecules such as fibronectin and members of the cadherin and integrin families are expressed, and regulate, cell migration and intercalation during vertebrate gastrulation (reviewed by Winklbauer et al., 1996). The ability of activated EphA4 and over-expressed ephrin-B1 to cause a loss of cell adhesion in the *Xenopus* blastula (Winning et al., 1996; Jones et al., 1998) indicates that perturbation of Eph/ephrin signaling can lead to defective adhesion in the embryo, albeit at developmental times earlier than the defects observed here. In contrast, loss of the function of the cell adhesion molecule paraxial protocadherin (*papc*) in both zebrafish and *Xenopus* leads to defects in convergence of the trunk mesoderm highly reminiscent of those observed in this study (Kim et al., 1998; Yamamoto et al., 1998). Further, expression of *papc* drives the elongation of sensitised animal cap explants by causing the cells to intercalate in the same way as seen during convergent extension (Kim et al., 1998). Together these findings would support an alternative mechanism of EphA/ephrin-A activity, whereby the gastrulation defects observed after disruption of EphA/ephrin-A interactions may be due to a change in cell-cell adhesion, preventing correct migratory and perhaps intercalation behaviour. For example, both *EphA3* and *ephrin-A-L1* are radially expressed in the hypoblast of the early gastrula, and *EphA3* is found in addition in the overlying epiblast. Loss of EphA3/ephrin-A-L1 interaction between these cell layers may result in an inability of cells at the margin to de- and re-adhere during involution and ingression, producing the aberrant epibolic margin and *ntl* expression patterns we observed. We must offer the caveat that our analysis is based on the movements of cells as large groups in the embryo, and that we cannot comment on the migratory behaviour of single cells under the effect of disrupted EphA-ephrin-A interactions during gastrulation. We are currently testing these ideas to determine the mechanisms of perturbation in detail.

Finally, we note that a loss-of-function-mutation in the *C. elegans* Eph homologue, *vab-1*, results in a failure in the movements of neuronal cells in gastrulation cleft closure, and in the migration of epidermal cells to complete ventral enclosure of the epidermis immediately thereafter (George et al., 1998). The similarity of these defects and those evident in vertebrate embryos with disrupted EphA-ephrinA interaction shown here implies an ancient evolutionary usage of Eph receptors in the execution of the complex morphogenetic movements of gastrulation, and suggests

that Eph-ephrin interaction may be a general mechanism for regulation of cell movement.

4. Experimental procedures

4.1. Fish care and embryo collection

Wildtype zebrafish were obtained from St. Kilda Aquarium (Melbourne) and kept essentially as described (Westerfield, 1995). Embryos were obtained by natural spawning between a small number (4–10) of male and female fish. Embryos were removed from the spawning tanks within 20 min of fertilisation, cleaned in system water, and transferred to the injection apparatus.

4.2. Screening of a zebrafish cDNA library

A 28 h zebrafish embryo cDNA library cloned into the ZAP vector was screened using a 660 bp human EphA3 probe generated by PCR from primers at either end of the third exon encoding the ligand binding domain (Lackmann et al., 1998). The probe was ^{32}P labelled using a Megaprime labelling kit (Amersham). A total of 2×10^6 plaques were transferred onto duplicate filters which were then pre-hybridized ($5 \times$ Denhardt's solution, $5 \times$ SSPE, 0.1 mg/ml salmon sperm DNA, 0.5% SDS) for 4 h and hybridized with ^{32}P labelled probe over-night. The filters were washed in SSPE/0.1% SDS, twice at room temperature and twice at 60°C . Duplicate positive plaques were identified by autoradiography and isolated for purification of positive clones. Bestfit analysis of the amino acid sequence encoded by the clone identified amino acids 214–477 of the published hEphA3 sequence (Wicks et al., 1992). This includes the C terminal third of exon 3, exons 4, 5 and 6 and the beginning of exon 7 (Lackmann et al., 1998). Bestfit analysis was performed against homologous sequences from human (hEphA3) and chicken (c EphA3) (Sajjadi et al., 1991).

4.3. RNA synthesis and microinjection

Constructs equivalent to FLAG-tagged, soluble human EphA3 extracellular domain (sh EphA3) and soluble ephrin-A5 (sh ephrin-A5) were generated by PCR from cDNA constructs encoding the FLAG-tagged soluble human proteins (Lackmann et al., 1997). In each case the 5' oligonucleotide was based on the IL-3 signal sequence and the 3' oligos were as above, except that BglII sites were used to clone the PCR products into the pSP64TK vector. The cDNA encoding truncated, soluble ephrin-A-L1 was prepared as described (Durbin et al., 1998). mRNA from the EphA3, ephrin-A5 and ephrin-A-L1 constructs and control GFP and mDCC cDNA constructs were transcribed in vitro (message maker kit, Ambion, Texas) and resuspended in water at 0.1 mg/ml. Integrity of the mRNA was checked by denaturing gel electrophoresis. Immediately prior to injection, aliquots of sh EphA3-RNA or sh

ephrin-A5-RNA were thawed and adjusted with water and GFP mRNA to deliver either 10 pg, 1 pg, or 0.1 pg of the sh EphA3-RNA, 10 pg or 100 pg of the sh ephrin-A5-RNA and 5 pg of the GFP mRNA or 10 pg of the sh EphA3-RNA and 100 pg of the sh ephrin-A5-RNA to each embryo. Approximately 600 pl of RNA solution was injected into the blastoderm or yolk of one, two or four cell embryos under a Wild stereo microscope using Leitz micromanipulators (Leitz, Wetzlar, Germany) and compressed nitrogen. Uptake and translation of mRNA by the embryo was measured by including 5 pg mRNA encoding EGFP as a marker in each injection.

4.4. Analysis of sh EphA3 and sh ephrin-A5 production in zebrafish embryos by Western blot and BIAcore analysis

Translation of EphA3, ephrin-A5 and DCC mRNA was measured at intervals during embryogenesis by Western blotting and the abundance of functionally-active proteins by BIAcore analysis of whole embryo lysates. Ten embryos per 0.1 ml sample were lysed in buffer (25 mM Tris-HCl, pH 7.4, 0.5 M NaCl, 1% Triton X-100) containing protease inhibitors (1 mM PMSF/1 mM EDTA/5 μM E64 (trans-epoxysuccinyl-L-3-methyl-butane, Boehringer Mannheim)/10 μM leupeptin, 10 μM pepstatin/1 mM 1,10-Phenanthroline), the lysate cleared by centrifugation (60 min, $1 \times 10^5 \times g$) and stored at -80°C until use. For comparison, CHO cell-derived sh EphA3 and sh ephrin-A5 (as indicated) were added to lysates of non-injected embryos. Samples were extracted individually using 7.5 μl of packed anti-FLAG MAb (M2) agarose (IBI, Kodak), washed (0.5 ml each) with lysis buffer and Tris-buffered saline (TBS) and eluted with $2 \times 15 \mu\text{l}$ of 0.15 mg/ml FLAG peptide in TBS. Parallel samples were analysed either by SDS-PAGE and Western blot using biotinylated anti-FLAG M2 MAb (IBI, Kodak) and HRP/streptavidin (Boehringer, Mannheim) for enhanced chemiluminescence detection (ECL, Pierce) or analysed on the BIAcore. BIAcore sensor chips were derivatised with anti-EphA3 MAb IIIA4 or sh EphA3 as described (Lackmann et al., 1996; Lackmann et al., 1997). Lysates of zebrafish embryos which had been injected with sh EphA3-RNA or sh ephrin-A5-RNA were analysed in parallel with samples of zebrafish lysates containing known concentrations of the CHO cell-derived proteins. A linear correlation ($r = 0.998$) between increasing concentration of added protein and BIAcore response was obtained routinely.

4.5. Kinetic BIAcore analysis of the interaction between ephrin-A-L1, ephrin-A-L3, ephrin-A-L4 or sh ephrin-A5 and sh EphA3

The methodology for the expression, purification and kinetic analysis of FLAG-tagged ephrins has been described previously in detail (Lackmann et al., 1997). Briefly, recombinant, soluble FLAG-tagged forms of ephrin-A-L1, ephrin-A-L3, ephrin-A-L4 or ephrin-A5 were obtained from

culture supernatants of CHO cells which had been stably transfected with the pEFBOS vector containing the relevant cDNA: homogenous preparations of these proteins were obtained by affinity and size-exclusion chromatography and the protein concentration determined as described previously (Lackmann et al., 1997). The binding of the various ephrins to the sh EphA3-coated BIAcore sensor chip surface (Lackmann et al., 1997) was performed at 25 μ l/min to avoid ambiguities due to mass-transport problems as instructed by the manufacturer (BIAcore AB, Sweden).

The interaction kinetics were derived from the BIAcore raw data essentially as described (Lackmann et al., 1997) and by global fitting analysis using the BIA evaluation software (version 2.1 and version 3.0).

4.6. Whole mount RNA in situ hybridisation

The effects of each of the injected mRNAs on embryonic development was measured at 6–15 hpf, i.e. from the shield stage to five to eight somite stage (Kimmel et al., 1995) by light microscopy and in situ hybridisation with probes to *hlx1* (Fjose et al., 1994), *pax2.1* (Krauss et al., 1991), *krox20* (Oxtoby and Jowett, 1993), *myoD* (Weinberg et al., 1996) and *ntl* (Schulte-Merker et al., 1994). Embryos were scored as defective if the wildtype pattern of gene expression was disrupted. Riboprobe synthesis and in situ hybridization were carried out essentially as described (Schulte-Merker et al., 1992) with the following modifications: riboprobes were purified before use over RNA sephadex G-50 columns (Boehringer, Mannheim). Using estimates of RNA synthesis based on 32 P-CTP incorporation, probes were resuspended in HYB⁺ at a concentration of 1 ng/ml for use. Embryos were not proteinase K digested. Hybridization and washing was carried out at temperatures of 65–70°C. Non-specific binding of anti-digoxigenin Fab-AP (Boehringer Mannheim), used at a dilution of 1/5000, was blocked with 10% w/v Blocking Reagent (Boehringer Mannheim)/25 heat-inactivated sheep serum/MABT (100 mM Maleic acid, 150 mM NaCl, 0.1% Tween-20, pH 7.5) for 1 h at room temperature. Color detection reactions utilized BM purple substrate (Boehringer Mannheim), and were developed for up to 2 days before fixing in 4% paraformaldehyde/PBT. Embryos were either cleared in glycerol or benzyl benzoate: benzyl alcohol (2:1) and photographed using a Leitz Wild T stereo dissection microscope or a Nikon Microphot AX compound microscope.

Acknowledgements

We thank Dr. H.M. Cooper and J.G. Gad for the kind gift of murine DCC cDNA and Janna Stickland and Pierre Smith for help in the preparation of the figures. We are grateful to Prof. Tony Burgess, Prof. Ashley Dunn, Prof. Robert Ho, Dr. Ashley Bruce and Dr. Andrew Wilks for constructive criticism of the manuscript. We thank Dr. Graham Lieschke for providing an environment in which these studies were in

part pursued. This work was supported in part by the National Health and Medical Research Council of Australia and the Leukaemia Foundation of Queensland. A.C.O was supported by an Anti Cancer Council of Victoria Post Graduate Research Scholarship.

References

- Beckmann, M.P., Cerretti, D.P., Baum, P., Vanden Bos, T., James, L., Farrah, T., Kozlosky, C., Hollingsworth, T., Shilling, H., Maraskovsky, E., et al., 1994. Molecular characterization of a family of ligands for eph-related tyrosine kinase receptors. *EMBO J.* 13, 3757–3762.
- Boyd, A.W., Ward, L.D., Wicks, I.P., Simpson, R.J., Salvaris, E., Wilks, A., Welch, K., Loudovaris, M., Rockman, S., Busmanis, I., et al., 1992. Isolation and characterization of a novel receptor-type protein tyrosine kinase (hek, from a human pre-B cell line). *J. Biol. Chem.* 267, 3262–3267.
- Brambilla, R., Schnapp, A., Casagrande, F., Labrador, J.P., Bergemann, A.D., Flanagan, J.G., Pasquale, E.B., Klein, R., 1995. Membrane-bound LERK2 ligand can signal through three different Eph-related receptor tyrosine kinases. *EMBO J.* 14, 3116–3126.
- Brennan, C., Monschau, B., Lindberg, R., Guthrie, B., Drescher, U., Bonhoeffer, F., Holder, N., 1997. Two Eph receptor tyrosine kinase ligands control axon growth and may be involved in the creation of the retinotectal map in the zebrafish. *Development* 124, 655–664.
- Bruckner, K., Klein, R., 1998. Signaling by Eph receptors and their ephrin ligands. *Curr. Opin. Neurobiol.* 8, 375–382.
- Cheng, H.J., Flanagan, J.G., 1994. Identification and cloning of ELF-1, a developmentally expressed ligand for the Mek4 and Sek receptor tyrosine kinases. *Cell* 79, 157–168.
- Cheng, H.J., Nakamoto, M., Bergemann, A.D., Flanagan, J.G., 1995. Complementary gradients in expression and binding of ELF-1 and Mek4 in development of the topographic retinotectal projection map. *Cell* 82, 371–381.
- Concha, M.L., Adams, R.J., 1998. Oriented cell divisions and cellular morphogenesis in the zebrafish gastrula and neurula: a time-lapse analysis. *Development* 125, 983–994.
- Cooke, J.E., Xu, Q., Wilson, S.W., Holder, N., 1997. Characterisation of five novel zebrafish Eph-related receptor tyrosin kinases suggests roles in patterning the neural plate. *Dev. Genes Evol.* 206, 515–531.
- Cooper, H.M., Armes, P., Britto, J., Gad, J., Wilks, A.F., 1995. Cloning of the mouse homologue of the deleted in colorectal cancer gene (mDCC) and its expression in the developing mouse embryo. *Oncogene* 11, 2243–2254.
- Daniel, T.O., Stein, E., Cerretti, D.P., St. John, P.L., Robert, B., Abrahamson, D.R., 1996. ELK and LERK-2 in developing kidney and microvascular endothelial assembly. *Kidney Int Suppl.* 57, S73–S81.
- Davis, S., Gale, N.W., Aldrich, T.H., Maisonnier, P.C., Lhotak, V., Pawson, T., Goldfarb, M., Yancopoulos, G.D., 1994. Ligands for EPH-related receptor tyrosine kinases that require membrane attachment or clustering for activity. *Science* 266, 816–819.
- Donoghue, M.J., Lewis, R.M., Merlie, J.P., Sanes, J.R., 1996. The Eph kinase ligand AL-1 is expressed by rostral muscles and inhibits outgrowth from caudal neurons. *Mol. Cell. Neurosci.* 8, 185–198.
- Drescher, U., Kremoser, C., Handwerker, C., Loschinger, J., Noda, M., Bonhoeffer, F., 1995. In vitro guidance of retinal ganglion cell axon by RAGS, a 25 kDa tectal protein related to ligands for Eph receptor tyrosine kinases. *Cell* 82, 359–370.
- Dumont, D.J., Gradwohl, G., Fong, G.H., Puri, M.C., Gertsenstein, M., Auerbach, A., Breitman, M.L., 1994. Dominant-negative and targeted null mutations in the endothelial receptor tyrosine kinase, tek, reveal a critical role in vasculogenesis of the embryo. *Genes Dev.* 8, 1897–1909.

- Durbin, L., Brennan, C., Shiomi, K., Cooke, J., Barrios, A., Shanmugalingam, S., Guthrie, B., Lindberg, R., Holder, N., 1998. Eph signaling is required for segmentation and differentiation of the somites. *Genes Dev.* 12, 3096–3109.
- Fjose, A., Izpisua-Belmonte, J.C., Fromental-Ramain, C., Duboule, D., 1994. Expression of the zebrafish gene *hlx-1* in the prechordal plate and during CNS development. *Development* 120, 71–81.
- Flanagan, J.G., Vanderhaeghe, P., 1998. The ephrins and Eph receptors in neural development. *Annu. Rev. Neurosci.* 21, 309–345.
- Flentgen, A.M., Gale, N.W., Yancopoulos, G.D., Wilkinson, D.G., 1997. Distinct and overlapping expression patterns of ligands for Eph-related receptor tyrosine kinases during mouse embryogenesis. *Dev. Biol.* 179, 382–401.
- Frattali, A.L., Treadway, J.L., Pessin, J.E., 1992. Transmembrane signaling by the human insulin receptor kinase. Relationship between intramolecular beta subunit trans- and cis-autophosphorylation and substrate kinase activation. *J. Biol. Chem.* 267, 1–19528.
- Friedman, G.C., O'Leary, D.D., 1996. Eph receptor tyrosine kinases and their ligands in neural development. *Curr. Opin. Neurobiol.* 6, 127–133.
- Frisen, J., Yates, P.A., McLaughlin, T., Friedman, G.C., O'Leary, D.D.M., Barbacid, M., 1998. Ephrin-A5 (AL-1/RAGS) is essential for proper retinal axon guidance and topographic mapping in the mammalian visual system. *Neuron* 20, 235–243.
- Gale, N.W., Holland, S.J., Valenzuela, D.M., Flenniken, A., Pan, L., Ryan, T.E., Hirai, H., Wilkinson, D.G., Pawson, T., Davis, S., Yancopoulos, G., 1996. EPH Receptors and Ligands Comprise Two Major Specificity Subclasses and are Reciprocally Compartmentalized during Embryogenesis. *Neuron* 17, 9–19.
- Ganju, P., Shigemoto, K., Brennan, J., Entwistle, A., Reith, A.D., 1994. The Eck receptor tyrosine kinase is implicated in pattern formation during gastrulation, hindbrain segmentation and limb development. *Oncogene* 9, 1613–1624.
- George, S.E., Simokat, K., Hardin, J., Chisholm, A.D., 1998. The VAB-1 Eph receptor tyrosine kinase functions in neural and epithelial morphogenesis in *C. elegans*. *Cell* 92, 633–643.
- Halpern, M.E., Ho, R.K., Walker, C., Kimmel, C.B., 1993. Induction of muscle pioneers and floor plate is distinguished by the zebrafish *no tail* mutation. *Cell* 75, 99–111.
- Harland, R., Gerhart, J., 1997. Formation and function of Spemann's organizer. *Annu. Rev. Cell Dev. Biol.* 13, 611–667.
- Heasman, J., 1997. Patterning the *Xenopus* blastula. *Development* 124, 4179–4191.
- Ho, R.K., 1992. Cell movements and cell fate during zebrafish gastrulation. *Dev. Suppl.*, 65–73.
- Honegger, A.M., Schmidt, A., Ullrich, A., Schlessinger, J., 1990. Evidence for epidermal growth factor EGF-induced intermolecular autophosphorylation of the EGF receptors in living cells. *Mol. Cell. Biol.* 10, 4035–4044.
- Jones, T.L., Chong, L.D., Kim, J., Xu, R.H., Kung, H.F., Daar, I.O., 1998. Loss of cell adhesion in *Xenopus laevis* embryos mediated by the cytoplasmic domain of XLerk, an erythropoietin-producing hepatocellular ligand. *Proc. Natl. Acad. Sci. USA* 95, 576–581.
- Kennedy, T.E., Tessier-Lavigne, M., 1995. Guidance and induction of branch formation in developing axons by target-derived diffusible factors. [Review] [48 refs]. *Curr. Opin. Neurobiol.* 5, 83–90.
- Kessler, D.S., Melton, D.A., 1994. Vertebrate embryonic induction: mesodermal and neural patterning. *Science* 266, 596–604.
- Kilpatrick, T.J., Brown, A., Lai, C., Gassmann, M., Goulding, M., Lemke, G., 1996. Expression of the *Tyro4/Mek4/Cek4* gene specifically marks a subset of embryonic motor neurons and their muscle targets. *Mol. Cell. Neurosci.* 7, 762–774.
- Kim, S.-H., Yamamoto, A., Bouwmeester, T., Agius, E., De Robertis, E.M., 1998. The role of Paraxial Protocadherin in selective adhesion and cell movements of the mesoderm during *Xenopus* gastrulation. *Development* 125, 4681–4691.
- Kimmel, C.B., Ballard, W.W., Kimmel, S.R., Ullmann, B., Schilling, T.F., 1995. Stages of embryonic development of the zebrafish. *Dev. Dyn.* 203, 253–310.
- Kimmel, C.B., Kane, D.A., Walker, C., Warga, R.M., Rothman, M.B., 1989. A mutation that changes cell movement and cell fate in the zebrafish embryo. *Nature* 337, 358–362.
- Kimmel, C.B., Warga, R.M., Schilling, T.F., 1990. Origin and organization of the zebrafish fate map. *Development* 108, 581–594.
- Krauss, S., Johansen, T., Korzh, V., Fjose, A., 1991. Expression of the zebrafish paired box gene *pax(zf-b)* during early neurogenesis. *Development* 113, 1193–1206.
- Lackmann, M., Bucci, T., Mann, R.J., Kravets, L.A., Viney, E., Smith, F., Moritz, R.L., Carter, W., Simpson, R.J., Nicola, N.A., Mackwell, K., Nice, E.C., Wilks, A.F., Boyd, A.W., 1996. Purification of a ligand for the EPH-like receptor HEK using a biosensor-based affinity detection approach. *Proc. Nat. Acad. Sci. USA* 93, 2523–2527.
- Lackmann, M., Mann, R.J., Kravets, L., Smith, F.M., Bucci, T.A., Maxwell, K.F., Howlett, G.J., Olsson, J.E., Vanden Bos, T., Cerretti, D.P., Boyd, A.W., 1997. Ligand for EPH-related kinase LERK. 7 is the preferred high affinity ligand for the HEK receptor. *J. Biol. Chem.* 272, 16521–16530.
- Lackmann, M., Oates, A.C., Dottori, M., Smith, F.M., Do, C., Power, M., Kravets, L., Boyd, A.W., 1998. Distinct subdomains of the EphA3 receptor mediate ligand binding and receptor dimerization. *J. Biol. Chem.* 273, 20228–20237.
- McGrew, M.J., Pourquie, O., 1998. Somitogenesis: segmenting a vertebrate [In Process Citation]. *Curr. Opin. Genet. Dev.* 8, 487–493.
- Melby, A.E., Warga, R.M., Kimmel, C.B., 1996. Specification of cell fates at the dorsal margin of the zebrafish gastrula. *Development* 122, 2225–2237.
- Monschau, B., Kremoser, C., Ohta, K., Tanaka, H., Kaneko, T., Yamada, T., Handwerker, C., Hornberger, M.R., Loschinger, J., Pasquale, E.B., Siever, D.A., Verderame, M.F., Muller, B.K., Bonhoeffer, F., Drescher, U., 1997. Shared and distinct functions of RAGS and ELF-1 in guiding retinal axons. *EMBO J.* 16, 1258–1267.
- Müller, B.K., Bonhoeffer, F., Drescher, U., 1996. Novel gene families involved in neural pathfinding. *Curr. Opin. Genet. Dev.* 6, 469–474.
- Nakamoto, M., Cheng, H.J., Friedman, G.C., McLaughlin, T., Hansen, M.J., Yoon, C.H., O'Leary, D.M., Flanagan, J.G., 1996. Topographically specific effects of ELF-1 on retinal axon guidance in vitro and retinal axon mapping in vivo. *Cell* 86, 755–766.
- Nieto, M.A., 1996. molecular biology of axon guidance. *Neuron* 17, 1039–1048.
- Oxtoby, E., Jowett, T., 1993. Cloning of the zebrafish *krox-20* gene (*krx-20*) and its expression during hindbrain development. *Nucleic Acids Res.* 21, 1087–1095.
- Pandey, A., Shao, H., Marks, R.M., Poverini, P.J., Dixit, V.M., 1995. Role of B61, the ligand for the Eck receptor tyrosine kinase, in TNF-alpha-induced angiogenesis. *Science* 268, 557–569.
- Pasquale, E., 1997. The Eph family of receptors. *Curr. Opin. Cell. Biol.* 5, 608–615.
- Peters, K., Werner, S., Liao, X., Wert, S., Whitsett, J., Williams, L., 1994. Targeted expression of a dominant negative FGF receptor blocks branching morphogenesis and epithelial differentiation of the mouse lung. *EMBO J.* 13, 3296–3301.
- Reith, A.D., Ellis, C., Maro, N., Pawson, T., Bernstein, A., Dubreuil, P., 1993. 'W' mutant forms of the Fms receptor tyrosine kinase act in a dominant manner to suppress CSF-1 dependent cellular transformation. *Oncogene* 8, 45–53.
- Robinson, V., Smith, A., Flenniken, A.M., Wilkinson, D.G., 1997. Roles of Eph receptors and ephrins in neural crest pathfinding. *Cell Tissue Res.* 290, 265–274.
- Ruiz, J.C., Conlon, F.L., Robertson, E.J., 1994. Identification of novel protein kinases expressed in the myocardium of the developing mouse heart. *Mech. Dev.* 48, 153–164.
- Sajjadi, F.G., Pasquale, E.B., Subramani, S., 1991. Identification of a new eph-related receptor tyrosine kinase gene from mouse and chicken that

- is developmentally regulated and encodes at least two forms of the receptor. *New Biol.* 3, 769–778.
- Schauerte, H.E., van Eeden, F.J., Fricke, C., Odenthal, J., Strahle, U., Haffter, P., 1998. Sonic hedgehog is not required for the induction of medial floor plate cells in the zebrafish. *Development* 125, 2983–2993.
- Schulte-Merker, S., Ho, R.K., Hermann, B.G., Nusslein-Volhard, C., 1992. The protein product of the zebrafish homologue of the mouse *T* gene is expressed in nuclei of the germ ring and the notochord of the early embryo. *Development* 116, 1021–1032.
- Schulte-Merker, S., van Eeden, F.J., Halpern, M.E., Kimmel, C.B., Nusslein-Volhard, C., 1994. no tail (*ntl*) is the zebrafish homologue of the mouse *T* (*Brachyury*) gene. *Development* 120, 1009–1015.
- Shih, J., Fraser, S.E., 1995. Distribution of tissue progenitors within the shield region of the zebrafish gastrula. *Development* 121, 2755–2765.
- Slack, J.M., Isaacs, H.V., Johnson, G.E., Lettice, L.A., Tannahill, D., Thompson, J., 1992. Specification of the body plan during *Xenopus* gastrulation: dorsoventral and anteroposterior patterning of the mesoderm. *Dev. Suppl.*, 143–149.
- Solnica-Krezel, L., Stemple, D.L., Driever, W., 1995. Transparent things: cell fates and cell movements during early embryogenesis of zebrafish. *Bioessays* 17, 931–939.
- Spritz, R.A., Giebel, L.B., Holmes, S.A., 1992. Dominant negative and loss of function mutations of the *c-kit* (mast/stem cell growth factor receptor, proto-oncogene in human piebaldism). *Am. J. Human Genet.* 50, 261–269.
- Stein, E., Lane, A.A., Cerretti, D.P., Schoecklmann, H.O., Schroff, A.D., Van Etten, R.L., Daniel, T.O., 1998. Eph receptors discriminate specific ligand oligomers to determine alternative signaling complexes, attachment, and assembly responses. *Genes Dev.* 12, 667–678.
- Tam, P.P., Quinlan, G.A., 1996. Mapping vertebrate embryos. *Curr. Biol.* 6, 104–106.
- Tanaka, M., Wang, D.Y., Kamo, T., Igarashi, H., Wang, Y., Xiang, Y.Y., Tanioka, F., Naito, Y., Sugimura, H., 1998. Interaction of EphB2-tyrosine kinase receptor and its ligand conveys dorsalization signal in *Xenopus laevis* development. *Oncogene* 17, 1016–1509.
- Taneja, R., Thisse, B., Rijli, F.M., Thisse, C., Bouillet, P., Dolle, P., Chambon, P., 1996. The expression pattern of the mouse receptor tyrosine kinase gene *MDK1* is conserved through evolution and requires *Hoxa-2* for rhombomere-specific expression in mouse embryos. *Dev. Biol.* 177, 397–412.
- Tessier-Lavigne, M., Goodman, C.S., 1996. The molecular biology of axon guidance. *Science* 274, 1123–1133.
- van der Geer, P., Hunter, T., 1994. Receptor protein kinases and their signal transduction pathways. *Annu. Rev. Cell. Biol.* 10, 251–337.
- van Eeden, F.J., Granato, M., Schach, U., Brand, M., Furutani-Seiki, M., Haffter, P., Hammerschmidt, M., Heisenberg, C.P., Jiang, Y.J., Kane, D.A., Kelsh, R.N., Mullins, M.C., Odenthal, J., Warga, R.M., Nusslein-Volhard, C., 1996. Genetic analysis of fin formation in the zebrafish, *Danio rerio*. *Development* 123, 255–262.
- van Eeden, F.J., Holley, S.A., Haffter, P., Nusslein-Volhard, C., 1998. Zebrafish segmentation and pair-rule patterning. *Dev. Genet.* 23, 65–76.
- Wang, H.U., Chen, Z.F., Anderson, D.J., 1998. Molecular distinction and angiogenic interaction between embryonic arteries and veins revealed by ephrin-B2 and its receptor Eph-B4. *Cell* 93, 741–753.
- Warga, R.M., Kimmel, C.B., 1990. Cell movements during epiboly and gastrulation in zebrafish. *Development* 108, 569–580.
- Weinberg, E.S., Allende, M.L., Kelly, C.S., Abdelhamid, A., Murakami, T., Andermann, P., Doerre, O.G., Grunwald, D.J., Riggleman, B., 1996. Developmental regulation of zebrafish *MyoD* in wild-type, no tail and spadetail embryos. *Development* 122, 271–280.
- Westerfield, M., 1995. *The Zebrafish Book*. University of Oregon Press, Oregon.
- Wicks, I.P., Wilkinson, D., Salvaris, E., Boyd, A.W., 1992. Molecular cloning of HEK, the gene encoding a receptor tyrosine kinase expressed by human lymphoid tumor cell lines. *Proc. Natl. Acad. Sci. USA* 89, 1611–1615.
- Winklbauer, R., Nagel, M., Selchow, A., Wacker, S., 1996. Mesoderm migration in the *Xenopus* gastrula. *Int. J. Dev. Biol.* 40, 305–311.
- Winning, R.S., Sargent, T.D., 1994. Pagliaccio, a member of the Eph family of receptor tyrosine kinase genes, has localized expression in a subset of neural crest and neural tissues in *Xenopus laevis* embryos. *Mech. Dev.* 46, 219–229.
- Winning, R.S., Scales, J.B., Sargent, T.D., 1996. Disruption of cell adhesion in *Xenopus* embryos by Pagliaccio, an Eph-class receptor tyrosine kinase. *Dev. Biol.* 179, 309–319.
- Winslow, J.W., Moran, P., Valverde, J., Shih, A., Yuan, J.Q., Wong, S.C., Tsai, S.P., Goddard, A., Henzel, W.J., et al., 1995. Cloning of *AL-1*, a ligand for an Eph-related tyrosine kinase receptor involved in axon bundle formation. *Neuron* 14, 973–981.
- Woo, K., Fraser, S.E., 1995. Order and coherence in the fate map of the zebrafish nervous system. *Development* 121, 2595–2609.
- Xu, Q., Alldus, G., Holder, N., Wilkinson, D.G., 1995. Expression of truncated *Sek-1* receptor tyrosine kinase disrupts the segmental restriction of gene expression in the *Xenopus* and zebrafish hindbrain. *Development* 121, 4005–4016.
- Xu, Q., Alldus, G., Macdonald, R., Wilkinson, D.G., Holder, N., 1996. Function of the Eph-related kinase *rtk1* in patterning of the zebrafish forebrain. *Nature* 381, 319–322.
- Xu, Q., Holder, N., Patient, R., Wilson, S.W., 1994. Spatially regulated expression of three receptor tyrosine kinase genes during gastrulation in the zebrafish. *Development* 120, 287–299.
- Yamamoto, A., Amacher, S.L., Kim, S.H., Geisser, D., Kimmel, C.B., De Robertis, E.M., 1998. Zebrafish paraxial protocadherin is a downstream target of spadetail involved in morphogenesis of gastrula mesoderm. *Development* 125, 3389–3397.

D13

Protein Tyrosine Kinase cDNAs from Amphioxus, Hagfish, and Lamprey: Isoform Duplications Around the Divergence of Cyclostomes and Gnathostomes

Hiroshi Suga,¹ Daisuke Hoshiyama,¹ Shigehiro Kuraku,¹ Kazutaka Katoh,¹ Kaoru Kubokawa,² Takashi Miyata¹

¹ Department of Biophysics, Graduate School of Science, Kyoto University, Kyoto 606-8502, Japan

² Ocean Research Institute, The University of Tokyo, Nakano-ku, Tokyo 164-8639, Japan

Received: 28 April 1998 / Accepted: 30 June 1999

Abstract. Animals evolved a variety of gene families involved in cell–cell communication and developmental control by gene duplication and domain shuffling. Each family is made up of several subtypes or subfamilies with distinct structures and functions, which diverged by gene duplications and domain shufflings before the divergence of parazoans and eumetazoans. Since the separation from protostomes, vertebrates expanded the multiplicity of members (isoforms) in the same subfamily by further gene duplications in their early evolution before the fish–tetrapod split. To know the dates of isoform duplications more closely, we have conducted isolation and sequencing cDNAs encoding the fibroblast growth factor receptor, Eph, *src*, and platelet-derived growth factor receptor subtypes belonging to the protein tyrosine kinase family from *Branchiostoma belcheri*, an amphioxus, *Eptatretus burgeri*, a hagfish, and *Lampetra reissneri*, a lamprey. From a phylogenetic tree of each subfamily inferred from a maximum likelihood (ML) method, together with a bootstrap analysis based on the ML method, we have shown that the isoform duplications frequently occurred in the early evolution of vertebrates around or just before the divergence of cyclo-

stomes and gnathostomes by gene duplications and possibly chromosomal duplications.

Key words: Protein tyrosine kinases — isoforms — hagfish — lamprey — amphioxus — gene duplication — phylogenetic tree — evolution

Introduction

Multicellular animals evolved a variety of gene families involved in cell–cell communication and developmental control by gene duplication and domain shuffling. Each family diverged from one or a few ancestral genes, which are shared with plants and fungi, or from an ancestral gene created uniquely in animal lineage (e.g., Iwabe et al. 1996). From phylogenetic analyses of several gene families involved in the signal transduction and developmental control, we recently showed that the pattern of gene diversification is characterized by two active periods in gene duplication interrupted by considerably long periods of silence, instead of proceeding gradually (Suga et al. 1997, 1999; Koyanagi et al. 1998a, 1998b; Hoshiyama et al. 1998; Ono et al. 1999). In the early period before the parazoan–eumetazoan split, animals underwent extensive gene duplications (subtype duplications) that gave rise to different subtypes with diverse functions. Almost complete sets of present-day subtypes had been established within that period. After the divergence

Data deposition: The nucleotide sequence data reported in this paper have been deposited in the DDBJ, EMBL, and GenBank nucleotide sequence databases (accession nos. AB025534–AB025557)

Correspondence to: T. Miyata; e-mail: miyata@biophys.kyoto-u.ac.jp

Table 1. Degenerate primers used for the cloning of cDNAs from cyclostomes and amphioxus

		Primer		
Subtype		Name	Sequence	Amino acid sequence
FGFR	sense	S0	5'-GGTAARCCYITGGIGARGGIKSNNTTYGG-3'	GKPLGEG(C/A)FG
		S1	5'-GGCAAGCAYAARAAATIRTTIAAAYT-3'	GKHKN(I/V)NL
	antisense	A1	5'-GACGACICCIWRISHCCANAYRTC-3'	D(V/I)W(S/A)(F/Y/L)GVV
Eph	sense	S0	5'-GTIATIGGIGNIGGNGARTTYGG-3'	VIGXGEFG
		S1	5'-GTICAYMGIGAYYTIGCIRCNMGNAA-3'	VHRDLA(A/T)RN
	antisense	A1	5'-GCYTCIGGIGCIGTCCANC-3'	RWTAPEA
		A2	5'-GTCCAICKIAYIGGIATYTT-3'	KIP(I/V)RWT
src	sense	S1	5'-GGAVMNGGIYRITTYGGIGANGTNTGG-3'	GXG(Q/C)FG(E/D)VW
		S2	5'-GGNGARGTNTGGATGGGNACNTGGAAAYGG-3'	GEVWMGTWNG
	antisense	A1	5'-GCYTCIGGNGCIGTCCAYTTDATNGG-3'	PIKWTAPEA
		A2	5'-GGYTCNGTNGCNGTRAARTARTCYTCNARRAA-3'	FLEDYFTATEP
PDGFR	sense	S0	5'-GGTMRACCIYITGGINVIIGGICNTTYGG-3'	G(K/R)PLGXGAFG
		S1	5'-GGCAAGCAYAARAAATIRTTIAAAYT-3'	GKHKN(I/V)NL
	antisense	A1	5'-GACGACICCIWRISHCCANAYRTC-3'	D(V/I)W(S/A)(F/Y/L)GVV

The identical primer is used for the cloning of cDNAs from *Branchiostoma belcheri* (amphioxus), *Eptatretus burgeri* (hagfish), and *Lampetra reissneri* (lamprey), except for the lamprey Eph (see Materials and Methods).

of protostomes and deuterostomes, the multiplicity of members in the same subtype rapidly increased in the first half of chordate evolution before the fish-tetrapod split by further gene duplications (isoform duplications), which gave rise to different isoforms; in most cases, different isoforms in the same subfamily are virtually identical in structure and function, but differ in tissue distribution (for isoforms in the protein tyrosine kinase [PTK] family, see Kraus et al. 1989; Partanen et al. 1991; Shier and Watt 1992; Mustelin and Burn 1993; Takahashi and Shirasawa 1994; Fox et al. 1995). A remarkable consequence suggested by these analyses is that there might be no direct link between the Cambrian explosion and the burst of subtype duplication.

The extensive isoform duplication in the first half of chordate evolution has been identified in many subtypes belonging to various gene families (Miyata et al. 1994; Iwabe et al. 1996; Suga et al. 1997, 1999; Hoshiyama et al. 1998). To know the dates of the active period of isoform duplication more closely, we have conducted isolation and sequencing cDNAs encoding the fibroblast growth factor receptor (FGFR), Eph, *src*, and platelet-derived growth factor receptor (PDGFR) subtypes of the PTK family from an amphioxus, a hagfish, and a lamprey. We report here that the extensive isoform duplication is observed in a period around or immediately before the cyclostome-gnathostome split.

Materials and Methods

Isolation and Sequencing of Cyclostome and Amphioxus cDNAs

Total RNA of *Eptatretus burgeri*, a hagfish, was extracted from each of the liver, brain, and vestigial eye, and those of *Branchiostoma belcheri*

an amphioxus, and larva of *Lampetra reissneri*, a lamprey, were extracted from the whole body using TRIZOL Reagent (Gibco BRL). These total RNAs were reverse-transcribed to cDNAs using oligo(dT) primer with reverse transcriptase (SuperScript II, Gibco BRL) and were used as templates for PCR amplifications with Expand High-Fidelity PCR System (Roche). The sense and antisense degenerate primers were designed from conserved amino acid residues as shown in Table 1. PCR amplifications were carried out under annealing condition of 46°C with the primers S1 and A1 (see Table 1) for all subtypes shown in Table 1, followed by nested PCR with S1 and A2 for the Eph subtype of *L. reissneri*. In *E. burgeri*, cDNAs prepared from the liver, brain, and vestigial eye were used as templates, except for the Eph subtype, for which the cDNA from the brain was used. For the *src* subtype, we carried out another PCR procedure with the primers S1 and A2 under annealing condition of 46°C, followed by nested PCR with S2 and A1 under 50°C.

The PCR-amplified fragments were purified and cloned into the pT7Blue vector (Novagen). More than three independent clones were isolated for each gene and sequenced using BigDye Terminator Cycle Sequencing Ready Reaction Kit and ABI PRISM 377 DNA Sequencer (Perkin-Elmer).

The 3' ends of cDNAs were amplified using 3' RACE System for Rapid Amplification of cDNA Ends (Gibco BRL). The 5' portions of cDNAs belonging to the FGFR, PDGFR, and Eph subtypes were amplified by PCR using respective subtype-specific sense primers (S0) and gene-specific antisense primers. These amplified fragments were purified, subcloned, and sequenced in the same way as above.

Sequence Alignment and Phylogenetic Tree Inference

Alignments were made by the methods of Needleman and Wunsch (1970) and Berger and Munson (1991), together with manual inspection.

The method of phylogenetic tree inference we adopted here is an approximate method for inferring the maximum likelihood (ML) tree of protein phylogeny (Kishino et al. 1990). This method consists of performing rearrangement of tree topology for a limited number of initial trees by the methods of nearest-neighbor interchange (NNI; Swofford et al. 1996; Adachi and Hasegawa 1996) and subtree pruning and regrafting (SPR; Swofford et al. 1996). The calculation procedure is as follows:

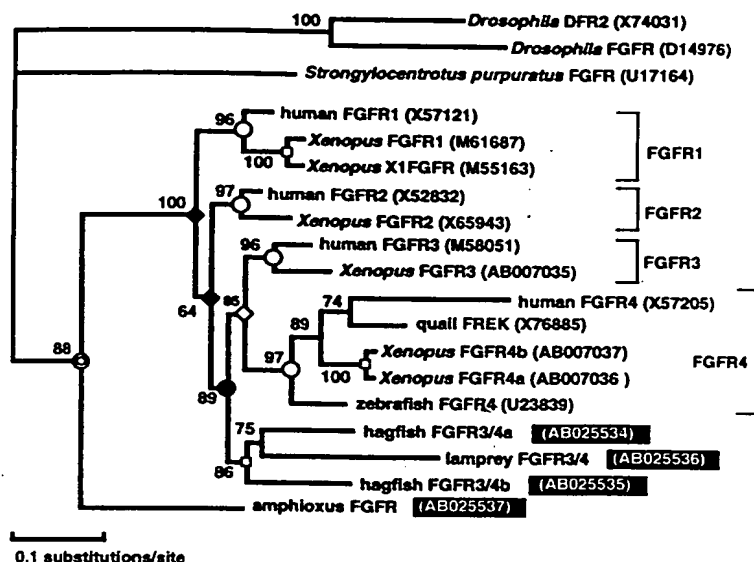


Fig. 1. Maximum likelihood tree of FGFR subfamily. From a comparison of the kinase domain sequences, the tree was inferred by an approximate ML method described in Materials and Methods, using *Drosophila* FGFRs as an outgroup. The number at each branch node represents the local bootstrap probability estimated by the RELL method (Kishino et al. 1990; Hasegawa and Kishino 1994). Open circles, fish-tetrapod split or amphibian-amniote split; filled circle, cyclostome-gnathostome split; double circle, cephalochordate-vertebrate split; open rhombus, gene duplication that postdates the cyclostome-gnathostome split, but antedates the fish-tetrapod split; filled rhombi, gene duplications that antedate the cyclostome-gnathostome split; open boxes, gene duplications on the lineage leading to cyclostomes or *Xenopus*. Accession numbers of sequences are shown in parentheses; reverse letters, present work.

1. Based on the neighbor joining (NJ) method (Saitou and Nei 1987) using the distance matrix estimated by the ML method (Adachi and Hasegawa 1996), 4,000 tree topologies, including that inferred from actual alignment are generated by the bootstrap resampling procedure (Felsenstein 1985).
2. For each of the 4,000 trees, the log-likelihood value is calculated by the ML method of protein phylogeny (Kishino et al. 1990; Adachi and Hasegawa 1996) based on the JTT model (PROTML version 2.3 in Adachi and Hasegawa's program package MQLPHY), and the top 40 trees are selected by log-likelihood criterion.
3. The tree topology with the largest log-likelihood value (approximate ML tree) is searched through repeated local rearrangements (Adachi and Hasegawa 1996) by NNI for all the 40 trees obtained in step 2.
4. To exclude a possibility that the approximate ML tree obtained in step 3 is local optimum, the approximate ML tree is subjected to further rearrangements by SPR. If no tree with log-likelihood value being larger than that of the approximate ML tree in step 3 is generated by SPR, the calculation procedure is completed. Alternatively if trees with larger log-likelihood value are obtained, the procedures in steps 3 and 4 are repeated for these trees.

The local bootstrap probability (LBP) at each node of a tree was calculated by the RELL method (Kishino et al. 1990; Hasegawa and Kishino 1994).

Results and Discussion

Each of the animal gene families involved in cell-cell communication and developmental control diverged from one or a few ancestral genes during animal evolution by gene duplications and domain shufflings. The family tree comprises several independent clusters corresponding to different subtypes or subfamilies that diverged before the divergence of parazoans and eumetazoans, the earliest divergence among extant animal phyla (Koyanagi et al. 1998a, 1998b; Hoshiyama et al. 1998; Siga et al. 1999; Ono et al. 1999). After the separation from protostomes, chordates expanded the multiplicity of members in the same subfamily by further gene dupli-

cations (isoform duplications). These isoform duplications have been completed until dates before the fish-tetrapod split (Miyata et al. 1994; Iwabe et al. 1996; Suga et al. 1997, 1999; Hoshiyama et al. 1998).

To determine the divergence times of these isoforms more closely, we have conducted isolation and sequencing cDNAs encoding the FGFR, Eph, *src*, and PDGFR subtypes belonging to the PTK family from *B. belcheri*, *E. burgeri*, and *L. reissneri* by the method described in Materials and Methods. Including these sequences, phylogenetic trees of the four subfamilies have been inferred by the ML analysis described in Materials and Methods.

Phylogenetic Tree of FGFR Subfamily

At least four distinct members (FGFR1–FGFR4) belonging to the FGFR subfamily have already been identified in gnathostomes, and they exhibit different tissue distribution (Partanen et al. 1991). We have isolated two cDNAs from *E. burgeri*, one cDNA from *L. reissneri*, and one cDNA from *B. belcheri*, and their nucleotide sequences have been determined for regions encoding the kinase domain. The amino acid sequences encoded by these cDNAs were aligned with known FGFR sequences for a highly conserved region corresponding to amino acid positions 491–780 in human FGFR1, for which unambiguous alignment is possible (alignment not shown). On the basis of the alignment comprising 270 amino acid sites, excluding gap positions, a phylogenetic tree was inferred, using two *Drosophila* FGFRs as an outgroup. The obtained ML tree is shown in Fig. 1.

According to Fig. 1, the three gene duplications that gave rise to the four gnathostome FGFRs obviously antedate the divergence of amphibian and amniotes, as previously shown (Iwabe et al. 1996; Suga et al. 1997). It is also evident that these gene duplications postdate the

cephalochordate-vertebrate split. In the accompanying paper (Kuraku et al. 1999), we have shown that lampreys and hagfishes form a monophyletic group (see also Stock and Whitt 1992; Mallatt and Sullivan 1998). The FGFR tree also supports the cyclostome monophyly: the hagfish FGFR3/4a shows a close association with the lamprey FGFR3/4, although the bootstrap probability is not significantly high. It is therefore likely that the hagfish FGFR3/4a and the lamprey FGFR3/4, together with the hagfish FGFR3/4b that was generated in the cyclostome lineage by gene duplication, are the cyclostome homologs of vertebrate FGFR3 and FGFR4. Thus, Fig. 1 suggests that, of the three gene duplications that generated the four gnathostome FGFRs, two gene duplications antedate the cyclostome-gnathostome split, but the latest gene duplication that gave rise to FGFR3 and FGFR4 occurred after the cyclostome-gnathostome split.

Two more gene duplications were observed on *Xenopus* lineage (Fig. 1). Such gene duplications were also observed in other genes, which might be derived by very recent chromosomal duplications (Suga et al. 1997). The gene duplications on *Xenopus* lineage were also observed in Eph4 (Sek-1/Pag) and src (*src-1/2*) (see below). We do not discuss further these recent gene duplications in *Xenopus*. In addition to the gene duplication in hagfish (FGFR3/4a and 3/4b), two more gene duplications were also observed in Eph subfamily (hagfish EphC1/2) and in PGDFR subfamily (lamprey *kit*-like receptor A/B) (see below). Divergence of the hagfish EphC1 and EphC2 may have occurred by a very recent gene duplication, judging from the number (k_s) of synonymous substitution per site (Miyata and Yasunaga 1980); the value is only 0.67, which is comparable to the corresponding value (0.64 ± 0.18 on the average of 574 genes) between human and rodents (unpublished data).

Phylogenetic Tree of Eph Subfamily

A similar analysis was carried out for Ephs, members of the PTK family. At least 13 gnathostome Ephs have been identified to date (Flanagan and Vanderhaeghen 1998); because EphB6 is highly divergent and the structure is unusual, this member was excluded from all the analyses (Matsuoka et al. 1997). We have isolated four cDNAs from *E. burgeri*, two cDNAs from *L. reissneri*, and two cDNAs from *B. belcheri*, and their nucleotide sequences have been determined for regions encoding the kinase domain. The amino acid sequences of the cyclostome and amphioxus Ephs were aligned with those of known Ephs for regions corresponding to amino acid positions 632–973 in human EphB1. On the basis of the alignment of 306 sites in total, excluding gap sites, a phylogenetic tree of Eph subfamily was inferred, using nematode and sponge Ephs as an outgroup (Fig. 2).

The phylogenetic tree of Fig. 2 shows that all gene

duplications occurred after the divergence of cephalochordates and vertebrates. The tree also shows that all gene duplications (represented by rhombi in Fig. 2) that gave rise to known Eph isoforms (EphA1–EphA8 and EphB1–EphB5) antedate the amphibian-amniote split or the fish-tetrapod split, as expected (Iwabe et al. 1996; Suga et al. 1997); for four gene duplications that gave rise to EphA3 and EphA5–EphA8, their divergence times are unknown. The hagfish EphA and the hagfish and lamprey EphBs are likely homologs of gnathostome EphA4 and EphB2/5, respectively; note that the cyclostome EphBs support the cyclostome monophyly. Of the 14 gene duplications, excluding gene duplications on the *Xenopus*, zebrafish, hagfish, and amphioxus lineages (represented by open boxes), six gene duplications (filled rhombi) antedate the cyclostome-gnathostome split, and one gene duplication (open rhombus) postdates that split: for the remaining seven gene duplications (half-filled rhombi), the divergence times are unknown, although three antedate the fish-tetrapod split. It is therefore likely that, since the separation from cephalochordates, vertebrates created many Eph isoforms by gene duplications, most of which occurred at dates before the divergence of cyclostomes and gnathostomes.

In addition to gene duplications on *Xenopus* and cyclostome lineages (see above), one gene duplication was observed in each of the amphioxus and zebrafish lineages (Eph1/2 and *rik5/8*, respectively). The amphioxus Eph1 and Eph2 might diverged recently, judging from the k_s value (0.79) between them. One more example of gene duplication (*src*-like protein A/B) on amphioxus lineage was found in the *src* subfamily (see below).

Phylogenetic Tree of *src* Subfamily

We have isolated three cDNAs from *E. burgeri*, two cDNAs from *L. reissneri*, and two cDNAs from *B. belcheri* and compared these sequences with known sequences belonging to the *src* subfamily. On the basis of the sequence alignment for regions corresponding to the amino acid positions 292–531 in human *src* (238 amino acid sites total, excluding gap sites), a phylogenetic tree of *src* subfamily was inferred, using hydra and sponge *src*-related sequences as an outgroup (Fig. 3). The hagfish *src*-like protein C might be orthologous to the gnathostome *srcs*. The hagfish and lamprey *src*-like protein As are possibly paralogous, if the cyclostome monophyly is correct, and the former is the ortholog of human *lck*. There is, however, still a possibility that the two cyclostome sequences form a cluster.

The ML tree revealed that all gene duplications (represented by rhombi in Fig. 3) that gave rise to known isoform genes belonging to the *src* subfamily postdate the cephalochordate-vertebrate split, but antedate the amphibian-amniote split or the fish-tetrapod split. The

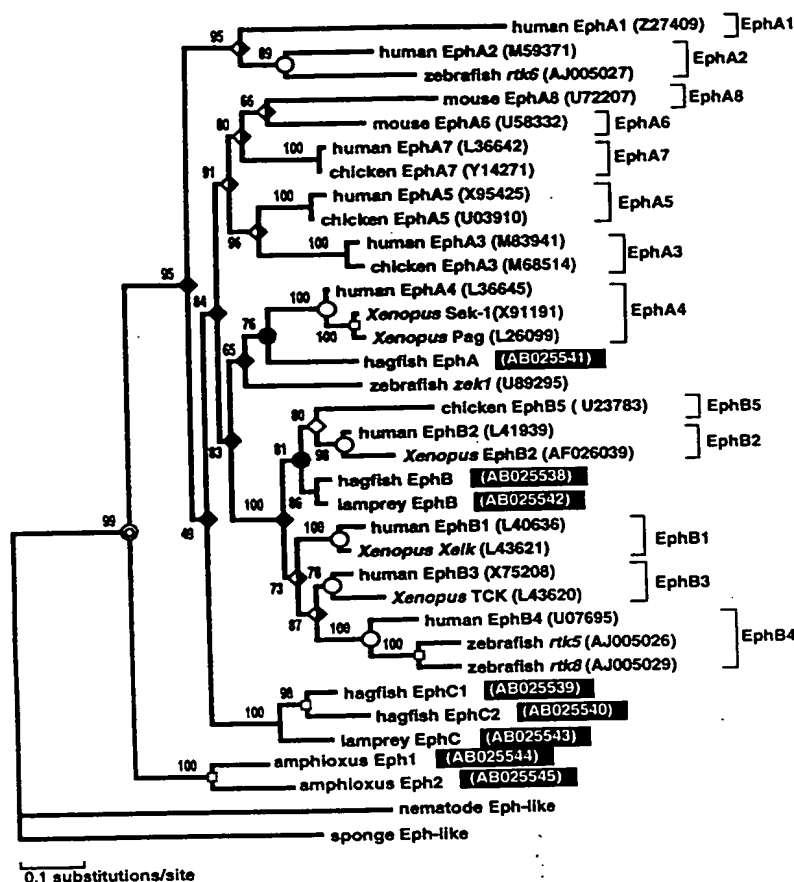


Fig. 2. Maximum likelihood tree of Eph subfamily. From a comparison of the kinase domain sequences, the tree was inferred by an approximate ML method described in Materials and Methods, using nematode and sponge Eph-like sequences as an outgroup. The number at each branch node represents the local bootstrap probability estimated by the RELL method (Kishino et al. 1990; Hasegawa and Kishino 1994). Open circles, fish-tetrapod split or amphibian-amniote split; filled circles, cyclostome-gnathostome split; double circle, cephalochordate-vertebrate split; filled rhombi, gene duplications that antedate the cyclostome-gnathostome split; open rhombus, gene duplication that postdates the cyclostome-gnathostome split, but antedates the amphibian-amniote split; half-filled rhombi, gene duplications whose divergence times are unknown; open boxes, gene duplications on the lineage leading to cyclostomes, *Xenopus*, fish, or cephalochordates. Accession numbers of sequences are shown in parentheses: reverse letters, present work.

seven gene duplications out of 10 antedate the cyclostome-vertebrate split: for the remaining three, their divergence times are unknown.

Phylogenetic Tree of PDGFR Subfamily

We have isolated two cDNAs from *E. burgeri*, two cDNAs from *L. reissneri*, and one cDNA from *B. belcheri*. These sequences were aligned with those reported to date for regions corresponding to the amino acid positions 606–953 in human PDGF α R (245 amino acid sites total, excluding gap sites). Figure 4 shows the ML tree inferred by using human, purple urchin, and *Drosophila* FGFRs as an outgroup. According to Fig. 4, the hagfish *kit*-like receptor and the lamprey *kit*-like receptor A support the cyclostome monophyly, although the bootstrap probability is not high enough. Unlike the above three subfamilies, the deepest gene duplication antedates the cephalochordate-vertebrate split. Because the group of five isoforms, PDGF α / β R, Flt3, CSF-1R, and *c-kit*, has five immunoglobulin (Ig)-like repeats in the extracellular region, whereas the group of VEGFR, FLT4, and Flk1 has seven Ig-like repeats (van der Geer et al. 1994), it remains possible that they comprise separate subfamilies. In the former group, all the four gene

duplications that gave rise to distinct isoforms antedate the cyclostome-gnathostome split.

Bootstrap Analysis for Estimating the Number of Isoform Duplications

The above phylogenetic analyses of the four subfamilies provides clear evidence that most if not all isoform duplications occurred in a period between the cephalochordate-vertebrate split and the amphibian-amniote split. It is, however, not obvious whether the majority of isoform duplications predate or postdate the cyclostome-gnathostome split. This may be due to simultaneous isoform duplications around the cyclostome-gnathostome split, judging from the short branch lengths and the low bootstrap probabilities around that split on trees. It is therefore necessary to estimate the number of isoform duplication on a solid statistical basis. For this purpose, we carried out a bootstrap analysis similar to that described previously (Suga et al. 1997). Based on the standard bootstrap procedure (Felsenstein 1985), we generated 100 ML trees with the largest log-likelihood value by repeated local rearrangements (Adachi and Hasegawa 1996), using the NJ trees as initial trees. From these set of ML trees, the numbers of isoform duplications that

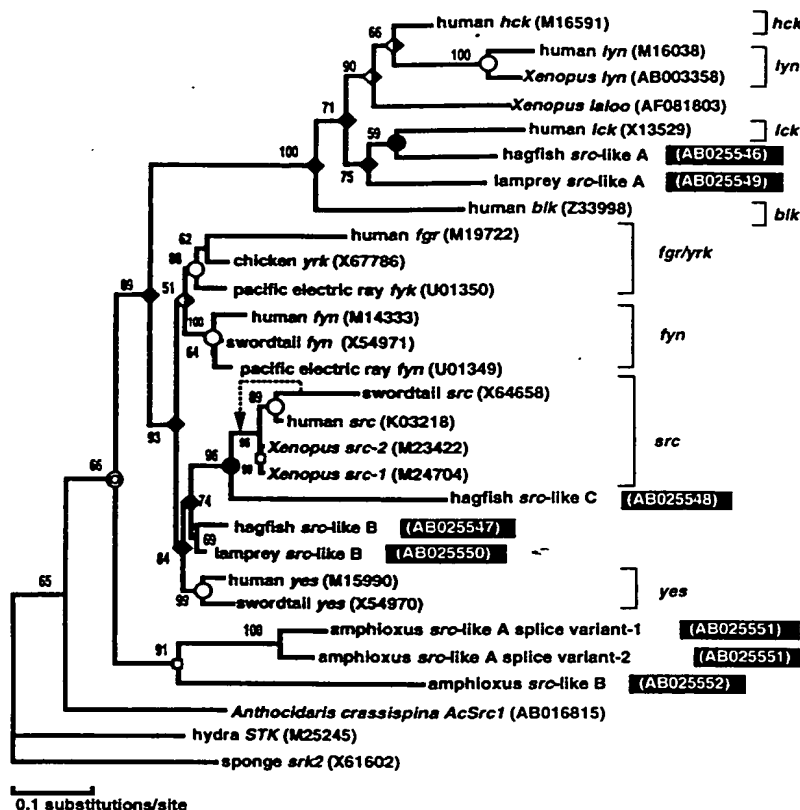


Fig. 3. Maximum likelihood tree of *src* subfamily. From a comparison of the kinase domain sequences, the tree was inferred by an approximate ML method described in Materials and Methods, using hydra and sponge sequences as an outgroup. The number at each branch node represents the local bootstrap probability estimated by the RELL method (Kishino et al. 1990; Hasegawa and Kishino 1994). The dotted arrow means that the swordtail *src* is the outgroup of the human and *Xenopus* *srcs*, when their complete sequences are compared. Open circles, fish–tetrapod split or amphibian–amniote split; filled circles, cyclostome–gnathostome split; double circle, cephalochordate–vertebrate split; filled rhombi, gene duplications that antedate the cyclostome–gnathostome split; half-filled rhombi, gene duplications whose divergence times are unknown; open boxes, gene duplications on the lineage leading to *Xenopus* or cephalochordates. Accession numbers of sequences are shown in parentheses; reverse letters, present work.

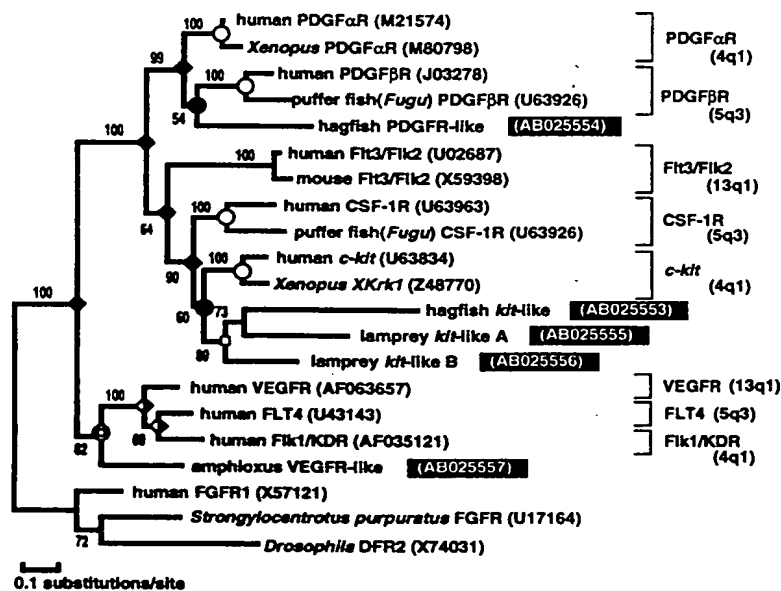


Fig. 4. Maximum likelihood tree of PDGFR subfamily. From a comparison of the kinase domain sequences, the tree was inferred by an approximate ML method described in Materials and Methods, using human, purple urchin, and *Drosophila* FGFR sequences as an outgroup. The number at each branch node represents the local bootstrap probability estimated by the RELL method (Kishino et al. 1990; Hasegawa and Kishino 1994). Open circles, fish–tetrapod split or amphibian–amniote split; filled circles, cyclostome–gnathostome split; double circle, cephalochordate–vertebrate split; filled rhombi, gene duplications that antedate the cyclostome–gnathostome split; half-filled rhombi, gene duplications whose divergence times are unknown. Data on chromosomal mapping of human genes were taken from van der Geer et al. (1994). Accession numbers of sequences are shown in parentheses; reverse letters, present work.

took place at dates before and after the cyclostome–gnathostome split were counted (designated as N_b and N_a , respectively).

Table 2 shows the results of the four subfamilies, together with those of the other three protein groups. In the seven gene groups examined here, N_b is always larger than N_a ; the former is three times larger in value

than the latter, on the average. Since the value of N_a is not negligibly small, it may be reasonable to conclude that extensive isoform duplications occurred in a limited period around or just before the divergence of cyclostomes and gnathostomes.

There is a possibility that these isoform duplications were derived from chromosomal duplications in part

Table 2. The numbers of isoform duplications in evolutionary periods before and after the divergence of cyclostomes and gnathostomes

	N_b	N_a	N_b/N_a
PTK subfamily			
FGFR	2.6 ± 1.2	1.3 ± 1.0	2.0
Eph	6.5 ± 1.4	2.3 ± 1.8	2.8
src	7.2 ± 1.4	1.7 ± 1.5	4.2
PDGFR	3.9 ± 1.1	0.8 ± 0.9	4.9
Other proteins			
Aldolase	1.3 ± 0.9	1.2 ± 0.9	1.1
Enolase	2.1 ± 0.9	1.1 ± 1.0	1.9
Complements	2.4 ± 0.5	0.1 ± 0.3	24
Total	26.0	8.5	3.1

N_b and N_a , the numbers of isoform duplications that occurred at dates before and after the cyclostome–gnathostome split, respectively. Isoform duplications whose divergence times are unknown were excluded from the calculations of N_b and N_a . For the calculation procedures, see text. Complements, gene groups encoding the complement components C3, C4, and C5. For the phylogenetic trees of three gene groups in other proteins, see the accompanying paper (Kuraku et al. 1999).

(Ohno 1970; Lundin 1993; Rousset et al. 1995; Bailey et al. 1997; Pébusque et al. 1998; Amores et al. 1998). From a structural and phylogenetic analysis of PDGFR subfamily, together with the chromosomal mappings of the family members, Rousset et al. (1995) suggested that the present-day PDGFR subfamily diverged by gene duplications and chromosomal duplications, although it is generally difficult to infer the chromosomal duplication events on ancient lineages because of frequent translocation and deletion events during evolution. Figure 4 supports the argument by Rousset et al. (1995). According to Fig. 4, PDGFR subfamily comprises three separate groups, PDGF α / β R group, CSF-1R group (Flt3/Flk2, CSF-1R, and *c-kit*), and VEGFR group (VEGFR, FLT4, and Flk1/KDR), which were generated by the first and second gene duplications. Each group has two more isoform duplications, which gave rise to three different isoforms (in PDGF α / β R group one member might be deleted during evolution). Their chromosomal locations on the human genome differ in the same group, but coincide to each other between different groups. It is therefore likely that two chromosomal duplications are responsible for the two isoform duplications in each group.

In conclusion, after the separation from cephalochordates, vertebrates evolved a variety of tissue-specific genes with virtually identical structure and function in each subfamily in a limited period around or just before the divergence of cyclostomes and gnathostomes by gene duplications and possibly chromosomal duplications. Cephalochordates are likely to have multiple isoforms generated by gene duplications on cephalochordate lineage, independently from vertebrates, although less frequent. Cyclostomes also increased the multiplicity of family members by such lineage-specific gene duplications. From phylogenetic analyses of several gene fam-

lies involved in the signal transduction and developmental control, we recently showed that most subtype duplications that gave rise to different subfamilies with diverse functions had been completed before the para-zoan–eumetazoan split, the earliest divergence of extant animal phyla (Suga et al. 1997, 1999; Koyanagi et al. 1998a, 1998b; Hoshiyama et al. 1998; Ono et al. 1999). These results suggest that the Cambrian explosion, the burst of diversification of the major group of animal phyla at the Cambrian/Vendian boundary (Conway Morris 1993), has been accomplished without creating further new genes. Thus, the molecular mechanism of the Cambrian explosion should be understood based on mechanisms that could generate organismal diversity by utilizing or recruiting preexisting genes, but not by creating new genes with novel functions.

Acknowledgments. We thank Prof. M. Hasegawa, Dr. N. Iwabe, and Dr. K. Kuma for discussion. This work was supported by grants from the Ministry of Education, Science, Sports and Culture of Japan.

References

- Adachi J, Hasegawa M (1996) Computer science monographs, no. 28. MOLPHY version 2.3: Programs for molecular phylogenetics based on maximum likelihood. Institute of Statistical Mathematics, Tokyo
- Amores A, Force A, Yan Y-L, Joly L, Amemiya C, Fritz A, Ho RK, Langeland J, Prince V, Wang Y-L, Westerfield M, Ekker M, Postlethwait JH (1998) Zebrafish *hox* clusters and vertebrate genome evolution. *Science* 282:1711–1714
- Bailey WJ, Kim J, Wagner GP, Ruddle FH (1997) Phylogenetic reconstruction of vertebrate Hox cluster duplications. *Mol Biol Evol* 14:843–853
- Berger MP, Munson PJ (1991) A novel randomized iterative strategy for aligning multiple protein sequences. *CABIOS* 7:479–484
- Conway Morris S (1993) The fossil record and the early evolution of the Metazoa. *Nature* 361:219–225
- Felsenstein J (1985) Confidence limits on phylogenies: an approach using the bootstrap. *Evolution* 39:783–791
- Flanagan JG, Vanderhaeghen P (1998) The ephrins and Eph receptors in neural development. *Ann Rev Neurosci* 21:309–345
- Fox GM, Holst PL, Chute HT, Lindberg RA, Janssen AM, Basu R, Welcher AA (1995) cDNA cloning and tissue distribution of five human EPH-like receptor protein-tyrosine kinases. *Oncogene* 10: 897–905
- Hasegawa M, Kishino H (1994) Accuracies of the simple methods for estimating the bootstrap probability of a maximum likelihood tree. *Mol Biol Evol* 11:142–145
- Hoshiyama D, Suga H, Iwabe N, Koyanagi M, Nikoh N, Kuma K, Matsuda F, Honjo T, Miyata T (1998) Sponge *Pax* cDNA related to *Pax-2/5/8* and ancient gene duplications in the *Pax* family. *J Mol Evol* 47:640–648
- Iwabe N, Kuma K, Miyata T (1996) Evolution of gene families and relationship with organismal evolution: rapid divergence of tissue-specific genes in the early evolution of chordates. *Mol Biol Evol* 13:483–493
- Kishino H, Miyata T, Hasegawa M (1990) Maximum-likelihood inference of protein phylogeny and the origin of chloroplasts. *J Mol Evol* 30:151–160
- Koyanagi M, Suga H, Hoshiyama D, Ono K, Iwabe N, Kuma K, Miyata T (1999) Ancient gene duplication and domain shuffling in

- animal cyclic nucleotide phosphodiesterase family. *FEBS Lett* 436: 323–328
- Koyanagi M, Ono K, Suga H, Iwabe N, Miyata T (1998b) Phospholipase C cDNAs from sponge and hydra: antiquity of genes involved in the inositol phospholipid signaling pathway. *FEBS Lett* 439:66–70
- Kraus MH, Issing W, Miki T, Popescu NC, Aaronson SA (1989) Isolation and characterization of *ERBB3*, a third member of the *ERBB*/epidermal growth factor receptor family: evidence for overexpression in a subset of human mammary tumors. *Proc Natl Acad Sci USA* 86:9193–9197
- Kuraku S, Hoshiyama D, Katoh K, Suga H, Miyata T (1999) Monophyly of lampreys and hagfishes supported by nuclear DNA-coded genes. *J Mol Evol* (in press)
- Lundin LG (1993) Evolution of the vertebrate genome as reflected in paralogous chromosomal regions in man and the house mouse. *Genomics* 16:1–19
- Mallatt J, Sullivan J (1998) 28S and 18S rDNA sequences support the monophyly of lampreys and hagfishes. *Mol Biol Evol* 15:1706–1718
- Matsuoka H, Iwata N, Ito M, Shimoyama M, Nagata A, Chihara K, Takai S, Matsui T (1997) Expression of a kinase-defective Eph-like receptor in the normal human brain. *Biochem Biophys Res Comm* 235:487–492
- Miyata T, Yasunaga T (1980) Molecular evolution of mRNA: a method for estimating evolutionary rates of synonymous and amino acid substitutions from homologous nucleotide sequences and its application. *J Mol Evol* 16:23–36
- Miyata T, Kuma K, Iwabe N, Nikoh N (1994) A possible link between molecular evolution and tissue evolution demonstrated by tissue specific genes. *Jpn J Genet* 69:473–480
- Mustelin T, Burn P (1993) Regulation of *src* family tyrosine kinases in lymphocytes. *Trends Biochem Sci* 18:215–220
- Needleman SB, Wunsch CD (1970) A general method applicable to the search for similarities in the amino acid sequence of two proteins. *J Mol Biol* 48:443–453
- Ohno S (1970) Evolution by gene duplication. Springer Verlag, New York, NY
- Ono K, Suga H, Iwabe N, Kuma K, Miyata T (1999) Multiple protein tyrosine phosphatases in sponge and explosive gene duplication in the early evolution of animals before the parazoan-eumetazoan split. *J Mol Evol* 48:654–662
- Partanen J, Mäkelä TP, Eerola E, Korhonen J, Hirvonen H, Claesson-Welsh L, Alitalo K (1991) FGFR-4, a novel acidic fibroblast growth factor receptor with a distinct expression pattern. *EMBO J* 10:1347–1354
- Pébusque M-J, Coulier F, Birnbaum D, Pontarotti P (1998) Ancient large-scale genome duplications: phylogenetic and linkage analyses shed light on chordate genome evolution. *Mol Biol Evol* 15:1145–1159
- Rousset D, Agnès F, Lachaume P, André C, Galibert F (1995) Molecular evolution of the genes encoding receptor tyrosine kinase with immunoglobulin like domains. *J Mol Evol* 41:421–429
- Saitou N, Nei M (1987) The neighbor-joining method: a new method for reconstructing phylogenetic trees. *Mol Biol Evol* 4:406–425
- Shler P, Watt VM (1992) Tissue-specific expression of the rat insulin receptor-related receptor gene. *Mol Endocrinol* 6:723–729
- Stock DW, Whitt GS (1992) Evidence from 18S ribosomal RNA sequences that lampreys and hagfishes form a natural group. *Science* 257:787–789
- Swofford DL, Olsen GJ, Waddell PJ, Hillis DM (1996) Phylogenetic inference. In: Hillis DM, Moritz C, Mable BK (eds) *Molecular systematics*. 2d edition. Sinauer Associates, Sunderland, MA. pp 407–514
- Suga H, Kuma K, Iwabe N, Nikoh N, Ono K, Koyanagi M, Hoshiyama D, Miyata T (1997) Intermittent divergence of the protein tyrosine kinase family during animal evolution. *FEBS Lett* 412:540–546
- Suga H, Koyanagi M, Hoshiyama D, Ono K, Iwabe N, Kuma K, Miyata T (1999) Extensive gene duplication in the early evolution of animals before the parazoan-eumetazoan split demonstrated by G proteins and protein tyrosine kinases from sponge and hydra. *J Mol Evol* 48:646–653
- Takahashi T, Shirasawa T (1994) Molecular cloning of rat JAK3, a novel member of the JAK family of protein tyrosine kinases. *FEBS Lett* 342:124–128
- van der Geer P, Hunter T, Lindberg RA (1994) Receptor protein-tyrosine kinases and their signal transduction pathways. *Ann Rev Cell Biol* 10:251–337

Expression of truncated *Sek-1* receptor tyrosine kinase disrupts the segmental restriction of gene expression in the *Xenopus* and zebrafish hindbrain

Qiling Xu^{1,*}, Graham Alldus^{2,*}, Nigel Holder¹ and David G. Wilkinson^{2,†}

¹Developmental Biology Research Centre, Division of Biomedical Sciences, Randall Institute, Kings College, 26-29 Drury Lane, London WC2B 5RL, UK

²Laboratory of Developmental Neurobiology, National Institute for Medical Research, The Ridgeway, Mill Hill, London NW7 1AA, UK

*These authors contributed equally to this work

†Author for correspondence (e-mail: d-wilkin@nimr.mrc.ac.uk)

SUMMARY

During development of the vertebrate hindbrain regulatory gene expression is confined to precise segmental domains. Studies of cell lineage and gene expression suggest that establishment of these domains may involve a dynamic regulation of cell identity and restriction of cell movement between segments. We have taken a dominant negative approach to interfere with the function of *Sek-1*, a member of the Eph-related receptor tyrosine kinase family expressed in rhombomeres r3 and r5. In *Xenopus* and zebrafish embryos expressing truncated *Sek-1*, lacking kinase sequences, expression of r3/r5 markers occurs in

adjacent even-numbered rhombomeres, in domains contiguous with r3 or r5. This disruption is rescued by full-length *Sek-1*, indicating a requirement for the kinase domain in the segmental restriction of gene expression. These data suggest that *Sek-1*, perhaps with other Eph-related receptors, is required for interactions that regulate the segmental identity or movement of cells.

Key words: segmentation, rhombomere, *Sek-1*, Eph, cell-cell interactions, community effect, zebrafish, *Xenopus*

INTRODUCTION

In many animal phyla, certain tissues are subdivided during embryogenesis into repeated morphological units, or segments, that then differentiate to generate a series of homologous structures. The molecular mechanisms underlying segmentation are best understood in the *Drosophila* embryo. In this system, the embryo is subdivided into presumptive segments at syncytial stages by a cascade of interactions between genes encoding transcription factors. This cascade establishes the expression of short-range signalling molecules in adjacent cells at the parasegment border, and these signals regulate the positional identity of neighbouring cells, as marked by segmental gene expression, and stabilise the boundary region (reviewed by Ingham and Martinez Arias, 1992; DiNardo et al., 1994). In contrast, little is known regarding the molecular mechanisms regulating the positional identity of cells during segmentation in the vertebrate embryo.

In recent years it has been shown that segmentation occurs in the vertebrate hindbrain and underlies the specification of nerves (Metcalf et al., 1986; Hanneman et al., 1988; Lumsden and Keynes, 1989; Clarke and Lumsden, 1993) and of neural crest cells migrating to the branchial arches (Noden, 1983, 1988; Lumsden et al., 1991; Serbedzija et al., 1992; Sechrist

et al., 1993). A molecular correlate of this cellular patterning is provided by the segment-restricted expression domains of genes, including *Krox-20* and *Hox* genes, encoding transcription factors required for the formation of the anterior-posterior (A-P) specification of segments (reviewed by McGinnis and Krumlauf, 1992; Wilkinson, 1993). For example, the *Krox-20* gene, required for r3 and r5 formation (Schneider-Maunoury et al., 1993), is up-regulated in the early neural plate prior to segmentation in two fuzzy domains that then become progressively sharper and restricted precisely to definitive r3 and r5 (Wilkinson et al., 1989; Nieto et al., 1991; Irving et al., 1995). This raises the question as to how the fuzzy expression domains are sharpened to become segment-restricted.

Studies in the chick embryo provide evidence for cellular mechanisms that might underlie the segmental restriction of gene expression. Transplantation experiments indicate that a regional specification of presumptive r4 occurs prior to segmentation (Guthrie et al., 1992). However, the clonal progeny of a single neuroepithelial cell labelled before segmentation disperse widely and frequently contribute to more than one segment (Fraser et al., 1990). After boundary formation most clonal progeny are confined to a single rhombomere (Fraser et al., 1990), but even at this stage some contribute to an adjacent segment (Birgbauer and Fraser, 1994). A potential mechanism

for the restriction of cell movement is indicated by the finding that cells from r3 and r5 mix more readily with each other than they do with cells from r2, r4 and r6 (Guthrie et al., 1993). Similarly, cells from r2, r4 and r6 are more miscible with each other than they are with r3 or r5. Cell adhesion properties that alternate between rhombomeres may therefore restrict cell movement across boundaries, and cell sorting could contribute to the sharpening of gene expression domains. However, since individual cells are not irreversibly committed to a specific rhombomere there must also be a dynamic regulation of the segmental identity of cells.

Based upon the critical roles of receptor tyrosine kinases (RTKs) in transducing signals that regulate cell fate in other systems (reviewed by Pawson and Bernstein, 1990; Dickson and Hafen, 1994; van der Geer et al., 1994), genes mediating cell-cell interactions during hindbrain segmentation might be found among the RTK superfamily. Indeed, in recent work, we and others have identified a number of RTKs segmentally expressed in the hindbrain that are members of the *Eph*-related family. *Eph*-related genes make up the largest known family of RTKs and their expression in the developing and mature CNS suggests potential roles in neural development and function (for review see van der Geer et al., 1994). However, little is known regarding the roles of *Eph*-related RTKs. Recently, several ligands have been identified and shown to constitute a family of structurally related proteins, all anchored in the plasma membrane, either via a transmembrane domain or a glycosylphosphatidyl inositol linkage (Bartley et al., 1994; Beckmann et al., 1994; Cheng and Flanagan, 1994; Davis et al., 1994). It is therefore likely that *Eph*-related RTKs mediate cell contact-dependent signalling.

Studies of *Eph*-related RTKs in the mouse have shown that, in addition to expression elsewhere in the early embryo, *Sek-1* (Nieto et al., 1992) and *Sek-2/leck* (Becker et al., 1994; Ganju et al., 1994; Ruiz and Robertson, 1994) are up-regulated in the hindbrain prior to segmentation, in pre-r3 plus pre-r5 and in pre-r4, respectively. In contrast, expression of *Sek-3/nuk* (Becker et al., 1994; Henkemeyer et al., 1994) and *Sek-4* (Becker et al., 1994) is restricted to r3 plus r5 later, after segmentation. Three *Eph*-related zebrafish genes, *rtk1-3* (Xu et al., 1994), also have segmental expression in the hindbrain (Q.X. and N.H., unpublished observations). These studies suggest that several members of the *Eph* family have segment-restricted roles in transducing signals, possibly cell contact-dependent, during hindbrain patterning.

To analyse the function of *Sek-1* protein in the hindbrain we have taken a dominant negative approach. We find that microinjection of RNA encoding truncated *Sek-1* receptor into *Xenopus* and zebrafish embryos leads to disruption of the spatial restriction of r3/r5 gene expression in the hindbrain. These data suggest that *Sek-1*, perhaps together with other *Eph*-related RTKs, mediates interactions that are required for the segmental restriction of gene expression, and we discuss possible roles of *Sek-1* in this restriction.

MATERIALS AND METHODS

Cloning and sequencing of *Sek-1* cDNAs

A neurula-stage *Xenopus* cDNA library was screened at high stringency (0.2× SSC, 60°C) with a probe including the kinase domain of

mouse *Sek-1*. Positives were picked, subcloned into Bluescript, and sequenced using the dideoxy chain termination method, either with fragments generated by exonuclease deletion or using oligonucleotides corresponding to previously determined sequence.

Generation of RNA encoding full-length and mutant *Sek-1*

Sequences were subcloned into pSP64TK, a derivative of pSP64T (which flanks the coding region with β-globin untranslated sequences; Krieg and Melton, 1984) modified to include a Kozak consensus sequence at the initiation codon, which is within an *NcoI* site, and stop codons in all three frames immediately downstream from the coding sequence. The truncated mouse *Sek-1* sequences correspond to a *NcoI*-*BamHI* fragment, and the truncated *XSek-1* sequences correspond to an *NcoI*-*DraI* fragment. Both of these fragments start at the initiation codon and terminate just downstream from the transmembrane domain (as indicated in Fig. 1). Capped RNA was synthesised by the in vitro transcription of linearised plasmids (Moon and Christian, 1989), dissolved at 1 µg/µl and stored in aliquots at -70°C. The sizes of the encoded polypeptides were analysed by in vitro translation with rabbit reticulocyte lysate (Promega) and gel electrophoresis. Immediately before use for microinjection an aliquot of RNA was mixed with 10 µg/µl lysinated rhodamine dextran (LRD) in a 4:1 ratio.

Microinjection of *Xenopus* and zebrafish embryos

Fertilised and dejellied (Smith and Slack, 1983) *Xenopus* eggs were equilibrated with 4% Ficoll in 3/4 NAM at least 5 minutes before injection. 5-10 nl of RNA/LRD mixture was microinjected into fertilised *Xenopus* embryos (Moon and Christian, 1989), either at the one cell stage, or into one cell at the two cell stage. In pilot experiments we found it necessary to inject 5-10 ng RNA in order to obtain phenotypes, and that at mid-neurula stages the concentration of residual injected RNA was similar to that of endogenous *XSek-1* transcripts. Embryos were gradually equilibrated with 1/10 NAM 6 hours after injection (prior to gastrulation), and harvested at various neurula stages by manually removing the vitelline membrane and fixing overnight in MEMFA.

Zebrafish embryos were produced by natural spawning and microinjected at the two cell stage using a glass capillary needle attached to a Picospritzer. Approximately 0.3-1 ng of RNA was injected and embryos were allowed to develop to various neurula stages before fixation in 4% paraformaldehyde in PBS. Manual dechorionation was carried out before in situ hybridisation or immunocytochemical analysis.

Whole-mount in situ hybridisation and immunocytochemistry

The analysis of *Xenopus* embryos by whole-mount in situ hybridisation was carried out essentially as described by Harland (1991), except that the post-hybridisation RNase treatment was omitted. The *XKrox-20* probe has been described previously (Bradley et al., 1992). The *XSek-1* probe is a 2.6 kb fragment including extracellular domain and kinase domain sequences. An identical pattern is observed using a probe against 3' untranslated sequences, but this short probe gave weaker signals. Whole mount in situ hybridisation and immunocytochemistry of zebrafish embryos was performed as described (Xu et al., 1994), using *kxx20* (Oxtoby and Jowett, 1993) or *rtk1* (Xu et al., 1994) probes, or anti-Pax6 (Macdonald et al., 1994) antibody. In order to examine segmental expression patterns in detail, *Xenopus* or zebrafish embryos were partially dissected such that the hindbrain could be mounted under a coverslip, either in a dorsal or lateral view.

Retrograde tracing of reticulospinal neurons

Retrograde tracing with LRD was carried out as described by Hill et al. (1995) except that low melting temperature agarose in 10% Hank's saline was used to immobilise the embryos.

RESULTS

Cloning of *Xenopus* and zebrafish orthologues of *Sek-1*

We cloned the *Xenopus* orthologue of *Sek-1* by screening a neurula-stage cDNA library with a probe corresponding to the tyrosine kinase domain of mouse *Sek-1*. Sequence analysis revealed an open reading frame with high sequence identity to mouse *Sek-1* (Fig. 1A). Sequence comparisons also showed a strong identity with *Cek8*, the chick orthologue of *Sek-1*, but less similarity with *Ehk-1*, *Ehk-2* and *Hek*, the *Eph*-related genes most closely related to *Sek-1* (Fig. 1B). Taken together with the similarity between the expression pattern of this gene

in *Xenopus* and *Sek-1* in mouse (see below), these data indicate that we have cloned the *Xenopus* orthologue of *Sek-1*, which we designate *XSek-1*. While our functional studies were in progress, a very similar cDNA, named *Pag*, was reported (Winning and Sargent, 1994); *Pag* and *XSek-1* are probably polymorphic alleles of the same gene, perhaps reflecting the tetraploidy of the *Xenopus laevis* genome.

In earlier studies, zebrafish cDNA clones related to *Sek-1* were isolated by screening of a neurula-stage library with sequences from the tyrosine kinase domain of *XSek-1* (Xu et al., 1994). As previously described, partial sequencing and the expression pattern indicates that one of these, named *rtk1*, corresponds to the zebrafish orthologue of *Sek-1*.

A

```

xsek  MAGIVHGILFCGLEGLCWAVTGSRIYPASEVTLLDSRSVQGELGWIASPLEGGWEEVSIMDEKNTPIRTYQVCNVMESSQNNWLR
sek   MAGIFYFILESFLEGLICDAVTGSRVYPANEVTLLDSRSVQGELGWIASPLEGGWEEVSIMDEKNTPIRTYQVCNVMESQNNWLR

xsek  DWIPRSGAQRVYVEIKFTLRDCNSLPGVMGTCKETFNLYYYESNNDKERFIRETQYVKIDTIAADESFTQVDIGDRIMKLNTEVRD
sek   DWITREGAQRVYIEIKFTLRDCNSLPGVMGTCKETFNLYYYESDNDKERFIRESQFGKTDIAADESFTQVDIGDRIMKLNTEIRD

xsek  VGPLSKKGFYLAQVDGACIALVSVRVFYKKCPLTVRNLAQFPDITGSDTSSLVEVRGSCVDNSEKDVPKMYCGADGEWLVPIC
sek   VGPLSKKGFYLAQVDGACIALVSVRVFYKKCPLTVRNLAQFPDITGADTSSLVEVRGSCVNSEKDVPKMYCGADGEWLVPIC

xsek  NCLCNAGFEEHNGGCQACKVGYKALSTDAACSKCPPHSYALREGSTCTCDRGYFRADTDPASMPCTRPPSAPQNLISNVNETSV
sek   NCLCNAGHEEQNGECQACKIGYKALSTDAACSKCPPHSYSVWEGATSCCTCDRGFFRADNDAASMPCTRPPSAPLNLISNVNETSV

xsek  NLEWSPQNSGGRPDVSYNLWCKRCG.SDLTRCRPCGSGVHYSPQNGKLKTKVSITDLQAHTNYTFEVSINGVSKQNPQDQAV
sek   NLEWSPQNTGGRQDISYNVCKKCGAGDPSKCRPCGSGVHYTPQNGKLKTRVSITDLLAHTNYTFEIVAVNGVSKYNPSPDQSV

xsek  SVTVTTNQAAPSTVTQIQPKDITRHSVSLTWPEPERPNGVILEYEVKYYEKDQNERITYRIVKTSRSADIKGLNPLTAYVFHVRAR
sek   SVTVTTNQAAPSSIALVQAKE/TRYVALAWLEPDRPNGVILEYEVKYYEKDQNERISYRIVRTAARNTDIKGLNPLTSYVFHVRAR
                                     ↓
xsek  TAAGYGEFSGPFETTTNTVPSPMIGEGASPTVLLVSVAGSIVLVVILIAAFVISRRRSKYSKAKQEADEEKHLNQGVKTYVDPFTY
sek   TAAGYGDFSEPLEVTTNTVPSPMIGGANSTVLLVSVSGSVLVVILIAAFVISRRRSKYSKAKQEADEEKHLNQGVRTYVDPFTY
                                     ↑

xsek  EDPNQAVREFAKEIDASCIKIEKVIGVGEFGEVCSGRLKVPKGKREIYVAIKTLKAGYTDKQRRDFLSEASIMGQFDHPNIIHLEGV
sek   EDPNQAVREFAKEIDASCIKIEKVIGVGEFGEVCSGRLKVPKGKREICVAIKTLKAGYTDKQRRDFLSEASIMGQFDHPNIIHLEGV

xsek  VTHCKPMMIITEYMENGSLDAFLRKNDGRFTVIQLVGLIRGIGSGMKYLSDMSYVHRDLAARNILVNSNLVCKVSDFGMSRVLEDD
sek   VTHCKPMMIITEYMENGSLDAFLRKNDGRFTVIQLVGLIRGIGSGMKYLSDMSYVHRDLAARNILVNSNLVCKVSDFGMSRVLEDD

xsek  PEAAVTTTRGGKIPIRWTAPEAAVYRKFTSASDVWSYGIWMVEVMSYGERPYWDMNQDVIIKAEEGYRLPPPMDCPIALHQLMLDC
sek   PEAAVTTTRGGKIPIRWTAPEAAVYRKFTSASDVWSYGIWMVEVMSYGERPYWDMNQDVIIKAEEGYRLPPPMDCPIALHQLMLDC

xsek  MQKERSDRPKFGQIVSMLEKLIIPNPNSLKRTGLDNSSRTNTLLDPSSPEWSQVAVSLDWLQAIKMERYKDNFTAAGYTSLEAVVH
sek   MQKERSDRPKFGQIVSMLEKLIIPNPNSLKRTG.SESSRPNTALLDPSSPEFSVAVSVGDWLQAIKMDRYKDNFTAAGYTTLAVVH

xsek  VHQDDLTRIGISSPSHQNKILSSVQGMRTQMQQIQGRMPVP
sek   MSQDDLARIGITAITHQNKILSSVQAMRTQMQQMHGRMPVP
  
```

B

	XSek-1	Sek-1	Cek8	Ehk1	Hek	Ehk2
XSek-1	-					
Sek-1	89	-				
Cek8	90	95	-			
Ehk1	66	66	66	-		
Hek	63	64	64	68	-	
Ehk2	63	63	64	64	67	-

Fig. 1. Amino acid sequence of *XSek-1*. (A) The deduced amino acid sequence of *XSek-1* is shown aligned with mouse *Sek-1*. The signal peptide and transmembrane domain are indicated by double underlining, and the kinase domain by single underlining. The C termini of the truncated proteins encoded by the constructs used in this study are indicated with an arrow. (B) The percentage amino acid sequence identity between *Eph*-related RTKs most closely related to *XSek-1* is tabulated. These genes are more closely related to each other than they are to any other published *Eph*-related RTKs.

Developmental regulation of *Sek-1/rtk1* in the *Xenopus* and zebrafish hindbrain

To characterise the expression patterns of *Sek-1* orthologues in *Xenopus* and zebrafish embryos we carried out whole mount in situ hybridisation analysis. Many, but not all, aspects of *Sek-1* expression found in the mouse (Nieto et al., 1992) are conserved in *Xenopus*, including expression in early mesoderm and the notochord (not shown), r3, r5, and neural crest adjacent to r5 (Fig. 2A-F), the otic placode (Fig. 2D), the forebrain and the olfactory placode (Fig. 2A,B). In the hindbrain, *XSek-1* transcripts are first detected at stage 14 in presumptive r3, and by stage 14.5 have been up-regulated in presumptive r5 (Fig.

2A). Expression is detected in neural crest adjacent to pre-r5 just prior to expression in pre-r5 itself, as seen in embryos with a slight asynchrony in development between left and right (Fig. 2A). At stages 15-16, *XSek-1* expression is not sharply restricted and low levels of transcripts are detected in presumptive r4 (Fig. 2B,C). By stage 20 the expression domains have become precisely restricted to r3 and r5, with a lower-level domain in r2 (Fig. 2D,E). Neural crest cells expressing *XSek-1* migrate into the third branchial arch (Fig. 2D). Whereas *XSek-1* transcripts persist in r3 and r5, expression in r2 is transient, and a third, more rostral stripe of *Sek-1* expression appears in the dorsal part of r1 between stages 31-33 (Fig. 2F).

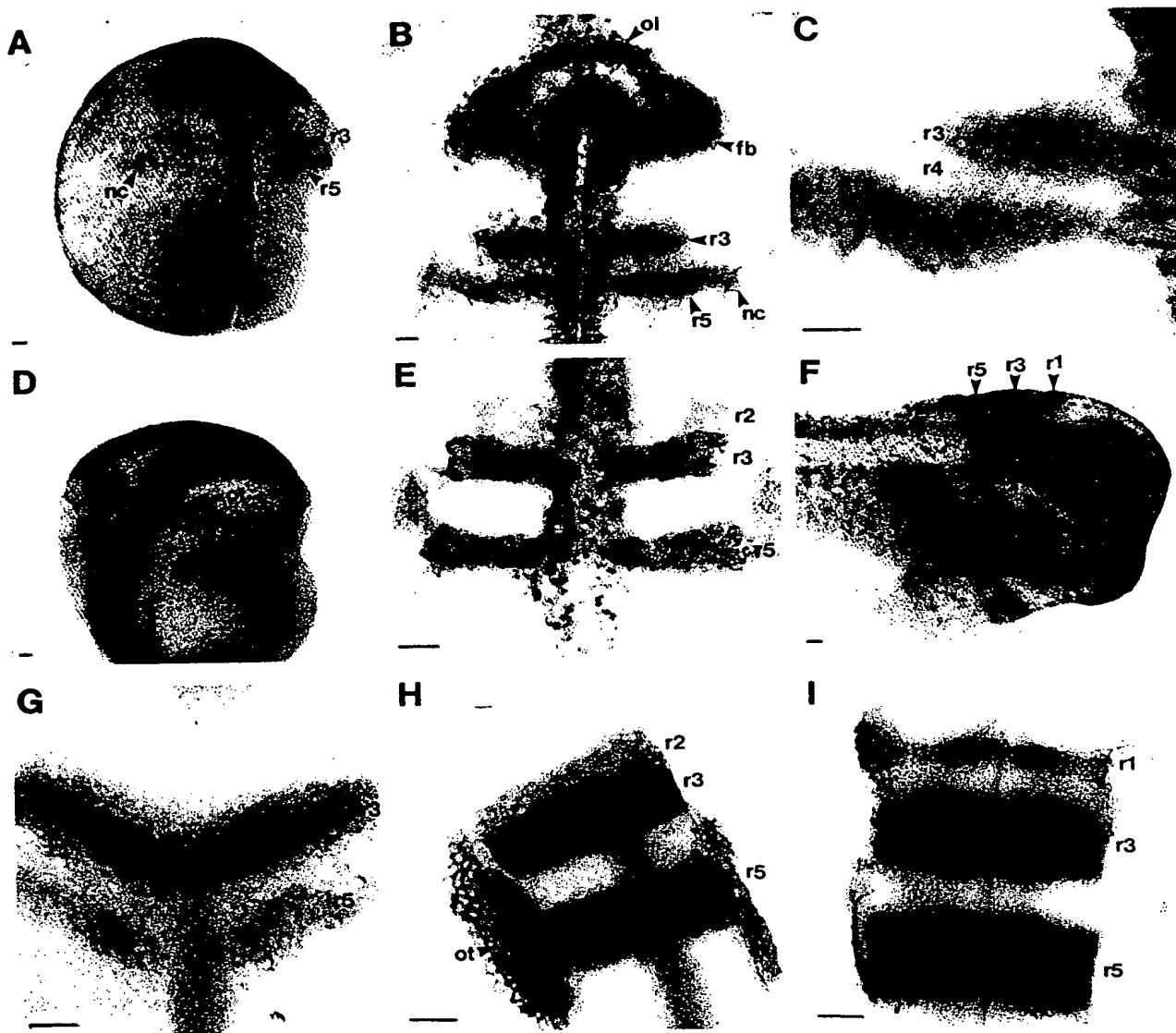


Fig. 2. Expression patterns of *XSek-1* and *rtk1* in the developing hindbrain. (A-F) The expression pattern of *XSek-1* during *Xenopus* development was analysed by whole mount in situ hybridisation. Photographs were taken of either cleared whole embryos (A,D,F), or of the neural epithelium after mounting under a coverslip (B,C,E). (A) Stage 14.5. (B) Rostral neural epithelium at stage 15. (C) Higher magnification view of hindbrain at stage 15. (D) Stage 20. (E) Hindbrain at stage 20. (F) Stage 33. (G-I) The expression pattern of *rtk1* during zebrafish development was analysed by whole mount in situ hybridisation. Photographs from a dorsal view were taken after mounting of the hindbrain under a coverslip. (G) 11.5 h. (H) 17 h. (I) 24 h. r, rhombomere; fb, forebrain; nc, neural crest; ol, olfactory placode; ot, otic placode; p, pronephros. Scale bars, 50 μ m.

In zebrafish, *rtkl* is expressed in a similar pattern in mesoderm, the hindbrain, otic placode and forebrain as *Sek-1* in higher vertebrates (Fig. 2G-I; Macdonald et al., 1994; Xu et al., 1994). In the hindbrain, *rtkl* expression is up-regulated in pre-r3 at 10h (10 hours of development; not shown), and then in pre-r5 at 11.5h (Fig. 2G). These expression domains become sharply restricted to r3 and r5 at 14h, and at 17h low levels of transcripts are also detected in r2 (Fig. 2H). Expression in r2 is transient, whereas transcripts continue to be expressed in r3 and r5. A third, narrow stripe of *rtkl* expression appears in r1 at 24h (Fig. 2I).

These studies indicate that in *Xenopus* and zebrafish, as in higher vertebrates, expression of *Sek-1/rtkl* occurs in r3, r5 and transiently at lower levels in r2. However, the later expression in r1 in zebrafish and *Xenopus* does not occur in the mouse.

Strategy to interfere with Sek-1 function

We investigated the function of *Sek-1* by taking a dominant negative approach analogous to that used to study the role of signalling through the FGF, activin and BMP4 receptors in the *Xenopus* embryo (Amaya et al., 1991; Hemmati-Brivanlou and Melton, 1992; Graff et al., 1994). Receptor kinases are activated by a ligand-induced dimerisation of receptor leading to trans-phosphorylation and activation of the intracellular catalytic domain (Ullrich and Schlessinger, 1990). Activation can therefore be disrupted by the over-expression of truncated receptor, comprising the extracellular and transmembrane domains, but lacking kinase function. Upon binding of the ligand this truncated receptor is capable of dimerising with the endogenous receptor to form a complex that, because of the absence of kinase function, cannot activate the catalytic domain of the endogenous protein (Amaya et al., 1991; Ueno et al., 1991, 1992).

To interfere with Sek-1 function, we cloned sequences encoding truncated mouse and *Xenopus* Sek-1 (see Fig. 1) into

a modified version of the pSP64T vector (Krieg and Melton, 1984), from which capped RNA can be transcribed. A construct to provide a negative control for any non-specific effects of RNA injection was generated by introducing a frame shift mutation 3' to the signal peptide sequence of truncated Sek-1. *In vitro* transcription and translation confirmed that polypeptides of the predicted length are encoded by these sequences (data not shown). These reagents allowed us to ascertain whether there is any difference in the effects of expressing, in *Xenopus* embryos, truncated mouse Sek-1, compared with the homologous truncated XSek-1. Full-length *rtkl* sequences have not yet been obtained, so expression of homologous truncated receptor has not been carried out in the zebrafish embryo.

Truncated Sek-1 disrupts segmental gene expression in the *Xenopus* hindbrain

RNA encoding truncated mouse or *Xenopus* Sek-1 was microinjected together with lineage tracer into *Xenopus* embryos, either at the 1 cell stage, or into one cell at the 2 cell stage; the latter injections provide an internal comparison of any phenotype generated because the injected RNA is present only in the left or right half of the embryo. Detection of this RNA revealed a uniform distribution at higher levels than endogenous *Sek-1* RNA within the injected half at early-mid neurula stages (not shown). Embryos were fixed at neurula stages and analysed by *in situ* hybridisation with *XKrox-20*, a molecular marker of r3 and r5 identity.

During normal development, *XKrox-20* expression is up-regulated first in pre-r3 at stage 14 and then in pre-r5 at stage 14.5, and by stage 17 has become sharply restricted to r3 and r5 (Bradley et al., 1992). Following the injection of RNA encoding truncated Sek-1 receptor into *Xenopus* embryos, an altered pattern of *XKrox-20* gene expression was observed in 12% (15/124) of embryos analysed at neurula stages. We

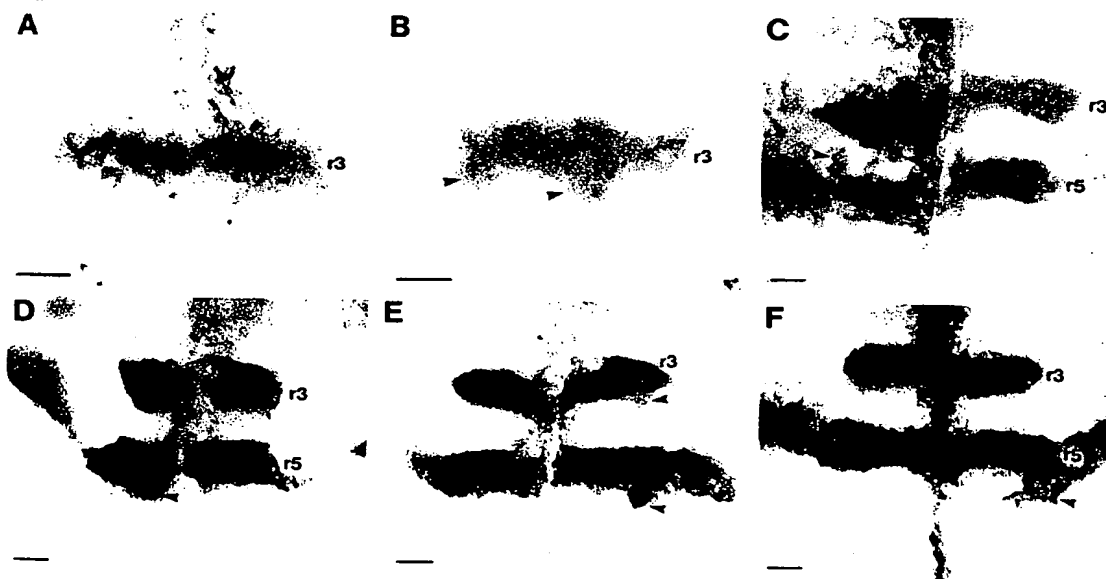


Fig. 3. Effect of truncated Sek-1 on *XKrox-20* gene expression in the *Xenopus* hindbrain. RNA encoding truncated Sek-1 was microinjected into 1 cell of 2 cell *Xenopus* embryos, so that one half of the embryo received injected RNA. The embryos were allowed to develop to various neurula stages and fixed. *In situ* hybridisation was then carried out to analyse the expression pattern of *XKrox-20*, a molecular marker of r3 and r5. Photographs were taken of the mounted hindbrain. (A) Uninjected half of stage 14 embryo.

(B) Injected half of stage 14 embryo. (C) Stage 15 embryo; the injected half is on the left. (D-F) Stage 16 embryos, with injected RNA present in the left (D) or right (E,F) half. r, rhombomere. The arrowheads indicate *XKrox-20*-expressing cells in even-numbered rhombomeres. Scale bars, 50 µm.

observed similar phenotypes when RNA encoding truncated *Xenopus* (Fig. 3B,F) or mouse (Fig. 3C-E) Sek-1 was injected, and in embryos injected at the 2 cell stage, the affected side always correlated with the presence of co-injected lineage tracer. At stage 14, the pre-r3 expression domain of *XKrox-20* forms a narrow band (Fig. 3A), whereas after injection of RNA encoding truncated receptor some expressing cells encroach into the adjacent non-expressing territory (Fig. 3B). At stage 15, after the up-regulation of pre-r5 expression, a similar encroachment of cells expressing *XKrox-20* into presumptive even-numbered rhombomeres is observed in the injected, but not the control half embryo (Fig. 3C). At later stages, coherent groups of cells expressing *XKrox-20* are observed extending from r3/r5 into adjacent even-numbered territory (Fig. 3D-F).

Truncated Sek-1 disrupts segmental gene expression in the zebrafish hindbrain

Although it was unclear why, despite the uniform over-expression of truncated Sek-1, disruption occurred only in a low proportion of embryos, these results suggest that Sek-1 function is required for the segmental restriction of gene expression to r3/r5 in *Xenopus*. To examine whether this function is conserved in a different vertebrate class, we carried out analogous experiments in the zebrafish. RNA encoding truncated *Xenopus* or mouse Sek-1 was microinjected into 1 cell of the 2 cell zebrafish embryo. At early blastula stages, cleavage is initially partial so RNAs could diffuse between cells, but in pilot experiments we nevertheless observed a mosaic inheritance of the injected RNA (data not shown). Injected embryos were allowed to develop to various neurula stages, fixed and then analysed by in situ hybridisation with *rtk1* or *krox20* probes, as markers of r3/r5. The *rtk1* probe corresponds to 3' untranslated sequences not present in the injected *Sek-1* RNA.

At early neurula stages (14h), shortly after the onset of *rtk1* and *krox20* expression, >50% of embryos expressing truncated Sek-1 or XSek-1 receptor had major disruptions to the spatial restriction of *krox20* expression. In contrast to normal embryos, in which *krox20* expression occurs in parallel, narrow bands (Fig. 4A; Oxtoby and Jowett, 1993), in embryos expressing truncated receptor these domains are irregular in shape, and often overlap (Fig. 4B,C). Similar severe disruptions are also observed when *rtk1* expression is used as a marker (not shown). We observed no difference between truncated mouse or *Xenopus* Sek-1 in their effects at this or later stages. Analysis of 18-24h embryos, when in normal development r3/r5 gene expression has become sharply restricted (Fig. 4D), revealed disruptions to *rtk1* or *krox20* expression in 55% (41/74) of embryos, and these fell into two classes of phenotypes (Fig. 4E-L). In 65% (27/41) of the affected embryos, cells were observed extending from an apparently normal r3/r5 expression domain into the adjacent r2 or r6 territory (Fig. 4E,F). 35% (14/41) of the affected embryos showed a more drastic phenotype, with an apparent fusion between r3 and r5, as seen in dorsal views (Fig. 4G,H,J) and sections (Fig. 4I). In many of these embryos the shape of r3 or r5 is altered, for example with one side narrower than normal (Fig. 4H,I). In all cases, cells ectopically expressing r3/r5 markers were not isolated, but formed coherent and sharply restricted populations intruding into even-numbered territory. Lateral views revealed that in both classes of embryos, the ectopic gene

Table 1. Rescue of disruption in the zebrafish hindbrain by full-length Sek-1

Amount RNA injected		Number affected	% affected
Truncated	Full length		
1	0	13/24	54
1	1	6/17	35
1	2	11/48	23
0.5	0	16/30	53
0.5	0.5	8/24	33
0.5	1	3/14	21
0.5	2.5	0/35	0

RNA encoding truncated Sek-1 was mixed with various amounts of RNA encoding full-length Sek-1 and co-injected into zebrafish embryos. The embryos were then analysed at 24 hours of development by in situ hybridisation for disruptions to the segmental restriction of *rtk1* or *krox20* expression. The amounts of injected RNA are normalised relative to the maximum amount (0.3 ng) of truncated receptor RNA injected in this experiment. The amounts of RNA injected may not reflect the relative amounts of full-length and truncated protein generated, as there could be differences in RNA stability, protein stability, and/or translational efficiency.

expression and fusions are dorsally located, and non-expressing cells are present ventrally in presumptive r4 (Fig. 4K,L). We therefore infer that r4 is still present, but no molecular markers are currently available to assess this directly. In summary, expression of truncated Sek-1 in zebrafish leads to a similar disruption of the spatial restriction of r3/r5 markers as in *Xenopus*, but with more severe phenotypes and in a higher proportion of embryos.

If Sek-1/*rtk1* has any adhesive role, it is possible that the disruption was due to the ectopic expression of extracellular domain rather than inhibition of signal transduction. However, no effects on segmental gene expression occurred in >300 zebrafish embryos injected with RNA encoding full-length Sek-1. This enabled us to test whether expression of full-length Sek-1 could rescue the effects of truncated Sek-1. We found that co-injection of increasing amounts of RNA encoding full-length Sek-1 lead to a progressive suppression of the disruption to the segmental restriction of gene expression (Table 1). These data indicate that Sek-1 is capable of homodimerisation and confirm that the disruption caused by truncated Sek-1 is due to a requirement for the cytoplasmic domain.

Disruption of boundary formation and neuronal organisation by truncated Sek-1

In the chick, morphological boundaries at the interface of odd and even numbered rhombomeres exhibit several distinctive cellular and antigenic properties (Lumsden and Keynes, 1989; Heyman et al., 1993). We found that, in addition to uniform expression up to the r1/r2 boundary, zebrafish Pax6 (*PaxA*; Krauss et al., 1991; Puschel et al., 1992) protein is expressed at higher levels at rhombomere boundaries in 24h embryos (Fig. 5A). We analysed whether expression of truncated Sek-1 receptor affected the expression pattern of this boundary marker. In 30% of embryos, lower levels of Pax6 expression occurred in certain rhombomere boundaries, for example at the r2/r3 (Fig. 5B) and r5/r6 (Fig. 5C) boundary. In some of these embryos, for example in rostral part of hindbrain shown in Fig. 5C, certain boundaries are distorted, perhaps reflecting the altered shape of rhombomeres detected by *rtk1* and *krox20* expression (Fig. 4E-L).

Previous studies have shown a segmental organisation of identified reticulospinal neurons in the zebrafish hindbrain that can be revealed by retrograde labelling from the spinal cord (Metcalf et al., 1986; Fig. 6A). These neurons are therefore amenable markers of regional specification in the hindbrain (Hill et al., 1995). We examined whether expression of truncated *Sek-1* had effects on the organisation of reticulospinal neurons by using lysinated rhodamine dextran for retrograde labelling. Many embryos expressing truncated *Sek-1* had the normal number and organisation of reticulospinal neurons indicating that, as suggested by the gene expression data, rhombomere specification has not been altered. However, in some embryos, the spacing of these neurons within rhombomeres is abnormal; for example, r5 neurons (MiD2cm and MiD2cl; Metcalf et al., 1986) which are close together in the normal hindbrain (Fig. 6A) are further apart in some embryos expressing truncated *Sek-1* (Fig. 6B). 10% of injected embryos had a duplication of the Mauthner neuron in r4, as identified by its location and contralateral projection (Fig. 6C).

DISCUSSION

It was possible that the expression of *Sek-1* in r3 and r5 correlated with a role in establishing or maintaining the segmental identity of cells within these rhombomeres. However, our data argue against such a role, since we do not observe a deficiency in r3/r5 after injection of RNA encoding truncated *Sek-1*. Rather, we find an ectopic expression of markers of r3/r5 in the *Xenopus* and zebrafish hindbrain. Unlike the situation in normal development, cells expressing *Krox-20* or *Sek-1/rtk1* are found in r2, r4 or r6, and in a high proportion of injected zebrafish embryos an apparent fusion occurs between r3 and r5. These ectopic cells occur in a variable pattern in a coherent group co-extensive with r3/r5, and might underlie the distortions of rhombomere boundaries and altered spacing of reticulospinal neurons observed at later stages. To interpret these results, we will first discuss the potential effects of truncated *Sek-1*, and then consider what mechanisms could underlie the restriction of segmental gene expression.

Specificity of truncated *Sek-1*

Our strategy is based upon the assumption that, as for other RTKs, activation of *Sek-1* occurs through a ligand-induced dimerisation. Although this has not been directly shown for Eph-related RTKs, in cells expressing a fusion protein of EGF receptor ligand binding domain and Elk receptor kinase domain, the latter is phosphorylated upon EGF treatment (Lhotak and Pawson, 1993). Therefore the kinase domain of this Eph-related RTK can be activated by dimerisation. Furthermore, whereas soluble Elk receptor ligand is inactive, a dimerised form of this activates Elk, suggesting that activation involves receptor homodimerisation (Davis et al., 1994). Our finding that co-injection of RNA encoding full-length *Sek-1* rescues the phenotype caused by truncated *Sek-1* indicates that these can bind to each other and thus provides further evidence for homodimerisation.

The use of truncated receptors has provided important insights into the roles of receptor kinases in *Xenopus* mesoderm patterning (Amaya et al., 1991; Hemmati-Brivanlou

and Melton, 1992; Graff et al., 1994), but have revealed some potential limitations to this approach. In particular, the truncated receptor may interfere with the function of several endogenous receptors by heterodimerisation (Ueno et al., 1992). It is not known whether Eph-related RTKs can heterodimerise, such that truncated *Sek-1* could interfere with the function of other family members; the rescuing effects of full-length *Sek-1* do not address this since it could compete for binding of truncated *Sek-1* to a heterologous partner. If truncated *Sek-1* does inhibit the function of several RTKs the effects we observe could involve related genes co-expressed with *Sek-1*, such as *Sek-3/nuk*, *Sek-4*, and zebrafish *rtk3* (Becker et al., 1994; Henkemeyer et al., 1994; Q. X. and N. H., unpublished observations). However, these genes are expressed after segmentation, and no Eph-related RTKs have been found that are co-expressed with *Sek-1* in pre-r3/r5, when we first observe disrupted gene expression. If receptor heterodimerisation occurs, less severe effects may result from disruption of the *Sek-1* gene compared with the use of a dominant negative approach. Since the phenotype correlates with *Sek-1* expression, for simplicity we will not refer below to the possibility of effects on multiple receptors.

Potential mechanisms restricting segmental gene expression

Whereas regional specification occurs prior to segmentation in the chick hindbrain (Guthrie et al., 1992), the progeny of an individual cell marked at this stage disperse considerably, and often contribute to two adjacent rhombomeres (Fraser et al., 1990). Since *Krox-20* transcripts are up-regulated in pre-r3 and -r5 at this stage (Nieto et al., 1991), it seems that expression does not correlate with an irrevocable commitment to an r3/r5 identity. Although after segmentation, most clonal progeny are restricted to a single rhombomere (Fraser et al., 1990), in 10–20% of clones some cells cross rhombomere boundaries (Birgbauer and Fraser, 1994). Thus the observation of sharp r3/r5 domains of *Krox-20* expression implies that cells are not committed even after segmentation. It therefore seems that there is a dynamic regulation of cell identity. We suggest that restricted domains of *Krox-20* gene expression might be maintained by local interactions acting in a community effect (Gurdon, 1988; Gurdon et al., 1993), in which as intermingling occurs between presumptive or definitive rhombomeres, cells switch their segmental identity to that of their neighbours. It is also possible that rather than switching identity, cell death occurs. However, cell death is unlikely to account for the restriction of gene expression prior to segmentation, when individual cells can contribute many progeny to each of two rhombomeres.

The partial restriction of cell movement across rhombomere boundaries (Fraser et al., 1990; Birgbauer and Fraser, 1994) is also likely to contribute to the formation of sharp segmental domains of gene expression. Transplantation experiments in the chick suggest that this restriction involves cellular properties, perhaps adhesion, that to a first approximation alternate between rhombomeres (Guthrie et al., 1993) and might lead to a sorting of cells with odd and even segmental identity. Taken together, these data suggest roles of both identity switching and constraints on cell mixing, but the relative contribution of these mechanisms is not known and may vary during the establishment of segments. Current data are consistent with a critical

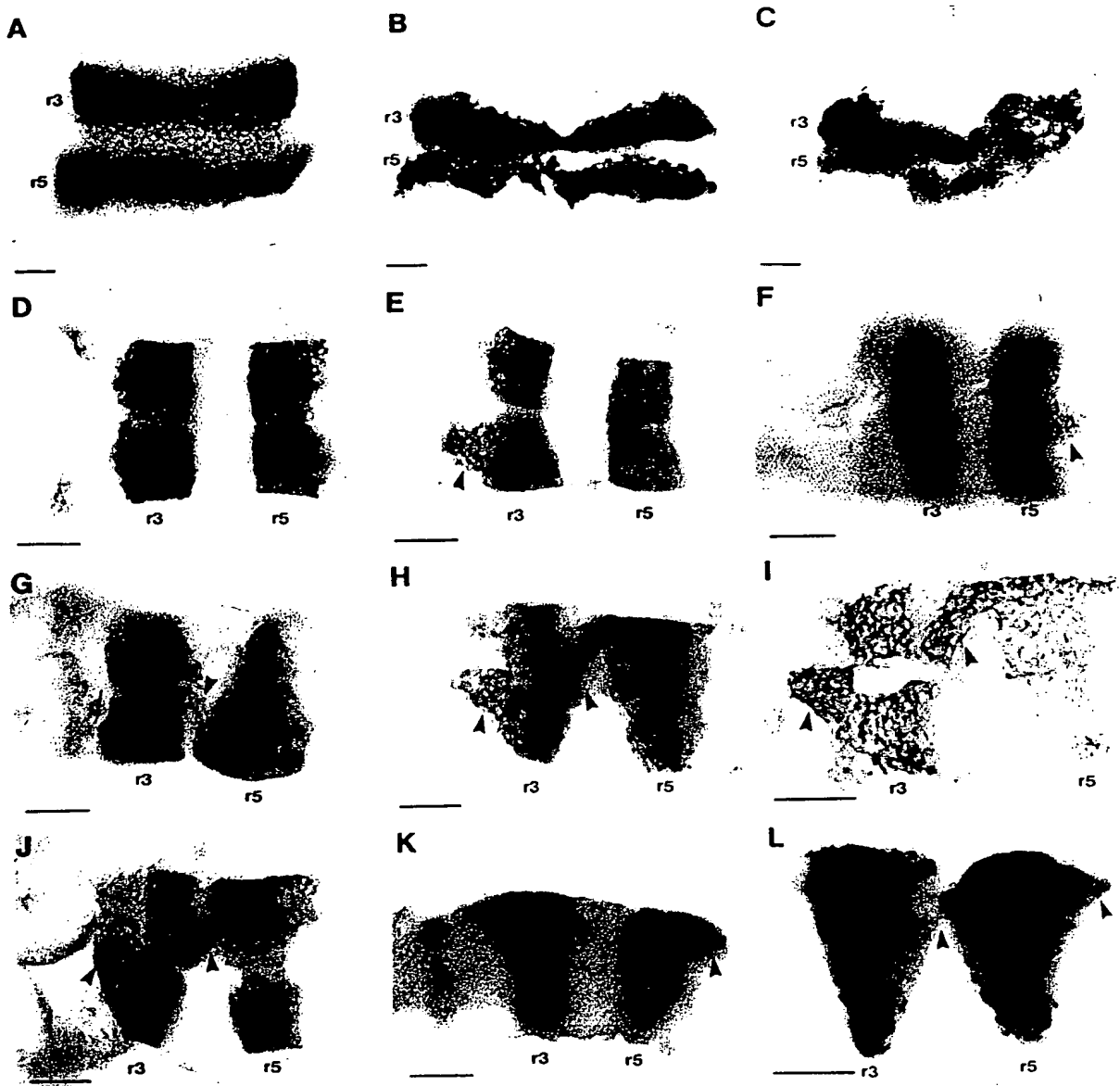


Fig. 4. Effect of truncated Sek-1 on *krx20* and *rtk1* expression in the zebrafish hindbrain. RNA encoding truncated Sek-1 was microinjected into 1 cell of zebrafish embryos at the 2 cell stage. Embryos were allowed to develop to neurula stages, fixed and either *krx20* or *rtk1* expression analysed by in situ hybridisation. Photographs were taken either of the hindbrain from a dorsal (A-H,J) or lateral view (K,L), or after sectioning in the coronal plane (I). *krx20* expression was analysed in (A) uninjected or (B,C) injected embryos fixed at 14 hours of development. *rtk1* expression was analysed in uninjected (D) or injected (E-K) embryos analysed at 24 hours of development. (L) *krx20* expression in injected 18h embryo. The arrowheads indicate cells expressing *krx20* or *rtk1* in even-numbered rhombomeres. Scale bars 50 µm.

role of cell identity switching in the maintenance of gene expression domains, with cell adhesion serving to sharpen and stabilise the pattern upon segmentation. Indirect support for this is provided by the phenotype of mice in which r3 and r5 are missing due to inactivation of the *Krox-20* gene (Schneider-Maunoury et al., 1993). The juxtaposed r2/r4/r6 in these mutants are predicted to have greater intermingling than odd and even rhombomeres (Guthrie et al., 1993), yet r4-specific gene expression is as sharp as in normal embryos. However, these studies do not rule out the possibility that there is a partial

restriction of cell movement at early stages, which has a critical role.

Disruption of segmentally restricted gene expression by truncated Sek-1

We suggest three possible mechanisms by which expression of truncated Sek-1 could lead to cells expressing *Krox-20/Sek-1* in even-numbered rhombomeres: a switch of r2/r4/r6 cells to an r3/r5 identity; an increased mixing of cells between odd and even rhombomeres; or a block in the switching of r3/r5 cells

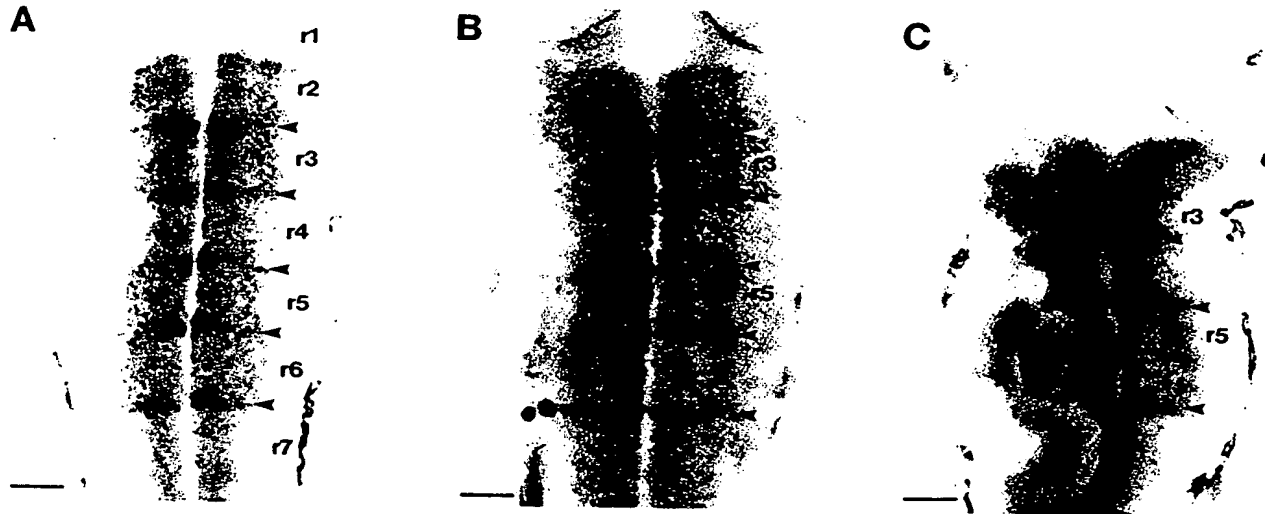


Fig. 5. Effect of truncated Sek-1 on Pax6 expression at rhombomere boundaries in the zebrafish. Immunocytochemistry was carried out to examine Pax6 expression in (A) uninjected 24h embryos or (B,C) 24h embryos injected with RNA encoding truncated Sek-1. The black arrowheads indicate rhombomere boundaries. all of which, in control embryos, express Pax6 at higher levels than within rhombomeres. The white arrowheads indicate rhombomere boundaries in injected embryos in which Pax6 expression appears deficient. Scale bars, 50 μ m.

that have intermingled into r2/r4/r6. These are discussed below.

According to the first hypothesis, expression of truncated Sek-1 has lead to a de novo up-regulation of *Krox-20/Sek-1* expression in even-numbered rhombomeres. Such a mechanism requires that truncated Sek-1 has not disrupted Sek-1 function, but rather an RTK expressed in r2/r4/r6. However, this explanation seems very unlikely since the cells ectopically expressing r3/r5 markers are always found contiguous with r3 or r5. Although ectopic cells with r3/r5 identity might preferentially adhere to r3/r5 during cell mixing, this intermingling would have to be very extensive and rapid to account for the complete absence of isolated ectopic cells in even-numbered rhombomeres: this is especially unlikely in *Xenopus*, in which little intermingling occurs (Wetts and Fraser, 1989). Furthermore, this hypothesis does not account

for the variability in the disrupted pattern of gene expression or the difference in the proportion of affected embryos in zebrafish and *Xenopus*.

The second hypothesis proposes that presumptive r3/r5 cells are present in r2/r4/r6 due to increased mixing between odd and even rhombomeres. Indeed, since ligands for Eph-related receptors are membrane bound (Bartley et al., 1994; Beckmann et al., 1994; Cheng and Flanagan, 1994; Davis et al., 1994), they could mediate adhesive interactions, and the r3/r5 expression of Sek-1 thus contributes to the adhesive differences between odd- and even-numbered segments. Widespread expression of the extracellular domain of Sek-1 could therefore lessen the adhesive difference between r3/r5 and adjacent rhombomeres, leading to increased mixing of these cell populations. However, we find injection of RNA encoding full-length Sek-1 has no effect on the segmental restriction of gene

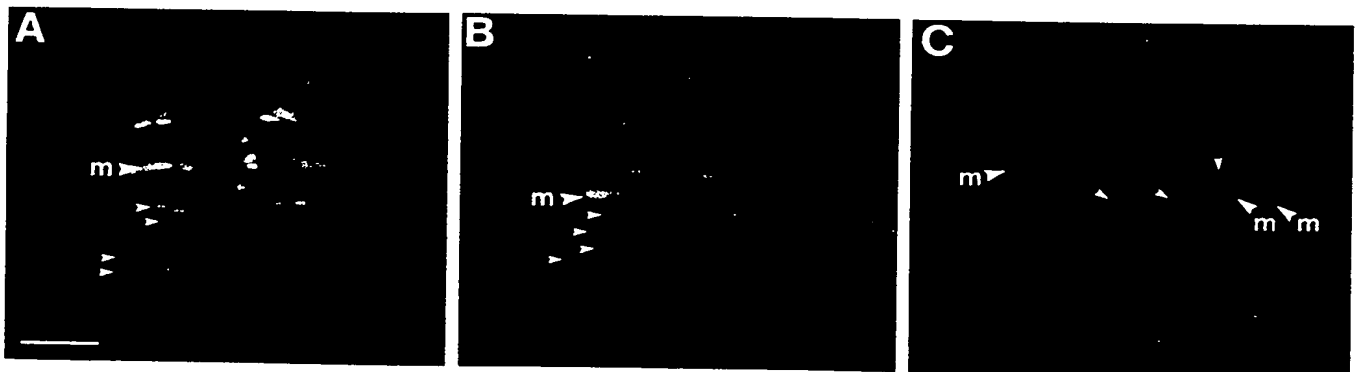


Fig. 6. Effect of truncated Sek-1 on reticulospinal neurons in the zebrafish embryo. Reticulospinal neurons were revealed in 3 day zebrafish embryos by retrograde labelling from the spinal cord using LRD (A) Uninjected embryo. (B,C) Embryos injected with RNA encoding truncated Sek-1. The small arrowheads in A and B indicate the locations of corresponding pairs of reticulospinal neurons in r5 and r6. The spacing of these neurons is altered in the injected embryo shown in B. The small arrowheads in C indicate the axons of the duplicated Mauthner neurons in r4. The large arrows labelled 'm' indicate the Mauthner neuron. Scale bar, 50 μ m.

expression, suggesting that the effect of truncated receptor is not due to ectopic expression of the extracellular domain. Indeed, full-length Sek-1 rescues the effect of truncated Sek-1, indicating that if this RTK does have a role in restricting cell movement from odd to even rhombomeres, it requires the kinase domain. Thus, rather than mediating a passive adhesion, any role of Sek-1 in lineage restriction might involve an active process, such as a contact dependent repulsion of r3/r5 cells by r2/r4/r6 cells.

According to the third hypothesis, truncated Sek-1 protein interferes with signal transduction and disrupts the ability of presumptive r3/r5 cells to switch segmental identity if, during intermingling, they cross into presumptive r2/r4/r6. The fusion of r3 and r5 observed in many zebrafish embryos may be a consequence of pre-r3/r5 cells encroaching sufficiently into pre-r4 to bridge the normal 3-4 cell wide gap between these odd-numbered rhombomeres in the early neural plate. Since cells from r3 and r5 will mix with each other relatively freely (Guthrie et al., 1993), touching of these rhombomeres could lead to an irreversible fusion. This model suggests that during normal development, activation of Sek-1 receptor occurs in any cells that move from odd- to even-numbered territory and is required for a switch in phenotype to that of the local community. The switch in phenotype is accompanied by the down-regulation of *Sek-1/rtk1* and *Krox-20* transcripts, which must occur rapidly to account for the sharp expression domains. This model predicts that the ligand for Sek-1 is expressed in even-numbered rhombomeres and that the signalling interactions are short-range. Indeed, ligands for Eph-related RTKs are active only when membrane-bound and not in soluble form (Davis et al., 1994). Recently, a ligand, Elf-1, has been identified that binds Sek-1 and another Eph-related RTK, Mek-4 (Cheng and Flanagan, 1994). However, expression of Elf-1 does not occur within, or adjacent to r3/r5, and it is therefore unlikely that Elf-1 activates Sek-1 in the hindbrain.

An important question arising from this model is how boundaries are stabilised, since at this interface pre-r3/r5 cells are in contact with pre-r2/r4/r6. One possibility is that a switch from odd to even identity requires contact with more than a critical ratio of pre-r2/r4/r6 cells relative to r3/r5 cells. It may be significant that after segmentation in the chick hindbrain a distinct population of cells is formed at boundaries, across which there is less cell contact compared to within rhombomeres (Martinez et al., 1992), perhaps due to larger intercellular spaces (Lumsden and Keynes, 1989; Heyman et al., 1993). It is possible that this relative lack of cell contact might stabilise domains of gene expression after segmentation, and thus it is intriguing that we find truncated Sek-1 leads to a deficiency in the higher-level expression of Pax6 in rhombomere boundary cells in the zebrafish. Studies in the chick indicate that boundaries form at the interface between any combination of odd- and even-numbered rhombomeres (Guthrie and Lumsden, 1991), so boundary cells may be induced by local interactions between these populations. We speculate that the decrease in Pax6 expression in some boundary cells may reflect a role of Sek-1 in such interactions between adjacent rhombomeres. If boundary cells stabilise gene expression domains, might disruption of their formation underlie the ectopic expression of r3/r5 markers in the presence of truncated Sek-1? Although this cannot be ruled out, current data do not

support this possibility since we observe disruptions at early stages whereas boundary cells have only been detected after segmentation. The effects of truncated Sek-1 on boundary cells may therefore reflect a distinct, later role.

Variations in the extent and pattern of disruption

Our data raise the questions as to why the extent of disruption and proportion of affected embryos is low in *Xenopus* despite the uniform distribution of injected RNA, why it is lower than in zebrafish, and why in both species the patterns of disruption are variable. These may relate to the extent and variability of cell mixing normally occurring in the hindbrain, and are consistent with models in which ectopic gene expression derives from r3/r5. Clonal analyses in the zebrafish have shown that during convergent extension there is considerable intermingling of cells along the A-P axis (Kimmel et al., 1994). This occurs because the progeny of a cell division often lie along the A-P axis, and are subsequently separated by the intercalation of other cells. Although the dispersal of clones has not been followed after the 16th cell division (8-9 h), convergent extension is still occurring after the onset of *krox20* expression (Oxtoby and Jowett, 1993), so substantial intermingling along the A-P axis seems likely to occur. As a consequence, blocking of the restriction of cell movement between presumptive rhombomeres or of cell identity switching will frequently lead to severe disruption of spatially restricted gene expression, and since the patterns of cell division and intercalation are stochastic (Kimmel et al., 1994) the extent of this disruption is variable. In contrast, little cell intermingling occurs in *Xenopus*, even during the major morphogenetic movements between blastula and mid-neurula stages (Wetts and Fraser, 1989). Moreover, only one cell division occurs in the neural epithelium between stages 13 and 16 (Hartenstein, 1989), the period when *Krox-20/Sek-1* expression is established and sharpened. There is therefore little opportunity for the dispersal of clonally-related cells along the A-P axis by division and intercalation. As a consequence, movement of cells between presumptive rhombomeres and a switching of segmental identity is likely to occur infrequently in *Xenopus*.

If substantial cell mixing is occurring in the zebrafish hindbrain, why do we find that cells expressing r3/r5 markers in an ectopic location always form a coherent group, rather than being interspersed with non-expressing cells? One possibility is that due to turnover of the injected RNA encoding truncated Sek-1 there is only a transient inhibition of lineage restriction or of cell identity switching which causes the severe scrambling seen in the 12h embryo. From this the coherent arrangement of r3/r5 cells seen at 18-24h could then emerge by a sorting of odd- and even-numbered cells and/or because ectopic communities, but not isolated cells, can maintain r3/r5 phenotype. According to this, the variable and abnormal shapes of r3/r5 seen at later stages may reflect the stochastic nature of the initial scrambling of cells with presumptive odd- and even-numbered identity, due to variability in planes of cell division (Kimmel et al., 1994).

Concluding remarks

Our results indicate that Sek-1 function is required for the restriction of *Krox-20* and *Sek-1* gene expression to r3/r5, and suggest a role either in a dynamic regulation of cell identity in a segmental community effect or in a restriction of cell

movement from odd to even presumptive segments. The relative contribution of these mechanisms to the establishment of segmental gene expression domains is unknown, and further understanding of the role of Sek-1 will therefore require cell lineage analysis and transplantation experiments.

REFERENCES

- Amaya, E., Musci, T. J. and Kirschner, M. W. (1991). Expression of a dominant negative mutant of the FGF receptor disrupts mesoderm formation in *Xenopus* embryos. *Cell* **66**, 256-270.
- Bartley, T. D., Hunt, R. W., Welcher, A. A., Boyle, W. J., Parker, V. P., Lindberg, R. A., Lu, H. S., Colombero, A. M., Elliott, R. L., Guthrie, B. A., Holst, P. L., Skrine, J. D., Toso, R. J., Zhang, M., Fernandez, E., Trail, G., Varnum, B., Yarden, Y., Hunter, T. and Fox, G. M. (1994). B61 is a ligand for the ECK receptor protein-tyrosine kinase. *Nature* **368**, 558-560.
- Becker, N., Seitanidou, T., Murphy, P., Mattei, M.-G., Topilko, P., Nieto, M. A., Wilkinson, D. G., Charnay, P. and Gilardi-Hebenstreit, P. (1994). Several receptor tyrosine kinase genes of the *Eph* family are segmentally expressed in the developing hindbrain. *Mech. Dev.* **47**, 3-17.
- Beckmann, M. P., Cerretti, D. P., Baum, P., Vanden Bos, T., James, L., Farrah, T., Kozlosky, C., Hollingsworth, T., Shilling, H., Maraskovsky, E., Fletcher, F. A., Lhotak, V., Pawson, T. and Lyman, S. D. (1994). Molecular characterisation of a family of ligands for eph-related tyrosine kinase receptors. *EMBO J.* **13**, 3757-3762.
- Birgbauer, E. and Fraser, S. E. (1994). Violation of cell lineage restriction compartments in the chick hindbrain. *Development* **120**, 1347-1356.
- Bradley, L. C., Snape, A., Bhatt, S. and Wilkinson, D. G. (1992). The structure and expression of the *Xenopus* *Krox-20* gene: conserved and divergent patterns of expression in rhombomeres and neural crest. *Mech. Dev.* **40**, 73-84.
- Cheng, H.-J. and Flanagan, J. G. (1994). Identification and cloning of ELF-1, a developmentally expressed ligand for the Mek4 and Sek receptor tyrosine kinases. *Cell* **79**, 157-168.
- Clarke, J. D. W. and Lumsden, A. (1993). Segmental repetition of neuronal phenotype sets in the chick embryo hindbrain. *Development* **118**, 151-162.
- Davis, S., Gale, N. W., Aldrich, T. H., Maisonnier, P. C., Lhotak, V., Pawson, T., Goldfarb, M. and Yancopoulos, G. D. (1994). Ligands for EPH-related receptors that require membrane attachment or clustering for activity. *Science* **266**, 816-819.
- Dickson, B. and Hafen, E. (1994). Genetics of signal transduction in invertebrates. *Curr. Opin. Genet. Dev.* **4**, 64-70.
- DiNardo, S., Heemskerk, J., Dougan, S. and O'Farrell, P. H. (1994). The making of a maggot: patterning the *Drosophila* embryonic epidermis. *Curr. Opin. Genet. Dev.* **4**, 529-534.
- Fraser, S., Keynes, R. and Lumsden, A. (1990). Segmentation in the chick embryo hindbrain is defined by cell lineage restrictions. *Nature* **344**, 431-435.
- Ganju, P., Shigemoto, K., Brennan, J., Entwistle, A. and Reith, A. D. (1994). The Eck receptor tyrosine kinase is implicated in pattern formation during gastrulation, hindbrain segmentation and limb development. *Oncogene* **9**, 1613-1624.
- Graff, J. M., Thies, R. S., Song, J. J., Celeste, A. J. and Melton, D. A. (1994). Studies with a *Xenopus* BMP receptor suggest that ventral mesoderm-inducing signals override dorsal signals in vivo. *Cell* **79**, 169-179.
- Gurdon, J. B. (1988). A community effect in animal development. *Nature* **336**, 772-774.
- Gurdon, J. B., Lemaire, P. and Kato, K. (1993). Community effects and related phenomena in development. *Cell* **75**, 831-834.
- Guthrie, S. and Lumsden, A. (1991). Formation and regeneration of rhombomere boundaries in the developing chick hindbrain. *Development* **112**, 221-229.
- Guthrie, S., Muchamore, I., Marshall, H., Kuroiwa, A., Krumlauf, R. and Lumsden, A. (1992). Neuroectodermal autonomy of *Hox-2.9* expression revealed by rhombomere transpositions. *Nature* **356**, 157-159.
- Guthrie, S., Prince, V. and Lumsden, A. (1993). Selective dispersal of avian rhombomere cells in orthotopic and heterotopic grafts. *Development* **118**, 527-538.
- Hanneman, E., Trevarrow, B., Metcalfe, W. K., Kimmel, C. B. and Westerfield, M. (1988). Segmental pattern of development of the hindbrain and spinal cord of the zebrafish embryo. *Development* **103**, 49-58.
- Harland, R. M. (1991). In situ hybridisation: an improved whole mount method for *Xenopus* embryos. In *Xenopus laevis: Practical Uses in Cell and Molecular Biology*. Methods in Cell Biol. vol. 36 (ed. B. K. Kay and H. B. Peng), pp. 685-695. San Diego: Academic Press.
- Hartenstein, V. (1989). Early neurogenesis in *Xenopus*: the spatio-temporal pattern of proliferation and cell lineages in the embryonic spinal cord. *Neuron* **3**, 399-411.
- Hemmati-Brivanlou, A. and Melton, D. A. (1992). A truncated activin receptor inhibits mesoderm induction and formation of axial structures in *Xenopus* embryos. *Nature* **359**, 609-614.
- Henkemeyer, M., Marengere, L. E., McGlade, J., Olivier, J. P., Conlon, R. A., Holmyard, D. P., Letwin, K. and Pawson, T. (1994). Immunolocalisation of the Nuk receptor tyrosine kinase suggests roles in segmental patterning of the brain and axonogenesis. *Oncogene* **9**, 1001-1014.
- Heyman, I., Kent, A. and Lumsden, A. (1993). Cellular morphology and extracellular space at rhombomere boundaries in the chick embryo hindbrain. *Dev. Dynamics* **198**, 241-253.
- Hill, J., Clarke, J. D. W., Vargesson, N., Jowett, T. and Holder, N. (1995). Exogenous retinoic acid causes specific alterations in the development of the midbrain and hindbrain of the zebrafish embryo including positional respecification of the Mauthner neuron. *Mech. Dev.* **50**, 3-16.
- Ingham, P. W. and Martinez Arias, A. (1992). Boundaries and fields in early embryos. *Cell* **68**, 221-235.
- Irving, C., Nieto, M. A., DasGupta, R., Charnay, P. and Wilkinson, D. G. (1995). Progressive spatial restriction of *Sek-1* and *Krox-20* gene expression during hindbrain segmentation. *Dev. Biol.* (in press).
- Kimmel, C. B., Warga, R. M. and Kane, D. A. (1994). Cell cycles and clonal strings during formation of the zebrafish central nervous system. *Development* **120**, 265-276.
- Krauss, S., Johansen, T., Korzh, V., Moens, U., Ericson, J. U. and Fjose, A. (1991). Zebrafish *pax1/f-a*: a paired box-containing gene expressed in the neural tube. *EMBO J.* **10**, 3609-3619.
- Krieg, P. A. and Melton, D. A. (1984). Functional messenger RNAs are produced by SP6 *in vitro* transcription of cloned cDNAs. *Nucl. Acids Res.* **12**, 7057-7070.
- Lhotak, V. and Pawson, T. (1993). Biological and biochemical activities of a chimeric epidermal growth factor-Elk receptor tyrosine kinase. *Mol. Cell Biol.* **13**, 7071-7079.
- Lumsden, A. and Keynes, R. (1989). Segmental patterns of neuronal development in the chick hindbrain. *Nature* **337**, 424-428.
- Lumsden, A., Sprawson, N. and Graham, A. (1991). Segmental origin and migration of neural crest cells in the hindbrain region of the chick embryo. *Development* **113**, 1281-1291.
- Maddonald, R., Xu, Q., Barth, K. A., Mikkola, I., Holder, N., Fjose, A., Krauss, S. and Wilson, S. W. (1994). Regulatory gene expression boundaries demarcate sites of neuronal differentiation in the embryonic zebrafish forebrain. *Neuron* **13**, 1039-1053.
- Martinez, S., Geijo, E., Sanchez-Vives, M. V., Puelles, L. and Gallego, R. (1992). Reduced junctional permeability at interrhombomeric boundaries. *Development* **116**, 1069-1076.
- McGinnis, W. and Krumlauf, R. (1992). Homeobox genes and axial patterning. *Cell* **68**, 283-302.
- Metcalfe, W. K., Mendelson, B. and Kimmel, C. B. (1986). Segmental homologies among reticulospinal neurons in the hindbrain of the zebrafish larva. *J. Comp. Neurol.* **251**, 147-159.
- Moon, R. T. and Christian, J. L. (1989). Microinjection and expression of synthetic mRNAs in *Xenopus* embryos. *Technique* **1**, 76-89.
- Nieto, M. A., Bradley, L. C. and Wilkinson, D. G. (1991). Conserved segmental expression of *Krox-20* in the vertebrate hindbrain and its relationship to lineage restriction. *Development* **Supplement 2**, 59-62.
- Nieto, M. A., Gilardi-Hebenstreit, P., Charnay, P. and Wilkinson, D. G. (1992). A receptor protein tyrosine kinase implicated in the segmental patterning of the hindbrain and mesoderm. *Development* **116**, 1137-1150.
- Noden, D. (1983). The role of the neural crest in patterning of avian cranial skeletal, connective, and muscle tissues. *Dev. Biol.* **96**, 144-165.
- Noden, D. (1988). Interactions and fates of avian craniofacial mesenchyme. *Development* **103** Supplement 121-140.
- Oxtoby, E. and Jowett, T. (1993). Cloning of the zebrafish *krox-20* gene (*kx-20*) and its expression during hindbrain development. *Nucl. Acids Res.* **21**, 1087-1095.
- Pawson, T. and Bernstein, A. (1990). Receptor tyrosine kinases: genetic evidence for their role in *Drosophila* and mouse development. *Trends Genet.* **6**, 350-356.
- Puschel, A. W., Gruss, P. and Westerfield, M. (1992). Sequence and

- expression pattern of *pax-6* are highly conserved between zebrafish and mice. *Development* **114**, 643-651.
- Ruiz, J. and Robertson, E. J. (1994). The expression of the receptor-protein tyrosine kinase gene, *ecf*, is highly restricted during early mouse development. *Mech. Dev.* **46**, 87-100.
- Schneider-Maunoury, S., Topilko, P., Seitanidou, T., Levi, G., Cohen-Tannoudji, M., Pournin, S., Babinet, C. and Charnay, P. (1993). Disruption of *Krox-20* results in alteration of rhombomeres 3 and 5 in the developing hindbrain. *Cell* **75**, 1199-1214.
- Sechrist, J., Serbedzija, G. N., Scherson, T., Fraser, S. E. and Bronner-Fraser, M. (1993). Segmental migration of the hindbrain neural crest does not arise from its segmental generation. *Development* **118**, 691-703.
- Serbedzija, G. N., Bronner-Fraser, M. and Fraser, S. E. (1992). Vital dye analysis of cranial neural crest cell migration in the mouse embryo. *Development* **116**, 297-307.
- Smith, J. C. and Slack, J. M. W. (1983). Dorsalisation and neural induction: properties of the organiser in *Xenopus laevis*. *J. Embryol. exp. Morph.* **78**, 299-317.
- Ueno, H., Colbert, H., Escobedo, J. A. and Williams, L. T. (1991). Inhibition of PDGF β receptor signal transduction by coexpression of a truncated receptor. *Science* **252**, 844-848.
- Ueno, H., Gunn, M., Dell, K., Tseng, A. and Williams, L. T. (1992). A truncated form of fibroblast growth factor receptor 1 inhibits signal transduction by multiple types of fibroblast growth factor receptor. *J. Biol. Chem.* **267**, 1470-1476.
- Ullrich, A. and Schlessinger, J. (1990). Signal transduction by receptors with tyrosine kinase activity. *Cell* **61**, 203-212.
- van der Geer, P., Hunter, T. and Lindberg, R. A. (1994). Receptor protein tyrosine kinases and their signal transduction pathways. *Ann. Rev. Cell Biol.* **10**, 251-337.
- Wetts, R. and Fraser, S. E. (1989). Soggy intermixing of cells during *Xenopus* embryogenesis contributes to the consistency of the blastomere fate map. *Development* **105**, 9-15.
- Wilkinson, D. G. (1993). Molecular mechanisms of segmental patterning in the vertebrate hindbrain and neural crest. *BioEssays* **15**, 499-505.
- Wilkinson, D. G., Bhatt, S., Chavrier, P., Bravo, R. and Charnay, P. (1989). Segment-specific expression of a zinc finger gene in the developing nervous system of the mouse. *Nature* **337**, 461-464.
- Winning, R. S. and Sargent, T. D. (1994). *Pagliaccio*, a member of the *Eph* family of receptor tyrosine kinase genes, has localised expression in a subset of neural crest and neural tissues in *Xenopus laevis* embryos. *Mech. Dev.* **46**, 219-229.
- Xu, Q., Holder, N., Patient, R. and Wilson, S. W. (1994). Spatially regulated expression of three receptor tyrosine kinase genes during gastrulation in the zebrafish. *Development* **120**, 287-299.

(Accepted 22 August 1995)

Note added in proof

The nucleotide sequence of *XSek-1* will appear in the EMBL, GenBank and DDBJ Nucleotide Sequence Databases under the accession number X91191.

Eph Receptors and Ligands Comprise Two Major Specificity Subclasses and Are Reciprocally Compartmentalized during Embryogenesis

Nicholas W. Gale,* Sacha J. Holland,†
David M. Valenzuela,* Ann Flenniken,‡ Li Pan,*
Terrence E. Ryan,* Mark Henkemeyer,†
Klaus Strebhardt,§ Hisamaru Hirai,||
David G. Wilkinson,‡ Tony Pawson,† Samuel Davis,*
and George D. Yancopoulos*

*Regeneron Pharmaceuticals, Incorporated
777 Old Saw Mill River Road
Tarrytown, New York 10591-6707

†Samuel Lunenfeld Research Institute
Mount Sinai Hospital

600 University Avenue
Toronto, Ontario M5G 1X5
Canada

‡Medical Research Council
National Institute for Medical Research
The Ridgeway
Mill Hill
London NW7 1AA
United Kingdom

§Chemotherapeutisches Forschungsinstitut
Georg-Speyer-Haus
Paul-Ehrlich Strasse 42-44
6000 Frankfurt
Federal Republic of Germany

||The Third Department of Internal Medicine
Faculty of Medicine
University of Tokyo
Hongo, Tokyo 113
Japan

Summary

We report that the many Eph-related receptor tyrosine kinases, and their numerous membrane-bound ligands, can each be grouped into only two major specificity subclasses. Receptors in a given subclass bind most members of a corresponding ligand subclass. The physiological relevance of these groupings is suggested by viewing the collective distributions of all members of a subclass. These composite distributions, in contrast with less informative patterns seen with individual members of the family, reveal that the developing embryo is subdivided into domains defined by reciprocal and apparently mutually exclusive expression of a receptor subclass and its corresponding ligands. Receptors seem to encounter their ligands only at the interface between these domains. This reciprocal compartmentalization implicates the Eph family in the formation of spatial boundaries that may help to organize the developing body plan.

Introduction

Factors that bind and activate receptor tyrosine kinases (RTKs) play key roles during development as well as in the adult (Schlessinger and Ullrich, 1992). The known RTKs can be grouped into families based on structural

considerations. The Eph family of RTKs, named for its first described member (Hirai et al., 1987), is the largest known family of RTKs with at least 13 distinct members (Tuzi and Gullick, 1994). Members of the Eph receptor family display dynamic and spatially restricted expression patterns during embryogenesis, which originally suggested that they might be involved in a variety of developmental processes. For example, segmental expression of various Eph receptors such as murine Sek1 (also known as Hek8 in humans and Cek8 in chick) and Eck (also known as Sek2, Mpk5, and Myk2) in early somites and in the rhombomeres of the developing hind-brain suggested that they may be involved in formation of body segments or in regulating segment-specific characteristics (Nieto et al., 1992; Gilardi-Hebenstreit et al., 1992; Ruiz and Robertson, 1994). Expression of Eph family members in the limb and particular neural structures suggested additional roles (Nieto et al., 1992; Ganju et al., 1994; Cheng and Flanagan, 1994), with the expression of the murine Nuk receptor (also known as Hek5 and Erk in humans, Sek3 in mice, and Cek5 in chick) on initial axonal outgrowths, suggesting a role for this RTK in early axonal pathfinding or in the fasciculation stages of axonogenesis (Henkemeyer et al., 1994). Several of the Eph receptors have also generated interest because of their restricted expression to the nervous system in the adult, such as for Etk1 (alternately dubbed Bsk or Rek7 in rats, and also known as Hek7 in humans) Etk2, Etk3 (with the mouse ortholog also referred to as MDK1 or Etk and the human version Hek11), and Etk4 (also known as Cek6 in chick), (Lhotak et al., 1991; Maisonnier et al., 1993; Zhou et al., 1994; Taylor et al., 1994; Valenzuela et al., 1995; Ciossek et al., 1995; Ellis et al., 1995).

Members of the Eph receptor family were all initially identified as "orphan receptors," because at the time of their identification they had no known ligands. Recently however, protein factors that bind these receptors have been molecularly cloned at an impressive rate. B61 was initially cloned as a TNF-inducible sequence of unknown function (Holzman et al., 1990), but was subsequently recloned by a number of groups as the ligand for the Eck receptor (Bartley et al., 1994), as a binding protein for the Hek receptor (also referred to as Hek4 in humans, Mek4 in mouse, and Cek in chicken) and termed LERK (Beckmann et al., 1994), or as a ligand for both Eck and Etk1 and termed Etk-1 (Davis et al., 1994). Six additional ligands for Eph receptor have been published, with each of these ligands (like B61) having been independently cloned by several different groups based on binding to different members of the Eph receptor family (Beckmann et al., 1994; Davis et al., 1994; Cheng and Flanagan, 1994; Shao et al., 1994, 1995; Kozlosky et al., 1995; Bennett et al., 1995; Winslow et al., 1995; Drescher et al., 1995; Cerretti et al., 1995; Lackmann et al., 1996). Perhaps surprisingly, no ligands have been reported to bind to the original and prototypical member of this RTK subfamily, Eph. The seven published ligands comprise a family, with members sharing between 23% and 56% amino acid identity. The most striking unifying feature of

all the Eph family ligands is that they are all membrane-attached, either because they are transmembrane proteins (as for Htk-L/ELF-2/LERK5 and Elk-L/LERK2/Elf-3/Cek-5L, hereafter referred to as Htk-L and Elk-L/LERK2) or because they are bound to the surface via a glycosylphosphatidylinositol (GPI) linkage (as is the case for B61/LERK1/Elf-1, Ehk1-L/Elf-2/LERK3, LERK4, ELF-1/Cek7-L and AL-1/RAGS, hereafter referred to as B61, Ehk1-L, LERK4, ELF-1, and AL-1). While ligands for several other families of RTKs can have membrane-bound and soluble forms that are both active, the Eph family ligands are unusual in that only their membrane-bound forms are active while soluble forms are not only inactive but in fact may act as antagonists (Davis et al., 1994; Winslow et al., 1995). However, the soluble forms can be artificially activated by deliberate dimerization or higher order oligomerization, leading to the proposal that these ligands are active in their membrane-attached forms because membrane attachment normally serves to facilitate their oligomerization (Davis et al., 1994). The strict requirement for membrane attachment seems to provide for a specialized mechanism that ensures that receptor activation is coupled to direct cell-to-cell contact (Davis et al., 1994) and is consistent with findings that Eph family receptors can be highly localized to patches of cell-to-cell contact (Henkemeyer et al., 1994).

In contrast with other ectopically expressed neural RTKs such as the Trk receptors used by the neurotrophins, when Eph family receptors are ectopically expressed in non-neuronal cells they can not elicit conventional growth responses (Lhotak and Pawson, 1993; Davis et al., 1994; Brambilla et al., 1995). Because of these findings, together with the unusual requirement that the ligands act as obligate membrane-attached factors (Davis et al., 1994; Winslow et al., 1995), it may not be too surprising that emerging functional evidence (Winslow et al., 1995; Drescher et al., 1995; Cheng et al., 1995) indicates that Eph family ligands elicit responses from neurons and their precursors that are quite different from those seen in response to classical neurotrophic and survival factors such as the neurotrophins. The Eph family may instead be involved in axonal bundling or guidance, perhaps by providing repulsive signals, and has been specifically implicated as providing positional cues for establishing retinotectal projection patterns (reviewed by Tessier-Lavigne, 1995).

The very large size of the Eph family of receptors and ligands initially seemed well-suited for providing the diversity necessary to mediate distinct and specific recognition events in the nervous system and elsewhere (reviewed by Tessier-Lavigne, 1995). Early hints, however, suggested that the number of distinct binding specificities encoded by this family might be much smaller than that predicted based on family size. For example, as noted above, several of the ligands were independently identified using different Eph family receptors, indicating that the ligands could bind multiple receptors. Direct comparison has indeed shown that this can be the case, finding that particular ligands can indeed have rather similar affinities for several receptors (e.g., Davis et al., 1994; Beckmann et al., 1994; Kozlosky et al., 1995; Cheng and Flanagan, 1994; Brambilla et al., 1995). Here, we report that all the Eph family ligands identified to date, as well as most of the known Eph

family receptors, can each be functionally divided into only two major specificity subclasses. Thus, one subclass of ligands binds and activates one subclass of receptors, while the second subclass of ligands binds and activates the other subclass of receptors. The composite distributions of these subclasses during embryogenesis suggest that the Eph family is involved in formation of spatial boundaries that may help to organize the developing body plan.

Results

Eph Family Ligands and Receptors Each Segregate into Only Two Major Subclasses Based on Binding Specificities

To determine the binding specificities of the various Eph family receptor and ligands, we first transiently expressed each of the ligands on the surface of COS7 cells, and then assayed for the binding of saturating concentrations of soluble receptor-antibody fusion proteins (dubbed receptor-bodies, consisting of the extracellular domain of the receptor fused to the Fc portion of human IgG1) to these cells (Figure 1A; summarized in Figure 6A). These binding studies revealed that all the Eph family ligands identified to date, as well as most of the known Eph family receptors, can each be functionally divided into only two major specificity subclasses. One subclass of ligands (Elk-L/LERK2 and Htk-L, as well as a novel ligand dubbed Elk-L3 to be described in detail elsewhere; Gale et al., 1996) binds to one subclass of receptors (Elk and Nuk), while the other subclass of ligands (B61, Ehk1-L, LERK4, AL-1, and ELF-1) binds to the other subclass of receptors (Eck, Ehk1, Ehk2, Ehk3/MDK1, and Sek1); the Eph receptor proved unique in that it only binds to a single ligand, B61. Interestingly, the ligand subclasses as defined by binding specificities also correspond to subclasses defined by the type of membrane linkages used by the ligands, that is, all members of one subclass of ligands (Elk-L/LERK2, Htk-L, and Elk-L3) are transmembrane proteins, while all the members of the other subclass (B61, Ehk1-L, LERK4, AL-1, and ELF-1) are GPI anchored. Furthermore, the binding specificity subclasses of both the ligands and receptors also correlate with groupings that can be made based on homologies displayed by these proteins (see Figures 6A and 6B).

Although we did not directly test the interaction of Hek/Mek4 with this panel of ligands, Hek/Mek4 is most homologous to Ehk2, and others have shown that Hek/Mek4 can interact with B61 (Beckmann et al., 1994), Ehk1-L/LERK3 and LERK4 (Kozlosky et al., 1995), and ELF-1 (Cheng and Flanagan, 1994; Lackmann et al., 1996). Thus, Hek/Mek4 can be included among the receptor subclass that includes Eck, Ehk1, Ehk2, Ehk3/MDK1, and Sek1. Similarly, it has previously been shown that the Htk (also known as Myk1 and MDK2) receptor binds to Htk-L (Bennett et al., 1995; Bergemann et al., 1995) and the chicken ortholog (Cek10, and also known as Sek4 and MDK5 in mouse) of Hek2 binds Elk-L/LERK2 (Brambilla et al., 1995) and Htk-L (Bergemann et al., 1995), indicating that Htk and Hek2 should be grouped with the Elk and Nuk subclass of receptors (Figure 6A; also see below for further data in this regard).

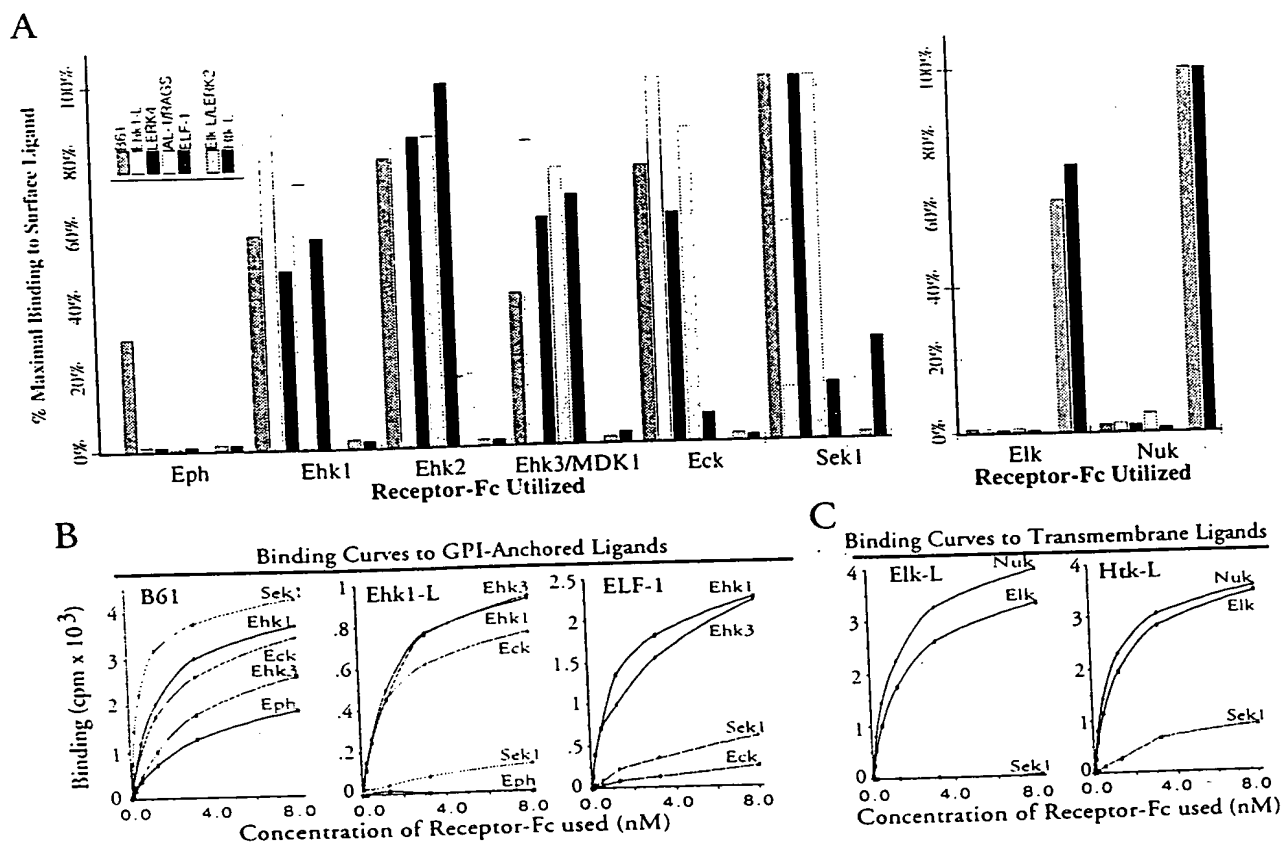


Figure 1. Binding Analyses Reveal Two Major Specificity Subclasses for the Eph Family

(A) Saturation binding of receptor-Fc to surface ligands. Binding of the indicated receptor-bodies, each at saturating concentrations, to a panel of transiently transfected COS cells expressing the indicated cell-surface bound ligands. (B and C) Indirect scatchard analysis of receptor/ligand binding. Analysis performed by measuring binding of varying concentrations of receptor-Fc fusions, as labeled on each binding curve, to transiently expressed surface bound ligand, indicated in the upper left corner of each graph.

Differences in Binding Specificities and Affinities of Members of the Same Subclass

Although different members of a particular subclass appear to have remarkably similar overall binding specificities as determined using saturating concentrations of receptor-bodies (Figure 1A), notable differences can also be seen. For example, Eck and Sek1 bind rather poorly to ELF-1, and Sek1 binds poorly to Ehk1-L, although Eck and Sek1 bind well to all the other GPI-anchored ligands. Furthermore, Sek1 appears to "cross" subclasses by exhibiting appreciable binding to the transmembrane ligand Htk-L. To explore further such differences in the binding specificities and affinities of members of the same subclass, sets of ligand-receptor pairings were selected for indirect scatchard analysis performed by measuring binding of varying concentrations of receptor-bodies (Figures 1B and 1C). Such binding analysis did indeed reveal clear differences in binding specificities and affinities of members of the same ligand or receptor subclass (Figure 2). Thus, B61 was bound with decreasing affinity by Sek1, Ehk1, Eck, Ehk3, and Eph; there was an approximately 10-fold difference in the binding affinity of B61 in the case of its highest

affinity interaction (to Sek1, $K_d \sim 0.395$ nM) compared with its lowest affinity interaction (to Eph, $K_d \sim 2.67$). There were similar variations in the binding affinities of Ehk1-L and ELF-1 by the various receptors, except that each displayed different relative preferences for the various receptors.

These data demonstrate that although members of a particular ligand subclass exhibit similar overall patterns of binding that are generally restricted to members of the corresponding subclass of receptors, each ligand displays a different set of preferences for these receptors, with the affinity of interaction ranging from the subnanomolar range to undetectable. Sek1 and Htk-L provide examples that "cross" subclasses by binding to each other with appreciable affinity, while Eph provides an example of a receptor with a very limited binding repertoire restricted to B61.

Eph Family Ligands Induce "Subclass-Specific" Receptor Activation

To determine whether the subclasses defined based on binding specificities correspond to functionally relevant groupings, we examined whether Eph family ligands

Receptors And Transmembrane Ligands

Rec/Lig Pair	Elk-L	Htk-L
Elk	1.16 nM	1.12 nM
Nuk	0.81	0.77
Sek1	n/a	8.60

Receptors And GPI-Anchored Ligands

Rec/Lig Pair	B61	Ehk1-L	ELF-1
Ehk1	1.19 nM	1.78 nM	1.31 nM
Ehk3/MDK1	2.41	1.47	1.03
Eck	1.33	0.95	20.10
Sek1	0.395	3.0	3.95
Eph	2.67	n/a	n/d

Figure 2. Calculated K_D s for Receptor-Fc Binding to Surface Ligands

Results of indirect scatchard analysis for the receptor/ligand pairs in Figures 1B and 1C are shown in matrix form and are expressed as K_D s (nM); n/a, too low to be determined accurately; n/d, not determined.

could indeed generally activate members of the corresponding subclass of receptors to which they could bind. Thus, deliberately clustered soluble ligands were assessed for their ability to induce phosphorylation of several members of the Eph receptor family; for these experiments, we employed MG mouse fibroblast cells stably expressing the Elk receptor (MG-Elk cells), COS1 monkey kidney cells endogenously expressing Nuk receptors, NIH 3T3 mouse fibroblast cells endogenously expressing Hek2 receptors, or CHP100 human neuroepithelial cells endogenously expressing Ehk1 receptors. The receptor phosphorylation results proved to be entirely consistent with the above binding studies. Thus, the transmembrane class of ligands (Elk-L/LERK2 and Htk-L) induced phosphorylation of Elk, Nuk and Hek2, while the GPI-anchored class of ligands (B61, Ehk1-L, Elf-4, or AL-1) did not (Figure 3, top). In contrast, the GPI-anchored ligands all induced activation of Ehk1 (and also Ehk2 and Eck; data not shown) while the transmembrane ligands did not (Figure 3, bottom). The findings for Hek2 also confirm the assumption made above, based on the binding specificities of the presumed chicken ortholog of Hek2 (Brambilla et al., 1995), that the mammalian Hek2 receptor can be placed into the group of receptors interacting with transmembrane ligands that also includes Elk, Nuk, and Htk.

Subclass Groupings Are Consistent with Binding Profiles in Whole Embryos

We next attempted to determine whether the Eph family ligand and receptor subclasses, defined based on the in vitro binding and receptor activation assays described above, were relevant to the specificities of these ligands and receptors for their in vivo counterparts. Toward this end, we stained whole embryos (embryonic day ~10.5) with either soluble receptor-bodies to define the embryonic distribution of their ligands, or soluble "ligand-bodies" (soluble ligand-antibody fusion proteins consisting of the soluble portion of the ligand fused to the antibody Fc domain) to define the embryonic distribution of their corresponding receptors. Consistent with the

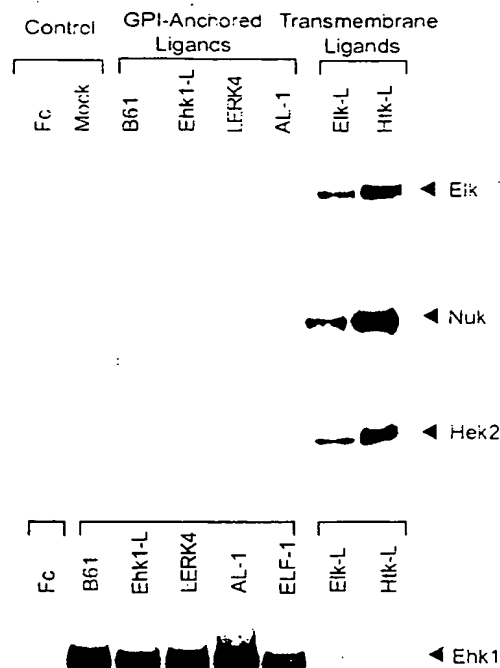


Figure 3. Eph Family Ligands Induce "Subclass-Specific" Receptor Activation

Receptor activation assayed by anti-phosphotyrosine immunoblotting of receptor precipitates from MG cells transfected with an expression construct to allow for stable expression of the Elk receptors, COS cells endogenously expressing Nuk receptors, NIH 3T3 cells endogenously expressing Hek2 receptors, or CHP100 cells endogenously expressing Ehk1 receptors. Cells stimulated with either control reagents (Fc alone, or Mock treated) or clustered ligand-bodies, as indicated.

subclass groupings determined above by the in-vitro binding and phosphorylation studies, receptors in a particular subclass all identified similar ligand patterns in the embryo, while ligands in a particular subclass also all detected rather uniform receptor profiles (Figure 4). However, consistent with the differences in relative affinities of members of a particular subclass for their counterparts, there were also occasional notable differences in the patterns identified by members of the same receptor or ligand subclass. Strikingly, the distribution of a given receptor subclass often seemed to be complementary to the distribution of its corresponding ligand subclass, suggesting that these receptors and their ligands mark or define boundaries in the embryo (this point addressed in detail below).

Elk and Nuk receptor-bodies, representing receptors interacting with transmembrane ligands when assayed on cell lines, both detected similar ligand patterns in the embryo (Figure 4B) that consisted of staining in the forebrain, lateral nasal process, dorsal midbrain/tectum, anterior dorsal hindbrain, eye regions, a dorsal stripe along the entire spinal cord, distinctive portions of the branchial arches, proximal limb bud, tail somites, and umbilical cord. Ligand-bodies representing the corresponding subclass of ligands, including Elk-L/LERK2

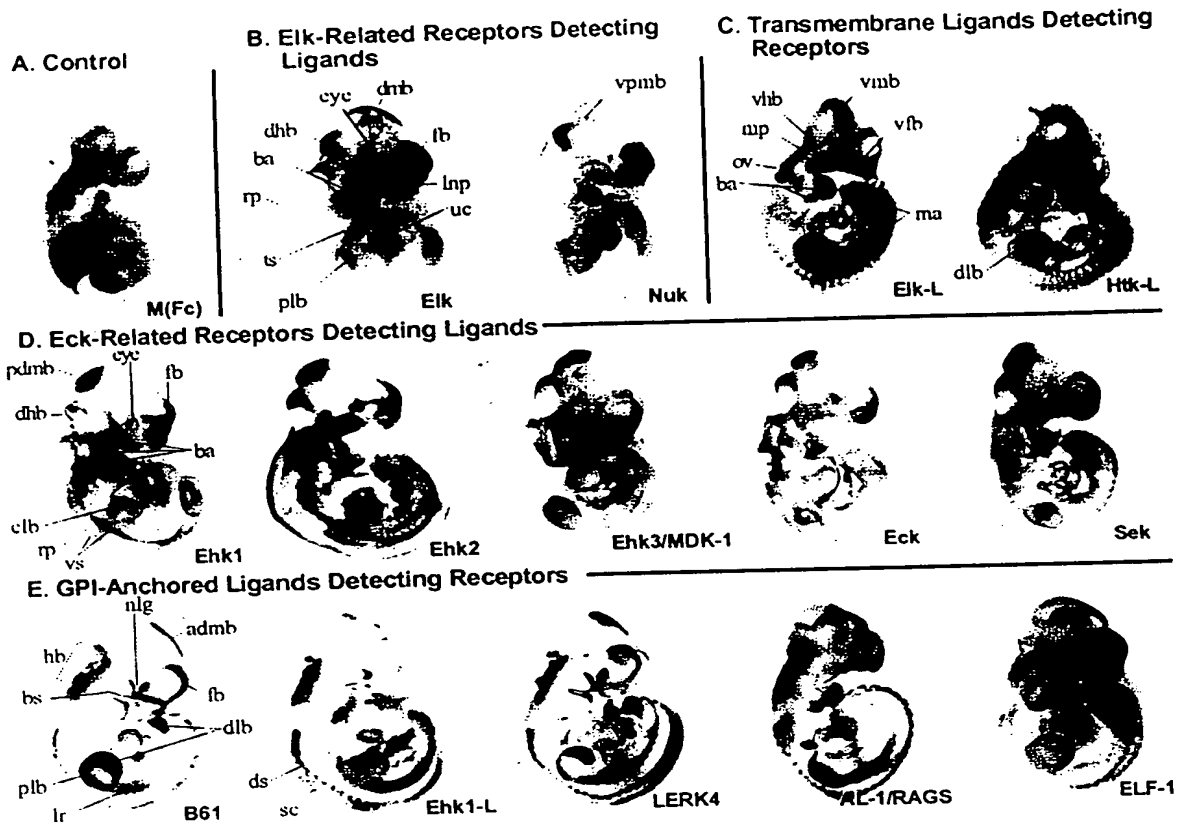


Figure 4. In Situ Binding Specificities of Eph Family Receptors and Ligands
 Receptor-Fc and ligand-Fc fusions were bound to whole 10.5 dpc embryos, and sites of binding were visualized by immunohistochemistry using an alkaline phosphatase-conjugated anti-human Fc secondary antibody.

- (A) Embryos bound with Fc alone, showing no detectable background binding.
- (B) Embryos bound with Elk-Fc or Nuk-Fc to localize the in situ distribution of their ligands.
- (C) Embryos bound with Elk-L/LERK2-Fc and Htk-L-Fc, two transmembrane ligands, to localize the distribution of their receptors.
- (D) Embryos bound with Fc fusions to the Eck-related receptors Ehk1, Ehk2, Ehk3/MDK-1, Eck, and Sek1 to localize the in situ distribution of their ligands.
- (E) Embryos bound with Fc fusions of the GPI-anchored ligands (B61, Ehk1-L, LERK4, AL-1/RAGS, and ELF-1) to localize distribution of their receptors.

Abbreviations: forebrain (fb), ventral forebrain (vfb), dorsal midbrain (dmb), anterior dorsal midbrain/pretectum (admb), posterior dorsal midbrain/tectum (pdmb), ventral midbrain (vmb), hindbrain (hb), dorsal hindbrain or cerebellar anlage (dhub), ventral hindbrain (vhb), spinal cord (sc), roof plate of spinal cord (rp), motor axons (ma), otic vesicle (ov), lateral nasal process (lnp) regions of the branchial arches (ba), nasolacrimal groove (nlg), slits/grooves of branchial arches (bs), maxillary process of the first branchial arch (mp), umbilical cord (uc), a body proximal band in the limb buds (plb), distal limb bud (dlb), central limb bud region (clb), dorsal region of the somites (ds), ventral region of the somites (vs), the lateral mesodermal ridge (lr), and a region of the newly formed tail somites (ts).

and Htk-L, both identified a characteristic receptor pattern distinguished by staining in the ventral region of the midbrain and diencephalon, the most ventral region of the hindbrain, otic vesicles, the maxillary process and branchial arches, and in segmentally expressed dorso-ventral stripes, which correspond to motor neuronal processes (Figure 4C; data not shown). A panel of receptor-bodies corresponding to the other subclass of receptors, that bind GPI-linked ligands *in vitro*, all identified largely similar ligand patterns in the embryo that were quite distinct from the ligand patterns detected by receptor-bodies representing the other subclass (Figure 4D). The ligand patterns detected by this panel of receptor-bodies was highlighted by staining in regions including the eye, the surface of the branchial arches (i.e., not in the slit/groove area of the arches), forebrain, dorsal posterior midbrain, dorsal anterior hindbrain, roof plate

of the spinal cord, in a ventral stripe along the somites, and within the limb bud in regions apparently exclusive of both the tip and the region most proximal to the body (Figure 4D and see below for further details). Finally, ligand–bodies representing the GPI-anchored ligands all exhibited remarkably similar binding patterns representing sites of expression of their receptors, which often seemed reciprocal to the distributions of the ligands themselves (Figure 4E and see below for further details). Receptors were detected in the forebrain, dorsal anterior midbrain/pretectum, in the hindbrain in the area of the rhombomeres, in the branchial arches within the slit/groove area exclusive of the surface of the arches and in the nasolacrimal groove, in a stripe along the dorsal region of the somites, and along the lateral mesodermal ridge (Figure 4E and see below). In the limb, sites of receptor expression were revealed in the distal

limb bud as well as in a body proximal location within the bud (Figure 4E and see below). Receptor expression was also prominently detected in the tail bud (not visible in the figure).

Despite the similar overall patterns detected by members of the same subclass, members did exhibit occasional notable differences, consistent with the above described binding assays, demonstrating that members of a given subclass could indeed display distinctive differences in their relative affinities for their counterparts. For example, in contrast with B61 ligand-bodies, ELF-1 ligand-bodies did not appreciably stain the tips of limb buds or tail buds and appeared to detect a more posterior region of the hindbrain (Figure 4E); the particular inability of ELF-1 ligand-bodies to stain limb buds can be explained by previous findings (Ganju et al., 1994; Cheng and Flanagan, 1994) that *Eck* and *Sek1*, which we have shown bind well to all GPI-linked ligands except for ELF-1, are localized to the limb bud tip. Eph receptor-bodies did not show detectable binding to whole embryos (data not shown).

Reciprocal Expression of Eph Receptors and Ligands Compartmentalize the Developing Body Plan and Suggest Dynamic Roles in Boundary Formation

The embryonic distributions of Eph receptors and ligands, as revealed by receptor body and ligand body staining experiments described in the previous section, suggested that these molecules might be involved in subdividing the body plan and perhaps in defining embryonic boundaries. Initial impressions that Eph receptors and ligands might be forming boundaries came from comparing distributions in the developing brain. Thus, receptors noted in the ventral midbrain by *Elk-L*/*LERK2* and *Htk-L* ligand-bodies appeared to be clearly bounded on either side by ligands expressed in the forebrain and the ventral posterior midbrain/hindbrain border as detected by *Elk* and *Nuk* receptor-bodies (compare Figures 4B and 4C); consistent with reciprocity in their expression, the ventral distributions of this class of receptors in the forebrain, midbrain and hindbrain are contrasted by dorsal locations of the corresponding ligands in these brain regions. Similarly, GPI-linked ligands and their receptors also seemed to define a complementary boundary between the dorsal posterior midbrain and the dorsal anterior midbrain (compare Figures 4D and 4E).

More apparent and dramatic examples of complementary domains and boundaries involving this subclass of ligands and their receptors were noted in the limb buds, in the branchial arches, in the spinal cord, and in somite regions. These domains and boundaries appeared quite dynamic, with dramatic changes occurring as development proceeds. For example, in the limb buds at embryonic day 10.5, GPI-anchored ligands were only detected in the central portion of the limb (prospective zeugopod) and were bounded by receptors expressed at the distal tip (prospective autopod) as well as in body-proximal areas (prospective stylopod; compare high power views provided in Figure 5A). Strikingly, reciprocal expression of receptors and ligands was also

noted later in limb development, forming different but still dramatic boundaries. Thus, in the distal limb at embryonic day 13.5, the GPI-anchored class of ligands could only be detected between the developing digits and not in the apical ectodermal ridge (AER), while receptors for these ligands were only noted in the digits themselves and in the AER (Figure 5B).

In the branchial arches, receptors for GPI-linked ligands were detected within the slit regions of the arches, while the ligands were noted primarily on the surface but not within the slit area of the arch (Figure 5C). Complementary binding patterns were also observed in the somites where the GPI-linked ligands appeared to be expressed in the ventral region of the somites, bounded on either side by receptors expressed in the dorsal region of the somite, as well as in the lateral ridge mesoderm (Figures 4D and 4E). To explore further the impression that the GPI-linked ligands and their receptors formed complementary boundaries in the somite regions of the embryos, the stained embryos were sectioned to allow for a more detailed comparison of ligand and receptor distributions in the trunk. Examination of such sections confirmed the precisely reciprocal nature of the expression patterns of these ligands and their receptors (Figure 5D). Thus, receptors for GPI-linked ligands were found in the dorsomedial region of the somite and were directly bounded by ligands expressed in dorsal root ganglion, the ventrolateral region of the somite as well as the lateral ridge mesoderm. Within the spinal cord, multiple striking boundaries could also be noted. Thus, receptors could be seen across the ventral spinal cord, exclusive of the floor plate. This receptor expression appeared to be capped by a thin layer of ligand expression, which was in turn overlaid by dense receptor expression that extended up to, but did not include, the roof plate area, which in turn strongly expressed the ligands.

Altogether, this analysis reveals that members of a particular Eph receptor subclass and their corresponding ligands are expressed in reciprocal and apparently mutually exclusive patterns that subdivide the embryo into clear domains that seem to form precise and dynamic boundaries in many different embryonic structures. Interestingly, it appears as if receptors may only encounter their ligands at the boundaries between the domains, although it remains possible that receptors and ligands interact within broader regions that appear to form sharp boundaries only because coexpressed partners interact and thus "mask" detection of each other. It is worth noting that distribution analysis of individual members of a subclass would not have readily revealed these domains, since each member accounts for only a portion of the composite pattern representing an entire subclass (data not shown; A. F. et al., unpublished data).

Discussion

Our results demonstrate that all the Eph family ligands identified to date, as well as most of the known Eph family receptors, can each be functionally divided into only two major specificity subclasses (Figure 6A). The

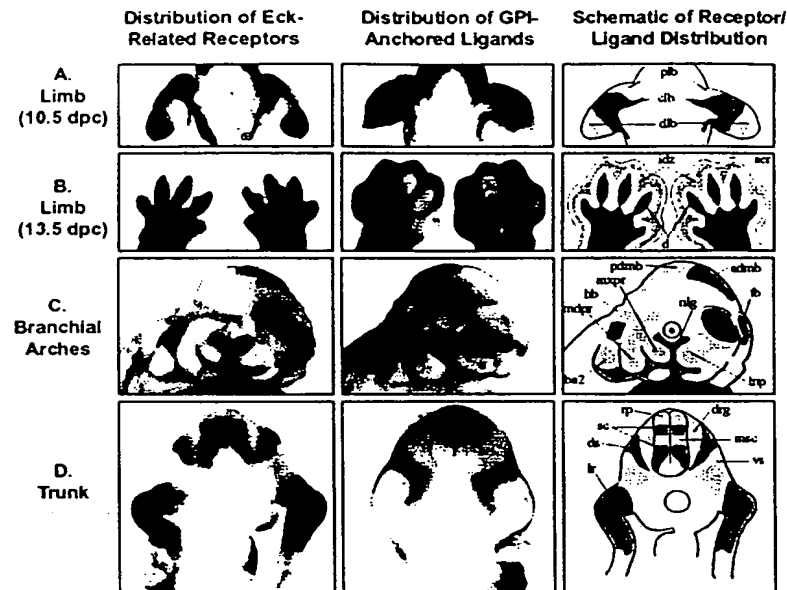


Figure 5. GPI-Anchored Ligands and Their Receptors Compartmentalize the Developing Body Plan and Form Dynamic Boundaries during Embryogenesis

Embryos were stained with an Fc fusion of a representative GPI-anchored ligand (B61, LERK4, or AL-1/RAGS) to reveal the composite distribution of the receptors binding this ligand subclass (left panels), or with an Fc fusion of one of these receptors (Ehk1 or Ehk2) to reveal the composite distribution of the GPI-anchored ligands themselves (middle panels). Binding was performed as in Figure 4, but embryos are shown at high power and/or sectioned through the trunk to allow for optimal comparison of receptor and ligand distribution. Schematic representations of the reciprocal patterns observed are provided in right panels.

(A) Forelimb buds of 10.5 dpc embryos depicting receptor expression in proximal and distal limb bud regions (plb and dlb, presumptive autopod and stylopod) with reciprocal ligand expression in the central limb bud region (clb, presumptive zeugopod). (B) Developing hands of 13 dpc embryos reveals receptor expression in the digits (d) and

in the apical ectodermal ridge (aer) and reciprocal ligand expression in the interdigital zone (idz).

(C) Views of the branchial arch region of embryos reveal receptor expression within the grooves of the branchial arches and in the nasolacrimal groove and olfactory pits, while ligand expression is reciprocally noted on the surface of the branchial arches exclusive of the grooves and in the lateral nasal process exclusive of the nasolacrimal groove and olfactory pits.

(D) Embryos sections from immediately posterior to the forelimb, and the trunk region viewed in cross section reveals complementary localization of receptors and ligands within the spinal cord, somites, and lateral mesoderm. Note that ligand expression within the dorsal root ganglion (drg) adjacent to the spinal cord, as noted in the schematic summary, was only noted in sections containing the drg (weak staining noted), although the drg is not visible in the section shown in the left panel. Abbreviations are as above and for Figure 4, with the following additions: maxillary process of the first branchial arch (mxpr), mandibular process of the first branchial arch (mdpr), second branchial arch (ba2), mid stripe in spinal cord (msc).

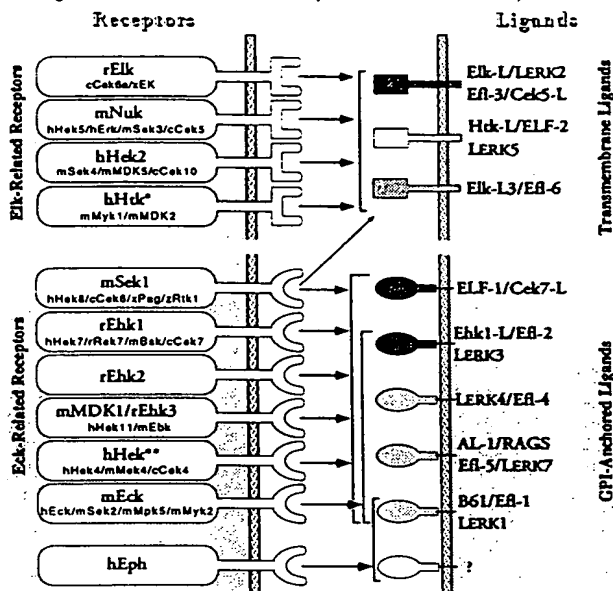
ligand subclasses correlate with the manner in which the ligands are anchored to the membrane. Thus, Elk-L/LERK2, Htk-L, and Elk-L3 are members of the "transmembrane class" of ligands, while B61, Ehk1-L, LERK4, ELF-1, and AL-1 are members of the "GPI-anchored class" of ligands. Not surprisingly, these ligand subclasses also reflect the degree of homology the ligands share with each other, with members of a subclass being most related (Figure 6B). Similarly, the two receptor subclasses defined based on their binding and activation specificities also generally reflect the relatedness of their extracellular domains, with the Elk-related subclass (comprised by Elk, Nuk, Hek2, and Htk) being rather specific for "transmembrane class" ligands and the Eck-related subclass (consisting of Eck, Ehk1, Ehk2, Ehk3/MDK-1, Sek1, and Hek) for "GPI-anchored" ligands (Figure 6). The only known Eph-related receptors that have not been grouped according to ligand specificity now include the Cek9 (which appears most homologous to the Elk subclass) and Eek receptors; full ectodomain sequences have not yet been reported for either of these receptors. The division of both Eph family receptors and ligands into the two major subclasses defined here seems quite important biologically, since the observed binding specificities have been preserved evolutionarily in all cases where the same receptor has been studied from both mammals and lower vertebrates.

Eph fits outside of the major subclasses because it has a very limited binding repertoire, thus far restricted

only to B61; it remains possible that this receptor may bind to yet undescribed ligands and may thus comprise an entirely separate subclass. Sek1 and Htk-L "cross" subclasses by binding to each other with appreciable affinity ($K_d \sim 8.6$ nM). An additional recently cloned ligand of the transmembrane subclass, Elk-L3, also binds Sek1 as well as Elk and Nuk, extending the notion that Sek1 "crosses" subclasses (Gale et al., 1996; Figures 6A and 6B). Within a particular ligand subclass, individual members clearly display a different set of preferences for their corresponding receptors, with the affinity of interaction ranging from the subnanomolar range to undetectable. In contrast with soluble ligands, whose affinity for their receptors reflects whether this binding can occur at physiologic levels of the ligand, it is much more difficult to predict whether particular Eph family receptor-ligand pairings are biologically relevant based on their affinity of interaction. This is because Eph receptor-ligand interactions occur at cell-to-cell interfaces, and therefore cooperative interactions due to multiple simultaneous receptor-ligand pairings may stabilize even weakly interacting partners. Thus, while binding and receptor activation studies reveal whether an exogenously provided ligand can pharmacologically interact with a particular Eph receptor, conclusions that this ligand and receptor normally pair in vivo will probably require that they are shown to colocalize to adjacent cells in vivo.

Why is it that such a large family of ligands has such a limited set of binding specificities? Unlike soluble li-

A. Binding and Activation Assays Reveal That Eph Family Receptors and Ligands Can Each Be Functionally Divided Into Two Major Subclasses



B. Cladograms of Eph Family Receptors and Ligands

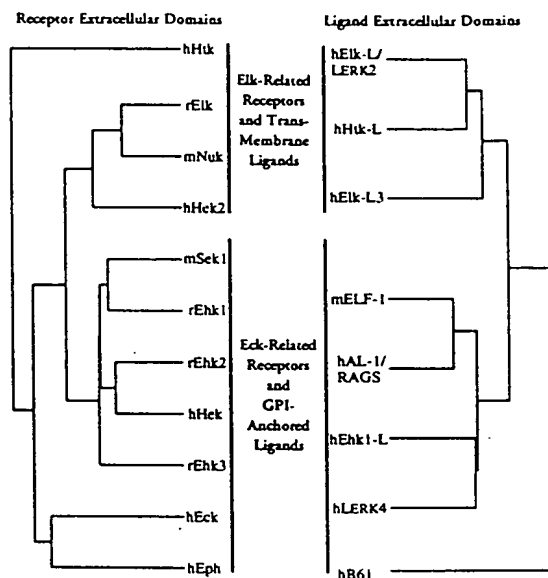


Figure 6. Groupings Made Based on Binding and Activation Assays Reflect the Relatedness of the Ectodomains of the Eph Receptors and Their Ligands

(A) Schematic summary of known receptor and ligand interactions. Arrows drawn from a receptor to a ligand group denote binding of that receptor to the ligands indicated by the brackets. The initial names of each receptor are provided in large bold type, with other names under which the receptors have been published indicated in smaller type; these names are prefixed with a lower case letter designating the species of origin for these receptors as follows: h, human; r, rat; m, mouse; c, chicken; x, Xenopus; z, zebrafish. Following the initial published names of the various ligands, additional published names of the various ligands are provided.

(B) Cladograms comparing the ectodomains of the Eph receptors and Eph ligands. Cladograms were generated by multiple amino acid sequence alignments using DNASTar Megalign program.

gands, which are free to access distant cells and thus may require exquisite receptor specificity to limit their actions, Eph family ligands can normally only act in membrane-anchored form (Davis et al., 1994). Thus, despite their ability to recognize many different receptors throughout the body, the actions of individual ligands may be restricted by simply limiting the distribution of the cells expressing the ligand, abrogating the need for exquisite receptor specificity. The evolutionary expansion of this family may have been driven not by the selection for new binding diversities, but rather by the selection for new distributions of old binding activities, or perhaps the association of new signaling capabilities with old binding activities. Regardless, the surprising lack of binding diversity in this large family raises issues concerning shared activities and redundancy; the fact that a given ligand maintains the ability to bind multiple receptors suggests that these interactions occur in vivo. Along these lines, it must also be considered that the subtle differences in the binding characteristics of members of the same subclass may prove to be functionally critical. For example, since this family has been implicated in the formation of gradients (Cheng et al., 1995; Drescher et al., 1995), it should be noted that "functional gradients" could, for example, either be formed by the graded distribution of an individual ligand, or by more uniform expression of several ligands in series, with each ligand having successively different affinities for a receptor recognizing the gradient; this may well be the

case in the tectum, where AL-1/RAGS and ELF-1 display overlapping gradients of expression. In any case, our data demand that future functional analyses simultaneously consider the potential roles of all members of a particular subclass when examining a given-biologic process in which one member of that subclass has been functionally implicated. The ability of any member of a given ligand or receptor subclass to mimic other members, at least pharmacologically, should also prove useful for addressing the roles of Eph family members in vivo.

The subclass designations we initially made based on in vitro binding and activation profiles were strikingly confirmed by staining whole embryos with receptor-bodies to define the in situ distribution of their ligands, or ligand-bodies to define the in situ distribution of their corresponding receptors. All receptors of a particular subclass identified similar ligand patterns in the embryo, while all ligands of a particular subclass detected similar receptor profiles. The distributions of receptors and ligands were in many cases consistent with emerging evidence that Eph family members may be involved in axonal outgrowth or guidance (Henkemeyer et al., 1994; Winslow et al., 1995; Drescher et al., 1995); for example, receptors recognizing the transmembrane class of ligands were noted on peripheral sensory ganglia and motor axons, and receptors for both classes of ligands were found in many regions of the developing brain. However, the most striking impression resulting from

the examination of receptor and ligand distributions was that expression of a receptor subclass was often quite complementary and reciprocal to that of its cognate ligand subclass, such that mutually exclusive receptor and ligand expression seems to subdivide much of the developing embryo into discrete domains. These subdivisions would not have been as readily apparent from distribution analysis of only individual members of a subclass, since each member accounts for only a portion of the composite pattern for that subclass.

Eph receptors seem to encounter their ligands primarily at the interfaces of the domains defined by the Eph subclasses, apparently demarcating precise boundaries throughout the developing embryo. These boundaries were noted in the developing brain and spinal cord, in the limb, in the branchial arches, in the somites, and elsewhere, implicating the Eph family in the formation, maintenance, or refinement of domains and boundaries in multiple embryonic structures, both within and outside of the developing nervous system. The strongest evidence for such a role for Eph family members has been obtained in the developing hindbrain. The binding studies presented here reveal that both the Eph ligands recently shown to be expressed in even-numbered rhombomeres (Htk-L/ELF-2 and Elk-L3; Bergemann et al., 1995; Gale et al., 1996) can bind to the Eph receptors (Sek1, Nuk/Sek3, and Htk/Sek4) previously shown to be expressed in odd-numbered rhombomeres. Dysregulation of these reciprocal expression domains, by uniformly expressing dominant negative versions of Sek1 throughout the hindbrains of developing *Xenopus* and zebrafish embryos, disrupts rhombomere specification (Xu et al., 1995), consistent with the notion that reciprocal expression of Eph receptors and ligands in adjacent rhombomeres is critical for normal segmentation in the hindbrain; earlier findings (Davis et al., 1994) that Eph family ligands can function only when presented in a membrane-bound form may be critical for their precise actions only at boundaries between distinct rhombomeres.

The developing limb presents an important example, with many analogies to the emerging hindbrain story, of how the dynamic boundaries and domains defined by Eph family expression can be compared with previous domains defined by fate-mapping studies and by the expression of other important regulatory molecules. Early in development, Eph-definable domains in the limb bud appeared to correlate with the three presumptive proximodistal subdivisions of the developing limb defined by fate-mapping studies, the autopod, the zeugopod, and the stylopod. Later in limb development, the Eph-definable domains in the distal limb precisely distinguished the developing cartilagenous digits from intervening regions that eventually regress and also marked the apical ectodermal ridge (at a stage in which it no longer has the ability induce outgrowth of the underlying mesenchyme). Interestingly, expression of a member of the Wnt gene family, Wnt-5a, seems to similarly distinguish the three proximodistal regions of the early limb and later specifically marks the developing digits (Dealy et al., 1993); the expression of particular Hox genes has been correlated with these areas of Wnt-5a expression (Dealy et al., 1993). Retinoic acid receptors (RARs) can also form proximodistal gradients in early

limb, and different members of this transcription factor family seem to distinguish the developing cartilagenous digits from the interdigital necrotic zone in later limbs (Tabin, 1991); in fact, expression of Eph family members can be regulated by retinoic acid (Bouillet et al., 1995). Thus, in the developing limb, the domains and boundaries reciprocally marked by Eph receptors and ligands appear to correspond to those previously defined by fate mapping and by the expression of other regulatory molecules such as the Wnts, homeobox genes, or retinoic acid-binding transcription factors. These findings are very reminiscent of those in the hindbrain and suggest that the Eph family may be regulated by, and/or collaborate with, other signaling molecules, and in turn contribute to the process of shaping the developing limb, perhaps by refining or maintaining boundaries by providing repulsive or attractive cues, by regulating cell migration or axonal guidance into or out of particular domains, or perhaps by helping to specify domain-specific characteristics.

Our expression patterns also suggest major roles for the Eph family in the dorsoventral patterning of the spinal cord. The thin stripe of GPI-linked ligand expression that appears to bisect the developing neural tube dorsoventrally (Figure 5D) may correspond to a boundary, previously marked by the expression of the cell-adhesion molecule F-cadherin as well as by members of the paired box (Pax) transcription factor family, across which cell mixing is restricted (Espeseth et al., 1995). This possibility suggests that other dorsoventral divisions marked by reciprocal expression of Eph receptors and ligands in the developing neural tube may also have functional significance consistent with the proposed roles of the Eph family in regulating cell migration, mixing, or specification and that the Eph family may critically interplay with particular cell-adhesion molecules and transcription factors in mediating these functions.

The reciprocal expression patterns of Eph family receptors and ligands seem to mark boundaries corresponding to several previously noted functional compartments in the developing limb, hindbrain, and spinal cord. However, reciprocal Eph expression patterns we have noted also define many new boundaries in these and other structures that seem just as likely to be functionally important. We and others have noted intriguing relationships between the compartmentalization of Eph family members and an assortment of developmentally important transcription factors, such as members of the Hox, Krox, Pax, and RAR gene families. Since the actions of these transcription factors depends on cell-to-cell communication, they must specify signals at the cell surface that mediate their actions. The Eph family, which provides an example of cell-surface receptors and their ligands that are reciprocally compartmentalized in the developing embryo, become prime candidates to provide such cell surface signals, perhaps in collaboration with other important regulatory molecules such as members of the Wnt family and cell adhesion molecules.

Experimental Procedures

Construction and Preparation of Receptor- and Ligand-Fcs
Ehk1-Fc, Eck-Fc, and Elk-Fc receptor-bodies have previously been described (Davis et al., 1994), and Nuk-Fc, Sek1-Fc, Ehk2-Fc, Eph-

Fc, and Ehk3-Fc receptor-bodies and B61-Fc, Ehk1L-Fc, Elf-4/LERK4-Fc, AL1-Fc, HtkL-Fc, ELF1-Fc, and ElkL-Fc were similarly engineered and produced.

Cloning of Eph Family Ligands

The Elf-4 cDNA (subsequently found to be identical to LERK4) was originally cloned by an expression cloning strategy essentially as described (Davis et al., 1994), except that the cDNA library was constructed from the human osteosarcoma cell line 143B, which exhibited binding to several Eph family receptors including Ehk1, Ehk2, Ehk3, and Eck. An Elf-5 cDNA fragment originally amplified from mouse hindbrain cDNA using degenerate primers (A. F. et al., unpublished data) was used as a probe to isolate a full-length Elf-5 human coding region subsequently found to be identical to AL-1. ELF-1 and Htk-L coding regions were amplified from embryonic mouse cDNA sources based on published sequence information (GenBank accession numbers U14941 and L38847).

Cell Transfections and Binding Analysis

COS7 cells transient transfections were done using LipofectAMINE reagent and Opti-MEM I (GIBCO BRL) according to the instructions of the manufacturer. Binding to transfected cells was performed as previously described (Davis et al., 1994). Fc-fusion proteins were quantitated by ELISA using anti-human antibody (Jackson Immunoresearch) coated plates and an alkaline phosphatase-conjugated anti-human antibody (Promega) with the soluble substrate pNPP (Sigma).

Receptor Phosphorylation Assays

Receptor phosphorylation was determined as previously described (Davis et al., 1994) on cells that were 80%–90% confluent at the time of treatment and changed into serum-free media for 1–2 hr prior to stimulation. Cells were stimulated at 37°C for 30 min using ligand-bodies at 500 ng/ml and clustering antibody at a final concentration of 17 µg/ml (Jackson Immunoresearch, goat anti-human antibody).

Whole-Mount Embryo Staining

Embryos of the indicated stage were dissected in ice-cold PBS, blocked in blocking solution (BS: 10% goat serum, 2% BSA, 0.02% Na azide in PBS) for 1 hr, and then incubated with either COS cell supernatants (with 10% calf serum) containing ligand-Fc or receptor-Fc, or purified Fc fusions at a concentration of 5 µg/ml in BS. Embryos were then washed extensively with PBS and fixed with fresh 4% paraformaldehyde overnight. (Alternatively, to enhance visualization of surface staining, embryos were fixed briefly with -20°C methanol and subsequently rehydrated in PBS.) Fixed embryos were heat treated at 70°C for 60 min in PBS to kill endogenous phosphatases, reblocked in BS plus 0.1% Triton X-100 overnight, and then incubated with goat anti-human (alkaline phosphatase conjugated; Promega) at a 1:1000 dilution in BS. Embryos were then extensively washed in TBS plus 0.1% Triton X-100 and, following color development, embryos were postfixed in 4% paraformaldehyde for 3 hr to overnight and were subsequently equilibrated in 50% glycerol followed by 70% glycerol.

Acknowledgments

Correspondence should be addressed to G. D. Y. We thank L. S. Schleifer, P. Roy Vagelos, and the rest of the Regeneron community for ardent support, particularly E. Rojas, J. Rojas, J. Griffiths, M. Simmons, L. DeFeo, R. Rossman, K. Tucci, M. McGlynn, E. Navarro, and C. Hughes for expert technical assistance and C. Murphy and E. Hubel for excellent graphics work. We also thank M. Goldfarb and M. Tessier-Lavigne for valuable insights and assistance in evaluating embryo staining results.

The costs of publication of this article were defrayed in part by the payment of page charges. This article must therefore be hereby marked "advertisement" in accordance with 18 USC Section 1734 solely to indicate this fact.

Received April 23, 1996; revised June 6, 1996.

References

- Bartley, T.D., Hunt, R.W., Welcher, A.A., Boyle, W.J., Parker, V.P., Lindberg, R.A., Lu, H.S., Colombero, A.M., Elliot, R.L., Guthrie, B.A., Holst, P.L., Skrine, J.D., Toso, R.J., Zhang, M., Fernandez, E., Trail, G., Varnum, B., Yarden, Y., Hunter, T., and Fox, G.M. (1994). B61 is a ligand for the ECK receptor protein-tyrosine kinase. *Nature* 368, 558–560.
- Beckmann, M.P., Cerretti, D.P., Baum, P., Vanden Bos, T., James, L., Farrah, T., Kozlosky, C., Hollingsworth, T., Shilling, H., Maraskovsky, E., Fletcher, F.A., Lhotak, V., Pawson, T., and Lyman, S.D. (1994). Molecular characterization of a family of ligands for the Eph-related tyrosine kinase receptors. *EMBO J.* 13, 3757–3762.
- Bennett, B.D., Zeigler, F.C., Gu, Q., Fendly, S., Goddard, A.D., Gillett, N., and Matthews, W. (1995). Molecular cloning of a ligand for the EPH-related receptor protein-tyrosine kinase Htk. *Proc. Natl. Acad. Sci. USA* 92, 1866–1870.
- Bergemann, A.D., Cheng, H.-J., Brambilla, R., Klein, R., and Flanagan, J.G. (1995). ELF-2, a new member of the Eph ligand family, is segmentally expressed in mouse embryos in the region of the hindbrain and newly forming somites. *Mol. Cell. Biol.* 15, 4921–4929.
- Bouillet, P., Oulad-Abdelghani, M., Vicaire, S., Garnier, J.M., Schuhbauer, B., Dolle, P., and Chambon, P. (1995). Efficient cloning of cDNAs of retinoic acid-responsive genes in P19 embryonal carcinoma cells and characterization of a novel mouse gene, Stra1 (mouse LERK-2/Eplg2). *Dev. Biol.* 170, 420–433.
- Brambilla, R., Schnapp, A., Casagrande, F., Labrador, J.P., Bergemann, A.D., Flanagan, J.G., Pasquale, E.B., and Klein, R. (1995). Membrane-bound LERK2 ligand can signal through three different Eph-related receptor tyrosine kinases. *EMBO J.* 14, 3116–3126.
- Cerretti, D.P., Vanden Bos, T., Nelson, N., Kozlosky, C.J., Reddy, P., Maraskovsky, E., Park, L.S., Lyman, S.D., Copeland, N.G., and Gilbert, D.J. (1995). Isolation of LERK-5: a ligand of the Eph-related receptor tyrosine kinases. *Mol. Immunol.* 32, 1197–1205.
- Cheng, H.-J., and Flanagan, J.G. (1994). Identification and cloning of ELF-1, a developmentally expressed ligand for the Mek4 and Sek receptor tyrosine kinases. *Cell* 79, 157–168.
- Cheng, H.-J., Nakamoto, M., Bergemann, A.D., and Flanagan, J.G. (1995). Complementary gradients in expression and binding of ELF-1 and Mek4 in development of the topographic retinotectal projection map. *Cell* 82, 371–381.
- Ciossek, T., Millauer, B., and Ullrich, A. (1995). Identification of alternatively spliced mRNAs encoding variants of MDK1, a novel receptor tyrosine kinase expressed in the murine nervous system. *Oncogene* 10, 97–108.
- Davis, S., Gale, N.W., Aldrich, T.H., Maisonpierre, P.C., Lhotak, V., Pawson, T., Goldfarb, M., and Yancopoulos, G.D. (1994). Ligands for the EPH-related receptor tyrosine kinases that require membrane attachment or clustering for activity. *Science* 266, 816–819.
- Dealy, C.N., Roth, A., Ferrari, D., Brown, A.M.C., and Koshier, R.A. (1993). Wnt-5a and Wnt-7a are expressed in the developing chick limb bud in a manner suggesting roles in pattern formation along the proximodistal and dorsoventral axes. *Mech. Dev.* 43, 175–186.
- Drescher, U., Kremoser, C., Handwerker, C., Löscher, J., Noda, M., and Bonhoeffer, F. (1995). In vitro guidance of retinal ganglion cell axons by RAGS, a 25 kDa tectal protein related to ligands for Eph receptor tyrosine kinases. *Cell* 82, 359–370.
- Ellis, J., Liu, Q., Breitman, M., Jenkins, N.A., Gilbert, D.J., Copeland, N.G., Tempest, H.V., Warren, S., Muir, E., Schilling, H., Fletcher, F.A., Ziegler, S.F., and Rogers, J.H. (1995). Embryo brain kinase: a novel gene of the eph/elk receptor tyrosine kinase family. *Mech. Dev.* 52, 319–341.
- Espeseth, A., Johnson, E., and Kintner, C. (1995). *Xenopus* F-cadherin, a novel member of the cadherin family of cell adhesion molecules, is expressed at boundaries in the neural tube. *Mol. Cell. Neurosci.* 6, 199–211.
- Gale, N.W., Flenniken, A., Compton, D.C., Jenkins, N., Copeland, N.G., Gilbert, D.J., Davis, S., Wilkinson, D.G., and Yancopoulos, G.D. (1996). Elk-L3, a novel transmembrane ligand for the Eph family of

- receptor tyrosine kinases, expressed in embryonic hindbrain, floor plate, and roof plate. *Oncogene*, in press.
- Ganju, P., Shigemoto, K., Brennan, J., Entwistle, A., and Reith, A.D. (1994). The *Eck* receptor tyrosine kinase is implicated in pattern formation during gastrulation, hindbrain segmentation and limb development. *Oncogene* 9, 1613-1624.
- Gilardi-Hebenstreit, P., Nieto, M.A., Frain, M., Mattei, M.-G., Chestier, A., Wilkinson, D.G., and Charnay, P. (1992). An Eph-related receptor protein tyrosine kinase segmentally expressed in the developing mouse hindbrain. *Oncogene* 7, 2499-2506.
- Henkemeyer, M., Marengere, L.E.M., McGlade, J., Olivier, J.P., Conlon, R.A., Holmyard, D.P., Letwin, K., and Pawson, T. (1994). Immunolocalization of the *Nuk* receptor tyrosine kinase suggests roles in segmental patterning of the brain and axonogenesis. *Oncogene* 9, 1001-1014.
- Hirai, H., Maru, Y., Hagiwara, K., Nishida, J., and Takaku, F. (1987). A novel putative tyrosine kinase receptor encoded by the *eph* gene. *Science* 238, 1717-1720.
- Holzman, L.B., Marks, R.M., and Dixit, V.M. (1990). A novel immediate-early response gene of endothelium is induced by cytokines and encodes a secreted protein. *Mol. Cell. Biol.* 10, 5830-5838.
- Kozlosky, C.J., Maraskovsky, E., McGrew, J.T., Vanden Bos, T., Teppe, M., Lyman, S.D., Srinivasan, S., Fletcher, F.A., Gayle, R.B., III, Cerretti, D.P., and Beckmann, M.P. (1995). Ligands for the receptor tyrosine kinases *hek* and *elk*: isolation of cDNAs encoding a family of proteins. *Oncogene* 10, 299-306.
- Lackmann, M., Bucci, T., Mann, R.J., Kravets, L.A., Viney, E., Smith, F., Moritz, R.L., Carter, W., Simpson, R.J., Nicola, N.A., Mackwell, K., Nice, E., Wilks, A.F., and Boyd, A.W. (1996). Purification of a ligand for the EPH-like receptor HEK using a biosensor-based affinity detection approach. *Proc. Natl. Acad. Sci. USA* 93, 2523-2527.
- Lhotak, V., and Pawson, T. (1993). Biological and biochemical activities of a chimeric epidermal growth factor-Elk receptor tyrosine kinase. *Mol. Cell. Biol.* 13, 7071-7079.
- Lhotak, V., Greer, P., Letwin, K., and Pawson, T. (1991). Characterization of *Elk*, a brain-specific receptor tyrosine kinase. *Mol. Cell. Biol.* 11, 2496-2502.
- Maisonpierre, P.C., Barrezuela, N.X., and Yancopoulos, G.D. (1993). *Ehk-1* and *Ehk-2*: two novel members of the Eph receptor-like tyrosine kinase family with distinctive structures and neuronal expression. *Oncogene* 8, 3277-3288.
- Nieto, M.A., Gilardi-Hebenstreit, P., Charnay, P., and Wilkinson, D.G. (1992). A receptor tyrosine kinase implicated in the segmental patterning of the hindbrain and mesoderm. *Development* 116, 1137-1150.
- Ruiz, J.C., and Robertson, E.J. (1994). The expression of the receptor-protein tyrosine kinase gene, *eck*, is highly restricted during early mouse development. *Mech. Dev.* 46, 87-100.
- Schlessinger, J., and Ullrich, A. (1992). Growth factor signaling by receptor tyrosine kinases. *Neuron* 9, 383-391.
- Shao, H., Lou, L., Pandey, A., Pasquale, E.B., and Dixit, V.M. (1994). cDNA cloning and characterization of a ligand for the *Cek5* receptor protein-tyrosine kinase. *J. Biol. Chem.* 269, 26606-26609.
- Shao, H., Lou, L., Pandey, A., Verderame, M.F., Siever, D.A., and Dixit, V. (1995). cDNA cloning and characterization of a *Cek7* receptor protein-tyrosine kinase ligand that is identical to the ligand (ELF-1) for the *Mek-4* and *Sek* receptor protein-tyrosine kinases. *J. Biol. Chem.* 270, 3467-3470.
- Tabin, C.J. (1991). Retinoids, homeoboxes, and growth factors: toward molecular models for limb development. *Cell* 66, 199-217.
- Taylor, V., Miescher, G.C., Pfarr, S., Honegger, P., Breitschopf, H., Lassmann, H., and Steck, A.J. (1994). Expression and developmental regulation of *Ehk-1*, a neuronal *Elk*-like receptor tyrosine kinase in brain. *Neuroscience* 63, 163-178.
- Tessier-Lavigne, M. (1995). Eph receptor tyrosine kinases, axon repulsion, and the development of topographic maps. *Cell* 82, 345-348.
- Tuzi, N.L., and Gullick, W.J. (1994). Eph, the largest known family of putative growth factor receptors. *Br. J. Cancer* 69, 417-421.
- Valenzuela, D.M., Rojas, E., Griffiths, J.A., Compton, D.L., Gisser, M., Ip, N.Y., Goldfarb, M., and Yancopoulos, G.D. (1995). Identification of full-length and truncated forms of *Ehk-3*, a novel member of the Eph receptor tyrosine kinase family. *Oncogene* 10, 1573-1580.
- Winslow, J.W., Moran, P., Valverde, J., Shih, A., Yuan, J.Q., Wong, S.C., Tsai, S.P., Goddard, A., Henzel, W.J., Hefti, F., Beck, K.D., and Caras, I.W. (1995). Cloning of *AL-1*, a ligand for an Eph-related tyrosine kinase receptor involved in axon bundle formation. *Neuron* 14, 973-981.
- Xu, Q., Alldus, G., Holder, N., and Wilkinson, D.G. (1995). Expression of truncated *Sek-1* receptor tyrosine kinase disrupts the segmental restriction of gene expression in the *Xenopus* and zebrafish hindbrain. *Development* 121, 4005-4016.
- Zhou, R., Copeland, T.D., Kromer, L.F., and Schulz, N.T. (1994). Isolation and characterization of *Bsk*, a growth factor receptor-like tyrosine kinase associated with the limbic system. *J. Neurosci. Res.* 37, 129-143.

EphA4 (Sek1) receptor tyrosine kinase is required for the development of the corticospinal tract

MIRELLA DOTTORI*, LYNNE HARTLEY†, MARY GALEA‡, GEORGE PAXINOS§, MARK POLIZZOTTO†, TREVOR KILPATRICK†, PERRY F. BARTLETT†, MARK MURPHY¶, FRANK KÖNTGEN†, AND ANDREW W. BOYD*||

*Queensland Institute for Medical Research, Royal Brisbane Hospital, Herston, Queensland 4029, Australia; †Walter and Eliza Hall Institute of Medical Research, Royal Melbourne Hospital, Victoria 3050, Australia; ‡School of Physiotherapy and §Department of Anatomy and Cell Biology, University of Melbourne, Victoria 3020, Australia; and ¶School of Psychology, University of New South Wales, New South Wales 2052, Australia

Communicated by Gustav J. V. Nossal, University of Melbourne, Parkville, Australia, August 24, 1998 (received for review February 27, 1998)

ABSTRACT Members of the Eph family of tyrosine kinase receptors have been implicated in the regulation of developmental processes and, in particular, axon guidance in the developing nervous system. The function of the EphA4 (Sek1) receptor was explored through creation of a null mutant mouse. Mice with a null mutation in the EphA4 gene are viable and fertile but have a gross motor dysfunction, which is evidenced by a loss of coordination of limb movement and a resultant hopping, kangaroo-like gait. Consistent with the observed phenotype, anatomical studies and anterograde tracing experiments reveal major disruptions of the corticospinal tract within the medulla and spinal cord in the null mutant animals. These results demonstrate a critical role for EphA4 in establishing the corticospinal projection.

Recent studies show that axons are guided to their targets by a system of guidance molecules, including Eph receptors and their ligands (1–3). The role of these molecules has been studied intensely in development of the visual system (4–6), where the reciprocal gradient expression of the Eph receptors in the retina and of their ligands in the optic tectum is the suggested basis for the formation of the retinotectal topographic map. Other observations pertinent to the role of these molecules in the developing nervous system include axonal fasciculation and establishing brain commissures (7–9).

The Eph family receptors can be divided into two groups, EphA and EphB, based on the sequence similarities of their extracellular domain (10). Each EphA receptor is able to bind several Ephrin A ligands that are associated with the membrane via a GPI-linkage; these receptors show little or no binding to the transmembrane Ephrin B ligands (11, 12). The EphB group of receptors show the reverse pattern, binding predominantly to Ephrin B ligands. An exception to this “rule” is the EphA4 (previously known as Sek1) receptor, which was found to bind significantly to some of the transmembrane ligands in addition to all of the GPI-linked ligands (11–13).

EphA4 expression during development shows a defined spatiotemporal pattern within the developing forebrain, hindbrain, and mesoderm (14, 15). In the final stages of embryogenesis, expression of EphA4 is found predominantly within regions of the central nervous system, including the cerebral cortex, striatum, thalamus, hippocampus, and ventral spinal cord. In the hindbrain, EphA4 shows restricted expression to rhombomeres 3 and 5 (14), which suggests a role of this receptor in establishing boundaries during embryogenesis. This notion is supported by overexpression of dominant negative, truncated EphA4 receptor in zebrafish embryos. The resultant mutant embryos were found to have disruption in the

rhombomere boundaries and an expansion of the developing retina into the diencephalon (16, 17). The expression pattern of EphA4 coupled with the unique binding characteristics of this receptor suggests that loss of function of the EphA4 gene may affect neural patterning events.

This report describes the generation of mice deficient in the EphA4 receptor. The EphA4 mutant mice displayed a gross motor abnormality in the hindlimbs. Anatomical analyses and anterograde tracing of cortical neurons demonstrated a severe disruption of the corticospinal tract (CST) in these animals. The CST is the single longest axonal projection in the mammalian central nervous system (18). CST neurons arise from layer V in the neocortex and extend their axons through the forebrain, midbrain, and hindbrain and terminate at various levels of the spinal cord. In primates, the CST axons predominantly synapse directly with the spinal motor neurons whereas in the rodent, most of the cortical axons synapse with interneurons, which then connect to the spinal motor neurons. The EphA4 null mutant mice showed specific defects in the CST both at the level of the medulla and the spinal cord, which indicates that EphA4 is required for the correct formation of the CST, possibly by guidance of CST axons.

MATERIALS AND METHODS

Targeted Disruption of EphA4 Gene. For homologous recombination, 5' *HindIII*-*SacI* 3-kilobase (kb) sequence and 3' *Eco47III*-*BamHI* 5.5-kb sequence flanking exon III were subcloned into the pKJ1 vector (Fig. 1). The vector contains the neomycin-resistance gene (*neo*) with the phosphoglycerate kinase (*pgk*) promoter and *pgk* polyadenylation signal. The W9.5 embryonic stem cell line was electroporated with the *SalI* linearized targeting construct and was selected with G418 for 10 days. A total of 480 surviving clones were expanded, and homologous recombinants were identified by Southern blot analysis of genomic DNA from single clones digested with *EcoRI*. Two isolated clones with a single targeted mutation of EphA4 gene each were injected into (C57BL/6 × C57BL/10)F₂ blastocysts. Chimeras were mated to C57BL/6 mice to produce heterozygotes. Southern blot analysis of tail DNA was used for genotyping the offspring.

Whole-Mount and Tissue Immunocytochemistry and PCR Genotyping of Embryos. Whole-mount immunocytochemistry was performed with anti-EphA4 antibody (provided by D.G. Wilkinson of National Institute of Medical Research, Mill Hill, U.K.) as described (19), and color detection was carried out by

The publication costs of this article were defrayed in part by page charge payment. This article must therefore be hereby marked “advertisement” in accordance with 18 U.S.C. §1734 solely to indicate this fact.

© 1998 by The National Academy of Sciences 0027-8424/98/9513248-6\$2.00/0
PNAS is available online at www.pnas.org.

Abbreviations: AC, anterior commissure; CST, corticospinal tract; kb, kilobase; E, embryonic day.

Data deposition: The sequence reported in this paper has been deposited in the GenBank database (accession no. 65138).

To whom reprint requests should be addressed at: Queensland Institute of Medical Research, The Bancroft Centre, PO Royal Brisbane Hospital, Herston, Queensland 4029, Australia. e-mail: andrewBo@qimr.edu.au.

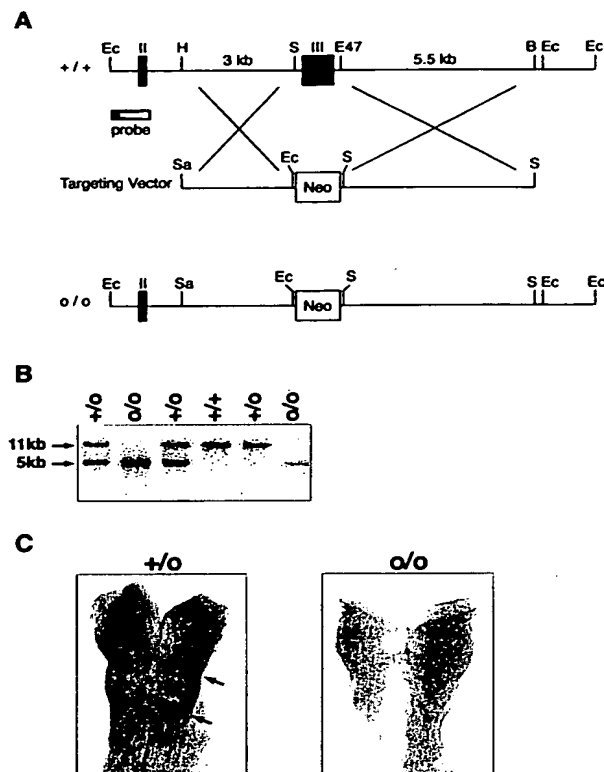


FIG. 1. Targeted disruption of EphA4 gene. **(A)** Partial map of the *ephA4* genomic locus (+/+) with the targeting construct and the resulting targeted loci (o/o). The EphA4 targeting vector was designed to replace exon III (217–880 bp of EphA4 cDNA) (38) with the 1.8-kb neomycin selection gene. For homologous recombination, 5' *HindIII*–*SacI* 3-kb sequence and 3' *Eco47III*–*BamHI* 5.5-kb sequence flanking exon III were subcloned into the pKJ1 vector. Homologous recombination would cause a frame shift in the EphA4 gene, resulting in a null mutant protein. The probe used for all Southern blot analyses was a 1-kb genomic fragment containing exon II (149–216 bp) and *EcoRI* site. Ec, *EcoRI*; H, *HindIII*; S, *SacI*; E47, *Eco47III*; B, *BamHI*; Neo, neomycin gene; II, exon II; and III, exon III. **(B)** Genotype analysis of EphA4 homozygous (o/o), heterozygous (+/o), and wild-type (+/+) animals. Genomic DNA was isolated from 0.5 cm tail tissue (39), was digested with *EcoRI*, and was subjected to Southern blot analysis using the 5' external probe shown in A. Alleles bearing the *ephA4* mutation results in a 5-kb band whereas an 11-kb band was observed in the wild-type alleles. **(C)** Whole-mount immunocytochemistry of E 8.5 embryos by using anti-EphA4 antibody. EphA4 is expressed in rhombomeres 3 and 5 (arrows) in heterozygotes (+/o), but no EphA4 protein is detected in homozygous (o/o) mutants. The embryos were genotyped by PCR from yolk sac DNA.

using 5-bromo-4-chloro-3-indolyl-phosphate/nitro blue tetrazolium (Promega) as substrate. For tissue sections, tissues were fixed for 24 hours in 4% paraformaldehyde and then another 24 hours in fixative containing 30% sucrose. Frozen tissue was sectioned serially 50 μ m thick. Immunohistochemistry was performed by using anti-EphA4 antibody, and the same protocol as for whole mounts, except the ABC Elite detection system (Vector Laboratories) was used to detect color staining.

Embryos were genotyped by PCR of yolk sac DNA (20) by using primer pairs P1 CGTGCTACTTCCATTTGT-CACGTCCTG and P2 TGCCGTGATAGCAATTGAG or P3 AGGAAGTGAGCATTATGGATGA and P4 TGCTC-CTCGTGCCGACGTT. A 600-bp band was generated from the mutant allele between the neomycin primer P1 and *ephA4* endogenous primer P2; a 645-bp product was generated from the wild-type allele between exon III primers P3 and P4. The

PCR reaction was in a total volume of 50 μ l and consisted of 50–500 ng DNA, 30 pmol of each primer, 2.0 mM MgCl₂, 100 μ M dNTPs, and 1 unit *Taq* polymerase (Roche, Gifp-Oberfrick, Switzerland), with the appropriate reaction buffer supplied by the manufacturer. The cycling reaction was 15 cycles of 96°C for 30 sec, 70°C for 30 sec (–1°C per cycle), and 72°C for 1 min, followed by 20 cycles of 96°C for 30 sec, 55°C for 30 sec, and 72°C for 1 min.

Histology. Histological examination was carried out on EphA4 homozygous, heterozygous, and wild-type littermates of embryonic day (E) 16 and 8- and 24-day-old mice. Embryos and adult tissues were fixed overnight in 10% formalin, were paraffin-embedded, and were sectioned serially 4 μ m thick. Sections were stained with either haematoxylin and eosin or luxol fast blue.

In Situ Hybridization. For EphA4 mRNA expression, tissues were fixed overnight in 10% formalin, were paraffin-embedded, and were sectioned serially 4 μ m thick. *In situ* hybridization was performed as described (21) by using ³³P-radiolabeled complementary EphA4 RNA probe. The antisense probe was synthesized with T7 polymerase from the *HindIII*-linearized plasmid Bluescript KS, containing a 1.5-kb *EcoRI* fragment of 3' untranslated and C-terminal coding sequences of EphA4 (provided by D.G. Wilkinson).

For expression of EphrinB3 mRNA, digoxigenin-labeled *in situ* hybridization was performed on frozen 20- μ m tissue sections as described (22). To generate the Ephrin B3 probe, Ephrin B3 cDNA was amplified by PCR from adult mouse brain cDNA by using primers TTAGAATTCCCCGAGGAG-GAGCTGTAC and CTAGAATTCTGCAGTCCCACCAC-CCCG. The PCR product, which spans 551 to 953 bp of Ephrin B3 cDNA (13), was cloned into *EcoRI* site of Bluescript SK and was sequenced. The antisense probe then was synthesized with T3 polymerase from the *HindIII*-linearized plasmid.

Surgery, Anterograde Tracing, and Tissue Processing. Corticospinal axons and their terminal projections were labeled in 5-week-old mice by using the anterograde tracer biotinylated dextran amine (15%; (Molecular Probes). Two wild-type, one heterozygous, and three homozygous EphA4 mutant mice were used for these studies. The animals were anesthetized by injecting i.p. (10 μ l/g of body weight) a 1:1:6 ratio mixture of Hypnorm (Janssen), Hypnovel (Roche), and distilled H₂O. Anesthetized animals had their head positioned in a stereotaxic frame, and a craniotomy (3–4 mm in diameter) was made to expose the rostral half of the left cerebral hemisphere. Seven injections of 0.3 μ l of tracer were made into the cerebral cortex at a depth of 0.5–1.0 mm below its surface by using a glass pipette (tip diameter of 50 μ m) attached to a Hamilton syringe (23). The injections covered the whole sensorimotor region of the cerebral cortex. The number of injections, the injection sites, and the amount of tracer used per injection were kept consistent between control and mutant animals. The brain and spinal cord were perfused 7 days after the injection with 0.9% phosphate buffered saline and 4% paraformaldehyde in phosphate buffer. The tissue was postfixed for 24 hours in 30% sucrose in buffered fixative.

The free-floating sections were processed according to the method as described (24) to visualize the axons and terminals labeled by biotinylated dextran amine. Phosphate buffer (0.1 M) was the vehicle for the immunoreagents and for rinsing after each of the following steps: (i) incubation in 0.3% hydrogen peroxide in methanol for 20 min to block any endogenous peroxidase activity; (ii) incubation in Avidin-peroxidase (Sigma) diluted 1:5,000 in 0.1 M phosphate buffer and 0.75% Triton X-100 for 2 hours; and (iii) processing for horseradish peroxidase histochemistry by using cobalt-enhanced diaminobenzidine reaction (25) for 8–10 min. This process stained the axons and terminals labeled with biotinylated dextran amine black. Transverse spinal cord sections were counterstained with haematoxylin.

A Corticospinal projections in the mouse

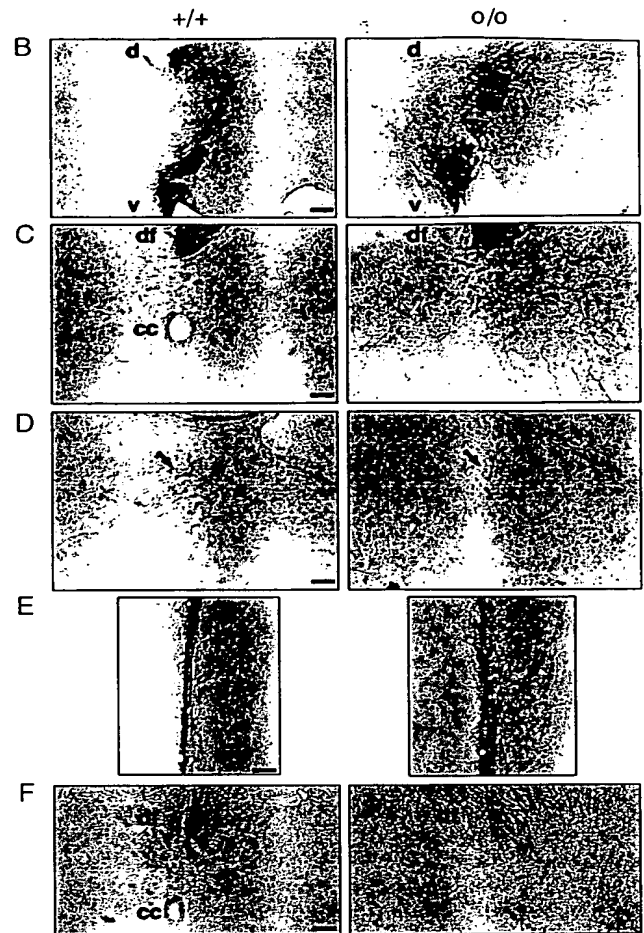
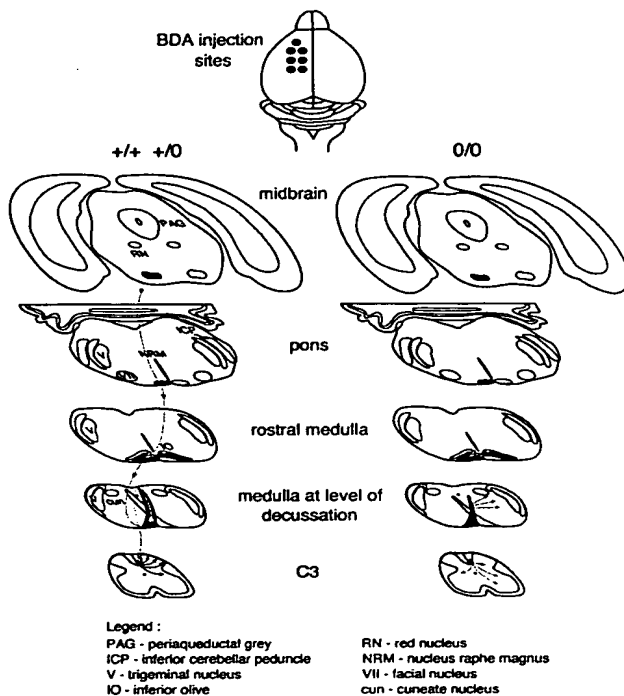


FIG. 3. Labeled CST in normal (+/+ and +/o) and EphA4 null mutant (o/o) mice. (A) Schematic representation of the corticospinal projection traced in mice. Multiple injections of the tracer were made in the motor cortex in the left cerebral hemisphere of adult mice. The labeled CST axons descend through the midbrain, pons, and pyramid in the medulla. In wild-type and heterozygous mice, the CST axons decussate at the medulla, crossing the midline traveling from left ventral to right dorsal, enter the dorsal funiculus of the spinal cord, and terminate predominantly in the dorsal horn contralateral to the tracer injections. In EphA4 null mutant mice, labeled CST axons appeared to terminate in the medulla and intermediate and ventral region of the spinal gray matter. Some labeled fibers were observed to recross the midline. (B) Transverse sections of medulla showing the decussation of labeled CST fibers travelling from left ventral (v) to right dorsal (d). In EphA4 o/o mice, many CST axons do not enter the dorsal column area. (Bar = 450 μ m.) (C and D) Transverse sections of cervical spinal cord showing area of dorsal funiculus (C) and dorsal horn (D). In wild-type animals, labeled CST axons terminate in the right dorsal horn (arrow). In homozygotes, axons project predominantly into the intermediate and ventral regions of the gray matter, and no labeled axons were observed terminating in the dorsal horn. cc, central canal; df, dorsal funiculus. (Bar = 125 μ m.) (E) Longitudinal sections of cervical spinal cord. CST axons in the right dorsal funiculus are seen in the midline. In homozygous animals, some CST fibers recross the midline and project to the gray matter ipsilateral to the tracer injections. (Bar = 300 μ m.) (F) Transverse sections of lumbar spinal cord. A reduced number of labeled CST axons was observed in the dorsal funiculus of the null mutant mice compared with normal. (Bar = 125 μ m.)

expression in the dorsal horns (Fig. 4C). These data indicate that EphA4 is not expressed in the CST axons but is found expressed in surrounding structures.

To determine whether a ligand for EphA4 may be expressed in the CST, we analyzed the expression of Ephrin B3 within E 18.5 mouse brain tissue (Fig. 5). Of the transmembrane ligands, Ephrin B3 binds to EphA4 with the highest affinity (12, 13). *In situ* hybridization with digoxigenin-labeled Ephrin B3 antisense probe detected strong expression within the sensorimotor cortex region (Fig. 5A), thereby suggesting that Ephrin B3 is expressed in the motor neurons of the CST during its development.

DISCUSSION

The EphA4 null mutant mice were the first Eph receptor null mice to display a motor phenotype (7–9). This motor defect was more marked in the hindlimbs and the animals have an

abnormal hopping gait. Analysis of the CST in these animals reveal a reduced number of CST axons in the lower spinal cord segments and an abnormal pattern of termination at higher segments of the spinal cord and medulla. This progressive diminution of the CST, relative to normal animals, along the length of the cord is consistent with the more marked motor defect observed in the lower limbs of these animals. There may be other motor defects in the mutant animals; however, preliminary tracing studies on spinal motor neurons have not detected aberrant projections to muscle (J. Coonan and M.G., unpublished observations). Additionally, it has been observed that some rats that have had their CST disrupted by transection also show a phenotype with a hopping gait similar to the EphA4 null mutants (B. Bregman, personal communication). Thus, a defective CST can account for the motor defect, albeit other unrecognized defects in the motor system also may be present in these mice.

The perturbation of the CST in null mutant animals establishes that EphA4 is required for CST development. During

7. Henkemeyer, M., Orioli, D., Henderson, J. T., Saxton, T. M., Roder, J., Pawson, T. & Klein, R. (1996) *Cell* **86**, 35–46.
8. Orioli, D., Henkemeyer, M., Lemke, G., Klein, R. & Pawson, T. (1996) *EMBO J.* **15**, 6035–6049.
9. Park, S., Frisen, J. & Barbacid, M. (1997) *EMBO J.* **16**, 3106–3114.
10. Orioli, D. & Klein, R. (1997) *Trends Genet.* **13**, 354–359.
11. Gale, N. W., Holland, S. J., Valenzuela, D. M., Flenniken, A., Pan, L., Ryan, T. E., Henkemeyer, M., Strebhardt, K., Hirai, H., Wilkinson, D. G., *et al.* (1996) *Neuron* **17**, 9–19.
12. Gale, N. W., Flenniken, A., Compton, D. C., Jenkins, N., Copeland, N. G., Gilbert, D. J., Davis, S., Wilkinson, D. G. & Yancopoulos, G. D. (1996) *Oncogene* **13**, 1343–1352.
13. Bergemann, A. D., Zhang, L., Chiang, M., Brambilla, R., Klein, R. & Flanagan, J. G. (1998) *Oncogene* **16**, 471–480.
14. Nieto, M. A., Gilardi-Hebenstreit, P., Charnay, P. & Wilkinson, D. G. (1992) *Development (Cambridge, U.K.)* **116**, 1137–1150.
15. Mori, T., Wanaka, A., Taguchi, A., Matsumoto, K. & Tohyama, M. (1995) *Brain Res. Mol. Brain Res.* **29**, 325–335.
16. Xu, Q., Alldus, G., Holder, N. & Wilkinson, D. G. (1995) *Development (Cambridge, U.K.)* **121**, 4005–4016.
17. Xu, Q., Alldus, G., Macdonald, R., Wilkinson, D. G. & Holder, N. (1996) *Nature (London)* **381**, 319–322.
18. Stanfield, B. B. (1992) *Prog. Neurobiol.* **38**, 169–202.
19. Irving, C., Nieto, M. A., DasGupta, R., Charnay, P. & Wilkinson, D. G. (1996) *Dev. Biol.* **173**, 26–38.
20. Robb, L., Lyons, I., Ruili, L., Hartley, L., Kontgen, F., Harvey, R. P., Metcalf, D. & Begley, C. G. (1995) *Proc. Natl. Acad. Sci. USA* **92**, 7075–7079.
21. Lyons, I., Parsons, L. M., Hartley, L., Li, R., Andrews, J. E., Robb, L. & Harvey, R. P. (1995) *Genes Dev.* **9**, 1654–1666.
22. Schaeren-Wiemers, N. & Gerfin-Moser, A. (1993) *Histochemistry* **100**, 431–440.
23. Galca, M. & Darian-Smith, I. (1997) *J. Comp. Neurol.* **381**, 282–306.
24. Rees, S., Rawson, J., Nitsos, I. & Brumley, C. (1994) *Brain Res.* **642**, 185–198.
25. Adams, J. (1981) *J. Histochem. Cytochem.* **29**, 775.
26. Capecchi, M. R. (1989) *Science* **244**, 1288–1292.
27. DeFries, J., Gervais, M. & Thomas, E. (1978) *Behav. Genet.* **8**, 3–13.
28. Bregman, B. S. & Goldberger, M. E. (1982) *Science* **217**, 553–555.
29. Bregman, B. S., Kunkel-Bagden, E., Schnell, L., Dai, H. N., Gao, D. & Schwab, M. E. (1995) *Nature (London)* **378**, 498–501.
30. Casale, E. J., Light, A. R. & Rustioni, A. (1988) *J. Comp. Neurol.* **278**, 275–286.
31. Cohen, N. R., Taylor, J. S. H., Scott, L. B., Guillery, P., Soriano, P. & Furley, A. J. W. (1997) *Curr. Biol.* **8**, 26–33.
32. Bastmeyer, M. & O'Leary, D. D. M. (1996) *J. Neurosci.* **16**, 1450–1459.
33. Holland, S. J., Gale, N. W., Mbamalu, G., Yancopoulos, G. D., Henkemeyer, M. & Pawson, T. (1996) *Nature (London)* **383**, 722–725.
34. Brückner, K., Pasquale, E. B. & Klein, R. (1997) *Science* **275**, 1640–1643.
35. Ohta, K., Iwamasa, H., Drescher, U., Terasaki, H. & Tanaka, H. (1997) *Mech. Dev.* **64**, 127–135.
36. Wang, H. U. & Anderson, D. J. (1997) *Neuron* **18**, 383–396.
37. Richards, L. J., Koester, S. E., Tuttle, R. & O'Leary, D. D. M. (1997) *J. Neurosci.* **17**, 2445–2458.
38. Gilardi-Hebenstreit, P., Nieto, M. A., Frain, M., Mattei, M. G., Chestier, A., Wilkinson, D. G. & Charnay, P. (1993) *Oncogene* **8**, 1103.
39. Laird, P. W., Ziderveld, A., Linders, K., Rudnicki, M. A., Jaenisch, R. & Berns, A. (1991) *Nucleic Acids Res.* **19**, 4293.

Distinct Subdomains of the EphA3 Receptor Mediate Ligand Binding and Receptor Dimerization*

(Received for publication, January 12, 1998, and in revised form, May 4, 1998)

Martin Lackmann[‡], Andrew C. Oates^{‡§}, Mirella Dottori[¶], Fiona M. Smith[¶], Cuong Do[‡],
Maryanne Power[¶], Lucy Kravets[‡], and Andrew W. Boyd[¶]

From the [‡]Ludwig Institute for Cancer Research (Melbourne Branch), Post Office, Royal Melbourne Hospital, Victoria 3050 and the [¶]Queensland Institute for Medical Research, The Bancroft Centre, Post Office, Royal Brisbane Hospital, 4029 Queensland, Australia

Eph receptor tyrosine kinases and their ligands (ephrins) are highly conserved protein families implicated in patterning events during development, particularly in the nervous system. In a number of functional studies, strict conservation of structure and function across distantly related vertebrate species has been confirmed. In this study we make use of the observation that soluble human EphA3 (HEK) exerts a dominant negative effect on somite formation and axial organization during zebrafish embryogenesis to probe receptor function. Based on exon structure we have dissected the extracellular region of EphA3 receptor into evolutionarily conserved subdomains and used kinetic BIAcore analysis, mRNA injection into zebrafish embryos, and receptor transphosphorylation analysis to study their function. We show that ligand binding is restricted to the N-terminal region encoded by exon III, and we identify an independent, C-terminal receptor-dimerization domain. Recombinant proteins encoding either region in isolation can function as receptor antagonists in zebrafish. We propose a two-step mechanism of Eph receptor activation with distinct ligand binding and ligand-independent receptor-receptor oligomerization events.

The Eph family of receptors signal by binding cell-surface proteins known as ephrins. Cell contact is thought essential for this process, as only membrane-associated or artificially clustered forms of the ephrins, which mimic cell-cell apposition, can cause receptor transphosphorylation and activation (1–3). Inferred from sequence homologies, the structure of the Eph family is typified by an extracellular domain (ECD)¹ compris-

ing an N-terminal, cysteine-rich region, an EGF-like motif, and two fibronectin III repeats (4–6); however, the structural requirements and mechanism of receptor activation remain to be elucidated.

Studies measuring Eph/ephrin binding affinities using artificially clustered receptor ECDs suggest that Eph receptors and ephrins fall into the following two groups: EphA receptors interact preferentially with glycosylphosphatidylinositol-linked ephrins (ephrin-A), whereas those interacting preferentially with transmembrane ligands (ephrin-B) are called EphB receptors (7). Within each group, Eph receptors display cross-reactivity with multiple ephrins (1, 8–12). However, receptors and ligands within a class do not show equivalent affinities, but rather display a distinct ordering (3, 12–14). These findings are in keeping with the specialized roles in the development of the visual system, observed for EphA3 receptors (MEK4/CEK4) and ephrin-A2 (ELF1) and -A5 ligands (AL1/RAGS) (14–18). Very similar functional and structural characteristics have been described for the zebrafish ephrin zEphL4, suggesting it as the orthologue of ephrin-A5 (19).

The activation mechanisms for a number of other RTK subfamilies have been elucidated. These include dimerization/activation of individual class I receptor chains through conformational changes upon binding of soluble ligands, ligand-induced activation of preassociated, disulfide-stabilized heterotetrameric type II receptors, and ligand dimer-induced activation of type III receptors (reviewed in Ref. 20). Both monomeric and dimeric ligands are known to induce rapid receptor dimerization, and for some monovalent RTK ligands, the critical role of an intrinsic receptor dimerization interface for receptor activation and biological function has been demonstrated (21). Little is known about the composition of Eph-ephrin signaling complexes. Importantly, the demonstration of stable human EphA3-ephrin-A5 complexes in solution, revealing a strict 1:1 stoichiometry (3), the ability of soluble forms of ephrin-A5 to act as a signaling antagonist (2), and the notion of distinct signaling pathways for dimeric and higher oligomeric receptor complexes (22) suggest that models of dimerization/activation for other RTK may not adequately describe the formation of active signaling complexes for Eph receptors.

To understand further Eph/ephrin interactions and the mechanisms of Eph receptor activation, we dissected the human EphA3 (h-EphA3) ECD into structural subdomains, and through BIAcore analysis we identified a unique N-terminal domain that is sufficient for h-ephrin-A5 (LERK7) binding. By adopting a dominant negative approach to disrupt zebrafish embryogenesis (23, 24), we confirmed the function of the ligand-binding domain *in vivo*. The same approach allowed characterization of a distinct C-terminal domain which mediates ligand-independent dimerization of the EphA3 ECD. The role

* This work was supported in part by the National Health and Medical Research Council of Australia, the Leukaemia Foundation of Queensland, the Queensland Cancer Fund, and the Australian Government Cooperative Research Centres scheme. The costs of publication of this article were defrayed in part by the payment of page charges. This article must therefore be hereby marked "advertisement" in accordance with 18 U.S.C. Section 1734 solely to indicate this fact.

§ Recipient of an Anti-cancer Council of Victoria Postgraduate Research Scholarship.

¶ To whom correspondence should be addressed: Queensland Institute for Medical Research, The Bancroft Centre, Post Office, Royal Brisbane Hospital, 4029, Queensland, Australia. E-mail: andrewBo@qimr.edu.au.

¹ The abbreviations used are: ECD, extracellular domain; DCC, deleted in colo-rectal cancer; FLAGTM, refers to the amino acid sequence DYKDDDDK; mAb, monoclonal antibody; PAGE, polyacrylamide electrophoresis; RTK, receptor tyrosine kinase; sh-EphA3, soluble h-EphA3 extracellular domain; PDGFR, platelet-derived growth factor receptor; EGF, epidermal growth factor; CHO, Chinese hamster ovary; PCR, polymerase chain reaction; bp, base pair; oligos, oligonucleotides; hpf, hours post-fertilization; GFP, green fluorescent protein; DiG, digoxigenin.

of these two domains in receptor activation was confirmed in transphosphorylation assays. By taking into account the 1:1 stoichiometry of the h-EphA3/h-ephrin-A5 interaction (3), the "mass action" model suggested by Nakamoto *et al.* (17) from functional studies, the receptor dimerization mechanism of the PDGF receptors (25), and the data presented here, we propose a stepwise receptor activation mechanism. In our model, high affinity interactions between ephrin-A on the leading edge of migrating cells and the N-terminal ligand binding domain of EphA receptors on opposing cells leads to clustering of EphA receptors. A sufficiently high local concentration of ephrin-A will facilitate accumulation of receptors to a critical concentration that triggers oligomerization through their C-terminal receptor/receptor interaction domain and leads to receptor transphosphorylation and signal transduction.

MATERIALS AND METHODS

Isolation and Mapping of hEphA3 Genomic Clones—The h-EphA3 cDNA probes used to screen the human genomic library were PCR fragments amplified from plasmids containing full-length h-EphA3 cDNA. The primers used were probe A (spans 74–1161 bp as described by Wicks *et al.* (58) GTAGGAATTCCTCTCACTGCCCTCTGC and GTAGGATCCGGCCTCTGTTCAG, probe B (1053–1124 bp) GTAGGAATTCATGG CTTGTACCCGAC and GTAGGGATCCATAATGCTTGCTTCTC, probe C (2–186 bp) ATGG ATGGTAACCTTCACAG and TCATTGGAAGGCTGCGGAAT, and probe D (spans 909–1404 bp) GTAGTCTAGACAAGCTTGTGCGACCAGGTTT and GTAGTCTAGATCAAGCCTGATTAGTTG TGATGC. The mouse genomic library was screened with a MEK4 fragment cut from a plasmid subcloned with MEK4 cDNA (kindly provided by E. Pasquale, University of California, San Diego). The cDNA fragment spans 582–899 bp of MEK4 sequence (26).

The genomic libraries used were as follows: human in λ FIX II vector (Stratagene Cloning Systems, La Jolla), mouse in λ FIX II vector (Stratagene), and λ DASH II vector (kindly provided by F. Köntgen). Approximately 10^6 plaques from each library were screened by high stringency hybridization with radiolabeled probes as described above. Positive clones were identified by autoradiography, purified by subsequent screenings, and isolated using standard methodology (27). Exon-intron boundaries were determined by a combination of direct DNA sequencing, PCR, restriction analyses, and Southern blotting. Direct DNA sequencing of the genomic λ phages and subcloned plasmid was performed using the ABI 373 DNA sequencer (Applied Biosystems, Melbourne, Australia). Sequencing and PCR primers used to characterize the h-EphA3 gene from human genomic clones were based on the h-EphA3 cDNA sequence.

The exons found within the mouse genomic clones were amplified by PCR using degenerate primers specific to EPH-like RTKs. GTAGGCATGCAAGGAGA C(ACT)TCTAACC and CC(AG)ATGGGNACCAGC-CA(CT)TC. The PCR products were then directly sequenced as described above (Applied Biosystems) using the degenerate primers.

Production of sh-EphA3 and sh-EphA3 Subdomains in CHO Cells—The h-EphA3 ECD and N-terminally FLAG-tagged h-EphA3 proteins were prepared from transfected Chinese Hamster ovary (CHO) cell supernatants as described (3, 28). Deletion mutants of h-EphA3 were prepared by PCR using oligos based on the exon boundaries. h-EphA3 III and IV were constructed using a 5' oligo based on the N terminus of the mature protein (29) with a 5' XbaI site (GTAGTCTAGAGAACTGATTCGCGACGCTTCCAA) and 3' oligos based on sequences spanning exon IV (GTAGTCTAGATCATGGAGGTGCGGTACAAGC) and 3 (GTAGTCTAGATCAAGCTTGGCACATAAAACCTC), respectively, followed by a stop codon and an XbaI site. Construct IX used a 5' oligo designed to span the 5' end of exon IV with a 5' XbaI site (GTAGTCTAGACAAGCTTGTGCGACCAGGTTTC) and a 3' oligo based on the C terminus of the exodomain with a stop codon and flanking XbaI site (GTAGTCTAGATCATTGGCTACTTTCACCAAGAG). In each case the PCR products were cloned into the interleukin-3 signal-FLAG-pEFBOS vector as described previously (3, 28). DNA was electroporated into CHO cells, and high producer clones were selected by "dot blot" screening of culture supernatants on polyvinylidene difluoride membranes and the expected size of the recombinant proteins confirmed by SDS-PAGE and Western blot analysis using M2 anti-FLAG mAb and rabbit anti-mouse AP-tagged mAb for detection by enhanced chemiluminescence (ECL; Amersham).

Deletion mutants were purified on M2 anti-FLAG affinity columns

and eluted with FLAG peptide according to the manufacturer's instructions. Homogenous preparations (>95% by SDS-PAGE and silver staining) were obtained by anion exchange (Mono Q, 5 \times 50 mm, Pharmacia, Uppsala, Sweden) and size exclusion chromatography (Superose 12, 10 \times 300 mm, Pharmacia, Uppsala, Sweden). The identity and concentration of the purified h-EphA3 proteins in the final preparations were confirmed by N-terminal amino acid sequence analysis and amino acid analysis, and where applicable, their native conformation was confirmed on the BIAcore as described (28).

Production of FLAG-tagged Ephrin-A5—h-Ephrin-A5 containing an N-terminal FLAG peptide was purified from transfected CHO cells and tested for its specific binding to sh-EphA3 as described (3).

Synthesis of sh-EphA3-derived Peptides—The peptides according to the amino acid sequence encompassing residues Glu¹ to Gly³¹ (h-EphA3 1–31) of sh-EphA3 was assembled by solid-phase peptide synthesis according to standard protocols, purified by reverse phase-high pressure liquid chromatography, and their masses confirmed by mass spectrometry.

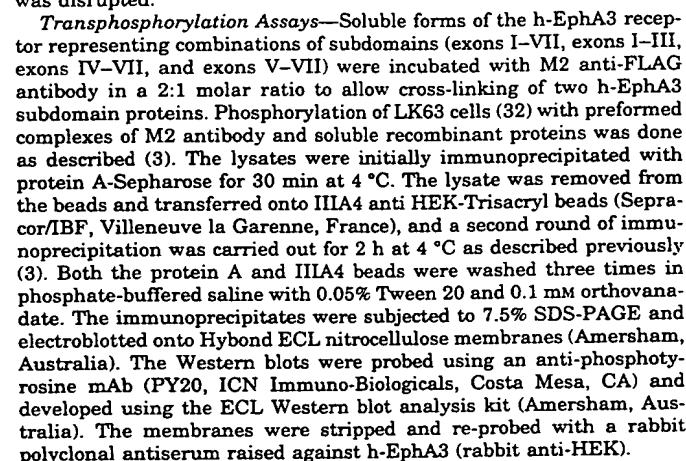
Analysis of the Interaction between sh-EphA3 Constructs and Ephrin-A5—The binding of various h-EphA3 constructs and derived peptides was analyzed on the BIAcore optical biosensor (Pharmacia Biosensor Sweden) using purified h-EphA3 ECD or ephrin-A5-FLAG-derivatized CM 5 sensor chips, and the interaction kinetics were determined as described (3). For the analysis of the binding of the h-EphA3 constructs to h-EphA3 (subdomain)-derivatized sensor surfaces, difference sensorgrams were derived by subtraction of the response on a parallel channel containing a non-relevant protein as described (28). The effect of h-EphA3-derived peptides on the interaction of h-EphA3 with ephrin-A5 was tested by incubating a constant concentration of the ligand with increasing amounts of peptide prior to analysis on a h-EphA3 ECD-derivatized sensorchip. The affinity surface was regenerated between subsequent injections of samples with a 35- μ l injection of 50 mM 1,2-diethylamine, 0.1% Triton X-100, followed by two washes with BIAcore running buffer (Hepes buffered saline, 0.005% Tween 20).

Fish Care and Embryo Collection—Wild type zebrafish were obtained from St. Kilda Aquarium (Melbourne, Australia) and were kept essentially as described (30). Embryos were obtained by natural spawning between a small number (4–10) of male and female fish. Embryos were removed from the spawning tanks within 20 min of fertilization, cleaned in system water, and transferred to the injection apparatus.

RNA Synthesis—Constructs equivalent to full-length h-EphA3 ECD (h-EphA3 I–VII) and h-EphA3 IV–VII were generated by PCR from the constructs described above. In each case the 5' oligo was based on the interleukin-3 signal sequence and the 3' oligos were as above except that BglII sites were used to clone the PCR products into the pSP64T vector. mRNA from the h-EphA3 constructs and a control E-GFP cDNA construct were transcribed *in vitro* using the mMessage mMaker kit (Ambion, Texas) and resuspended in water at a concentration of 0.1 mg/ml in small aliquots. Integrity of the RNA was checked by denaturing gel electrophoresis of the resulting products. Immediately prior to injection, aliquots of h-EphA3 I–III, h-EphA3 I–IV, or h-EphA3 IV–VI were thawed and mixed with water and E-GFP mRNA to a final concentration such that either 100, 10, or 1 pg of the receptor mRNA and 5 pg of the E-GFP mRNA were delivered to each embryo.

RNA Microinjection—Approximately 600 μ l of RNA dissolved in water at various concentrations was injected into one, two, or four cell embryos under a Wild stereo microscope using Leitz micromanipulator (Leitz, Wetzlar, Germany) and compressed nitrogen. The needle was positioned under the blastoderm in the region of cytoplasmic streaming. Successful injection was judged in the first instance by a visible bolus of fluid in the embryo. Uptake and translation of mRNA by the embryo was measured by including 5 pg of mRNA encoding E-GFP as a marker in each injection. Injection of over 100 pg of E-GFP mRNA per embryo does not cause developmental defects. The translation of the injected h-EphA3 mRNA was measured at intervals during embryogenesis by Western blotting and BIAcore analysis.

Western Blot and BIAcore Analysis of Zebrafish Lysates—Ten embryos per sample were lysed in embryo lysis buffer (0.1 M, 25 mM Tris-HCl, pH 7.4, 0.5 M NaCl, 1% Triton X-100), and the lysate was cleared by centrifugation (60 min, 1 \times 10⁵ \times g) and stored at –80 °C until use. For comparison, CHO cell-derived h-EphA3 I–VII and subdomain constructs (as indicated) were added to zebrafish lysate, and all samples were extracted individually using 7.5 μ l of packed anti-FLAG (M2) agarose (IBI, Kodak), washed (0.5 ml each) with lysis buffer and buffer, and eluted from the affinity resin with 2 \times 15 μ l of 0.15 mg/ml FLAG peptide in buffer. Parallel samples were either separated by SDS-PAGE, electroblotted and probed with biotinylated anti-FLAG M2 mAb (IBI, Kodak) followed by horseradish peroxidase-derivatized



Expression of Receptor ECD Subdomains—To analyze the structural basis of the h-EphA3 receptor/ephrin-A5 ligand interaction and receptor activation, we analyzed the function of isolated subdomains derived from the complete h-EphA3 ECD.

were inferred from the 5' and 3' junctions of exon I and exon III, respectively. Introns interrupting h-EphA3 cDNA coding sequence as described (58) were found to occur at 89 bp (5' of exon II), 155 bp (5' of exon III), 817 bp (5' of exon IV), 974 bp (5' of exon V), 1311 bp (5' of exon VI), 1438 bp (5' of exon VII), and 1601 bp (5' of exon VIII). The exons found within the mouse genomic clones of SEK1, BSK, and ESK were found to have identical borders as h-EphA3 with respect to the protein coding sequence. *b*, ECD subdomains according to the exon structure of sh-EphA3, depicted in Fig. 2*a*. The domains are illustrated as differently shaded bars: □, exons I and II; ▤, exon III; ■, exon IV; ▨, exon V; ▩, exons VI and VII. *c*, recombinant h-EphA3 proteins, encoded by exons I-VII, I-IV, I-III, IV-VII, and produced as described under "Materials and Methods" were analyzed by SDS-PAGE and silver staining. The doublet bands of h-EphA3, h-EphA3 I-VII, and h-EphA3 IV-VII are due to glycosylation heterogeneity.⁸ In CHO cells appreciable expression levels and the expected apparent molecular sizes were found for h-EphA3 I-VII (the FLAG-tagged version of h-EphA3 encoded by exons 1-7, 68 kDa), h-EphA3 I-IV (36 kDa), h-EphA3 I-III (33 kDa), h-EphA3 IV-VII (40 kDa), and h-EphA3 V-VII (36 kDa, not shown). *d*, association rate constants (■), derived from BIAcore raw data using the BIA evaluation software for the binding of h-EphA3 subdomain proteins (15.6-500 nM) to h-ephrin-A5-derivatized sensorchips. *e*, apparent dissociation constants were estimated from the kinetic rate constants according to $K_D = k_d/k_a$. The mean and standard deviation from estimates at five different concentrations are shown (■). In addition, equilibrium responses were used to estimate the apparent equilibrium dissociation constants (□). *f*, samples containing 40 nM h-ephrin-A5 and 1 nM to 10 μM of a synthetic peptide according to the h-EphA3 sequence encoded by exons I and II (Δ), 1 nM to 1 μM sh-EphA3 I-III (□), 10 nM to 5 μM sh-EphA3 IV-VII (×), or 10 nM to 1 μM sh-EphA3 I-VII (○) were injected onto a sh-EphA3-derivatized sensorchip. The residual responses are illustrated as percent of total response in the absence of competitor.

For the design of stable subdomains, we analyzed the h-EphA3 gene structure and found that exon-intron boundaries of h-EphA3 ECD genomic clones aligned with clones of the mouse EphA4 (SEK1), EphA5 (BSK), and EphA1 (ESK) genes.² Together with data on the chicken EphB2 (CEK5) gene (33) and splice variants of other Eph-like RTK (26, 34), this suggests a highly conserved exon structure within the Eph subfamily (Fig. 1a). Comparison of ECD sequences of h-EphA3 and its mouse (MEK4) and chicken (CEK4) homologues (26) demonstrates the highest amino acid sequence identity (99.5 and 98.3%, respectively) is found in the exon III-encoded domain (Fig. 1b). The structure of the domain encoded by exons II and III was analyzed in detail, addressing previous reports that this region consisted of an N-terminal Ig-like domain and a C-terminal cysteine-rich region. Sequence data base comparisons and alignment of the h-EphA3 exon II and III sequences with known C1, C2, and V set Ig domains and a number of EGF domains using the ALIGN program (35) showed features of the C-terminal half of an EGF domain in the most C-terminal exon III-encoded region, but no homology more N-terminally, whereas homology to an Ig-like motif was not found within this region.

The defined exon boundaries were used to demarcate cDNA domain deletion mutants of the h-EphA3 ECD for expression as FLAG epitope-tagged proteins in CHO cells (Fig. 1c) and, following *in vitro* transcription into mRNA, for expression in zebrafish embryos (Fig. 2). The proteins are identified throughout by roman numbers according to their corresponding exons. The exon III- and exon IV-encoded portions of the h-EphA3 receptor correspond to domains described as globular and cysteine-rich domains in a recent report on the functional dissection of the EphB2 receptor (36). Thus, the FLAG fusion proteins h-EphA3 I-III, h-EphA3 I-IV, and h-EphA3 VI-VII directly relate to the EphB2-alkaline phosphatase (AP) fusion proteins "280-AP," "331-AP," and "CEK5ΔGlob-AP" (which includes an exon III-encoded part), respectively (36).

We obtained homogenous proteins from CHO cell supernatants by anti-FLAG affinity and size exclusion chromatography; SDS-PAGE and silver staining of the purified proteins revealed apparent molecular sizes as predicted from the amino acid sequence and putative glycosylation sites (Fig. 1c). Doublet protein bands for h-EphA3, h-EphA3 I-VII, and h-EphA3 IV-VII are likely due to the glycosylation heterogeneity of these proteins; h-EphA3 derived from transfected glycosylation-deficient Lec4 CHO cells (37), with unchanged ability to bind h-ephrin-A5, appear as single bands on silver-stained SDS-PAGE.³ Interestingly, no expression was observed for any of the protein constructs containing the exon III-encoded domain, but lacking the first 31 amino acids of h-EphA3 (encoded by exons I and II), suggesting impaired translation or stability of these constructs.

Identification of the EphA3 Ligand-binding Domain—In order to characterize the ligand-binding region of the h-EphA3 receptor, the individual binding affinity of each of the ECD subdomains for the h-EphA3 ligand was assayed using an h-ephrin-A5-derivatized BIAcore sensorchip. A kinetic analysis demonstrates high affinity interactions for the binding of h-EphA3 I-VII (the FLAG-tagged version of the h-EphA3 ECD encoded by exons I-VII), h-EphA3 I-IV, and h-EphA3 I-III, with affinities in the same range (K_d , 18–72 nM, Fig. 1, d and e) reported previously for the binding of h-ephrin-A5 to sensor chip-immobilized h-EphA3 (3). No binding of h-EphA3 IV-VII was observed at any of the tested concentrations (16–500 nM).

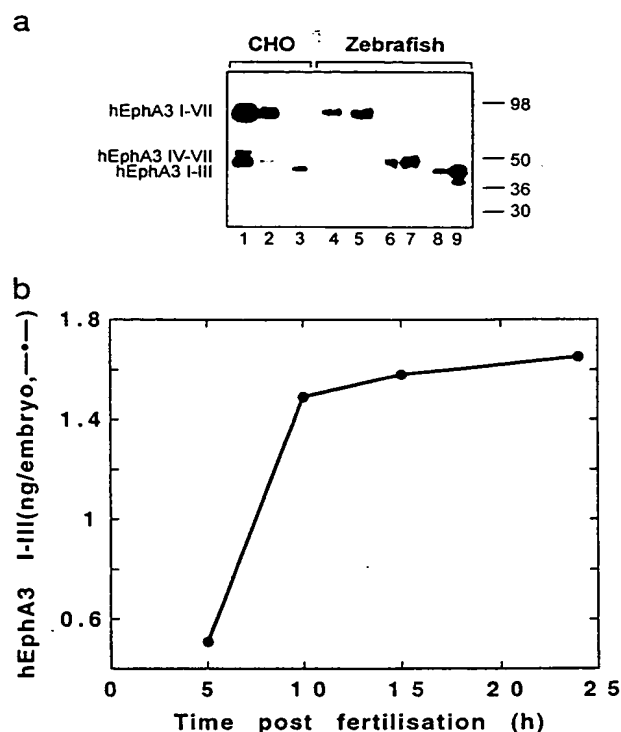


FIG. 2. Expression of exogenous h-EphA3 I-VII, h-EphA3 I-III, and h-EphA3 VI-VII in zebrafish embryos by Western blot and BIAcore analysis. *a*, samples of 12 hpf zebrafish lysate (10 embryos/0.1 ml) containing defined amounts of CHO cell-derived h-EphA3 I-VII, h-EphA3 I-III, and h-EphA3 IV-VII were immunoprecipitated with anti-FLAG mAb (M2) agarose and analyzed by Western blots with anti-FLAG mAb, visualized by enhanced chemiluminescence (lanes 1–3). Zebrafish embryos injected with 10 pg of either h-EphA3 I-VII, h-EphA3 I-III, or h-EphA3 IV-VII mRNA were lysed after 5 or 10 h (10 embryos/0.1 ml) and analyzed in parallel lanes of the gel (lanes 4–9). Lanes 1 and 2, CHO cell h-EphA3 I-VII and h-EphA3 IV-VII, 15 and 10 ng, respectively; lane 3, 10 ng of CHO cell h-EphA3 I-III; lanes 4 and 5, h-EphA3 I-VII RNA injections, 5 and 10 hpf; lanes 6 and 7, h-EphA3 I-VII RNA injections; lanes 8 and 9, h-EphA3 I-III RNA injections, 5 and 10 hpf. *b*, parallel samples of zebrafish lysates from h-EphA3 I-III RNA-injected embryos (100 pg/embryo), collected 5, 10, 15, and 24 h post-fertilization were extracted on M2 agarose, and the FLAG peptide eluate was analyzed on a BIAcore sensorchip which had been derivatized with the conformation-specific anti h-EphA3 mAb IIIA4. The BIAcore response was used to estimate the h-EphA3 I-III abundance by comparison with identically treated samples of CHO cell-derived h-EphA3 III at a known concentration.

localizing the ligand binding site to the exon I-III-encoded N terminus of h-EphA3. Very similar apparent dissociation constants for the h-EphA3 ECD and h-EphA3 I-VII (72 ± 15 and 62 ± 12 nM, Fig. 1e) suggest that an N-terminal addition of the FLAG peptide has no effect on the interaction between h-EphA3 and its ligand. Substantially lower dissociation constants (*i.e.* higher affinities) of 18–29 nM due to increased association rate constants (Fig. 1d) were observed for the h-EphA3 subdomain constructs h-EphA3 I-IV and h-EphA3 I-III. In-solution competition with an exons I- and II-encoded synthetic h-EphA3_{1–31} peptide, and with the FLAG-tagged h-EphA3 IV-VII construct, did not inhibit the receptor/ligand interaction at concentrations up to 10 μ M, whereas addition of h-EphA3 I-VII or h-EphA3 I-III resulted in a dose-dependent reduction of the BIAcore response (Fig. 1f). Taken together, these results imply that the cysteine-rich domain encoded by exon III of h-EphA3 is necessary and sufficient for ligand binding.

Soluble EphA3 Ligand Binding Subdomain Induces a Dominant Negative Phenotype in Zebrafish—To confirm the binding

² M. Dottori and A. W. Boyd, unpublished observations.

³ M. Lackmann and L. Kravets, unpublished observations.

studies we analyzed the effect of ectopic expression of receptor constructs h-EphA3 I–III (ligand binding domain) or h-EphA3 IV–VII, which shows no ephrin-A5 binding, on zebrafish development. We have recently characterized developmental defects in the formation of somite boundaries in zebrafish embryos induced by introduction of either soluble h-EphA3 ECD or h-ephrin-A5 as signaling antagonists.⁴ A similar dominant negative approach has been used earlier to evaluate the role of EphA4 signaling in forebrain and hindbrain formation (23). These authors expressed kinase domain deletion constructs of m-EphA4 in zebrafish embryos to disrupt the function of the endogenous orthologue by forcing heterodimerization with the exogenous mutant receptor (23, 24). In a modification of this approach, we anticipated that expression of the h-EphA3 ligand binding domain during zebrafish development should be sufficient to block endogenous receptor/ligand interactions by competing for binding to endogenous ligand. On the other hand, expression of the regions of the ECD that cannot bind ligand should not mediate these antagonistic effects.

Thus, the effects of constructs h-EphA3 I–VII, containing the entire ECD, h-EphA3 I–III, encompassing the ligand binding domain, and h-EphA3 IV–VII, encompassing the remainder of the ECD (and incapable of h-ephrin-A5 binding) on zebrafish development were analyzed. The corresponding mRNAs, denoted h-EphA3 I–VII RNA, h-EphA3 I–III RNA, and h-EphA3 IV–VII RNA, respectively, were introduced into zebrafish embryos by microinjection. A widespread distribution of the exogenous proteins throughout the embryo was observed as indicated by the uniform expression pattern of the GFP protein (Fig. 3f). FLAG epitope-containing proteins with the same molecular weights as the corresponding proteins expressed in CHO cells were detected by Western blot (Fig. 2a) at similar abundance of all three constructs in the embryos at 5 and 10 hours post-fertilization. This suggests equivalent expression of all mRNAs throughout the time frame of the experiment. By using the native conformation-specific, anti-h-EphA3 mAb, IIIA4 (28, 29), we quantitated the expression level of exogenous, biologically active h-EphA3 I–III by BIAcore analysis of lysates from zebrafish embryos, which had been injected with h-EphA3 I–III RNA (Fig. 2b). As shown previously for h-EphA3 I–VII and h-ephrin-A5,⁴ there was an initial steep rise in expression h-EphA3 I–III leading to a plateau after 15 h (Fig. 2b).

Embryos injected with 1 pg or 10 pg of sh-EphA3 I–III RNA per embryo developed a syndrome indistinguishable from that described for the full-length h-EphA3 I–VII RNA (Fig. 3 c and d).⁴ The defects noticed in embryos between 11 and 15 h post-fertilization (hpf), by comparison with non-injected control embryos (Fig. 3, a and b), included most prominently a disruption of somite boundaries (Fig. 3, c and d) coincident with a reduced height of the dorsal axis from the surface of the yolk cell (Fig. 3c). Furthermore, a disorganized anterior neuraxis and retarded tailbud development were observed (Fig. 3c). To monitor nonspecific effects on embryogenesis, which may have been caused by injection of mRNA and expression of foreign protein, embryos were injected with E-GFP or the soluble, FLAG-tagged ECD of deleted in colo-rectal cancer (DCC) (38), a major guidance receptor known to be involved in embryogenesis. Although expression of the soluble FLAG-tagged DCC construct induces a defined nerve guidance defect in *Xenopus* embryos,⁵ and despite high levels of exogenous protein expression, we could not detect any developmental defects in E-GFP or DCC

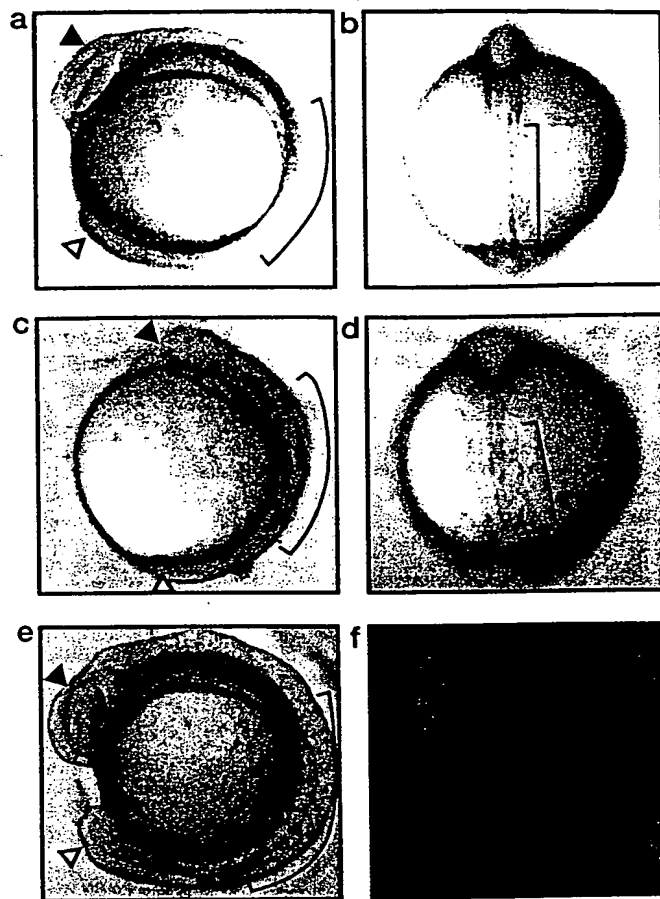


FIG. 3. Ectopic expression of the exon I–III- but not of the exon IV–VII-encoded h-EphA3 subdomain affects the development of zebrafish embryos. a–f, zebrafish embryos, uninjected or injected with 5 pg of marker mRNA and with 10 pg of either h-EphA3 I–III or h-EphA3 VI–VII RNA during the first two cleavage divisions, were raised at 28 °C. After 12–13 h embryos viewed by light microscopy were photographed from a lateral perspective in a, c, e, and f with dorsal to the right and anterior up, and from a dorsal perspective (b and d) with anterior up in each frame. The areas of somite development are indicated by brackets. Embryos shown are representative of the phenotype in groups of 29–89 embryos as indicated in Fig. 5. a, a non-injected zebrafish embryo at 12–13 hpf showing normally developed optic vesicle, forebrain, and tail-bud. The embryo has covered more than ¾ of the perimeter of the yolk cell with head and tail approaching each other. Somite formation in the trunk in a regular, periodic pattern is indicated by the bracket. b, dorsal view of the same embryo revealing clearly distinguishable neuraxis and somites. The bracket on the right-hand side indicates a region of paraxial mesoderm that underwent somite formation. c, a zebrafish embryo at 12–13 hpf after microinjection with 10 ng of h-EphA3 I–III RNA displaying severe anterior defects, including a reduced size of the optic vesicle as well as an absence of mid- and hindbrain segmentation. The gap between the tail region (tail bud is missing, open arrowhead) and the head region (optic vesicle barely visible, closed arrowhead) is widened substantially compared with the non-injected embryo (a). The region of the trunk that normally would form somites is indicated by the bracket (compare with a). The dark line around perimeter of the yolk is a photographic artifact due to the contrast needed to show the details of somite formation in the embryo during light microscopy. d, dorsal view of the h-EphA3 I–III RNA-injected embryo. Comparison of the left and right sides of the trunk region of affected embryos as indicated by the bracket reveals heavily disorganized somite boundaries. e, a 13-hpf embryo after injection with 10 pg of h-EphA3 I–III RNA. The morphology of this embryo is indistinguishable from the non-injected control shown in a. As in c, the dark line around perimeter of the yolk is a photographic artifact due to the contrast needed to show the details of the embryo during light microscopy. f, the same embryo viewed under epifluorescence illumination to illustrate the translation of co-injected E-GFP marker mRNA demonstrating widespread and high level expression of the exogenous proteins.

⁴ M. Lackmann, A. C. Oates, M. Dottori, F. M. Smith, C. Do, L. Kravets, C. Brennan, M. Power, N. Holder, and A. W. Boyd, manuscript submitted for publication.

⁵ J. M. Gad and H. M. Cooper, personal communication.

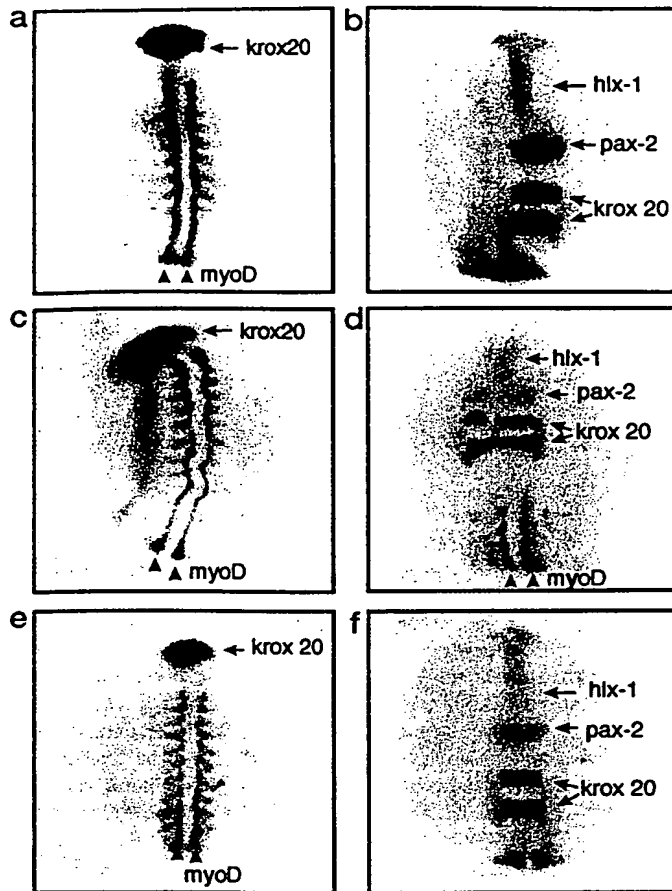


FIG. 4. *In situ* hybridization analysis of h-EphA3 mRNA injected embryos. Embryos were left untreated (a and b) or injected with 10 pg of either h-EphA3 I-III RNA (c and d) or h-EphA3 IV-VII RNA (e and f), allowed to develop for 12 to 13 hpf, and fixed for *in situ* hybridization with *pax-b*, *hlx-1*, *kroxo20*, and *myoD* DIG-labeled riboprobes. Embryos are photographed from a dorsal perspective with anterior to the top and posterior to the bottom of each frame; a, c, and e, postero-dorsal view; b, d and f, antero-dorsal view. a and b, uninjected embryo at 12 hpf showing normal expression of *hlx-1* in the ventral forebrain, *pax-b* in the midbrain, *kroxo20* in rhombomeres 3 and 5 of the hindbrain and *myoD* in the paraxial mesoderm. A regular, serially repeated pattern of *myoD* staining illustrates the somites. Cells expressing *pax-b*, *hlx-1*, and *kroxo20* have migrated toward the midline and form tight bands marking forebrain (*hlx-1*), midbrain (*pax-b*), and hindbrain (*kroxo20*). c and d, h-EphA3 I-III RNA (10 pg)-injected embryo at 12 hpf showing *pax-b* and *kroxo20* expressing cells in the left part of the mid- and hindbrain displaced from the midline. An intact *hlx-1* stripe is present anteriorly. The *myoD* staining of the paraxial mesoderm suggest that the somite boundaries are out of register across the midline and reveal a distinctly twisted midline. e and f, dorsal views of embryos injected with h-EphA3 IV-VII RNA, demonstrating normal expression of *hlx-1*, *pax-b*, *kroxo20* (e), and *myoD* (f). The distinctive twist in the neuraxis of affected embryos is missing and the *pax-b* and *kroxo20* expressing cells are also symmetrically distributed lateral to the midline.

mRNA-injected embryos as judged by the criteria of our experiments (Fig. 3f and data not shown).

The similarity of the phenotype due to h-EphA3 I-VII RNA and h-EphA3 I-III RNA injection was also evident by analysis of marker gene expression; *in situ* hybridization with probes to *hlx-1* (39), *paxb* (40), *kroxo20* (41), and *myoD* (42) revealed abnormal patterns consistent with the morphological defects observed in the live embryos (Fig. 4, c and d). In particular, *myoD*-expressing cells were disarrayed along the paraxial mesoderm indicating a disruption of somite formation, giving the track formed by *myoD*-expressing, adaxial mesoderm cells ad-

jacent to the midline a distinctive twist (Fig. 4c). A single axially located stripe of *hlx-1* expression suggested an intact ventral forebrain region. Non-injected control embryos (Fig. 4, a and b) or embryos injected with E-GFP alone (not shown) did not show these defects in the expression of *myoD*. In contrast, no apparent developmental defects were detected in embryos injected with either 1 or 10 pg of h-EphA3 IV-VII RNA per embryo, either by gross morphological criteria (Fig. 3e) or by analysis of marker gene expression (Fig. 4, e and f). Ubiquitous expression of the co-injected E-GFP mRNA (Fig. 3f) and Western blot analysis (Fig. 2a) during the period of development under analysis indicated that the protein was both widely and highly expressed.

The ability of h-EphA3 I-III but not of h-EphA3 IV-VII to mimic the developmental disruption caused by h-EphA3 I-VII implies that the subdomain responsible for mediating the specific, dominant negative effect of the EphA3 ECD on zebrafish development is encoded in the first three exons. This finding is consistent with assignment of the ligand-binding domain to exon III by BIAcore analysis of ligand binding affinities.

High Concentration of C-terminal Domain Protein Induces Disruption of Somite Formation.—We observed a linear, dose-dependent increase in the number of affected embryos when the amount of injected h-EphA3 I-III RNA was increased from 1 to 100 ng per embryo, whereby the increase in defective embryos paralleled the increase in concentration of the expressed protein (Fig. 5a). As before, only a small number of defective embryos were observed at low and moderate concentrations of h-EphA3 IV-VII RNA (1 and 10 pg/embryo, Fig. 4, e and f and Fig. 5a), whereas at high concentrations, the proportion of affected embryos injected with sh-EphA3 IV-VII RNA was similar to the proportion of defective sh-EphA3 I-III RNA-injected embryos (Fig. 5a, 100 pg/embryo). Importantly, the phenotype of animals injected with 100 pg of sh-EphA3 IV-VII RNA was indistinguishable from the defects resulting from injection of either the entire h-EphA3 ECD or the ligand-binding domain alone, as judged by morphology and the expression of marker genes (Fig. 5b). Thus the C-terminal portion of the receptor ECD encoded by exons IV-VII mediates a ligand-independent dominant negative effect on zebrafish somite formation and axial organization.

Transphosphorylation Assays Suggest Ligand-independent h-EphA3 Dimerization.—This dominant negative effect at high h-EphA3 IV-VII concentration can be explained by the occurrence of heterodimers between intact endogenous receptors and the h-EphA3 IV-VII protein which are acting to block receptor function. This notion, implying the existence of a dimerization interface outside the ligand-binding region was supported by BIAcore analysis of the binding of h-EphA3 I-VII, h-EphA3 I-III, and h-EphA3 IV-VII to a sensorchip derivatized with h-EphA3. We demonstrated binding of h-EphA3 IV-VII at micromolar concentrations that was characterized by a slow off rate, yielding an apparent dissociation constant of 3 μ M. Marginally weaker binding was observed for the h-EphA3 IV-VII construct, whereas the interaction of h-EphA3 I-III had a substantially lower affinity (Table I).

To test further the hypothesis of a dimerization interface, we performed *in vitro* transphosphorylation assays of h-EphA3, constitutively expressed in LK 63 cells (29). Transphosphorylation of the receptor by cross-linking with anti-h-EphA3 mAb IIIA4 during immunoprecipitation or by incubation with mAb cross-linked ephrin-A5-FLAG complexes has been demonstrated previously (3, 29). In the latter experiments 20–30 nM ephrin-A5-mAb complex had been used to induce receptor transphosphorylation. The approximately 100-fold lower affinity of the receptor/receptor interaction (Table I) compared with

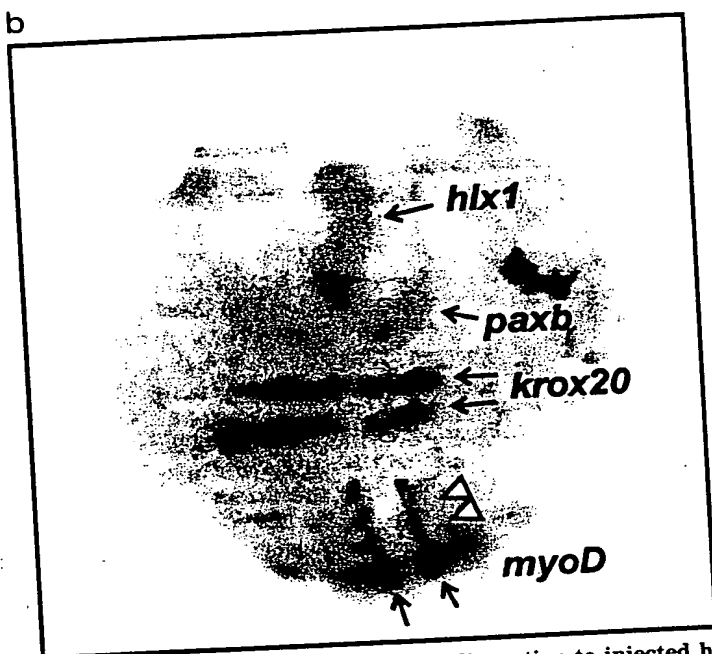
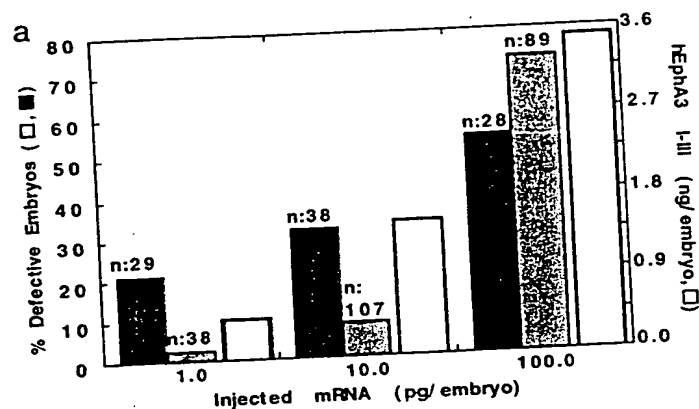


FIG. 5. Dose-response of embryonic disruption to injected h-EphA3 I-III or h-EphA3 IV-VII RNA. *a*, batches of embryos ($n = 29-107$) were injected with decreasing concentrations (from 100 to 1 pg) of h-EphA3 I-III (■) or h-EphA3 IV-VII RNA (□), and a constant amount of E-GFP mRNA (5 pg). The embryos were allowed to grow for 12 to 13 hpf before fixation. They were then hybridized with *pax-b*, *hlx-1*, *krox20*, and *myoD* DIG-labeled riboprobes. Embryos were observed under a dissecting microscope and scored for disrupted patterns of gene expression. To control for potential defects due to the genetic background of particular parents in our strain, a number of embryos that were transferred to the injection stage were not injected but were handled identically to the injected embryos and were scored as described for defects. Parallel samples of h-EphA3 I-III RNA-injected embryos were lysed at 10 hpf (10 embryos/100 μ l), the exogenous FLAG-tagged protein extracted on M2-agarose, and its concentration in the lysate determined on an anti-h-EphA3 mAb-derivatized BIAcore sensorchip. The concentration of h-EphA3 I-III per embryo is shown (□). *b*, *in situ* hybridization analysis of 100 pg of h-EphA3 IV-VII RNA-injected embryo. An injected embryo at 12-13 h of development was fixed for *in situ* hybridization with *pax-b*, *hlx-1*, *krox20*, and *myoD* DIG-labeled riboprobes. The photograph represents an antero-dorsal view with anterior to the top and posterior to the bottom. Disorganization of *pax-b* and *krox20* expressing cells similar to the pattern observed in h-EphA3 I-III RNA-injected embryos (Fig. 4d) is illustrated. Staining with *myoD* reveals defects in somite organization, whereby open arrowheads indicate missing somites in the right-hand part of the embryo.

the ligand binding reaction (Fig. 1e) suggested that concentrations of the EphA5 constructs in the 10-30 μ M range would be necessary to inhibit ligand-induced receptor transphosphoryla-

TABLE I
Binding of h-EphA3 I-VII to sensorchip-immobilized receptor subdomains

Sensor surface	Association rate ^a k_a ($M^{-1}s^{-1}$)	Dissociation rate ^a k_d (s^{-1})	Dissociation constant ^b K_D (M)
s h-EphA3 I-VII	399	$1.5 \cdot 10^{-3}$	$3.7 \cdot 10^{-6}$
s h-EphA3 I-III	99	$8.1 \cdot 10^{-4}$	$8.2 \cdot 10^{-6}$
s h-EphA3 IV-VII	303	$8.1 \cdot 10^{-4}$	$2.7 \cdot 10^{-6}$

^a The response of serial dilutions of h-EphA3 I-VII (2-10 μ M) to a BIAcore sensorchip derivatized with bovine serum albumin was subtracted from the BIAcore signal measured on parallel channels immobilized with approximately equimolar concentrations of h-EphA3 I-VII, h-EphA3 I-III, and h-EphA3 IV-VII. The association and dissociation rate constants were derived from the raw data of difference sensorgrams using a linear, one-component interaction model as described previously (3).

^b The apparent dissociation constant of the interaction is estimated as ratio $K_D = k_d/k_a$.

tion. As we were unable to provide these high protein concentrations for this competition assay, in an alternative approach we analyzed ligand-independent receptor dimerization by assessing receptor binding of h-EphA5 constructs. Thus, in the following experiments we prepared immune complexes of FLAG peptide-tagged receptor ECD or the derived subdomain deletion constructs with M2 antibody. These preformed, divalent receptor ECD-M2 complexes were used at a low micromolar concentration to induce receptor dimerization and transphosphorylation by the endogenous receptor kinase. Incubation of LK63 cells with h-EphA3 I-VII-M2 mAb complex resulted in a substantial phosphorylation of the endogenous h-EphA3. This confirms that the soluble, exogenous mAb cross-linked receptor dimer binds and tethers endogenous h-EphA3 receptors in the absence of ligand and facilitates their transphosphorylation. The interaction between the endogenous receptors and the exogenous receptor ECD-M2 complex was sufficiently stable to withstand cell lysis and immunoprecipitation with protein A-Sepharose (Fig. 6b, lane C). Importantly, incubation of the cells with the h-EphA3 IV-VII subdomain gave a virtually identical result (lane A), confirming that this domain harbors the suggested receptor dimerization interface. Notably, in both cases no additional phosphorylated h-EphA3 was recovered on immunoprecipitation of the protein A-completed lysates with anti-h-EphA3 mAb IIIA4 and confirms that only endogenous receptors, which had been dimerized by the h-EphA3 IV-VII-M2 mAb complex, underwent transphosphorylation. Western blot analysis with an anti-h-EphA3 polyclonal antiserum indicated that only a small (virtually undetectable) proportion of the total endogenous receptor population had been captured into the M2-protein A complex. In contrast to these results, analysis of a parallel sample of cells treated with an identical concentration of h-EphA3 I-III-M2 complex (lane B) revealed phosphorylated h-EphA3 in the anti-h-EphA3 mAb precipitate but not in the protein A-precipitate. This indicates that h-EphA3 I-III can induce dimerization at high concentrations, but in keeping with BIAcore results, this interaction is notably weaker, leading to dissociation of endogenous phosphorylated h-EphA3 from h-EphA3-M2 complex during cell lysis. In a control experiment LK63 cells were treated with M2 mAb on its own, but yielded no phosphorylated endogenous receptor in either the protein A- or IIIA4 precipitates (lane D). Taken together, our experiments suggest that the exon IV-VII-encoded subdomain with the contribution of the exon III-encoded region provide the dimerization interface of the h-EphA3 receptor, which is functional in the absence of ligand.

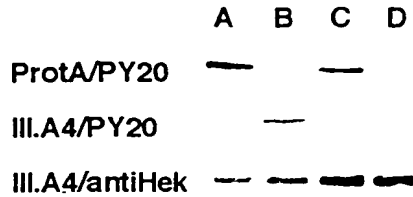


FIG. 6. Transphosphorylation analysis of ligand-independent receptor dimerization. Induction of phosphorylation of endogenous h-EphA3 in parallel cultures of LK63 cells with preformed M2-mAb complexes of FLAG-tagged h-EphA3 IV-VII (lane A), h-EphA3 I-III (lane B), or h-EphA3 I-VII (lane C). The endogenous receptor bound to the exogenous receptor-subdomain complex is recovered by immunoprecipitation with protein A (ProtA) and analyzed by Western blot with PY20 anti-phosphotyrosine antibody (top panel). The corresponding supernatant is extracted with anti-h-EphA3 IIIA4 mAb and again analyzed by PY20 Western blot (middle panel). This blot is stripped and further probed with a polyclonal anti-h-EphA3 antiserum (bottom panel).

DISCUSSION

While Eph receptors have been shown to mediate key functions in embryogenesis, the mechanisms of ligand binding and receptor activation underlying these functions remain to be defined in detail. It is clear that only membrane-bound or artificially dimerized or clustered soluble ligands will mediate activation of Eph receptors (43) including h-EphA3 (3), and soluble monomeric h-ephrin-A5 has been shown to act as antagonist of receptor activation (2). Recently the role of higher order receptor oligomers has been studied, demonstrating that full biological activation is only achieved once a tetrameric receptor aggregate is generated (22). Our analysis of the stoichiometry of soluble h-ephrin A5 binding to the h-EphA3 ECD unambiguously confirmed a one-to-one interaction (3). The event(s) that follow ligand binding, leading to receptor oligomerization and cell signaling, remain to be defined. This study sought to further our understanding of this first step of receptor activation through the analysis of functional domains of the h-EphA3 ECD both *in vitro* and *in vivo*.

The highly conserved subdomain architecture of the ECD of Eph receptors coincides with a conserved exon structure (this paper and Ref. 33). A study of interspecies sequence homologies between human, murine, and chicken EphA3 revealed high homology throughout but with a ranking of exon sequence identities, the strongest evolutionary constraint (>99% identity between mouse and human) being on exon III (Fig. 1, a and b). Regions of the ECD demarcated by exon boundaries were expressed in CHO cells, and the proteins were purified to homogeneity. A kinetic analysis, using plasmon resonance detection of binding of the various subdomains to BIAcore sensorchip-immobilized h-ephrin-A5 clearly localized the ligand binding sequences to those encoded by exons I-III. The affinity for the interaction of this smaller ligand binding domain of $K_D = 18$ nM was well within the range reported previously for the binding of ephrin-A5 to sensorchip-immobilized h-EphA3 ($K_D = 12$ nM (3)) but was somewhat higher than the affinity estimated for the binding of the h-EphA3 ECD to sensorchip-immobilized ephrin-A5 ($K_D = 62$ – 72 nM, Fig. 1e). Correspondingly increased association rates of the smaller subdomain constructs (Fig. 1d) and of the ligand (3) suggest that higher diffusion rates and improved access to the binding interface of the smaller proteins may explain this apparent affinity increase.

In seeking to further narrow the binding region, we note that exon I contributes only seven non-conserved residues, but both exons II and III show very high sequence identity across species (Fig. 1). Attempts to express exon III without exon II

sequences were unsuccessful, and expression of protein was not detected. However, in-solution competition experiments with a peptide corresponding to the exon I- and II-encoded residues of the receptor ECD showed no effect on binding. Taken together with the homology data, these results suggest that exon III-encoded sequences are directly involved in ligand binding, whereas exon II is not involved but is required for a stable protein domain structure. Furthermore, attempts to express a C-terminal truncated form of exon III, terminating after cysteine 186 (corresponding to cysteine 191 of EphB2), resulted in low yields of high molecular weight protein aggregates, suggesting the importance of this C-terminal sequence for the structural integrity of this domain. These findings are in general agreement with a recent study of the chicken EphB2 and EphA3 receptors (36). By using a different approach the authors also identified the critical role of the N-terminal region in ligand binding. Although they did not analyze the contribution to protein secretion, stability, or ligand binding of the N-terminal, exon I- and II-encoded subdomain denoted in their report as "signal peptide," successful expression of N-terminally FLAG-tagged proteins in our study suggests that this signal peptide is not cleaved from the receptor ECD during secretion. Furthermore, restricted C-terminal truncations of exon III sequences in their study resulted in reduced ligand binding affinity (36), suggesting that most or all of exon III is required for high affinity binding. Together, these findings, emphasizing the structural importance of the N- and C-terminal sequence of the N-terminal half of the EphA3 ECD, support our conclusion that exons II and III encode an integral structure rather than, as previously assumed, discrete globular and cysteine rich subdomains.

Organization from defined structural building blocks with distinct regions of sequence conservation is a common feature of RTKs (44). As our data imply for EphA receptors, the region of highest sequence conservation within several subfamilies including the fibroblast growth factor receptors delineates the ligand-binding interface. In the case of the fibroblast growth factor receptors, ligand binding is encoded by Ig domains II and III, both of which independently bind fibroblast growth factors. Similarly, the PDGFR, c-Kit, TrkR, and Flt1 RTKs use multiple Ig repeats to bind ligand (21, 45–47), whereas the insulin I ligand-binding site spans two unique N-terminal α -subunit domains (48) and ErbB binds EGF through the region between two Cys-rich domains, with some contribution from the N terminus (49–51). In the Eph family the ligand-binding site is characterized as a single structural domain which, despite reported weak similarities to Ig-like (4, 52) or laminin VI (36) domains, appears to be unique to this family. The notion of a single exon II- and III-encoded protein domain is also supported by an evolutionary argument based on intron phase analysis (53). The 5' end of exon II and the 3' end of exon III are phase 1 (i.e. interrupting the coding triplet after one base) whereas the intron between exons II and III is phase 0, implying that it arose through insertion into an ancestral coding sequence.

To analyze further the role of isolated receptor ECD subdomains *in vivo*, we modified a dominant negative strategy in zebrafish, previously used to study EphA4 signaling in fore and hindbrain formation during zebrafish embryogenesis (24). Inhibition of RTK signaling by expression of kinase-deleted or truncated forms of the receptor, either in a ligand-dependent (23, 24, 54) or -independent manner (55, 56), is well established (reviewed in Ref. 44). We used our observation that expression of exogenous soluble EphA3 or ephrin-A5 resulted in a characteristic developmental defect in somite development and axis organization⁴ to probe the function of ECD subdomains. A

anticipated from the BIAcore analysis. embryos injected with h-EphA3 I-III RNA show the same phenotype as h-EphA3 I-VII or soluble ephrin-A5 RNA-injected embryos, consistent with a dominant negative effect by the soluble EphA3 ligand binding domain. By contrast, injection of the h-EphA3 IV-VII RNA, encoding all regions except the ligand-binding domain, was not expected to alter the normal phenotype. At low and medium concentrations no abnormality in embryo development was observed. Extended dose-response studies revealed that both h-EphA3 I-VII or h-EphA3 I-III exhibited the expected dose-dependent increase in the number of developmentally defective embryos (Fig. 5).⁴ Although the severity of the effects also increased (an increasing number of somites were disrupted at higher concentrations of RNA; data not shown), the defects were confined exclusively to those tissues that had been perturbed also at low concentrations of injected RNA. Importantly, at high concentrations of h-EphA3 IV-VII RNA and h-EphA3 I-III RNA, injections resulted in a similar proportion of identically defective embryos. The complete overlap of phenotypes resulting from these injections of either h-EphA3 I-VII RNA, h-EphA3 I-III RNA, or high concentrations of h-EphA3 IV-VII RNA implied that the same signaling processes had been disrupted by all receptor constructs.

Since the h-EphA3 IV-VII protein cannot bind ephrin-A5 (Fig. 1, *d* and *e*), this finding suggested that h-EphA3 can bind to endogenous receptor to produce functionless heterodimers, thus disrupting Eph signaling in a ligand-independent manner. An approximation of the abundance of the exogenous receptor proteins on the basis of Western blot and BIAcore data (Figs. 2, *a* and *b*, 5*a*), and by assuming the extracellular space of a 10 hpf embryo as 5 pl (1/100th of the total volume of a 1-mm diameter embryo), suggests a concentration of 10–20 μ M h-EphA3 IV-VII in 100 pg of mRNA-injected embryos. This high concentration of expressed protein required to achieve the dominant negative effect (Fig. 5, *a* and *b*) implies a significantly lower affinity of the receptor/receptor interaction than for the receptor-ligand binding. This notion was confirmed by BIAcore studies of h-EphA3 I-VII or h-EphA3 IV-VII binding to h-EphA3 I-VII derivatized sensor surfaces, indicating that ligand-independent receptor dimerization occurred at micromolar concentrations (Table I). Although we were not able to achieve high enough concentrations of monomeric h-EphA3 IV-VII to block ligand-induced h-EphA3 transphosphorylation in LK63 cells, we confirmed the ligand-independent receptor dimerization through a direct *in vitro* binding experiment. Anti-FLAG mAb cross-linked forms of either soluble h-EphA3 I-VII or the ligand binding domain-deficient h-EphA3 IV-VII construct (Fig. 6) induced transphosphorylation of endogenous receptors, demonstrating their competence for a ligand-independent interaction. A slow dissociation rate from the h-EphA3 I-VII sensor surface during BIAcore experiments and immunoprecipitation of phosphorylated endogenous h-EphA3 with mAb-dimerized h-EphA3 ECD constructs from a detergent lysate of LK63 cells suggest that the interaction is stable, once the critical receptor concentration is reached. On the other hand, a weak interaction of h-EphA3 I-III with h-EphA3 I-VII inferred from BIAcore and transphosphorylation experiments (Table I, Fig. 6) did not withstand the immunoprecipitation and indicates a minor contribution of this domain to the dimerization. Thus, our experiments provide several lines of evidence suggesting the presence of a low affinity dimerization domain which is encoded by exons IV–VII and functions independently of ligand binding. Exons IV–VII encode an EGF domain and two Fibronectin type III domains, the latter having been implicated in receptor dimerization in the cytokine receptor family (57). Although the data presented in this report do not

precisely define the region mediating dimerization, preliminary zebrafish studies with h-EphA3 IV–V and h-EphA3 V–VII suggest that dimerization is mediated by exon IV sequences.

The presence of a ligand-independent dimerization domain in EphA3 invites comparison with activation of the c-Kit and PDGFR. Experiments with c-Kit-specific mAbs which block dimerization, and analysis of c-Kit ECD deletion mutants, define an Ig domain C-terminal to the ligand binding interface which is required for receptor dimerization (21). This dimerization domain is essential for biological effects of the Kit ligand. Of most relevance to the results presented, ligand-independent activation at high receptor density has been demonstrated using high level expression of PDGFR in SF9 cells (25).

The identification of distinct receptor subdomains that mediate ligand-binding and receptor dimerization at different concentrations suggests a stepwise mechanism of receptor activation for EphA receptors and ephrin-A ligands. In our model, an EphA-expressing cell or axon moving into a gradient generated by differentially expressing ephrin-A-positive cells encounters progressively higher ephrin-A concentrations. As EphA receptors engage ephrin through high affinity interaction of the N-terminal ligand-binding domain at the cell-cell interface (step 1), the reduced mobility of the receptor-ligand complexes *versus* free receptor or ligand results in their accumulation at the interface. At some position in the ephrin-A gradient, a critical receptor concentration (dependent on receptor-ligand affinity) obtains at the interface between the cells such that receptor-receptor interaction through the C-terminal dimerization domain (step 2) allows the generation of multimeric complexes. EphA signaling is activated by transphosphorylation of the oligomerized receptors (step 3), and the resulting signal halts migration of the EphA-expressing cell. Recent observations indicating that multimeric complexes (tetramers) of EphB1 and EphB2 receptors are required for full biological function (22) is of interest in regard to the experiments presented here, in which transphosphorylation is induced by heterotetramer formation and might involve even higher order aggregates. It seems reasonable to speculate that the low affinity dimerization domain is involved in mediating the formation of these higher order structures and thus provides a critical component of the Eph-receptor signaling system.

Acknowledgments—We thank Caroline Brennan and Nigel Hold for helpful discussions and critical comments on the manuscript. Thanks to Jacqueline Gad and Helen Cooper for sharing unpublished results and to Janna Stickland for preparation of figures.

REFERENCES

1. Davis, S., Gale, N. W., Aldrich, T. H., Maisonpierre, P. C., Lhotak, V., Pawson, T., Goldfarb, R. H., and Yancopoulos, G. D. (1994) *Science* 266, 816–819.
2. Winslow, J. W., Moran, P., Valverde, J., Shih, A., Yuan, J. Q., Wong, S. C., Tsai, S. P., Goddard, A., Henzel, W. J., Hefti, F., Beck, K. D., and Caras, W. (1995) *Neuron* 14, 973–981.
3. Lackmann, M., Mann, R. J., Kravets, L., Smith, F. M., Bucci, T. A., Marx, K. F., Howlett, G. J., Olsson, J. E., Vanden Bos, T., Cerretti, D. P., and Brown, A. W. (1997) *J. Biol. Chem.* 272, 16521–16530.
4. Tuzi, N. L., and Gullick, W. J. (1994) *Br. J. Cancer* 69, 417–421.
5. Henkemeyer, M., Marengere, L. E., McGlade, J., Olivier, J. P., Conlon, R., Holmyard, D. P., Letwin, K., and Pawson, T. (1994) *Oncogene* 9, 1001–1011.
6. Pandey, A., Lindberg, R. A., and Dixit, V. M. (1995) *Curr. Biol.* 5, 986–990.
7. The Eph Nomenclature Committee (1997) *Cell* 90, 403–404.
8. Beckmann, M. P., Cerretti, D. P., Baum, P., Vanden Bos, T., James, L., Far, T., Kozlosky, C., Hollingsworth, T., Shilling, H., Maraskovsky, E., Fletcher, F. A., Lhotak, V., Pawson, T., and Lyman, S. D. (1994) *EMBO J.* 13, 3757–3762.
9. Pandey, A., Lazar, D. F., Saltiel, A. R., and Dixit, V. M. (1994) *J. Biol. Chem.* 269, 30154–30157.
10. Cerretti, D. P., Vanden Bos, T., Nelson, N., Kozlosky, C. J., Reddy, Maraskovsky, E., Park, L. S., Lyman, S. D., Copeland, N. G., Gilbert, Jenkin, N. A., and Fletcher, F. A. (1995) *Mol. Immunol.* 32, 1197–1207.
11. Pandey, A., Duan, H., and Dixit, V. M. (1995) *J. Biol. Chem.* 270, 19201–19207.
12. Brambilla, R., Schnapp, A., Casagrande, F., Labrador, J. P., Bergemann, J., Flanagan, J. G., Pasquale, E. B., and Klein, R. (1995) *EMBO J.* 14, 3116–3126.
13. Cheng, H. J., and Flanagan, J. G. (1994) *Cell* 79, 157–168.

14. Monschau, B., Kremoser, C., Ohta, K., Tanaka, H., Kaneko, T., Yamada, T., Handwerker, C., Hornberger, M. R., Loschinger, J., Pasquale, E. B., Siever, D. A., Verderame, M. F., Muller, B. K., Bonhoeffer, F., and Drescher, U. (1997) *EMBO J.* 16, 1258-1267
15. Cheng, H. J., Nakamoto, M., Bergemann, A. D., and Flanagan, J. G. (1995) *Cell* 82, 371-381
16. Drescher, U., Kremoser, C., Handwerker, C., Loschinger, J., Noda, M., and Bonhoeffer, F. (1995) *Cell* 82, 359-370
17. Nakamoto, M., Cheng, H. J., Friedman, G. C., McLaughlin, T., Hansen, M. J., Yoon, C. H., O'Leary, D. M., and Flanagan, J. G. (1996) *Cell* 86, 755-766
18. Frisen, J., Yates, P. A., McLaughlin, T., Friedman, G. C., O'Leary, D. D. M., and Barbacid, M. (1998) *Neuron* 20, 235-243
19. Brennan, C., Monschau, B., Lindberg, R., Guthrie, B., Drescher, U., Bonhoeffer, F., and Holder, N. (1997) *Development* 124, 655-664
20. Ullrich, A., and Schlessinger, J. (1990) *Cell* 61, 203-212
21. Blechman, J. M., Lev, S., Barg, J., Eisenstein, M., Vaks, B., Vogel, Z., Givol, D., and Yarden, Y. (1995) *Cell* 80, 103-113
22. Stein, E., Huynh-Do, U., Lane, A. A., Cerretti, D. P., and Daniel, T. O. (1998) *J. Biol. Chem.* 273, 1303-1308
23. Xu, Q., Alldus, G., Holder, N., and Wilkinson, D. G. (1995) *Development* 121, 4005-4016
24. Xu, Q., Alldus, G., Macdonald, R., Wilkinson, D. G., and Holder, N. (1996) *Nature* 381, 319-322
25. Herren, B., Rooney, B., Weyer, K. A., Iberg, N., Schmid, G., and Pech, M. (1993) *J. Biol. Chem.* 268, 15088-15095
26. Sajjadi, F. G., Pasquale, E. B., and Subramani, S. (1991) *New Biol.* 3, 769-778
27. Sambrook, J., Fritsch, E. F., and Manniatis, T. (1989) *Molecular Cloning: A Laboratory Manual*, pp. 2.82-2.118. Cold Spring Harbor Laboratory, Cold Spring Harbor, NY
28. Lackmann, M., Bucci, T., Mann, R. J., Kravets, L. A., Viney, E., Smith, F., Moritz, R. L., Carter, W., Simpson, R. J., Nicola, N. A., Mackwell, K., Nice, E. C., Wilks, A. F., and Boyd, A. W. (1996) *Proc. Natl. Acad. Sci. U. S. A.* 93, 2523-2527
29. Boyd, A. W., Ward, L. D., Wicks, I. P., Simpson, R. J., Salvaris, E., Wilks, A., Welch, K., Loudovaris, M., Rockman, S., and Busmanis, I. (1992) *J. Biol. Chem.* 267, 3262-3267
30. Westerfield, M. (1995) *The Zebrafish Book*. University of Oregon Press
31. Kimmel, C. B., Ballard, W. W., Kimmel, S. R., Ullmann, B., and Schilling, T. F. (1995) *Dev. Dyn.* 203, 253-310
32. Salvaris, E., Novotny, J. R., Welch, K., Campbell, L., and Boyd, A. W. (1992) *Leuk. Res.* 16, 655-663
33. Connor, R. J., and Pasquale, E. B. (1995) *Oncogene* 11, 2429-2438
34. Maisonnier, P. C., Barrezaeta, N. X., and Yancopoulos, G. D. (1993) *Oncogene* 8, 3277-3288
35. Williams, A. F., and Barclay, A. N. (1988) *Annu. Rev. Immunol.* 6, 381-405
36. Labrador, J. P., Brambilla, R., and Klein, R. (1997) *EMBO J.* 16, 3889-3897
37. Stanley, P. (1989) *Mol. Cell. Biol.* 9, 377-383
38. Cooper, H. M., Armes, P., Britto, J., Gad, J., and Wilks, A. F. (1995) *Oncogene* 11, 2243-2254
39. Fjose, A., Izpisua-Belmonte, J. C., Fromental-Ramain, C., and Duboule, D. (1994) *Development* 120, 71-81
40. Krauss, S., Johansen, T., Korzh, V., and Fjose, A. (1991) *Development* 113, 1193-1206
41. Oxtoby, E., and Jowett, T. (1993) *Nucleic Acids Res.* 21, 1087-1095
42. Weinberg, E. S., Allende, M. L., Kelly, C. S., Abdelhamid, A., Murakami, T., Andermann, P., Doerre, O. G., Grunwald, D. J., and Riggleman, B. (1996) *Development* 122, 271-280
43. Tessier-Lavigne, M. (1995) *Cell* 82, 345-348
44. van der Geer, P., and Hunter, T. (1994) *Annu. Rev. Cell Biol.* 10, 251-337
45. Heidaran, M. A., Pierce, J. H., Jensen, R. A., Matsui, T., and Aaronson, S. A. (1990) *J. Biol. Chem.* 265, 18741-18744
46. Davis-Smyth, T., Chen, H., Park, J., Presta, L. G., and Ferrara, N. (1996) *EMBO J.* 15, 4919-4927
47. Perez, P., Coll, P. M., Hempstead, B. L., Martin-Zanca, D., and Chao, M. V. (1995) *Mol. Cell. Neurosci.* 6, 97-105
48. Wedekind, F., Baer-Pontzen, K., Bala-Mohan, S., Choli, D., Zahn, H., and Brandenburg, D. (1989) *Biol. Chem. Hoppe-Seyler* 370, 251-258
49. Lax, I., Burgess, W. H., Bellot, F., Ullrich, A., Schlessinger, J., and Givol, D. (1988) *Mol. Cell. Biol.* 8, 1831-1834
50. Lax, I., Bellot, F., Howk, R., Ullrich, A., Givol, D., and Schlessinger, J. (1989) *EMBO J.* 8, 421-427
51. Woltjer, R. L., Lukas, T. J., and Staros, J. V. (1992) *Proc. Natl. Acad. Sci. U. S. A.* 89, 7801-7805
52. Pandey, A., Shao, H., Marks, R. M., Poverini, P. J., and Dixit, V. M. (1995) *Science* 268, 567-569
53. Patthy, L. (1987) *FEBS Lett.* 214, 1-7
54. Ueno, H., Escobedo, J. A., and Williams, L. T. (1993) *J. Biol. Chem.* 268, 22814-22819
55. Frattali, A. L., Treadway, J. L., and Pessin, J. E. (1992) *J. Biol. Chem.* 267, 19521-19528
56. Levy-Toledano, R., Caro, L. H., Accili, D., and Taylor, S. I. (1994) *EMBO J.* 13, 835-842
57. Somers, W., Ultsch, M., De Vos, A. M., and Kossiakoff, A. A. (1994) *Nature* 372, 478-481
58. Wicks, I. P., Wilkinson, D., Salvaris, E., and Boyd, A. W. (1992) *Proc. Natl. Acad. Sci. U. S. A.* 89, 1611-1615
59. Dayhoff, M. O., Barker, W. C., and Hunt, L. T. (1983) *Methods Enzymol.* 91, 524-595
60. Bell, G. I., Fong, N. M., Stempien, M. M., Wormsted, M., Caput, D., Ku, L., Urdea, M. S., Rall, L. B., and Sanchez-Pescador, R. (1986) *Nucleic Acids Res.* 14, 8427-8446
61. Oldberg, A., and Ruoslahti, E. (1986) *J. Biol. Chem.* 261, 2113-2116
62. Mount, S. M. (1982) *Nucleic Acids Res.* 10, 459-472



Genomic organization and alternatively processed forms of Cek5, a receptor protein-tyrosine kinase of the Eph subfamily

Robert J Connor and Elena B Pasquale

La Jolla Cancer Research Foundation, La Jolla, California 92037, USA

D19

The genomic organization of Cek5, a receptor tyrosine kinase of the Eph subfamily, was elucidated utilizing a strategy involving PCR amplification of Cek5 genomic DNA. Cek5 is the first Eph-related kinase for which the exon-intron structure of the entire coding region has been determined. The Cek5 gene spans over 35 kb and comprises at least 16 exons. The exon-intron structure of Cek5 can be correlated with the proposed domain structure of the Eph subfamily, with the exception of an Ig motif in the extracellular domain. Intron positions in the Cek5 gene coincide with the locations of the deletions, substitutions, or insertions that have been described in a number of Eph-related kinases. This suggests that alternative processing plays a major role in generating the structural variability observed in the Eph subfamily. Consistent with this hypothesis, analysis of the Cek5 gene indicated that: (i) a variant form of Cek5 containing an insertion in the juxtamembrane region (Cek5+) arises through the use of alternative 5' splice sites, and (ii) a soluble form of Cek5 comprising only the extracellular domain (Cek5s) may exist, which originates by a native polyadenylation. RT-PCR analysis and RNase protection assays revealed the expression of both Cek5+ and Cek5s at various stages of chicken development.

Keywords: exon-intron structure; alternative splicing; alternative polyadenylation; domain structure; gene family

Introduction

Receptor protein tyrosine kinases transduce signals across the plasma membrane: the binding of their cognate ligands to the extracellular domain results in catalytic activation, autophosphorylation and phosphorylation on tyrosine of cytoplasmic substrates (van der Geer *et al.*, 1994). They are categorized into subfamilies based upon structural similarities (van der Geer *et al.*, 1994). Receptor tyrosine kinases of the Eph subfamily are characterized by a conserved cysteine-rich region and two fibronectin type III repeats in the extracellular domain and a highly conserved cytoplasmic kinase domain (Tuzi and Gullick, 1994; van der Geer *et al.*, 1994). In addition, a juxtamembrane domain and a carboxy-terminus flank the kinase domain and are not highly conserved. The presence of an Ig-like domain at the extreme amino-terminus of the extracellular domain has also been tentatively

proposed (O'Bryan *et al.*, 1991). The Eph subfamily currently represents the largest branch of receptor tyrosine kinases, comprising at least thirteen distinct genes. Based on their expression patterns, the Eph-related kinases are likely to be important in developmental processes as well as in the maintenance of adult tissues and in cell transformation (Tuzi and Gullick, 1994). Although the specific functions of individual members of the Eph subfamily are still undefined, the preferential expression of many Eph-related kinases in embryonic as well as adult neural tissues suggests important functions in the nervous system (Sajjadi and Pasquale, 1993; Tuzi and Gullick, 1994; van der Geer *et al.*, 1994). Roles for the Eph subfamily in pattern formation, neuronal survival, axon growth and pathfinding have been proposed (Nieto *et al.*, 1992; Pasquale *et al.*, 1992, 1994; Becker *et al.*, 1994; Henkemeyer *et al.*, 1994). Direct evidence that the Eph-related kinases are indeed receptors was provided by the recent identification of their activating ligands (Bartley *et al.*, 1994; Beckmann *et al.*, 1994; Cheng and Flanagan, 1994; Davis *et al.*, 1994; Bennet *et al.*, 1995; Kozlosky *et al.*, 1995; Winslow *et al.*, 1995), including the Cek5 ligand (Shao *et al.*, 1994).

Cek5 (Chicken embryo kinase 5) is a member of the Eph subfamily that was identified by screening a 10-day chicken embryo cDNA expression library with an anti-phosphotyrosine antibody (Pasquale, 1991). Cek5 is expressed throughout embryogenesis in nearly all the chicken tissues examined, whereas in the adult it is predominantly expressed in the nervous system (Pasquale, 1991). The amino acid sequences of the mouse (Nuk) and human (Erk) homologs of Cek5 (Henkemeyer *et al.*, 1994; Kiyokawa *et al.*, 1994) indicate a high level of conservation for this gene. Erk mRNA is normally expressed in various adult human organs and exhibits highest expression levels in the placenta, brain, colon and thyroid (Kiyokawa *et al.*, 1994). Cek5 and Erk are overexpressed in a number of tumor cell lines and tissues (Kiyokawa *et al.*, 1994; Soans *et al.*, 1994), suggesting a possible role for the Cek5/Erk gene in cell transformation. The human Erk gene has been localized to chromosome 1p34-35 (Kiyokawa *et al.*, 1994).

Two different forms of Cek5, designated Cek5 and Cek5+, were previously identified by screening a 10-day whole chicken embryo cDNA expression library (Sajjadi and Pasquale, 1993). Cek5+ contains 48 additional nucleotides which encode a sixteen amino acid insertion located in the juxtamembrane region. Variant forms of other Eph-like receptors have been reported. Variant forms of chicken Cek7 (Siever and Verderame, 1994; and unpublished observations) and its rat homolog Ehk-1 (Maisonpierre *et al.*, 1993) contain deletions in their extracellular regions and

Correspondence: EB Pasquale

Received 19 July 1995; revised 1 September 1995; accepted 1 September 1995

truncations or substitutions in their carboxy-termini. In addition, variant forms of Cek7 and Cek10 contain an insertion in their juxtamembrane regions which is distinct from that of Cek5+ (Sajjadi and Pasquale, 1993; Siever and Verderame, 1994). Finally, a soluble form of Mek4 is comprised of the truncated extracellular domain of the Mek4 receptor and seven unique amino acids at the carboxy-terminus (Sajjadi *et al.*, 1991) and transmembrane forms of Ehk-3/MDK1 lack the catalytic domain and the carboxy-terminus (Ciossek *et al.*, 1995; Valenzuela *et al.*, 1995). To determine whether these different forms of the Eph-related kinases arise as a result of alternative splicing or are the products of distinct genes, the genomic organization of the kinases of the Eph subfamily requires analysis. Here we describe the genomic organization of the Cek5 gene and propose that it is representative of that of the other genes of the Eph subfamily. The exon-intron structure of the Cek5 gene corresponds to the proposed structural domains of the Eph subfamily, with the exception of the extracellular domain Ig motif. The genomic sequence of Cek5 predicts the existence of at least three different Cek5 alternatively processed forms, which presumably have distinct functions. The expression of each Cek5 variant form during embryonic development was demonstrated using reverse transcription-polymerase chain reaction (RT-PCR) analysis and ribonuclease (RNase) protection assays.

Results

Southern blot analysis

Since two different Cek5 cDNAs, Cek5 and Cek5+, have been identified (Sajjadi and Pasquale, 1993), Southern blot analysis of chicken genomic DNA was carried out to determine whether Cek5 is a single gene. Recombinant λ phage containing a genomic fragment of Cek5 (see Figure 2) was also used for comparison. Both the phage and chicken genomic DNAs were digested using various restriction enzymes and transferred to nylon membranes for probing. When a cDNA probe to the extracellular region of Cek5 was used (comprising nucleotides 212 to 566), single bands of the same size were observed for both chicken genomic DNA (Figure 1B) and recombinant λ phage (Figure 1A). With a probe comprising genomic sequences between nucleotides 1627 and 1795, single bands were also observed (Figure 1C). These data confirm that a single Cek5 gene is present in the chicken genome.

Exon-intron organization of the Cek5 gene

PCR was used to analyse the genomic organization of the Cek5 gene. Either genomic DNA or λ phage DNA containing Cek5 genomic sequences were used as templates for PCR amplification. By amplifying using various sets of primers and sequencing the resultant PCR products, as well as by directly sequencing λ phage DNA, the locations and sizes of introns and exons were determined throughout the coding sequence of the Cek5 gene (Figure 2 and Table 1). In some cases primers were designed by predicting intron positions based on the domain structure of Cek5, while in other

cases primers were designed according to the known locations of the few introns previously identified in other Eph-related kinases (Maru *et al.*, 1988; Chan and Watt, 1991; Sajjadi *et al.*, 1991). The Cek5 gene is comprised of at least 16 exons and 15 introns and spans a minimum of 35 kb. Since genomic sequences upstream of the initiation ATG were not identified, exon numbering was based on the assumption that the first exon contains the 5' untranslated sequences as well as the sequences encoding the signal peptide. Exon 16 encodes the carboxy-terminus of Cek5 and at least 1055 nucleotides of 3' untranslated sequence. A polyadenylation signal is present downstream of the stop codon (Pasquale, 1991). However, this polyadenylation signal is not followed by a poly(A) tail in the available cDNA clone that contains this region (Pasquale, 1991), suggesting the presence of at least one additional polyadenylation signal in exon 16. Amplification with primers flanking three introns did not result in detectable products, even under conditions which allowed the amplification of control templates of at least 11 kb (not shown). Therefore, the sizes of these three introns are probably too large for PCR amplification. Minimum size estimations for these introns were based on the mapping of phage genomic clones (Figure 2). The sequences of the exon/intron junctions are shown in Table 1. The dinucleotide sequences at the beginning of all the introns match the consensus sequence characteristic of a 5' splice donor site (gt), while the final two nucleotides of all introns match the consensus sequence characteristic of a 3' splice acceptor site (ag).

Members of the Eph family of receptor tyrosine kinases have been suggested to contain an Ig domain (O'Bryan *et al.*, 1991), a cysteine rich region and two fibronectin type III repeats in the extracellular domain (Pasquale, 1991). When intron positions are compared to the location of these domains (Figure 3), it is

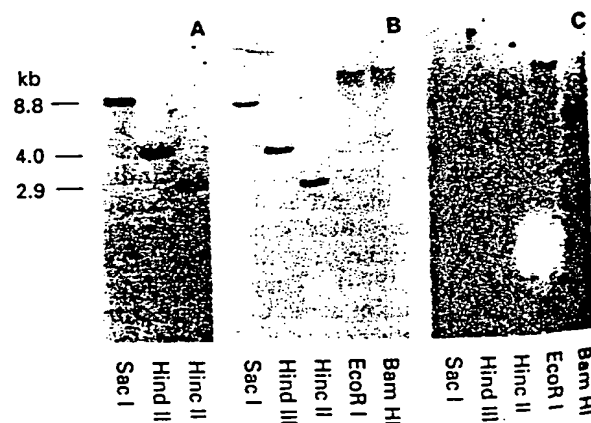


Figure 1 Southern analysis of genomic DNA. (A) λ phage clone containing Cek5 5' end genomic sequences (shown schematically in Figure 2B); (B and C), chicken genomic DNA. The DNA in each lane was digested with the restriction enzymes indicated. (A) and (B) were probed using a 32 P-labeled cDNA probe corresponding to residues 212–566 of Cek5. The probe for C was prepared by random priming of chicken genomic DNA that was amplified by PCR using primers corresponding to residues 1627–1646 of the Cek5 sense strand and 1776–1795 of the antisense strand. A was exposed for 1 h without intensifying screen; B and C were exposed for 2 days with intensifying screen.

appa
dom:
or t
intr
the
split
nuch
1). T
of fi
Exon
1
2
3
4
5
6
7
8
9
10
11
12
13
14
15
16

parent that the proposed fibronectin type III domains are encoded by either one (amino-terminal) or two (carboxy-terminal) discrete exons. The three exons at positions 1000, 1336 and 1624, which are at the boundaries of the two fibronectin type III repeats, shift the reading frame between the first and second nucleotide of a codon (phase 1) (Patthy, 1991) (Table 1). This arrangement typifies the genomic organization of fibronectin type III modules (Schwarzbauer *et al.*,

1987; Patthy, 1991; O'Grady *et al.*, 1994). In contrast, the 5' end of the Cek5 coding sequence contains an unusually large exon (exon 3, 685 bp) (Blake, 1985) and no exon/intron junction is found at the carboxy-terminal boundary of the postulated Ig domain. This is not consistent with the expected genomic organization of sequences encoding Ig domains, which are typically comprised within one or two discrete exons (Williams and Barclay, 1988).

Table 1 Summary of exon/intron junctions

Exon	Exon size (bp)	5' Splice donor	Intron size (bp)	3' Splice acceptor	Intron position	Phase
1	-	GTGGAAG	> 2.5 k	tcctgcagAGACGCT	94	1
2	65	CTCAGGGgtgagagt	4.0 k	gtctccagTGGGAAG	159	0
3	685	TGCAGAGgtaacccc	> 12 k	GCTGCCC	844	1
4	156	TGCACCAgtattttgg	950	ccttatagCCATCCC	1000	1
5	336	CAGGCTG	> 2.5 k	tcttgacagTCCTTC	1336	1
6	125	TGAGAAGgtactgag	4.3 k	ccttgacagAACCTGA	1461	0
7	163	ACTGAAGgtgagttct	619	cctttcagCCGAGTA	1624	1
8	109	GCAACAGgttaggtca	341	ctttccagAAGACGG	1733	2
9	116	CTCTTCGgtttgtgt	2.5 k	ttacacagTGACTCC	1801	1
10	124	GGGGCAGgttaggtga	380	gttcacagGGGAGTT	1924	1
11	247	CTTGAGGgtatgaaa	700	tttcctagCAAAATG	2172	0
12	217	CGCACTGgttaaagct	1.0 k	tcctgtagGGTGGAA	2388	0
13	149	TCAAGATgtgagttg	1.3 k	tgctgcagGTGATAA	2538	0
14	194	CCTCTGGgtatgcat	300	tgtttcagGGTTAAC	2732	2
15	157	CTGTAGAgtaagtgc	2.9 k	ctccaaagGGACATT	2888	2
16	> 1104					

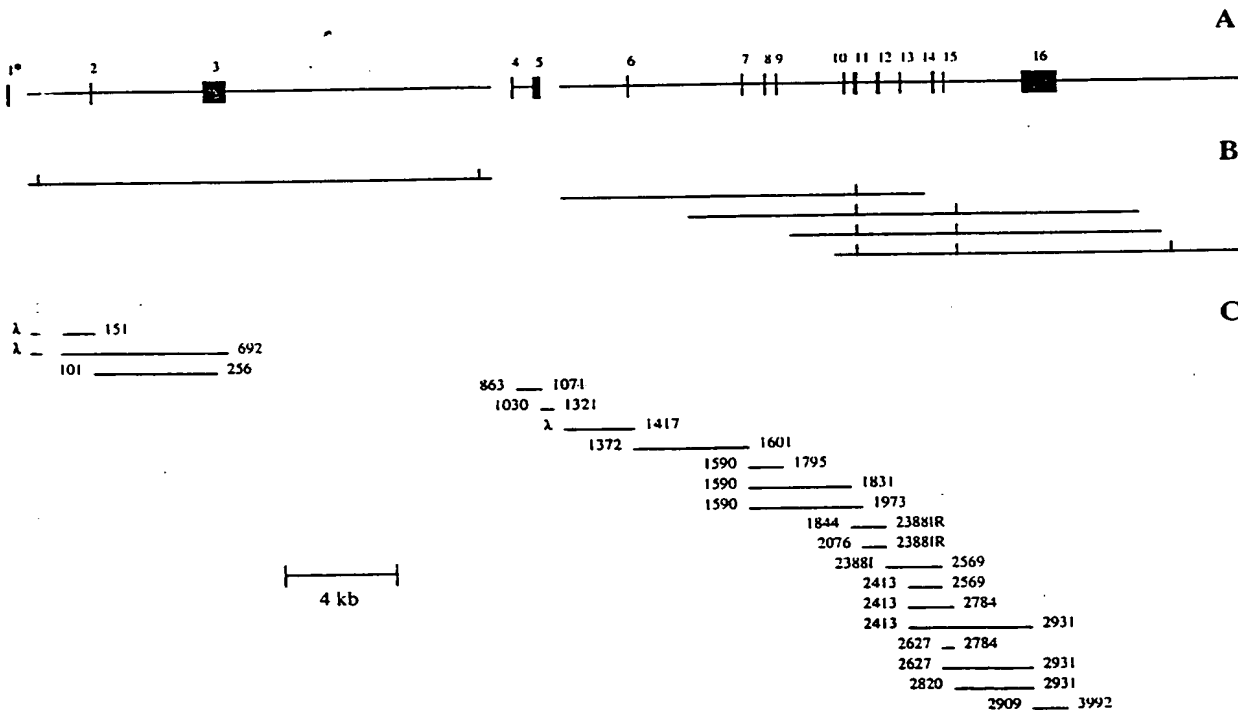


Figure 2 Genomic organization of Cek5. (A) schematic representation of the exon/intron organization of the Cek5 gene. The positions and approximate sizes of the exons are shown by filled boxes. Exon numbering was based on the minimal assumption that the first exon contains the 5' untranslated sequences as well as the sequences encoding the signal peptide. Since this was not verified directly, exon 1 is marked by an asterisk. Introns are indicated by horizontal lines. The segments that have not been characterized (all within introns) are indicated by gaps. (B) recombinant λ phage clones used for mapping the Cek5 gene. Recognition sites for the restriction enzyme EcoRI are indicated by vertical bars. (C) PCR products used for mapping the Cek5 gene. The numbering indicates the location of the most 5' nucleotide of the forward and reverse primers with respect to the Cek5 cDNA sequence (Pasquale, 1991). λ indicates that the λ gt11 reverse primer TTGACACCAGACCAACTGGTAATG was used as the forward primer; 2388I indicates that a primer located within the intron at position 2388 (CTTTTCGACAGCAGGAGTGA) was used as the forward primer; 2388IR indicates that a primer located within the intron at position 2388 (TCACTCCTGCTGTCGAAAAG) was used as the reverse primer for amplification. Templates for PCR amplification were either the phage clones shown in B or chicken genomic DNA.

To determine whether other known protein motifs are present in the extracellular region of Cek5 following the signal peptide and preceding the fibronectin type III motifs, the amino acid sequences encoded by exons 2, 3 and 4 were used separately to search protein databases for homologous sequences. This strategy was chosen because protein motifs are typically encoded by discrete exons (Patthy, 1991; Bork, 1992; Doolittle, 1992). Exon 2 did not exhibit significant homologies with other known protein sequences. The carboxy-terminal portions of exons 3 and 4 contain the sequence CnCx_nCn (where C represents cysteine, n a stretch of 12 to 15 amino acids and x any amino acid), which is similar to the sequence found at the carboxy-terminus of epidermal growth factor (EGF) modules (Sudhof *et al.*, 1985; Davis, 1990). Highest similarity scores were obtained between the consensus sequences CxCxxG(Y/F)xxxxGxxC (residues 261–277 in exon 3) and GxxxCxCxxG(Y/F) (residues 307–317 in exon 4) and the corresponding regions of the EGF repeats of extracellular matrix proteins such as fibrillin, tenascin and thrombospondin. These sequence similarities suggest that exon 4 and the carboxy-terminal

portion of exon 3 (corresponding to residues 205–276 of Cek5) have a structure related to that of EGF modules.

Genomic sequences involved in generating a Cek5 juxtamembrane region variant

Since Cek5 was shown to be a single copy gene by Southern analysis (Figure 1), Cek5 and Cek5+, the two variant forms of Cek5 previously identified by screening a 10-day embryo cDNA library (Sajjadi and Pasquale, 1993), must be derived from the same genomic DNA as a result of alternative splicing. Cek5+ is characterized by a 48 nucleotide insertion in the juxtamembrane region. To investigate the splicing mechanism by which this insertion is generated, Cek5 genomic DNA was amplified by PCR using primers which flank the juxtamembrane region. A single product was obtained (data not shown). Its sequence revealed that the insertion immediately follows the sequence of exon 9 and corresponds to the first 48 bp at the 5' end of a 2.5 kb intron located between bases 1801 and 1802 of the Cek5 cDNA sequence (Figure 4A). The first two

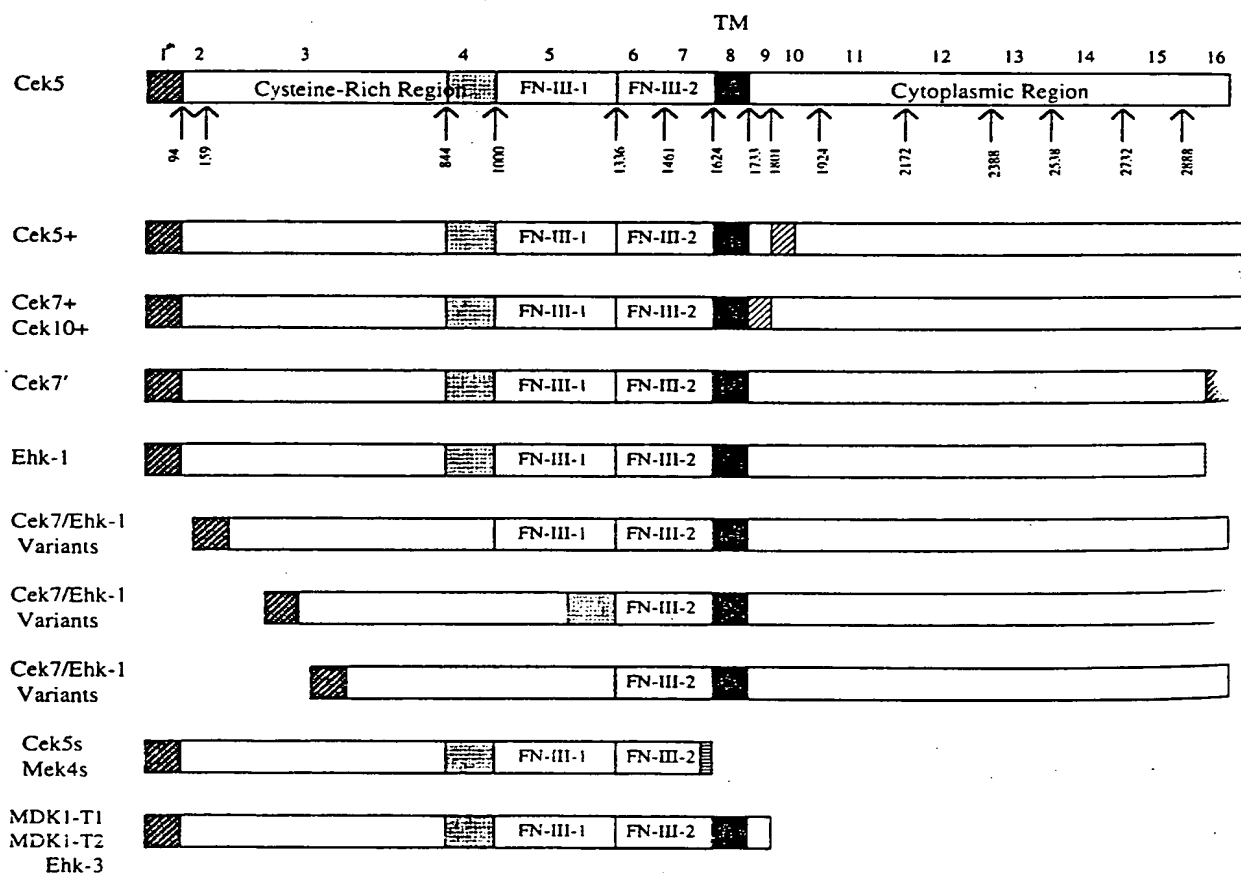


Figure 3 Position of the introns in the Cek5 gene relative to the domain structure of the Eph subfamily. The domain structure of Cek5, which is conserved within the Eph subfamily and consists of a signal peptide, a cysteine-rich region, two fibronectin type III repeats (FN-III-1 and FN-III-2), a transmembrane domain (TM), and a cytoplasmic region (Pasquale, 1991), is shown schematically. The position of the introns relative to the domain structure of Cek5 are indicated by arrows. Exon numbering is indicated. Variant forms that have been identified for a number of the Eph-related genes (Sajjadi *et al.*, 1991; Maisonpierre *et al.*, 1993; Sajjadi and Pasquale, 1993; Siever and Verderame, 1994; Ciossek *et al.*, 1995; Valenzuela *et al.*, 1995) are also shown. The positions of insertions (Cek5+, Cek7+ and Cek10+), deletions (Ehk-1/Cek7 variants) or substitutions (Cek7', Cek5s, Mek4s and Ehk-3/MDK1) are coincidental with the location of the exon-intron junctions in Cek5.

nucleotides of the insertion as well as the first two nucleotides immediately following the insertion both conform to the 'gt' consensus sequence of 5' splice donor sites (underlined in Figure 4A). Therefore, the structure of the Cek5 gene indicates that Cek5 and Cek5+ transcripts are generated by the alternative use of distinct 5' splice sites (McKeown, 1992).

To examine the expression of Cek5 and Cek5+ during embryonic development, RT-PCR was used to analyse mRNAs from whole chicken embryo as well as embryonic brain for the presence of Cek5 and Cek5+ transcripts at different developmental stages. Primers were used to amplify the juxtamembrane region between nucleotide residues 1697 and 1793 (Figure 4B). Using mRNA from 5 and 10 day whole embryos, as well as from 6, 10 and 20 day embryonic brain, amplified products of the predicted sizes for both Cek5 and Cek5+ were obtained (Figure 4C, lanes 2–6). The two PCR products were confirmed to correspond to the juxtamembrane domain region of Cek5 by Southern analysis (data not shown). Bands of the expected size for both Cek5 and Cek5+ were also obtained with mRNAs from 3 and 4 day whole embryos (not shown).

Cek7 and Cek10, two receptor tyrosine kinases closely related to Cek5, contain insertions in the juxtamembrane region, but at a location different from that of Cek5 (Maisonpierre *et al.*, 1993; Sajjadi

and Pasquale, 1993). To determine if an additional alternatively spliced form of Cek5 exists with an insertion similar to that of Cek7 and Cek10, the PCR products shown in lanes 2–6 of Figure 4C were used as templates for PCR amplification with nested primers flanking the region where the Cek7 and Cek10 insertion is located (Figure 4B). After the second amplification a single band of the expected size for Cek5 was detected (Figure 4C, lanes 8–12). This PCR product was confirmed to correspond to the appropriate juxtamembrane domain region of Cek5 by Southern analysis (not shown). Therefore, we have found no evidence supporting the existence of Cek5 variants containing juxtamembrane domain insertions other than the one in Cek5+.

Genomic sequences involved in generating a Cek5 variant transcript by selective use of an alternative polyadenylation signal

Analysis of the exon/intron structure of the Cek5 gene revealed that a 0.6 kb intron is located at position 1624, immediately prior to the exon encoding the transmembrane region (exon 8). To examine the possibility that a truncated form of Cek5 lacking the transmembrane and cytoplasmic regions is generated by a mechanism analogous to that previously described

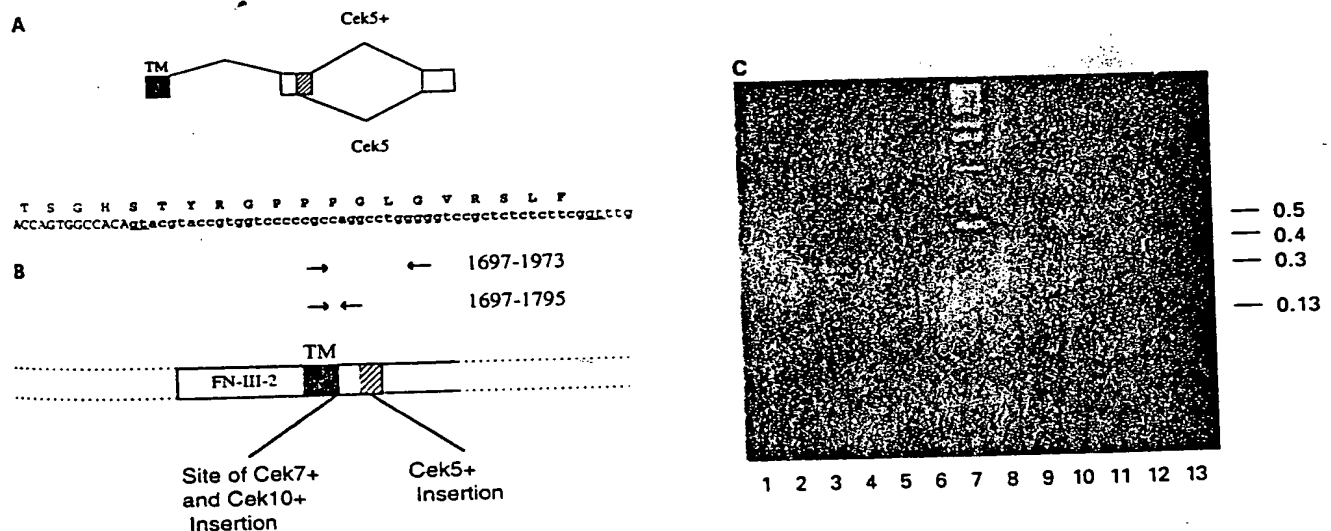


Figure 4 Genomic organization and RT-PCR analysis of the juxtamembrane domain of Cek5. (A) schematic representation of the genomic organization of the juxtamembrane domain region of Cek5. The sequence of the 48 bp insertion characteristic of Cek5+ (small letters, bold) was found to be contiguous with the cDNA sequence of Cek5 at residue 1801 (capital letters). A 2.5 kb intron follows the sequence of the insertion. Both the insertion and the intron contain the consensus sequence characteristic of a 5' splice donor site (underlined). This indicates that Cek5+ arises through the use of alternative 5' splicing, as shown. (B) Strategy used for the detection of Cek5 juxtamembrane region variant forms by RT-PCR. Arrows mark the location of the primers used with respect to the domain structure of Cek5+. The most 5' nucleotide of the forward and reverse primers are indicated at the right. FN-III-2, second fibronectin type III repeat; TM, transmembrane domain. (C) RT-PCR analysis of chicken embryo mRNAs. The primer corresponding to residues 1954–1793 of Cek5 (antisense strand) was used for the reverse transcription reaction. Primers flanking the corresponding to residues 1954–1793 of Cek5 (antisense strand) were used for amplification in lanes 1–6. Lane 1: negative control lacking cDNA template; lanes 2 and 3: 5 day and 10 day whole embryo, respectively; lanes 4, 5 and 6: 5 day, 10 day and 20 day embryonic brain, respectively. The products shown in lanes 2–6 were re-amplified using an antisense nested primer (1776–1795, antisense strand) and the same forward primer used in the previous reaction (1697–1716), as shown in lanes 8–13. Lanes 8 and 9: 5 day and 10 day whole embryo, respectively; lanes 10, 11 and 12: 6 day, 10 day and 20 day embryonic brain, respectively. Lane 13: re-amplification of the negative control shown in lane 1. The single product detected has the predicted size for Cek5 (99 bp). Larger products, which would result if an insertion was present in the region amplified, were not detected. Lane 7: 1 kb molecular weight ladder (Gibco BRL). Selected molecular weights, in kb, are indicated at the right.

for the related kinase Mek4 (Sajjadi *et al.*, 1991), the entire intron was sequenced (Figure 5A). A consensus polyadenylation sequence was identified within the

intron (bold in Figure 5A). Polyadenylation of sequences within the intron would result in a transcript retaining a portion of the intron, which

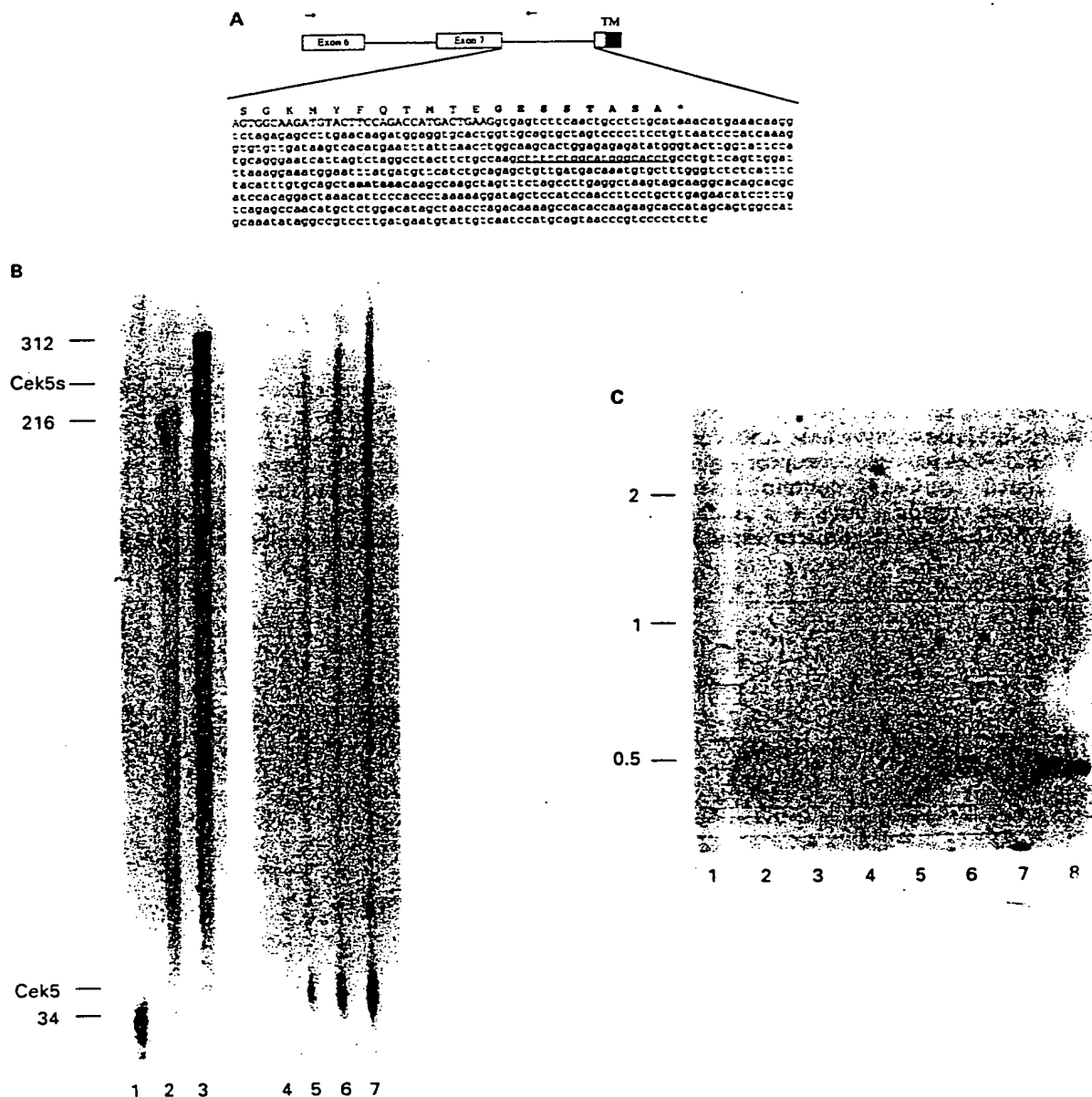


Figure 5 Sequence and expression of the variant transcript Cek5s. (A) Genomic organization in the region that regulates the generation of Cek5s transcripts. The complete sequence of the intron following exon 7 is shown in small letters. The sequences within the intron encode the amino acids indicated in bold, followed by a stop codon (*). A consensus polyadenylation site which is located within the intron is indicated in bold. The sequence complementary to that of the primer used for the detection of Cek5s mRNA by RT-PCR (see C) is underlined. The location of this primer and of the primer corresponding to residues 1372–1391 of the sense strand of Cek5, which were used for PCR amplification of Cek5s sequences (see C), are indicated by arrows. TM, transmembrane domain. (B) Relative abundance of Cek5 and Cek5s mRNAs in the 11 day chicken embryo by RNase protection analysis. Lanes 1–3, transcripts prepared with T7 RNA polymerase in the presence of radiolabelled UTP. Lane 1, transcript from pBluescript SK+ digested with HincII (34 bases); lane 2, β -actin transcript (216 bases); and lane 3, Cek5s probe (312 bases). Lane 4 represents the Cek5s probe mixed with torula yeast RNA and digested with RNase as a control. Lanes 5–7 represent 1 μ g, 2 μ g, 4 μ g of 11 day chicken embryo mRNA hybridized with the Cek5s probe and digested with RNase. The predicted size of the Cek5s protected fragment is 266 bases (Cek5s) and that of the Cek5 protected fragment is 41 bases (Cek5) (see Materials and methods). The amount of probe loaded in lane 3 represents 1/6 of the amount of probe used for the hybridizations that were loaded in lanes 4–7. Lanes 1–3 and lanes 4–7 are from the same gel, however lanes 1–3 were exposed for 2 h and lanes 4–7 for 24 h, respectively, at -70°C with intensifying screen. (C) Amplification of Cek5s sequences from chicken embryo mRNAs using the primers indicated in A. Lane 1: negative control lacking cDNA template; lanes 2–6: 3, 4, 5, 6 and 10 day whole embryo, respectively; lanes 7 and 8, 6 day and 10 day embryonic brain, respectively. The amplification of a product of the expected size (492 bp) in all the lanes was confirmed by Southern analysis using a ^{32}P -labelled probe. This probe was generated from Cek5 genomic DNA amplified with a primer corresponding to bases 1590–1609 of the sense strand and the antisense primer corresponding to the sequence underlined in Figure 5A. Selected molecular weight standards, in kb, are indicated at left

encodes eight unique amino acids in frame with the extracellular domain sequence of Cek5 followed by a stop codon (Figure 5A). This predicts the existence of another variant form of Cek5 comprised of the extracellular domain of the receptor, which may represent a secreted form of Cek5 and has been designated Cek5s.

To determine whether transcripts encoding Cek5s exist *in vivo* and to quantitate the relative abundance of the Cek5s variant with respect to Cek5, mRNA from 11 day whole chicken embryo was examined using RNase protection assays (Figure 5B). The probe used contains, in addition to vector sequences, 266 bases of the Cek5s antisense sequence, 41 bases of which are also expected to hybridize with the Cek5 mRNA (see Material and methods). The amount of probe used was in large molar excess over both the Cek5 and Cek5s target mRNAs (see Figure 5B legend). As shown in Figure 5B lanes 4–7, the band corresponding to Cek5 is considerably more prominent than that corresponding to Cek5s, even though the Cek5 protected fragment only contains 12 UTPs, compared to 73 UTPs in the Cek5s protected fragment. Hence, at embryonic day 11 the message for Cek5s in the whole embryo is substantially less abundant than that for Cek5.

To determine whether transcripts encoding Cek5s are present in the chicken embryo at different developmental stages, RT-PCR was used to amplify various embryonic mRNAs. Using an antisense primer located within the intron which follows exon 7 (underlined in Figure 5A), cDNA was generated for PCR. The 5' primer was designed to hybridize with sequences located in exon 6 (nucleotides 1372 to 1391), to insure that the products amplified from the cDNA would be different in size from the products resulting from the amplification of possible contaminating genomic DNA. mRNAs from 3 to 10 day old whole chicken embryos as well as from 6 and 10 day old embryonic brain were used for cDNA synthesis. Subsequent amplification yielded a product of the predicted size for the Cek5s cDNA in all the samples examined, which was confirmed to contain Cek5s sequences by Southern analysis (Figure 5C).

Discussion

In this report we have investigated the structural organization of the Cek5 gene in order to identify the molecular mechanisms by which diverse forms of Cek5 and other Eph-related kinases originate. Cek5 is the first receptor tyrosine kinase of the Eph gene subfamily for which the exon-intron structure of the entire coding region has been elucidated. The existence of a transcript encoding a previously undescribed soluble form of Cek5 (Cek5s) was predicted based on the genomic sequence of Cek5 and was confirmed by RT-PCR and RNase protection analysis. Cek5s does not contain a consensus sequence for glycosyl phosphatidylinositol-linkage at its carboxy-terminus and is thus expected to be secreted. Extracellular domain soluble forms of other receptor tyrosine kinases have been described which arise as a result of alternative splicing (Petch et al., 1990), proteolytic cleavage (Downing et al., 1989) or an alternative polyadenylation mechanism similar to that proposed for Cek5s (Johnson et al.,

1991; Sajjadi et al., 1991; Flickinger et al., 1992; Kendall and Thomas, 1993). Based on its structure, Cek5s may modulate the activity of the full-length receptor by competitively binding its ligand or by acting as a 'dominant negative' (Flickinger et al., 1992; Kendall and Thomas, 1993; Li et al., 1994). Furthermore, the intriguing possibility exists that binding of Cek5s to the Cek5 ligand, which is a transmembrane protein (Shao et al., 1994), generates a signal mediated by the cytoplasmic domain of the ligand. While the only notable feature recognized in the 83 amino acid long cytoplasmic domain of the Cek5 ligand is the presence of numerous Ser, Thr and Tyr residues, which may be phosphorylated (Brambilla et al., 1995), interactions with cytoplasmic signal transduction molecules remain to be investigated. Although the overall levels of Cek5s expression in the 11 day chicken embryo are low relative to full-length Cek5, Cek5s transcripts may be concentrated in specific cell types, or they may be more abundant at specific developmental stages. Hence, understanding the expression and localization of this variant truncated protein in normal and tumor tissues will be important for understanding the function of the Cek5 gene.

We have also identified the genomic sequences responsible for the generation of Cek5+, an alternatively spliced form of Cek5 characterized by an insertion within the juxtamembrane region of the receptor and showed that both Cek5+ and Cek5 are expressed in the chicken embryo at various developmental stages. The relative levels of Cek5+ and Cek5 amplified products suggest a generally lower expression of Cek5 compared to Cek5. In addition, we have previously reported that Cek5+ transcripts are detectable by Northern analysis in brain, but not body tissues, of the 10 day chicken embryo (Sajjadi and Pasquale, 1993). While the precise function of juxtamembrane domain insertions remains to be elucidated, several hypotheses are possible. The insertion in Cek5+ contains two serines, a tyrosine and a threonine residue and phosphorylation of these residues may modulate Cek5 function. For example, the Ser and Thr in the insertion are part of a protein kinase C (PKC) consensus phosphorylation site (Ser/Thr-(X)₂-Lys/Arg). Hence, the insertion in Cek5+ introduces potential PKC phosphorylation sites in the juxtamembrane domain. Since PKC phosphorylation has been shown to downregulate the activity of the EGF and hepatocyte growth factor (HGF) receptors (Downward et al., 1985; Gandino et al., 1994), phosphorylation by PKC may differentially regulate the catalytic activity of Cek5 and Cek5+. Phosphorylation of tyrosines in the juxtamembrane region, which may occur as a result of ligand binding, has also been suggested to be important in the signal transduction of receptor tyrosine kinases, such as the insulin and EGF receptors (Segatto et al., 1991; Feener et al., 1993). The insertion may also provide Cek5+ with an additional binding site for cytoplasmic targets. Phosphorylated tyrosines in the juxtamembrane domains of other tyrosine kinase receptors, such as the platelet-derived growth factor (PDGF) and insulin receptors, have been implicated in the binding of cytoplasmic target molecules (Mori et al., 1993; Staubs et al., 1994). However, the sequence of the amino acid insertion of Cek5+ does not conform to known SH2

(Src homology 2) or PTB (phosphotyrosine binding) domain consensus sequences (Songyang *et al.*, 1992; Kavanaugh *et al.*, 1995).

The location of the insertion within the juxtamembrane region of Cek5+ is unique among the members of the Eph subfamily. At least two other members of the Eph subfamily, Cek7 and Cek10, contain insertions, but at a different location within the juxtamembrane region. Whether the insertions in Cek7 and Cek10, like the one in Cek5, also arise by the use of distinct 5' splice sites remains to be elucidated. In addition, amplification with appropriate primers did not reveal Cek5 transcripts containing a second juxtamembrane domain insertion similar to those of Cek7 and Cek10. Insertions in the juxtamembrane region appear to be peculiar to members of the Eph subfamily, with the exception of the receptor tyrosine kinase met (HGF receptor) (Lee and Yamada, 1994). However, the insertion in met is longer and generated by the alternative use of a discrete exon, rather than by the alternative use of 5' splice sites. Since alternative splicing can be spatially and temporally regulated (Smith *et al.*, 1989), differential regulation of the structure/function of at least several Eph-related kinases may be achieved through the use of insertions in various regions of the juxtamembrane domain.

The genomic organization of the Cek5 gene demonstrates that the structural variability of Cek5 arises as a result of alternative splicing. When the location of the Cek5 introns is compared to the position of the insertions, deletions, or substitutions reported for other Eph-related kinase genes (Figure 3), the position of the Cek5 introns coincides with the location of these protein structural alterations. Furthermore, the phases of the exon-intron junctions in Cek5 are compatible with the preservation of the reading frame in the deletion variants of other Eph-like receptors. Hence, the structural diversity observed among members of the Eph subfamily is likely to arise as a result of alternative processing from genes that have a structural arrangement similar to that of the Cek5 gene.

Information about the genomic organization of several other Eph-related kinases is fragmentary, but provides an opportunity to determine whether the exon/intron organization is conserved between members of the Eph subfamily, yielding information on their evolutionary relationships. If the Eph-related kinases are derived from a single ancestral gene, the location of most introns is expected to be conserved. This has been demonstrated for other subfamilies of tyrosine kinases, such as the src (Rouet *et al.*, 1989), insulin receptor (Abbott *et al.*, 1992) and PDGF receptor (André *et al.*, 1992; Pajusola *et al.*, 1993; Agnès *et al.*, 1994) gene families. For example, the catalytic domain of Eph is divided into five domains (D1 through D5) by four introns (Maru *et al.*, 1988) and the exon/intron organization of the catalytic domain is conserved between Eph and Cek5, with one exception. The Cek5 gene lacks the intron corresponding to that which separates domains D1 and D2 of the Eph gene. The Erk gene, the human homolog of the Cek5 gene (Kiyokawa *et al.*, 1994), also lacks this same intron (Chan and Watt, 1991). It is likely that exon fusion has occurred in the catalytic

domain of the Cek5/Erk gene, rather than intron gain in the Eph gene (Rogers, 1989), since the intron between the D1 and D2 domains of Eph is conserved in another Eph-related kinase, Eek (Chan and Watt, 1991) and in the tie (Korhonen *et al.*, 1994) and UFO (Schulz *et al.*, 1993) genes, which belong to different subfamilies of receptor tyrosine kinases. Although differences in the structural organization of their catalytic domains suggests an early evolutionary divergence of the different subfamilies of protein tyrosine kinases, the positions of several introns in the catalytic domain of both Cek5 and Eph are conserved in other families of receptor tyrosine kinases. The intron between exons 10 and 11 of Cek5 is conserved in UFO (Schulz *et al.*, 1993), the intron between exons 12 and 13 is conserved in ret (Ceccarelli *et al.*, 1993), tie (Korhonen *et al.*, 1994), the EGF receptor (Semba *et al.*, 1985) and fibroblast growth factor (FGF) receptor 1 (Johnson *et al.*, 1991) and the intron between exons 11 and 12 is at a similar, although not identical, position of the catalytic domain as introns in the tie, insulin receptor (Seino *et al.*, 1989) and UFO genes. Hence, based upon the information available from the Eph (Maru *et al.*, 1988), Eek (Chan and Watt, 1991), Erk (Chan and Watt, 1991) and Mek4 (Sajjadi *et al.*, 1991) genes, the exon/intron structure of the Eph-related kinase genes appears to be conserved, with the exception of one intron which is present in the Eph and Eek genes, but not in the Cek5/Erk gene. In all cases in which comparisons could be made, the phases of corresponding introns in different genes are also conserved.

In summary, by delineating the genomic organization of Cek5 we have established the close evolutionary relationship of the Eph-related kinases and gained insight into the mechanisms involved in creating their structural diversity. Alternative splicing and polyadenylation likely have important implications in the functions of the Eph-related kinases.

Materials and methods

Southern hybridization of genomic DNA

Ten μ g of chicken genomic DNA or 2 μ g of phage DNA, which were purified using gravity-flow columns (Qiagen), were digested twice with restriction enzymes, separated on 0.75% agarose gels and transferred to nylon membranes (MSI) according to standard protocols (Ausubel *et al.*, 1995). The membranes were prehybridized in 0.5 M Na₂HPO₄, pH 7.2, 9% SDS, 1 mM EDTA for 1 h at 60°C, followed by overnight hybridization in the same buffer containing ³²P-labeled probes at a concentration of 2–3 $\times 10^6$ c.p.m./ml. The radioactive probes were generated by random priming of cDNA or genomic DNA PCR fragments. Nylon membranes were washed twice at 42°C for 15 min using 2 \times SSPE, 0.1% SDS and once at 42°C for 5 min using 0.1% SSPE, 0.1% SDS. Membranes were exposed at –70°C with an intensifying screen (Figure 1B and C) or at room temperature without intensifying screen (Figure 1A) using Kodak XAR film.

Isolation and characterization of Cek5 genomic clones

A chicken genomic library in the λ vector Charon 4A was generously provided by Dr Jerry Dodgson, Michigan State University. This library was screened by filter hybridization under stringent conditions (50% formamide, 50% SSPE, 50% formamide, 50% SSPE).

Denhardt's, 0.5% SDS and 200 µg/ml sheared salmon sperm DNA, 42°C) using digoxigenin-labeled probes (Boehringer Mannheim). These probes were generated by PCR using as templates either plasmid DNA (cDNA probes encoding the extracellular domain of Cek5) or genomic DNA (corresponding to the sequence of PCR product 2076-2388IR in Figure 2). After hybridization the filters were washed with 2×SSPE, 0.2% SDS at 42°C, blocked in 5% milk in TBST (Tris buffered saline with 0.1% TX100) for a minimum of 30 min and incubated with 0.15 U/ml anti-digoxigenin-alkaline phosphatase antibodies (Boehringer Mannheim) in 0.2% milk in TBST for 1 h. Filters were then washed and developed in a X-phosphate/NBT solution. Positive plaques were subjected to several rounds of purification prior to λ phage DNA purification using gravity-flow columns (Qiagen).

Sequencing of about 10⁶ clones yielded 17 Cek5 genomic clones, which were subsequently characterized by restriction mapping and Southern analysis. The λ phage inserts corresponded to the five unique Cek5 genomic fragments shown in Figure 2. Purified λ phage DNA containing Cek5 genomic sequences was used either for direct sequencing or for PCR amplification. One µg of chicken genomic DNA or 0.1 µg of λ phage DNA were used as templates for PCR amplification using the following program: one cycle for 1.5 min at 95°C, 1 min at 60°C and 3 min at 72°C, followed by 34 cycles for 1 min at 95°C, 2 min at 58°C and 3 min at 72°C and a final extension of 10 min at 72°C. PCR fragments were either sequenced directly or subcloned into a TA cloning vector (pCRII vector, Invitrogen) and the regions of interest sequenced in several plasmids. Primers used for direct sequencing of λ phage DNA corresponded to nucleotides 101-120, 371-390 and 648-667 (sense strand) and 100-119, 27-256, 386-405 and 673-692 (antisense strand) of Cek5 (Pasquale, 1991). DNA sequences were determined by the dideoxy-chain termination method (Sanger *et al.*, 1977) using plasmid DNA, or by linear amplification sequencing with Exo⁻Pfu polymerase (Stratagene) using purified λ phage DNA or PCR products.

RT-PCR analysis

For RT-PCR, mRNA was prepared from tissue homogenates by hybridization to biotinylated oligo(dT) and adsorption to streptavidin paramagnetic particles (Promega). Two µg of each mRNA were used for cDNA synthesis with Superscript II reverse transcriptase (BRL/Life Technologies, Inc.), using primers specific to Cek5. PCR was performed as described above for genomic DNA, using 1/4 of the cDNA synthesized in the reverse transcription reaction. The following two primer combinations were used for PCR: (i) for amplification of the juxtamembrane domain region, the primers TCATTGCTGTTGTCGT-CATC (corresponding to residues 1697-1716 of the Cek5 sense strand) and CTTTGGCCAGGAAGCTTGAG (corresponding to residues 1954-1973 of the antisense strand); and (ii) for amplification of Cek5s specific sequences, the primers CGCACTGTGGACAGCATTAC (corresponding

to residues 1372-1391 of the Cek5 sense strand) and AGGTGCCCATGCCAGAAAAG (corresponding to the non-coding strand, 242 nucleotides within the intron which follows exon 7 (Figure 5A)). One µl of a 20-fold dilution of the PCR products obtained from the amplification described in (i) above was used as template for amplification with the primer corresponding to residues 1697-1716 of the Cek5 sense strand (see (i) above) and primer CACTGGTATAGTGCTGCAGC (corresponding to residues 1776-1795 of the antisense strand). Products were separated on 1.5% agarose gels, photographed, denatured, and transferred to nylon membranes (MSI) for Southern analysis with ³²P-labeled DNA probes, as described above.

RNase protection assays

PolyA RNA was extracted from whole chicken embryo homogenates at day 11 of development as described above. For the synthesis of a Cek5/Cek5s antisense transcript, the cDNA predicted to encode Cek5s (comprising nucleotides 1 to 1624 in common with Cek5, followed by 225 bp of the intron following exon 7, which are unique to Cek5s (Figure 5A)) was subcloned in the EcoRI (5' end) and HindIII (3' end) sites of pBluescript SK⁺. This plasmid was linearized by digestion with BsrFI, which cleaves the Cek5 cDNA at position 1584, and transcribed with T7 RNA polymerase (Promega) in the presence of [α-³²P]UTP (800 Ci/mmol, New England Nuclear) following the instructions of the manufacturer (Promega). The resulting probe contains 312 bases, including 266 bases corresponding to the 3' end of the cDNA insert and 46 bases corresponding to vector sequences. Two protected fragments are expected with this probe, a Cek5s protected fragment of 266 bases and a Cek5 protected fragment of 41 bases (residues 1584-1624). Two additional transcripts were prepared for use as molecular size markers. A fragment of the chicken β-actin cDNA (Cleveland *et al.*, 1980) subcloned in the HindIII and EcoRV sites of the vector pSP72 (Promega), was linearized with TaqI and the plasmid pBluescript SK⁺ was linearized with HincII. Both plasmids were transcribed as described above, to produce transcripts of 216 and 34 bases, respectively. Hybridizations were allowed to proceed for 24 h and were followed by RNase digestion, using an RPA II RNase protection assay kit (Ambion) and following the recommendations of the manufacturer. Protected fragments were analysed on 6% sequencing gels. DNase I treatment of the mRNA prior to hybridization, to eliminate possible contaminating genomic DNA, did not produce detectable differences in the results obtained.

Acknowledgements

We thank H Baribault and M Wilson-Heiner for help with Southern blotting, J Dodgson for the gift of the chicken genomic library, R Doolittle and L Chong for helpful comments on the manuscript. This work was supported by National Institutes of Health Grant CA56721.

References

- Abbott AM, Bueno R, Pedrini MT, Murray JM and Smith R J. (1992). *J. Biol. Chem.*, 267, 10759-10763.
- Agnes F, Shamoon B, Dina C, Rosnet O, Birnbaum D and Galibert F. (1994). *Gene*, 145, 283-288.
- André C, Martin E, Cornu F, Hu W-X, Wang X-P and Galibert F. (1992). *Oncogene*, 7, 685-691.
- Ausubel FM, Brent R, Kingston RE, Moore DD, Seidman JG, Smith JA and Struhl K. (1995). *Current Protocols in Molecular Biology*, Jon Wiley & Sons: New York.
- Bartley TD, Hunt RW, Welcher AA, Boyle W, Parker VP, Lindberg RA, Lu HS, Colombero AM, Elliot RL, Guthrie BA, Holst PL, Skrine JD, Toso RJ, Zhang M, Fernandez E, Trail G, Varnum B, Yarden Y, Hunter T and Fox GM. (1994). *Nature*, 368, 558-560.
- Becker N, Seitanidou T, Murphy P, Mattèi M-G, Topilko P, Nieto MA, Wilkinson D G, Charnay P and Gilardi-Hebenstreit P. (1994). *Mech. Devel.*, 47, 3-17.

- Beckmann MP, Cerretti DP, Baum P, Vanden Bos T, James L, Farrah T, Kozlosky C, Hollingsworth T, Shilling H, Marakovsky E, Fletcher FA, Lhotak V, Pawson T and Lyman SD. (1994). *EMBO J.*, 13, 3757-3762.
- Bennett BD, Zeigler FC, Gu Q, Fendly B, Goddard AD, Gillett N and Matthews W. (1995). *Proc. Natl. Acad. Sci. USA*, 92, 1866-1870.
- Blake CCF. (1985). *International Review of Cytology*, 93, 149-185.
- Bork P. (1992). *Current Biology*, 2, 413-421.
- Brambilla R, Schnapp A, Casagrande F, Labrador JP, Bergemann AD, Flanagan JG, Pasquale EB and Klein R. (1995). *EMBO J.*, 14, 3116-3126.
- Ceccherini I, Boccardi R, Luo Y, Pasini B, Hofstra R, Takahashi M and Romeo G. (1993). *Biochem. Biophys. Res. Comm.*, 196, 1288-1295.
- Chan J and Watt VM. (1991). *Oncogene*, 6, 1057-1061.
- Cheng H-J and Flanagan JG. (1994). *Cell*, 79, 157-168.
- Ciossek T, Millaüer B and Ullrich A. (1995). *Oncogene*, 9, 97-108.
- Cleveland DW, Lopata MA, MacDonald RJ, Cowan NJ, Rutter WJ and Kirschner MW. (1980). *Cell*, 20, 95-105.
- Davis CG. (1990). *New Biol.*, 2, 410-419.
- Davis S, Gale NW, Aldrich TH, Maisonpierre PC, Lhotak V, Pawson T, Goldfarb M and Yancopoulos GD. (1994). *Science*, 266, 816-819.
- Doolittle RF. (1992). *Protein Science*, 1, 191-200.
- Downing JR, Roussel MF and Sherr CJ. (1989). *Mol. Cell. Biol.*, 9, 2890-2896.
- Downward J, Waterfield MD and Parker PJ. (1985). *J. Biol. Chem.*, 260, 14538-14546.
- Feener EP, Backer JM, King GL, Wilden PA, Sun XJ, Kahn CR and White MF. (1993). *J. Biol. Chem.*, 268, 11256-11264.
- Flickinger TW, Maihle NJ and Kung H-J. (1992). *Mol. Cell. Biol.*, 12, 883-893.
- Gandino L, Longati P, Medico E, Prat M and Comoglio PM. (1994). *J. Biol. Chem.*, 269, 1815-1820.
- Henkemeyer M, Marengere LEM, McGlade J, Olivier JP, Conlon RA, Holmyard DP, Letwin K and Pawson T. (1994). *Oncogene*, 9, 1001-1014.
- Johnson DE, Lu J, Chen H, Werner S and Williams LT. (1991). *Mol. Cell. Biol.*, 11, 4627-4634.
- Kavanaugh WM, Turck CW and Williams LT. (1995). *Science*, 268, 1177-1179.
- Kendall RL and Thomas KA. (1993). *Proc. Natl. Acad. Sci. USA*, 90, 10705-10709.
- Kiyokawa E, Takai S, Tanaka M, Iwase T, Suzuki M, Xiang Y-Y, Naito Y, Yarnada K, Sugimura H, and Kino I. (1994). *Cancer Research*, 54, 3645-3650.
- Korhonen J, Polvi A, Partanen J and Alitalo K. (1994). *Oncogene*, 9, 395-403.
- Kozlosky CJ, Maraskovsky E, McGrew T, VandenBos T, Teepe M, Lyman SD, Srinivasan S, Fletcher FA, Gayle RB, Cerretti DP and Beckmann MP. (1995). *Oncogene*, 10, 299-306.
- Lee C-C and Yamada KM. (1994). *J. Biol. Chem.*, 269, 19457-19561.
- Li Y, Basilico C and Mansukhani A. (1994). *Mol. Cell. Biol.*, 14, 7660-7669.
- Maisonpierre PC, Barrezueta NX and Yancopoulos GD. (1993). *Oncogene*, 8, 3277-3288.
- Maru Y, Hirai H, Yoshida MC and Takaku F. (1988). *Mol. Cell. Biol.*, 8, 3770-3776.
- McKeown M. (1992). *Annu. Rev. Cell Biol.* 8, 133-155.
- Mori S, Rönstrand L, Yokote K, Engström A, Courtneidge SA, Claesson-Welsh L and Heldin C-H. (1993). *EMBO J.*, 12, 2257-2264.
- Nieto MA, Gilardi-Hebenstreit P and Charnay P, W. Kinson D G. (1992). *Development*, 116, 1137-1150.
- O'Bryan JP, Frye RA, Cogswell PC, Neubauer A, Kitch B, Prokop C, Espinosa III R, Le Beau M M, Earp HS and Liu ET. (1991). *Mol. Cell. Biol.* 11, 5016-5031.
- O'Grady P, Krueger NX, Streuli M and Saito H. (1994). *J. Biol. Chem.*, 269, 25193-25199.
- Pajusola K, Aprelikova O, Armstrong E, Morris S and Alitalo K. (1993). *Oncogene*, 8, 2931-2937.
- Pasquale EB. (1991). *Cell Regulation*, 2, 523-534.
- Pasquale EB, Deerinck TJ, Singer SJ and Ellisman MH. (1992). *J. Neurosci.*, 12, 3956-3967.
- Pasquale EB, Connor RJ, Rocholl D, Schnürch H and Risan W. (1994). *Dev. Biol.*, 163, 491-502.
- Patthy L. (1991). *Curr. Opin. Struct. Biol.*, 1, 351-361.
- Petch LA, Harris J, Raymond VW, Blasband A, Lee DC and Earp HS. (1990). *Mol. Cell. Biol.*, 10, 2973-2982.
- Rogers JH. (1989). *Trends Genet.*, 5, 213-216.
- Rouer E, Van Huynh T, Lavareda de Souza S, La 1 M-C, Fisher S and Benarous R. (1989). *Gene*, 84, 105-113.
- Sanger F, Nicklen S and Coulson AR. (1977). *Proc. Natl. Acad. Sci. USA*, 74, 5463-5468.
- Sajjadi FG and Pasquale EB. (1993). *Oncogene*, 8, 1807-1813.
- Sajjadi FG, Pasquale EB and Subramani S. (1991). *New Biol.*, 3, 769-778.
- Schulz AS, Schleithoff L, Faust M, Bartrarn CR and Janssen JWG. (1993). *Oncogene*, 8, 509-513.
- Schwarzbauer JE, Patel RS, Fonda D and Hynes RO. (1987). *EMBO J.*, 6, 2573-2580.
- Segatto O, Lonardo F, Wexler D, Fazioli F, Pierce JH, Bottaro DP, White MF and Di Fiore PP. (1991). *Mol. Cell. Biol.*, 11, 3191-3202.
- Seino S, Seino M, Nishi S and Bell GI. (1989). *Proc. Natl. Acad. Sci. USA*, 86, 114-118.
- Semba K, Kamata N, Toyoshima K and Yamamoto T. (1985). *Proc. Natl. Acad. Sci. USA*, 82, 6497-6501.
- Shao H, Lou L, Pandey A, Pasquale EB and Ditt VM. (1994). *J. Biol. Chem.*, 269, 26606-26609.
- Siever DA and Verderame MF. (1994). *Gene*, 148, 219-226.
- Smith CW, Patton JG and Nadal-Ginard B. (1989). *Annu. Rev. Genet.*, 23, 527-577.
- Soans C, Holash JA and Pasquale EB. (1994). *Oncogene*, 9, 3353-3361.
- Songyang Z, Shoelson SE, Chaudhuri M, Gish G, Pawson T, Haser WG, King F, Roberts T, Ratnofsky S, Schleider RJ, Neel BG, Birge RB, Fajardo JE, Chou MM, Darnay H, Schaffhausen B and Cantley LC. (1993). *Cell*, 72, 767-778.
- Staub PA, Reichart DR, Saltiel AR, Milarski KL, Maegawa H, Berhanu P, Olefsky JM and Seely BL. (1994). *J. Biol. Chem.*, 269, 27186-27192.
- Sudhof TC, Russel DW, Goldstein JL, Brown MS, Sanchez-Pescador R and Bell GI. (1985). *Science*, 228, 893-895.
- Tuzi NL and Gullick WJ. (1994). *Br. J. Cancer*, 69, 417-421.
- Valenzuela DM, Rojas E, Griffiths JA, Compton E, Gissel M, Ip NY, Goldfarb M and Yancopoulos GD. (1993). *Oncogene*, 10, 1573-1580.
- van der Geer P, Hunter T and Lindberg RA. (1994). *Annu. Rev. Cell Biol.*, 10, 251-337.
- Williams AF and Barclay AN. (1988). *Annu. Rev. Immunol.*, 6, 381-405.
- Winslow JW, Moran P, Valverde J, Shih A, Yuan JQ, Wong SC, Tsai SP, Goddard A, Henzel WJ, Hefti F, Reck M and Caras IW. (1995). *Neuron*, 14, 973-981.

Nuk Controls Pathfinding of Commissural Axons in the Mammalian Central Nervous System

Mark Henkemeyer,*§|| Donata Orioli,‡||
Jeffrey T. Henderson,* Tracy M. Saxton,*†
John Roder,*† Tony Pawson,*†
and Rüdiger Klein‡

*Programme in Molecular Biology and Cancer
Samuel Lunenfeld Research Institute
Mount Sinai Hospital
Toronto, Ontario
M5G 1X5 Canada

†Department of Molecular and Medical Genetics
University of Toronto
Toronto, Ontario
M5S 1A8 Canada

‡European Molecular Biology Laboratory
Meyerhofstrasse 1
D-69117 Heidelberg
Germany

Summary

Eph family receptor tyrosine kinases have been proposed to control axon guidance and fasciculation. To address the biological functions of the Eph family member Nuk, two mutations in the mouse germline have been generated: a protein null allele (*Nuk*[−]) and an allele that encodes a Nuk-βgal fusion receptor lacking the tyrosine kinase and C-terminal domains (*Nuk*^{lacZ}). In *Nuk*[−] homozygous brains, the majority of axons forming the posterior tract of the anterior commissure migrate aberrantly to the floor of the brain, resulting in a failure of cortical neurons to link the two temporal lobes. These results indicate that Nuk, a receptor that binds transmembrane ligands, plays a critical and unique role in the pathfinding of specific axons in the mammalian central nervous system.

Introduction

Receptor tyrosine kinases are involved in controlling cell growth and developmental fate decisions, in directing cell movement and migration, and in tissue morphogenesis (Pawson and Bernstein, 1990; Dickson and Hafen, 1994). The Eph family of receptor tyrosine kinases, which possesses at least 13 members, has been circumstantially implicated in regulating cell movement and axonal pathfinding (reviewed by Tuzi and Gullick, 1994; Brambilla and Klein, 1995; Tessier-Lavigne, 1995). Recently, considerable progress has been made in the identification of ligands for Eph receptors (or LERs; Bartley et al., 1994; Beckmann et al., 1994; Cheng and Flanagan, 1994; Davis et al., 1994; Shao et al., 1994, 1995; Bennett et al., 1995; Bergemann et al., 1995; Drescher et al., 1995; Kozlosky et al., 1995; Winslow et al., 1995; Gale et al., submitted). All LERs are anchored to the cell

surface, either through a transmembrane segment in the case of LER2 (Elk-L/Elf-3/Cek5-L), LER5 (Htk-L/Elf-2), and Elk-L3, or through a glycosyl phosphatidylinositol (GPI) linkage for the other five known LERs. Eph receptors can be subdivided into two classes based on their interactions with the various LERs. The Elk, Nuk/Cek5, Sek4/Hek2, and Htk receptors (Elk subclass) all preferentially bind to and are activated by the transmembrane LERs. Conversely, the remaining Eph receptors interact promiscuously with the GPI-linked LERs (Brambilla et al., 1995; Gale et al., submitted). Interestingly, strong catalytic activation of Eph receptors can only be achieved by coculturing ligand-expressing cells with receptor-expressing cells, or by artificially oligomerizing soluble forms of the ligands (Davis et al., 1994). These results, as well as the immunolocalization of the Nuk receptor to specific sites of cell-cell contact, are consistent with the idea that this receptor-ligand family mediates close-range cellular interactions (Henkemeyer et al., 1994).

The properties of GPI-linked LERs and their cognate receptors have provided clues to possible biological activities. B61 induces endothelial cell migration and can act as an angiogenic factor when applied to the rat cornea (Pandey et al., 1995). Two other GPI-linked LERs, RAGS and Elf-1, are expressed in a posterior-to-anterior gradient in the chick tectum, and one of their receptors, Mek4, is expressed in a temporal-to-nasal countergradient in the retina (Drescher et al., 1995; Cheng et al., 1995). Moreover, membranes from the posterior tectum cause growth cone collapse of axons from the temporal retina, while recombinant RAGS repels the growth of retinal axons in vitro (Drescher et al., 1995). These observations have raised the possibility that Eph receptors and their ligands function as guidance molecules to establish a retinal-tectal topographic map. In separate studies, the human homolog of RAGS, AL-1, has been implicated in promoting the fasciculation of cultured cortical axons in vitro (Winslow et al., 1995).

We have previously identified and characterized Eph receptors of the Elk subclass, which bind to transmembrane ligands and are expressed to high levels in the nervous system (Letwin et al., 1988; Lhotak et al., 1991; Lhotak and Pawson, 1993; Henkemeyer et al., 1994; Gale et al., submitted). To investigate the biological functions of these receptors, we have introduced two mutations into the mouse *Nuk* gene and examined their effects on development of the nervous system. We find that Nuk plays a unique role during the pathfinding of a specific set of central nervous system axons forming the anterior commissure, a major interhemispheric connection between the two temporal lobes of the cerebral cortex.

Results

Nuk Mutations

The *Nuk*[−] mutation was generated through homologous recombination in embryonic stem (ES) cells by deleting a 5' segment of the *Nuk* locus and inserting a neomycin resistance cassette (Figure 1A). This deletion, which encompasses the exon for Nuk amino acids 29–50, was

§Present address: Center for Developmental Biology, University of Texas Southwestern Medical Center, Dallas, Texas 75235-9133

||The first two authors made equal contributions to this work.

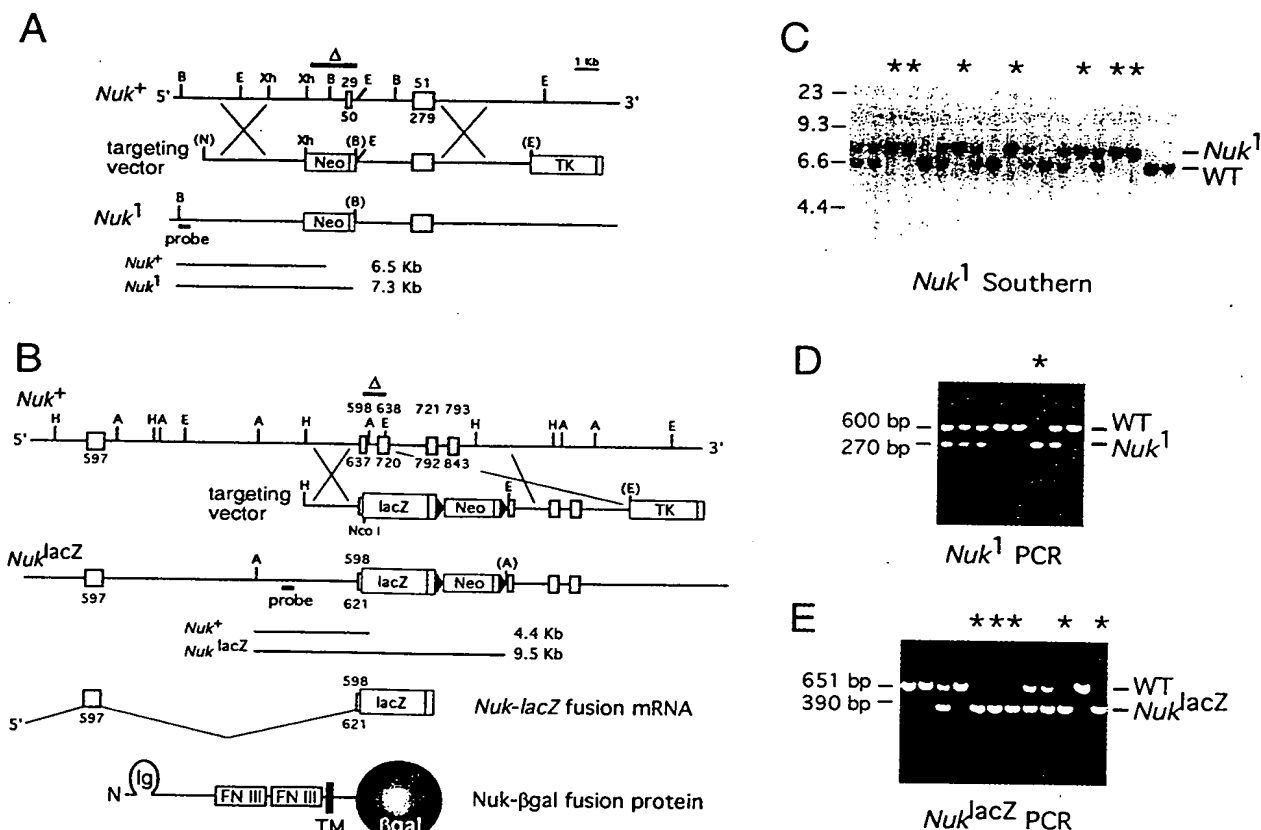


Figure 1. Generation of *Nuk*¹ and *Nuk*^{lacZ} Mutations

(A) *Nuk*¹ mutation. Genomic restriction map and targeting strategy used to delete a 1.4 kb region of *Nuk* containing the coding exon for *Nuk* amino acids 29–50. The *Nuk*¹ targeting vector, including the PGK-neo and PGK-tk cassettes (boxes) and their transcription termination sequences (stippled boxes) are shown. Homologous recombinants were identified by hybridizing a 5' external probe to BamHI digests of genomic DNA, resulting in a wild-type band of 6.5 kb and a *Nuk*¹ mutant band of 7.3 kb. Pertinent restriction sites are indicated; those in brackets are derived from vector sequences. A, Asp-718; B, BamHI; E, EcoRI; H, HindIII; Xh, XhoI.

(B) *Nuk*^{lacZ} mutation. Genomic restriction map of a 3' region of the *Nuk* locus containing exons encoding the *Nuk* juxtamembrane and tyrosine kinase domains. A group of four exons encoding *Nuk* amino acids 598–843 were identified (shaded boxes). A *Nuk-lacZ* targeting strategy was designed to delete 1 kb of *Nuk*, including codons for the ATP binding region of the tyrosine kinase domain (residues 622–707), while inserting in-frame bacterial *lacZ* including codons for the ATP binding region of the tyrosine kinase domain (residues 622–707). Homologous recombinants were identified by hybridizing a 5' external probe with Asp-718 digests of genomic DNA, resulting in a wild-type band of 4.4 kb and a *Nuk*^{lacZ} mutant band of 9.5 kb. The predicted *Nuk-lacZ* mRNA and *Nuk-βgal* fusion protein are shown (TM, transmembrane).

(C–E) Genotype analysis of *Nuk*¹ and *Nuk*^{lacZ} mutations.

(C) Southern blot analysis of *Nuk*¹ mutant mice. Tail DNA from the offspring of intercrosses between *Nuk*^{1/+} heterozygous males and females were digested with BamHI and subjected to Southern blot analysis, using the external probe shown in (A).

(D and E) Polymerase chain reaction analysis of *Nuk*¹ (D) and *Nuk*^{lacZ} (E) mutant mice. The positions of wild-type (WT) and mutant bands are indicated, and asterisks denote the lanes where homozygote samples were loaded.

expected to generate a protein null allele, as sequence analysis indicated that any aberrant splicing around the *neo*^r cassette would result in a mutant transcript containing a frameshift in the *Nuk* open reading frame. The *Nuk*^{lacZ} mutant allele was designed to encode a fusion protein, comprised of the extracellular, transmembrane, and juxtamembrane domains of *Nuk* (amino acids 1–621) linked to β-galactosidase (βgal; Figure 1B). This *Nuk-βgal* fusion receptor lacks the entire tyrosine kinase catalytic and C-terminal domains of *Nuk*. Aggregation chimeras of three *Nuk*^{1/+} and two *Nuk*^{lacZ/+} targeted ES cell lines were generated, and germline transmission of the mutant alleles was obtained. Animals homozygous

for either *Nuk* mutation were observed at the expected frequency in the progeny of heterozygous intercrosses and were identified by either Southern blot analysis or *Nuk*-specific polymerase chain reactions (Figures 1C–1E). *Nuk*¹/*Nuk*¹ and *Nuk*^{lacZ}/*Nuk*^{lacZ} homozygotes were long-lived and fertile in 129 inbred and 129 × C57BL/6 or 129 × CD1 mixed backgrounds.

Biochemical Characterization of *Nuk*¹ and *Nuk*^{lacZ} Alleles

To determine whether the *Nuk*¹ mutation abrogated expression of the wild-type *Nuk*⁺ protein, antiserum raised

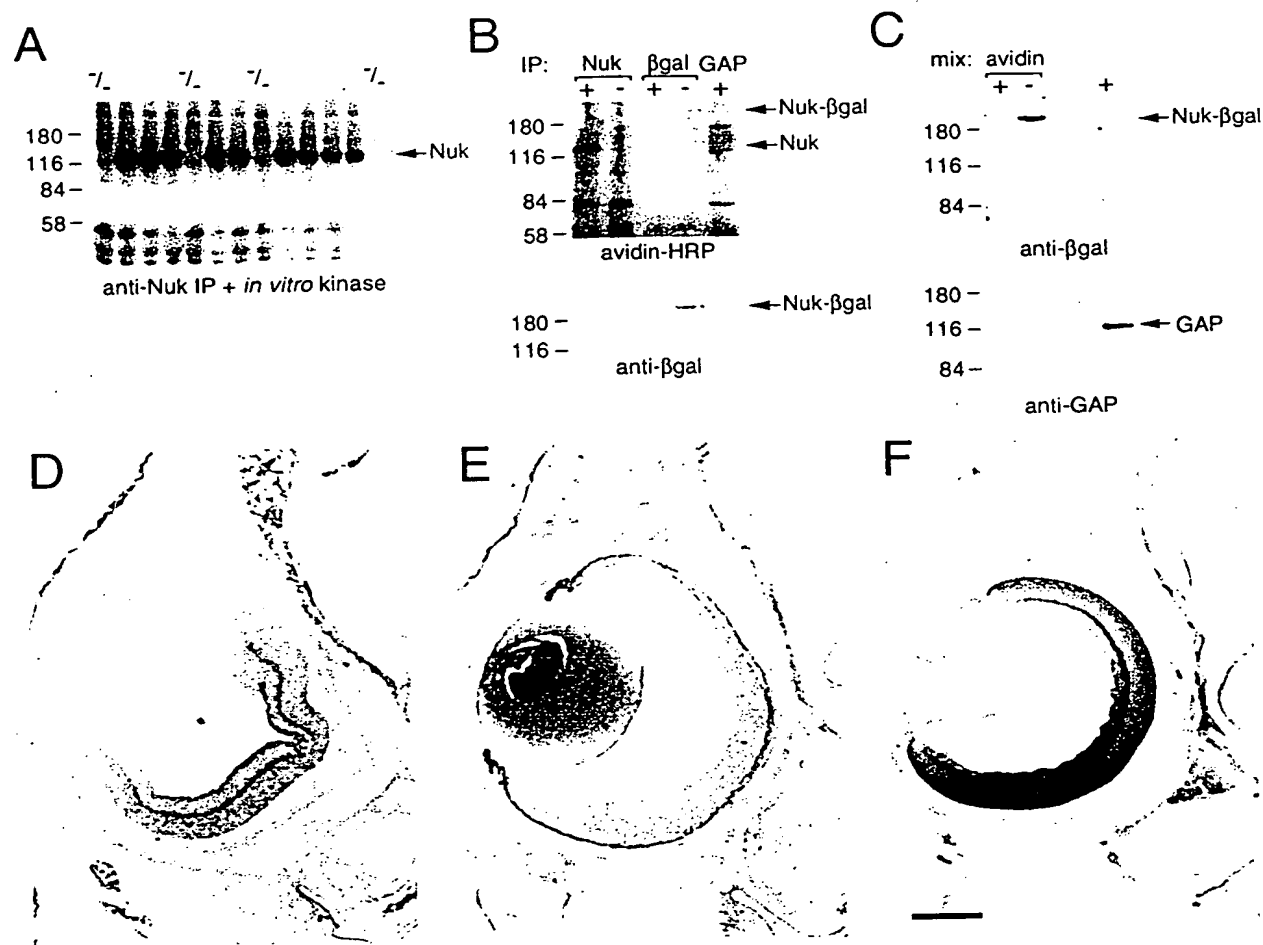


Figure 2. Biochemical Characterization of *Nuk*¹ and *Nuk*^{lacZ} Mutations

(A) *Nuk*-specific in vitro kinase assays from E10.5 mouse embryos. Total protein lysates were prepared from individual embryos resulting from an intercross of *Nuk*^{1/+} heterozygous males and females. *Nuk* protein was immunoprecipitated using anti-*Nuk* antibodies and subjected to in vitro kinase assays with γ -³²P ATP. Lanes containing homozygous ($-/-$) embryos are indicated.

(B and C) Biotinylation of cell-surface proteins from wild-type and *Nuk*^{lacZ} homozygous mutant brains. Cell-surface proteins from primary cultures of postnatal day 4 (P₄) brains were specifically biotinylated. In (B), total protein lysates from wild-type (+) and *Nuk*^{lacZ} homozygous cultures were immunoprecipitated with anti-*Nuk*, anti- β gal, or anti-GAP antibodies and subjected to Western blot analysis with avidin conjugated to horseradish peroxidase or anti- β gal antibodies. In (C), total protein lysates from the cell surface biotinylated (+) and ($-$) cultures were incubated with avidin-agarose beads. The precipitated biotinylated proteins were then subjected to Western blot analysis using anti- β gal antibodies. The filter was subsequently stripped and reprobed with anti-GAP antibodies. The far right lane contains total cell protein lysate.

(D-F) *Nuk*¹ and *Nuk*- β gal expression in coronal sections of the eye. Dorsal is up.

(D and E) Anti-*Nuk* antibody staining of $+/+$ (D) and *Nuk*^{lacZ}/*Nuk*^{lacZ} (E) newborn mouse heads.

(F) *Nuk*- β gal staining of a *Nuk*^{lacZ}/*Nuk*^{lacZ} newborn. Scale bar D-F, 400 μ m.

against the *Nuk* C-terminus was used in an immune-complex in vitro tyrosine kinase assay. An autophosphorylated 130 kDa *Nuk*⁺ protein was specifically detected in $+/+$ and *Nuk*^{1/+}, but not in *Nuk*¹/*Nuk*¹ embryo protein lysates (Figure 2A). No abnormally sized gene product was observed in *Nuk*¹/*Nuk*¹ embryos that might result from readthrough past the *neo*^r cassette or from aberrant transcripts initiating downstream of the cassette. These results indicate the *Nuk*¹ mutation is a protein null.

To investigate whether the *Nuk*^{lacZ} mutation led to the production of the expected 200 kDa membrane-bound

Nuk- β gal fusion receptor, primary brain cultures from neonatal wild-type and homozygous mutants were obtained, and cell-surface proteins were specifically biotinylated. Total protein lysates were immunoprecipitated with polyclonal antibodies directed against *Nuk* or β gal, and biotinylated species were detected in Western blots with avidin conjugated to horseradish peroxidase (HRP; Figure 2B). A 130 kDa protein that bound avidin was specifically precipitated from $+/+$ cells with anti-*Nuk* antibodies, indicating that *Nuk*⁺ was biotinylated and therefore exposed on the cell surface. In contrast, no biotinylated protein was precipitated with the anti-*Nuk*

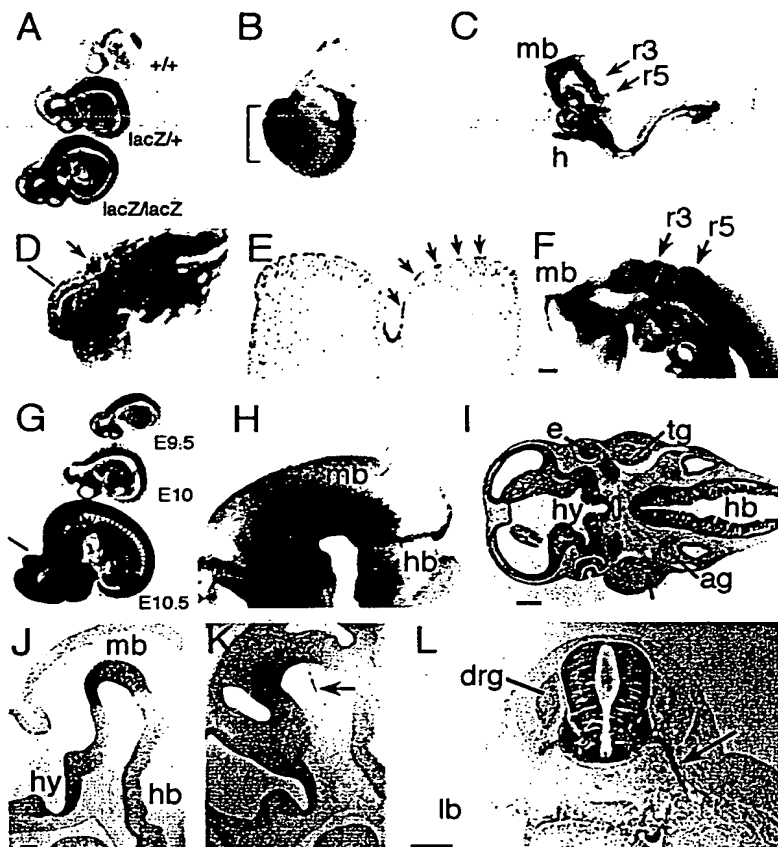


Figure 3. Expression of Nuk-βgal in the Developing Nervous System

Embryos containing the *Nuk^{lacZ}* mutation were collected and stained for Nuk-βgal activity and viewed as whole-mount specimens (A–D, F–H) or as tissue sections (E, I–L). Dorsal is up and anterior is left.

(A) *+/+*, *Nuk^{lacZ}/+* and *Nuk^{lacZ}/Nuk^{lacZ}* E10 littermates. Nuk-βgal staining in *Nuk^{lacZ}/+* and *Nuk^{lacZ}/Nuk^{lacZ}* embryos is mainly confined to the developing nervous system.

(B) At E7.5, Nuk-βgal was detected in the headfold process of the early nervous system (bracket).

(C) E8.5 embryos with 4 somites show Nuk-βgal staining in the neuroectoderm and heart (h). In the neural groove, staining was localized to the future forebrain, midbrain (mb) and hindbrain rhombomeres r3 and r5.

(D) Dorsal view looking down into the neural groove; the arrow points to r3, and the line indicates the plane of the transverse section shown in (E). (D) and (E) detail the repeating pattern of dorsal–ventral stripes of Nuk-βgal expression, localized to the apical/future ventricular surface of the neuroectodermal cells (arrows in E).

(F) At E9.25, Nuk-βgal intensely labeled specific ventral cells within the closed neural tube, including the hypothalamic region of the diencephalon, the tegmental region of the midbrain, and hindbrain rhombomeres.

(G) Between E9.5 to E10.5 days of development, embryos continue to express Nuk-βgal in the nervous system. (H–L) Nuk-βgal expression at E10.5.

(I and L) Transverse sections with the plane for (I) indicated by the line in (G) and the plane for (L) through the spinal region at the forelimb buds (lb).

(J and K) Two sagittal sections of the same embryo with (J) slightly off the midline and (K) approximately 200 μm lateral to (J). Nuk-βgal staining was intense in the preoptic area and hypothalamus (hy; I, J, K), the ventral midbrain (H, J, K), the ventral hindbrain (hb; H, I, and J), and the posterior neural tube (L). Note the near total absence of staining in dorsal cells. In (I), Nuk-βgal was also detected in the eye (e), the trigeminal (tg) and acoustic/vestibular (ag) ganglia, and the otic vesicle. Nuk-βgal localized within the axons of the PNS as shown for the trigeminal nerve entering branchial arch 1 (arrow in I), the oculomotor nerve whose cell bodies lie in the ventral midbrain (arrow in K), and the spinal motor nerves whose cell bodies lie in the ventral neural tube (arrow in L). The dorsal root ganglion (drg) did not express Nuk-βgal at E10.5. Scale bar F, J–L, 100 μm; I, 200 μm.

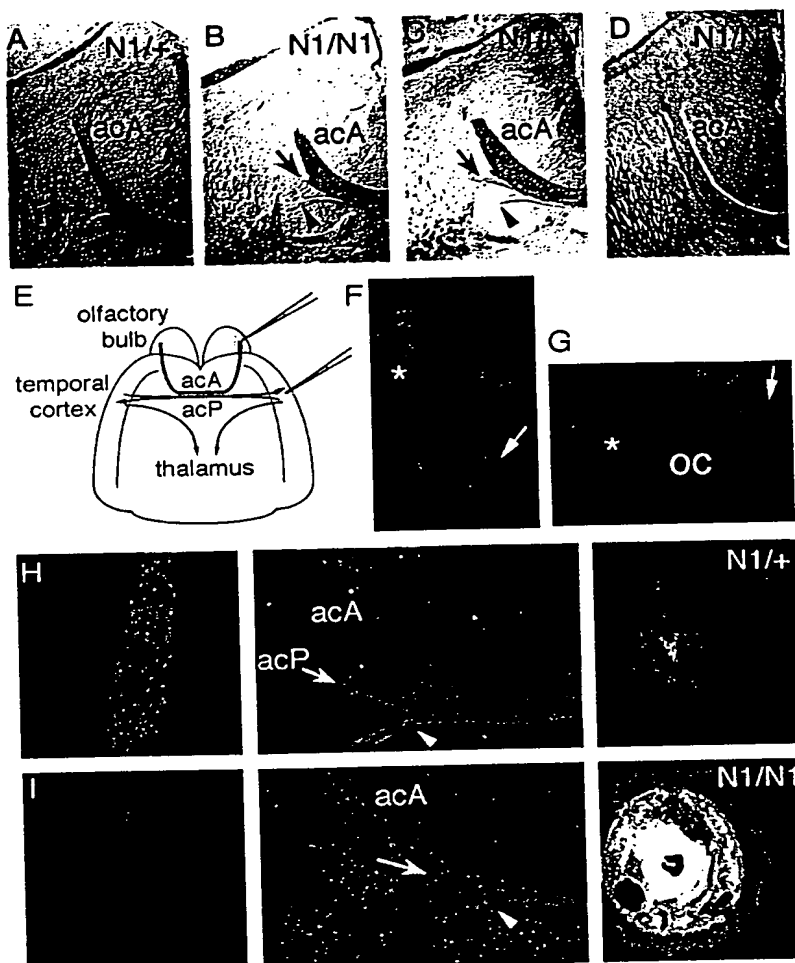
antibodies from *Nuk^{lacZ}/Nuk^{lacZ}* cells, as anticipated from the fact that the Nuk-βgal fusion protein lacks the C-terminal domain recognized by the anti-Nuk antibodies. However, the *Nuk^{lacZ}/Nuk^{lacZ}* cells did express a novel 200 kDa biotinylated polypeptide that was precipitated by anti-βgal antibodies. In the converse experiment, immobilized avidin precipitated a 200 kDa biotinylated protein specifically from *Nuk^{lacZ}/Nuk^{lacZ}* cultures that was recognized by anti-βgal antibodies (Figure 2C). The intracellular protein GAP did not become biotinylated, indicating that the labeling was indeed specific for proteins expressed on the surface of the plasma membrane. Thus, the *Nuk^{lacZ}* mutation leads to the expression of a 200 kDa Nuk-βgal fusion protein at the cell surface.

To test the fidelity with which the *Nuk^{lacZ}* allele was expressed, coronal sections of newborn eyes were subjected to anti-Nuk immunohistochemical analysis or stained for Nuk-βgal activity using the chromogenic substrate X-gal. Anti-Nuk antibodies revealed a ventral-to-dorsal gradient of Nuk⁺ expression in wild-type eyes

(Figure 2D). In the retina, intense staining for Nuk⁺ protein was observed in the axon and dendrite-rich plexiform layer and in the ganglion cell axons forming the optic nerve. In eyes of a *Nuk^{lacZ}* homozygote no anti-Nuk immunoreactivity was detected (Figure 2E); however, staining for Nuk-βgal activity revealed an expression gradient and subcellular localization identical to Nuk⁺ (Figure 2F). This result and analysis of other specimens (see below) demonstrate that the Nuk-βgal fusion receptor is expressed in the same cell types and subcellular localizations previously described for the endogenous Nuk⁺ protein (Henkemeyer et al., 1994).

Nuk-βgal Expression in the Early Nervous System

The Nuk-βgal fusion receptor provides a very precise and sensitive means to characterize Nuk expression. As shown for mid-gestation E10 specimens, Nuk-βgal staining was detected in *Nuk^{lacZ}/+* and *Nuk^{lacZ}/Nuk^{lacZ}*, but not *+/+*, embryos (Figure 3A). At earlier stages, Nuk-βgal was confined to the headfolds (Figure 3B), which by



(I) In a *Nuk'/Nuk'* mutant, dye did not label the reduced acP tract (arrow) or cells in the contralateral cortex (left panel). Note that the small posterior tract unaffected by the *Nuk'* mutation also was labeled by the injections into the temporal cortex (arrowhead in middle panels). The acA tract was not labeled by injections into the temporal cortex.

E8.5 resolved into a highly ordered expression pattern in the neuroectodermal cells of the neural plate (Figures 3C–3E). Intense staining was detected in specific anterior–posterior regions of the future brain, including the ventral midbrain and hindbrain rhombomeres r3 and r5. Interestingly, this staining also revealed at high resolution a pattern of longitudinal stripes of *Nuk*- β gal-expressing and nonexpressing cells down the length of the future brain (see Figures 3D and 3E). Thus, *Nuk* expression in the open neural groove marks specific anterior–posterior and dorsal–ventral cells.

Following dorsal closure, *Nuk*- β gal expression intensified in defined regions of the forebrain, midbrain, and rhombomeres r3 and r5, with relatively lower expression detected in the other hindbrain segments and in the posterior neural tube (Figures 3F–3L). The most intense *Nuk*- β gal staining was restricted to ventral structures, most notably in the preoptic area and hypothalamus of the forebrain (Figures 3I and 3J), the tegmental region of the midbrain (Figures 3H and 3J), the ventral hindbrain (Figure 3I), and the ventral neural tube throughout the

length of the spinal cord (Figure 3L). Like the *Nuk*⁺ receptor (Henkemeyer et al., 1994), the *Nuk*- β gal fusion protein localized to early axon fibers of the peripheral nervous system (PNS), including the trigeminal nerves (Figure 3I), the oculomotor nerves (Figure 3K), and the spinal motor nerves (Figure 3L). *Nuk* is therefore most highly expressed in ventral cells of the neural tube and within axons of the PNS.

Axon Pathfinding Defect in *Nuk'* Mutant Brains

Histological analysis of serial sections through a number of *Nuk'/Nuk'* brains revealed defects in a specific axon tract of the forebrain. In all 16 specimens examined, there was a striking reduction in the lateral projection of the anterior commissure. A section through the forebrain of a *Nuk'/+* adult mouse (Figure 4A) exhibited a normal anterior commissure, composed of two major axon pathways: a horseshoe-shaped tract connecting the two olfactory bulbs (pars anterior, acA) and a lateral tract with projections between the two temporal lobes (pars posterior, acP). Sections at similar levels through

Figure 4. Defective Anterior Commissure in *Nuk'* Homozygotes

(A–D) Horizontal sections through the anterior commissure in a *Nuk'/+* (A) and three different *Nuk'/Nuk'* (B–D) adult brains. Anterior is up, and only the left hemisphere of each forebrain is shown. Axon bundles were visualized using interference microscopy. In (A), large acA and acP (arrow) tracts can be observed. In (B)–(D), axon fibers forming the acP tract were absent or much reduced (arrows). A third much smaller tract that is not affected by the *Nuk'* mutation can also be identified behind the acP fibers (arrowheads).

(E–I) *In vivo* dye tracing of the anterior commissure and optic nerve in adult mice.

(E) Diagram outlining the brain and the strategy used to trace the acP and acA axons with fluorescent dyes. The left olfactory bulb and temporal cortex are indicated, as are their associated commissural axon tracts.

(F) Dye injection into an olfactory bulb of a *Nuk'/Nuk'* animal properly traced the axons in the acA tract (arrow) and labeled cells in the contralateral olfactory bulb (asterisk).

(G) Dye injection into the retina of a *Nuk'/Nuk'* animal traced the axons in the optic nerve (arrow) as they near the optic chiasma (oc). As in wild-type mice, a majority of the labeled retinal ganglion cell axons in *Nuk'* mutants crossed the midline in the chiasma (asterisk).

(H and I) Injections of dye into the temporal cortex were used to label the acP axons. The right panels show the site of injection, the middle panels show sections at the midline where the acA and acP tracts converge, and the left panels show sections of the contralateral temporal cortex.

(H) In a *Nuk'/+* specimen, the acP tract was labeled (arrow), as were cells in the contralateral anterior commissure (left panel), indicating a functional anterior commissure.

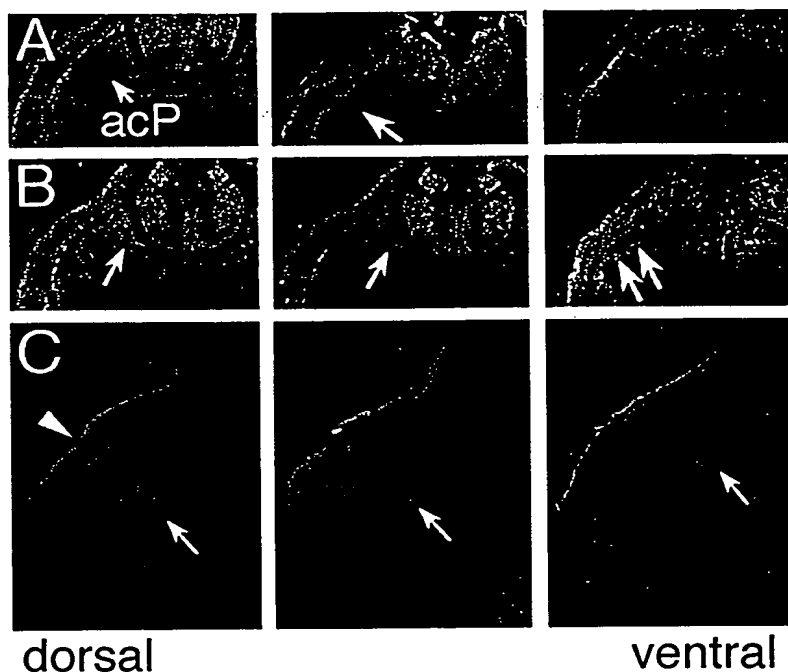


Figure 5. Abnormal Migration of acP Axons in *Nuk1* Homozygotes

(A and B) Serial horizontal sections of neonatal (P_0) brains at the level of the anterior commissure viewed under interference contrast microscopy. Sections (3) of each specimen are shown with the most ventral section depicting the floor of the brain on the right and more dorsal sections to the left.

(A) In a *Nuk1/+* brain, the acA and acP tracts have formed thick bands of fibers crossing the midline. The acP tract is marked by arrows.

(B) A much reduced acP tract was evident in the brain of a *Nuk1/Nuk1* littermate (arrows). In the most ventral section, groups of bundled axons were observed to have abnormally migrated towards the floor of the brain (paired arrows).

(C) Dye tracing of the temporal cortex in a *Nuk1/Nuk1* neonatal (P_0) brain. Dil crystals were placed into the temporal cortex of fixed brains and allowed to trace the cortical axon fibers. Fluorescent images of horizontal sections corresponding to the ventral-most floor of the brain of one mutant are shown. The site of Dil placement in the temporal cortex is indicated (arrowhead). These sections document accumulations of Dil-labeled cortical axons that have migrated improperly towards the floor of the brain (arrows).

Nuk1/Nuk1 adult brains revealed a marked reduction of the acP axon tract (Figures 4B–4D). In adult brains, the acP tract was over 300 μ m thick, whereas, in all cases examined, the acP in *Nuk1/Nuk1* homozygotes was reduced to less than 100 μ m. The specificity of this defect to the acP tract was highlighted by the presence of a normal acA tract in the mutants.

To analyze this phenotype in greater detail, in vivo axon tracing experiments were performed on major forebrain commissures, using vital fluorescent dyes. In separate experiments, axons corresponding to the acP tract, acA tract, corpus callosum, or optic nerve were labeled by injecting a small amount of dye into the appropriate location of deeply anesthetized mice (Figure 4E). Injected dye was then allowed to trace the axons in revived animals for 48 hr, after which brain tissues were serially sectioned and viewed under fluorescent microscopy. For the acA tract (Figure 4F), the corpus callosum (data not shown), and the optic nerve (Figure 4G), dye-tracing experiments revealed that labeled axons had properly crossed the midline to form normal functional pathways. To analyze the axonal projections of the acP tract, Fast Blue was injected into the pyramidal layer of the temporal cortex. As shown for a *Nuk1/+* brain, a small amount of injected Fast Blue readily traced the acP tract and labeled neurons in the contralateral temporal cortex (Figure 4H). However, as the acP tract is much reduced in *Nuk1/Nuk1* homozygotes, few if any Fast Blue-labeled neurons were observed in the contralateral temporal lobe of mutant brains even when greater amounts of the dye were injected ($n = 6$; Figure 4I).

To understand whether the acP tract forms normally and then degenerates later in life or whether it fails to

form during embryonic development, we analyzed neonatal brains by serial sectioning and dye-tracing studies. In brains from $+/+$ and *Nuk1/+* animals, the acA and acP tracts were well formed, projecting through the midline into their contralateral targets (Figure 5A). However, in brains from *Nuk1/Nuk1* littermates, only the acA tract was well developed (Figure 5B). In all mutants examined, a much reduced number of acP axon fibers was observed to have migrated towards the midline. Instead, the majority of these axons appeared to have migrated as fasciculated bundles into the ventral floor of the forebrain (Figure 5B, right). To confirm that these axons were inappropriate projections of cortical neurons, Fast Dil was stereotactically placed into the temporal cortex of neonatal brains and allowed to trace in vitro for 6 weeks. For all four *Nuk1/Nuk1* brains analyzed, misdirected axonal material was observed to label the ventral forebrain adjacent to the site of dye placement (Figure 5C). This confirms that the defect in the acP tract associated with the *Nuk1* mutation is primarily due to a failure of the temporal cortical neurons to extend axons laterally towards the midline and subsequently into the contralateral cortex.

Nuk1^{lacZ} Homozygotes Can Exhibit a Normal Anterior Commissure

The brains of adult and newborn mice homozygous for the *Nuk1^{lacZ}* mutation were also analyzed for the presence of an intact anterior commissure. Since the *Nuk1^{lacZ}* fusion protein lacks the *Nuk* tyrosine kinase catalytic domain, it might be anticipated that *Nuk1^{lacZ}* homozygotes would show the same defect as the *Nuk1* mutants. However, in 129 inbred or 129 \times CD1 mixed backgrounds, all *Nuk1^{lacZ}/Nuk1^{lacZ}* adult brains examined ($n = 12$) had

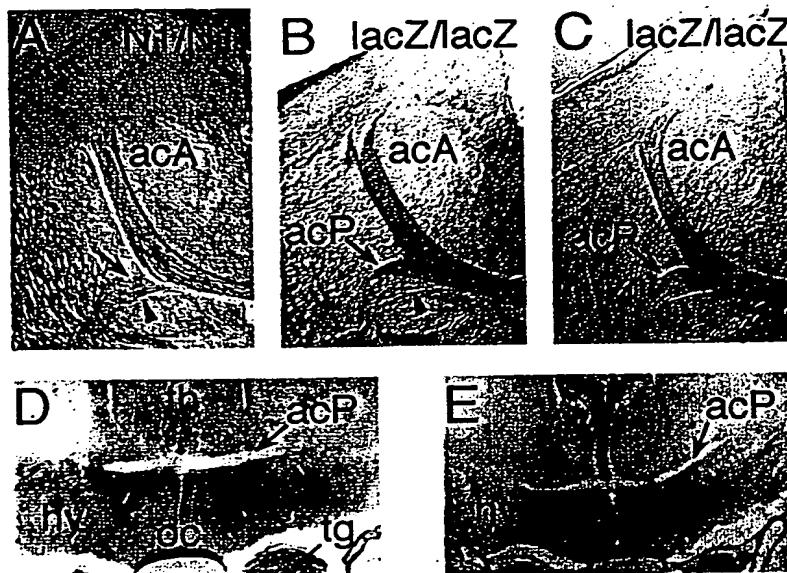


Figure 6. *Nuk^{lacZ}* Homozygotes Exhibit a Normal acP Pathway

(A–C) Horizontal sections through the anterior commissure of a *Nuk^{+/Nuk⁺}* (A) and two different 129 × CD1 *Nuk^{lacZ}/Nuk^{lacZ}* (B and C) adult brains. Interference microscopy revealed a normal bundle of acP axons crossing the midline in the *Nuk^{lacZ}* homozygotes (arrows). (D and E) Coronal sections of *Nuk^{lacZ}/Nuk^{lacZ}* newborn (D) and E16.5 day (E) specimens. The acP tracts were well formed, appearing as a white bundle crossing the midline. These sections were stained for Nuk-βgal, indicating that in this region of the brain, Nuk is most highly expressed in cells of the preoptic area and hypothalamus (hy), which lie directly underneath the acP tract. The acP axons did not stain for Nuk-βgal activity. In these sections, Nuk-βgal staining was localized to retinal ganglion axons in the optic chiasma (oc), in the trigeminal ganglia (tg), and, to a lesser extent, in the thalamus (th).

a normal acP fiber tract (Figure 6). Dye tracing of the temporal cortex further confirmed the presence of a normal acP axon pathway in these brains (data not shown). Volumetric reconstructions from morphometric analysis of the acP tract showed no difference between wild-type and *Nuk^{lacZ}/Nuk^{lacZ}* mice, while *Nuk^{+/Nuk⁺}* mice exhibited up to an 80% reduction in the morphometric volume of the tract (data not shown). The acP tract in the *Nuk^{lacZ}/Nuk^{lacZ}* mutants formed normally during embryonic development and could easily be detected in newborn and E16.5 day specimens (Figures 6D and 6E). These results indicate that a truncated Nuk receptor lacking the tyrosine kinase catalytic domain retains functions required for the pathfinding of temporal cortical axons.

Nuk Expression Marks the Path of acP Axons in the Forebrain

The expression of Nuk in the embryonic forebrain during the stages of acP axon migration and pathfinding was carefully analyzed using both anti-Nuk immunohistochemistry (data not shown) and by staining for Nuk-βgal activity (Figure 7). At E14.5, high expression of Nuk was detected specifically within the cells of the hypothalamus and preoptic area directly underneath the acP axon fibers. Remarkably, there was very little to no expression in the acP axon bundles or in the cells of the brain directly above the commissure (see also Figure 6D). The acP axons appear to have traversed above the Nuk-expressing cells in the hypothalamus and preoptic area such that by E14.5 the leading growth cones have reached the midline, which has yet to fuse and remains separated by the third ventricle. As these axons accumulate near the midline, transient structures form similar to Probst's bundles (Probst, 1901), which appear to be bounded both below and above by Nuk-expressing cells (see Figures 7D and 7G). By E15.5, acP axons from both sides will have crossed the midline to migrate along the tract set up by the corresponding contralateral part-

ner tract. Thus, the acP axons appear to migrate preferentially along a pathway defined by Nuk expression in the basal forebrain, in such a fashion that these axons do not migrate into the Nuk expression domain. Moreover, in *Nuk⁺* homozygotes, the acP axons inappropriately migrate into this region, which would normally express Nuk.

Transmembrane Ligands Are Detected in the Anterior Commissure

The apparent lack of Nuk expression in the axons forming the acP tract prompted us to examine the expression of the transmembrane ligands that bind Nuk. Antibodies raised against a peptide corresponding to a unique region of the Lerk2 extracellular domain were used to characterize its expression in the forebrain. To test the specificity of this antibody, protein lysates of Lerk2 and Lerk5-transfected Cos1 cells were immunoblotted, and a protein of the expected 38 kDa was detected only in Lerk2-transfected cells (S. Holland, G. Mbamalu, N. Gale, G. Yancopoulos, M. H., and T. P. unpublished data). Anti-Lerk2 immunohistochemistry specifically labeled the acA and acP tracts of the anterior commissure (Figure 8). In related experiments, the extracellular portions of the Elk and Nuk receptors were used as Fc-conjugated affinity reagents to probe for expression of Lerks. These reagents also labeled the anterior commissure, providing further evidence for Lerk expression in this particular axon tract (data not shown).

Discussion

Over the past century, a key interest of developmental neurobiology has been the formation of commissural axon tracts in the brain and spinal cord (Mihalkovics, 1877; His, 1889; Langelaan, 1908; Von Szily, 1912; Johnston, 1913; Suitsu, 1920; Silver et al., 1982; Katz et al., 1983). The results presented in this paper show that Nuk, a member of the Eph receptor tyrosine kinase family that

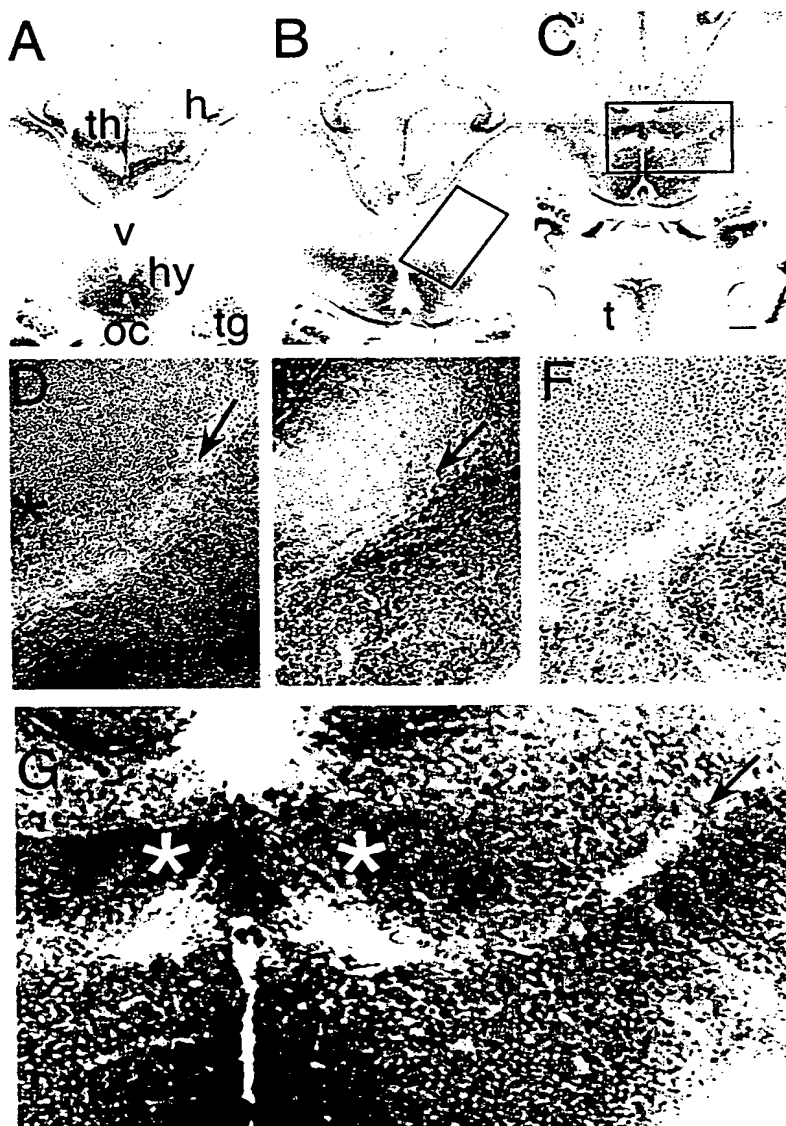


Figure 7. Expression of Nuk-βgal in the Forebrain at E14.5

Coronal sections through the forebrain of 129 × CD1 *Nuk^{lacZ}/Nuk^{lacZ}* embryos were stained for Nuk-βgal activity.

(A–C) Low magnification sections through the forebrain with (A) a more caudal/posterior section than (B) or (C). Nuk-βgal staining was detected in the hypothalamus (hy), the thalamus (th), the hippocampus (h), the optic chiasma (oc), the trigeminal ganglion (tg), and tongue (t). In the more posterior section (A), Nuk expression was detected throughout the hypothalamus, while in sections bisecting the acP tract (B and C), Nuk is restricted to ventral cells.

(D–G) High magnification views of the acP tract. The boxed area in (B) is shown in (D), and the boxed area in (C) is shown in (F) and (G). The axons forming the acP tract appear as white bundled fibers migrating from the temporal cortex through the forebrain, gradually curving toward the midline (arrows). Nuk-βgal was detected in the cells of the hypothalamus underneath the acP and was not observed to label the axons themselves. The only region where strong Nuk-βgal staining was detected above the acP axon fibers was in a patch of cells at the midline, directly above the growth cones that accumulate prior to midline fusion (asterisks in [D] and [G]). Scale bars: A–C, 200 μm; D, E, 50 μm; F, 25 μm.

binds transmembrane ligands, plays a unique role in the guidance of cortical axons that form the anterior commissure. The normal trajectory of these axons correlates with a boundary of Nuk expression in the ventral region of the brain, underlying the path of this commissure.

Nuk Is Required for Pathfinding of the Anterior Commissure

In mice homozygous for the *Nuk*¹ protein-null mutation, the cortical axons forming the acP tract are misrouted and appear to project as fasciculated bundles into the ventral floor of the brain. Fluorescent dye-tracing studies of the cortical neurons that form the anterior commissure have confirmed a functional defect in communication between the two lobes of the temporal cortex. These observations provide direct evidence that Eph receptors are involved in the guidance and pathfinding of central nervous system axons. For Nuk, this function appears

to be specific for the acP tract, as other axon pathways appeared normal in the mutant brains, including the partner acA component of the anterior commissure.

A surprising finding is that correct pathfinding of the acP axons in 129 or CD1 mice can be supported by a truncated Nuk receptor that lacks the kinase domain. These results are not without precedent. In *Drosophila*, the essential functions of the *abl* cytoplasmic tyrosine kinase are also independent of its catalytic activity (Henkemeyer et al., 1990). Indeed, tyrosine kinase-inactive forms of *abl* that exhibit proper subcellular localization to axons can rescue the lethality, sterility, and rough-eye phenotypes of *abl* mutant flies. The *abl* kinase activity does become essential when the *abl* mutations are combined with mutations in interacting loci, including the gene *disabled*. Similarly, essential functions for Nuk tyrosine kinase activity have been revealed by the finding that both the *Nuk*¹ and *Nuk^{lacZ}* mutations exhibit similar double-mutant phenotypes when combined with a

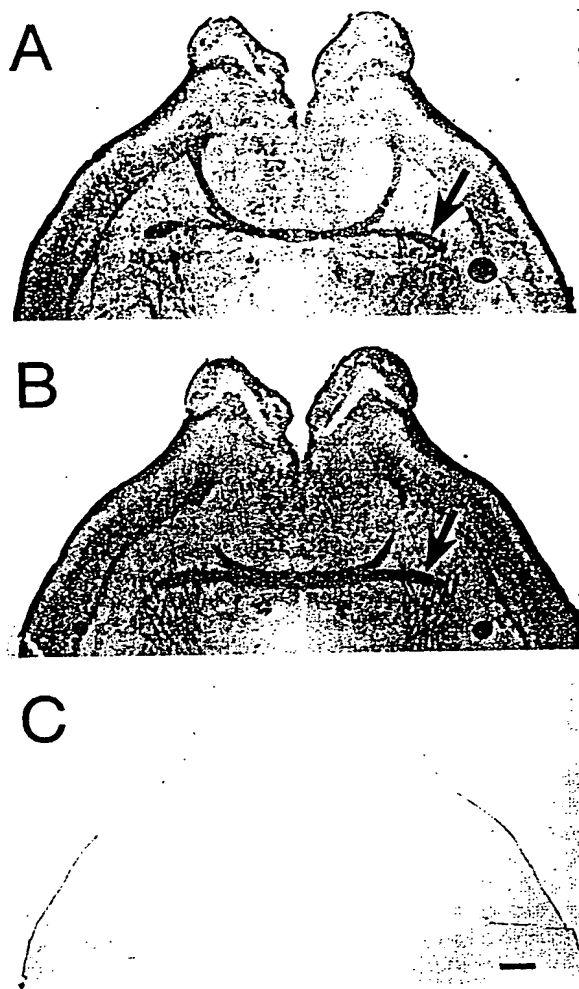


Figure 8. Expression of Lerk2 in the Forebrain
Horizontal sections of newborn brains were probed with affinity-purified anti-Lerk2 antibodies.
(A and B) The acP (arrows) and acA tracts of the anterior commissure were labeled.
(C) Preincubating the anti-Lerk2 antibody with the immunizing peptide abolished all staining. Scale bar: 400 μ m.

mutation in the related *Sek4* gene (Orioli et al., submitted). Furthermore, in a C57BL/6 genetic background, the *Nuk^{lacZ}* mutation induced a defect in the anterior commissure (our unpublished data), suggesting that the Nuk kinase domain may play a role in acP pathfinding that is only evident in specific mouse strains.

How Does Nuk Guide acP Axons?

The defective pathfinding of the acP axons is consistent with the restricted expression of Nuk in the ventral forebrain. Even during early stages of neural development, the highest levels of Nuk protein are found in the ventral-most cells along the midline of the neural plate. Moreover, as the neural tube closes (and throughout embryonic development), the brain and spinal cord continue to express Nuk almost solely in ventral-cell types, with the most intense levels being detected in the forebrain and midbrain (see Figures 3H and 3J). Well before the

birth of the cortical neurons that will extend acP axons, the early expression of Nuk in the ventral forebrain marks cells that will eventually form the preoptic area and hypothalamus.

An expectation arising from the defect in acP axon guidance in *Nuk¹* homozygous mice is that Nuk should be expressed in the commissural axons and function in these cells to control growth cone motility in response to transmembrane ligands in surrounding cells. However, expression analysis of Nuk and its ligands in the region of the developing commissure indicates that this scheme may be too simplistic. Nuk was not detected at significant levels in the acP axon fibers themselves. Instead, we found high levels of Nuk expressed specifically in cells of the preoptic area and hypothalamus immediately ventral to the commissure. In contrast, transmembrane ligands (i.e., Lerk2) were identified in the acP axons. Hence, although it is possible that a low level of Nuk is present and functions in the acP axons, an alternative model is that correct pathfinding of axons forming the anterior commissure depends on Nuk expression in the ventral cells over which the acP axons migrate. This latter hypothesis is more consistent with the expression data of Nuk and its ligands. Thus, the role of Nuk in guiding acP axons may not be cell-autonomous, in the sense that Nuk is not significantly expressed in the axons that are affected by the *Nuk¹* mutation.

As shown in Figure 7, by E14.5 the axons of the anterior commissure have migrated from the temporal cortex across one side of the brain, and their growth cones accumulate near the midline. In these sections, Nuk expression in the preoptic area and hypothalamus appeared to mark a pathway along which the acP axons migrate. In wild-type and *Nuk^{lacZ}* homozygotes, very few axon fibers were observed to stray from this trajectory and project into the Nuk-expression domain. However, in *Nuk¹* homozygotes, the great majority of the acP axons migrated aberrantly, projecting down into the region of the ventral forebrain that would normally express Nuk. The most straightforward interpretation of these observations is that the Nuk receptor exerts a repulsive function that prevents acP axons from migrating ventrally into the preoptic area and hypothalamus.

Support for the idea that Nuk provides a cue to guide acP axons came from a close examination of Nuk expression along the path of the developing axon tract, which indicated that a small pocket of nonexpressing cells formed near the midline (Figure 7G). The growth cones of the acP axon fibers appear to migrate into this pocket and to accumulate prior to fusion of the midline, in an area where they are bounded by Nuk-expressing cells on all sides. Midline fusion would then provide a route for the axons to cross and migrate towards the contralateral cortex. In the scheme proposed above in which Nuk may have a repulsive effect on axon migration, Nuk expression can be envisaged as forming a conduit that, through its inhibitory effects, would force the migration of acP axons towards and ultimately across the midline.

The suggestion that Nuk acts in cells in the brain ventral to the acP tract, rather than in the axons themselves, may explain the finding that these axons project normally to their contralateral targets in 129 and CD1

Nuk^{lacZ} homozygotes. The ability of the *Nuk-βgal* fusion to promote normal pathfinding of the anterior commissure suggests that the extracellular, transmembrane, or juxtamembrane regions of *Nuk* are critical for acP guidance, and that the tyrosine kinase catalytic domain is not.

How might the kinase-defective *Nuk-βgal* fusion protein control axon guidance? It is possible that *Nuk-βgal*, which retains the juxtamembrane region containing potential autophosphorylation sites, can form heterodimers with other Eph receptors such as *Sek4* and thereby contribute to intracellular signaling and axon pathfinding. However, as neither *Nuk⁺* nor *Nuk-βgal* are significantly localized to the acP axons, they are unlikely to act in a cell-autonomous fashion within the anterior commissure. Conceivably, *Nuk-βgal*, by heterodimerizing with other Eph family receptors, could function in the preoptic area and hypothalamus to regulate cell adhesion molecules involved in axon migration. However, since *βgal* is only catalytically active as a tetramer, the *Nuk-βgal* fusion protein must homooligomerize through its *βgal* moiety, perhaps interfering with its ability to heterodimerize with other Eph receptors. This may explain why *Nuk-βgal* does not exhibit a dominant-negative phenotype, even though this might have been anticipated (Xu et al., 1995).

An alternative explanation for our observations is that the extracellular domain of *Nuk⁺* or *Nuk-βgal*, when expressed on the surface of cells in the preoptic area and hypothalamus, provides a direct signal that guides the migration of acP axons. This could be achieved if transmembrane Lerks, which are apparently expressed on acP axons, themselves function as signaling molecules upon interaction with the *Nuk* extracellular domain. Both *Lerk2* and *Lerk5* have highly conserved 83 amino acid cytoplasmic domains and are identical in their C-terminal 33 residues, including several potential tyrosine phosphorylation sites (Beckmann et al., 1994; Davis et al., 1994; Fletcher et al., 1994; Shao et al., 1994; Bennett et al., 1995; Bergemann et al., 1995; Kozlosky et al., 1995). Furthermore, we have noted that both *Lerk2* and *Lerk5* become highly phosphorylated on tyrosine when coexpressed in Cos cells with an activated Src cytoplasmic tyrosine kinase (S. Holland, G. Mbamalu, N. Gale, G. Yancopoulos, M. H., and T. P., unpublished data). By receiving guidance cues from the *Nuk* extracellular domain, transmembrane Lerks might then transduce these signals into the acP axons, potentially in conjunction with a tyrosine kinase, resulting in a modification of their migration and pathfinding. This scheme is clearly not incompatible with a signal being transmitted by *Nuk* into the *Nuk*-expressing cells upon contact with the corresponding Lerks. *Nuk* has been shown to localize at sites of cell-cell contact (Henkemeyer et al., 1994), and Lerks are known to stimulate the tyrosine kinase activity of receptors only upon clustering or membrane attachment (Davis et al., 1994). Thus, it is possible that *Nuk* and its transmembrane ligands function in bidirectional signal transduction pathways activated at sites of cell-cell junctions.

Multiple Functions for Eph Receptors and Their Ligands

Nuk is highly localized in the axons of retinal ganglion cells and in the axonal compartment of a broad range

of sensory and motor neurons in the PNS (Henkemeyer et al., 1994; data not shown). This suggests that *Nuk* may act directly within these axons to control neuronal pathfinding or targeting. The lack of any obvious phenotype affecting these structures in *Nuk⁺* or *Nuk^{lacZ}* homozygous mutant mice may be due to the compensating effects of other Eph receptors. The Eph receptor *Mek4*, which binds GPI-linked ligands, is expressed in a temporal-to-nasal gradient in the chick retina, and the Lerks, RAGS, and ELF-1 have been detected in posterior-to-anterior gradients in the tectum (Cheng et al., 1995; Drescher et al., 1995). Furthermore, cells expressing RAGS induce retinal axons to undergo growth cone collapse in vitro (Drescher et al., 1995). These observations have led to suggestions that Eph receptors act in retinal axons to control pathfinding and that repulsive activities of the GPI-linked Lerks may function to establish a topographic map of the retina in the brain. Interestingly, we have also observed a gradient of *Nuk* expression in the retina; however, this receptor forms a ventral-to-dorsal gradient. This raises the possibility that the two different classes of Eph receptors and ligands may serve complementary functions during the pathfinding of retinal ganglion cell axons. Experiments are in progress to investigate whether the retinal-tectal map is affected in *Nuk*-mutant mice.

A direct analysis of Eph receptor function by targeted mutation of the *Nuk* gene in mice has revealed a profound defect in the pathfinding of a specific axon tract of the anterior commissure. While our results show that Eph receptors are indeed important for directing axon migration in the central nervous system, they also indicate that the functions of Eph receptors and their ligands in the brain may be more complex than proposed for the PNS or retinal-tectal system. This is suggested by the finding that *Nuk* is strongly expressed by cells of the brain immediately ventral to the acP migration route, while the transmembrane Lerks are highly localized to the axons of cortical neurons, and by the observation that a kinase-defective form of *Nuk* can suffice to support normal pathfinding of the acP fibers. These results suggest that Eph receptors and their ligands play a dynamic role in controlling cell movements in the developing nervous system.

Experimental Procedures

Nuk Gene Targeting

The *Nuk⁺* targeting vector was constructed by inserting 4 kb and 6.6 kb fragments of cloned 129 strain genomic DNA from the 5' end of the *Nuk* gene into pPNT (Tybulewicz et al., 1991). To construct the *Nuk-lacZ* targeting vector, we first modified a 2.5 kb genomic fragment of *Nuk* by site-specific mutagenesis to contain an *NcoI* restriction site in the exon sequence at codon 622. The *NcoI* site was then used to fuse this *Nuk* exon in-frame with a 3.5 kb *lacZ* cassette (pATG*lacZ*) that also contains at the 3' end an SV40 eukaryotic polyadenylation sequence (Calzonetti et al., 1995). This 6 kb *Nuk-lacZ* fragment served as the 5' arm and was cloned into pPNT. The 3' arm consisting of a 5 kb *Nuk* genomic fragment was subsequently inserted between the *neo* and *tk* selection cassettes. Linearized targeting vectors were electroporated into the ES cell line R1 (Nagy et al., 1993), and colonies were isolated following selection in G418 and gancyclovir (Wurst and Joyner, 1993), expanded, and genomic DNA screened by Southern blotting. The frequency of homologous recombination was 10 of 215 (*Nuk⁺*) and 3 of 125 (*Nuk^{lacZ}*) cell lines screened. Germline transmission was obtained by generating congenic chimera with targeted ES cells (Nagy et al., 1993).

Biochemical Analysis

For the *in vitro* kinase assay, individual embryos were collected, and yolk sac DNA was used to genotype for the *Nuk*⁻ mutation. Embryo lysates were prepared, and *in vitro* kinase assays were performed essentially as described (Henkemeyer et al., 1994).

For biotinylation of cell-surface proteins, primary cultures of brain cells were obtained by treating postnatal day 4 (P₄) brains with trypsin/EDTA and plating in Dulbecco's modified Eagle's medium supplemented with 20% fetal calf serum. After 2 days, adherent cells were passaged onto two plates and allowed to recover for a further 2 days. The extracellular region of cell-surface proteins from these cultures was labeled with N-hydroxy succinimide-biotin (Calbiochem). Adherent cells were washed two times in phosphate-buffered saline (PBS) containing Ca²⁺ and Mg²⁺ and then incubated two times with rocking for 30 min each at room temperature in freshly diluted 0.5 mg/ml N-hydroxy succinimide-biotin in PBS containing Ca²⁺ and Mg²⁺. Cells were washed by rocking for 10 min at room temperature in Dulbecco's modified Eagle's medium plus 10% fetal calf serum to quench excess N-hydroxy succinimide-biotin and then washed two times in PBS containing Ca²⁺ and Mg²⁺. Cells were lysed in TxLB (1% Triton X-100, 138 mM NaCl, 20 mM Tris [pH 8.0], 2 mM EDTA, 10% glycerol, plus protease inhibitors) and protein concentrations determined by a bicinchoninic acid assay (Pierce). Immunoprecipitations were performed with 250 µg/ml of lysate and either anti-Nuk (Henkemeyer et al., 1994) or anti-βgal (Cappel #55976) rabbit antisera and Protein A-sepharose. Alternatively, avidin-agarose beads were used to precipitate biotinylated proteins. Immunoprecipitates were washed three times in TxLB, denatured, resolved on 8% polyacrylamide gels, and transferred to Immobilon-P membranes (Millipore). The membranes were blocked using 1% gelatin in TBST (0.05% Tween-20) and then Western-blotted in TBST plus 0.5% gelatin with avidin-HRP (BioRad, 1:50,000) followed by chemiluminescence (ECL, Amersham). Anti-βgal or anti-GAP (Ellis et al., 1990) Western blots utilized Protein-A-HRP (BioRad) as the secondary reagent.

Nuk-βgal Staining

For whole-mount staining, embryos were collected in 0.1 M PBS (pH 7.3), incubated at room temperature for 30 min in fresh lacZ fix buffer (0.2% glutaraldehyde, 5 mM EGTA, 2 mM MgCl₂ in PBS), rinsed several times in wash buffer (2 mM MgCl₂, 0.02% NP-40 in PBS), and incubated at 37°C overnight in lacZ staining buffer (wash buffer containing 1 mg/ml X-gal, 2.12 mg/ml potassium ferrocyanide, and 1.64 mg/ml potassium ferricyanide). Embryos were then rinsed in wash buffer, postfixed in formalin, dehydrated in an ethanol series, and cleared in benzyl alcohol:benzyl benzoate (1:2) immediately prior to observation and photography. For histochemical analysis, embryos were dehydrated in ethanol, embedded in paraffin, sectioned at 6 µm, and counterstained with nuclear-fast red.

For later stages of development, unfixed specimens were embedded in OCT and immediately cryosectioned at 15 µm. Air-dried sections were immersed in lacZ fix buffer for 8–10 min at room temperature, rinsed through multiple changes in wash buffer for 20 min, incubated at 37°C overnight in lacZ staining buffer, rinsed in wash buffer, postfixed in formalin, and counterstained with nuclear-fast red.

Bright-field photography was carried out with a Wild M10 microscope or a Leitz DMRXE compound microscope using Kodak EPY 64 tungsten slide film.

Immunohistochemistry

Newborn mouse heads were fixed at 4°C for 24 hr in 4% paraformaldehyde in PBS, washed at 4°C in PBS, embedded in OCT, cryosectioned at 15 µm, and allowed to air dry overnight. Immunohistochemistry using 4 µg/ml of affinity-purified anti-Nuk antibodies (Henkemeyer et al., 1994) or anti-Lerk2 (A-20) antibodies (Santa Cruz Biochemicals) was performed with the ABC Elite detection system (Vector Laboratories).

Morphological Analysis of Mutant Brains

Adult mice were anesthetized and perfused with 20 ml PBS, followed by 40 ml of 4% paraformaldehyde. Tissues were then dissected, postfixed in 4% paraformaldehyde, equilibrated in 30% sucrose, and embedded in OCT, and 30 µm serial horizontal sections were

obtained through the desired region using a Reichert-Jung model 2800 frigocut E cryostat. Samples were photographed using a Leitz wetzlar scope equipped with interference contrast optics mounted on a 360° rotating slide platform.

Dye Tracing of Mutant Brains

Axons forming the optic nerve were labeled by injecting approximately 1 µl of 1% rhodamine B dextran (Molecular Probes) into the retina of anesthetized adult mice through a microneedle that obliquely penetrated the corneal-scleral boundary. Axons forming the acA tract were labeled by injecting into anesthetized mice approximately 1 µl of 1% rhodamine B dextran into the anterior portion of the olfactory bulb. Axons forming the acP tract in adult mice were labeled by injecting into anesthetized mice 0.4–1.8 µl of 3% Fast Blue (Gross Umstat) stereotactically into the temporal cortex (0.5 mm ventral to the ventral boundary of the junction of the frontal and parietal bones, immediately anterior to the zygomatic arch; at an angle of 110° from the vertical, at a depth of 1.0 mm). Injected dye was allowed to trace axons *in vivo* in resuscitated animals for 48 hr. The animals were then perfused with paraformaldehyde, and serial sections through the appropriate brain tissue were obtained and viewed under fluorescence microscopy.

Acknowledgments

Correspondence should be addressed to T. P. We thank D. Rossi for assistance with ES cell cultures, K. Harpel for paraffin sections, T. Calzonetti for the pATG/lacZ plasmid, and G. Yancopoulos and T. Hunter for discussion. Postdoctoral support for M. H. came from the Medical Research Council of Canada (MRC) and for J. T. H. from the Rick Hansen Society. Predoctoral support for T. M. S. came from an MRC studentship and for D. O. from an EMBL fellowship. This work was supported by a grant from Bristol-Myers-Squibb, a Terry Fox programme grant from the National Cancer Institute of Canada (NCIC), a Howard Hughes International Research Scholar Award to T. P., and a grant from the Deutsche Forschungsgemeinschaft to R. K. T. P. is a Terry Fox Cancer Research Scientist of the NCIC.

Received February 1, 1996; revised May 17, 1996.

References

- Bartley, T.D., Hunt, R.W., Weicher, A.A., Boyle, W.J., Parker, V.P., Lindberg, R.A., Lu, H.S., Colombero, A.M., Elliott, R.L., Guthrie, B.A., and 10 others. (1994). B61 is a ligand for the ECK receptor protein-tyrosine kinase. *Nature* 368, 558–560.
- Beckmann, M.P., Cerretti, D.P., Baum, P., Vanden Bos, T., James, L., Farrah, T., Kozlosky, C., Hollingsworth, T., Shilling, H., Maraskovsky, E., Fletcher, F.A., Lhotak, V., Pawson, T., and Lyman, S.D. (1994). Molecular characterization of a family of ligands for the eph-related tyrosine kinase receptors. *EMBO J.* 13, 3757–3762.
- Bennett, B.D., Zeigler, F.C., Gu, Q., Fendly, B., Goddard, A.D., Gillett, N., and Matthews, W. (1995). Molecular cloning of a ligand for the Eph-related receptor protein-tyrosine kinase Htk. *Proc. Natl. Acad. Sci. USA* 92, 1866–1870.
- Bergemann, A.D., Cheng, H.J., Brambilla, R., Klein, R., and Flanagan, J.G. (1995). ELF-2, a new member of the Eph ligand family, is segmentally expressed in mouse embryos in the region of the hindbrain and newly forming somites. *Mol. Cell. Biol.* 15, 4921–4929.
- Brambilla, R., and Klein, R. (1995). Telling axons where to grow: a role for Eph receptor tyrosine kinases in guidance. *Mol. Cell. Neurosci.* 6, 487–495.
- Brambilla, R., Schnapp, A., Casagrande, F., Labrador, J.P., Bergemann, A.D., Flanagan, J.G., Pasquale, E.B., and Klein, R. (1995). Membrane-bound LERK2 ligand can signal through three different Eph-related receptor tyrosine kinases. *EMBO J.* 14, 3116–3126.
- Calzonetti, T., Stevenson, L., and Rossant, J. (1995). A novel regulatory region is required for trophoblast-specific transcription in transgenic mice. *Dev. Biol.* 171, 615–626.
- Cheng, H.J., and Flanagan, J.G. (1994). Identification and cloning of ELF-1, a developmentally expressed ligand for the Mek4 and Sek receptor tyrosine kinases. *Cell* 79, 157–168.

- Cheng, H.J., Nakamoto, M., Bergemann, A.D., and Flanagan, J.G. (1995). Complementary gradients in expression and binding of *Elk-1* and *Mek4* in development of the topographic retinotectal projection map. *Cell* 82, 371-381.
- Davis, S., Gale, N., Aldrich, T.H., Maisonpierre, P.C., Lhotak, V., Pawson, T., Goldfarb, M., and Yancopoulos, G.D. (1994). Ligands for the EPH-related receptor tyrosine kinases that require membrane attachment or clustering for activity. *Science* 266, 816-819.
- Dickson, B., and Hafen, E. (1994). Genetics of signal transduction in invertebrates. *Curr. Opin. Genet. Dev.* 4, 64-70.
- Drescher, U., Kremoser, C., Handwerker, C.J.L., Noda, M., and Bonhoeffer, F. (1995). In vitro guidance of retinal ganglion cell axons by RAGS, a 25 kDa tectal protein related to ligands for Eph receptor tyrosine kinases. *Cell* 82, 359-370.
- Ellis, C., Moran, M.F., McCormick, F., and Pawson, T. (1990). Phosphorylation of GAP and GAP-associated proteins by transforming and mitogenic tyrosine kinases. *Nature* 343, 377-381.
- Fletcher, F.A., Carpenter, M.K., Shilling, H., Baum, P., Ziegler, S.F., Gimpel, S., Hollingsworth, T., Vanden Bos, T., James, L., Hjermild, K., Davison, B.L., Lyman, S.D., and Beckmann, M.P. (1994). Lerk-2, a binding protein for the receptor tyrosine kinase ELK, is evolutionarily conserved and expressed in a developmentally regulated pattern. *Oncogene* 9, 3241-3247.
- Henkemeyer, M., West, S.R., Gertler, F.B., and Hoffmann, F.M. (1990). A novel tyrosine kinase-independent function of *Drosophila* *abl* correlates with proper subcellular localization. *Cell* 63, 949-960.
- Henkemeyer, M., Marengere, L.E.M., McGlade, J., Olivier, J.P., Conlon, R.A., Holmyard, D.P., Letwin, K., and Pawson, T. (1994). Immunolocalization of the Nuk receptor tyrosine kinase suggests roles in segmental patterning of the brain and axonogenesis. *Oncogene* 9, 1001-1014.
- His, W. (1889). Die Formentwicklung des menschlichen Vorderhirns vom Ende des ersten bis zum Beginne des dritten Monates. Abhandl. D. Math. Phys. Kl. Kon. Sachs. Akad. Wissensch. Bd. 15, 675-735.
- Johnston, J.B. (1913). The morphology of the septum, hippocampus, and pallial commissures in reptiles and mammals. *J. Comp. Neurol.* 23, 371-478.
- Katz, M.J., Lasek, R.J., and Silver, J. (1983). Ontophyetics of the nervous system: development of the corpus callosum and evolution of axon tracts. *Proc. Natl. Acad. Sci. USA* 80, 5936-5940.
- Kozlosky, C.J., Maraskovsky, E., McCrew, J.T., Vanden Bos, T., Teppe, M., Lyman, S.D., Srinivasan, S., Fletcher, F.A., Gayle, R.B., III, Cerretti, D.P., and Beckmann, M.P. (1995). Ligands for the receptor tyrosine kinases *hek* and *elk*: isolation of cDNAs encoding a family of proteins. *Oncogene* 10, 299-306.
- Langelaan, J.W. (1908). On the development of the large commissures of the telencephalon in the human brain. *Brain* 31, 221-241.
- Letwin, K., Yee, S.-P., and Pawson, T. (1988). Novel protein-tyrosine kinase cDNAs related to *fps/fes* and *eph* cloned using antiphosphotyrosine antibody. *Oncogene* 3, 621-627.
- Lhotak, V., and Pawson, T. (1993). Biological and biochemical activities of a chimeric epidermal growth factor-ELK receptor tyrosine kinase. *Mol. Cell. Biol.* 13, 7071-7079.
- Lhotak, V., Greer, P., Letwin, K., and Pawson, T. (1991). Characterization of Elk, a brain-specific receptor tyrosine kinase. *Mol. Cell. Biol.* 11, 2496-2502.
- Mihalkovics, V. (1877). Entwicklungsgeschichte des Gehirns: Nach Untersuchungen an höheren Wurbeltieren und den Menschen. (Leipzig: W. Engelmann.)
- Nagy, A., Rossant, J., Nagy, R., Abramow-Newerly, W.A., and Roder, J.C. (1993). Derivation of completely cell culture-derived mice from early-passage embryonic stem cells. *Proc. Natl. Acad. Sci. USA* 90, 8424-8428.
- Pandey, A., Shao, H., Marks, R.M., Polverini, P.J., and Dixit, V.M. (1995). Role of B61, the ligand for the Eck receptor tyrosine kinase, in TNG- α -induced angiogenesis. *Science* 268, 567-569.
- Pawson, T., and Bernstein, A. (1990). Receptor tyrosine kinases: genetic evidence for their role in *Drosophila* and mouse development. *Trends Genet.* 6, 350-356.
- Probst, M. (1901). Über den Bau des balkenlosen Grosshirns, sowie über Mikroglyrie und Heterotopie der grauen Substanz. *Arch. F. Psychiatr.* 34, 709-786.
- Shao, H., Lou, L., Pandey, A., Pasquale, E.B., and Dixit, V.M. (1994). Cloning and characterization of a ligand for the *Cek5* receptor protein-tyrosine kinase. *J. Biol. Chem.* 269, 26606-26609.
- Shao, H., Lou, L., Pandey, A., Verderame, M.F., Siever, D.A., and Dixit, V. (1995). cDNA cloning and characterization of a *Cek7* receptor protein-tyrosine kinase ligand that is identical to the ligand (ELF-1) for the *Mek4* and *Sek* receptor protein-tyrosine kinases. *J. Biol. Chem.* 270, 3467-3470.
- Silver, J., Lorenz, S.E., Wahisten, D., and Coughlin, J. (1982). Axonal guidance during development of the great cerebral commissures: descriptive and experimental studies, in vivo, on the role of preformed glial pathways. *J. Comp. Neurol.* 210, 10-29.
- Suitsu, N. (1920). Comparative studies on the growth of the corpus callosum. *J. Comp. Neurol.* 32, 35-60.
- Tessier-Lavigne, M. (1995). Eph receptor tyrosine kinases, axon repulsion, and the development of topographic maps. *Cell* 82, 345-348.
- Tuzi, N.L., and Gullick, W.J. (1994). Eph, the largest known family of putative growth factor receptors. *Br. J. Cancer* 69, 417-421.
- Tybulewicz, V.L.J., Crawford, C.E., Jackson, P.K., Bronson, R.T., and Mulligan, R.C. (1991). Neonatal lethality and lymphopenia in mice with a homozygous disruption of the *c-abl* proto-oncogene. *Cell* 65, 1153-1163.
- Von Szily, A. (1912). Über die einleitenden Vorgänge bei der ersten Entstehung der Nervenfasern im Nervus opticus. *Graefes Arch. Ophthalmol.* 81, 67-86.
- Winslow, J.W., Moran, P., Valverde, J.A.S., Yuan, J.Q., Wong, S.C., Tsai, S.P., Goddard, A., Henzel, W.J., Hefti, F., Beck, K.D., and Caras, I.W. (1995). Cloning of AL-1, a ligand for an Eph-related tyrosine kinase receptor involved in axon bundle formation. *Neuron* 14, 973-981.
- Wurst, W., and Joyner, A.L. (1993). *Gene Targeting: A Practical Approach*. (Cambridge: Oxford University Press).
- Xu, Q., Alldus, G., Holder, N., and Wilkinson, D.G. (1995). Expression of truncated *Sek-1* receptor tyrosine kinase disrupts the segmental restriction of gene expression in the *Xenopus* and zebrafish hindbrain. *Development* 121, 4005-4016.

Note Added in Proof

The data referred to throughout as Gale et al., submitted, are now in press: Gale, N.W., Holland, S.J., Valenzuela, D.M., Flenniken, A., Pan, L., Ryan, T.E., Henkemeyer, M., Strebhardt, K., Hirai, H., Wilkinson, D.G., Pawson, T., Davis, S., and Yancopoulos, G.D. Eph receptors and ligands comprise two major specificity subclasses and are reciprocally compartmentalized during embryogenesis. *Neuron* 17, in press.



D 21

Genomic structure of the *EPHA1* receptor tyrosine kinase gene

D. Owshalimpur and M. J. Kelley*

Lung Cancer Biology Section, National Cancer Institute,
Bethesda, MD 20889-5105, USA

Copied by uni. of Qld Library
Herston Medical Library for Supply
under S.50 of Copyright Act 1968

22 FEB 2000

(Received 26 October 1998, Accepted 30 December 1998)

Some receptor tyrosine kinase genes are mutated in inherited and somatically acquired human cancers. To permit mutational analysis, the complete genomic structure of the human *EPHA1* gene on chromosome 7q34 was determined and oligonucleotide pairs were designed to amplify coding regions. The gene contains 18 exons, two more than the related tyrosine kinase, *EPHB2*. Presumed sequencing errors in the published cDNA sequence of *EPHA1* were identified in exons 10 and 11. Availability of this information will facilitate mutational analysis of *EPHA1*.

KEYWORDS: exon, intron, mutation, evolution, genomic structure.

INTRODUCTION

Receptor tyrosine kinases are a large family of transmembrane molecules that includes the platelet-derived growth factor (PDGF), epidermal growth factor (EGF), fibroblast growth factor/heparin binding growth factor (FGF/HBGF), and insulin receptor subfamilies. These molecules transduce extracellular signals involved in various cellular processes.¹ Mutation of tyrosine kinases have been implicated in pathogenesis of human cancer. Germline mutations of *MET* and *RET* proto-oncogenes have been found in hereditary papillary renal cancer¹ and multiple endocrine neoplasia type II,² respectively, and acquired mutations of *MET* have been found in sporadic papillary renal cell cancer.¹ Mutations of *MET* in hereditary papillary renal cell cancer are associated with trisomy of chromosome 7, on which *MET* is located, suggesting that duplication of the mutated copy of *MET* is a second alteration necessary for malignant transformation. Thus, trisomy may be associated with tyrosine kinase mutation.

About 30% of sporadic colon, lung and kidney tumours have trisomy of chromosome 7.³ However, *MET* mutations were found in only 3 of 60 (5%) sporadic papillary renal tumours¹ and have not been reported in colon and lung tumours. Thus, mutations of other tyrosine kinase receptors on chromosome 7 may be found in these tumour types.

EPHA1 (also known as eph) is located at chromosome 7q34 and is the prototype for a 14 member subfamily of the tyrosine kinase receptor family.^{4,5} When bound to the appropriate ligand (known as ephrins) these receptors have been shown to modulate cellular growth, differentiation and mitogenic activities.⁶ Some members of the eph family, including *EPHA1*, have been implicated in carcinogenesis.⁷ *EPHA1* is expressed in a subset of human cancer cell lines,⁸ and transfection of the full length cDNA into NIH-3T3 cells results in increased colony formation in soft agar and development of tumours in nude mice.⁸ The genomic structure of only the tyrosine kinase domain of the *EPHA1* has previously been determined.⁸ Therefore, as a prerequisite to mutational analysis of

*Author to whom all correspondence should be addressed at: Hematology/Oncology (111G), Duke University/V.A. Hospital, 508 Fulton Street, Durham, NC 27705, USA. Tel: +1 919 286 6944; Fax: +1 919 286 6896; E-mail: kelleym@duke.edu

Table 1. Exon characteristics and amplification primers for *EPHA1*

Number	Exon size (bp)	Intron ^a size (bp)	Amplification primers	Annealing temperature	Amplified size ^b (bp)
1	82	ND	TCCCTTGCAACCTGGCGCTG GGTCGGTACCTTCCTTGGCG	70	154
2	68	ND	TTAGGAACAGGATGTTGCAGC ACTGGCCTTCCAGGAGTTTT	60	227
3	282	~1160	TCTACTGTCCTGGAGCTGAGG CATTCCCAAACTCAGTGCCA	65	1254
4	403	237	AAAATCACCTGGGCATGGTG GGAGAGAGAACGCAGCAGAG	65	1539
5	156	312	GAGATGTTTCCAGTAGAAGGG CAGAGAAGCTCAGGTTTCGG	65	605
6	345	152	ACATGGACACACCCCATTTG GTCCAGAGGGATAAGGTTGG	65	932
7	125	250	GAAGCCCAAAATGGAGTGTC GGAAAACGAGAATCCCAAGC	65	1112
8	154	250	GAAGCCCAAAATGGAGTGTC GGAAAACGAGAATCCCAAGC	65	1112
9	97	198	AACTCAGCTCCTGTTCACG GTAGCAAAACACAAGAGCCC	60	731
10	59	793	AACTCAGCTCCTGTTCACG GTAGCAAAACACAAGAGCCC	60	731
11	126	~943	AAACAGGAGTCACCTTGGGAAAC AACTCTTGGACCAGAGAAGCCAG	65	375
12	186	136	GGGAGACAGTGGTGAATAGG CTGTGATGATCATGATCGGC	65	559
13	186	106	CAGTGGTGGAACCTTCCTTCG GAAGCTTCTGGAAGTGTTGGC	65	1669
14	207	464	CAGTGGTGGAACCTTCCTTCG GAAGCTTCTGGAAGTGTTGGC	65	1669
15	150	329	CAGTGGTGGAACCTTCCTTCG GAAGCTTCTGGAAGTGTTGGC	65	1669
16	194	ND	TTATCTTGTGTGACCGTCGG CGTCTTGCCCTCATACACTGG	60	406
17	156	ND	TTCAGCTTCCTCTCAGACAGG AAGAATGCGCTTCTGGTGC	65	649
18	79		GACACCATGGAGTGTGTGCT CCCCACCTCCCTTTTAAAC	65	386

^aSize of intron following indicated exon; introns with exact sizes stated were completely sequenced, while others were partially sequenced.

^bExons 7–8, 9–10 and 13–15 are amplified with a single polymerase chain reaction each.

ND=no data

EPHA1 in cancer, we determined the complete intron/exon structure of this gene to allow amplification of the coding regions using genomic DNA as template.

MATERIALS AND METHODS

Polymerase chain reaction (PCR) was performed in 100 µl reaction volume containing 1X PCR buffer, 1.5 mM MgCl₂, 5 units *Taq* platinum (Life Technologies, Gaithersburg, MD, USA), 0.2 mM each dNTP, and 0.2 µM each oligonucleotide primer. Typical cycling conditions were initial denaturation of 94°C for 2 min followed by 30–40 cycles of 94°C for

30 s, annealing temperature (see Table 1) for 30 s, and 72°C for 2 min and final extension time of 10 min at 72°C. Polymerase chain reaction products were purified using QIAquick Spin PCR Purification Columns (Qiagen, Santa Clarita, CA, USA) per manufacturer's recommendations. An *EPHA1* BAC clone was obtained by screening a human BAC library (Research Genetics, Huntsville, AL, USA) with *EPHA1* oligonucleotides from both the 5' and 3' end of the cDNA. Approximately 400 ng of the PCR product or 2 µg of BAC plasmid DNA was sequenced using BigDye terminator kit (Perkin Elmer, Norwalk, CT, USA). DNA sequences have been submitted to GenBank (AF101165–AF101171).

Exon 1	gcccggagctATGGAGCGCGCTGGCCCTGGGCTAGGGCTGGTGGTCTGCTCT GGCCCCCGCTGCCCGGGGGGCGCGCCCAAGGAAGgtaccgacc	GGTGGAACTTCTTCGAGAGGCAACTATCATGGGCGCATTTAGCCACCCGCATTT CTGCATCTGGAAGCGCTCGTCACAAAGgtacgagag	
Exon 2	ccacttttcagTTACTCTGTAGGACACAAGCAAGSCACAGGAGAGCTGGGCTGGCT GCTGGATCCCCCAAAGATGGGgttaagtgc	Exon 13	tgtgtctcagGAAAGCGATCATGATCATACAGAATTATGGAGAATGGAGCCCT GGATGCCTTCTGAGGgtgagggag
Exon 3	ctctctgcagTGGAGTGAACAGCAACAGATACTGAATGGGACACCCCTGTACATGT ACCAGGACTGCCCAATGCAAGGACGACAGACTGACCACTGGCTTCGCTCCAAT TGGATCTACCGCGGGGAGGAGCTTCCCGCTCAGCTGGAGCTGACGTTACCGT CGGGAGCTGCAAGAGTTTCCCTGGGGAGCGGGCTCTGGGCTGCAAGGAGACCT TCAACCTTCTGTACATGGAGAGTACCAAGATGTTGGCATTcagctccgac	Exon 14	cctgtctcagGAGCGGGAGGACAGCTGTTCTCTGGGACAGTAGTGGCCATGCTGC AGGGCATAGCATCTGGCATGAACTACCTGAGTAATCACAATTATGCCACCGGAC CTGGCTGCCAGAAACATCTTGGTGAATCAAACTGTGCTGCAAGGTGTCTGACTT TGGCCTGACTCGCCTCTGGATGACTTGTATGGACATACGAAACCAAGgttagag gcc
Exon 4	ttctaccagGTAACACGGTGGCTGCAGACAGAGCTTCAACATTGAGACCTTG CGTCTGGCTCCGTGAAGCTGAATGTGGAGCGCTGCTCTCTGGGCGCTGACCCGC CGTGGCTCTACCTCGCTTCCACAACCGGGTGCCTGTGTGGCCCTGGTGTCTGT CCGGTCTTCTACCAAGCTGTCTGAGACCTGAATGGCTTGGCCAATTCCCAAG ACACTCTGCTGGCCCGCTGGTGGTGGTGAAGTGGCGGGGactgcttgc	Exon 15	gccttcttagGGAGAAAGATCCCTATCCCTTGGACAGCCCTGAAGCCATTGCC ATCGGATCTTACCACAGCCAGCGATGTGTGGAGCTTGGGATTGTGATGTGGAG GTGCTGAGCTTTGGGGACAAGCCTTATGGGAGATGAGCAATCAGGAGgtgagccc ag
Exon 5	ctctctccagCCTGCCCTAGCGCTCTACCGGATGGACATGGAACACCCCATG TCTACGTGCCCGCAGCAGAGCACTGCTGAGTCTGAGGGGGCCACCATCTGTACCT GTGAGAGCGGCATTACAGAGCTCCCGGGGAGGGCCCCAGGTGGCATGCACAGgt gagtcag	Exon 16	cgcctgcagGTTATGAAGAGCATTGAGGATGGGTACCGTTGCCCTCTGTGG ACTGCCCTGCCCTCTGTATGAGCTCATGAAGACTGCTGGGCATATGACCGTGC CGCGGCCACACTTCCAGAGCTTCAAGGACATCTGGAGCAACTGCTGCCAACCC CCACTCCCTGCGGACATTGCCAATTGACCCAGgttaaccatgc
Exon 6	ttctccacagTCCCCCTCGGCCCCCGAAACCTGAGTCTCTGCTCAGGGAC TCAGTCTCCCTGCGTGGGAACCCCGCAGCAGTACGGGGGACGCCAGGATGTCA GATACAGTGTGAGGTGTCCAGGTGTGAGGGACAGCAGGACGGGGGGCCCTGC CAGCCCTGTGGGTGGGCGTCACTTCTCGCGGGGGCGGGCGCTACCAACACC TGCAGTGCATGTCAATGGCTTGAACCTTATGCCAATACactttaagt	Exon 17	tgtccacagGGTACTCTTGGCTGCCAGCCTGAGTGGCTCAGATGGGATCCCG TATCGAACCGTCTCTGAGTGGCTGAGTCCATACGCATGAAACGTATCTCTGCA CTTCCACTCGGCTGGGCTGGACACCATGAGTGTGTGCTGGAGCTGACCGTGAgt aaggagct
Exon 7	ggacccccagAGTCACTGTGAGGCTGTCTCTGAGACTGGTGAAGAAAGACCGAG GCAACTAGAGCTGACCTGGGCGGGTCCCGCCCCGAAGCCTGGGGGGAACCTGA CCTATGAGCTGCACGTGCTGAACcaggtcagga	Exon 18	ttgcccacagGGACCTGACGAGTGGGAATCACACTGCCCGGGCACCAGAGCGC ATTCTTTGAGTATTACAGGATTAAGGACTGATCCCTCTCTCACCCCATGCCCA GTCAGGTGCAAGGAGCAAGGACGGGGCCAGGTGGCTCATGTCCTCTCCCTGCGC CCCTTCCCAACCTGCCAGACTAGGCTATCGGTGTGCTTCTGCCACTTTCAGG AGAACCTGTCTGCACCCAGAAACCTCTTTGTTTAAAgggaggtgg
Exon 8	ctccacccacCAGGATGAAGAACCGTACCAGATGGTCTAGAACCCAGGGTCTTGC TGACAGAGCTGCAGCTGACACCATACATCGTCAGAGTCCGAATGTGACCCCA CTGGGCTCTGGCCCTTCTCCCTGATCATGAGTTTCGGACACCCACAGgttg ggatc		
Exon 9	gtgctacagTGTCCAGGGGCTGACTGGAGGAGAGATTGAGCCGTATCTTTGG GCTGCTGCTTGGTGACGCTTGTGCTGGGATCTCTGTTTCCGCTCCAGgtgccc agctc		
Exon 10	AcccccacagGAGAGCCAGCGGCAGAGGAGAGAGGCAAGCTGACCGCCACC GATGTGGATCGAGgtgagtcagg		
Exon 11	ctgcccacagAGGACAAGCTGTGGCTGAAGCCTTATGTGGACCTCCAGGCATAG AGGACCTGACAGGAGCCTTGGACTTTA_CCGGGAGCTTGTATCCAGCTGGCT GATGGTGACACTGTATAGGAGAgtgagtcctg		
Exon 12	ttctaccagGAGAGTTTGGGGAAGTGTATGAGGAGACCTCAGGCTCCCCAGCCA GGAGTCAAGACTGTGGCCATTAAAGCCTTAAAGACACATCCCCAGGTGGCAGT		

Fig. 1. Partial Genomic Sequence of *EPHA1*. Intron sequence is in lower case, exon sequence in upper case. The bold nucleotides in exon 10 and 11 indicate the location of an inserted base pairs compared to the previously published cDNA sequence (GenBank accession number M18391). Underscores in exon 11 indicate the location of deletion of 1 bp and 25 bp, respectively. These sequences and additional intron sequence has been submitted to GenBank (accession numbers AF101165-AF101171).

cDNA by alignment to *EPHB2* [cek5 (Chicken embryo kinase 5)], for which intron/exon borders have been determined.⁹ Using oligonucleotides designed to amplify across the presumed introns, PCR products containing *EPHA1* cDNA sequence were amplified from genomic DNA. Inspection of DNA sequence identified intron/exon borders (Fig. 2).

No PCR products were obtained using this strategy for introns following exons 1, 2, 9, 10 and 17. Instead

RESULTS/DISCUSSION

To determine the intron/exon borders of *EPHA1*, we first predicted the location of introns within the *EPHA1*

Fig. 1. Partial Genomic Sequence of *EPHA1*. Intron sequence is in lower case, exon sequence in upper case. The bold nucleotides in exon 10 and 11 indicate the location of an inserted base pairs compared to the previously published cDNA sequence (GenBank accession number M18391). Underscores in exon 11 indicate the location of deletion of 1 bp and 25 bp, respectively. These sequences and additional intron sequence has been submitted to GenBank (accession numbers AF101165-AF101171).

cDNA by alignment to *EPHB2* [ck5 (Chicken embryo kinase 5)], for which intron/exon borders have been determined.⁹ Using oligonucleotides designed to amplify across the presumed introns, PCR products containing *EPHA1* cDNA sequence were amplified from genomic DNA. Inspection of DNA sequence identified intron/exon borders (Fig. 2).

No PCR products were obtained using this strategy for introns following exons 1, 2, 9, 10 and 17. Instead, a human genomic BAC clone, 494m18, which contains the entire *EPHA1* gene, was obtained and partially sequenced. Intron/exon borders were identified for all exons. Only 9 bp of sequence could be obtained from the 5' end of intron 1, probably due to strong secondary structure in this area. Primers capable of

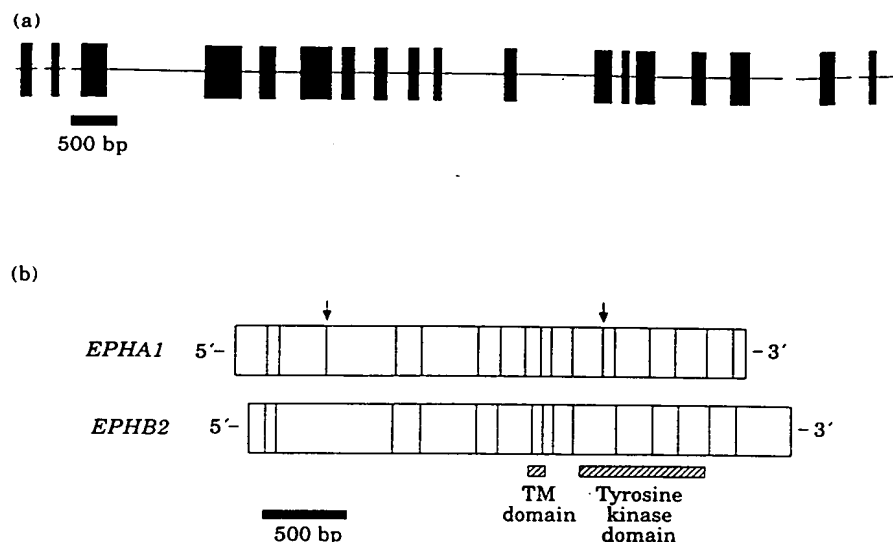


Fig. 2. Schematic representation of the relative size of *EPHA1* introns and exons (a) and relative size and position of *EPHA1* and *EPHB2* exons (b). Only coding regions of exons are shown. Arrows indicate position of *EPHA1* introns not found in *EPHB2*. *EPHB2* based on previously published genomic structure from chicken.⁹

amplifying each exon and adjacent splice sites from genomic DNA were designed (Table 1), with the exception of exon 1, where the primers do not amplify the 11 bp at the 3' end of the exon.

Eighteen coding exons were identified, two more than the related *EPHB2*. There may also be non-coding exons upstream of exon 1, as this region was not sequenced. Alignment of *EPHA1* and *EPHB2* cDNAs indicates that *EPHA1* exons 3–4 and 12–13 correspond to a single exon each in *EPHB2*. Thus, the two additional exons of *EPHA1* (one in the extracellular domain and one in the tyrosine kinase domain) arise by replacement of one *EPHB2* exon with two in *EPHA1*, or conversely, the joining of two exons of *EPHA1* into a single exon in *EPHB2*. Determination of the genomic structure of additional members of this subfamily might distinguish these alternative evolutionary events.

The coding regions contained multiple sequence variations from the published *EPHA1* cDNA sequence.¹⁰ Four of these variations (insertion of G after nucleotide 1835, insertion of G after nucleotide 1876, deletion of nucleotide 1893, and deletion of nucleotides 1939–1963; Fig. 1) result in reading frame shifts and likely represent sequencing errors in the original cDNA sequence. Alternate splicing of the involved exons (10 and 11) was excluded by complete sequencing of the intervening introns. These four frameshifts are absent from an unreferenced partial *EPHA1* cDNA (GenBank accession number Z27409). Therefore, the correct *EPHA1* protein contains a

unique stretch of 36 amino acids between the transmembrane and tyrosine kinase domains in place of 44 amino acids in the published sequence.

Additional variations noted were three missense changes (nucleotide 1286, GCG Ala to GGG Gly; nucleotide 2240, GCA ala to GGA Gly; and nucleotide 2340, GCA Ala to GGA Gly), three silent changes (nucleotide 282, C to G; nucleotide 780, C to G; and nucleotide 1929, T to C), and three changes in the 3' untranslated region (nucleotide 3072, A to G; nucleotide 3175, G to A; and nucleotide 3180, A to C). Each of these variants may represent sequencing errors or polymorphisms. The determination of the correct cDNA sequence and complete genomic structure, as well as identification of primers capable of amplifying the coding regions, will now allow analysis of the role intragenic mutation of *EPHA1* plays in human cancer.

©1999 US Government

REFERENCES

- Schmidt, L., Duh, F. M., Chen, F. *et al.* (1997). Germ-line and somatic mutations in the tyrosine kinase domain of the MET proto-oncogene in papillary renal carcinomas. *Nature Genetics* 16, 68–73.
- Mulligan, L. M., Kwok, J. B., Healey, C. S. *et al.* (1993). Germ-line mutations of the RET proto-oncogene in multiple endocrine neoplasia type 2A. *Nature* 363, 458–60.

3. Mertens, F., Johansson, B., Hoglund, M. & Mitelman, F. (1997). Chromosomal imbalance maps of malignant solid tumours: a cytogenetic survey of 3185 neoplasms. *Cancer Research* **57**, 2765–80.
4. Pasquale, E. B. (1997). The Eph family of receptors. *Current Opinion in Cell Biology* **9**, 608–15.
5. Zisch, A. H. & Pasquale, E. B. (1997). The Eph family: a multitude of receptors that mediate cell recognition signals. *Cell and Tissue Research* **290**, 217–26.
6. Sajjadi, F. G., Pasquale, E. B. & Subramani, S. (1991). Identification of a new eph-related receptor tyrosine kinase gene from mouse and chicken that is developmentally regulated and encodes at least two forms of the receptor. *New Biology* **3**, 769–78.
7. Tuzi, N. L. & Gullick, W. J. (1994). eph, the largest known family of putative growth factor receptors. *British Journal of Cancer* **69**, 417–21.
8. Maru, Y., Hirai, H., Yoshida, M. C. & Takaku, F. (1988). Evolution, expression, and chromosomal location of a novel receptor tyrosine kinase gene, eph. *Molecular and Cellular Biology* **8**, 3770–6.
9. Connor, R. J. & Pasquale, E. B. (1995). Genomic organization and alternatively processed forms of Cek5, a receptor protein-tyrosine kinase of the Eph subfamily. *Oncogene* **11**, 2429–38.
10. Hirai, H., Maru, Y., Hagiwara, K., Nishida, J. & Takaku, F. (1987). A novel putative tyrosine kinase receptor encoded by the eph gene. *Science* **238**, 1717–20.

The N-terminal globular domain of Eph receptors is sufficient for ligand binding and receptor signaling

D23

Juan Pablo Labrador, Riccardo Brambilla and Rüdiger Klein¹

European Molecular Biology Laboratory, Meyerhofstrasse 1,
D-69117 Heidelberg, Germany

¹Corresponding author

The Eph family of receptor protein-tyrosine kinases (RTKs) have recently been implicated in patterning and wiring events in the developing nervous system. Eph receptors are unique among other RTKs in that they fall into two large subclasses that show distinct ligand specificities and for the fact that they themselves might function as 'ligands', thereby activating bidirectional signaling. To gain insight into the mechanisms of ligand–receptor interaction, we have mapped the ligand binding domain in Eph receptors. By using a series of deletion and domain substitution mutants, we now report that an N-terminal globular domain of the Nuk/Cek5 receptor is the ligand binding domain of the transmembrane ligand Lerk2. Using focus formation assays, we show that the Cek5 globular domain is sufficient to confer Lerk2-dependent transforming activity on the Cek9 orphan receptor. Extending our binding studies to other members of both subclasses of receptors, it became apparent that the same domain is used for binding of both transmembrane and glycosylphosphatidyl-anchored ligands. Our studies have determined the first structural elements involved in ligand–receptor interaction and will allow more fine-tuned genetic experiments to elucidate the mechanism of action of these important guidance molecules.

Keywords: Eph/ligand/receptor/signal transduction/tyrosine kinase

Introduction

Axonal guidance during the development of the nervous system is controlled by both soluble (long-range) and surface-bound (short-range) cues located in the trajectories of navigating axons (Tessier-Lavigne and Goodman, 1996). The Eph family of receptor tyrosine kinases and their cell surface-bound ligands have recently been implicated in short-range control of axon guidance during retinotectal map formation and in guidance of commissural axon projections across the midline (Cheng *et al.*, 1995; Drescher *et al.*, 1995; Henkemeyer *et al.*, 1996; Nakamoto *et al.*, 1996; Orioli *et al.*, 1996). In addition, they have roles in axon fasciculation (Winslow *et al.*, 1995; Orioli *et al.*, 1996) and in patterning of forebrain and hindbrain structures (Xu *et al.*, 1995, 1996).

The Eph receptor family falls into two subclasses based on their interactions with ligands that are tethered to the

cell surface either by a single transmembrane domain (TM) or by a glycosylphosphatidyl (GPI) anchor (Brambilla and Klein, 1995; Brambilla *et al.*, 1995; Gale *et al.*, 1996). Whereas cross-reactive binding between the two subclasses is rare and of low affinity, ligand–receptor interactions within a subclass are rather promiscuous (Brambilla *et al.*, 1996; Gale *et al.*, 1996). However, small differences in binding affinities observed *in vitro* may result in different biological responses *in vivo*. Genetic evidence suggests that this is indeed the case. The two Eph receptors Nuk (Henkemeyer *et al.*, 1994) and Sek4 (Becker *et al.*, 1994; Ciossek *et al.*, 1995) (in this report referred to as Cek5 and Cek10, respectively) both bind the transmembrane ligands Lerk2 (Beckmann *et al.*, 1994; Shao *et al.*, 1994; Brambilla *et al.*, 1995) and Elf2 (also referred to as Lerk5 or Htk-L) (Bennett *et al.*, 1995; Bergemann *et al.*, 1995; Kozlosky *et al.*, 1995). However, the analysis of Nuk and Sek4-deficient mice has revealed that, despite being co-expressed, each receptor has unique roles in the guidance of commissural axons and that both receptors cooperate in axon guidance and fasciculation, as well as in the development of midline structures outside the nervous system (Henkemeyer *et al.*, 1996; Orioli *et al.*, 1996). These results are consistent with the idea that small differences in ligand interaction may influence in subtle ways the guidance of navigating growth cones *in vivo*.

Despite the rapidly accumulating knowledge of the biological functions of Eph receptors and their ligands, the precise mechanism of guidance is poorly understood. Two GPI-anchored ligands, Rags and Elf1, have been shown to be contact repellents for retinal ganglion cell axons (Drescher *et al.*, 1995; Nakamoto *et al.*, 1996); other ligands may behave in similar ways or be contact attractants for certain cells. Little information is available on the signaling events triggered by activated Eph receptors after ligand-induced receptor autophosphorylation (Brambilla and Klein, 1995; Ellis *et al.*, 1996).

Both genetic and biochemical evidence suggests that TM ligands are also actively involved in signaling during axonal pathfinding. Mice expressing a kinase-defective version of Nuk have a normal anterior commissure, at least in certain genetic backgrounds, suggesting that reverse signaling through TM ligands on the surface of the navigating axon may help to guide it properly across the midline (Henkemeyer *et al.*, 1996). Consistent with the idea of ligand signaling, TM ligands carry within their cytoplasmic domains a set of conserved tyrosine residues, which become phosphorylated after receptor contact (Holland *et al.*, 1996; Brückner *et al.*, 1997). This suggests that receptor contact causes ligand clustering and subsequent phosphorylation by an as yet unknown cytoplasmic tyrosine kinase endogenous to the ligand-expressing cells (Orioli and Klein, 1997).

Elucidating the structural elements involved in ligand–

receptor interaction is essential for our understanding of the sequence of events which result in bidirectional signaling by Eph receptors and their ligands. In this report, we have determined the domain of Eph receptors responsible for ligand binding by constructing a series of Eph receptor deletion and domain swapping mutants, which were then analyzed for ligand binding and subsequent receptor signaling. We conclude that the same domain is used by all Eph receptors to interact with their respective ligand subclass.

Results

An N-terminal globular domain allows Lerk2 to bind to the *Cek5* receptor

Our mapping studies of the ligand interaction domain in Eph receptors were guided by the recently published genomic organization of the chicken *Cek5* gene (Connor and Pasquale, 1995) and by information on sequence homologies and structural domains. The C-terminal half of the *Cek5* ectodomain encompassing amino acid (aa) residues 332–549 contains two fibronectin type III (FN III) domains whose boundaries can be clearly defined based on high sequence conservation with other FN III domains (O'Bryan *et al.*, 1991). The N-terminal half of the *Cek5* ectodomain is encoded by two exons: a large exon 3 (aa 42–279) and exon 4 (aa 280–331), which can be alternatively spliced in other Eph receptors (Valenzuela *et al.*, 1995). The C-terminal portion of exon 3 and exon 4 contain two stretches of cysteine-rich sequences with characteristically spaced cysteine residues bearing significant homology to epidermal growth factor (EGF)-like modules from tenascin and thrombospondin (Connor and Pasquale, 1995) (J.P.Labrador and R.Klein, unpublished observations). The N-terminal portion of exon 3 has previously been proposed to have weak homology to immunoglobulin (Ig)-like domains (O'Bryan *et al.*, 1991; see also Tessier-Lavigne and Goodman, 1996), although this similarity is controversial (Connor and Pasquale, 1995). Secondary structure predictions for this region suggest that it is exclusively composed of β -sheet segments separated by loops (Rost, 1996). This is characteristic not only of Ig-like, but also of several other extracellular globular domains. In the absence of any structural data, we will refer to this domain as the N-terminal globular domain.

We constructed a series of soluble deletion mutants of the *Cek5* ectodomain fused to heat-stable alkaline phosphatase (AP) (Flanagan and Leder, 1990). Such *Cek5*-AP fusion proteins, when expressed and secreted by COS cells, bind to membrane-bound Lerk2 ligand with nanomolar affinity (Brambilla *et al.*, 1995). As indicated in Figure 1, the N-terminal half of the *Cek5* ectodomain including the globular domain and cysteine-rich regions (331-AP) specifically bound to NIH 3T3 cells expressing Lerk2, while showing no specific binding to wild-type NIH 3T3 cells (data not shown). The reciprocal deletion mutant containing both FN III domains fused to the *Cek5* signal peptide (2FN-AP), despite being efficiently secreted by COS cells (data not shown), did not bind to Lerk2. The amount of binding of 2FN-AP was comparable to that of unfused AP protein (Figure 1). Further removal of the cysteine-rich sequences encoded by the alternatively spliced exon (280-AP) did not affect Lerk2 binding, nor

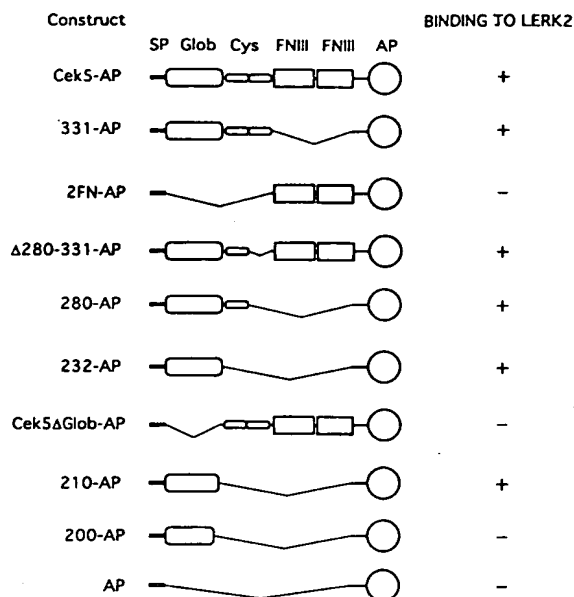


Fig. 1. An N-terminal globular domain is the primary ligand binding determinant in *Cek5* receptors. Schematic representation of *Cek5* deletion mutants fused to AP. Deleted regions are indicated by thin bent lines. The individual domains are drawn to scale. Mutant names correspond to the most C-terminal aa residue fused to AP, e.g. 200-AP: the most N-terminal 200 aa residues of *Cek5* fused to AP. Internal or N-terminal deletions are expressed as Δ followed by the name of the domain or aa residues deleted. The indicated fusion proteins were assayed for binding to wild-type NIH 3T3 cells or NIH 3T3 cells stably expressing Lerk2. Binding activity is expressed qualitatively as + when the binding affinity of the mutant was in the nanomolar range and was scored as - when no binding was detected above background ($K_D > 100$ nM). None of the mutants bound to wild-type NIH 3T3. cys, cysteine-rich region; FN III, fibronectin type III domain; glob, globular domain; SP, signal peptide.

did the specific deletion of this exon in the context of the entire *Cek5* ectodomain (Δ 280–331-AP). Specific binding to Lerk2-expressing cells was still observed after removal of the entire cysteine-rich region (232-AP) up to residue 210. A reciprocal deletion mutant to 232-AP containing the cysteine-rich regions and both FN III domains fused to the *Cek5* signal peptide (*Cek5* Δ Glob-AP) did not bind to Lerk2. Further C-terminal deletion (200-AP) including the conserved cysteine at position aa 205 abolished Lerk2 binding without affecting secretion of the fusion protein. 200-AP was the smallest peptide that could be expressed as an AP fusion protein. Further C- and N-terminal deletions did not produce active AP fusion proteins, suggesting that these peptides were not properly folded (data not shown).

For those AP fusion proteins that showed specific binding, Scatchard analyses were performed to determine binding affinities. As shown in Figure 2, the entire *Cek5*-AP fusion protein bound with subnanomolar affinity to Lerk2-expressing NIH 3T3 cells. *Cek5* mutants lacking both FN III domains and carrying partial or complete deletions of the cysteine-rich domain showed comparable affinities, with K_D between 2 and 3 nM. Similar values were also observed with the globular domain alone generated as *Cek5*-TrkB chimeric receptor, when expressed in NIH 3T3 cells and tested with Lerk2-AP fusion proteins (data not shown).

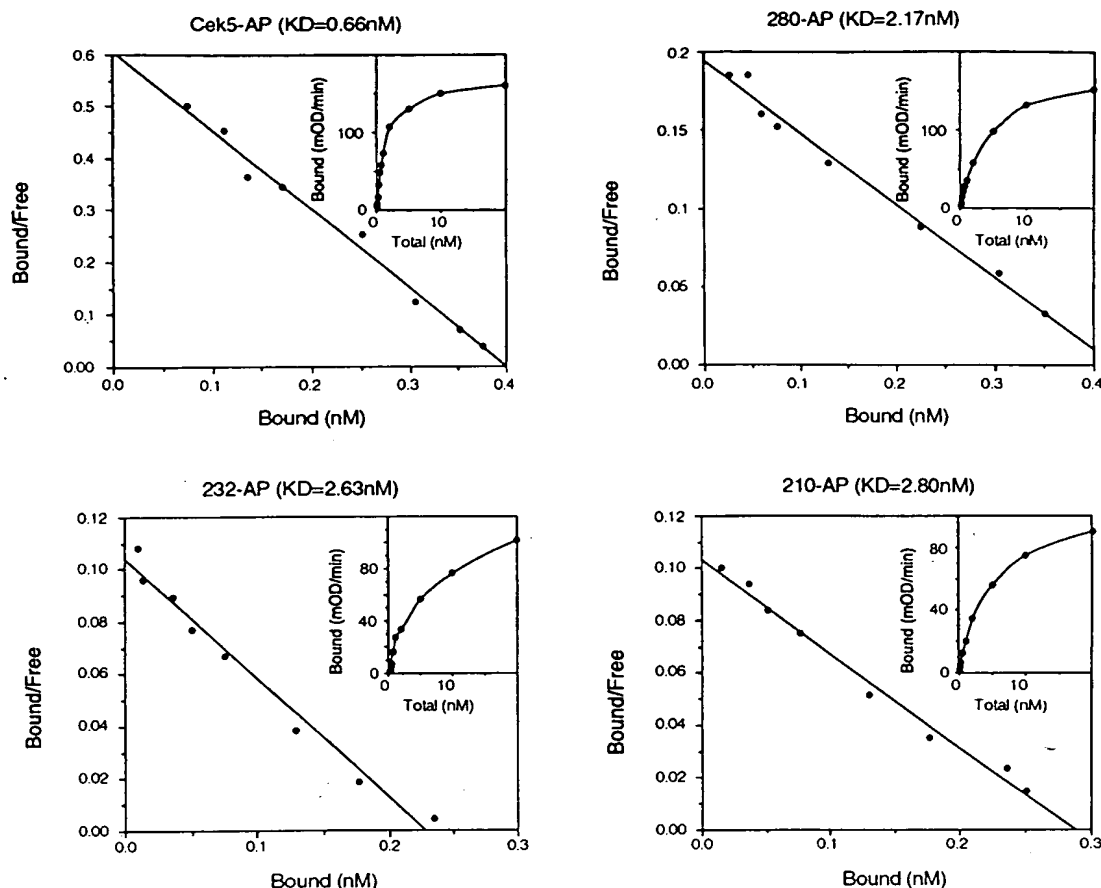


Fig. 2. The globular domain of Cek5 retains full binding activity to Lerk2. Scatchard analyses of the binding of full-length Cek5-AP, and the Cek5 deletion mutants 280-AP, 232-AP and 210-AP to membrane-bound Lerk2 expressed in NIH 3T3 cells. Dissociation constants are indicated above each graph.

The N-terminal globular domain of Cek5 is sufficient to confer Lerk2 binding on the Cek9 orphan receptor

To determine whether N-terminal sequences contain the primary determinants of ligand binding in the context of entire receptor ectodomain and whether they are sufficient to change the specificity of an orphan receptor into that of a Lerk2 receptor, we generated chimeric receptor ectodomains using sequences from the Cek9 orphan receptor (Sajjadi and Pasquale, 1993). Substitution of the N-terminal and cysteine-rich sequences of Cek5 for those of Cek9 into a Cek9-AP fusion protein or a Cek9-TrkB chimeric receptor (Brambilla *et al.*, 1995) resulted in high-affinity binding to Lerk2-expressing NIH 3T3 cells or soluble Lerk2-AP protein (Figure 3 and data not shown). Specific high-affinity binding to Lerk2 was still observed after the Cek5 contribution to the swapped ectodomain was progressively reduced from the N-terminal 331 to 232 aa (SW331-AP, SW280-AP, SW249-AP and SW232-AP) (Figure 3A). All the mutants displayed similar affinities with K_D values within 0.3 and 0.5 nM (Figure 3B). Taken together with the data from the deletion mutants, these results strongly suggest that the N-terminal globular domain is the main determinant for Lerk2 specific binding.

The N-terminal globular domain of Cek5 is sufficient to trigger Lerk2-dependent receptor signaling

To examine the ability of Cek5/9 chimeric ectodomains to trigger a functional response after Lerk2 binding, we generated Cek5/9-TrkB chimeric receptors and expressed them in NIH 3T3 cells (Figure 4A). Chimeras of Eph receptor ectodomains and TrkB kinase produce ligand-dependent transformation of NIH 3T3 cells (Brambilla *et al.*, 1995). As shown in Figure 4B, wild-type Cek5-TrkB very efficiently induces focus formation in the presence of its ligand Lerk2, whereas the orphan Cek9-TrkB chimeric receptor is completely inactive independent of the presence or absence of Lerk2. The substitution of the N-terminal globular and cysteine-rich domains of Cek5 confers transforming activity on the Cek9-TrkB chimeric receptor. Moreover, transforming activity is observed with the N-terminal globular domain of Cek5 alone (SW232-TrkB), in the context of a Cek9 ectodomain, indicating that these sequences are sufficient to bind Lerk2 and to induce receptor signaling. Transforming activity of the chimeric receptors containing swapped ectodomains was lower compared with wild-type Cek5 at low plasmid concentrations, but was only 2- to 4-fold lower at near-saturating conditions (Table I).

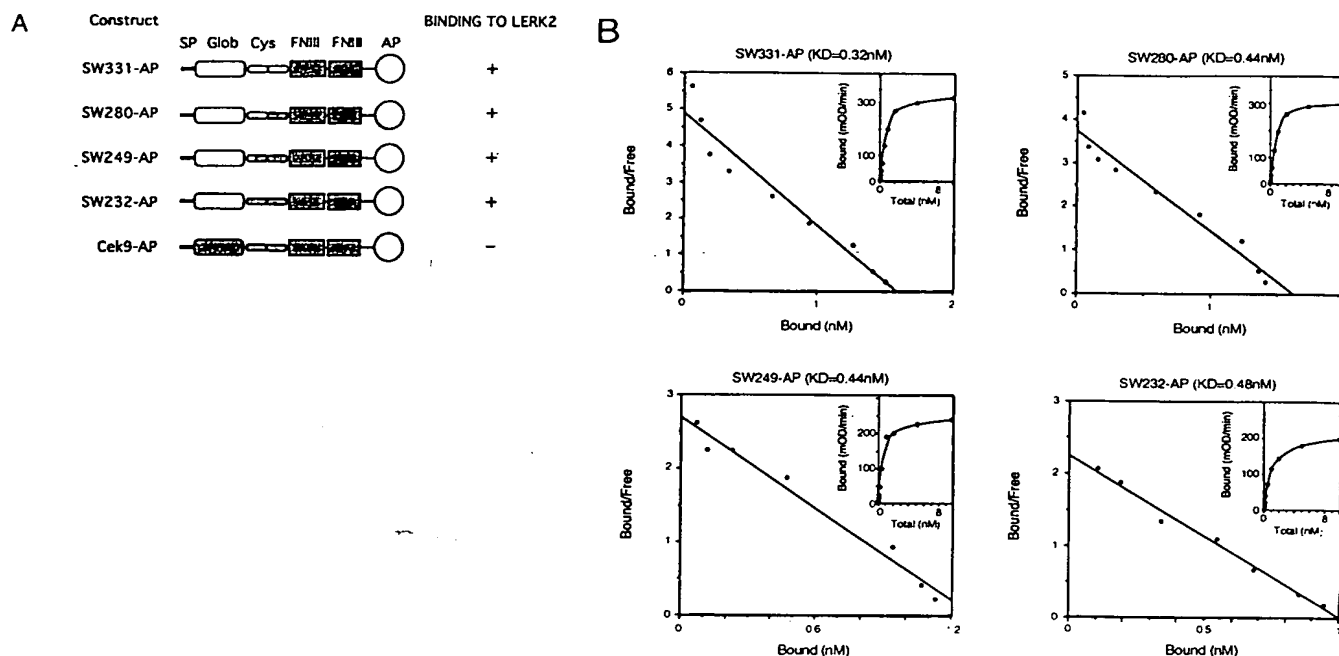


Fig. 3. The N-terminal globular domain of Cek5 confers specific Lerk2 binding on the Cek9 orphan receptor. (A) Schematic representation of Cek5/Cek9 chimeric mutants fused to AP. Cek5 sequences are in white, Cek9 sequences are in gray. The names of the mutants begin with SW (swapping) followed by the aa residue where the junction between Cek5 and Cek9 occurred. Abbreviations are as in Figure 1. (B) Scatchard analyses of the binding of Cek5/Cek9-AP chimeric mutants to membrane-bound Lerk2 expressed in NIH 3T3 cells. Dissociation constants are indicated above each graph.

The corresponding ligand-binding domain is used by other Eph receptors including those interacting with GPI-anchored ligands

We next investigated whether the same ligand-binding domain is used (i) by other receptors of the same subclass (e.g. Elk; Lhotak *et al.*, 1991) to bind transmembrane ligands and (ii) by Eph receptors, such as Cek4 (Sajjadi *et al.*, 1991), which interact with GPI-anchored ligands. We constructed and expressed deletion mutants of Elk and Cek4 as AP fusion proteins and tested their ability to bind surface-bound ligands. As shown in Figure 5A, specific Lerk2 binding was observed with the Elk deletion mutant containing only N-terminal sequences encoded by putative exon 3 (inferred from the Cek5 gene structure). Specific binding was also observed for Elf2, a second transmembrane ligand, indicating that both ligands use the same or largely overlapping binding regions in the Elk ectodomain (Figure 5B).

Cek4-AP deletion mutants were assayed for binding to the GPI-anchored ligand, Elf1 (Cheng and Flanagan, 1994). Elf1 was expressed in COS cells, since NIH 3T3 cells express endogenous Cek4-binding activity (Brambilla *et al.*, 1995). Cek4-AP deletion constructs containing the N-terminal globular domain as well as the cysteine-rich sequences (Cek4 Δ 331-AP and Cek4 Δ 280-AP) or the globular domain alone (Cek4 Δ 232-AP) bound to the GPI-anchored ligand Elf1, but not to untransfected COS cells (data not shown). As depicted in Figure 6, Scatchard analysis revealed that the binding affinities for the full-length Cek4 ectodomain and the Cek4-AP deletion mutants were in the subnanomolar range. These results indicate that the determinants of specific ligand binding in all Eph receptors lie in the globular domain.

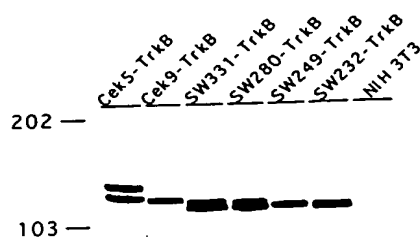
The N-terminal globular domain of Cek4 is sufficient to confer Elf1 specific binding on Cek5

To analyze further whether the globular domain alone contains all elements for specific ligand binding, we generated a chimeric receptor ectodomain replacing the globular domain of Cek5 with the corresponding sequence from Cek4 into a Cek5-AP fusion protein (Cek4-GlobGek5-AP). Whereas wild-type Cek5 fails to bind Elf1 ligand, this chimeric Cek4/5 protein binds Elf1 with high affinity ($K_D = 0.76\text{ nM}$; Figure 7), but shows no specific binding to untransfected COS cells.

Discussion

Given the large number of Eph receptors and their surface-bound ligands and recent functional data, it seems likely that these molecules are major determinants of axon pathfinding and fasciculation events in the developing nervous system (Cheng *et al.*, 1995; Drescher *et al.*, 1995; Winslow *et al.*, 1995; Henkemeyer *et al.*, 1996; Nakamoto *et al.*, 1996; Orioli *et al.*, 1996). Moreover, Eph receptors and transmembrane ligands may be unique among receptor tyrosine kinases (RTKs) in mediating bidirectional signaling both in the receptor and ligand-expressing cells (Holland *et al.*, 1996; Brückner *et al.*, 1997). To gain insight into the structural elements of ligand-receptor interactions, we have mapped the binding site for both transmembrane and GPI-anchored ligands on Eph receptors. The specific binding activity resides in the most N-terminal 183 aa (excluding the signal peptide). According to secondary structure predictions, this portion of the ectodomain is composed of β -sheet segments interspersed with loops, a structure characteristic of extracellular globular

A



B

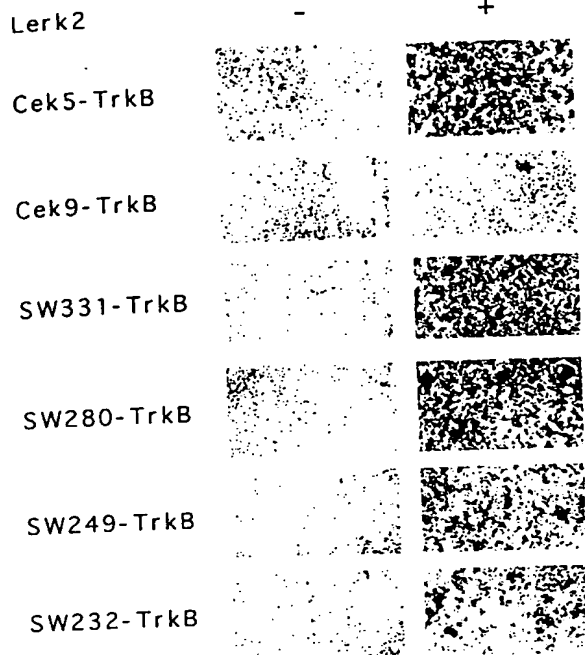


Fig. 4. The N-terminal globular domain of Cdk5 is sufficient to trigger receptor signaling. (A) NIH 3T3 cells were transfected with pMEX-neo-derived expression plasmids containing the cDNAs of the indicated wild-type Cdk5, Cdk9, and Cdk5/Cdk9 chimeric mutants fused to the cytoplasmic domain of TrkB, selected for 1 week in G418-containing medium, lysed and immunoprecipitated with a pan-Trk specific antiserum. Immunoblotting was performed with a TrkB-specific antiserum. Double bands can be detected for some of the constructs, probably corresponding to differentially glycosylated forms of the receptor. The sizes of the molecular mass markers are indicated. (B) Transformation of NIH 3T3 cells by Cdk5/9 chimeric receptors. NIH 3T3 cells were co-transfected with 500 ng of expression plasmids encoding Cdk5, Cdk9 and Cdk5/Cdk9 chimeric mutants fused to the TrkB cytoplasmic domain together with 100 ng of an expression plasmid encoding the membrane-bound Lerk2 ligand. Plates were stained with Giemsa 10 days later. Each photograph shows an area of ~40 cm².

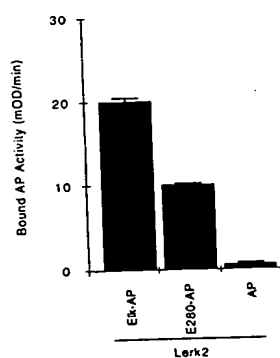
domains. In addition to the globular domain (aa 27–210), the adjacent cysteine-rich domain (aa 211–331) may play a minor role in ligand binding, since we observed a 3- to 4-fold reduction in the K_D for those mutants lacking the cysteine-rich domain, in comparison to wild type Cdk5. However, the globular domain of Cdk5 renders the Cdk9 orphan receptor competent for Lerk2-induced signaling. Likewise, the globular domain of Cdk4 renders the Cdk5 receptor competent to bind to the GPI-anchored Elk1. The calculated K_D values of receptor swapping mutants are all in the subnanomolar range. This suggests that the cysteine-rich region is dispensable for ligand

Table 1. Transformation of NIH 3T3 cells by co-transfection of expression plasmids encoding Lerk2 (100 ng) and Cdk5/9–TrkB chimeric mutants (indicated amounts)

Transfected DNAs		Transforming activity (foci per 1.5×10^5 cells)	
Receptor	DNA (ng)	Exp. 1	Exp. 2
Cdk5–TrkB	500	102	>500
SW280–TrkB	500	>500	>500
SW249–TrkB	500	>500	306
SW232–TrkB	500	128	202
Cdk5–TrkB	50	>500	>500
SW280–TrkB	50	206	194
SW249–TrkB	50	250	236
SW232–TrkB	50	150	163
Cdk5–TrkB	5	122	40
SW280–TrkB	5	8	32
SW249–TrkB	5	8	38
SW232–TrkB	5	6	22
Cdk5–TrkB	0.5	0	ND
SW280–TrkB	0.5	0	ND
SW249–TrkB	0.5	0	ND
SW232–TrkB	0.5	0	ND

500 ng of Cdk9–TrkB co-transfected with Lerk2 failed to show any transforming activity. ND, not done.

A



B

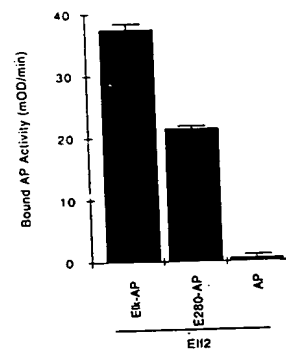


Fig. 5. The same ligand binding domain is used by Elk, another member from the same subclass as Cdk5. Deletion mutants of Elk were constructed as AP fusion proteins containing either the full-length ectodomain or the sequences encoded by exon 3 (of Cdk5), the N-terminal globular and part of the cysteine-rich region (Elk: E280–AP). 0.5 nM of AP activity of the indicated fusion proteins and soluble AP were assayed for binding to NIH 3T3 cells expressing Lerk2 (A) or Elk2 (B). Binding activity is expressed as the AP activity bound to a monolayer of cells in a six-well dish.

binding and specificity, but may be involved in stabilization of the ligand–receptor complex. Whether or not the natural splice variants of other Eph receptors lacking the second cysteine-rich cluster (aa 280–331) are fully active *in vivo* remains to be analyzed.

The FN III domains are dispensable for ligand binding and receptor signaling, and may play a structural role, e.g. providing an optimal distance between interacting cells *in vivo*. FN III domains are found in ectodomains of cell adhesion molecules, RTKs and receptor protein tyrosine phosphatases (Bork *et al.*, 1996), and have been suggested

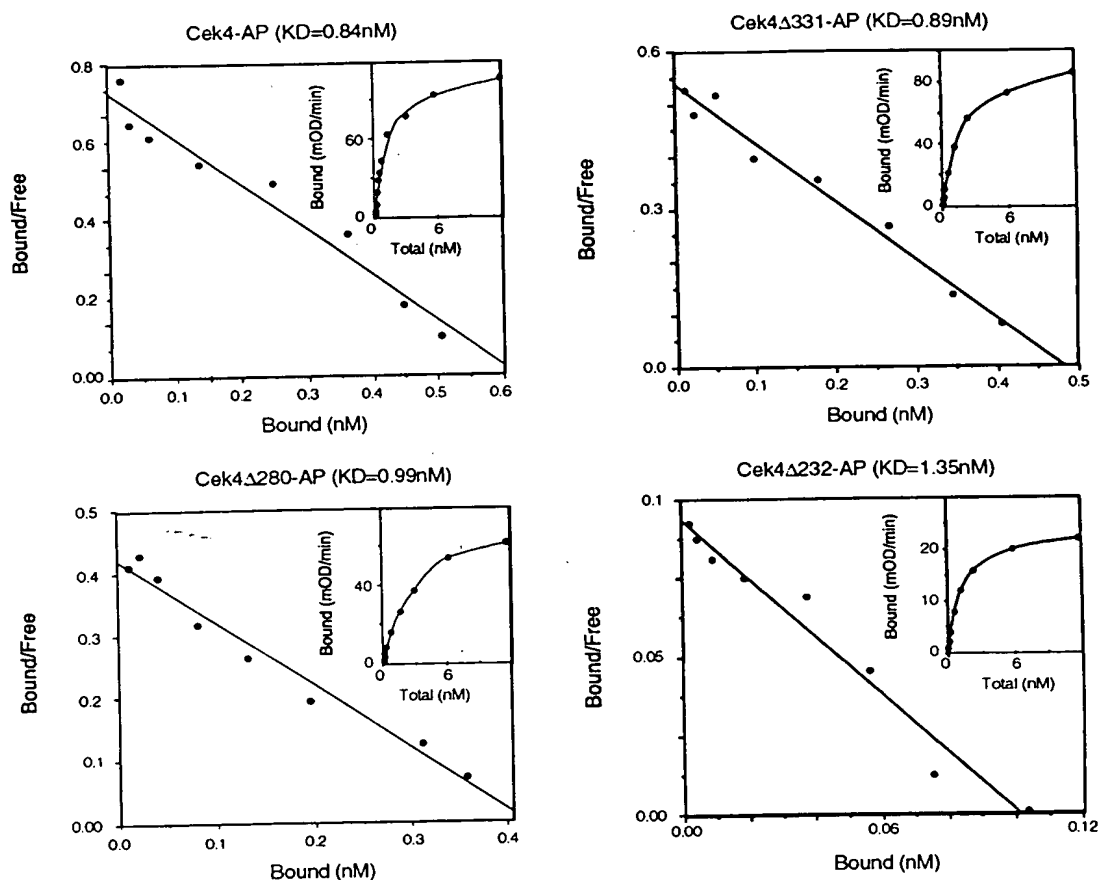


Fig. 6. The globular domain of Cdk4 shows full binding activity to the GPI-anchored ligand Elf1. Binding of Cdk4-AP was analyzed on wild-type COS cells and COS cells expressing Elf1. Cdk4 deletion mutants were made (Cdk4Δ331-AP, Cdk4Δ280-AP and Cdk4Δ232-AP) analogous to Cdk5. Scatchard analyses were performed and dissociation constants are indicated above each graph.

to play a role in dimerization (Sommers *et al.*, 1994), similar to Ig-like domains (Blechman *et al.*, 1995).

Consistent with its important function in receptor signaling, the Cdk5 ligand binding domain, when compared with other Eph receptors of the same or related species, reveals a higher degree of sequence conservation than the two FN III domains. For instance, the human Cdk5 (also known as Erk; Kiyokawa *et al.*, 1994) ligand binding domain is 75.9% identical to rat Elk, 70.9% to human Cdk10 (also known as Hek2; Böhme *et al.*, 1993) and 44.5% to human Eph (Hirai *et al.*, 1987). In contrast, both FN III domains of human Cdk5 are 64.9% identical to Elk, 59.3% to human Cdk10, and 29.1% to human Eph.

Ligand binding to single domains appears to be the exception rather than the rule among members of the superfamily of RTKs. RTKs with Ig domains in their extracellular portions, such as fibroblast growth factor receptors (with two or three Ig domains), platelet-derived growth factor receptors and c-Kit (with five Ig domains), and receptors for vascular endothelial growth factor (with seven Ig domains) all have non-contiguous ligand binding regions (Heidaran *et al.*, 1990; Lev *et al.*, 1993; Wang *et al.*, 1995; Davis-Smyth *et al.*, 1996). Whereas one Ig domain constitutes the core of the binding site, adjacent Ig domains greatly influence ligand binding, presumably by folding over the binding cleft and thereby reducing ligand dissociation.

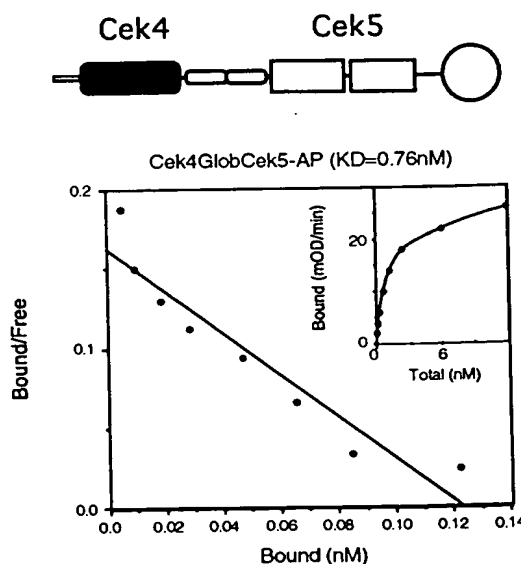


Fig. 7. The Cdk4 globular domain confers specific Elf1 binding on the Cdk5 receptor. The globular domain of Cdk5 was replaced by the corresponding sequences of Cdk4. The resulting chimeric receptor was fused to AP (Cdk4GlobCdk5-AP) and assayed for binding to Elf1 expressed in COS cells. The dissociation constant is indicated above the Scatchard plot.

The binding region of the Trk receptors maps to the most C-terminal Ig domain located closest to the transmembrane region of Trk receptors (Urfer *et al.*, 1995). However, based on cross-linking experiments, high-affinity binding appears also to require the adjacent N-terminal Ig domain (Perez *et al.*, 1995).

Among the RTKs that lack Ig domains, ligand binding regions were also found to be non-contiguous. EGF binding to the EGF receptor was mapped to sequences between two cysteine-rich regions with participation of the most N-terminal portion of the receptor ectodomain (Lax *et al.*, 1989, 1991). Similarly, both N-terminal and cysteine-rich sequences cooperate in high-affinity binding of insulin and insulin-like growth factor (IGF)-I to their respective receptors (Kjeldsen *et al.*, 1991; Yip *et al.*, 1991). In the case of Eph receptors, we report a ligand binding domain mapping to a single contiguous region apparently independent from the rest of the ectodomain.

It has been suggested that the N-terminal globular domain has certain features of an Ig-like structure (O'Bryan *et al.*, 1991). It is premature, however, to classify Eph receptors within the Ig superfamily of proteins (Tessier-Lavigne and Goodman, 1996). Instead, our own database searches with the minimal binding domain determined here revealed the highest similarity to the N-terminal globular domain VI of laminins (30% identity, 49% similarity over a stretch of 70 aa residues). This similarity also is not statistically significant. However, as in laminins, and other related molecules, such as netrins/unc-6 (Serafini *et al.*, 1994), this N-terminal domain is followed by cysteine-rich EGF-like sequences (domain V of laminin). Based on the similarity in modular architecture, it is likely that rather than resembling an Ig-like domain, the Eph ectodomain is structurally similar to domains V and VI of laminin-like molecules. Considering the apparent conservation of function between netrins and Eph receptors, this structural similarity may turn out to be physiologically relevant. Experiments to determine the crystal structure of the globular domain are in progress.

In conclusion, our characterization of the ligand binding domain will allow further studies on the mechanisms of Eph function *in vivo*. Subtle changes in the binding spectrum of Eph receptors may influence the behavior of growing axons. Fine mapping of the residues directly interacting with the ligand will allow us to produce gain-of-function molecules that will interact efficiently across subclass boundaries. Such receptor mutants will be extremely useful for genetic studies, in addition to loss-of-function mutations.

Materials and methods

Production of secreted alkaline phosphatase fused ectodomains

Deletion mutants and Cdk5/9 chimeric ectodomains were generated with the technique of gene splicing by overlap extension described previously (Horton *et al.*, 1989), with some modifications. Briefly, the mutant ectodomains are generated in two PCRs. In the first one, two fragments to be recombined are synthesized leaving complementary sequences in the ends to be fused. For the deletion mutants, the two fragments are the regions flanking the deletion. In Cdk5/9 chimeric mutants, one fragment comes from Cdk5 and the other from Cdk9. The two fragments are mixed and annealed one to the other by their complementary sequence. One becomes the primer of the other in a second PCR that gives the designed deletion or chimeric molecule. Pfu polymerase was

used in 7–10 cycle reactions to generate all the mutant ectodomains. A segment of the amino acid sequence at the junction region is listed below for each mutant.

Cdk5 deletions:			
331-AP:	MPCT/TSVQ	I 332 to T543 deletion	(pRB73)
2FN-AP:	LGWM/SAPQ	V 45 to S334 deletion	(pRB90)
Δ280-331-AP:	VCRG/TPSA	C 278 to T 331 deletion	(pRB70)
280-AP:	VCRG/TSVQ	C 278 to T 543 deletion	(pRB86)
232-AP:	AARG/TSVQ	T 232 to T 543 deletion	(pRB87)
Cdk5ΔGlobAP	IPNV/TCIS	V111 to T 233 deletion	(pJP79)
210-AP:	PRVI/TSVQ	Q 210 to T 543 deletion	(pRB89)
200-AP:	AVRV/TSVQ	F 200 to T 543 deletion	(pRB88)
Cdk5/9 chimeras:			
SW331-AP:	MPCT/GIPS		(pRB68)
SW280-AP:	VCRG/CPIG		(pRB84)
SW249-AP:	KILC/NGQG		(pRB83)
SW232-AP:	AARG/TCVA		(pRB82)

The numbers refer to the aa number in the Cdk5 sequence where the deletion has been introduced or, in the case of Cdk5/9 chimeras, where Cdk5 has been fused to Cdk9. The Cdk9 sequence is in italics and the plasmid names are in parentheses. All the ectodomains were synthesized by introducing an artificial *HindIII* site at the 5' end (nucleotide 304 of the published sequence) and an artificial *BglII* site at the end of the extracellular domain (nucleotide 1006 of the published sequence), and they were cloned into *HindIII/BglII*-digested pAPtag-2 (Cheng *et al.*, 1995) to produce AP fusion proteins, as previously described (Brambilla *et al.*, 1995). Elk and Cdk4 deletions were made in the same way, and the aa sequence at the junction region is as follows:

E280-AP:	CKAC/RSSG	deletion from C270	(pJP46)
Cdk4Δ331-AP	TRPP/RSSG	deletion from P318	(pJP59)
Cdk4Δ280-AP	CQAC/RSSG	deletion from C272	(pJP55)
Cdk4Δ232-AP	EVRG/RSSG	deletion from G226	(pJP81)

To construct Cdk4-AP (pJP47), an artificial *BglII* site was introduced in the sequence at the 5' end and another at the end of the extracellular domain in order to clone it in pAPtag-2. Cdk4GlobCdk5-AP (pJP82) was produced in the same way as the Cdk5/Cdk9 chimeras, introducing an artificial *HindIII* site upstream of the start codon and a *BglII* site at the end of Cdk5 ectodomain in order to fuse it with the AP from pAPtag-2. The sequence of the junction is VERG/SSGG. The Cdk5 sequence is in italics.

Cdk5-AP and Elk-AP have already been described (Brambilla *et al.*, 1995). The production of the AP fusion proteins was monitored by assaying the supernatant for heat-stable AP, as described previously (Cheng and Flanagan, 1994).

Binding assays

Binding assays were performed as described previously (Cheng and Flanagan, 1994). Briefly, NIH 3T3 and NIH 3T3-derived cell lines expressing either Lerk2 or Elf2 were seeded into six-well plates and used when confluent. For Cdk4 constructs, COS cells were transfected with an Elf1 expression vector (Cheng and Flanagan, 1994).

Generation of TrkB fusion receptors

The Cdk5/9 chimeric ectodomains, SW331 (pJP9), SW280 (pJP33), SW249 (pJP32) and SW232 (pJP31), were synthesized as described above including an artificial *BamHI* site 5' of the ATG start codon. They were cloned into *BamHI/SpeI*-digested pAS13 (Brambilla *et al.*, 1995), taking advantage of a natural *SpeI* site in the Cdk9 sequence.

Cell culture and gene transfer assays

COS cells (Gluzman, 1981), NIH 3T3 cells (Jainchill *et al.*, 1969) and NIH 3T3-derived cell lines were grown in Dulbecco's modified Eagle's medium (DMEM) containing 10% calf serum. Gene transfer assays in NIH 3T3 cells were performed by the calcium phosphate precipitation technique (Graham and van der Eb, 1973). Gene transfer assays in COS cells were carried out by using Lipofectamine (GibcoBRL), following the manufacturer's instructions.

Immunoprecipitation assays

Cell extracts from different NIH 3T3-derived cell lines were immunoprecipitated with a rabbit polyclonal antiserum raised against a peptide corresponding to the 14 C-terminal aa residues of human gp140^{TrkA} (Martin-Zanca *et al.*, 1989). The resulting immunoprecipitates were fractionated by 7.5% PAGE, transferred onto nitrocellulose filters, and incubated with an antiserum raised against the mouse TrkB tyrosine

kinase domain expressed in bacteria (Klein *et al.*, 1990). Further incubations were performed using rabbit anti-mouse horseradish peroxidase (HRP)-linked antibodies or HRP-linked protein A. Specific signals were revealed using the ECL detection system (Amersham).

Acknowledgements

We thank Francesca Diella for excellent technical assistance, Kelly McNagny, Angel Nebreda, Giulio Superti-Furga and members of the Klein laboratory for critical reading of the manuscript, and Peer Bork for his help with sequence comparisons. J.P.L. was funded by an EMBL predoctoral fellowship. Part of this work was funded by grant K1948/1-1 from the Deutsche Forschungsgemeinschaft and by a European Commission Biotechnology network grant.

References

- Becker, N., Seitanidou, T., Murphy, P., Mattei, M.-G., Topilko, P., Nieto, M.A., Wilkinson, D.G., Charnay, P. and Gilardi-Hebenstreit, P. (1994) Several receptor tyrosine kinase genes of the *Eph* family are segmentally expressed in the developing hindbrain. *Mech. Dev.*, **47**, 3–17.
- Beckmann, M.P. *et al.* (1994) Molecular characterization of a family of ligands for eph-related tyrosine kinase receptors. *EMBO J.*, **13**, 3757–3762.
- Bennett, B.D., Zeigler, F.C., Gu, Q., Fendly, B., Goddard, A.D., Gillett, N. and Matthews, W. (1995) Molecular cloning of a ligand for the Eph-related receptor protein-tyrosine kinase Htk. *Proc. Natl Acad. Sci. USA*, **92**, 1866–1870.
- Bergemann, A.D., Cheng, H.-J., Brambilla, R., Klein, R. and Flanagan, J.G. (1995) Elf-2, a new member of the Eph ligand family, is segmentally expressed in mouse embryos in the region of the hindbrain and newly forming somites. *Mol. Cell. Biol.*, **15**, 4921–4929.
- Blechman, J.M., Lev, S., Barg, J., Eisenstein, M., Vaks, B., Vogel, Z., Givol, D. and Yarden, Y. (1995) The fourth immunoglobulin domain of the stem cell factor receptor couples ligand binding to signal transduction. *Cell*, **80**, 103–113.
- Böhme, B., Holtrich, U., Wolf, G., Luzius, H., Grzeschik, K.-H., Strebhardt, K. and Rübsamen-Waigmann, H. (1993) PCR mediated detection of a new human receptor tyrosine kinase, HEK2. *Oncogene*, **8**, 2857–2862.
- Bork, P., Downing, A.K., Kieffer, B. and Campbell, I.D. (1996) Structure and distribution of modules in extracellular proteins. *Q. Rev. Biophys.*, **29**, 119–167.
- Brambilla, R. and Klein, R. (1995) Telling axons where to grow: a role for Eph receptor tyrosine kinases in guidance. *Mol. Cell. Neurosci.*, **6**, 487–495.
- Brambilla, R., Schnapp, A., Casagrande, F., Labrador, J.P., Bergemann, A.D., Flanagan, J.G., Pasquale, E.B. and Klein, R. (1995) Membrane-bound LERK2 ligand can signal through three different Eph-related receptor tyrosine kinases. *EMBO J.*, **14**, 3116–3126.
- Brambilla, R., Brückner, K., Orioli, D., Bergemann, A.D., Flanagan, J.G. and Klein, R. (1996) Similarities and differences in the way transmembrane-type ligands interact with the elk subclass of eph receptors. *Mol. Cell. Neurosci.*, **8**, 199–209.
- Brückner, K., Pasquale, E.B. and Klein, R. (1997) Tyrosine phosphorylation of transmembrane ligands for Eph receptors. *Science*, **275**, 1640–1642.
- Cheng, H.-J. and Flanagan, J.G. (1994) Identification and cloning of ELF-1, a developmentally expressed ligand for the Mek4 and Sek receptor tyrosine kinases. *Cell*, **79**, 157–168.
- Cheng, H.-J., Nakamoto, M., Bergemann, A.D. and Flanagan, J.G. (1995) Complementary gradients in expression and binding of Elf1 and Mek4 in development of the topographic retinotectal projection map. *Cell*, **82**, 371–381.
- Ciossek, T., Lerch, M.M. and Ullrich, A. (1995) Cloning, characterization, and differential expression of MDK2 and MDK5, two novel receptor tyrosine kinases of the eck/eph family. *Oncogene*, **11**, 2085–2095.
- Connor, R.J. and Pasquale, E.B. (1995) Genomic organisation and alternatively processed forms of Cek5, a receptor protein-tyrosine kinase of the Eph subfamily. *Oncogene*, **11**, 2429–2438.
- Davis-Smyth, T., Chen, H., Park, J., Presta, L.G. and Ferrara, N. (1996) The second immunoglobulin-like domain of the VEGF tyrosine kinase receptor Flt-1 determines ligand binding and may initiate a signal transduction cascade. *EMBO J.*, **15**, 4919–4927.
- Drescher, U., Kremoser, C., Handwerker, C., Löscher, J., Noda, M. and Bonhoeffer, F. (1995) In vitro guidance of retinal ganglion cell axons by RAGS, a 25kDa tectal protein related to ligands for Eph receptor tyrosine kinases. *Cell*, **82**, 359–370.
- Ellis, C., Kasmir, F., Ganju, P., Walls, E., Panayotou, G. and Reith, A. (1996) A juxtamembrane autophosphorylation site in the Eph family receptor tyrosine kinase, Sek, mediates high affinity interaction with p59fyn. *Oncogene*, **12**, 1727–1736.
- Flanagan, J. and Leder, P. (1990) The kit ligand: a cell surface molecule altered in Steel mutant fibroblasts. *Cell*, **63**, 185–194.
- Gale, N.W. *et al.* (1996) Eph receptors and ligands comprise two major specificity subclasses, and are reciprocally compartmentalized during embryogenesis. *Neuron*, **17**, 9–19.
- Gluzman, Y. (1981) SV40-transformed simian cells support the replication of early SV40 mutants. *Cell*, **23**, 175–182.
- Graham, F. and van der Eb, A. (1973) A new technique for the assay of infectivity of human adenovirus 5 DNA. *Virology*, **52**, 456–467.
- Heidaran, M.A., Pierce, J.H., Jensen, R.A., Matsui, T. and Aaronson, S.A. (1990) Chimeric alpha- and beta-platelet-derived growth factor (PDGF) receptors define three immunoglobulin-like domains of the alpha-PDGF receptor that determine PDGF-AA binding specificity. *J. Biol. Chem.*, **265**, 18741–18744.
- Henkemeyer, M., Marengere, L.E.M., McGlade, J., Olivier, J.P., Condeelis, R.A., Holmyard, D.P., Letwin, K. and Pawson, T. (1994) Immunolocalization of the Nuk receptor tyrosine kinase suggests roles in segmental patterning of the brain and axonogenesis. *Oncogene*, **9**, 1001–1014.
- Henkemeyer, M., Orioli, D., Henderson, J.T., Saxton, T.M., Roder, J., Pawson, T. and Klein, R. (1996) Nuk controls pathfinding of commissural axons in the mammalian central nervous system. *Cell*, **86**, 35–46.
- Hirai, H., Maru, Y., Hagiwara, K., Nishida, J. and Takaku, F. (1987) A novel putative tyrosine kinase receptor encoded by the *eph* gene. *Science*, **238**, 1717–1720.
- Holland, S.J., Gale, N.W., Mbamalu, G., Yancopoulos, G.D., Henkemeyer, M. and Pawson, T. (1996) Bidirectional signaling through the EPH-family receptor Nuk and its transmembrane ligands. *Nature*, **383**, 722–725.
- Horton, R.M., Hunt, H.D., Ho, S.N., Pullen, J.K. and Pease, L.R. (1989) Engineering hybrid genes without the use of restriction enzymes: gene splicing by overlap extension. *Gene*, **77**, 61–68.
- Jainchill, J., Aaronson, S. and Todaro, G. (1969) Murine sarcoma and leukemia viruses: assay using clonal lines of contact-inhibited cells. *J. Virol.*, **4**, 549–553.
- Kiyokawa, E. *et al.* (1994) Overexpression of ERK, an EPH family receptor protein tyrosine kinase, in various human tumors. *Cancer Res.*, **54**, 3645–3650.
- Kjeldsen, T., Andersen, A.S., Wiberg, F.C., Rasmussen, J.S., Schaffer, L., Balschmidt, P., Møller, K.B. and Møller, N.P. (1991) The ligand specificities of the insulin receptor and the insulin-like growth factor I receptor reside in different regions of a common binding site. *Proc. Natl Acad. Sci. USA*, **88**, 4404–4408.
- Klein, R., Conway, D., Parada, L.F. and Barbacid, M. (1990) The B tyrosine protein kinase gene codes for a second neurogenic receptor that lacks the catalytic kinase domain. *Cell*, **61**, 647–656.
- Kozlosky, C.J. *et al.* (1995) Ligands for the receptor tyrosine kinases hek and elk: isolation of cDNAs encoding a family of proteins. *Oncogene*, **10**, 299–306.
- Lax, J., Bellot, F., Howk, R., Ullrich, A., Givol, D. and Schlessinger, J. (1989) Functional analysis of the ligand binding site of EGF-receptor utilizing chimeric chicken/human receptor molecules. *EMBO J.*, **8**, 421–427.
- Lax, J., Fischer, R., Ng, C., Segre, J., Ullrich, A., Givol, D. and Schlessinger, J. (1991) Noncontiguous regions in the extracellular domain of EGF receptor define ligand-binding specificity. *Cell Regul.*, **2**, 337–345.
- Lev, S., Blechman, J., Nishikawa, S., Givol, D. and Yarden, Y. (1993) Interspecies molecular chimeras of kit help define the binding site of the stem cell factor. *Mol. Cell. Biol.*, **13**, 2224–2234.
- Lhotak, V., Greer, P., Letwin, K. and Pawson, T. (1991) Characterization of Elk, a brain-specific receptor tyrosine kinase. *Mol. Cell. Biol.*, **11**, 2496–2502.
- Martin-Zanca, D., Oskam, R., Mitra, G., Copeland, T. and Barbacid, M. (1989) Molecular and biochemical characterization of the human *erbB* proto-oncogene. *Mol. Cell. Biol.*, **9**, 24–33.

- Nakanishi, M., Cheng, H.-J., Friedman, G.C., McLaughlin, T., Hansen, M.J., Yoon, C.H., O'Leary, D.D.M. and Flanagan, J.G. (1996) Topographically specific effects of E1f-1 on retinal axon guidance *in vitro* and retinal axon mapping *in vivo*. *Cell*, **86**, 755–766.
- O'Bryan, J.P. *et al.* (1991) axl, a transforming gene isolated from primary human myeloid leukemia cells, encodes a novel receptor tyrosine kinase. *Mol. Cell. Biol.*, **11**, 5016–5031.
- Orioli, D. and Klein, R. (1997) The Eph receptor family: axonal guidance by contact repulsion. *Trends Genet.*, in press.
- Orioli, D., Henkemeyer, M., Lemke, G., Klein, R. and Pawson, T. (1996) Sek4 and Nuk receptors cooperate in guidance of commissural axons and in palate formation. *EMBO J.*, **15**, 6035–6049.
- Perletti, G.P., Coll, P.M., Hempstead, B.L., Martin Zanca, D. and Chao, M.V. (1995) NGF binding to the trk tyrosine kinase receptor requires the extracellular immunoglobulin-like domains. *Mol. Cell. Neurosci.*, **6**, 97–105.
- Rost, B. (1996) PHD: predicting one-dimensional protein structure by profile based neural networks. *Methods Enzymol.*, **266**, 525–539.
- Sajjadi, F.G. and Pasquale, E.B. (1993) Five novel avian Eph-related tyrosine kinases are differentially expressed. *Oncogene*, **8**, 1807–1813.
- Sajjadi, F.G., Pasquale, E.B. and Subramani, S. (1991) Identification of a new *epb*-related receptor tyrosine kinase gene from mouse and chicken. This is developmentally regulated and encodes at least two forms of receptor. *N. Biol.*, **3**, 769–778.
- Serafini, T., Kennedy, T.E., Galko, M.J., Mirzayan, C., Jessell, T.M. and Tessier-Lavigne, M. (1994) The netrins define a family of axon outgrowth-promoting proteins homologous to *C. elegans* UNC-6. *Cell*, **78**, 409–424.
- Shao, H., Lou, L., Pandey, A., Pasquale, E.B. and Dixit, V.M. (1994) cDNA cloning and characterization of a ligand for the Cek5 receptor protein-tyrosine kinase. *J. Biol. Chem.*, **269**, 26606–26609.
- Sommers, W., Ultsch, M., De Vos, A.M. and Kossiakoff, A.A. (1994) X-ray structure of a growth hormone-prolactin receptor complex. *Nature*, **371**, 478–481.
- Tessier-Lavigne, M. and Goodman, C.S. (1996) The molecular biology of axon guidance. *Science*, **274**, 1123–1133.
- Urfer, R., Tsoulfas, P., O'Connell, L., Shelton, D.L., Parada, L.F. and Presta, L.G. (1995) An immunoglobulin-like domain determines the specificity of neurotrophin receptors. *EMBO J.*, **14**, 2795–2805.
- Valenzuela, D.M., Rojas, E., Griffith, J.A., Compton, D.L., Gisser, M., Ip, N.Y., Goldfarb, M. and Yancopoulos, G.D. (1995) Identification of full-length and truncated forms of Ehk-3, a novel member of the Eph receptor tyrosine kinase family. *Oncogene*, **10**, 1573–1580.
- Wang, E., Kan, M., Xu, J., Yan, G. and McKeenan, W. (1995) Ligand-specific structural domains in the fibroblast growth factor receptor. *J. Biol. Chem.*, **270**, 10222–10230.
- Winslow, J.W. *et al.* (1995) Cloning of AL1, a ligand for an Eph-related tyrosine kinase receptor involved in axon bundle formation. *Neuron*, **14**, 973–981.
- Xu, Q., Alldus, G., Holder, N. and Wilkinson, D.G. (1995) Expression of truncated Sek1 receptor tyrosine kinase disrupts the segmental restriction of gene expression in the *Xenopus* and zebrafish hindbrain. *Development*, **121**, 4005–4016.
- Xu, Q., Alldus, G., Macdonald, R., Wilkinson, D.G. and Holder, N. (1996) Function of the Eph-related kinase rtk1 in patterning of the zebrafish forebrain. *Nature*, **381**, 319–322.
- Yip, C.C., Grunfeld, C. and Goldfine, I.D. (1991) Identification and characterization of the ligand-binding domain of insulin receptor by use of an anti-peptide antiserum against amino acid sequence 241–251 of the alpha subunit. *Biochemistry*, **30**, 695–701.

Received on December 20, 1996; revised on March 20, 1997

Note added in proof

After this paper was submitted, the community agreed on a new nomenclature for Eph receptors and their ligands [Tessier-Lavigne, M., Flanagan, J., Gale, N., Hunter, T. and Pasquale, E.B. (1997) A unified nomenclature for Eph receptors and their ligands. *Cell*, in press]. Following this nomenclature, the new names for receptors and ligands used in this study are indicated in parentheses: Elk (EphB1), Cek5 (EphB2), Cek9 (EphB5), Cek4 (EphA3), Lerk2 (ephrin-B1), ELJ (ephrin-B2), ELJ1 (ephrin-A2).

11. Oshima, Y. The phosphatase system in *Saccharomyces cerevisiae*. *Genes Genet. Syst.* 72, 323–334 (1997).
12. Ogawa, N. et al. Functional domains of Pho81p, an inhibitor of Pho85p protein kinase, in the transduction pathway of Pi signals in *Saccharomyces cerevisiae*. *Mol. Cell. Biol.* 15, 997–1004 (1995).
13. Schneider, K. R., Smith, R. L. & O'Shea, E. K. Phosphate-regulated inactivation of the kinase PHO80-PHO85 by the CDK inhibitor PHO81. *Science* 266, 122–126 (1994).
14. Kaffman, A., Rank, N. M. & O'Shea, E. K. Phosphorylation regulates association of the transcription factor Pho4 with its import receptor Pse1/Kap121. *Genes Dev.* 12, 2673–2683 (1998).
15. Lee, M. S., Henry, M. & Silver, P. A. A protein that shuttles between the nucleus and the cytoplasm is an important mediator of RNA export. *Genes Dev.* 10, 1233–1246 (1996).
16. Wimmer, C., Doye, V., Grandi, P., Nehrass, U. & Hurt, E. C. A new subclass of nucleoporins that functionally interact with nuclear pore protein NSP1. *EMBO J.* 11, 5051–5061 (1992).
17. Nehrass, U. et al. NSP1: a yeast nuclear envelope protein localized at the nuclear pores exerts its essential function by its carboxy-terminal domain. *Cell* 61, 979–989 (1990).
18. Doye, V., Wepf, R. & Hurt, E. C. A novel nuclear pore protein Nup133p with distinct roles in poly(A)⁺ RNA transport and nuclear pore distribution. *EMBO J.* 13, 6062–6075 (1994).
19. Aitchison, J. D., Blobel, G. & Rout, M. P. Kap104p: a karyopherin involved in the nuclear transport of messenger RNA binding proteins. *Science* 274, 624–627 (1996).
20. Xiao, Z., McGrew, A. J. & Fitzgerald-Hayes, M. CSE1 and CSE2, two new genes required for accurate mitotic chromosome segregation in *Saccharomyces cerevisiae*. *Mol. Cell. Biol.* 13, 4691–4702 (1993).
21. Stade, K., Ford, C. S., Guthrie, C. & Weis, K. Exportin 1 (Crm1p) is an essential nuclear export factor. *Cell* 90, 1041–1050 (1997).
22. Seedorf, M. & Silver, P. A. Importin/karyopherin protein family members required for mRNA export from the nucleus. *Proc. Natl Acad. Sci. USA* 94, 8590–8595 (1997).
23. Rout, M. P., Blobel, G. & Aitchison, J. D. A distinct nuclear import pathway used by ribosomal proteins. *Cell* 89, 715–725 (1997).
24. Kadowaki, T. et al. Isolation and characterization of *Saccharomyces cerevisiae* mRNA transport-defective (mtr) mutants. *J. Cell Biol.* 126, 649–659 (1994).
25. Arts, G. J., Fornerod, M. & Mattaj, J. W. Identification of a nuclear export receptor for tRNA. *Curr. Biol.* 8, 305–314 (1998).
26. Kutay, U., Bischoff, F. R., Kostka, S., Kraft, R. & Gorlich, D. Export of importin alpha from the nucleus is mediated by a specific nuclear transport factor. *Cell* 90, 1061–1071 (1997).
27. Kutay, U. et al. Identification of a tRNA-specific nuclear export receptor. *Mol. Cell* 1, 359–369 (1998).
28. Fornerod, M., Ohno, M., Yoshida, M. & Mattaj, J. W. CRM1 is an export receptor for leucine-rich nuclear export signals. *Cell* 90, 1051–1060 (1997).
29. Bischoff, F. R., Klebe, C., Kretschmer, J., Wittinghofer, A. & Ponstingl, H. RanGAP1 induces GTPase activity of nuclear Ras-related Ran. *Proc. Natl Acad. Sci. USA* 91, 2587–2591 (1994).
30. Chenervet, J., Valtz, N. & Herskowitz, I. Identification of genes required for normal pheromone-induced cell polarization in *Saccharomyces cerevisiae*. *Genetics* 136, 1287–1296 (1994).

Acknowledgements. We thank I. Herskowitz, J. Li, J. Weissman and members of the O'Shea laboratory for comments on the manuscript; R. Bischoff for the RanQ69L plasmid; M. Lenburg for the Pho85-GFP plasmid; and J. Aitchison, K. Weis, P. Silver, M. Fitzgerald-Hayes, E. Hurt and A. Tartakoff for yeast strains. A.K. is a fellow of the UCSF Medical Scientist Training Program. N.M.R. and L.S.H. were supported by fellowships from the NIH and E.M.O. was supported by a fellowship from the Jane Coffin Childs Foundation. This work was supported by the David and Lucile Packard Foundation and by an NSF Presidential Faculty Fellowship (E.K.O.).

Correspondence and requests for materials should be directed to E.K.O. (e-mail: oshea@biochem.ucsf.edu).

Crystal structure of the ligand-binding domain of the receptor tyrosine kinase EphB2

Juha-Pekka Himanen*, Mark Henkemeyer† & Dimitar B. Nikolov*

* Cellular Biochemistry and Biophysics Program, Memorial-Sloan-Kettering Cancer Center, 1275 York Avenue, New York, New York 10021, USA

† Center for Developmental Biology, University of Texas Southwestern Medical Center, Dallas, Texas 75235-9133, USA

The Eph receptors, which bind a group of cell-membrane-anchored ligands known as ephrins, represent the largest subfamily of receptor tyrosine kinases (RTKs)¹. They are predominantly expressed in the developing and adult nervous system² and are important in contact-mediated axon guidance^{3–6}, axon fasciculation^{5,7} and cell migration^{8–11}. Eph receptors are unique among other RTKs in that they fall into two subclasses with distinct ligand specificities¹², and in that they can themselves function as ligands to activate bidirectional cell-cell signalling^{4,13,14}. We report here the crystal structure at 2.9 Å resolution of the amino-terminal ligand-binding domain of the EphB2 receptor (also known as Nuk)^{15–17}. The domain folds into a compact jellyroll β -sandwich composed of 11 antiparallel β -strands. Using structure-based mutagenesis, we have identified an extended loop that is important for ligand binding and class

specificity. This loop, which is conserved within but not between Eph RTK subclasses, packs against the concave β -sandwich surface near positions at which missense mutations cause signalling defects¹⁸, localizing the ligand-binding region on the surface of the receptor.

The extracellular region of Eph receptors consists of two fibronectin type III repeats, a cysteine-rich region, and a conserved 180-amino-acid N-terminal 'globular' domain (Fig. 1) which is both necessary and sufficient for bindings of the receptors to their ephrin ligands¹⁶. Eph receptors bind their ephrin ligands with high affinity ($K_d = 0.5$ – 15.0 nM) and with one-to-one stoichiometry^{16,17,19} (Fig. 2).

We determined the structure of the biologically active (Fig. 2) ligand-binding domain of the murine EphB2 receptor by X-ray crystallography using the multiple isomorphous replacement (MIR) method (Table 1 and Figs 3, 4). Our model is refined at 2.9 Å resolution to an R-factor of 20.6% with tightly restrained temperature factors and good stereochemistry. The domain has dimensions of roughly $50 \text{ Å} \times 40 \text{ Å} \times 30 \text{ Å}$. It has two antiparallel β -sheets, with the usual left-handed twist, packed against each other to form a compact β -sandwich, and a short 3_{10} helix. The concave β -sheet is composed of strands C, F, F', L, H and I, and the convex β -sheet of strands D, E, A, M, G, K and J (Fig. 4c). The extensive hydrophobic core created by approximation of the two β -sheets and the short 3_{10} helix contains no cavities and is dominated by aromatic side chains. The β -strands are connected by loops of varying length, including a long loop (between strands H and I; coloured in orange and red in Fig. 4a) that packs against the full width of the concave β -sheet, and two loops (D–E and J–K) that protrude from the two sides of the β -sandwich, closing on the middle of the convex β -sheet. The H–I loop (in the front in Fig. 4a) is well-ordered, as are the loops running across the top, whereas the D–E and J–K loops at the back are disordered, with several residues that cannot be located in the electron-density map. Two disulphide bridges stabilize the loops at the top of the β -sandwich: Cys 105 binds Cys 115 in the longest of the top loops (G–H), and Cys 70, the first residue of loop E–F, binds Cys 192, the last residue of loop L–M.

The EphB2 ligand-binding domain has a jellyroll folding topology²⁰ (Fig. 4c). Comparison of this structure with the contents of the FSSP database²¹ reveals considerable similarity with the carbohydrate-binding domains of glucanases, legume lectins, β -galactosidases, sialidases, cellulases, bacterial toxins and influenza virus haemagglutinin. This raises two interesting possibilities, namely that the homology in molecular architecture includes the location of the ligand-binding site, or that the carbohydrate moieties at the putative glycosylation sites of the ephrins are directly involved in ligand-receptor recognition. Our results support the first possibility (see below); however, we suggest that the Eph receptors are not lectins. Indeed, the purified EphB2 globular domain forms a stable, high-affinity complex with a bacterially expressed non-glycosylated ephrin-B2 ligand preparation (Fig. 2) (K_d is within the range of values reported for recombinant glycosylated ephrins^{2,16,17,19}). Furthermore, addition of a tenfold molar excess of N-linked type oligosaccharides (Oxford GlycoSystem) has no effect on the *in vitro* Eph-receptor-ephrin interaction (data not shown). Beyond the similarity in overall topology between the EphB2 ligand-binding domain and the carbohydrate-binding proteins, the precise structures are quite different (Fig. 4d) and the best structural alignments include stretches of 100–120 amino acids with root mean square deviations between α -carbon positions of 3.0 Å.

The ligand-binding domain of Eph receptors is unique to this family of RTKs²² and shares no significant amino-acid-sequence homology with other known proteins. Nevertheless, jellyroll folding topology is observed in the extracellular domains of other proteins, including, in addition to the carbohydrate-binding proteins, the tumour-necrosis factor (TNF) family²³ (which includes TNF, lym-

Table 1 Crystallographic analysis

Crystal	Native	Sm1	Sm2	Os1	Os2	Au	Pt1	Pt2
Resolution (Å)	2.9	3.2	3.0	3.0	3.2	3.0	3.2	3.0
Redundancy	5.0	12.8	5.3	4.8	3.6	4.7	3.7	4.5
Data coverage (%)	95.1	94.0	98.2	90.7	90.1	89.4	80.6	89.3
R_{int} (%)	11.4	17.1	10.9	12.2	14.4	7.6	10.1	6.5
Multiple isomorphous replacement analysis (15.0–3.2 Å)								
Mean fractional isomorphous difference (%)†		19.5	19.4	19.2	20.7	13.7	15.1	15.2
Binding sites		3	3	3	3	4	3	7
Phasing power‡		2.07	2.13	1.60	1.31	0.84	0.96	1.00
R_{cs}		0.64	0.64	0.69	0.77	0.83	0.84	0.84
Mean overall figure of merit	0.72							
Refinement	Resolution (Å)	Reflections ($ F > 2.0\sigma(F)$ working/test)	Number of atoms	R value $R_{\text{cryst}}/R_{\text{free}}$	Bonds (Å)	R.m.s. deviations§ Angles (°)	B -factors (Å ²)	
	8.0–2.9	4,214/340	1,377	20.6/31.4	0.012	1.97	1.93	

The space group is $P4_22_1$ ($a = b = 55$ Å, $c = 159$ Å) with one molecule in the asymmetric unit. The heavy-metal compounds are Sm1 = Sm2 = samarium (III) acetate trihydrate, Os1 = Os2 = potassium hexachloroaurate (IV), Au = sodium tetrachloroaurate (III), Pt1 = diamine dichloroplatinate (II), and Pt2 = potassium tetrachloroplatinate (II).
 $R_{\text{int}} = \sum |I - \langle I \rangle| / \sum I$, where I is the observed intensity and $\langle I \rangle$ is the average intensity obtained from multiple observations of symmetry-related reflections.
 \dagger Mean fractional isomorphous difference = $\sum |F_{\text{H}} - \langle F_{\text{H}} \rangle| / \sum |F_{\text{H}}|$, where $|F_{\text{H}}|$ is the protein structure-factor amplitude and $\langle F_{\text{H}} \rangle$ is the heavy-atom-derivative structure-factor amplitude.
 \dagger Phasing power = root-mean-square ($|F_{\text{H}}|/E$), where $|F_{\text{H}}|$ is the heavy-atom structure-factor amplitude and E is the residual lack of closure.
 \dagger $R_{\text{cs}} = \sum |F_{\text{H}} - \langle F_{\text{H}} \rangle| / \sum |F_{\text{H}}|$, where $|F_{\text{H}}|$ is the observed heavy-atom structure-factor amplitude and $\langle F_{\text{H}} \rangle$ is the calculated heavy-atom structure-factor amplitude.
 \dagger R.m.s. deviations in bond lengths and angles are the respective root-mean-square deviations from ideal values. The r.m.s. thermal parameter (B -factor) is the r.m.s. deviation between the B -value of covalently bound atomic pairs.

phoetoxin, CD40 ligand and complement C1q) and several viral coat proteins. The TNF-family members are all trimeric and bind their receptors on the 'side' of the jellyroll, at the interface between trimer subunits²³. Eph receptors, on the other hand, are monomeric (including the full-length recombinant extracellular region)^{16,19}, and therefore their functional ligand-binding site is different from that of TNF proteins.

Discussion of the precise mechanisms of ligand recognition by the Eph RTKs must await high-resolution structures of appropriate

ephriin-Eph-receptor complexes. However, the structure of a functional ligand-binding core domain does allow us to predict the location of the ligand-recognition site on the receptor surface and to test our hypothesis using structure-based mutagenesis. Several results (see below) indicate that the ligand-binding surface of EphB2 is localized to the upper part of the concave β -sheet, including the H-I loop traversing the middle region of the structure as well as the loops running across the upper surface of the β -sandwich (Fig. 4d).

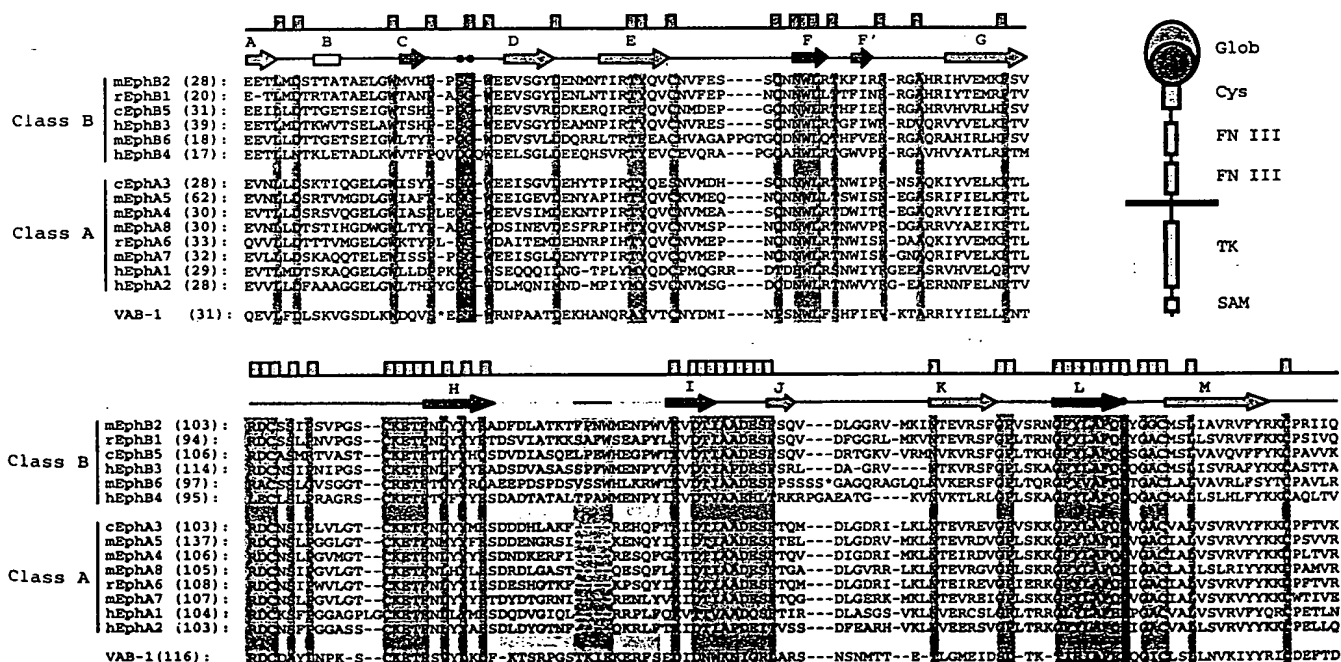


Figure 1 Alignment of amino-acid sequences of Eph globular domains. The sequences of the known Eph RTKs were aligned using the program DNASTar. The secondary-structure elements of the EphB2 crystal structure are shown using arrows for β -strands and a rectangle for the 3_{10} helix. The strands of the concave β -sheet are coloured blue and those in the convex β -sheet are coloured green. The locations of three different point mutations that affect the function of the C. elegans VAB-1 Eph receptor¹⁸ are indicated with purple dots and the Eph class-specificity loop is shown in orange, with the four residues by which the sub-

classes differ shown in red. The residues with the highest sequence conservation between RTKs (calculated with DNASTar) are indicated above the secondary structure and are also shaded in grey. Asterisks indicate the locations of a ten-amino-acid insertion in VAB-1 and a fifteen-amino-acid insertion in EphB6. The domain organization of the Eph receptors is shown at the right: Glob, globular domain; Cys, cysteine-rich linker; FN III, fibronectin type III motif; TK, tyrosine-kinase domain; SAM, sterile α -motif.

letters to nature

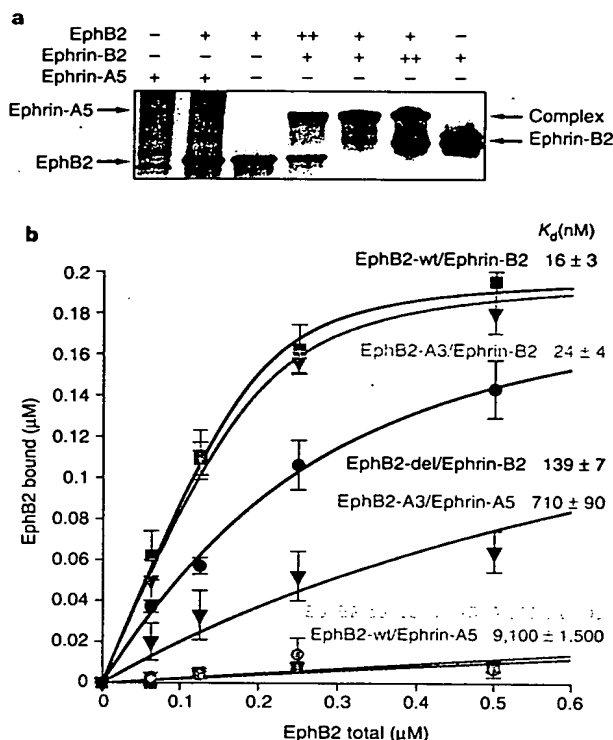


Figure 2 Eph-ephrin recognition. **a**, Gel mobility-shift experiment with the recombinant globular domain of EphB2 that was used in the structure determination and the recombinant extracellular domains of ephrin-B2 and ephrin-A5. The two bands in lanes with ephrin-B2 represent a monomer/dimer equilibrium that is also observed using size-exclusion chromatography. ++ indicates a twofold molar excess of the component. **b**, Binding of wild-type and mutant EphB2-receptor ligand-binding domains to class A and class B ephrins in Ni-affinity-bead pull-down experiments (see Methods). Data points represent the means of multiple measurements (typically $n = 3$) and the bars represent standard errors, $\sigma/(n-1)$ (where σ is the standard deviation). The curves represent unweighted least-squares fits to a standard dissociation equilibrium equation. The calculated apparent dissociation constants are somewhat overestimated because the post-binding washing of the Ni-affinity-beads is not accounted for in the calculations.

Eph receptors can be divided into two subclasses on the basis of their preference to bind ligands that are tethered to the cell surface either by a glycosylphosphatidylinositol (GPI) anchor (A-ephrins) or by a single transmembrane segment (B-ephrins)¹². In general, EphA subclass receptors bind to the five known A-ephrins, whereas the EphB subclass receptors interact with the three known B-ephrins¹². Analysis of all currently available ligand-binding-domain sequences (Fig. 1) shows that the length of the loop connecting strands H and I may determine Eph-receptor subclass. EphB members possess H-I loops that are 17 residues in length, whereas the H-I loops of EphA members are 4 residues shorter (orange/red loop in Fig. 4a). To understand better the role of this loop in ephrin recognition, we performed binding assays using two EphB2 mutants—one containing a deletion of the four extra class-B-specific amino acids (EphB2-del), and one in which the H-I loop of EphB2 was substituted with the corresponding loop of the A-class receptor EphA3 (EphB2-A3). As compared with the wild-type EphB2 protein, the EphB2-del mutant exhibited roughly ninefold reduced affinity for ephrin-B2, indicating that the H-I loop is directly involved in ligand binding. Furthermore, although both wild-type EphB2 and EphB2-del bind to ephrin-B2 only, the chimeric EphB2-A3 receptor recognizes not only ephrin-B2 but also ephrin-A5, albeit with much lower affinity than a wild-type receptor for ephrin-A5, indicating that the loop confers some degree of class specificity. The ability of the EphB2-A3 mutant to retain full affinity for ephrin-B2 while also binding to ephrin-A5 indicates that the H-I loop may be particularly important for recognition of A-type ligands.

Other regions on the molecular surface of the globular domain of Eph-family receptors must also be involved in ligand recognition. In our crystal structure, the H-I loop packs against the middle of the concave β -sheet only 13 Å away from the locations of known signalling-defective mutations¹⁸ in the *Caenorhabditis elegans* Eph RTK VAB-1. The locations of these point mutations are shown in magenta in Fig. 4a. All characterized missense mutations in the extracellular region map to loops at the top of the β -sandwich. The *ju8* allele, which causes a strong loss-of-function phenotype¹⁹, contains a Glu \rightarrow Lys substitution of a solvent-exposed residue (Ser 49 in EphB2) in the loop between strands C and D that will alter the local electrostatic potential. The intermediate alleles *e856* and *e699* contain a Thr \rightarrow Ile substitution of a partially buried residue inside the C-D loop (Gly 50 in EphB2), and a Glu \rightarrow Lys substitution of a residue buried inside the L-M loop (Asp 188 in EphB2), respectively. These mutations would probably alter the

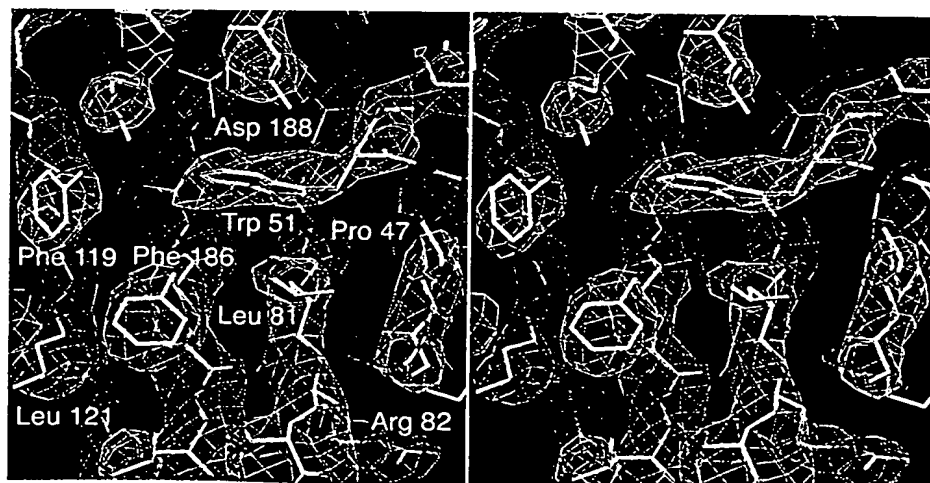


Figure 3 Stereo diagram of a representative region of the solvent-flattened experimental (MIR) electron-density map (contour level 1.2 σ) with the refined

EphB2 atomic model drawn as a stick figure.

conformation of the loops at the top of the β -sandwich (the exact nature of the perturbation is hard to predict, as EphB2 and VAB-1 have C-D loops of different lengths) but would probably not affect the overall folding of the domain. As Eph receptors also function as ligands in a bidirectional tyrosine-kinase signalling cascade^{4,13,14}, mutations in the ligand-binding region would affect signalling in

both directions, and indeed, the three described alleles produce stronger phenotypes than mutations that abolish the catalytic activity of VAB-1 (ref. 18).

In agreement with the direct evidence for the location of the ligand-binding region from the analyses of the VAB-1 and EphB2 H-I-loop mutants, the residues comprising the concave β -sheet

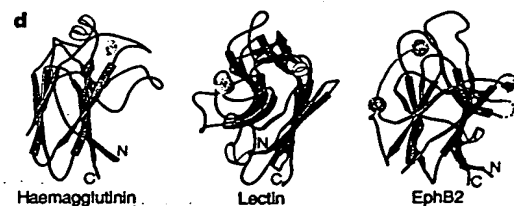
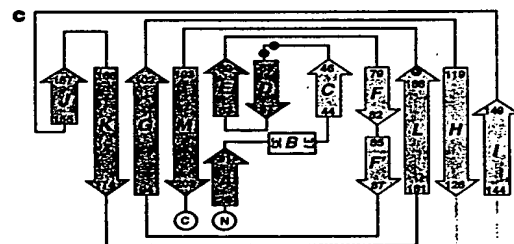
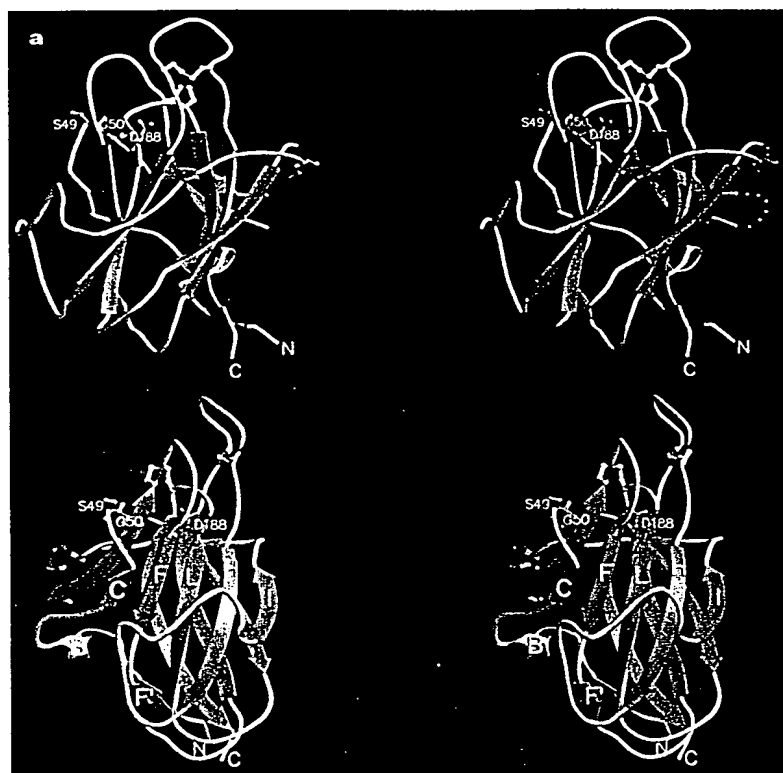


Figure 4 Structure of the N-terminal ligand-binding domain of EphB2. **a**, Two stereo views of the EphB2 ligand-binding domain. The N and C termini of the protein are labelled. The equivalent positions of VAB-1 point mutations are indicated as pink sidechain stick diagrams. The disulphide bridges are indicated as stick figures in white. The colour coding is as in Fig. 1. **b**, Stereo view of the α trace of the EphB2 ligand-binding domain; the colour is graduated from the N terminus, blue, to the C terminus, red. Every tenth residue is numbered. **c**, Diagram of the secondary structure. Residues were assigned to secondary-structure elements according to criteria defined in ref. 30. The N and C termini of

the protein are labelled, as are the residues at the ends of each β -strand and of the short 3_{10} helix. β -strands are shown as arrows and the helix as a rectangle. The colour coding is as in Fig. 1. **d**, Structures of two topological homologues of EphB2: left, the globular head of influenza virus haemagglutinin, with the location of the bound sialic acid shown in red²⁴; middle, *Griffonia simplicifolia* lectin, with the location of the bound human blood-group determinant shown in red²⁵; right, the globular domain of EphB2, with the proposed location for binding ephrin shown in red.

letters to nature

tend to be better conserved than those making up the convex β -sheet (Fig. 1). The secondary-structure elements that are most invariable are (Figs 1, 4) strand F, the G-H loop, strand I, the I-J loop, strand L and the L-M loop. Finally, the overall structural homology between the ligand-binding domain of EphB2 and the jellyroll carbohydrate-binding proteins indicates that they might use similar surface regions to bind their respective ligands. Several crystal and NMR structures reveal that the carbohydrates bind the receptors either at the top of the β -sandwich or at its concave face²⁰ and Fig. 4d shows two representative cases, haemagglutinin²⁴ and a legume-type lectin²⁵, for comparison with the ligand-binding domain of EphB2. Most structural studies of carbohydrate-binding proteins, however, involve low-affinity interactions ($K_d = 0.01$ – 0.1 mM) of mono-, di- or trisaccharides with a small region on the surface of the proteins, whereas a high-affinity interaction such as that between Eph receptors and their ligands would involve a larger protein-protein interface (Fig. 4d).

The structure of the globular domain of EphB2 is the first structure of a Eph RTK ligand-binding domain and reveals an unexpected molecular architecture. This is the first example, to our knowledge, of a *bona fide* protein-binding receptor with jellyroll folding topology. On the basis of the structure, published data and H-I-loop mutagenesis, we have located the surface region involved in ligand recognition, providing a starting point for further crystallographic, biochemical and genetic studies of Eph-receptor signalling. In particular, these data should aid directed, systematic analyses of ligand-receptor recognition to explain the high promiscuity within Eph subclasses but lack of interaction between subclasses. Furthermore, as we have already shown with the H-I loop, it should now be possible to design structure-based mutations that alter the affinity and specificity of receptor-ligand interactions to allow *in vivo* studies of how Eph receptor/ephrin expression boundaries and gradients direct the movement of cells and axons in the developing nervous system. □

Methods

Expression and crystallization. The sequence encoding the murine EphB2 globular domain (residues 28–210) was subcloned by the polymerase chain reaction (PCR) into a pET32 expression vector (Novagen), and overexpressed in *Escherichia coli* (strain AD494(DE3)) using the T7 RNA polymerase system. The protein was purified on a HiTrap Ni²⁺-chelating column (Pharmacia) and the histidine-containing N-terminal sequence was removed by thrombin proteolysis to yield EphB2(28–210) plus 36 N-terminal amino acids from the expression vector. A final anion-exchange chromatography step yielded material of homogeneity of 98% or greater. Mass spectrometry and DNA sequencing of the plasmid showed that the EphB2 ligand-binding domain used for crystallization was neither modified nor further proteolysed during expression and purification. Dynamic light scattering (Molecular Size Detector, Protein Solutions) showed that EphB2(28–210) was both monomeric and monodisperse at 1 mg ml⁻¹. The purified EphB2 protein was concentrated to 10 mg ml⁻¹ in a buffer containing 10 mM KCl, 2 mM MgCl₂ and 10 mM HEPES, pH 7.2, and crystallized in a hanging drop by vapour diffusion against reservoir containing 200 mM ammonium sulphate, 15% PEG 4000 and 50 mM sodium acetate, pH 4.8. Crystals grew in the tetragonal space group P4₂2₁2 (a = b = 55 Å, c = 159 Å) with one molecule in the asymmetric unit. Heavy-atom derivatives were prepared by soaking the crystals in the heavy-metal reagents at concentrations of 1–5 mM for 2–3 days.

Mutagenesis and ligand-binding assays. Gel mobility-shift assays, used to confirm the biological activity of the recombinant proteins, were done by incubating the components at 0.2 mM concentration for 10 min at room temperature and separating them on 10–20% gradient non-denaturing polyacrylamide gels. EphB2 ligand-binding domain mutants (EphB2-del has a deletion of Phe 135 to Trp 138; EphB2-A3 includes a substitution of EphB2 residues Phe 128 to Trp 143 with EphA3 residues Asp 128 to Phe 139) were generated by PCR and confirmed by automated sequencing. The mutant proteins were expressed and purified as before. Both mutant proteins were properly folded, as judged by the fact that they were monomeric and

monodisperse at 0.01–0.2 mM concentrations and formed stable 1:1 complexes with ephrin-B2 in gel mobility-shift and size-exclusion chromatographic assays. Ephrin-B2 and ephrin-A5 were expressed and purified as before but with the histidine tag left intact.

The pull-down experiments were done as follows: the Eph proteins were incubated (at room temperature, for 30 min, in 1 ml total reaction volume, in a binding buffer containing 150 mM KCl, 2 mM MgCl₂, 20 mM imidazole, 20 mM HEPES, pH 8.2) at various concentrations with ephrins that were prebound to Ni-affinity beads (Pharmacia) (fixed ephrin concentration of 0.2 μ M). The beads were then isolated by centrifugation and washed with 1 ml binding buffer. The bound proteins were separated on 10–20% gradient polyacrylamide gels. The amount of bound EphB2 was estimated by the intensity of the Coomassie-blue staining (Fotodyne FotoAnalyst scanner and MacBas software), and corrected for background. Dissociation constants were determined from unweighted least-squares fits of the data to the standard equilibrium binding equation $K_d = [L][R]/[RL]$, where [RL] is the concentration of the complex estimated from the amount of bound EphB2 [R] is the concentration of the free EphB2 and [L] is the concentration of free ephrin (in Fig. 2b, 'EphB2 bound' = [RL], and 'EphB2 total' = [RL] + [R]; [RL] + [L] = 0.2 μ M). The estimated apparent dissociation constants are not corrected for complex dissociation during the washing step and, therefore, are used as relative and not absolute measures of the binding affinities of the EphB2-ephrin constructs.

Data collection and structure determination. Diffraction was measured at room temperature using a Rigaku RAXIS-IV imaging plate area detector. Oscillation photographs were integrated, scaled and merged using DENZO and SCALEPACK²⁶. Subsequent calculations were done with the CCP4 program suite²⁷. An initial MIR electron-density map was calculated with data between 15 Å and 3.2 Å (mean figure of merit 0.72) and improved by density modification (Fig. 3) which allowed unambiguous tracing and sequence assignment of the globular EphB2 domain using program O (ref. 28). Refinement of the model by conventional least-squares algorithm was done with XPLOR²⁹. The final refined model at 2.9 Å resolution (Table 1) has a free R value²⁹ of 31.4% and comprises 1,377 non-hydrogen atoms in 172 well-defined amino acids in the electron density map, and no water molecules. No electron density is observed for the six carboxy-terminal residues, for loop residues 59–61 and 160–163, and for the 34 N-terminal fusion residues introduced by the expression vector. Tightly restrained refinement of temperature factors was monitored throughout by the free-R-factor criterion²⁹. Stereochemical analysis of the refined model using PROCHECK (CCP4 suite) revealed main-chain and sidechain parameters better than, or within the typical range of, values for protein structures determined at 2.9 Å resolution (overall G-factor, -0.14). Only two EphB2 residues (Ala 39 and Ala 91) fell in the disallowed region of the Ramachandran plot.

Received 2 September; accepted 14 October 1998.

1. Eph Nomenclature Committee. Unified nomenclature for Eph family receptors and their ligands, the ephrins. *Cell* 90, 403–440 (1997).
2. Flanagan, J. G. & Vandehaeghe, P. The ephrins and Eph receptors in neural development. *Annu. Rev. Neurosci.* 21, 309–345 (1998).
3. Drescher, U. et al. *In vitro* guidance of retinal ganglion cell axons by RAGS, a 25 kDa tectal protein related to ligands for Eph receptor tyrosine kinases. *Cell* 82, 359–370 (1995).
4. Henkemeyer, M. et al. Nuk controls pathfinding of commissural axons in the mammalian central nervous system. *Cell* 86, 35–46 (1996).
5. Orioli, D., Henkemeyer, M., Lemke, G., Klein, R. & Pawson, T. Sek4 and Nuk receptors cooperate in guidance of commissural axons and in palate formation. *EMBO J.* 15, 6035–6049 (1996).
6. Park, S., Frisen, J. & Barbacid, M. Aberrant axonal projections in mice lacking EphA8 (Eek) tyrosine protein receptors. *EMBO J.* 16, 3106–3114 (1997).
7. Winslow, J. W. et al. Cloning of AL-1, a ligand for an Eph-related tyrosine kinase receptor involved in axon bundle formation. *Neuron* 14, 973–981 (1995).
8. Smith, A., Robinson, V., Patel, K. & Wilkinson, D. G. The EphA4 and EphB1 receptor tyrosine kinases and ephrin-B2 ligand regulate targeted migration of branchial neural crest cells. *Curr. Biol.* 7, 561–570 (1997).
9. Xu, Q., Allidus, G., Holder, N. & Wilkinson, D. G. Expression of truncated *Sek-1* receptor tyrosine kinase disrupts the segmental restriction of gene expression in the *Xenopus* and zebrafish hindbrain. *Development* 121, 4005–4016 (1995).
10. Wang, H. U. & Anderson, D. J. Eph family transmembrane ligands can mediate repulsive guidance of trunk neural crest migration and motor axon outgrowth. *Neuron* 18, 383–396 (1997).
11. Krull, C. E. et al. Interactions of Eph-related receptors and ligands confer rostrocaudal pattern to trunk neural crest migration. *Curr. Biol.* 7, 571–580 (1997).
12. Gale, N. W. et al. Eph receptors and ligands comprise two major specificity subclasses and are reciprocally compartmentalized during embryogenesis. *Neuron* 17, 9–19 (1996).
13. Holland, S. J. et al. Bi-directional signalling through the EPH-family receptor Nuk and its transmembrane ligands. *Nature* 383, 722–725 (1996).
14. Bruckner, K., Pasquale, E. B. & Klein, R. Tyrosine phosphorylation of transmembrane ligands for Eph receptors. *Science* 275, 1640–1643 (1997).

- Acknowledgements.** We thank I. Berry for technical support; P. D. Jeffrey for help with X-ray measurements; U. Drescher for ephrin-A5 DNA; and S. K. Burley, J. Goldberg, N. P. Pavlitch and M. K. Rosen for useful suggestions. J.-P.H. is a Winston Foundation fellow. This work was supported by the DeWitt Wallace Fund and the V Foundation (D.B.N.), and by the Kent Waldrup National Paralysis Foundation for Basic Neuroscience Research (M.H.).

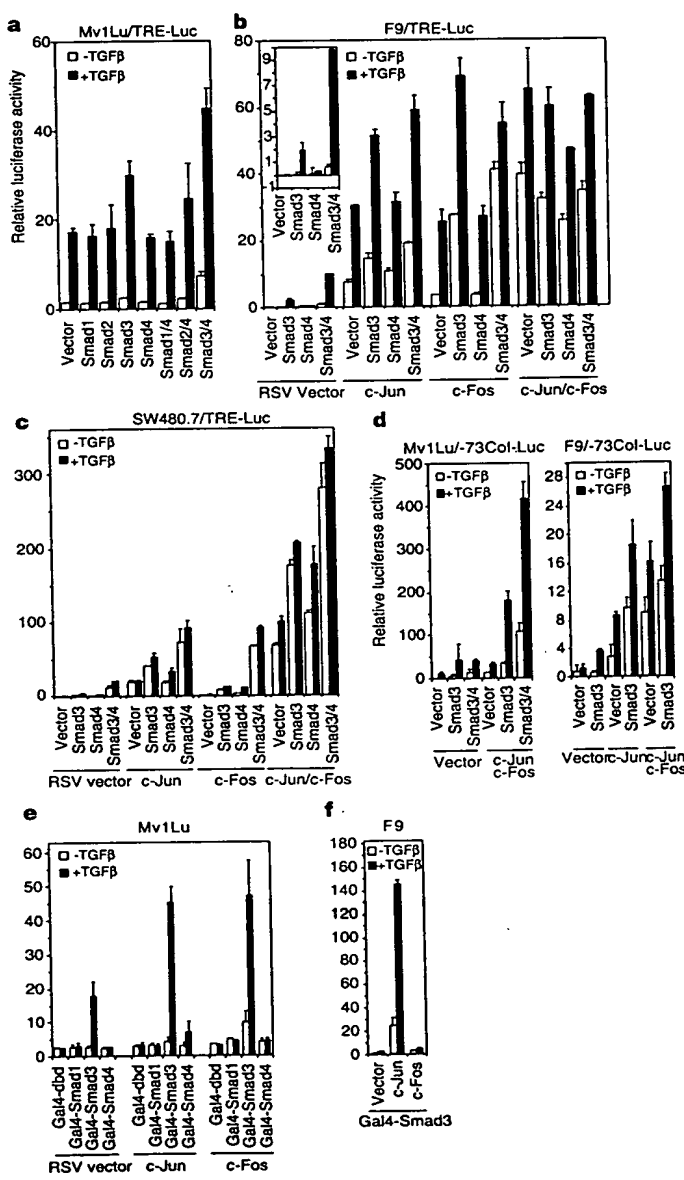
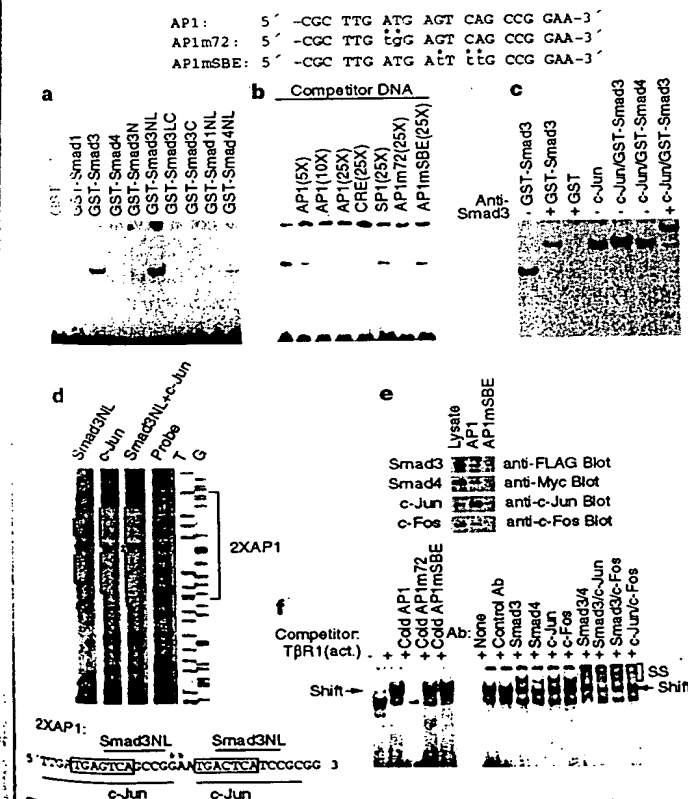
Correspondence and requests for materials should be addressed to D.B.N. (e-mail: Dimitar@ximpact3.ski.mskcc.org). Coordinates have been deposited with the Brookhaven Protein Data Bank under accession number 1nuk.

Smad3 and Smad4 cooperate with c-Jun/c-Fos to mediate TGF- β -induced transcription

Nature 394, 909–913 (1998)

In Fig. 1 of this Letter, the key in all panels was incorrect: black bars should be +TGF- β , and white bars should be -TGF- β ; in addition, the c-Fos Smad3/4 bar colours were transposed in panel b. The correct figure is shown here.

In Fig. 3f, right panel, the symbols should all have been plus signs, as shown here. There were also two typographical errors in Fig. 3a (1N: not 31NL; 4NL, not 34NL). ☐



**This Page is Inserted by IFW Indexing and Scanning
Operations and is not part of the Official Record**

BEST AVAILABLE IMAGES

Defective images within this document are accurate representations of the original documents submitted by the applicant.

Defects in the images include but are not limited to the items checked:

☐ BLACK BORDERS

☒ IMAGE CUT OFF AT TOP, BOTTOM OR SIDES

☐ FADED TEXT OR DRAWING

☐ BLURRED OR ILLEGIBLE TEXT OR DRAWING

☐ SKEWED/SLANTED IMAGES

☐ COLOR OR BLACK AND WHITE PHOTOGRAPHS

☐ GRAY SCALE DOCUMENTS

☐ LINES OR MARKS ON ORIGINAL DOCUMENT

☒ REFERENCE(S) OR EXHIBIT(S) SUBMITTED ARE POOR QUALITY

☐ OTHER: _____

IMAGES ARE BEST AVAILABLE COPY.

As rescanning these documents will not correct the image problems checked, please do not report these problems to the IFW Image Problem Mailbox.